

NASA-CR-3267 19800015748

NASA Contractor Report 3267

Application of Advanced Computational Procedures for Modeling Solar-Wind Interactions With Venus - Theory and Computer Code

Stephen S. Stahara, Daniel Klenke,
Barbara C. Trudinger, and John R. Spreiter

CONTRACT NASW-3182
MAY 1980

FOR REFERENCE

NOT TO BE TAKEN FROM THIS ROOM

LIBRARY COPY

MAY 20 1980

LANGLEY RESEARCH CENTER
LIBRARY, NASA
HAMPTON, VIRGINIA



NF02112



NASA Contractor Report 3267

Application of Advanced Computational
Procedures for Modeling Solar-Wind
Interactions With Venus -
Theory and Computer Code

Stephen S. Stahara, Daniel Klenke,
Barbara C. Trudinger, and John R. Spreiter
Nielsen Engineering & Research, Inc.
Mountain View, California

Prepared for
NASA Headquarters
under Contract NASW-3182

NASA

National Aeronautics
and Space Administration

**Scientific and Technical
Information Office**

1980

TABLE OF CONTENTS

<u>Section</u>	<u>Page No.</u>
LIST OF ILLUSTRATIONS	iv
SUMMARY	1
INTRODUCTION	2
LIST OF SYMBOLS	4
ANALYSIS	8
The Mathematical Model - Formulation of the Fluid Representation	8
<u>Governing equations</u>	8
<u>Conditions at discontinuities</u>	10
<u>Frozen-field approximation</u>	12
Determination of the Ionosphere Boundary	14
Calculation of the Gasdynamic Flow Properties	20
<u>Nose region solution - implicit unsteady Euler equation method</u>	21
<u>Downstream region solution - shock capturing marching method</u>	25
<u>Calculation of the streamlines</u>	27
Calculation of the Magnetic Field	27
Calculation of the Contour Lines	30
Solar-Ecliptic/Solar-Wind Coordinate Transformations	31
Properties Along a Spacecraft Trajectory	33
RESULTS	36
CONCLUDING REMARKS	47
ACKNOWLEDGEMENTS	48
APPENDIX A - COMPUTER PROGRAM USER'S MANUAL	49
APPENDIX B - LISTING OF COMPUTER PROGRAM	131
APPENDIX C - CATALOG OF TEST CASES	177
REFERENCES	287
TABLE 1	289
FIGURES 1 THROUGH 20	291

LIST OF ILLUSTRATIONS

<u>Figure</u>	<u>Page No.</u>
1. Illustration of ionopause shapes for atmospheres with various (i) constant scale heights H/R_0 and (ii) gravitational variation included in the scale height \bar{H}/R_0 .	291
2. Comparison of former and present computational procedures for determining the gasdynamic flow properties of solar wind-magneto/ionopause interactions	292
3. Transformation from physical domain to rectangular computational domain	293
4. Illustration of capability for providing an additional flow-field segment to the obstacle nose solution in the computational procedure for determining the gasdynamic flow properties of solar wind-ionopause interactions	294
5. Illustration of quantities used for streamline calculation	295
6. Illustration of quantities used for magnetic field-line calculation in the plane of magnetic symmetry	295
7. Illustration of the components of the three-dimensional magnetic field	296
8. Illustration of the sun-planet (x_s, y_s, z_s) and solar wind (x, y, z) coordinate systems and the azimuthal (Ω) and polar (ϕ_p) solar-wind angles, both shown in a positive sense	297
9. Illustration of solar-wind (x, y, z) and (X, Y, Z) coordinate systems and the interplanetary magnetic field and magnetic-field angles (α_p, α_n)	298
10. Bow shock locations for $M_\infty = 8.0$, $\gamma = 5/3$ flow past constant scale-height ionopause shapes with $H/R_0 = 0.5$ and 1.0	299
11. Bow shock shapes for flow past an ionopause shape with gravitational variation included in scale height with $H/R_0 = 0.25$, $\gamma = 5/3$ and $M_\infty = 2.0$ and 3.0	300
12. Overall features of Pioneer-Venus Orbiter trajectory crossings of solar-wind/Venus-ionosphere interaction region	301
13. Illustration of typical flow-field grid density for gasdynamic solution; $M_\infty = 3.0$, $\gamma = 5/3$	302
14. P-V Orbit 6 trajectories and observational bow shock crossings as viewed in solar-wind coordinates based on inbound and outbound interplanetary solar-wind directions; also, various bow shock shapes for different interplanetary solar-wind conditions	303

LIST OF ILLUSTRATIONS (Concluded)

<u>Figure</u>	<u>Page No.</u>
15. Comparison of observed (OPA) and theoretical time histories of ionosheath plasma properties for P-V Orbit 6 based on inbound and outbound interplanetary solar-wind conditions using a gasdynamic solution for $M_{\infty} = 13.3$, $\gamma = 2.0$	304
16. Comparison of observed (OMAG) and theoretical time histories for the magnitude of the magnetic field for P-V Orbit 6 based on inbound and outbound interplanetary conditions using gasdynamic solution for $M_{\infty} = 13.3$, $\gamma = 2$	305
17. P-V Orbit 3 trajectories and observational bow shock crossings as viewed in solar-wind coordinates based on inbound and outbound interplanetary solar-wind directions; also, various bow shock shapes for different interplanetary solar wind conditions	307
18. Comparison of observed and theoretical time histories of ionosheath plasma properties for P-V Orbit 3 based on inbound and outbound interplanetary solar-wind conditions	308
19. Comparison of observed (OMAG) and theoretical time histories for the magnetic field for P-V Orbit 3 based on inbound and outbound interplanetary solar-wind conditions using gasdynamic solutions $M_{\infty} = 7.38$, $\gamma = 2.0$ for inbound and $M_{\infty} = 5.96$, $\gamma = 2.0$ for outbound calculations	309
20. Comparison of observed (OMAG) and theoretical time histories of the magnetic field for P-V Orbit 3 based on inbound solar wind interplanetary conditions using a gasdynamic solution for $M_{\infty} = 3.0$, $\gamma = 5/3$	311

APPLICATION OF ADVANCED COMPUTATIONAL PROCEDURES FOR
MODELING SOLAR-WIND INTERACTIONS WITH VENUS - THEORY
AND COMPUTER CODE

by

Stephen S. Stahara, Daniel Klenke,
Barbara C. Trudinger, and John R. Spreiter

SUMMARY

Advanced computational procedures are developed and applied to the prediction of solar-wind interaction with nonmagnetic terrestrial-planet atmospheres, with particular emphasis to Venus. The theoretical method is based on a single-fluid, steady, dissipationless, magnetohydrodynamic continuum model, and is appropriate for the calculation of axisymmetric, supersonic, super-Alfvénic solar-wind flow past terrestrial planets. The procedures, which consist of finite-difference codes to determine the gasdynamic properties and a variety of special-purpose codes to determine the frozen magnetic field, streamlines, contours, plots, etc. of the flow, are organized into one computational program which has been extensively documented and is presented in a general user's manual included as part of this report.

Theoretical results based upon these procedures are reported for a wide variety of solar-wind conditions and ionopause obstacle shapes. Plasma and magnetic-field comparisons in the ionosheath are also provided with actual spacecraft data obtained by the Pioneer-Venus Orbiter. These results have verified the appropriateness of the basic theoretical model, and have indicated the importance of accounting for the variable oncoming direction of the interplanetary solar wind.

INTRODUCTION

The magnetohydrodynamic models (refs. 1-9) of solar-wind interaction with planetary magneto/ionospheres and their associated calculations of the detailed flow and magnetic-field properties provide the basis of the theoretical understanding and interpretation of phenomena occurring in space around terrestrial planets from the viewpoint of a fluid rather than particle description of the flow. The general value and usefulness of results based on these models are now well established, and have advanced to the point where theoretical calculations can be used to predict important planetary and magnetic-field characteristics.

Prior to the previous work reported in reference 9, the utility of calculations based on these models was severely restricted due both to the fact that the original solution techniques employed bordered on what was barely possible at the time, as well as that considerable hand computation and intervention was required. Moreover, reported results were carried out for only a limited set of solar-wind conditions such as obstacle shape, oncoming Mach number, interplanetary magnetic field, etc., and were presented in archival publications only in the form of plots from which results for other conditions had to be determined by interpolation. The importance of the preliminary work of reference 9 was that advanced computational methods, based on current state-of-the-art algorithms, were introduced to this problem to provide the basic gas-dynamic solutions. The frozen-in magnetic-field was then solved for on the high-resolution flow-field grid, and the entire computational procedure was assembled into a user-oriented program providing the detailed flow-field and magnetic-field properties in a convenient output format.

In the current work reported here, those basic procedures have been extended and generalized in several important directions. These include the capability for treating very low oncoming interplanetary gasdynamic Mach numbers ($M_\infty \approx 2.0$), as well as quite general ionopause shapes. A new family of ionopause shapes has been developed which accounts for the effect of gravitational variation in scale height. Additionally, the capability for determining the plasma gasdynamic and magnetic-field properties along an arbitrary spacecraft trajectory, simultaneously accounting

for an arbitrary oncoming direction of the solar wind, has been developed. Moreover, a large number of sample calculations have been performed for typical solar-wind conditions and, using the output contour-plot capability, a catalog of these cases were established and are archived here for convenient quick-look use. Finally, a number of successful comparisons were made by the present computational model with actual spacecraft observations obtained from initial orbits of the Pioneer-Venus Orbiter. These comparisons have both provided a verification of the basic theoretical model as well as demonstrated its value as a convenient research tool capable of routinely providing details of the solar-wind/planetary atmosphere interaction process not previously attainable--at modest computational cost and in a format directly compatible with observational data.

LIST OF SYMBOLS

a	speed of sound, $(\gamma p/\rho)^{1/2}$
A	Alfvén speed, $(B^2/4\pi\rho)^{1/2}$
\bar{A}	Jacobian matrix associated with IMP code, equal to $\partial\hat{E}/\partial\hat{U}$
\underline{B}	magnetic field vector
\bar{B}	Jacobian matrix associated with IMP code, equal to $\partial\hat{F}/\partial\hat{U}$
C_p	specific heat at constant pressure
C_v	specific heat at constant volume
D	distance defined by eq. (59)
e	internal energy, eq. (3)
e_t	total energy, eq. (44)
E	column matrix defined by eq. (42)
\hat{E}	column matrix associated with IMP code, equal to $(\xi_T U + \xi_X E + \xi_R F)/J$
F	column matrix defined by eq. (42)
\hat{F}	column matrix associated with IMP code, equal to $(\eta_T U + \eta_X E + \eta_R F)/J$
g	acceleration due to gravity
g_k	gravitational component, eq. (5)
G	column matrix defined by eq. (42)
h	enthalpy, eq. (47)
h_t	total enthalpy, eq. (47)
H	local scale height of atmosphere, $\bar{RT}/\bar{M}g$
\bar{H}	local scale height with gravitational variation, $H(R_R/R_S)^2$
J	Jacobian matrix, eq. (43)
K	constant defined by eq. (34)
$\Delta\ell$	vector length of elemental magnetic flux tube
M	local Mach number, $ \underline{v} /a$
\bar{M}	nondimensional mean molecular mass, equal to 1/2 for ionized atomic hydrogen

LIST OF SYMBOLS (Continued)

M_A	local Alfvén Mach number, $ v /A$
P	pressure
q	shock velocity
Q	dummy parameter
r	spherical radial distance
R	cylindrical radial distance
\bar{R}	gas constant, 8.315×10^7 ergs/gm $^\circ$ K
R_i	spherical radius of ionopause, eq. (39)
R_o	spherical distance from center of planet to ionopause nose
S_k	Poynting vector component
ΔS	incremental distance along streamline
t, T	time
(u, v, w)	velocity components associated with the (X, Y, Z) coordinate directions, respectively
U	column matrix defined by eq. (42)
\hat{U}	column matrix associated with IMP code, equal to U/J
v	velocity vector
(x, y, z) or (x_w, y_w, z_w)	solar-wind oriented Cartesian coordinates with origin at planetary center, x positive upstream and z positive northward
(x_s, y_s, z_s)	sun-planet oriented Cartesian coordinates with origin at planetary center, x_s positive toward sun, y_s positive opposite to planetary orbital motion, and z_s positive northward
(x', y', z')	solar-wind oriented Cartesian coordinates defined by an azimuthal rotation given by eq. (70)
(X, Y, Z)	solar-wind oriented Cartesian coordinates with origin at planetary center, X positive downstream and Z positive northward
α_p	interplanetary magnetic-field angle between perpendicular and parallel components, eq. (62)
α_n	interplanetary magnetic-field angle between normal and in-plane components, eq. (63)

LIST OF SYMBOLS (Continued)

β	spherical polar angle, measured with origin at planet center, from subsolar point away from undisturbed solar wind direction; varies from 0 in upstream direction to π in downstream direction; eq. (39)
γ	ratio of plasma specific heats
δ	angle defined by eq. (59)
δ_{ik}	Kronecker delta
δ_S	local angle of bow shock wave
$(\delta_\xi, \delta_\eta)$	second-order difference operators in (,) direction
ϵ	smoothing coefficient in IMP code
η	transformation variable, eqs. (40), (48)
θ	azimuthal rotation angle in solar-wind (X,Y,Z) system, eq. (69); also shock tangency angle, eq. (59)
Λ	quantity defined by eq. (36)
ξ	transformation variable, eqs. (40), (48)
ρ	density
σ	conductivity
τ	transformed time, eq. (40)
Φ	gravitational potential, eq. (5)
ϕ_p	solar-wind polar angle
ψ	angle between outward normal to magneto/ionosphere boundary and oncoming undisturbed solar wind, eq. (32); also, angle of magnetic component $(\underline{B}/B_\infty)_\perp$, eq. (58)

Subscripts

b	obstacle body
i	ionopause
n	normal direction
P	arbitrary point
R	reference quantity
s	planetary surface; also streamline
S	shock surface

LIST OF SYMBOLS (Concluded)

s_t	stagnation conditions
t	tangential direction
o	reference quantity at subsolar point
1	conditions upstream of a discontinuity
2	conditions downstream of a discontinuity
∞	interplanetary undisturbed quantity
(\parallel, \perp, n)	parallel, perpendicular, and normal magnetic-field components as defined in eq. (56)

Superscripts

\wedge	unit vector
$*$	relative to shock

ANALYSIS

The Mathematical Model - Formulation of the Fluid Representation

The fundamental assumption underlying the present work and that reported in all of the references cited above is that the average bulk properties of solar-wind flow around a planetary magneto/ionosphere can be adequately described by the continuum equations of magnetohydrodynamics for a single-component perfect gas having infinite electrical conductivity and zero viscosity and thermal conductivity. Theoretical justification of this point has not yet been established, and proof remains essentially qualitative at present. The primary justification for use of the continuum fluid model is the outstanding agreement of the qualitative results predicted on this basis with those actually measured in space. It appears that the continuum model is capable of accounting both for many of the details as well as the broad features of the observations.

Governing equations.- The equations which express the conservation of the average bulk mass, momentum, energy, and magnetic field of the solar-wind plasma are given by the following expressions:

$$\frac{\partial \rho}{\partial t} + \frac{\partial}{\partial x_k} (\rho v_k) = 0 \quad (1)$$

$$\frac{\partial}{\partial t} (\rho v_i) + \frac{\partial}{\partial x_k} \left[\rho v_i v_k + p \delta_{ik} - \frac{B_i B_k}{4\pi} + \frac{B^2}{8\pi} \delta_{ik} + \frac{g_i g_k}{4\pi G} - \frac{g^2}{8\pi G} \delta_{ik} \right] = 0 \quad (2)$$

$$\frac{\partial}{\partial t} \left[\frac{\rho v^2}{2} + \rho e + \rho \phi + \frac{B^2}{8\pi} \right] + \frac{\partial}{\partial x_k} \left[\rho v_k \left(\frac{v^2}{2} + e + \frac{p}{\rho} + \phi \right) + S_k \right] = 0 \quad (3)$$

$$\frac{\partial B_i}{\partial t} = \frac{\partial}{\partial x_k} (v_i B_k - v_k B_i) , \quad \frac{\partial B_i}{\partial x_i} = 0 \quad (4)$$

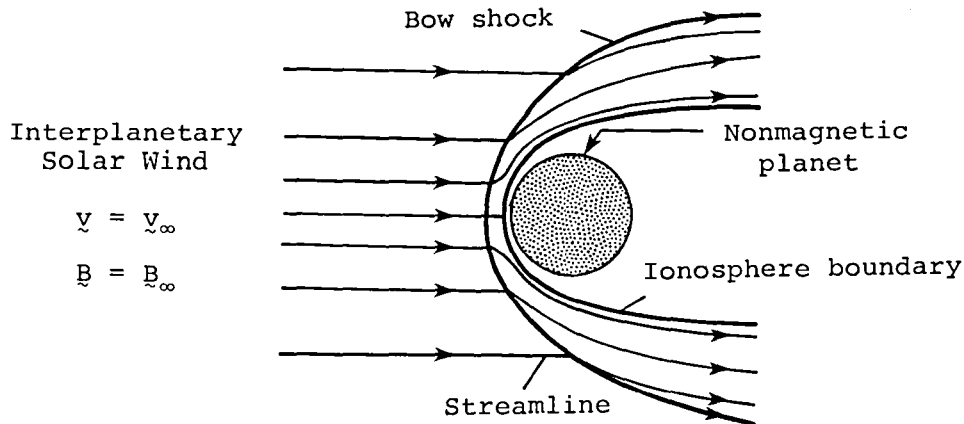
where

$$g_i = - \frac{\partial \phi}{\partial x_i} , \quad S_k = \frac{1}{4\pi} \left(v_k B^2 - B_k v_i B_i \right) \quad (5)$$

and the equation of state of a perfect gas is given by

$$p = \frac{\rho \bar{R} T}{\bar{M}} \quad (6)$$

In these equations and those to follow, the symbols ρ , p , v , T , $e = C_v T$, and $h = C_p T$ refer to the density, pressure, velocity, temperature, internal energy and enthalpy, and C_v and C_p refer to the specific heats at constant volume and pressure. We define the symbol $\bar{R} = (C_p - C_v) \bar{M} = 8.31 \times 10^7$ ergs/gm $^\circ$ K as the universal gas constant, and \bar{M} as the mean molecular weight nondimensionalized so that $\bar{M} = 16$ for atomic oxygen. For fully ionized hydrogen, \bar{M} is thus 1/2. The magnetic field \underline{B} and the Poynting vector \underline{S} for the flux of electromagnetic energy are expressed in terms of gaussian units. The gravitational potential ϕ and acceleration \underline{g} are assumed to be due to massive fixed bodies so that their time derivatives are zero. These equations apply in the region exterior to the ionosphere boundary, as shown in the sketch below, and also in a degenerate sense in the ionosphere.



Conditions at discontinuities.- Because of the omission of dissipative terms in these equations, surfaces of discontinuity may develop in the solution, across which the fluid and magnetic properties change abruptly, but in such a way that mass, momentum, magnetic flux, and energy are conserved. These are approximations to comparatively thin surfaces across which similar but continuous changes in the fluid and magnetic properties occur in the corresponding theory of a dissipative gas, and correspond physically to the bow wave, ionosphere boundary, and possibly other thin regions of rapidly changing properties. Across these surfaces, continuous solutions of the dissipationless differential equations cease to exist. The flow is no longer governed solely by the differential equations (1) to (4), but must be supplemented by additional considerations. The conservation of mass, momentum, magnetic flux, and energy lead to the following conditions which relate quantities on the two sides of any such discontinuity:

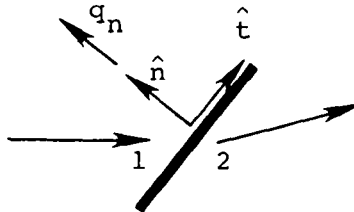
$$[\rho v_n^*] = 0 \quad (7)$$

$$[\rho \underline{v} \cdot \underline{v}_n^* + (p + B^2/8\pi)\hat{n} - B_n \underline{B}_t/4\pi] = 0 \quad (8)$$

$$[\underline{B}_t \cdot \underline{v}_n^* - B_n \cdot \underline{v}_t] = 0 \quad (9)$$

$$\left[\underline{v}_n^* \left(\frac{1}{2} \rho v^2 + \rho e + p + \frac{B^2}{4\pi} \right) + q_n \cdot \left(p + \frac{B^2}{8\pi} \right) - \frac{B_n (\underline{v} \cdot \underline{B})}{4\pi} \right] = 0 \quad (10)$$

Here, (\hat{n}, \hat{t}) denote unit vectors normal and tangential to the discontinuity surface, as sketched below,



where q_n represents the local normal velocity of the discontinuity surface, and $v_n^* = v_n - q_n$ is the fluid normal velocity component relative to the normal velocity q_n of the discontinuity surface. The square brackets are used to indicate the difference between the enclosed quantities on the two sides of the discontinuity, as in $[Q] = Q_2 - Q_1$ where subscripts 1 and 2 refer to conditions on the upstream and downstream sides, respectively, of the discontinuity.

Five classes of discontinuities are described by Eqs. (7-10). Those with $v_n^* = 0$ are called tangential discontinuities or contact discontinuities according to whether or not B_n vanishes. Discontinuities across which there is flow ($v_n^* \neq 0$) are divided into three categories called rotational discontinuities, and fast and slow shock waves. Some properties which distinguish the various discontinuities are indicated by the following relationships:

Tangential:

$$v_n^* = B_n = 0, [\underline{v}_t] \neq 0, [\underline{B}_t] \neq 0, [\rho] \neq 0, [p + B^2/8\pi] = 0 \quad (11)$$

Contact:

$$v_n^* = 0, B_n \neq 0, [\underline{v}] = [\underline{B}] = [p] = 0, [\rho] \neq 0 \quad (12)$$

Rotational:

$$v_n^* = \pm B_n / \sqrt{4\pi\rho}, [\underline{v}_t] = \pm [\underline{B}_t] / \sqrt{4\pi\rho} \quad (13)$$

$$[\rho] = [p] = [v_n] = [v^2] = [B^2] = [B_n] = 0$$

Fast and Slow Shock Waves:

$$v_n^* \neq 0, [\rho] > 0, [p] > 0, [B_n] = 0$$

$$\left(\rho v_n^* \right)_{\text{fast}} \geq \left(\rho v_n^* \right)_{\text{rot.}} \geq \left(\rho v_n^* \right)_{\text{slow}} \quad (14)$$

B_t and B^2 $\left\{ \begin{array}{l} \text{increase} \\ \text{decrease} \end{array} \right\}$ through $\left\{ \begin{array}{l} \text{fast} \\ \text{slow} \end{array} \right\}$ shock waves

Of the five classes of discontinuities possible, two of these, the fast shock wave and the tangential discontinuity, are of concern in the present applications. The first relates conditions on the two sides of the bow shock wave, and any other shock waves present, while the latter has properties required to describe a boundary surface (ionopause) that separates the flowing solar wind and the planetary ionosphere. More detailed consideration of the tangential discontinuity condition leads to a determination of the ionopause shape, as described in the following sections.

With regard to conditions at the bow wave, for solar-wind flows past Venus, as well as Mars and the Earth, that discontinuity can only be represented by a fast shock wave since the mass flux through each of the other possible choices is too small. With regard to conditions at the ionopause, of the various possibilities, only the tangential discontinuity has properties compatible with those required to describe a boundary surface that separates the externally flowing solar wind and the planetary atmosphere; that is, the condition $v_n^* = 0$ prohibits flow across the boundary, while the condition $B_n = 0$ must hold since by assumption no magnetic field exists interior to the ionopause and the solenoidal jump condition $[B_n] = 0$ always holds.

Frozen-field approximation.— Two important parameters characterize the solar-wind flow at any field point as described by eqs. (1-5). These are the Mach number $M = v/a$ and the Alfvén Mach number $M_A = v/A$. The former is the ratio of the flow velocity to the speed of sound $a = (\gamma p/\rho)^{1/2}$, while the latter is the ratio of the flow velocity to the speed $A =$

$(B^2/4\pi\rho)^{1/2}$ of a rotational or Alfvén wave propagating along the direction of the magnetic field.

For typical solar-wind conditions (refs. 5,6), both the oncoming Mach number and the Alfvén Mach number are high ($M_\infty \approx M_A \approx 0(10)$). In this instance, an important simplification of the magnetohydrodynamic equations occurs. This is so because the order of magnitude of the inertia term in differential equation (2) for the momentum is related to that of the magnetic terms by the square of the Alfvén Mach number. When the latter is large, therefore, the magnetic terms in eqs. (2), (3), (8), and (10) decouple from the gasdynamic portions of those equations. Furthermore, for Earth, Venus, or Mars, the strong interactive nature of the flow permits the terms involving \underline{g} and Φ to be disregarded because of the relative smallness of their effect on the fluid motion (ref. 5). The equations for the fluid motion thereby reduce to those of gasdynamics, while the magnetic field \underline{B} can be determined subsequently by solving the remaining equations using the values for \underline{v} already determined. The magnetic field, determined in this fashion, is usually interpreted as being "frozen-in" or moving with the fluid (ref. 5).

This then results in the following differential and conservation equations; for the flow field

$$\frac{\partial \rho}{\partial t} + \frac{\partial}{\partial x_k} (\rho v_k) = 0 \quad (15)$$

$$\frac{\partial}{\partial t} (\rho v_i) + \frac{\partial}{\partial x_k} (\rho v_i v_k + p \delta_{ik}) = 0 \quad (16)$$

$$\frac{\partial}{\partial t} \left(\frac{\rho v^2}{2} + \rho e \right) + \frac{\partial}{\partial x_k} \left[\rho v_k \left(\frac{v^2}{2} + e + p/\rho \right) \right] = 0 \quad (17)$$

$$[\rho v_n^*] = 0 \quad (18)$$

$$[\rho \underline{v} \cdot \underline{v}_n^* + p] = 0 \quad (19)$$

$$\left[\mathbf{v}_n^* \cdot \left(\frac{1}{2} \rho v^2 + \rho e + p \right) \right] = 0 \quad (20)$$

and for the magnetic field

$$\frac{\partial B_i}{\partial t} + \frac{\partial}{\partial x_k} (v_k B_i - v_i B_k) = 0 \quad (21)$$

$$\frac{\partial B_i}{\partial x_i} = 0 \quad (22)$$

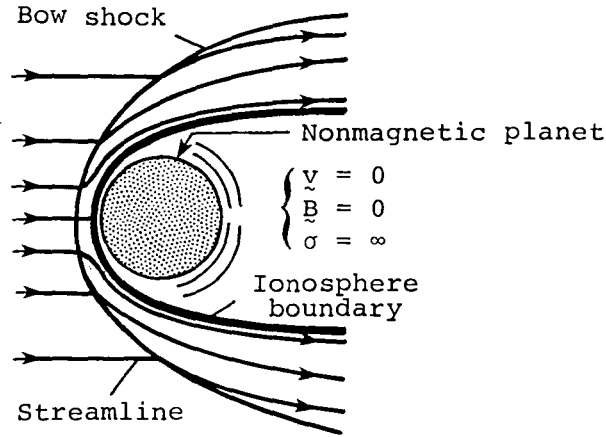
$$[B_n] = 0 \quad (23)$$

$$[B_n \cdot \mathbf{v}_t - B_t \cdot \mathbf{v}_n^*] = 0 \quad (24)$$

Equations (15) to (24) provide the governing equations which form the basis of the mathematical representation of the solar wind-magneto/ionosphere interaction problem considered here. For all of the results as well as the computer codes presented herein, we are interested exclusively in the steady-state solution to these equations which are obtained by setting $\partial/\partial t = 0$ and $\mathbf{v}_n^* = \mathbf{v}_n$, i.e. $q_n = 0$. We have presented the unsteady equations, however, since one of the computational methods used to determine the gasdynamic solution employs an unsteady procedure, integrating in time until the steady-state solution is asymptotically obtained.

Determination of the Ionosphere Boundary

The determination of the ionosphere boundary initiates from the assumptions that the ionosphere, or at least the outer part of it that participates in the interaction with the solar wind, is idealized as a spherically-symmetric and hydrostatically-supported plasma having infinite electrical conductivity, effectively bound to the planet and incapable of mixing with the solar wind, as indicated in the sketch below:



This interior plasma is separated from the flowing solar plasma by a tangential discontinuity across which the relations

$$v_n = B_n = [p + B^2/8\pi] = 0 \quad (25)$$

$$[\underline{v}_t] \neq 0; [B_t] \neq 0; [\rho] \neq 0$$

given previously (eq. (11)) must hold. The basis for important simplifying approximations to these conditions, which can be assumed to apply at the Venusian ionosphere boundary and possibly for that at Mars as well, is that the gas pressure p is much larger than the magnetic pressure $B^2/8\pi$ on both sides of the ionopause. Therefore, the discontinuity pressure balance relation $[p + B^2/8\pi] = 0$ of eq. (25) reduces to a simple equality between the ionosphere pressure and the static pressure of the flowing solar plasma adjacent to the ionopause, i.e.

$$(p)_{\text{atm.}} = (p)_{\text{flow}} \quad (26)$$

Determination of the ionospheric pressure in the vicinity of the ionopause for the ionosphere models chosen in this study proceeds from the assumption of hydrostatic support, which implies a quiescent ionosphere where the bulk motions of the gas with respect to the planet are sufficiently small ($\underline{v} = 0$) that equilibrium exists between the pressure gradient and gravity, viz.

$$dp/dr = -\rho g \quad (27)$$

where p and ρ are the gas pressure and density, r is the radial distance measured from the center of the planet, and g is the acceleration due to gravity. The variation of g is inversely proportional to r_s , so that $g = g_s (r_s/r)^2$ where the subscript s denotes values at the surface of the planet. Since the density ρ is related to the pressure according to the perfect gas law eq. (6), eq. (27) can be integrated to yield

$$p = p_R \exp \left[- \int_{R_R}^r \frac{dr}{H} \right] \quad (28)$$

where p_R is the pressure at some reference radius R_R and H is the local scale height of the atmosphere given by $H = \bar{R}T/\bar{M}g$.

If H is regarded as constant; that is, if variations of g and T with r are neglected, eq. (27) can be integrated directly to yield

$$p = p_R \exp \left[- \frac{r - R_R}{H} \right] \quad (29)$$

In view of uncertainties associated with measurements of the atmospheric properties of Venus and Mars, the variation of p with r as given by eq. (29) was adopted in the initial solar wind/ionosphere applications (ref. 6) and was also used in the previous study (ref. 9) involving the initial application of advanced computational methods to this problem. With preliminary ionospheric data now available from the Pioneer-Venus spacecraft (refs. 10 and 11), some of these uncertainties for Venus have been removed. It has been found that the assumption of an isothermal ($T = \text{constant}$) atmosphere at typical ionopause heights is quite reasonable. Consequently, there is no need to neglect the variation of gravity in the scale height in eq. (28). Including this effect leads to the following result for the pressure

$$p = p_R \exp \left[- \frac{R_R \cdot (r - R_R)}{\bar{H} \cdot r} \right] \quad (30)$$

where

$$\bar{H} = H_s \cdot (R_R/R_s)^2 \quad (31)$$

and R_s is the planetary radius and $H_s = \bar{RT}/\bar{M}g_s$. Equations (29) and (30) provide the two models employed in this study for the ionosphere pressure variation which is required in eq. (26) for the pressure balance condition at the ionopause.

For the a priori determination of the static pressure of the flowing solar-wind plasma on the exterior boundary of the ionosphere - $(p)_{\text{flow}}$ in eq. (26) - we use, as in all previous applications, the Newtonian approximation

$$p = p_{\text{st}} \cos^2 \psi \quad (32)$$

where ψ is the angle between the outward normal to the magnetosphere boundary and the flow direction of the oncoming undisturbed solar wind, and p_{st} is the stagnation or ram pressure exerted on the nose of the ionopause and is given by

$$p_{\text{st}} = K \rho_{\infty} v_{\infty}^2 \quad (33)$$

In this relation, K is a constant usually taken as one, but whose actual value is

$$K = \frac{1}{\gamma} \left[\frac{\left[\frac{(\gamma + 1)/2}{\gamma - (\gamma - 1)/2M_{\infty}^2} \right] (\gamma + 1)}{\gamma - (\gamma - 1)/2M_{\infty}^2} \right]^{\frac{1}{\gamma - 1}} \quad (34)$$

For the high Mach number flows typical of solar-wind conditions, K approaches 0.844 for $\gamma = 2$ and 0.881 for $\gamma = 5/3$. Modification of the product $K\rho_{\infty}$ in eq. (33) to account for the presence of minor constituents such as ionized helium in the solar wind, as well as a discussion of the differences in that product between a fluid and collisionless representative, is provided in reference 8. The important implication associated with the introduction of the Newtonian approximation is that the calculation of the shape of the ionosphere boundary decouples from the calcula-

tion of the external flow. We then arrive at the following equation for the pressure balance at the ionopause locations R_i :

$$K\rho_\infty v_\infty^2 \cos^2 \psi = p_R \Lambda(R_i) \quad (35)$$

where

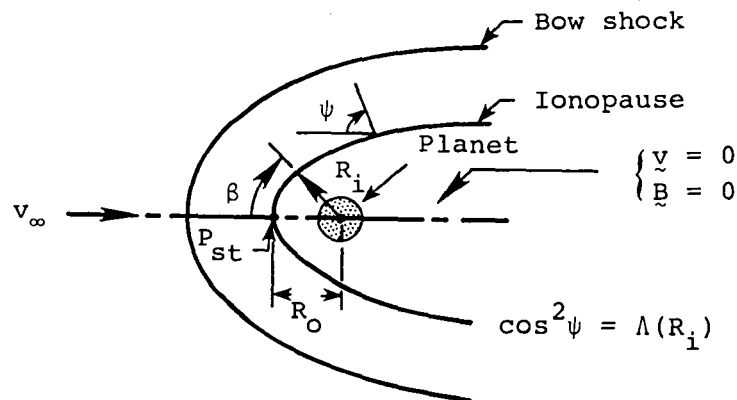
$$\Lambda(R_i) = \left\{ \begin{array}{l} \exp \left[- \left(\frac{R_i - R_R}{H} \right) \right] \\ \exp \left[- R_R \left(\frac{R_i - R_R}{H \cdot R_i} \right) \right] \end{array} \right\} \quad \begin{array}{l} g, T = \text{Const.} \\ g = g_S \left(\frac{r_S}{r} \right)^2, T = \text{Const.} \end{array} \quad (36a)$$

$$\Lambda(R_i) = \left\{ \begin{array}{l} \exp \left[- \left(\frac{R_i - R_R}{H} \right) \right] \\ \exp \left[- R_R \left(\frac{R_i - R_R}{H \cdot R_i} \right) \right] \end{array} \right\} \quad \begin{array}{l} g, T = \text{Const.} \\ g = g_S \left(\frac{r_S}{r} \right)^2, T = \text{Const.} \end{array} \quad (36b)$$

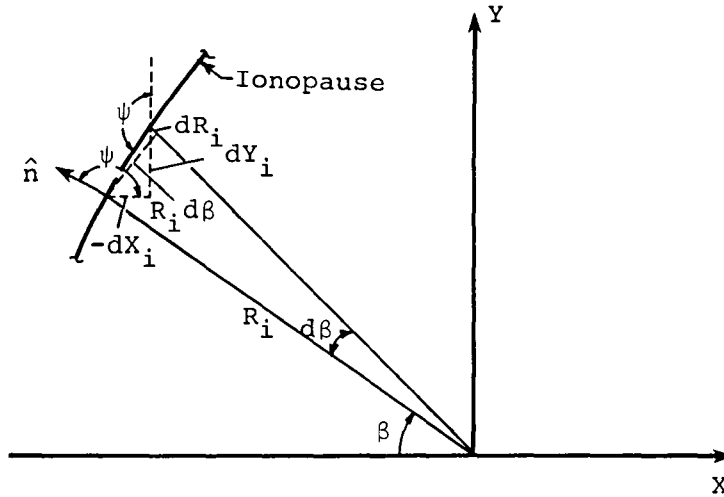
depending upon whether the gravitational variation is included in scale height or not. It is convenient to choose as the reference radius and location the stagnation point on the ionopause; that is, $R_R = R_O$ where R_O is the distance from the center of the planet to the nose of the ionopause. This implies that $p_R = p_O = K\rho_\infty v_\infty^2$ and that at all points along the ionosphere boundary

$$\cos^2 \psi = \Lambda(R_i) \quad (37)$$

The final mathematical statement of the free-boundary problem for determining the shape of the ionosphere boundary then is summarized in the sketch below:



In order to proceed to a final determination of the ionopause shape, it is necessary to relate the local angle ψ to the local coordinates (R_i, β) of the boundary. This is accomplished with the help of the following sketch



from which we find

$$\cos^2 \psi = \left(\frac{dY_i}{dS} \right)^2 = \frac{(R_i d\beta \cos \beta + dR_i \sin \beta)^2}{dR_i^2 + (R_i d\beta)^2} \quad (38)$$

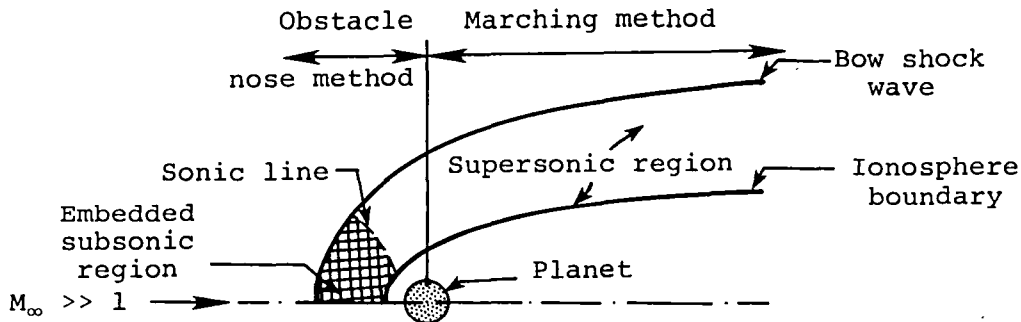
This results in the following ordinary differential equation for the ordinates of the ionosphere boundary

$$\frac{dR_i}{d\beta} = R_i \left[\frac{\sin 2\beta - 2\sqrt{\Lambda - \Lambda^2}}{2(\Lambda - \sin^2 \beta)} \right] \quad 0 \leq \beta \leq \pi \quad (39)$$

where Λ is defined by eqs. (36a,b) and β is the angle measured from the subsolar point as indicated above. Results for various ionopause shapes obtained by integrating eq. (39) for different values of H/R_0 using the constant scale-height model eq. (36a) were provided in ref. 9. Similar results using the isothermal model, eq. (36b) for different values of \bar{H}/R_0 in the range $0.01 \leq \bar{H}/R_0 \leq 0.5$ are provided in figure 1, where for comparison purposes the constant scale-height shapes for corresponding H/R_0 values are also illustrated. We note that the range of interest for planetary applications to Venus and Mars appears to be $0.01 \leq \bar{H}/R_0 \leq 0.10$. Tabulated ordinates of Y_i/R_0 vs. X/R_0 are provided in Table 1 for $\bar{H}/R_0 = 0.01, 0.05, 0.10, 0.20, \text{ and } 0.25$, where $Y_i = R_i \sin \beta$ is the cylindrical radial coordinate of the ionopause profile.

Calculation of the Gasdynamic Flow Properties

Determination of the gasdynamic flow properties is, both conceptually and computationally, the most difficult and time-consuming portion of the total calculation of the solar-wind/terrestrial-planet interaction; and represents the heart of the present modeling effort insofar as the application of advanced computational procedures is concerned. The calculation consists of determining solutions to the differential equations and discontinuity conservation equations given by eqs. (15-20). Since in solar-wind/terrestrial-planet interactions, both the downstream tail region (far field) as well as the region in the vicinity of the obstacle nose (near field) are generally of interest, the computational methods selected must be capable of efficiently determining this entire flow field. In view of the need to carry the flow calculation to an arbitrary downstream distance, the most computationally-expedient procedure is to subdivide the flow field into two regions, as indicated in the sketch below:



This sketch illustrates the essential features of the high-supersonic Mach number flow typical of solar-wind flows past terrestrial planets. Of particular note is the embedded subsonic pocket located at the nose of the ionopause. The presence of this subsonic pocket necessitates use of a computational method capable of treating mixed subsonic/supersonic flows. Downstream of this region, the flow becomes supersonic and remains so for the convex shapes typical of solar-wind/ionosphere boundaries. In that region, a more computationally-economical procedure than that required near the nose can be employed. Such a subdivision of both flow field and solution procedures is common practice for calculating such flows and was employed in the previous solar-wind applications as well as in a related application to space shuttle reentry flows (ref. 12). The precise surface on which the solutions are joined is relatively

arbitrary; in our procedure it was convenient to place it along a plane through the planet center and normal to the free-stream direction of the solar wind, i.e. the dawn-dusk terminator. As illustrated in fig. 2, this position is further downstream than used in the former work in which an inverse iteration method was used for the nose region and the method of characteristics was used for the remaining supersonic region. In light of recent advances, both of the techniques used in the former procedures, particularly the inverse method, are now considered obsolete and much inferior to more current methods. In the new code, those two methods have been superceded by: (1) a new axisymmetric implicit unsteady Euler-equation solver (IMP) specifically developed for the present application, which determines the steady-state solution in the nose region by an asymptotic time-marching procedure, and (2) a shock-capturing marching solution (SCT) which spatially advances the solution downstream as far as required by solving the steady Euler equations.

Nose region solution - implicit unsteady Euler equation method.- The partial differential equations employed in the implicit (IMP) code are the unsteady gasdynamic Euler eqs. (15-20) for axisymmetric flow. These equations may be written in conservation-law form under the generalized independent variable transformation

$$\tau = T, \quad \xi = \xi(T, X, R), \quad \eta = \eta(T, X, R) \quad (40)$$

as follows

$$(U/J)_{\tau} + \left[(\xi_T U + \xi_X E + \xi_R F) / J \right]_{\xi} + \left[(\eta_T U + \eta_X E + \eta_R F) / J \right]_{\eta} + G = 0 \quad (41)$$

where

$$U = \begin{bmatrix} \rho \\ \rho u \\ \rho v \\ \rho e_t \end{bmatrix} \quad E = \begin{bmatrix} \rho u \\ p + \rho u^2 \\ \rho uv \\ (\rho e_t + p) u \end{bmatrix} \quad (42)$$

$$F = \begin{bmatrix} \rho v \\ \rho uv \\ p + \rho v^2 \\ (\rho e_t + p) v \end{bmatrix} \quad G = \frac{1}{RJ} \begin{bmatrix} \rho v \\ \rho uv \\ \rho v^2 \\ (\rho e_t + p) v \end{bmatrix}$$

and the Jacobian

$$J = \xi_X \eta_R - \xi_R \eta_X \quad (43)$$

In eqs. (40) through (43), T denotes time, X is the axial downstream coordinate, and R the cylindrical radial distance; u and v the velocity components in the X and R directions; and e_t is the total energy per unit mass, which for a perfect gas is related to the other quantities by

$$e_t = p/[\rho(\gamma - 1)] + (u^2 + v^2)/2 \quad (44)$$

The subscripts in eqs. (41) and (43) denote partial derivatives with respect to the indicated variable.

The analysis commences by introducing a computational mesh in polar (r, β) coordinates such that one family of coordinates consists of rays from the planetary center spaced at equal increments of β measured from the obstacle nose, and the other of curved lines intersecting each ray so as to divide the portion of it between the ionopause and the shock wave into a fixed number of equal segments. The coordinate transformation eq. (40) is then used to map the portion of the X, R, T physical space bounded by (1) the bow wave, (2) the downstream outflow boundary at $\beta = \pi/2$, (3) the obstacle surface, and (4) the stagnation streamline at $\beta = 0$ into a rectangle in the ξ, η, τ computational space as illustrated in fig. 3. Generally, the transformation metrics at each time step are not known beforehand, and must be determined numerically as part of the solution. Integration step size is established by using the eigenvalues of the Jacobian matrices \bar{A} and \bar{B} , where $\bar{A} = \partial \hat{E} / \partial \hat{U}$, $\bar{B} = \partial \hat{F} / \partial \hat{U}$, and $\hat{U} = U/J$, $\hat{E} = (\xi_T U + \xi_X E + \xi_R F)/J$, and $\hat{F} = (\eta_T U + \eta_X E + \eta_R F)/J$.

Boundary conditions necessary for the specification of a properly-posed mathematical problem are that the flow (a) satisfy the axisymmetric Rankine-Hugoniot shock relations derivable from eq. (41) along (1), (b) be entirely supersonic along (2), (c) be parallel to boundaries (3) and (4), and (d) be symmetric about boundary (4). Initial flow-field conditions are determined by use of an approximating formula for the coordinates of the bow shock wave which is dependent on γ , M_∞ and the shape of the obstacle, and by prescribing a Newtonian pressure

distribution on the obstacle. Since the maximum entropy streamline wets the obstacle surface, that fact plus the known flow direction on the obstacle serve to determine the remainder of the flow properties on that surface. A linear variation for the flow properties between the bow shock and the obstacle is then prescribed. This provides the initial flow field which is then integrated in a time-asymptotic fashion until the steady-state solution is obtained.

The basic numerical algorithm used in the IMP code was developed by Beam and Warming (ref. 13) and is second-order accurate, noniterative, and spatially factored. In particular, the "delta form" with Euler time differencing is employed. When applied to eq. (41), the algorithm assumes the form

$$(I + \Delta\tau\delta_{\xi}\bar{A}^n)(I + \Delta\tau\delta_{\eta}\bar{B}^n)(\hat{U}^{n+1} - \hat{U}^n) = -\Delta\tau(\delta_{\xi}\hat{E}^n + \delta_{\eta}\hat{F}^n + G) \quad (45)$$

where \bar{A} and \bar{B} are the Jacobian matrices, I is the identity matrix, δ_{ξ} and δ_{η} are second-order, central-difference operators, $\hat{U}^{n+1} = \hat{U}(n\Delta\tau)$ and $\Delta\tau$ is the integration step size.

Equation (45) is solved at the interior points only. It requires two 4x4 block tridiagonal inversions at each time step of the integration. The solution proceeds as follows:

1. Define $\Delta\hat{U} = \hat{U}^{n+1} - \hat{U}^n$
2. Form the right-hand side of eq. (45) and store results in the \hat{U}^{n+1} array.
3. Apply smoothing $\hat{U}^{n+1} = \hat{U}^{n+1} - (\epsilon/8)S/J$.
4. Define $\bar{U} = (I + \Delta\tau\delta_{\eta}\bar{B}^n)\Delta\hat{U}$ and solve the matrix equation $(I + \Delta\tau\delta_{\xi}\bar{A}^n)\bar{U} = \hat{U}^{n+1}$ for \bar{U} storing the result in the \hat{U}^{n+1} array.
5. Solve the matrix equation $(I + \Delta\tau\delta_{\eta}\bar{B}^n)\Delta\hat{U} = \hat{U}^{n+1}$ for $\Delta\hat{U}$.
6. Obtain the values of \hat{U}^{n+1} from the relation $\hat{U}^{n+1} = \Delta\hat{U} + \hat{U}^n$.

7. Transfer contents of \hat{U}^{n+1} to \hat{U}^n and repeat all steps until satisfactory convergence is attained.

In step 3 a fourth-order smoothing term S is used to eliminate non-linear instabilities that may arise since the use of central differences in the spatial directions results in a neutrally stable algorithm. This smoothing term is given by

$$\begin{aligned}
 S_{jk} = & (\hat{U}_J)^{n+1}_{j+2,k} - 4 \left[(\hat{U}_J)^{n+1}_{j+1,k} + (\hat{U}_J)^{n+1}_{j-1,k} \right] + 12 (\hat{U}_J)^{n+1}_{j,k} + (\hat{U}_J)^{n+1}_{j-2,k} \\
 & + (\hat{U}_J)^{n+1}_{j,k+2} - 4 \left[(\hat{U}_J)^{n+1}_{j,k+1} + (\hat{U}_J)^{n+1}_{j,k-1} \right] + (\hat{U}_J)^{n+1}_{j,k-2}
 \end{aligned}
 \tag{46}$$

and ϵ , the smoothing coefficient, chosen from the range $0 \leq \epsilon \leq 0.4$ depending upon the size of the time step. The j and k indices correspond to the ξ and η directions, respectively. At the points adjacent to the boundaries a special form of the smoothing term is used.

At the boundaries, modification of the differencing algorithm to account for the particular conditions described above is accomplished as follows. The obstacle-surface flow-tangency condition is incorporated through the use of Kentzer's scheme (ref. 14), while at the symmetry plane, the variables are reflected according to whether they are odd or even. At the outflow boundary where the flow is entirely supersonic, the dependent variables are determined by extrapolation from the adjacent interior points. For the upstream boundary formed by the bow shock wave, the sharp discontinuity approach of reference 15 is used. The interior flow field bounded by these various boundaries is treated in shock-capturing fashion and, therefore, allows for the correct formation of secondary internal shocks.

In the initial development of the nose-region solution procedure (ref. 9), it was found that for certain ionopause obstacle shapes which have a significant amount of lateral flaring at the dawn-dusk terminator, for example, constant scale-height shapes for $H/R_0 \geq 0.5$, and/or cases involving low free-stream Mach numbers $M_\infty \leq 3$, the axial component of velocity at some points on the terminator plane $\beta = \pi/2$ may become

subsonic. Although this has no effect whatsoever on the nose-region solver, for these cases the downstream solution cannot be obtained since the marching-region solver which determines the solution downstream of this starting plane, and which is described in detail in the following section, requires supersonic axial velocities in order to proceed. Under the work reported here, this limitation has been removed by developing the capability for adding an additional portion of the flow field, located downstream of the terminator, to the blunt-body solution as illustrated in figure 4. This effectively generalizes the capability of the present procedures to treat a wide variety of ionopause shapes - including all of the shapes of interest described by the constant scale-height and scale-height with gravitational variation atmospheric models found from eqs. (36a,b) - as well as to treat relatively low free-stream Mach numbers, $M_\infty \approx 2.0$. Details of this capability are provided in the Computer Program Users Manual, Section A.2.1.1 of this report.

Downstream region solution - shock capturing marching method.- Since the shock-capturing technique employed has been described previously in references 16-18, only an outline of the salient features is provided here. The analysis is based on the conservation-law form of the gasdynamic Euler equations for steady axisymmetric flow, which can be readily obtained from eqs. (40) through (44) by setting the τ derivatives to zero. The fourth of this set of equations representing conservation of energy ρe_t can be integrated for steady flow to yield the following relation for the total enthalpy

$$h_t = h + (u^2 + v^2)/2 = \text{constant} \quad (47)$$

where $h = e + p/\rho = C_p T$ is the enthalpy per unit mass.

The computational mesh is defined by lines of constant X and $(R-R_b)/(R_s-R_b)$, where R_s and R_b are functions of X that describe the radial cylindrical coordinates of the ionopause and bow shock wave at the same X as the field point (X,R) . The three remaining partial differential equations for conservation of mass and of axial and radial momentum are then transformed to a rectangular computational space by the transformation

$$\xi = X, \quad \eta = \frac{R - R_b}{(R_s - R_b)} \quad (48)$$

to obtain

$$\partial \tilde{E} / \partial \xi + \partial \tilde{F} / \partial \eta + \tilde{G} = 0 \quad (49)$$

$$\begin{aligned} \tilde{E} &= E, \quad \tilde{F} = \left\{ F - \left[\frac{\partial}{\partial \xi} R_b + \eta \frac{\partial}{\partial \xi} (R_s - R_b) \right] \right\} / (R_s - R_b) \\ \tilde{G} &= G + \frac{E}{R_s - R_b} \frac{\partial}{\partial \xi} (R_s - R_b) \end{aligned} \quad (50)$$

The finite-difference counterpart of eq. (49) is integrated with respect to the hyperbolic coordinate ξ to yield values of the conservative variable E . Subsequent to each integration step, the physical flow variables p , ρ , u , and v must be decoded from the components e_i of E . This necessitates the solution of four simultaneous, nonlinear equations consisting of eq. (47) together with the three elements e_i . This can be done readily by using the relations $v = e_3/e_1$, $p = e_2 - e_1 u$, and $\rho = e_1/u$ together with the expression $h = \gamma/(\gamma-1)(p/\rho)$ for a perfect gas to determine the following quadratic equation for u

$$\begin{aligned} \frac{u^2}{2} + \frac{\gamma}{\gamma-1} \left(\frac{e_2 - e_1 u}{e_1} \right) u - h_t + \left(\frac{e_3}{e_1} \right)^2 \\ = - \frac{\gamma+1}{2(\gamma-1)} u^2 + \left(\frac{\gamma}{\gamma-1} \right) \frac{e_2}{e_1} u - h_t + \left(\frac{e_3}{e_1} \right)^2 = 0 \end{aligned} \quad (51)$$

Two roots exist; one corresponds to subsonic flow and is discarded since u is always supersonic in the present application, while the other corresponds to supersonic flow and gives the desired solution.

Since only the bow shock wave is treated as a sharp discontinuity and any others that may be present are "captured" by the difference algorithm, selection of the appropriate finite difference scheme to advance the calculation in the ξ direction is of prime importance. Following the analysis of refs. 16-18, the numerical integration of eq. (49) is accomplished using the finite-difference predictor-corrector

scheme of MacCormack (ref. 19), the most efficient second-order algorithm for shock-capturing calculations. General descriptions of the method can be found in the references cited.

Calculation of the streamlines.- The streamlines are determined by integrating fluid particle trajectories through the known velocity field since this procedure was found to be more accurate than the alternative mass-flow calculation. The calculation of a particular streamline is initiated at the point where the streamline crosses the bow shock, as illustrated in figure 5. At that point, exact values of the streamline slope dR_S/dX are known in terms of the local shock angle δ_S and free-stream quantities according to the relation

$$\frac{dR_S}{dX} = \frac{(2\cot \delta_S)(M_\infty^2 \sin^2 \delta_S - 1)}{2 + M_\infty^2(\gamma + 1 - 2\sin^2 \delta_S)} \quad (52)$$

which is contained implicitly in both the blunt-body (IMP) and marching (SCT) code solutions. At other points in the flow field, the local streamline slope is given by the ratio of radial to downstream velocity, i.e.,

$$dR_S/dX = v/u \quad (53)$$

and the streamline determination is made by stepwise integration in X using a modified third-order Euler predictor-corrector method. Bivariate linear interpolation from the flow-field grid points is employed to obtain the velocity components (u,v) required at the stepwise points along the streamline trajectory. Separate streamline calculations are made for the nose region (IMP results) and downstream region (SCT results) because of the different coordinate systems employed in those two regions.

Calculation of the Magnetic Field

With the flow properties known from the gasdynamic calculations, determination of the steady magnetic field B proceeds by integrating the

remaining magnetohydrodynamic equations not employed in the gasdynamic analysis, that is eqs. (21-24) with $\partial/\partial t = 0$:

$$\begin{aligned} \text{curl } (\underline{B} \times \underline{v}) &= 0, \quad \text{div } \underline{B} = 0 \\ [B_n v_t - B_t v_n] &= 0, \quad [B_n] = 0 \end{aligned} \quad (54)$$

These equations are commonly interpreted as indicating the field lines move with the fluid. The analysis associated with eqs. (54) leads to a straightforward calculation in which the vector distance from each point on an arbitrarily-selected field line to its corresponding point on an adjacent field line in the downstream direction is determined by numerically integrating $\int \underline{v} dt$ over a fixed time interval Δt . Once the coordinates of the field lines are determined, the magnetic field at any point may be calculated from the relation

$$\frac{\underline{B}}{|\underline{B}_\infty|} = \frac{\rho}{\rho_\infty} \frac{\Delta \underline{\ell}}{|\Delta \underline{\ell}_\infty|} \quad (55)$$

where $\Delta \underline{\ell}$ is the vector length of a small element of a flux tube. Figure 6 clarifies these quantities for the plane of magnetic symmetry defined by the plane containing the axis of symmetry of the obstacle and the magnetic-field lines upstream of the bow wave for the special case when the latter is perpendicular to the flow. In that figure the open symbol \circ denotes locations of points on the streamlines corresponding to the fixed-time interval $\Delta t = \Delta S_\infty / v_\infty$.

Such a procedure is valid generally, but its use in the present calculations is confined to only the component of the magnetic field $(\underline{B})_\perp$ just described. The remainder of the magnetic-field calculation makes use of a decomposition due to Alksne and Webster (ref. 20) in which the axisymmetric properties of the gasdynamic solution and the linearity of the magnetic-field eqs. (54) are employed to derive the following relationship for the magnetic field \underline{B}_P at any point P:

$$\underline{B}_P = \left(\frac{B_P}{B_\infty} \right)_{\parallel} B_{\infty \parallel} + \left(\frac{B_P}{B_\infty} \right)_{\perp} B_{\infty \perp} + \hat{e}_n \left(\frac{B_P}{B_\infty} \right)_n B_{\infty n} \quad (56)$$

As illustrated in figure 7, subscripts \perp , \parallel , and n refer to contributions associated with the components $B_{\infty\parallel}$ of B_{∞} parallel to v_{∞} ; the component $B_{\infty\perp}$ perpendicular to v_{∞} in the plane that contains the point P, the center of the planet, and the vector v_{∞} ; and the component $B_{\infty n}$ normal to the latter plane, and \hat{e}_n is a unit vector in the latter direction. The unit ratios $(B_P/B_{\infty})_{\parallel}$ and $(B_P/B_{\infty})_{\perp}$ can be calculated directly from the gas-dynamic solution by the expressions

$$\left(\frac{B_P}{B_{\infty}}\right)_{\parallel} = \frac{\rho_P v_P}{\rho_{\infty} |v_{\infty}|}, \quad \left(\frac{B_P}{B_{\infty}}\right)_{\perp} = \frac{R_P \rho_P}{R_P \rho_{\infty}} \quad (57)$$

where R_P is the radial cylindrical coordinate of the streamline through P, as indicated in figure 7.

In carrying out the determination of $(B_P/B_{\infty})_{\perp}$ using eq. (55), values for $\Delta \ell / |\Delta \ell_{\infty}|$ are determined initially at the points where the streamlines and perpendicular-component field lines intersect. A generalized quadrilateral interpolation scheme followed by a fifth-order smoothing is then employed to determine the corresponding values at the computational grid points where values for ρ/ρ_{∞} are available for calculation of $(B_P/B_{\infty})_{\perp}$. At the bow shock, an exact formula is used

$$\begin{aligned} (|\Delta \ell|/|\Delta \ell_{\infty}|)^2 &= 1 + \cot^2 \theta (1+D^2) - 2D \times \csc \theta \times \cot \theta \times \cos (\theta-\delta) \\ \psi &= \theta + \sin^{-1} \left\{ [D \times \cot \theta \times \sin (\theta-\delta)] / (|\Delta \ell|/|\Delta \ell_{\infty}|) \right\} \end{aligned} \quad (58)$$

where

$$\begin{aligned} D^2 &= 1 - 4(M_{\infty}^2 \sin^2 \theta - 1)(\gamma M_{\infty}^2 \sin^2 \theta + 1) / [(\gamma + 1)^2 M_{\infty}^4 \sin^2 \theta] \\ \cot \delta &= \tan \theta \times \left\{ (\gamma + 1) M_{\infty}^2 / [2(M_{\infty}^2 \sin^2 \theta - 1)] - 1 \right\} \\ \theta &= \tan^{-1} \left(\frac{dR_S}{dX} \right) \end{aligned} \quad (59)$$

Finally, the resultant magnetic field can then be expressed in components relative to any orthogonal (X,Y,Z) coordinate system. For convenience of illustration, we have chosen the point P to lie in the (X,Y) plane. Relative to this reference frame, the magnetic components are

$$\begin{aligned}
B_X/B_\infty &= \left[(|\underline{B}|/B_\infty)_n \cos \phi \cos \alpha_p + (|\underline{B}|/B_\infty)_\perp \cos \psi \sin \alpha_p \right] \cos \alpha_n \\
B_Y/B_\infty &= \left[(|\underline{B}|/B_\infty)_n \sin \phi \cos \alpha_p + (|\underline{B}|/B_\infty)_\perp \sin \psi \sin \alpha_p \right] \cos \alpha_n \\
B_Z/B_\infty &= (B/B_\infty)_n \sin \alpha_n
\end{aligned} \tag{60}$$

where ϕ is the local flow angle given by

$$\phi = \tan^{-1} \left(\frac{v}{u} \right) \tag{61}$$

and the interplanetary magnetic field angles α_p and α_n indicated in figure 7 are defined by

$$\alpha_p = \tan^{-1} \left[\frac{B_{\infty\perp}}{B_{\infty n}} \right] = \tan^{-1} \left[\frac{B_{Y_\infty}}{B_{X_\infty}} \right] \tag{62}$$

$$\alpha_n = \tan^{-1} \left[\frac{B_{\infty n}}{\sqrt{(B_{\infty n})^2 + (B_{\infty\perp})^2}} \right] = \tan^{-1} \left[\frac{B_{Z_\infty}}{\sqrt{(B_{X_\infty})^2 + (B_{Y_\infty})^2}} \right] \tag{63}$$

The generalizations of these results when the point P is at some arbitrary (Y,Z) location, i.e. not in the (X,Y) plane, are provided below in the spacecraft trajectory section.

Calculation of the Contour Lines

Contours are calculated for nondimensionalized velocity $|v|/v_\infty$, density ρ/ρ_∞ , magnetic field components $(|\underline{B}|/B_\infty)_n$, $(|\underline{B}|/B_\infty)_\perp$, and $(B/B_\infty)_n$ by application of a modified version of a contour procedure developed at NASA/Ames Research Center. After specifying a value for the contour line, the boundary is searched for intervals which bracket the selected value. After locating one such point by interpolation, the remainder of the contour is determined by 'walking' around the contour, searching at each step for the interval and then interpolating to find the point through which the contour line next passes. This is repeated until a boundary

point is reached. Then closed contours are found in a similar manner. Linear interpolation is used throughout the process. Since the temperature is a function of $|\underline{v}|/v_\infty$ only for a specified M_∞ and γ ,

$$T/T_\infty = 1 + \left[\left(\frac{\gamma - 1}{2} \right) M_\infty^2 \right] \left[1 - \left(\frac{|\underline{v}|}{v_\infty} \right)^2 \right] \quad (64)$$

velocity contours may also be considered as temperature contours with only a relabeling required. The coordinates of the contour lines are output either or both as listings and pen plots.

Solar-Ecliptic/Solar-Wind Coordinate Transformations

In order to facilitate comparison of results from the current theoretical model with actual observational data obtained by a spacecraft, it is necessary to consider the appropriate transformations between the spacecraft and solar-wind coordinate systems. Part of the data required as input to the theoretical model consists of oncoming interplanetary values of solar-wind temperature, density, and velocity and magnetic-field vector components. These are naturally obtained in the spacecraft coordinate system, and are usually reported in a sun-planet or solar-ecliptic reference frame. The key coordinate system for the theoretical model is one which aligns the axial direction with the oncoming solar wind, since the gasdynamic calculation is assumed to be axisymmetric about this direction. Thus, the interplanetary input data must be transformed to the solar-wind system to initiate the theoretical determination. Once the gasdynamic and magnetic-field calculations in the solar-wind system are complete, those results must then be transformed back to the sun-planet system to allow direct comparison with spacecraft data obtained at arbitrary locations in the solar-wind/ionosphere interaction region. Consequently, direct and inverse transformations for both spatial coordinates as well as vector quantities between these reference frames are required.

For the measurements of the oncoming interplanetary solar-wind velocity we have assumed that the velocity is obtained with reference to a

sun-planet (x_s, y_s, z_s) system with origin at planetary center and in which the x_s -axis points to the sun, the y_s -axis is opposite to the planetary orbital motion, and the z_s -axis points northward. The direction of the oncoming solar wind is such that the total aberration or azimuthal angle, including planetary orbital motion, of the solar-wind velocity vector in the plane of the ecliptic is Ω and the out-of-ecliptic plane or polar angle is ϕ_p . The positive sense of the azimuthal angle is for east-to-west flow and for the polar angle for north-to-south flow, as indicated in figure 8. In that figure we have also indicated the solar-wind (x, y, z) coordinate system so defined by (Ω, ϕ_p) . For the gas-dynamic calculation, the (x, y, z) system is somewhat inconvenient since the direction of solar-wind flow is in the negative x-direction. Hence, the internal gasdynamic and magnetic-field calculations are performed in an (X, Y, Z) system as shown in figure 9.

The coordinate and vector transformations from the ecliptic sun-planet (x_s, y_s, z_s) system to the (X, Y, Z) solar-wind system are given by

$$\begin{pmatrix} Q_X \\ Q_Y \\ Q_Z \end{pmatrix} = \begin{pmatrix} -\cos \Omega \cos \phi_p & -\sin \Omega \cos \phi_p & \sin \phi_p \\ \sin \Omega & -\cos \Omega & 0 \\ -\cos \Omega \sin \phi_p & \sin \Omega \sin \phi_p & \cos \phi_p \end{pmatrix} \begin{pmatrix} Q_{x_s} \\ Q_{y_s} \\ Q_{z_s} \end{pmatrix} \quad (65)$$

where (Q_X, Q_Y, Q_Z) represents the Cartesian components of any vector referred to the solar-wind (X, Y, Z) coordinate system, and $(Q_{x_s}, Q_{y_s}, Q_{z_s})$ represents the corresponding vector in the sun-planet ecliptic (x_s, y_s, z_s) system. Thus, for a transformation of coordinates

$$\begin{aligned} (Q_X, Q_Y, Q_Z) &= (X, Y, Z) \\ (Q_{x_s}, Q_{y_s}, Q_{z_s}) &= (x_s, y_s, z_s) \end{aligned} \quad (66)$$

while for a vector transformation of, say, the magnetic field

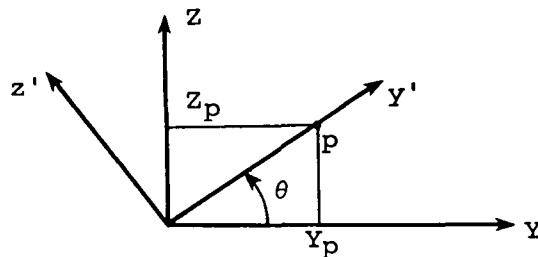
$$\begin{aligned} (Q_X, Q_Y, Q_Z) &= (B_X, B_Y, B_Z) \\ (Q_{x_s}, Q_{y_s}, Q_{z_s}) &= (B_{x_s}, B_{y_s}, B_{z_s}) \end{aligned} \quad (67)$$

The inverse transformation from the solar-wind to the sun-ecliptic system is given by

$$\begin{pmatrix} Q_{X_S} \\ Q_{Y_S} \\ Q_{Z_S} \end{pmatrix} = \begin{pmatrix} -\cos \Omega \cos \phi_p & \sin \Omega & -\cos \Omega \sin \phi_p \\ \sin \Omega \cos \phi_p & -\cos \Omega & \sin \Omega \sin \phi_p \\ \sin \phi_p & 0 & \cos \phi_p \end{pmatrix} \begin{pmatrix} Q_X \\ Q_Y \\ Q_Z \end{pmatrix} \quad (68)$$

Properties Along a Spacecraft Trajectory

One of the primary aims of the present effort has been the development of the capability to determine plasma and magnetic-field properties, as predicted by the present theoretical model, at locations specified along an arbitrary spacecraft trajectory, and in such a form as to enable comparisons to be made directly with actual spacecraft data. To this end, the following procedure has been developed and implemented in the associated computer code. First, from the known oncoming interplanetary conditions provided in a sun-planet reference frame, the azimuthal and polar solar-wind angles (Ω, ϕ_p) are employed to establish both the location of the trajectory point in the solar-wind (X, Y, Z) frame as well as the interplanetary magnetic-field components $(B_{X_\infty}, B_{Y_\infty}, B_{Z_\infty})$ using the transformation eq. (65). Next, the axisymmetric gasdynamic and unit magnetic-field calculations are carried out. Because the gasdynamic flow is axisymmetric in the (X, Y, Z) system, the internal coordinate system in which the trajectory calculations are actually performed may be rotated about the X axis into the most convenient orientation. If we consider a point P located at (X_p, Y_p, Z_p) , then the rotation most appropriate for the present application is indicated in the sketch below



where the angle θ is given by

$$\theta = \tan^{-1} \left[\frac{z_p}{y_p} \right] \quad (69)$$

This rotation defines a new coordinate system (x', y', z') where

$$\begin{pmatrix} x' \\ y' \\ z' \end{pmatrix} = \begin{pmatrix} 1 & 0 & 0 \\ 0 & \cos \theta & \sin \theta \\ 0 & -\sin \theta & \cos \theta \end{pmatrix} \begin{pmatrix} X \\ Y \\ Z \end{pmatrix} \quad (70)$$

in which

$$\begin{aligned} x' &= X_p \\ y' &= \sqrt{Y_p^2 + Z_p^2} \\ z' &= 0 \end{aligned} \quad (71)$$

Thus, the (x', y') plane which contains the X axis and the arbitrary point P corresponds directly to the plane $(X, R) = (X_p, \sqrt{Y_p^2 + Z_p^2})$ in which the axisymmetric gasdynamic flow properties are calculated. In particular, the velocity magnitude v , density ρ , and flow angle ϕ at the point P are found by bilinear interpolation through the (X, R) flow-field grid. The vector velocity in the (X, Y, Z) system is then given by the transformation

$$\begin{pmatrix} v_X \\ v_Y \\ v_Z \end{pmatrix} = \begin{pmatrix} 1 & 0 & 0 \\ 0 & \cos \theta & -\sin \theta \\ 0 & \sin \theta & \cos \theta \end{pmatrix} \begin{pmatrix} v \cos \phi \\ v \sin \phi \\ 0 \end{pmatrix} \quad (72)$$

and then in the sun-ecliptic system by the transformation given in eq. (68)

$$\begin{pmatrix} v_{x_s} \\ v_{y_s} \\ v_{z_s} \end{pmatrix} = \begin{pmatrix} -\cos \Omega \cos \phi_p & \sin \Omega & -\cos \Omega \sin \phi_p \\ \sin \Omega \cos \phi_p & -\cos \Omega & \sin \Omega \sin \phi_p \\ \sin \phi_p & 0 & \cos \phi_p \end{pmatrix} \begin{pmatrix} v_X \\ v_Y \\ v_Z \end{pmatrix} \quad (73)$$

Calculation of the magnetic field at an arbitrary point is somewhat more complicated since these components are dependent upon the orientation of the incident interplanetary magnetic field. With the known $(B_{X_\infty}, B_{Y_\infty}, B_{Z_\infty})$ components, the corresponding components $(B'_{X_\infty}, B'_{Y_\infty}, B'_{Z_\infty})$ in the rotated (x', y', z') system are given by

$$\begin{pmatrix} B'_{X_\infty} \\ B'_{Y_\infty} \\ B'_{Z_\infty} \end{pmatrix} = \begin{pmatrix} 1 & 0 & 0 \\ 0 & \cos \theta & \sin \theta \\ 0 & -\sin \theta & \cos \theta \end{pmatrix} \begin{pmatrix} B_{X_\infty} \\ B_{Y_\infty} \\ B_{Z_\infty} \end{pmatrix} \quad (74)$$

In this reference frame, the perpendicular, parallel, and normal interplanetary components are identified as

$$\begin{aligned} B_{\infty_{\parallel}} &= B'_{X_\infty} \\ B_{\infty_{\perp}} &= B'_{Y_\infty} \\ B_{\infty_n} &= B'_{Z_\infty} \end{aligned} \quad (75)$$

Then, the magnetic field angles α'_p and α'_n in the rotated system are given by

$$\alpha'_p = \tan^{-1} \left[\frac{B_{\infty_{\perp}}}{B_{\infty_{\parallel}}} \right] = \tan^{-1} \left[\frac{B'_{Y_\infty}}{B'_{X_\infty}} \right] \quad (76)$$

$$\alpha'_n = \tan^{-1} \left[\frac{B_{\infty_n}}{\sqrt{(B_{\infty_{\parallel}})^2 + (B_{\infty_{\perp}})^2}} \right] = \tan^{-1} \left[\frac{B'_{Z_\infty}}{\sqrt{(B'_{X_\infty})^2 + (B'_{Y_\infty})^2}} \right] \quad (77)$$

The magnetic angle ψ associated with the incident perpendicular component and the unit magnetic-field ratios $(|B|/B_\infty)_{\parallel}$, $(|B|/B_\infty)_{\perp}$, $(B/B_\infty)_n$ in the rotated system are next determined by bilinear interpolation through the flow-field grid. Then, the magnetic-field components (B'_x, B'_y, B'_z) in the rotated system are calculated from

$$B'_x = \cos \alpha'_n \left(\cos \phi \cdot \cos \alpha'_p \cdot \left| \frac{B}{B_\infty} \right|_{\parallel} + \cos \psi \cdot \sin \alpha'_p \cdot \left| \frac{B}{B_\infty} \right|_{\perp} \right) \cdot B_\infty \quad (78)$$

$$B'_Y = \cos \alpha'_n \left[\sin \phi \cdot \cos \alpha'_p \cdot \left| \frac{B}{B_\infty} \right|_{\parallel} + \sin \psi \cdot \sin \alpha'_p \cdot \left| \frac{B}{B_\infty} \right|_{\perp} \right] \cdot B_\infty \quad (79)$$

$$B'_Z = \sin \alpha'_n \cdot \left(\frac{B}{B_\infty} \right)_n \cdot B_\infty \quad (80)$$

The magnetic-field components in the solar-wind (X,Y,Z) system are then determined from the rotational transformation.

$$\begin{pmatrix} B_X \\ B_Y \\ B_Z \end{pmatrix} = \begin{pmatrix} 1 & 0 & 0 \\ 0 & \cos \theta & -\sin \theta \\ 0 & \sin \theta & \cos \theta \end{pmatrix} \begin{pmatrix} B'_X \\ B'_Y \\ B'_Z \end{pmatrix} \quad (81)$$

and finally in the sun-planet system from

$$\begin{pmatrix} B_{X_s} \\ B_{Y_s} \\ B_{Z_s} \end{pmatrix} = \begin{pmatrix} -\cos \Omega \cos \phi_p & \sin \Omega & -\cos \Omega \sin \phi_p \\ \sin \Omega \cos \phi_p & -\cos \Omega & \sin \Omega \sin \phi_p \\ \sin \phi_p & 0 & \cos \phi_p \end{pmatrix} \begin{pmatrix} B_X \\ B_Y \\ B_Z \end{pmatrix} \quad (82)$$

RESULTS

Using the computational procedures developed under the current modeling effort, a large variety and number of different solar-wind/planetary-ionosphere interaction results were systematically obtained. These results were directed toward the following specific objectives: (1) verification of the correctness of the procedures, (2) demonstration of their flexibility and generality for a variety of cases covering ranges typical of solar-wind conditions, (3) establishment of a catalog of flow and magnetic-field results for a large number of solar-

wind flows, and (4) comparisons of theoretical predictions with data obtained from spacecraft measurements. The results obtained associated with these objectives are discussed below.

Verification of the correctness of the procedures developed under the current effort primarily involved testing the computational extensions developed regarding both the gasdynamic and magnetic-field calculation methods reported in ref. 9. For the gasdynamic solver, this consists of demonstrating the extended blunt-body capability. As discussed previously in the section describing the nose-region solution and also in section A.2.1.1 of the computer manual, that extension involves the addition to the nose-region flow field of a region downstream of the dawn-dusk terminator - which is the usual plane terminating the nose-region solution. This added capability effectively removes any restriction with regard to obstacle shape and interplanetary gasdynamic Mach number of the previous procedures (ref. 9); and permits the calculation of ionopause shapes which have significant flaring in the radial direction at the dawn-dusk terminator, as well as flows at very low ($M_\infty \approx 2.0$) free-stream Mach numbers. In figure 10, we present results for the bow shock locations for $M_\infty = 8.0$, $\gamma = 5/3$ flow past constant scale-height ionopause shapes (see eq. (36a) with $H/R_0 = 0.5$ and 1.0. The downstream solutions for neither of these shapes could be determined with the previous procedures (ref. 9), whereas with the present method they present no problem. The downstream locations to which the nose-region solutions were extended were $X/R_0 = (0.54, 0.67)$, respectively, for the $H/R_0 = (0.5, 1.0)$ ionopause shapes - indicating that the addition of an extensive downstream region to the nose solution for such flows is unnecessary. This is important, as the nose-region solver requires significantly more computational time for a given flow-field region than the marching solver. Hence, minimization of the nose-region flow field is essential in minimizing the total computational time.

In figure 11, we display additional results using the extended nose-region grid capability to demonstrate the ability of the current method for calculating very low interplanetary gasdynamic Mach number flows. Bow shock locations are shown for $M_\infty = 2.0$ and 3.0, $\gamma = 5/3$ flows past an

ionopause obstacle shape with gravitational variation included in scale-height having $\bar{H}/R_0 = 0.25$ (see eq. (36b)). This particular obstacle is a relatively blunt shape, as can be observed from the ionopause profiles presented previously in figure 1, and, computationally, presents a more difficult flow to determine than flows for shapes having less flaring. For applications to terrestrial planets, such as Mars and Venus, typical ionopause shapes occurring in nature appear to lie in the range $0.01 \lesssim \bar{H}/R_0 \lesssim 0.10$. Consequently, demonstration of the ability of the current procedures to treat successfully such flows as shown in figures 10 and 11 - which lie at the limits of interest as far as applications to nonmagnetic terrestrial planets, indicates that these procedures will not be restricted insofar as ionopause geometry and interplanetary solar-wind conditions are concerned.

Corresponding verification of the extensions to the procedures for the magnetic-field calculation has involved demonstration of the correctness of the magnetic-field prediction at any arbitrary point in the solar-wind flow field. This was accomplished by consideration of a variety of special test cases in which the location in the flow field and the incident interplanetary magnetic-field orientation were systematically changed so as to produce both symmetric and antisymmetric changes in the resultant ionosheath magnetic field, as well as to reverse the roles of the perpendicular and normal components. All of these various permutations of the magnetic-field calculation procedure were successfully verified.

One of the primary objectives of the present work was to demonstrate the flexibility and generality of the present procedures by exercising them over a wide range of ionopause geometries and solar wind oncoming conditions so as to cover, insofar as possible, the entire range of practical interest of these parameters. These calculations were to be summarized in a convenient format and then archived so as to provide at-a-glance information regarding the variation of the flow-field and unit magnetic-field quantities. The output format selected was the automatic pen-plot output option of the program involving plots of the flow-field streamlines, and contours of the velocity magnitude $|\underline{v}|/v_\infty$, temperature T/T_∞ , density ρ/ρ_∞ , and the field-line locations and contours of the unit magnetic-field ratios $(|\underline{B}|/B_\infty)_\parallel$ and $(|\underline{B}|/B_\infty)_\perp$.

The test cases selected for this catalog involved a ratio of specific heats $\gamma = 5/3$ and the following matrix of free-stream Mach numbers M_∞ and ionopause shapes:

$$\begin{aligned}M_\infty &= \{2.0, 3.0, 5.0, 8.0, 12.0, 25.0\} \\H/R_O &= \{0.01, 0.10, 0.25\} \\\bar{H}/R_O &= \{0.10, 0.20, 0.25\}\end{aligned}$$

Thus, a total of 36 separate cases were calculated. The plot output for these cases is provided in Appendix B, which also presents a convenient page index to the individual results. These archived results provide an very convenient means of determining the overall dependence of flow-field and magnetic-field quantities with M_∞ and obstacle shape, in particular the variation of bow shock location and flow-field contour changes. We note that the range of free-stream Mach numbers selected easily spans the entire range of solar-wind conditions usually encountered, while the different obstacle shapes provide a wide variation as well, as can be observed from figure 1.

The final and ultimate check of the current procedures lies in the comparison of the results predicted by the present model with data actually measured by a spacecraft. To that end, we have made a number of preliminary comparisons with data obtained from orbits 3 and 6 of the Pioneer-Venus Orbiter spacecraft.

The overall features of the spacecraft trajectory crossings of the solar-wind/Venus-ionosphere interaction region are provided in the sketch given in figure 12. In that figure, which is referred to the sun-Venus solar-ecliptic coordinate system, we note in particular the highly elliptic spacecraft orbit (periapsis ≈ 200 Km, apoapsis $\approx 66,000$ Km) and the crossings of the bow shock and ionopause surfaces. The oncoming solar-wind direction, with arbitrary azimuthal (aberration) and polar angles (Ω, ϕ_p) is as indicated, with the ionopause and bow shock surfaces symmetric about that direction. The oncoming arbitrary interplanetary magnetic field \underline{B} is also as indicated.

The procedural outline employed for the theoretical comparisons is as follows:

I. Orbital data selection

Select data from an orbit when solar-wind conditions are relatively steady.

II. Theoretical calculations

Input:

Ionospheric ρ and T versus altitude from orbiter retarding potential analyzer (ORPA)

Solar wind v_{∞} , ρ_{∞} , T_{∞} from orbiter plasma analyzer (OPA)

Solar wind B_{∞} from orbiter magnetometer (OMAG)

Trajectory coordinates

Output: (Contours and/or time histories along orbital trajectory)

Ionosheath ρ , T , \underline{y} , \underline{B} and their scalar components in solar ecliptic coordinates

III. Comparisons with Spacecraft data

Observational ionosheath data for ρ , $|\underline{y}|$, T from OPA and for B from OMAG with two sets of theoretical predictions based on $\left\{ \begin{array}{l} \text{last} \\ \text{first} \end{array} \right\}$ interplanetary solar-wind properties (v_{∞} , T_{∞} , ρ_{∞} , B_{∞}) measured $\left\{ \begin{array}{l} \text{before} \\ \text{after} \end{array} \right\}$ bow shock $\left\{ \begin{array}{l} \text{inbound} \\ \text{outbound} \end{array} \right\}$ crossings.

First, the selection of the particular orbit for which theoretical calculations and data comparisons will be carried out must be made. This choice is based on spacecraft observations of the oncoming interplanetary solar wind, and for the cases reported here, the selections were made when conditions appeared relatively steady. In particular, the interplanetary conditions regarding solar-wind velocity, density, temperature and magnetic field based on the orbiter solar-wind plasma analyzer (OPA) and fluxgate magnetometer (OMAG) measurements just prior

to inbound bow shock crossing and immediately after outbound bow shock crossing were analyzed by the Pioneer-Venus investigators responsible for these instruments for a number of the initial orbits of the Pioneer-Venus spacecraft, and on this basis the selection of Orbits 3 and 6 were made.*

To initiate the theoretical calculations, information regarding both the ionospheric obstacle shape and the oncoming interplanetary conditions are required. The determination of the obstacle shape is based on measurements of atmospheric density and temperature as a function of altitude made by the orbiter retarding potential analyzer at (ORPA) locations interior to the ionopause boundary.** These measurements yield the variation of atmospheric pressure with altitude in the vicinity of ionopause altitudes. From this information, the value of the scale-height parameter from the atmospheric pressure model given by either eq. (29) or (30) can be determined. For Venus, it appears that the ionosphere/solar-wind interaction is such that the ionopause wraps tightly about the planet (ref. 10). Our calculations based on ORPA data for Orbits 3 and 6 indicate scale heights of approximately 200 Km, which yield a corresponding range of values for H and \bar{H} of $0.02 \lesssim H/R_0, \bar{H}/R_0 \lesssim 0.05$. We note that for such small values of scale height, the two ionospheric pressure models eqs. (29) and (30) yield essentially the same obstacle shape, as can be seen from figure 1. For the comparisons reported here for both Orbits 3 and 6, we have selected a value of $\bar{H}/R_0 = 0.03$. With regard to oncoming interplanetary conditions, we require as input the solar-wind bulk velocity v_∞ , density ρ_∞ , temperature T_∞ , and magnetic field B_∞ . The first three are provided by the orbiter plasma analyzer (OPA), while the magnetic field is given by the orbiter fluxgate magnetometer (OMAG). We note that the OPA provides either ion density and temperature or electron density and temperature, but not both simultaneously. For orbits 3 and

* Special thanks are due to J. H. Wolfe and J. P. Mihalov who provided information regarding the solar-wind plasma from OPA measurements (refs. 21,22) and to C. T. Russell, R. C. Elphic, and J. A. Slavin for magnetic-field information from OMAG measurements (refs. 23,24).

** Special thanks are due to W. C. Knudsen and K. Spenner for providing the ionospheric plasma information from ORPA measurements (refs. 10,11).

6, ion measurements were available and have been employed. Information regarding the oncoming direction of the solar wind, as given by the angles (Ω, ϕ_p) , defines the requisite coordinate rotations required to align the gasdynamic calculation in the oncoming solar-wind direction; while information of solar-wind speed, density, and temperature serve to define the oncoming gasdynamic Mach number required to initiate the gasdynamic calculations.

With this information, the detailed gasdynamic and unit magnetic-field calculations in the ionosheath region can be carried out. In order to provide an idea of the detail obtained by the present computational procedures in these calculations, we have displayed in figure 13 the flow-field grid for one of the gasdynamic flow solutions used in the data comparisons discussed below. The result shown is for $M_\infty = 3.0$, $\gamma = 5/3$ flow past an ionopause obstacle shape with $\bar{H}/R_0 = 0.03$, and is shown carried to a downstream location of $X/R_0 = 3.0$. The flow field properties $[\underline{v}/v_\infty, \rho/\rho_\infty, T/T_\infty]$ and the unit frozen magnetic-field ratios $[(B/B_\infty)_n, (B/B_\infty)_t, (B/B_\infty)_n]$ are determined at each intersection of the grid lines, including the bow shock, stagnation streamline, and ionopause boundaries. The final output of the calculation consists of detailed flow-field and magnetic-field properties in the ionosheath region, both in terms of tabular output and plotted contours and time histories along the orbital trajectory of the velocity magnitude and components, density, temperature, and magnetic-field magnitude and components. Complete details are provided in section A.4 of the Computer User's Manual.

For the comparisons with spacecraft data, the most convenient portion of the output format are the time-history predictions along the spacecraft orbit. The observational data used for comparisons with the theoretical predictions in the ionosheath region include plasma density, velocity, and temperature from OPA measurements and magnetic field from OMAG measurements. For the theoretical predictions, two sets of results are usually generated based on $\left\{ \begin{array}{l} \text{last} \\ \text{first} \end{array} \right\}$ interplanetary solar-wind properties $(\underline{v}_\infty, T_\infty, \rho_\infty, B_\infty)$ measured $\left\{ \begin{array}{l} \text{before} \\ \text{after} \end{array} \right\}$ bow shock $\left\{ \begin{array}{l} \text{inbound} \\ \text{outbound} \end{array} \right\}$ crossing.

In figure 14, we have displayed some overall flow-field results for Orbit 6. Indicated in that figure are bow shock locations for the three combinations of free-stream Mach number M_∞ and plasma specific heat ratio γ , i.e. $(M_\infty, \gamma) = (13.3, 5/3), (13.3, 2), (3.0, 5/3)$ for flow about an ionopause with $\bar{H}/R_\odot = 0.03$. Also indicated are two sets of points (-○-, -□-) representing the spacecraft trajectory for orbit 6 as viewed in two solar-wind oriented coordinate systems. The trajectory indicated by the solid lines and circles (-○-) is that based on the last measured direction $(\Omega, \phi_p) = (6.5^\circ, -1.4^\circ)$ of the interplanetary solar wind just prior to crossing the bow shock on the inbound leg, while the dashed line and squares (--□--) denotes the trajectory based on the first measured direction $(\Omega, \phi_p) = (4.9^\circ, 7.6^\circ)$ of the solar wind immediately after crossing the bow shock on the outboard leg. We note that the spatial location of the spacecraft trajectory in solar-wind coordinates depends only on the direction (Ω, ϕ_p) of the oncoming solar wind, but not on its magnitude. With regard to the results indicated in figure 14 for the spacecraft trajectory, we observe the extremely large dependence of spatial position of a trajectory point, as viewed in solar-wind coordinates, on solar-wind direction. For the particular inbound and outbound solar-wind angles indicated, the shift in X-coordinate of a trajectory point can be as high as a quarter of the Venusian planetary radius, which obviously results in substantial differences in predicted flow and magnetic-field properties. In previous work, the influence of the angular shift in the solar wind was generally considered to be small and negligible. The current results, however, indicate that this purely geometrical effect can be surprisingly large, even for directional shifts of less than 5° , and must be accounted for in any realistic theoretical comparison with data. See reference 7 for another example of the importance of this effect.

Finally, with regard to the three sets of bow shock results displayed in figure 14, these calculations represent an attempt to resolve the uncertainty in the oncoming free-stream Mach number and ratio of specific heats of the plasma. Because only solar-wind ion temperatures from the OPA were available for Orbit 6, the initial calculation of the free-stream Mach number was based on the assumption that $T_e = T_i$, which leads to $M_\infty = 13.3$. A ratio of specific heats $\gamma = 5/3$ was assumed, and these interplanetary values result in the bow shock indicated by the

dot-dash line. That shock location is in poor agreement with the observational shock crossings, indicated as occurring between the pairs of solid circles and squares. A separate uncertainty arises from the possibility that the magnetic field may act to align the plasma particle motion in its direction, thus effectively reducing the number of degrees of translational freedom from 3 to 2 and thereby increasing the ratio of specific heats from 5/3 to 2. To investigate this possibility, we have repeated the $M_\infty = 13.3$ calculation using $\gamma = 2$. That result is indicated by the dashed line, and is in better but still not completely satisfactory agreement with the observed shock locations. Finally, if it is assumed that the oncoming interplanetary electron temperature is not equal to the ion temperature, but is substantially higher, we are lead to low Mach numbers of the order of $M_\infty \approx 3-5$. We have displayed bow shock results of a $M_\infty = 3.0$, $\gamma = 5/3$ calculation in figure 14 as the solid line, and observe that based on this Mach number and the inbound solar-wind direction, the observational shock crossings display very good agreement with the theoretical results.

Figure 15 displays the time-history comparisons of the theoretically-predicted bulk plasma density, speed and temperature in the ionosheath region with OPA measurements of these quantities. These theoretical results were based on a gasdynamic flow solution with $M_\infty = 13.3$, $\gamma = 2.0$. In these results, the solid lines with circles correspond to results based on inbound interplanetary conditions, while the dashed lines with squares correspond to outbound conditions. We note that while the few data points available are in general agreement with the theoretical calculations, the lack of more detailed plasma measurements in the ionosheath prevents a definitive conclusion. The OPA instrument requires approximately 9 minutes to acquire sufficient data to enable predictions of the bulk plasma quantities. While this time lag presents no problem when the spacecraft is in the interplanetary solar wind, the large resolution time effectively averages the plasma quantities in the ionosheath over such a large spatial range that only overall comparisons of the bulk plasma properties are possible.

The situation is quite different for the magnetic field, as the OMAG instrument provides essentially instantaneous magnetic-field measurements. Comparisons of the frozen magnetic-field predictions with data

are displayed in figures 16(a,b). These comparisons employ the gas-dynamic solution $M_\infty = 13.3$, $\gamma = 2$ for which plasma properties were given in figure 15. In figure 16a, we display two sets of theoretical calculations for the magnitude of the magnetic field, based on the inbound and outbound interplanetary magnetic field conditions as indicated on the figure. In these comparisons, we observe very good agreement with both sets of predictions. In particular, on the inbound leg, the theoretical predictions based on the inbound interplanetary conditions are in very good agreement with the data, while the outbound-condition predictions are clearly not as favorable. On the other hand, as we proceed in time along the outbound leg, the opposite is true. Here, the outbound-condition predictions are in very good agreement with the data, while the inbound-condition predictions are notably inferior, particularly with regard to shock crossing. Corresponding results for the magnetic-field components are provided in figure 16b, and display a similar behavior. The agreement of the theoretical results with data for the individual components is remarkable, confirming the accuracy of the frozen-field model, as well as the shift of the ionosheath magnetic field from a solution related to inbound interplanetary conditions to one related to outbound conditions.

For Orbit 3, similar comparisons as those shown in figures 14-16 for Orbit 6 are given in figures 17 to 19. In figure 17, we have provided the bow shock locations for five different combinations of M_∞ and γ as indicated. The Mach numbers $M_\infty = 7.38, 5.96$ correspond, respectively, to the inbound and outbound interplanetary conditions for $|\underline{v}_\infty|, \rho_\infty, T_\infty$ as measured by the OPA, while the two values of $\gamma = 5/3, 2$ used in the calculations represent our uncertainty of the ratio of plasma specific heats. We have also indicated for reference the bow shock location for $M_\infty = 3.0, \gamma = 5/3$ as given previously in figure 14 for Orbit 6. Note that the observational shock crossings are again closest to the $M_\infty = 3.0, \gamma = 5/3$ shock. Also provided in figure 17 are the orbital trajectories as viewed in solar-wind coordinates for the inbound $(\Omega, \phi_p) = (3.3^\circ, 0.15^\circ)$ and outbound $(\Omega, \phi_p) = (3.7^\circ, 4.9^\circ)$ solar-wind directions.

The comparisons for the bulk plasma properties for Orbit 3 are provided in figure 18. Again we note an overall agreement for bulk plasma speed and density, but note an observable discrepancy in the temperature.

This is thought to be indicative of the manner in which the bulk properties from the theoretical model are being interpreted in relation to the observational measurements; i.e. the theoretical values correspond to those for a single-component plasma, while the measurements are in terms of a multi-component plasma. Whether the theoretical plasma properties require rescaling or reformulation, or whether their present formulation is appropriate for comparison with the multi-component data, appears to be a necessary and important subject for future study.

Results for the magnetic-field comparisons are displayed in figures 19(a,b), which provide time-histories of both the magnitude and the individual magnetic-field components based on both inbound and outbound interplanetary conditions. We note again, although the shock crossing comparisons are somewhat in disagreement since the gasdynamic flow fields used in these results were for $M_\infty = 7.56, 5.96$ and $\gamma = 2$, the reasonable comparisons are obtained for the ionosheath magnetic field. In particular, we observe the drift with time along the trajectory of the trajectory of the agreement of theory with data from the predictions based on inbound interplanetary conditions on the inbound leg, to those based on outbound conditions on the outbound leg.

In order to demonstrate the improvement obtained in magnetic-field results when a gasdynamic flow-field solution is employed which more closely agrees with the observational bow shock location, we have displayed in figure 20(a,b) the analogous time-history magnetic-field comparisons when using a $M_\infty = 3.0, \gamma = 5/3$ gasdynamic result. In this case, results were computed for only the inbound direction $(\Omega, \phi_p) = (3.3^\circ, 0.15^\circ)$ of the solar wind. As can be seen, there is a marked improvement in the agreement near the bow shock, and quite good agreement throughout the ionosheath as well as, for both the magnitude and the individual magnetic-field components. We note that the general agreement of theory and observation of the individual components demonstrates both the accuracy of the calculation and, in particular, the need for accounting in the theoretical results of the variable direction of the interplanetary solar wind.

CONCLUDING REMARKS

The application of advanced computational procedures was undertaken for the purpose of modeling the interaction of the solar wind with non-magnetic planets, with particular emphasis on Venus. Based on the successful theoretical model employed previously (ref. 9), i.e., the steady, dissipationless, magnetohydrodynamic model for axisymmetric, supersonic, super-Alfvénic solar-wind flow, a number of important theoretical extensions have been developed and included in the computational procedures. These include the capability for treating very low oncoming interplanetary gasdynamic Mach numbers ($M_\infty \approx 2.0$), as well as quite general ionopause shapes. A new family of ionopause shapes has been developed which includes the effect of gravitational variation in scale height, and has been incorporated in the computational program. Additionally, the capability for determining the plasma gasdynamic and magnetic-field properties along any arbitrary spacecraft trajectory, accounting for an arbitrary oncoming direction of the solar wind, has been developed. All of these developments have been incorporated into an assemblage of computer codes to enable detailed calculations of the solar-wind interaction with planetary atmospheres. The computer codes have been extensively documented and are described in a computer user's manual included as part of this report.

Comparisons are reported which verify the correctness of these new procedures, and which demonstrate their capability for computing a wide range of flows encompassing those typical of solar-wind conditions about terrestrial planetary atmospheres. A catalog of sample solar-wind flows covering a large number of flow conditions and ionopause geometries was established, and reported in summary format in the forms of contour plots of important flow-field and magnetic-field properties. Finally, successful comparisons of results from the theoretical model were made with actual spacecraft data obtained from initial orbits of the Pioneer-Venus Orbiter. These results have indicated the importance, heretofore largely neglected, of the directional variability of the oncoming solar wind. All of these results, taken in toto, serve to verify the basic theoretical model which underlies the present procedures. Furthermore, it demonstrates the value of the present computational procedures as a research tool capable of routinely providing - at small computation cost

and in a format directly compatible with experimental observations - details of the solar-wind/planetary atmosphere interaction process not previously attainable.

With regard to future uses as well as improvements of the present model, the obvious need for a detailed study involving comparisons between theory and observations for a large number of orbits of the Pioneer-Venus Orbiter is clear. Based on the preliminary comparisons for orbits 3 and 6, the frozen magnetic-field model appears to be remarkably accurate for relatively quiet-time conditions. Similar comparisons of the plasma properties indicate a need for an improved interpretation of the results from the single-fluid theory in terms of multi-component measurements. Questions regarding the possible suppression by the interplanetary magnetic field of the number of degrees of freedom of the plasma require further study and could be clarified through systematic comparisons with data. Additionally, observations from the Pioneer-Venus Orbiter of the nightside ionosphere of Venus have indicated a more complex and dynamic structure than suspected. These observations point, in particular, toward the need for improvement of the simple model used in the present method for the determination of the ionosphere boundary. This improved determination would involve an iterative procedure in which a balance of the sum of the solar-wind gasdynamic plus magnetic pressure along the ionopause surface would be maintained against the ionospheric pressure. The present method, which balances the Newtonian pressure distribution against the ionospheric pressure, represents the first step in this iteration.

ACKNOWLEDGEMENTS

Support for the research reported in this investigation was provided by National Aeronautics and Space Administration, Headquarters under Contract NASW-3182 with Robert Murphy as Technical Monitor. Special thanks are given to J. H. Wolfe and J. D. Mihalov for generously providing solar-wind plasma information from Pioneer-Venus Orbiter plasma analyzer measurements, to C. T. Russell and J. A. Slavin for magnetic field information from Pioneer-Venus Orbiter fluxgate magnetometer measurements, and W. C. Knudsen for ionosphere plasma information from Pioneer-Venus Orbiter retarding potential analyzer measurements.

APPENDIX A
COMPUTER PROGRAM USER'S MANUAL

APPENDIX A
COMPUTER PROGRAM USER'S MANUAL

TABLE OF CONTENTS

<u>Section</u>	<u>Page No.</u>
A.1 INTRODUCTION	53
A.2 PROGRAM DESCRIPTION	54
A.2.1 Calculation Procedure	56
A.2.1.1 Blunt-body calculation	56
A.2.1.2 Marching calculation	58
A.2.1.3 Streamline calculation	59
A.2.1.4 Magnetic-field calculation	61
A.2.1.5 Contour calculation and plot generation	64
A.2.1.6 Trajectory calculation	65
A.2.2 Rerun Option	70
A.2.3 Program Limitations and Precautions	70
A.2.4 Convergence Criteria for Blunt-Body Calculation	71
A.3 DESCRIPTION OF INPUT	72
A.3.1 Dictionary of Input Variables	72
A.3.2 Preparation of Input Data	77
A.3.3 Format of Input Data	81
A.4 DESCRIPTION OF OUTPUT	85
A.5 PROGRAM ERROR MESSAGES	87
A.6 SAMPLE CASE	90
FIGURES A.1 THROUGH A.6	92

This Page Intentionally Left Blank

APPENDIX A

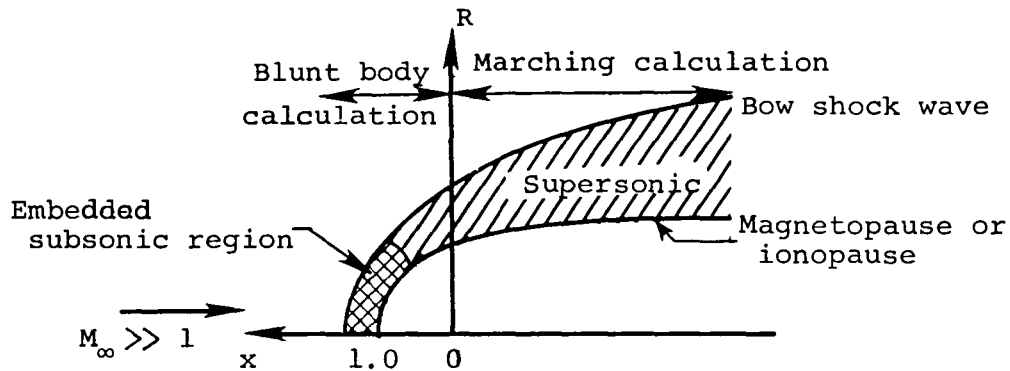
A.1 INTRODUCTION

The purpose of this appendix is to describe the operation of the assemblage of computer codes which were developed in conjunction with the theoretical work presented in this report and organized into one program, and to provide sufficient detail to permit understanding and use of the program. The program computes the flow field of the solar wind about a terrestrial planet, using a procedure for the calculation of supersonic/hypersonic flow about an axisymmetric blunt body. The corresponding frozen-in magnetic field is calculated from the previously-determined velocity and density fields. Streamlines and contour lines of various flow-field properties and magnetic-field components are also determined. Next, these flow-field and magnetic-field values are calculated for points along a user-specified trajectory.

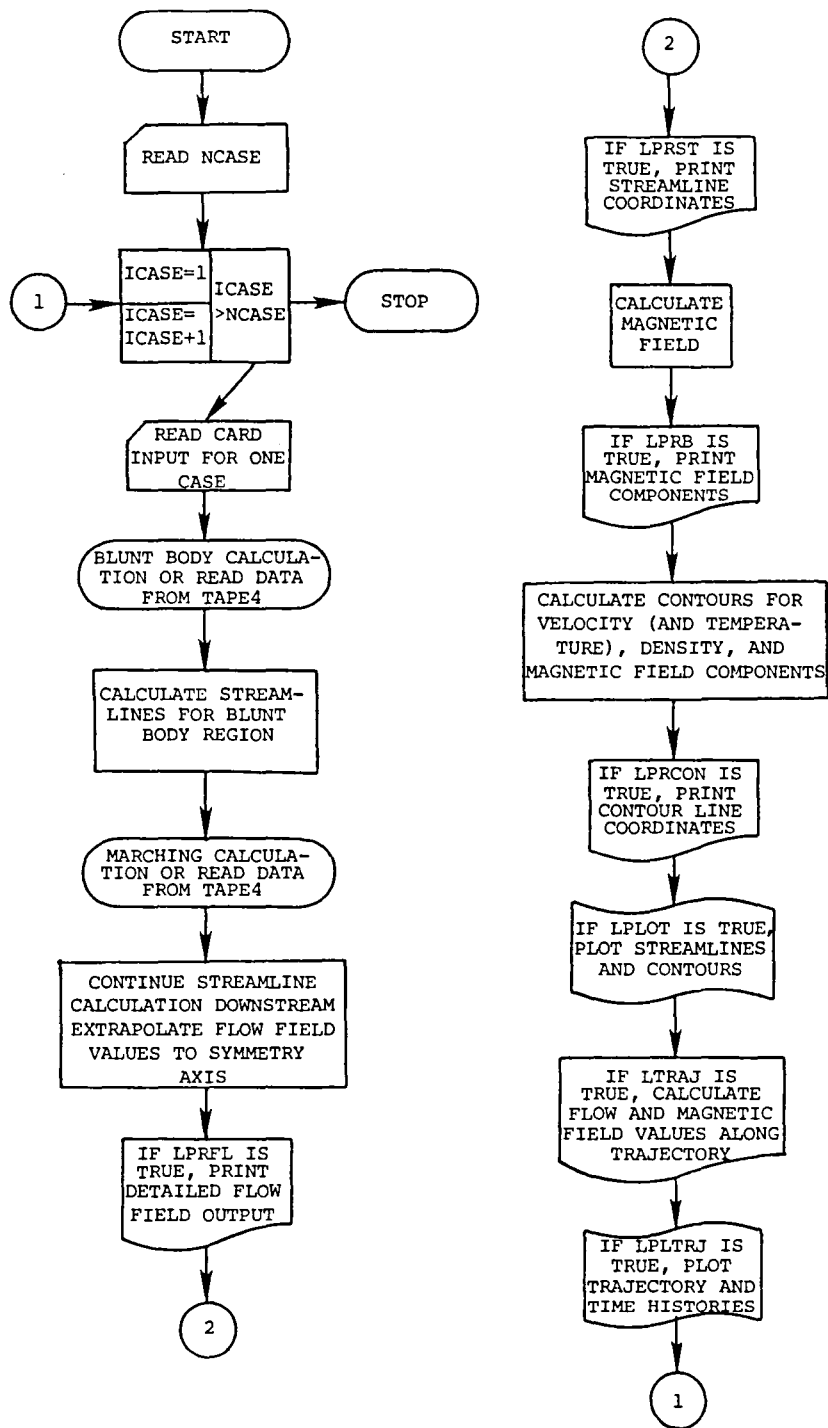
A description of the general operating procedure of the program is given, with descriptions of input and output. The program is written in FORTRAN IV and has been developed on a CDC 7600 computer. University Computing Company (UCC) Standard Plotting Software and Functional Software packages are used to produce automated plots. Files used, besides TAPE5 for INPUT and TAPE6 for OUTPUT, are TAPE1 for the plot file (system default), TAPE4 for input file for rerun option, and TAPE9 for storing data for rerun. Typical run times for cases using the default parameters are 110 to 120 seconds, using the OPT=2 compiler. For a case using the rerun option, which employs a previously-calculated flow field, the run time is approximately 15 seconds. The storage requirements are 146K₈ for small core memory and 273K₈ for large core memory.

A.2 PROGRAM DESCRIPTION

For computational purposes, the flow is subdivided into two regions, as indicated in the sketch below, with the center of the planet as origin.



The region near the nose of the magnetopause/ionopause includes all of the imbedded subsonic flow and part of the supersonic flow. An axisymmetric implicit unsteady Euler equation solver is used to calculate this part of the flow field. Using the solution plane at $x = 0.0$ to provide starting conditions, the flow field in the purely supersonic downstream region is determined by integrating the steady Euler equations using a spatial-marching procedure. Streamlines, the magnetic field, and contours are calculated using the entire flow field, distinguishing between the two regions as required by the different forms of the computational grids. A rerun capability is provided, where flow-field data is read from a file written on a previous run, rather than repeating the blunt-body and marching calculations. The computations proceed as shown in the sketch below, which provides an overall flow chart of the complete program. The program provides for several cases to be run consecutively.



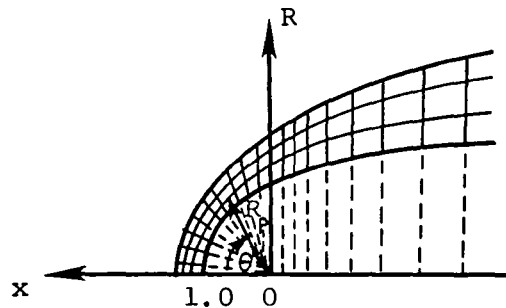
Program Flow Chart

A.2.1 Calculation Procedure

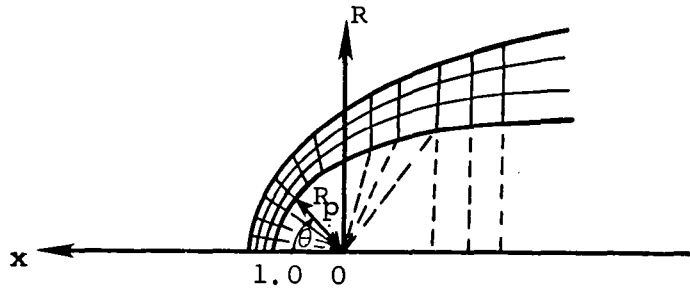
After reading in the number of cases in the run, each case is calculated independently. Subroutine INPUT reads in all card input required for one case, viz. a title, flow conditions, obstacle geometry, calculation and print control parameters, and desired contour values. The user may supply the obstacle geometry in the form of a shape table for an axisymmetric body, or use one of the default shapes which are calculated internally by the program. These default shapes are the magnetopause equatorial trace, constant scale-height ionopauses, and ionopauses having gravitational variation in scale-height. The input is printed as the first item of output.

A.2.1.1 Blunt-body calculation

A computational mesh in polar (R_p, θ) coordinates is established for the blunt-body calculation; then, for the marching calculation, this is extended into a cylindrical (x, R) system, as indicated below:



This method has proven effective except for certain obstacle shapes which have a significant amount of flaring at the terminator and/or cases involving low free-stream Mach numbers $M_\infty \leq 3$. Under such conditions, the axial component of velocity may become subsonic at the starting plane of a marching calculation (terminator) and the calculation cannot proceed. In this case the blunt-body grid must be extended past $\theta = 90^\circ$ as shown below:



The number of rays added to the blunt-body mesh is controlled by the input variable NXADD, and are limited by the requirement, $NBLUNT + NXADD \leq 39$.

All lengths, x , R , R_p , are normalized so that the nose of the obstacle is at $x = 1.0$. For the default shapes, rays at equal angular increments of $\Delta\theta$ are used, starting at $-\Delta\theta/2$, up to $90^\circ + \Delta\theta$, where $\Delta\theta = 90^\circ/(NBLUNT-1.5)$, and NBLUNT is an input parameter describing the number of angular mesh points to be used in the blunt-body calculation. Program default value is $NBLUNT = 24$, so that for the default mesh, $\Delta\theta = 4^\circ$. The obstacle shape is determined by integrating the appropriate differential equation by a trapezoidal predictor-corrector method. For a user-supplied shape, the θ grid is determined by rays from the origin through the first NBLUNT points, and the reflection of the first ray about the x -axis. Values for R_p are determined by dividing the line segments between the body and bow shock wave into $NR-1$ equal intervals. Thus, including the obstacle and bow shock wave, the grid forms NR arcs around the obstacle. A starting solution for the blunt-body calculation is obtained by guessing a bow shock shape and by prescribing a Newtonian pressure distribution on the body. Noting that the maximum entropy streamline wets the body, other flow properties on the body surface can then be calculated. An initial flow field is then established by linear interpolation between the obstacle and the guessed bow shock, where the Rankine-Hugoniot relations hold. The integration proceeds in time for ITER steps. The initial bow shock shape used for the magnetopause equatorial trace and for an

ionopause with $H/R_O \geq 0.1$ is a correlation shape depending on $(M_\infty, \gamma, H/R_O)$ and given by the parabola $R_p = \delta_1 \sqrt{\delta_O - x/\sqrt{\delta_O}}$ where

$$\delta_O = 1.0 + 1.1 \{ [(\gamma-1)M_\infty^2 + 2] / (\gamma+1)M_\infty^2 \} \times (0.9 + 0.5 H/R_O)$$

$$\delta_1 = \Delta_O \{ (1.273 + 0.009 M_\infty^2) (0.904 + 0.655 H/R_O) \\ \times [3.95 - 5.3 H/R_O + 3.85 (H/R_O)^2] \} + (R_{body})_{x=0.0}$$

$$\Delta_O = [(\gamma-1)M_\infty^2 + 2] / [(\gamma+1)M_\infty^2] \times 0.78$$

For a user-supplied obstacle shape and for an ionopause with $H/R_O < 0.1$, the initial shock shape used is the curve $R_p = \sqrt{[1 + \Delta_O (1 + 0.68 \theta^2 + 0.16 \theta^4)]}$. Information on convergence, the final sonic line locations, and the body and final bow shock shape are printed from this calculation.

The flow chart for the blunt-body code is shown in Figure A.1(a).

A.2.1.2 Marching calculation

The results at the $\theta = 90^\circ$ plane of the blunt-body calculation are used as starting conditions for the marching calculation, after proper variable normalization for the internal marching calculation. For default geometries, the obstacle shape is determined by integration of the appropriate differential equation proceeding from the nose downstream at equal θ increments to form a body-shape table. The stepsize along the x-axis is recalculated at every ICONST(49) with ICONST(49) being set to 10. At each x-location, R_{body} is determined by linear interpolation. The computational mesh is extended by adding the line perpendicular to the x-axis at each step, divided in the same manner as for the blunt nose. The calculation marches downstream with a maximum stepsize of 1.0 until the terminal location specified

by the user has been passed. However, the number of steps is limited to 75, after which the calculation will end regardless of the x-location. The coordinates of the obstacle and bow shock are printed at each step.

The grid coordinates and flow-field values are written to a file, TAPE9, which may be saved to use as input for a later run. This rerun option, which replaces construction of the computational mesh and performance of the blunt-body and marching calculations with the reading of the rerun input file TAPE4, is described in section A.2.2. The flow chart for the marching calculation is provided in figure A.1(b).

A.2.1.3 Streamline calculation

The streamlines are calculated in two sections, following each of the flow-field calculations. Using the results of the blunt-body calculation, i.e. the (x,R) grid coordinates, (R_p, θ) grid coordinates, density ρ/ρ_∞ , and velocity components v_x/v_∞ and v_R/v_∞ , the velocity magnitude $|v|/v_\infty$ and flow angle ϕ are calculated. Density ρ/ρ_∞ and velocity magnitude $|v|/v_\infty$ are first smoothed along the rays of constant- θ , using a third-degree least-squares fit with respect to R_p . Streamlines are then calculated downstream to $x = 0.0$, using the trajectory method and integrating through the velocity field by means of a third-order modified Euler integration procedure with the grid locations on the bow shock used as starting positions. The flow angle $\phi = \tan^{-1}(v_R/v_x)$ at each point is determined using bivariate linear interpolation first in θ , then R_p . Points for which $\theta < 0^\circ$ or $\theta > 90^\circ$ are discarded in the interpolation.

The marching calculation provides (x,R) grid coordinates, and values of density ρ/ρ_t , and velocity components v_x/v_t and v_R/v_t , where t denotes free-stream stagnation conditions. For compatibility with the blunt-body solution, the flow-field values are converted to ρ/ρ_∞ , v_x/v_∞ , v_R/v_∞ before calculating the resultant velocity magnitude

$|y|/v_\infty$ and flow angle ϕ . The streamline calculation is continued downstream, employing the same method as in the nose region. Starting positions on the shock wave for the streamline calculation in the marching zone are set at equal R-increments, with a maximum of 50 streamlines calculated. The flow angle is determined using bivariate linear interpolation first in x , then in R .

Along the symmetry axis, values of x , ρ/ρ_∞ , and $|y|/v_\infty$ are determined by extrapolation, using a third-order Lagrangian polynomial in θ on each arc of the computational grid. Exact values for the stagnation streamline are used where possible, viz. at the bow shock

$$\rho/\rho_\infty = (\gamma+1)M_\infty^2 / [(\gamma-1)M_\infty^2 + 2]$$

$$|y|/v_\infty = 1/(\rho/\rho_\infty)$$

at the body surface

$$\rho/\rho_\infty = (\rho/\rho_\infty)_{\text{shock}} \cdot \left\{ \left[\frac{(\gamma+1)M_\infty^2}{4\gamma M_\infty^2 - 2(\gamma-1)} \right]^{1/(\gamma-1)} \right\}$$

$$|y|/v_\infty = 0.0$$

$$x = 1.0$$

Detailed flow-field output may now be printed by subroutine FLOUT, with LPRFL as print control variable. In addition to grid coordinates, density, velocities and flow angle, values of temperature T/T_∞ and pressure P/P_∞ are output, where

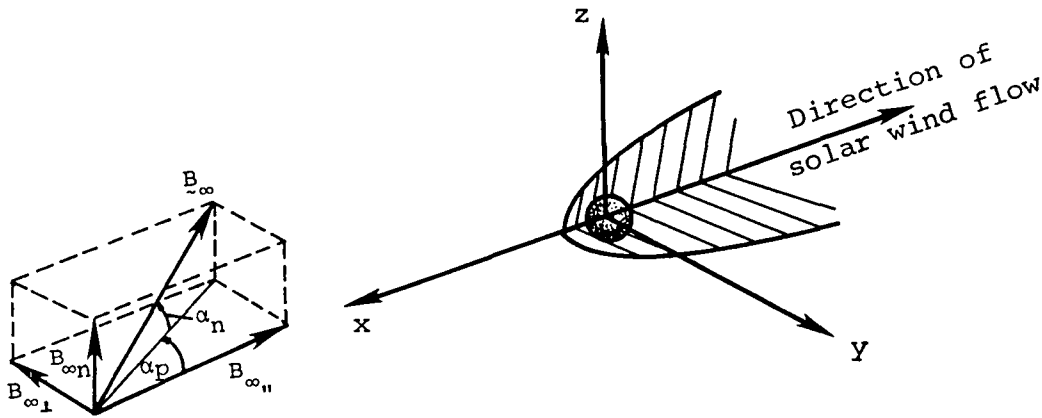
$$T/T_\infty = 1 + [(\gamma-1)/2] \cdot M_\infty^2 \cdot [1 - (|y|/v_\infty)^2]$$

$$P/P_\infty = (\rho/\rho_\infty) (T/T_\infty)$$

Streamline coordinates may also be printed by subroutine STOUT, with LPRST as print control variable. A plot of the streamlines is generated if the variable LPLOT is true. A flow chart of the streamline calculation is shown in figure A.1(c).

A.2.1.4 Magnetic-field calculation

The magnetic field is determined by separately calculating the unit components whose directions are parallel, perpendicular, and normal to the flow, in the undisturbed solar wind. These components are then added vectorially, the resultant being expressed in orthogonal (x,y,z) components. The angles in the free stream α_p and α_n between the magnetic field and the flow, as shown in the sketch below, are either input or, in the case of a trajectory calculation, are calculated internally from the input interplanetary magnetic field.



The magnetic-field components are calculated using the following formulae in which \underline{e} signifies a vector of magnitude e in the direction of the component field line, and \hat{n} the unit normal vector.

$$\left(\frac{\underline{B}}{B_\infty}\right)_{\parallel} = \left(\frac{\underline{v}}{v_\infty}\right) \left(\frac{\rho}{\rho_\infty}\right); \quad \left(\frac{\underline{B}}{B_\infty}\right)_{\perp} = \left(\frac{\Delta\tilde{\ell}}{\Delta\ell_\infty}\right) \left(\frac{\rho}{\rho_\infty}\right); \quad \left(\frac{\underline{B}}{B_\infty}\right)_n = \left(\frac{R}{R_\infty}\right) \left(\frac{\rho}{\rho_\infty}\right)$$

$$\left(\frac{\underline{B}}{B_\infty}\right) = \left(\frac{\underline{B}}{B_\infty}\right)_{\parallel} \left(\frac{B_{\infty\parallel}}{B_\infty}\right) + \left(\frac{\underline{B}}{B_\infty}\right)_{\perp} \left(\frac{B_{\infty\perp}}{B_\infty}\right) + \hat{n} \left(\frac{\underline{B}}{B_\infty}\right)_n \left(\frac{B_{\infty n}}{B_\infty}\right)$$

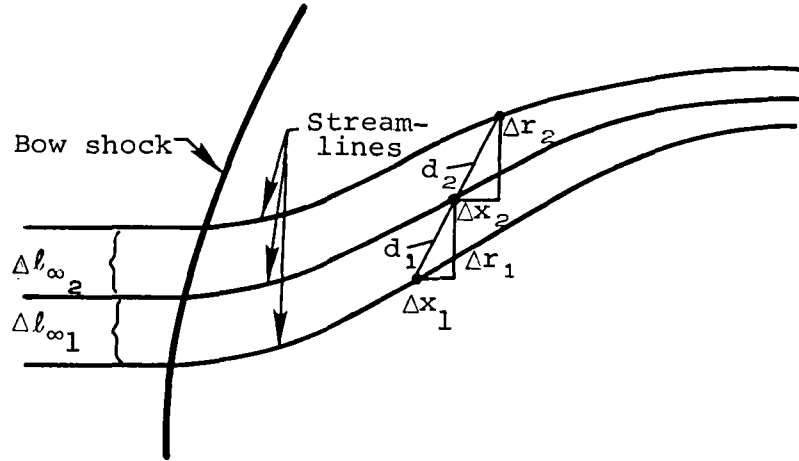
The magnetic-field line vector component $\underline{B}_{\parallel}$ which results from the interplanetary component $B_{\infty\parallel}$ that is parallel to the undisturbed solar flow has local magnitude given by $(|v|/v_\infty)(\rho/\rho_\infty)$, and the same local direction ϕ as the fluid flow. Determination of the normal magnetic-field component B_n requires calculation of R/R_∞ , where R_∞ is the free-stream cylindrical R-ordinate of the streamline through the point under consideration. This is calculated by linearly interpolating in the local radial cylindrical coordinate R between the streamlines, with $R/R_\infty = 1.0$ along the x-axis. The magnetic-field vector component \underline{B}_{\perp} resulting from the interplanetary component $B_{\infty\perp}$ which is perpendicular to the undisturbed solar-wind flow requires the distance vector $\Delta\tilde{\ell}/\Delta\ell_\infty$, whose magnitude is $|\Delta\tilde{\ell}|/\Delta\ell_\infty$ and direction is ψ , where $|\Delta\tilde{\ell}|/\Delta\ell_\infty$ is the stretching factor of the perpendicular field at the point, and ψ is the direction of the field line through the point. The magnitude and direction of $\Delta\tilde{\ell}/\Delta\ell_\infty$ are calculated according to

$$\frac{|\Delta\tilde{\ell}|}{\Delta\ell_\infty} = \frac{d_1 \cdot d_2}{d_1 + d_2} \cdot \frac{1}{\Delta\ell_{\infty 1} + \Delta\ell_{\infty 2}}$$

and

$$\psi = \frac{\tan^{-1} \left(\frac{\Delta r_1}{\Delta x_1} \right) \cdot d_2 + \tan^{-1} \left(\frac{\Delta r_2}{\Delta x_2} \right) \cdot d_1}{(d_1 + d_2)}$$

where the quantities d_1 , d_2 , Δx_1 , Δx_2 , Δr_1 , Δr_2 , $\Delta \ell_{\infty 1}$, and $\Delta \ell_{\infty 2}$ are described by the sketch below. The points marked (•) on the streamlines represent equal-time intervals in the flow.



The perpendicular field lines are determined by integrating $\int \underline{v} dt$ along each streamline, using trapezoidal integration to locate points along the streamline at regular increments in time, Δt , starting at a perpendicular field line ahead of the bow shock. Values for $|\Delta \underline{\ell}|/\Delta \ell_{\infty}$ and ψ are calculated at the points where the perpendicular field lines and streamlines intersect, interpolating only along the field lines. A generalized quadrilateral interpolation scheme is then employed to determine $|\Delta \underline{\ell}|/\Delta \ell_{\infty}$ and ψ at the computational grid points, using the quadrilateral containing the point formed by the intersection of pairs of adjacent streamlines and perpendicular field lines. At the bow shock, an exact formula is used, viz.

$$(|\Delta \underline{\ell}|/\Delta \ell_{\infty})^2 = 1 + \cot^2 \theta (1+D^2) - 2D \times \csc \theta \times \cot \theta \times \cos(\theta-\delta)$$

$$\psi = \theta + \sin^{-1} [D \times \cot \theta \times \sin(\theta-\delta) / (|\Delta \underline{\ell}|/\Delta \ell_{\infty})]$$

where

$$D^2 = 1 - 4(M_\infty^2 \sin^2 \theta - 1)(\gamma M_\infty^2 \sin^2 \theta + 1) / [(\gamma + 1)^2 M_\infty^4 \sin^2 \theta]$$

$$\cot \delta = \tan \theta \times \{(\gamma + 1)M_\infty^2 / [2(M_\infty^2 \sin^2 \theta - 1)] - 1\}$$

$$\theta = \tan^{-1} \left(\frac{dR_{\text{shock}}}{dx} \right)$$

The values of $|\Delta \underline{\ell}| / \Delta \ell_\infty$ at the grid points are smoothed using fifth-order least-squares fit with respect to arc length along the arcs of the grid. The resultant magnetic field can then be expressed in orthogonal (x, y, z) components. The code determines these components for the case when the field point is located in the (x, y) plane, i.e., $z = 0$. These components are given by

$$B_x / B_\infty = \cos \alpha_n \times [\cos \phi \times \cos \alpha_p \times (|\underline{B}| / B_\infty)_n + \cos \psi \times \sin \alpha_p \times (|\underline{B}| / B_\infty)_\perp]$$

$$B_y / B_\infty = \cos \alpha_n \times [\sin \phi \times \cos \alpha_p \times (|\underline{B}| / B_\infty)_n + \sin \psi \times \sin \alpha_p \times (|\underline{B}| / B_\infty)_\perp]$$

$$B_z / B_\infty = \sin \alpha_n \times (B / B_\infty)_n$$

Magnetic-field components may now be printed by subroutine BOUT, with LPRB as print control parameter. The magnetic field is not calculated when LPRB = .FALSE. and KBCON=0. A flow chart of the magnetic-field calculation is shown in figure A.1(d).

A.2.1.5 Contour calculation and plot generation

Contours are calculated for velocity $|v| / v_\infty$, density ρ / ρ_∞ , and magnetic components $(|\underline{B}| / B_\infty)_n$, $(|\underline{B}| / B_\infty)_\perp$, and $(|\underline{B}| / B_\infty)_n$. The method used is a modified version of a procedure developed by R. Sorenson

of NASA/Ames Research Center. The boundary is searched for intervals which bracket a contour point. Having found one point, the remainder of the contour is determined by 'walking' around the contour, searching at each step for the interval through which the contour line next passes, until a boundary point is reached. Then closed contours are found in a similar manner. Linear interpolation is used throughout the process. Note that since T/T_∞ is a function of $|v|/v_\infty$ only, velocity contours may also be considered as temperature contours. Temperature and velocity are related by the following function.

$$T/T_\infty = 1 + \frac{\gamma-1}{2} M_\infty^2 \left[1 - \left(\frac{|v|}{v_\infty} \right)^2 \right]$$

The coordinates of the contour lines can be printed by subroutine CONOUT, with LPRCON as print control parameter.

The program segment which controls the generation of contour plots is accessed only when LPLOT = .TRUE. The UCC Plot Routines used to produce these plots are AXIS, CHAR, DASH, DOTLN, ENPLT, GREEK, MATH, NUMPLT, PLOT, PLTLN, POLAR, RESET, SCALF, and VECTOR. A flow chart of the contour calculation and plot generation in figure A.1(e).

A.2.1.6 Trajectory calculation

This segment of the program provides theoretical plasma and magnetic-field properties in an output form that is useful for direct comparison with actual spacecraft data. Given a sequence of coordinates describing the spacecraft trajectory, the program calculates the density, temperature, and velocity and magnetic-field components at each point. Generation of trajectory plots is controlled by the logical variable LPLTRJ. The trajectory calculation proceeds as follows.

Input to this calculation includes interplanetary values of temperature, density, velocity, and magnetic field together with

the trajectory coordinates. The trajectory input is required as a function of time and normalized by planetary radius. If the logical variable LSUN is TRUE, then it is assumed that the trajectory coordinates and vector quantities are expressed in terms of a sun-planet (ecliptic) coordinate system. In this case, these quantities are converted by the program into a solar-wind coordinate system by the transformation

$$\begin{pmatrix} x_w \\ y_w \\ z_w \end{pmatrix} = \begin{pmatrix} \cos \Omega \cos \phi_p & -\sin \Omega \cos \phi_p & \sin \phi_p \\ \sin \Omega & \cos \Omega & 0 \\ -\cos \Omega \sin \phi_p & \sin \Omega \sin \phi_p & \cos \phi_p \end{pmatrix} \begin{pmatrix} x_s \\ y_s \\ z_s \end{pmatrix}$$

where (x_w, y_w, z_w) are coordinates in the solar-wind system and (x_s, y_s, z_s) are coordinates in the sun-planet system. The angles Ω and ϕ_p are the azimuthal (total aberration) and polar angles, respectively. The azimuthal angle, Ω , is the angle in the plane of the ecliptic between the sun-planet line and the oncoming solar-wind, i.e., the x_s -axis and the x_w -axis as shown in figure A.2. The angle ϕ_p , positive for southward solar-wind flow, measures the deviation of the solar-wind from the plane of the ecliptic. Figure A.2 illustrates the transformation from sun-planet ecliptic coordinates to solar-wind coordinates. In this case the azimuthal and polar angles indicated are both positive.

If LSUN is FALSE, it is assumed that all input data are referenced to the solar-wind coordinate system and this transformation is not performed.

In order to conform with the internal flow-field and magnetic-field calculations, the signs of the x and y components of the trajectory and vector quantities are reversed. This is, in effect, another coordinate transformation which is defined by

$$\begin{pmatrix} x_C \\ y_C \\ z_C \end{pmatrix} = \begin{pmatrix} -1 & 0 & 0 \\ 0 & -1 & 0 \\ 1 & 0 & 1 \end{pmatrix} \begin{pmatrix} x_W \\ y_W \\ z_W \end{pmatrix} = \begin{pmatrix} -\cos \Omega \cos \phi_p & -\sin \Omega \cos \phi_p & \sin \phi_p \\ \sin \Omega & -\cos \Omega & 0 \\ -\cos \Omega \sin \phi_p & \sin \Omega \sin \phi_p & \cos \phi_p \end{pmatrix} \begin{pmatrix} x_S \\ y_S \\ z_S \end{pmatrix}$$

where (x_C, y_C, z_C) are coordinates referenced to the internal calculation system. This transformation is illustrated in figure A.3. Also shown in figure A.3 is the relationship of the interplanetary parallel, perpendicular, and normal magnetic field components to the internal calculation system. Specifically,

$$B_{\infty n} = B_{x_C}, \quad B_{\infty \perp} = B_{y_C}, \quad \text{and} \quad B_{\infty p} = B_{z_C}$$

The angles α_p and α_n are now calculated from the relationships

$$\alpha_p = \tan^{-1} \left(\frac{B_{y_C}}{B_{x_C}} \right)$$

and

$$\alpha_n = \tan^{-1} \left(\frac{B_{y_C}}{\sqrt{(B_{x_C})^2 + (B_{y_C})^2}} \right)$$

At this point, all data is in a form compatible with the internal calculations and the program can interpolate for flow and magnetic-field values along the trajectory. The following procedure is repeated at each trajectory point. Noting that the flow is axisymmetric, the coordinate system may be rotated to the most convenient orientation for the calculation. The present (x_C, y_C, z_C) coordinates are converted to (x_C, R) coordinates by a rotation in the (y_C, z_C) plane about the x_C -axis through the angle $\theta = \tan^{-1}[z_C/y_C]$. This rotation defines a new coordinate system (x', y', z') in which $z' = 0$. Subroutine IJRAJ now locates the point with reference to the computational flow-field grid. The point is either within the ionopause, in the grid

region, or beyond the bow shock. If the point is within the ionopause, all values are set to zero. If the point lies beyond the bow shock, all quantities assume their free-stream values. For points within the grid, the velocity magnitude, density, and flow angle ϕ are found by interpolation using function FTRAJ. From the flow angle ϕ and the rotation angle θ , velocity components in the (x_c, y_c, z_c) system can be calculated according to

$$\begin{aligned}v_{x_c} &= v \cos \phi \\v_{y_c} &= v \sin \phi \cos \theta \\v_{z_c} &= v \sin \phi \sin \theta\end{aligned}$$

Calculation of the magnetic field is complicated somewhat because the components are dependent on the incident magnetic field. Using α_p and α_n , B'_{x_∞} , B'_{y_∞} , and B'_{z_∞} are calculated in the rotated (x', y', z') system by

$$\begin{aligned}B'_{x_\infty} &= B_{x_{c_\infty}} \\B'_{y_\infty} &= B_{y_{c_\infty}} \cos \theta + B_{z_{c_\infty}} \sin \theta \\B'_{z_\infty} &= -B_{y_{c_\infty}} \sin \theta + B_{z_{c_\infty}} \cos \theta\end{aligned}$$

Then α'_p and α'_n are defined by

$$\alpha'_p = \tan^{-1} \left(\frac{B'_{y_\infty}}{B'_{x_\infty}} \right) \text{ and } \alpha'_n = \tan^{-1} \left[\frac{B'_{z_\infty}}{\sqrt{(B'_{x_\infty})^2 + (B'_{y_\infty})^2}} \right]$$

Interpolation is then carried out to determine the magnetic angle ψ and the ratios $\left| \frac{\tilde{B}}{B_\infty} \right|_{\parallel}$, $\left| \frac{\tilde{B}}{B_\infty} \right|_{\perp}$, and $\left(\frac{B}{B_\infty} \right)_n$ in the rotated system again using the function FTRAJ. Next, the magnetic-field components B'_x , B'_y , B'_z in the rotated system are calculated from

$$B'_x = \cos \alpha'_n \left[\cos \phi \cdot \cos \alpha'_p \cdot \left| \frac{\tilde{B}}{B_\infty} \right|_{\parallel} + \cos \psi \cdot \sin \alpha'_p \cdot \left| \frac{\tilde{B}}{B_\infty} \right|_{\perp} \right] \cdot B_\infty$$

$$B'_y = \cos \alpha'_n \left[\sin \phi \cdot \cos \alpha'_p \cdot \left| \frac{\tilde{B}}{B_\infty} \right|_{\parallel} + \sin \psi \cdot \sin \alpha'_p \cdot \left| \frac{\tilde{B}}{B_\infty} \right|_{\perp} \right] \cdot B_\infty$$

$$B'_z = \sin \alpha'_n \cdot \left(\frac{B}{B_\infty} \right)_n \cdot B_\infty$$

Finally, these magnetic-field components are rotated back through the angle θ to yield magnetic-field components referenced to the internal calculation system (x_c, y_c, z_c) by

$$\begin{pmatrix} B_{x_c} \\ B_{y_c} \\ B_{z_c} \end{pmatrix} = \begin{pmatrix} 1 & 0 & 0 \\ 0 & \cos \theta & -\sin \theta \\ 0 & \sin \theta & \cos \theta \end{pmatrix} \begin{pmatrix} B'_x \\ B'_y \\ B'_z \end{pmatrix}$$

Subroutine TROUT now prints the trajectory output in both the solar-wind (x_c, y_c, z_c) and the sun-planet (x_s, y_s, z_s) coordinate systems using the transformation below to obtain sun-planet magnetic-field vector components from solar-wind magnetic-field vector components.

$$\begin{pmatrix} B_{x_s} \\ B_{y_s} \\ B_{z_s} \end{pmatrix} = \begin{pmatrix} -\cos \Omega \cos \phi_p & \sin \Omega & -\cos \Omega \sin \phi_p \\ \sin \Omega \cos \phi_p & -\cos \Omega & \sin \Omega \sin \phi_p \\ \sin \phi_p & 0 & \cos \phi_p \end{pmatrix} \begin{pmatrix} B_{x_c} \\ B_{y_c} \\ B_{z_c} \end{pmatrix}$$

The transformation of the solar-wind velocity components (v_{x_C} , v_{y_C} , v_{z_C}) into sun-planet components (v_{x_S} , v_{y_S} , v_{z_S}) is also done using the same transformation.

Finally, if LPLTRJ is true, a file of trajectory plots is created. A flow chart for this program segment is shown in figure A.1(f).

A.2.2 Rerun Option

The rerun option is used when LRERUN = .TRUE. The blunt-body and marching calculations are replaced with the reading of grid coordinates and flow-field values from the rerun file, TAPE4, which contains data written to TAPE9, then saved, on a previous run. Different values for any parameter not used in the flow-field calculations may be specified, viz. contour values, plot length, magnetic-field angles, and output options. Values of AMACH, GAMMA, and HRO are required input, to ensure that the input rerun file does contain the case desired for rerun. If the geometry is user-supplied, the body-shape table will be read from TAPE4, and should not be input from cards.

After reading the card input, MACH, GAMMA, and HRO are tested against values from TAPE4. The grid coordinates and flow-field values from the blunt-body calculation are read in, then smoothed, and streamlines calculated for this region, as previously described. The results of the marching calculation are then read, and the streamline calculation continued downstream. The calculations then proceed as described in section A.2.1.

A run must not contain more than one case which uses the rerun option.

A.2.3 Program Limitations and Precautions

The program makes some assumptions about the geometry of the obstacle shape around which flow is to be calculated, and about the

flow field. The obstacle shape is assumed to be monotonically increasing in cylindrical radius R, going downstream. The nose of the obstacle is at $x = 1.0$. The origin of the (x,R) coordinate system is the center of the planet. Obstacle shapes with sharp corners should be avoided. In the magnetic-field calculation, the first streamline is assumed to be inside the arc described by the grid points immediately off the body, downstream of $x = 0.0$. To reduce computational costs, a grid using $NR = 10$ may be used, in which case a lower value of CN may be required. This would reduce the running time by approximately 40 percent. A free-stream Mach number less than 2.0 is not advised.

A.2.4 Convergence Criteria for Blunt-Body Calculation

The output provides two measures of the convergence of the blunt-body calculation. The RMS of shock speed and maximum shock speed are printed at each iteration. These quantities should both tend to zero as the iterations proceed. A value for q_{RMS} , RMS of shock speed, of

$$q_{RMS} < \sqrt{\gamma} \times M_{\infty} \times 10^{-3}$$

where γ is the specific heat ratio, and M_{∞} is the free-stream Mach number, usually indicates a converged solution. The RMS of error in enthalpy, HT, should be less than 1 percent, with the maximum enthalpy error also of that order.

The Courant number, CN, determines the time step size used by the calculation. A value not greater than the default of 3.0 should be used. For low Mach numbers or a coarser mesh than the default grid, a lower value may be preferable. If the default value does not generate a converged solution, or if the error message from subroutine SHOCK is printed, try lowering CN in increments of 0.5 to find a better value of CN. User-supplied bodies may also require a lower Courant number.

A.3 DESCRIPTION OF INPUT

This section describes the card input for the program. An alphabetized dictionary of input variables is provided, defining the variables, listing default values and limitations. A discussion of the preparation of the card input is then presented, followed by a description of the input card format.

A.3.1 Dictionary of Input Variables

- AMACH free-stream Mach number; $3.0 \leq \text{AMACH} \leq 25.0$ is recommended
- ANGN the angle, in degrees, measuring the deviation of the free-stream magnetic field from the plane in which $B_{\infty n}$ and $B_{\infty \perp}$ lie; equal to $\tan^{-1} \left(B_{\infty n} / \sqrt{|B_{\infty n}^2| + |B_{\infty \perp}^2|} \right)$; see figure A.3, measured in the (x_c, y_c, z_c) coordinate system; only specified when interplanetary magnetic-field components not specified.
- ANGP the angle, in degrees, measuring the deviation of the in-plane magnetic component ($B_{\infty n} + B_{\infty \perp}$) from the direction of flow; equal to $\tan^{-1} (B_{\infty n} / B_{\infty \perp})$; see figure A.3, measured in the (x_c, y_c, z_c) coordinate system; only specified when interplanetary magnetic-field components not specified.
- AZANG angle in the ecliptic plane between the sun-planet line and the direction of solar-wind flow. See figure A.2 for positive direction.
- BCON(I) KBCON-dimensional array specifying values to be used for magnetic field strength contours
- BINF magnetic field strength free-stream value; set to 1.0 if plots desired in nondimensionalized units.

BX1 x_s -component of interplanetary magnetic field; referred to sun-planet coordinates
 BY1 y_s -component of interplanetary magnetic field; referred to sun-planet coordinates
 BZ1 z_s -component of interplanetary magnetic field; referred to sun-planet coordinates
 CN Courant number used for blunt-body calculation; program default value is 3.0
 GAMMA ratio of plasma specific heats
 HRO obstacle geometry indicator:
 HRO > 0. - ionopause with $H/R_o = HRO$
 HRO = 0. - magnetopause equatorial trace
 HRO < 0. - geometry is user-supplied
 ITER integer, number of iterations for blunt-body calculation; program default value is 300
 KBCON integer, number of values specified for magnetic-field contours; $0 \leq KBCON \leq 20$
 KRCON integer, number of values specified for density contours; $0 \leq KRCON \leq 20$
 KVCON integer, number of values specified for velocity magnitude contours; $0 \leq KVCON \leq 20$
 LGRAV logical variable indicating whether default ionopause is calculated with gravitational variation in scale height
 FALSE - no
 TRUE - yes

L PLOT logical variable indicating whether to create plots or plot
 file
 FALSE - no
 TRUE - yes

L PLTRJ logical variable indicating whether to create trajectory and
 time history plots
 FALSE - no
 TRUE - yes

L PRB logical variable indicating whether to print magnetic field
 output
 FALSE - no
 TRUE - yes

L PRCON logical variable indicating whether to print coordinates of
 contours lines
 FALSE - no
 TRUE - yes

L PRFL logical variable indicating whether to print detailed flow-
 field output
 FALSE - no
 TRUE - yes

L PRST logical variable indicating whether to print coordinates of
 streamlines
 FALSE - no
 TRUE - yes

L RERUN logical variable indicating whether this case uses rerun
 option
 FALSE - perform blunt-body and marching calculations
 TRUE - read results of a previous calculation from
 TAPE4

LRSTRT logical variable indicating whether to use previous shock shape as initial guess for blunt body
 TRUE - use shock shape from previous solution.
 (Must have a full solution as an earlier run in same job.)
 FALSE - use default initial guess for shock shape

LSUN logical variable indicating whether trajectory input is referenced to sun-planet coordinate system
 FALSE - trajectory input in solar-wind coordinates
 TRUE - trajectory input in sun-planet coordinates

LTRAJ logical variable indicating whether to perform a trajectory calculation
 TRUE - trajectory calculation, data provided
 FALSE - no trajectory calculation

MARKT(I) NMARKT - dimensional array specifying points to be marked for cross reference. If $K = \text{NMARKT}(I)$, the K th point of the trajectory is to be marked.

NBLUNT integer, number of angular mesh points for blunt-body calculation; for user-supplied geometry, $\text{XX}(\text{NBLUNT}-1)=0.0$; program default value, and maximum, is 24

NBOD integer, number of points in body-shape table when geometry is user-supplied; $1 \leq \text{NBOD} \leq 100$

NCASE integer, number of cases to be run consecutively; $\text{NCASE} > 1$

NMARKT integer, numbered values specified for cross reference points; $0 \leq \text{NMARKT} \leq 12$.

NR integer, number of radial mesh points; program default value, and maximum, is 19

NTRAJ integer, number of points specified in trajectory table

NXADD integer, number of points to be added to blunt-body grid past $\theta = 90^\circ$, default value is 0.

POLANG angle, measured in degrees, between the plane of the ecliptic and direction of solar-wind flow; positive for southward flow; see figure A.2

RCON(I) KRCON - dimensional array specifying values to be used for density contours

RHOINF density-free stream value; set to 1.0 if plots desired in nondimensional units

RPLNT radius of planet in units of nose radius, R_{PLNT}/R_O

RR(I) NBOD - dimensional array representing the R-locations, in cylindrical (x,R) coordinates, of the user-supplied body shape; in units of nose radius

TITLE descriptive heading of the case, to be printed on the first page of output; may contain up to 80 characters, including blanks

TMPINF free-stream temperature; set to 1.0 if plots desired in nondimensional units

TTRAJ(I) NTRAJ - dimensioned array specifying time locations of trajectory points

VCON(I) KVCON - dimensional array specifying values to be used for velocity contours

VINF free-stream velocity; set to 1.0 if plots desired in non-dimensional units

XCALC terminal downstream x-location for marching calculation of flow field; XCALC < 0.0; program default value is -1.0

XPLOT terminal downstream x-location for calculation of streamlines, magnetic field, and contours; XCALC \leq XPLOT \leq 0.0; program default value is -1.0

XTRAJ(I) NTRAJ - dimensioned array specifying x_s -locations of trajectory points; in units of planetary radius; when (ANGP,ANGN) are specified, XTRAJ(I) is referred to solar-wind x_c -locations; see figures A.2 and A.3

XX(I) NBOD - dimensional array representing the x-locations, in cylindrical (x,R) coordinates, of the user-supplied body shape; in units of nose radius. See figures A.2 and A.3

YTRAJ(I) NTRAJ - dimensioned array specifying y_s -locations of trajectory points; in units of planetary radius; when (ANGP,ANGN) are specified, YTRAJ(I) is referred to solar-wind y_c -locations; see figures A.2 and A.3

ZTRAJ(I) NTRAJ - dimensioned array specifying z_s -locations of trajectory points; in units of planetary radius; when (ANGP,ANGN) are specified, ZTRAJ(I) is referred to solar-wind z_c -locations; see figures A.2 and A.3

A.3.2 Preparation of Input Data

The card input for a run consists of one card containing the number of cases to be run consecutively, Item 0, followed by a set of input for each case, Item 1 through Item 7, and Item 8 if required. Where a default value is to be used, the input field should be left blank.

For each case, all required variables which do not assume their default values should be specified. The input format for all cards is described in section A.3.3.

Item 0 - This item consists of one card, containing the number of cases in this run, NCASE.

Item 1 - This card provides identification of the case, TITLE, which is printed on the first page of the output for this case.

Item 2 - This card contains information on the flow conditions and body geometry, and parameters required for the blunt-body and marching calculations. AMACH, GAMMA, and HRO must be specified for each case. For the rerun option, the values are tested against the values from the rerun file. The parameters XCALC, NR, NBLUNT, CN, ITER are used only when the flow field is to be calculated. These variables each assume a default value if the input field is blank.

Item 3 - This item consists of one card containing the rerun indicator, LRERUN, the output control variables LPRFL, LPRST, LPRCON, LPRB, and LPLOT, the trajectory indicator LTRAJ, and the restart indicator LRSTRT.

Item 4 - This card contains the variables XPLOT, ANGP, ANGN, NXADD, and LGRAV. The value for XPLOT is changed by the program to be the x-location of the marching calculation immediately upstream of the input value for XPLOT. The angles describing the deviation of the magnetic field from the flow, ANGP and ANGN, are not required when LPRB = .FALSE; KBCON = 0, and LTRAJ = .FALSE. since the magnetic field is not calculated under these conditions. ANGP is the angle between the vectors $(\underline{B}_{\infty n} + \underline{B}_{\infty \perp})$ and \underline{v}_{∞} , while ANGN is the angle between \underline{B}_{∞} and $(\underline{B}_{\infty n} + \underline{B}_{\infty \perp})$, where $\underline{B}_{\infty n}$, $\underline{B}_{\infty \perp}$, $\underline{B}_{\infty n}$ are the components of the free-stream magnetic field, \underline{B}_{∞} , which are parallel, perpendicular, and normal to \underline{v}_{∞} , and are as indicated in figure A.3. The two angles ANGP and ANGN fully determine the half plane for which the magnetic field

is to be calculated. The magnetic field for the other half of the plane may be calculated by rerunning with the sign of ANGP reversed. When $(\tilde{B}_{\infty 11} + \tilde{B}_{\infty 1}) = 0$, $ANGN = +90^\circ$, $ANGP = 0^\circ$; and, when $\tilde{B}_{\infty n} = 0$, $ANGN = 0^\circ$. Note that ANGP and ANGN are referenced to the (x_c, y_c, z_c) system and are specified only when the interplanetary magnetic-field components are not specified.

If both LTRAJ = .TRUE. and LSUN = .TRUE., then ANGP and ANGN are calculated internally from the interplanetary magnetic-field components BX1, BY1, and BZ1.

Item 5 - This item contains the values for the velocity contours. The first card contains KVCON, the number of values specified for VCON. If KVCON > 0, the contour values are then read. Up to three cards may be required to accommodate the values, eight per card, maximum of 20. The contour values should be monotonically increasing, with at least one value within the range of the magnitude of the velocity in the region for which contours are to be calculated.

Item 6 - This item contains the values for the density contours. The description is similar to that for Item 5, with KRCON being the number of values specified, and RCON the array of values.

Item 7 - This item contains the values for the magnetic-field contours. The description is similar to that for Item 5, with KBCON being the number of values specified, and BCON the array of values. Note that the same contour values are used for the parallel and perpendicular components.

Item 8 - This optional item is required when HRO < 0.0 and LRERUN = .FALSE., and contains the body-shape table for the user-supplied geometry. The first card contains NBOD, the number of points in the shape table. The next NBOD cards contain the cylindrical (x,R) coordinates of these points, [XX(I), RR(I)], one point per card. The points supplied by the user determine the θ -spacing of the mesh used for the

blunt-body calculation. The first point should be near, but not on, the x-axis. A suggested location is such that the θ -spacing between the first point and the x-axis is half the θ -spacing between the first two points. The blunt-body calculation adds a point which is the reflection about the x-axis of the first point in the body-shape table. The $(\text{NBLUNT}-1)^{\text{th}}$ point should be at $x = 0.0$. The BLUNT^{th} point is also used to create the grid for the blunt-body calculation. The coordinates must be normalized so that the planet center is at $(0.,0.)$ and the nose of the body at $(1.,0.)$.

Item 9 - This optional item is read only when LTRAJ is TRUE. The first card contains NTRAJ, the number of points in the trajectory. Then follows NTRAJ cards, each containing the time T, and location (x_s, y_s, z_s) of one point. The time values should be monotonically increasing. At present, $\text{NTRAJ} \leq 100$ is required. Note that when ANGP and ANGN are specified, the trajectory is specified in (x_c, y_c, z_c) coordinates.

Item 10 - This item is read only when LTRAJ is TRUE. The variable LPLTRJ indicates whether plots are to be produced of the trajectory and time histories. The relative size of the planet to the ionopause is given by RPLNT, which may be 0.0, in which case, a value of 1.0 is assumed in the calculations, but the planet is not drawn on the plots. Next are the four free-stream values $v_\infty, T_\infty, \rho_\infty, B_\infty$. If the plots are desired to be in nondimensional units, any or all of these values may be input as 1.0. Each quantity must have a value, zero is not permissible.

Item 11 - This item is read only when LTRAJ is TRUE. The first card contains NMARKT, the number of values specified for MARKT, (presently maximum of 12). If NMARKT = 0, only this card is required. If NMARKT > 0, the values of MARKT are read, 8 per card.

Item 12 - This item, which includes the variables LSUN, AZANG, POLANG, BX1, BY1, and BZ1, is read only when LTRAJ is true.

A.3.3 Format of Input Data

Four format types are used for the input data. For real numbers (F-format), a decimal point is required. Integers (I-format) should be right-adjusted in the field. For logical variables (L-format), the first non-blank character in the field, which should be 'T' or 'F', determines the value. Note that a blank input field is interpreted as 'FALSE'. The title, which is in A-format, may contain any valid character.

A description of the card format of the input data follows, with item numbers corresponding to those in section A.3.2:

Item No. 0: 1 card

Variable	NCASE
Card Column	10
Format type	I

Item No. 1: 1 card

Variable	Title						
Card Column	80						
Format type	A						

Item No. 2: 1 card

Variable	AMACH	GAMMA	HRO	XCALC	NR	NBLUNT	CN	ITER
Card column	10	20	30	40	50	60	70	80
Format type	F	F	F	F	F	F	F	F

Item No. 3: 1 card

Variable	LRERUN	LPRFL	LPRST	LPRCON	LPRB	LPLOT	LTRAJ	LRSTRT
Card column	10	20	30	40	50	60	70	80
Format type	L	L	L	L	L	L	L	L

Item No. 4: 1 card

Variable	XPLOT	ANGP	ANGN	NXADD	LGRAV
Card column	10	20	30	40	50
Format type	F	F	F	N	L

Item No. 5: a) 1 card

Variable	KVCON
Card column	10
Format type	I

b) 0 to 3 cards as needed for up to 20 values, 8 per card

Variable	VCON(1)	VCON(2)			VCON(KVCON)		
Card column	10	20	30	40	50	60	80
Format type	F	F	F	F	F	F	F

Item No. 6: a) 1 card

Variable	KRCON
Card column	10
Format type	I

b) 0 to 3 cards

Variable	RCON(1)	RCON(2)			RCON(KRCON)			
Card column	10	20	30	40	50	60	70	80
Format type	F	F	F	F	F	F	F	F

Item No. 7 a) 1 card

Variable	KBCON
Card column	10
Format type	I

b) 0 to 3 cards

Variable	BCON(1)	BCON(2)			BCON(KBCON)			
Card column	10	20	30	40	50	60	70	80
Format type	F	F	F	F	F	F	F	F

Item No. 8 a) 1 card (this item required only when HRO < 0.0 and LRERUN = .FLASE.)

Variable	NBOD
Card column	10
Format type	I

b) NBOD cards

XX(I)	RR(I)
10	20

Item No. 9: a) 1 card (this item read only when LTRAJ is TRUE)

Variable	NTRAJ
Card column	10
Format type	I

b) NTRAJ cards

Variable	TTRAJ(I)	XTRAJ(I)	YTRAJ(I)	ZTRAJ(I)
Card column	10	20	30	40
Format type	F	F	F	F

Item No. 10: 1 card (this item read only when LTRAJ is TRUE)

Variable	LPLTRJ	RPLNT	VINF	RHOINF	TMPINF	BINF
Card column	10	20	30	40	50	60
Format type	L	F	F	F	F	F

Item No. 11: a) 1 card (this item read only when LTRAJ is TRUE)

Variable	NMARKT
Card column	10
Format type	I

b) 0-2 cards

Variable	MARKT(1)	MARKT(2)			MARKT(NMARKT)			
Card column	10	20	30	40	50	60	70	80
Format type	I	I	I	I	I	I	I	I

Item No. 12: 1 card (this item read only when LTRAJ is TRUE)

Variable	LSUN	AZANG	POLANG	BX1	BY1	BZ1
Card column	10	20	30	40	50	60
Format type	L	F	F	F	F	F

A.4 DESCRIPTION OF OUTPUT

This section describes the output of the computer program. The contents of each output item are specified and discussed. The printed output consists of seven items, five of which are optional and are controlled with input parameters. Plotted output is also optional.

The first output item consists of a banner page and the input data. The input is presented in two forms: first, as images of the input cards, and then with identification of each variable. Default values are printed as if they were input. Parameters CN, NR, NBLUNT, ITER for the blunt-body calculation and XCALC, the terminal location for the marching calculation, are printed only when the flow field is to be calculated. When the obstacle geometry is user-supplied, the input body-shape table is printed. For a default geometry, the body shape is indicated by the description "default ionopause shape for constant scale height with $H/RO =$ ", or "default ionopause shape with gravitational variation in scale height, $H/RO =$ ". Trajectory input is printed only when LTRAJ is true.

The second output item is not printed when LRERUN = .TRUE. From the blunt-body calculation, the shock speed at each iteration, the final enthalpy error, final sonic-line location, and body and final bow-shock shape are printed. For the marching calculation, the downstream x-location and body and shock ordinates are output. There is no control variable allowing the user to suppress this item of output when the flow field is calculated.

Detailed flow-field output is the third item, and is printed only when LPRFL = .TRUE. Coordinates are labeled as X/D, R/D, RP/D, or X/RO, R/RO, RP/RO, to emphasize that distances are normalized by the distance from the center of the planet to the nose of the body, D for the magnetopause, RO for an ionopause. Along the symmetry axis, the values printed are velocity magnitude $V/VINF$, density $RHO/RHOINF$,

temperature $T/TINF$, and pressure $P/PINF$. Over the rest of the flow field, values are also given for velocity components $VX/VINF$, $VR/VINF$, and flow angle ϕ . Note that the flow angle is the deviation of the flow about the obstacle, and so $0^\circ \leq \phi \leq 90^\circ$.

The next output item is the (x,R) coordinates of the streamlines. For blunt-body region, the (R_p, θ) coordinates of the starting position on the bow shock wave are also given. This item is printed only when $LPRST = .TRUE$.

The magnetic-field components are then printed, if $LPPRB = .TRUE$. The location of each point is defined in (R_p, θ) coordinates for the blunt-body region, and (x,R) coordinates for the downstream marching region. The components along field lines parallel, perpendicular, and normal to the flow in the free stream are printed as $B/BINF(PARALLEL)$, $B/BINF(PERP)$, $B/BINF(NORMAL)$. The orthogonal (x_c, y_c, z_c) components of the resultant are printed as $BX/BINF(RESULTANT)$, $BY/BINF(RESULTANT)$, $BZ/BINF(RESULTANT)$. The magnetic field in the symmetry (x_c, y_c) plane, defined by the vector sum $[(\underline{B}/B_\infty)_\parallel + (\underline{B}/B_\infty)_\perp]$, is also printed, and is given by the magnitude $B/BINF(IN-PLANE)$ and direction $B-ANGLE(IN-PLANE)$ of the vector. We note, as pointed out in the text, that the orthogonal magnetic-field components printed here correspond to those in the (x_c, y_c) plane, i.e., $z_c = 0$.

The next item printed is the (x_c, R) coordinates of the contours, for which $LPRCON$ is the logical control variable. Noting that temperature and velocity contours coincide, the corresponding value of $T/TINF$ is printed along with $V/VINF$ for the velocity contours. There are three nonfatal error messages which may occur - see section A.5.

Trajectory output is the last item to be printed. This output is presented first in terms of the solar-wind coordinate system (x_c, y_c, z_c) , and then in terms of sun-planet coordinates (x_s, y_s, z_s) .

The trajectory coordinates are printed as a function of time and are shown normalized by both R_0 and the planetary radius. Next, flow and magnetic-field components are printed for each trajectory point. This output is presented in both nondimensional and dimensionalized forms and includes $|\underline{v}|$, v_x , v_y , v_z , density, temperature, $|\underline{B}|$, B_x , B_y , and B_z .

The program also has the capability to produce two sets of plotted output using UCC plot routines `AXIS`, `CHAR`, `DASH`, `DOTLN`, `ENPLT`, `GREEK`, `MATH`, `NUMPLT`, `PLOT`, `PLTLN`, `POLAR`, `SCALE`, and `VECTOR`. The first set of plots is generated when `L PLOT = .TRUE.` and provides a pictorial representation of the streamlines and contours with a maximum of seven frames produced. The first frame is a plot of the streamlines followed by contour plots of velocity magnitude, temperature, and density. The next three frames are contour plots of the unit parallel, perpendicular, and normal magnetic-field components. These plots are referred to the solar-wind (x,R) coordinate system.

The second set of plots is produced according to the value of the logical variable `LPLTRJ`. This set consists of twelve plots. The first frame is a projection of the trajectory rotated onto the $x-R$ plane. The second frame is a plot of the trajectory projected onto the y_c-z_c plane. The remaining frames are time-history plots of density, temperature, velocity, and magnetic field. The velocity plots include magnitude and three components as do the magnetic field plots. The vector components are referred to the sun-planet ecliptic (x_s, y_s, z_s) coordinates.

A.5 PROGRAM ERROR MESSAGES

This section lists the messages printed by the program, and indicates what action should be taken by the user.

(1) ***** EXECUTION TERMINATED *****
RERUN DATA ON TAPE4 DOES NOT AGREE
WITH CASE SPECIFIED ON CARD INPUT:
MACH NO. GAMMA H/RO

FROM CARDS
FROM TAPE4

The first three parameters of item 2 of the input for a case using the rerun option should agree with those used when creating the file. The tolerance used in comparing the values is 10^{-5} . For a user-supplied geometry, it is sufficient for both values of H/R_0 to be negative.

(2) ***** EXECUTION TERMINATED *****
 ARRAY OF CONTOUR VALUES IMPROPERLY SPECIFIED

When specified, the contour values should be monotonically increasing with at least one value in the range of the velocity, density, or magnetic-field strength for the region under consideration. This error does not inhibit generation of the rerun file.

(3) CONTOUR SEARCH ABORTED - TABLE OVERFLOW IN NAD

The program allows for 29 contour lines to be found, storing the starting address of each contour line in array NAD. This message indicates that at least one more contour line could be found. If the user requires all the contours of the levels specified, the case should be rerun in two parts. Otherwise, reduce the number of contour levels specified.

(4) CONTOUR SEARCH ABORTED - TABLE OVERFLOW IN (X,Y)

The contour lines may be described by up to 1000 points, stored in arrays X and Y. This message indicates that more points would be

required for the contour lines requested. The last contour line found will be incomplete. As with (3), either reduce the number of contour levels or run as two cases.

(5) NEGATIVE PRESSURE DETECTED BY SHOCK AT J=
 PN= PO= PTAU=

This message is printed by the blunt-body code when a negative pressure has been calculated at the shock on this iteration, at radial locations J. The quantities printed are: PN, the pressure calculated on this step; PO, the pressure from the previous step; and PTAU, the partial derivative of pressure with respect to time. This condition indicates that the shock wave motion is too extreme. Lowering the value of CN, and thus reducing the time step, may remove the problem.

The following messages (6)-(10) usually result from using an obstacle geometry which is in some way too severe for the program to handle in its present form. The obstacle slope may be sufficiently high at $x = 0.0$ that the axial Mach number becomes subsonic in the starting solution for the marching calculation, or there may be a sharp corner in the profile. Check input, particularly free-stream Mach number and body geometry.

(6) NEGATIVE PRESSURE ON BODY DETECTED BY BNDRY, PB= AT J=

This message indicates that a negative pressure on the body, PB, has been calculated at radial location J.

(7) NEGATIVE PRESSURE OR DENSITY ON BODY DETECTED BY BNDRYM AT X=
 PB= RHOB= VXB= VRB=

The program makes internal corrections when this condition occurs, resulting pressure PB, density RHOB, and velocity components VXB and VRB.

(8) NEGATIVE SIGMA-BAR-1 IN EIGENM INDICATES SUBSONIC FLOW AT I=

(9) NEGATIVE SIGMA-BAR-2 IN EIGENM INDICATES SUBSONIC FLOW AT I=

These messages are printed when subsonic flow is detected by the marching calculation. The computed stepsize for this region will be quite small.

(10) -----BODY TURN STOPPED AT M2=100-----

This message indicates that the body has a sharp corner, which has been limited to 100° when being transformed.

A.6 SAMPLE CASE

The sample case presented in this section is based on actual interplanetary conditions as measured by the solar-wind plasma analyzer, the fluxgate magnetometer, and retarding potential plasma analyzer on the Pioneer-Venus Orbiter for orbit 3.

The sample case is run alone and is set up to produce all possible output. The gasdynamic solution is to be calculated about a default ionopause shape with $H/R_\odot = 0.03$, $M_\infty = 3.0$, and $\gamma = 5/3$. The value of H/R_\odot is based on measurements of ionospheric density and temperature by the retarding potential plasma analyzer. Streamlines, magnetic-field components, and contours are desired to a downstream location of $-5.5 x/R_\odot$. Contour values are specified for all quantities. Interplanetary values for velocity magnitude and direction, density, and temperature were provided by the solar-wind plasma analyzer and for the magnetic field by the fluxgate magnetometer.

The input data is tabulated in figure A.4, with item numbers corresponding to those in sections A.3.2 and A.3.3. The first card, item 0, indicates that there is one case to run. The remaining

fifty-five cards provide the data for this case. Item 1 contains the identifying title. On the next card, item 2, values are specified for AMACH, GAMMA, HRO, and XCALC. The other data fields are left blank to indicate that the default values will be used. The values of the logical variables of item 3 specify that the flow field is to be calculated and that full printed and plotted output is to be produced. Item 4 defines the plot length to be $-5.5 x/R_0$. The fields for ANGP and ANGN are left blank as they are to be calculated internally by the program. Items 5, 6, and 7 specify the contour levels to be used - 14 for velocity and temperature, 11 for density, and 13 for magnetic-field strength. Item 8 is omitted because the obstacle geometry is one of the default shapes for which the coordinates are calculated internally. The next 37 cards, item 9, are the trajectory coordinates, indicating time (in minutes from periapsis and the three spacial coordinates normalized by planetary radius). Item 10 indicates that trajectory plots are to be generated. This item also specifies free-stream values of velocity, density, temperature, and magnetic-field strength. The next two cards, item 11, indicates that the fourth, ninth, eleventh, and nineteenth trajectory points are to be marked on the plots for cross-reference. The last input card, item 12 indicates that the given trajectory coordinates are expressed in sun-planet coordinates. The azimuthal and polar angles, Ω and ϕ_p , are also specified by this item as are the free-stream magnetic-field components.

Figure A.5 presents portions of the printed output from this sample case. The full printed output is approximately 6,000 lines. Figure A.6 shows the 19 plots which are produced by the program for this case.

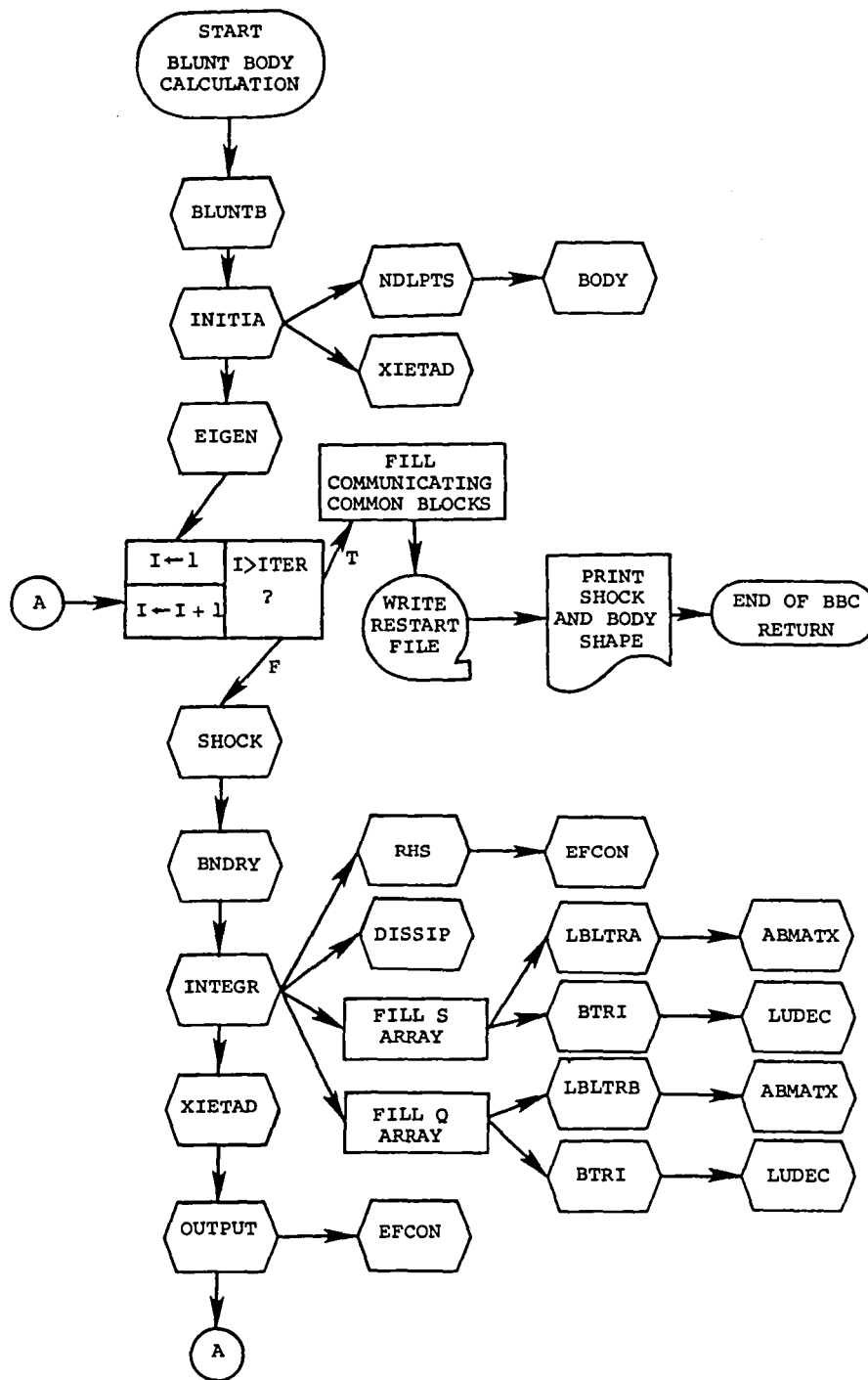


Figure A.1(a).- Flow chart for blunt-body calculation.

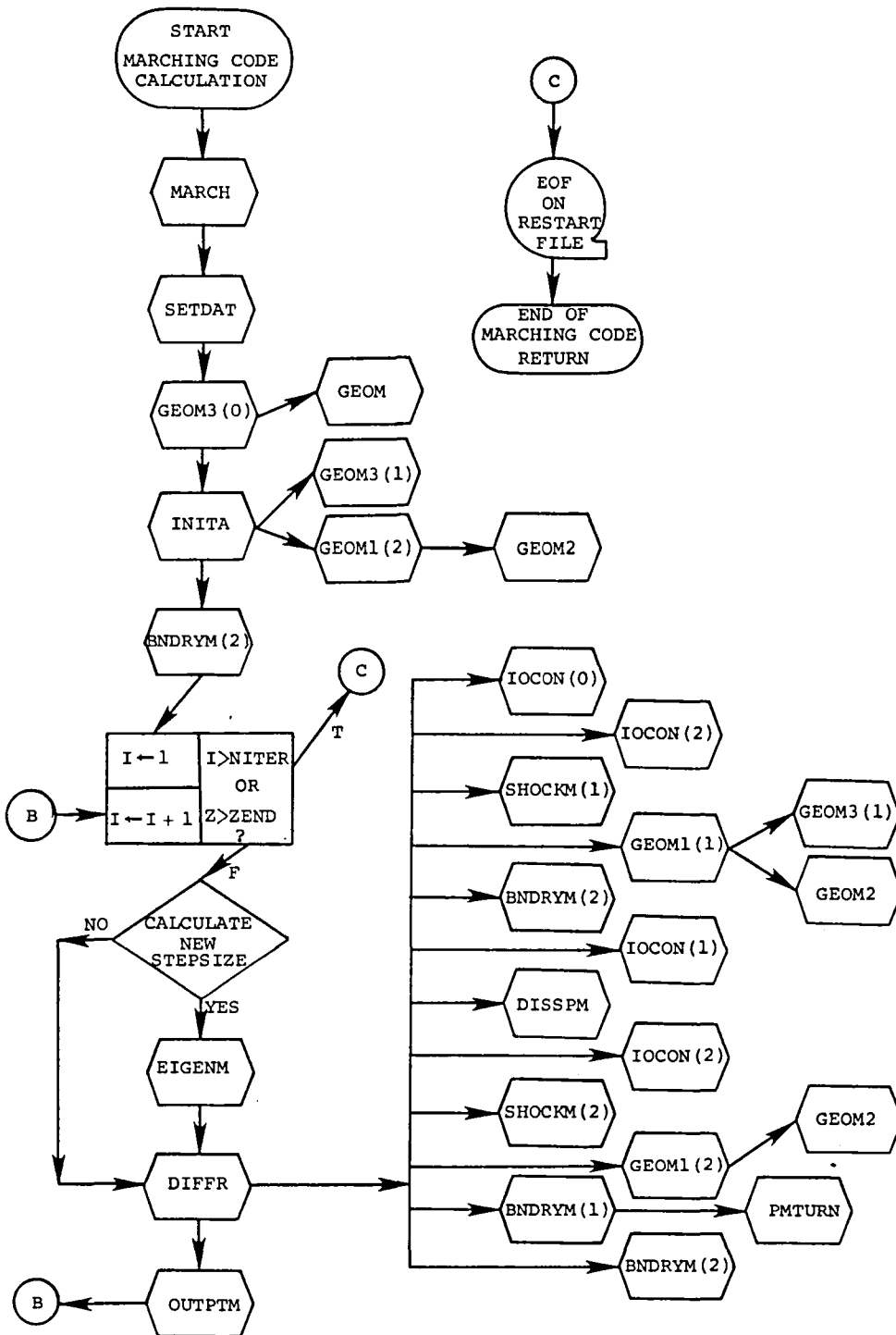


Figure A.1(b).- Flow chart for marching calculation.

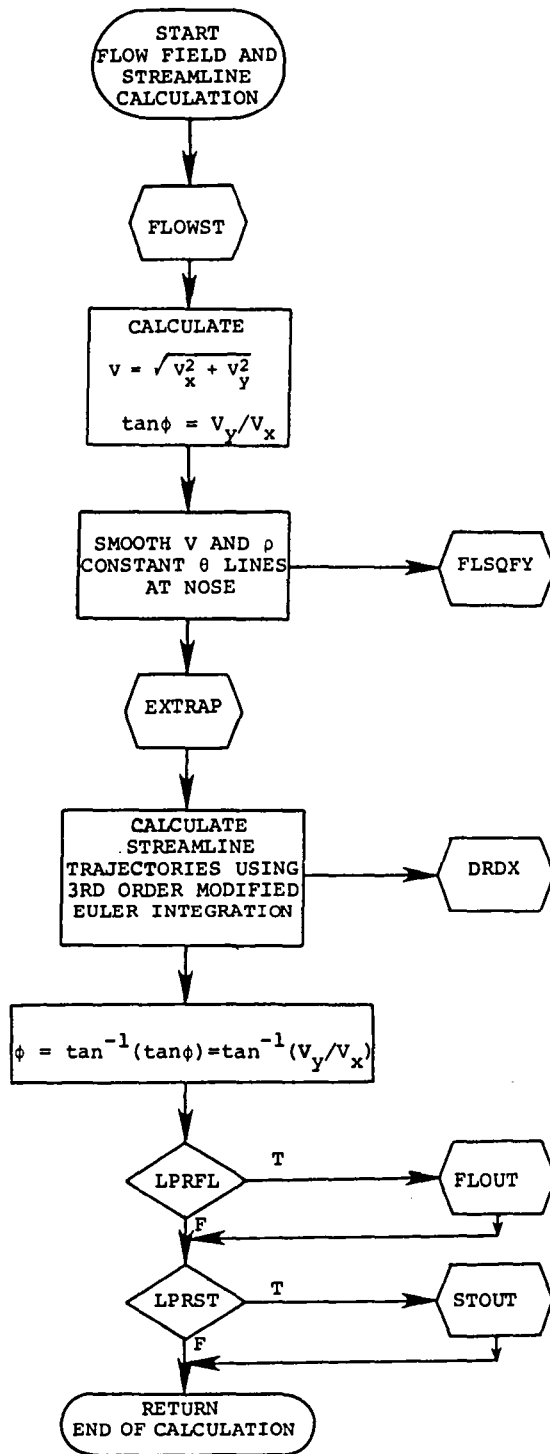


Figure A.1(c).- Flow chart of streamline calculation.

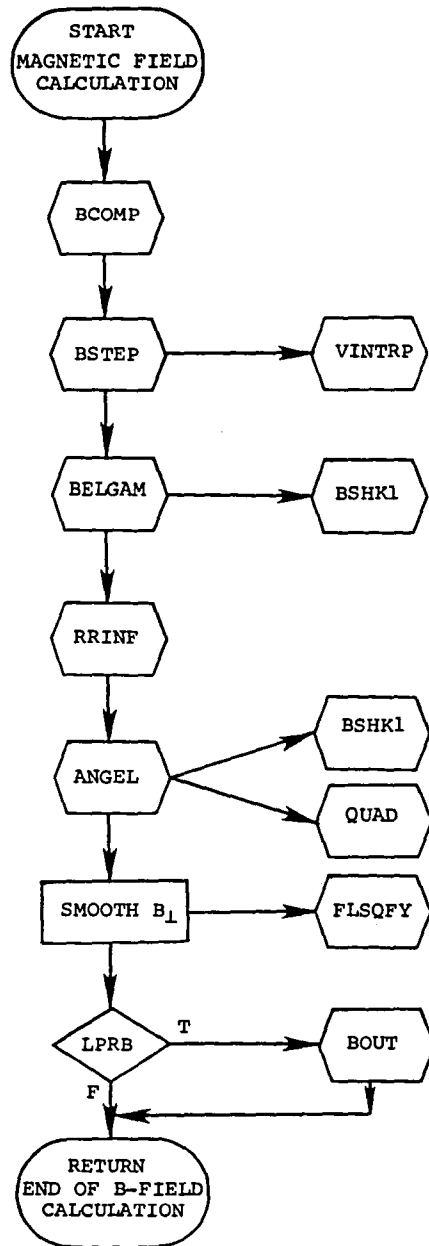


Figure A.1(d).- Flow chart of magnetic-field calculation.

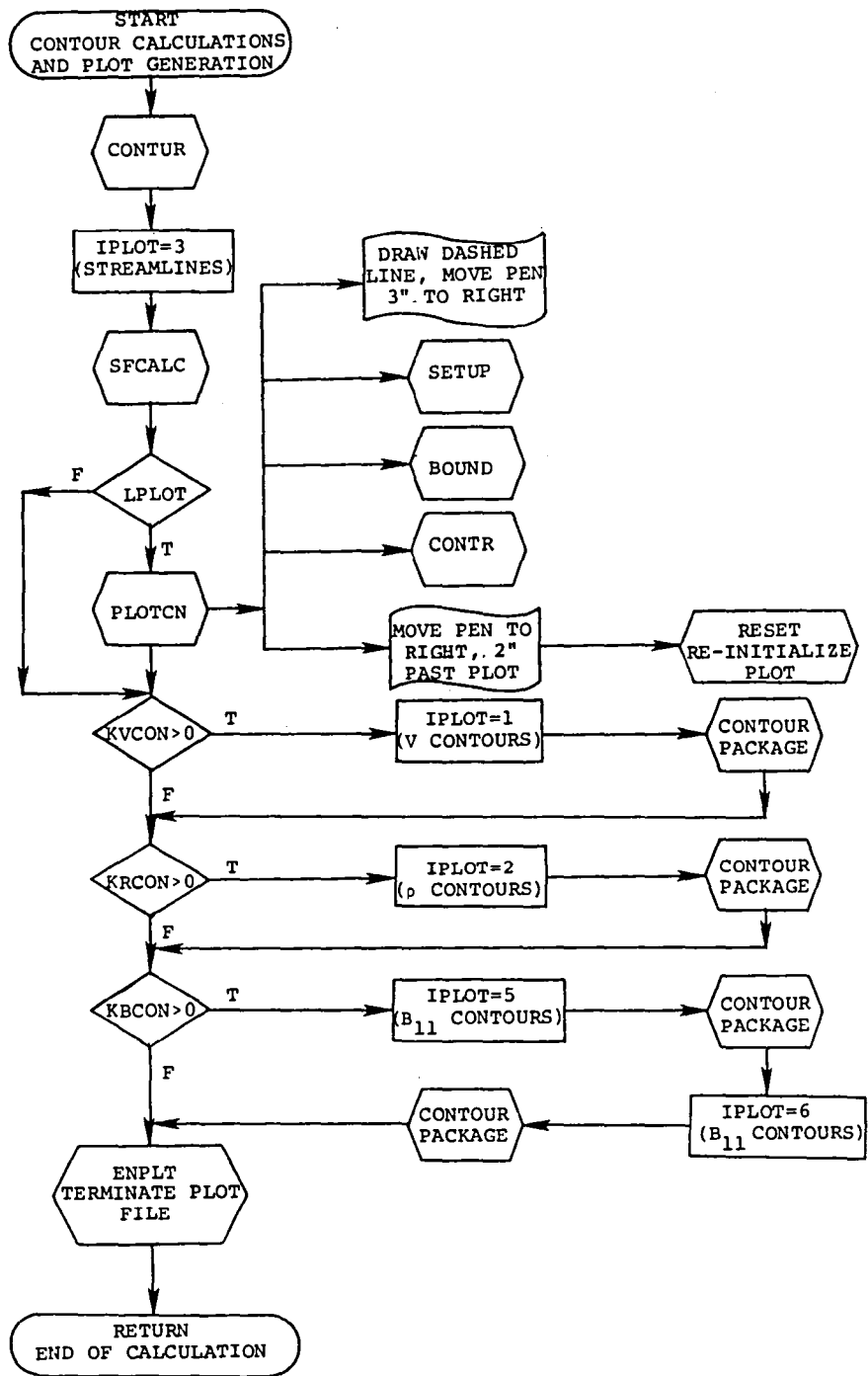


Figure A.1(e).- Flow chart of contour and plot generation calculation.

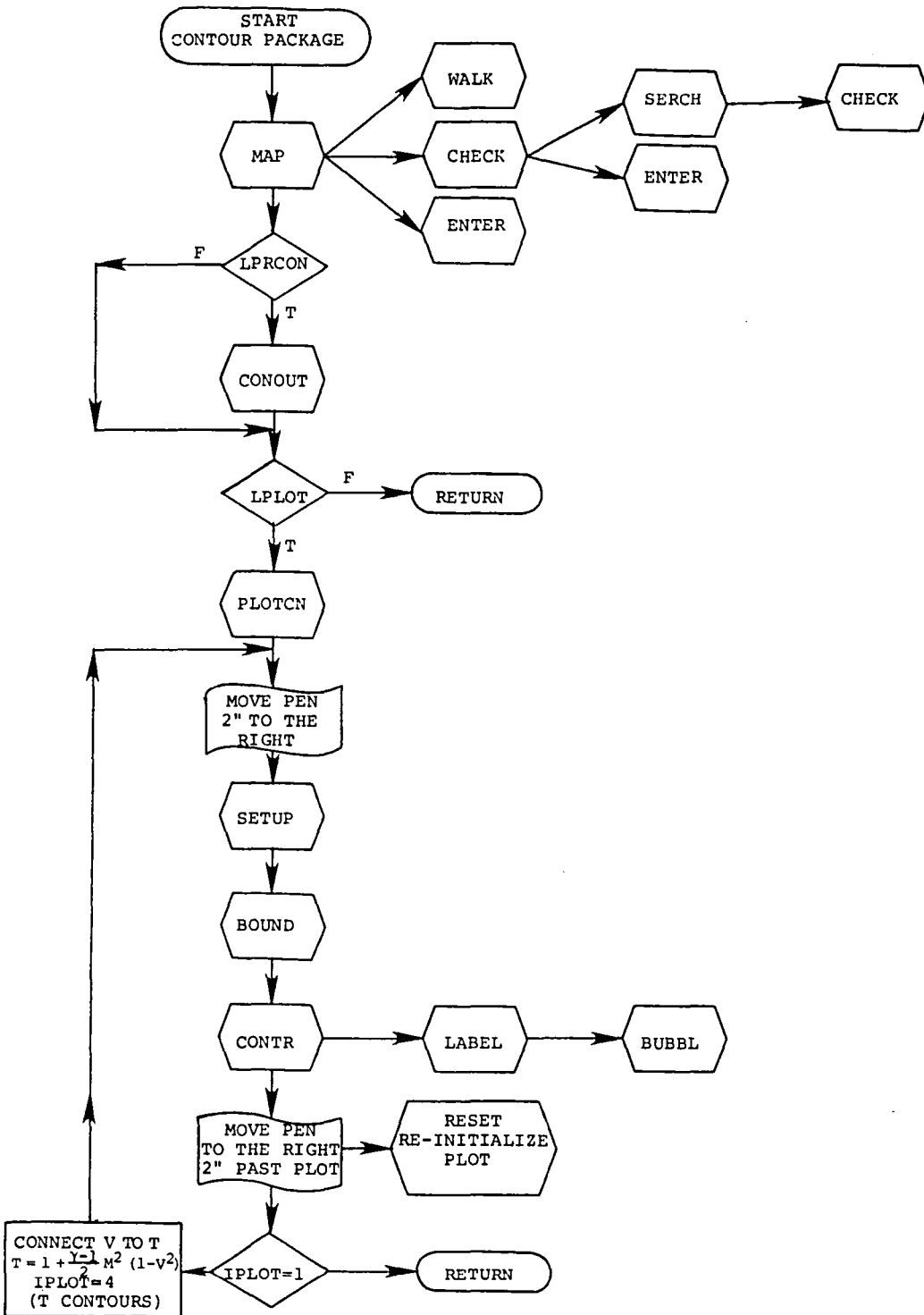


Figure A.1(e).- Concluded

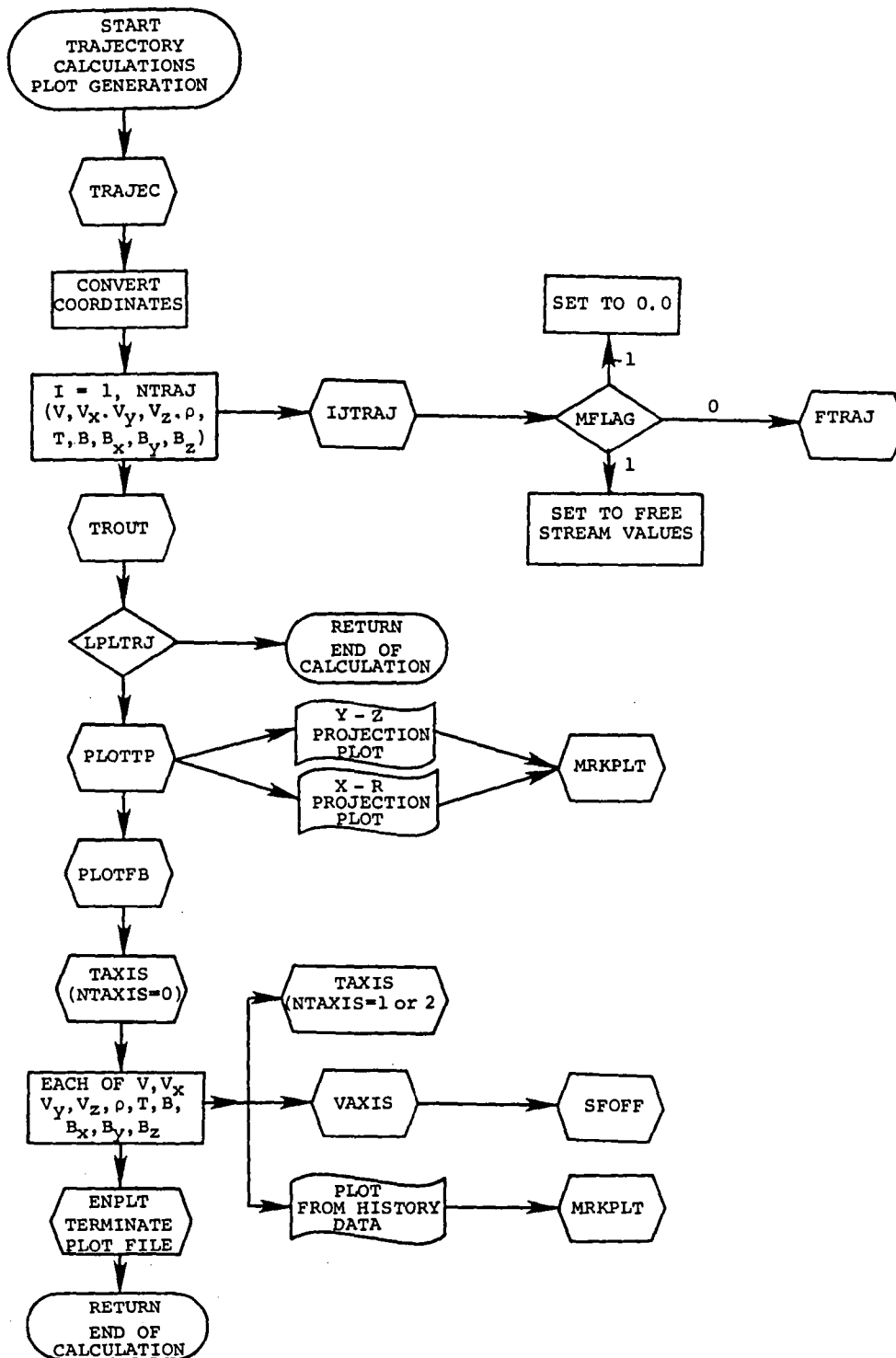


Figure A.1(f).- Flow chart of trajectory calculation.

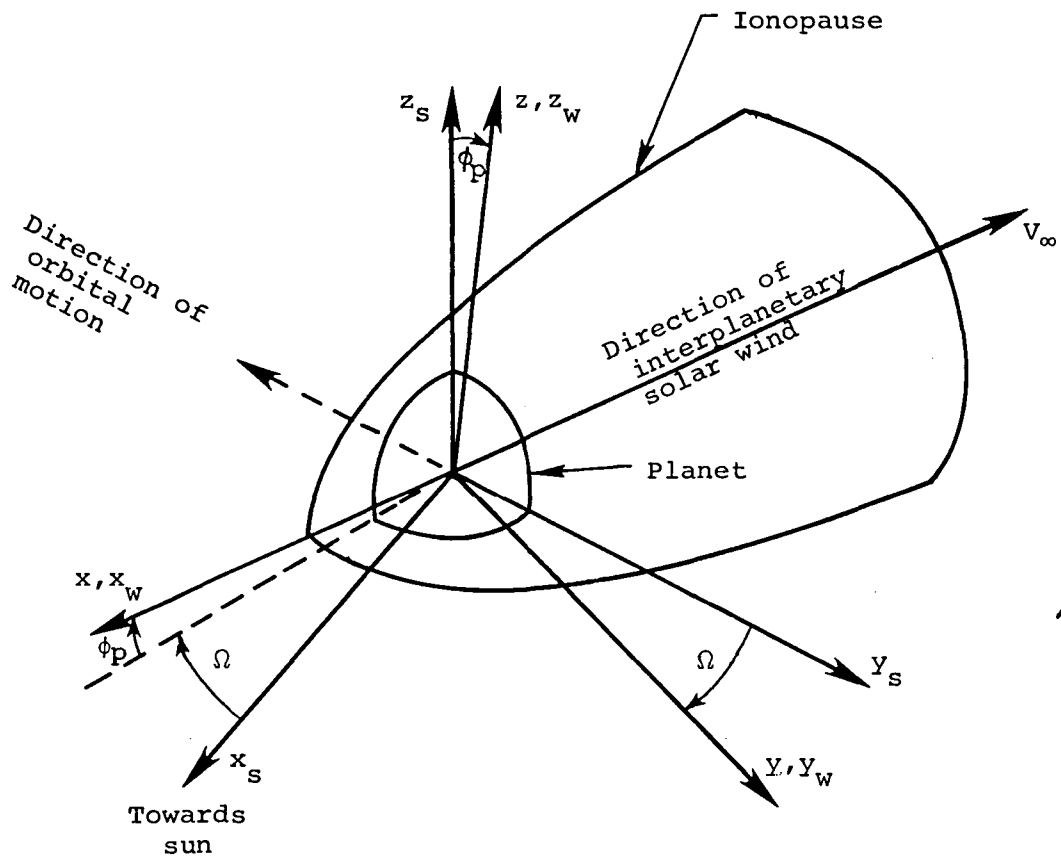


Figure A.2.- Illustration of the azimuthal (Ω) and polar (ϕ_p) solar-wind angles, both shown in a positive sense.

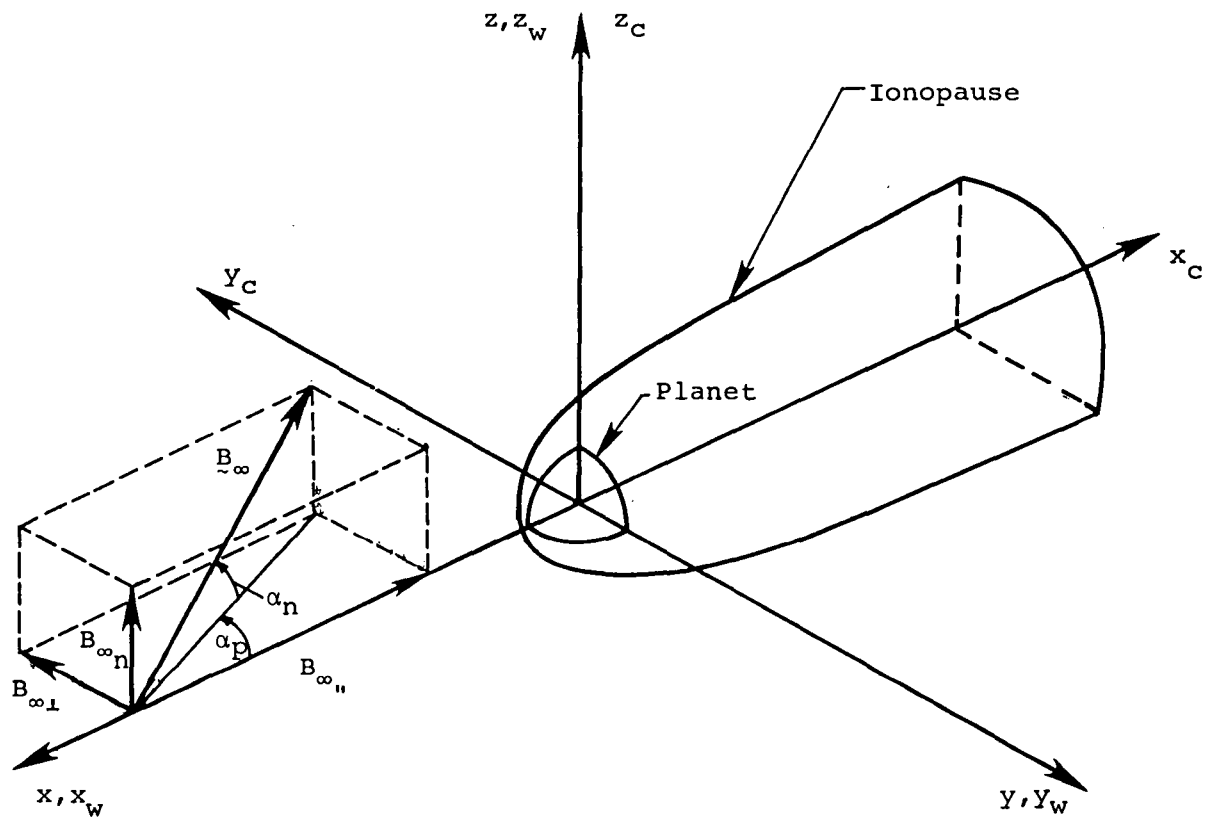


Figure A.3.- Illustration of the interplanetary magnetic field and magnetic-field angles (α_p, α_n) in the solar-wind aligned coordinate systems (x, y, z) , (x_w, y_w, z_w) , and (x_c, y_c, z_c) .

Item No.	Column No.	10	20	30	40	50	60	70	80
0									
1		1							
2		SAMPLE CASE (DEFAULT IONOPAUSE SHAPE WITH H/RO = 0.03)							
3		3.0	1.6666667	0.03	-10.0				
4		F	T	T	T	T	T	F	
5		-5.5							
6		14							
7		0.1	0.2	0.3	0.4	0.5	0.6	0.7	0.75
8		0.8	0.93	0.85	0.9	0.92	0.94		
9		11							
10		0.5	0.8	1.2	1.6	2.0	2.5	3.0	3.5
11		3.8	4.0	4.2					
12		13							
13		0.45	0.6	0.8	1.0	1.25	1.5	2.0	2.5
14		3.0	3.5	4.0	5.0	6.0			
15		37							
16		-90.870	-0.843	3.787	2.027				
17		-85.537	-0.765	3.600	2.045				
18		-80.203	-0.684	3.393	2.062				
19		-74.870	-0.600	3.177	2.073				
20		-70.603	-0.533	2.999	2.078				
21		-64.203	-0.430	2.721	2.079				
22		-57.802	-0.324	2.427	2.067				
23		-51.402	-0.217	2.118	2.043				
24		-40.735	-0.034	1.562	1.961				
25		-39.668	-0.017	1.509	1.951				
26		-38.602	-0.010	1.422	1.932				
27		-35.935	0.049	1.281	1.902				
28		-34.867	0.67	1.232	1.886				
29		-32.735	0.158	1.108	1.852				
30		-24.202	0.2456	0.5826	1.6658				
31		-21.002	0.2954	0.3749	1.5693				
32		-16.735	0.356	0.090	1.409				
33		-14.602	0.382	-0.052	1.315				
34		-11.402	0.415	-0.205	1.150				
35		-8.102	0.437	-0.478	0.945				
36		-4.900	0.442	-0.703	0.660				
37		6.298	0.309	-1.042	-0.266				
38		9.498	0.237	-1.055	-0.546				
39		12.593	0.160	-1.038	-0.801				
40		17.393	0.034	-0.966	-1.162				
41		29.127	-0.275	-0.673	-1.887				
42		34.460	-0.407	-0.512	-2.155				
43		43.860	-0.561	-0.312	-2.444				
44		47.260	-0.705	-0.108	-2.670				
45		53.660	-0.844	0.0982	-2.925				
46		56.862	-0.91	0.201	-3.031				
47		58.993	-0.954	0.269	-3.097				
48		60.060	-0.975	0.303	-3.131				
49		62.193	-1.018	0.371	-3.195				
50		67.528	-1.122	0.541	-3.347				
51		73.928	-1.241	0.739	-3.514				
52		80.328	-1.357	0.839	-3.671				
53		T	0.968	392.0	20.2	102000.	8.8225		
54		4							
55		4	9	11	19				
56		T	3.3	0.15	-1.74	-8.64	0.4		

Figure A.4.- Card input for sample case.

```

*****
PROGRAM SOLAR
**
** DETERMINES
**
** SOLAR WIND FLOW PAST PLANETARY MAGNETOIONOSPHERES
**
** USING
**
** FULLY CONSERVATIVE FINITE DIFFERENCE ALGORITHMS
**
**
** WRITTEN BY
**
** STEPHEN S. STAHARA, BARBARA C. TRUDINGER,
**
** AND DANTEL J. KLENKE
**
**
** NIELSEN ENGINEERING AND RESEARCH, INC.
**
** MOUNTAIN VIEW, CALIFORNIA
**
*****

```

LISTING OF INPUT CARDS FOR THIS RUN

```

1
SAMPLE CASE (DEFAULT TONTPAUSE SHAPE WITH H/R = 0.03)
3.C 1.6666667 0.03 -10.0
F T T T T T T F
-3.5
16
0.1 1.2 3.3 0.14 1.5 1.6 0.7 0.75
0.4 0.85 0.48 2.9 2.92 1.94
11
0.5 1.8 1.2 1.6 2.0 2.5 3.0 3.5
3.8 4.4 4.2
13
3.45 0.6 0.8 1.2 1.25 1.5 2.0 2.5
3.0 3.5 4.0 2.0
37
-90.470 -1.843 3.787 2.027
-89.337 -3.765 3.600 2.145
-80.203 -0.694 3.393 2.062
-74.470 -0.600 3.177 2.073
-70.523 -2.533 2.999 2.078
-64.203 -0.430 2.721 2.079
-57.432 -2.324 2.427 2.067
-51.452 -0.217 2.118 2.043
-47.735 -0.034 1.592 1.961
-39.668 -0.017 1.509 1.951
-38.602 -3.411 1.422 1.932
-35.935 0.649 1.291 1.902
-34.467 0.067 1.232 1.886
-32.775 0.158 1.108 1.852
-24.202 0.2456 0.5826 1.5658
-21.302 7.2054 0.3749 1.5693
-16.735 1.356 0.199 1.449
-14.632 0.382 -0.522 1.315
-11.402 0.415 -0.205 1.150
-3.102 1.437 -1.478 0.945
-4.900 0.442 -0.703 0.660
6.208 1.309 -1.047 -0.266
9.498 1.237 -1.655 -2.545
12.593 0.164 -1.134 -3.811
17.393 7.034 -0.966 -1.162
29.127 -0.275 -0.673 -1.687
34.453 -3.417 -0.512 -2.155
42.857 -1.561 -3.312 -2.444
47.260 -3.705 -0.164 -2.674
53.653 -0.844 0.182 -2.925
56.367 -0.91 0.201 -3.031
58.993 -0.454 0.259 -3.067
60.060 -1.975 0.203 -3.131
67.191 -1.018 0.371 -3.195
67.928 -1.122 0.541 -3.347
73.428 -1.241 0.739 -3.514
83.324 -1.317 0.939 -3.671
T 0.968 392.0 20.2 1023.0 8.0225
4
T 4 9 11 13
3.3 0.15 -1.74 -8.64 0.4

```

Figure A.5.- Abbreviated print output for sample case.

SAMPLE CASE: DEFAULT TORUSHAUSE SHAPE WITH $H/R = 0.021$

INPUT VARIABLES

INTERPLANETARY MACH NO. = 3.00

SPECIFIC HEAT RATIO = 1.667

GEOMETRY: DEFAULT TORUSHAUSE SHAPE
FOR CONSTANT SCALE HEIGHT WITH $H/R = 0.021$

PARAMETERS FOR BLUNT BODY CALCULATION

NO. OF RADIAL MESH POINTS = 16
NO. OF ANGULAR MESH POINTS = 24
NO. OF ADDITIONAL POINTS IN
BLUNT BODY MESH = 1
COMPACT NUMBER = 3.60
NO. OF ITERATIONS = 300

TERMINAL DOWNSTREAM LOCATION FOR MARCHING CALCULATION, $X/R = 1.000$

TERMINAL DOWNSTREAM LOCATION FOR PLOTTING, $X/R = 5.51$

LRFRN = F

LRFL = T

LRST = T

LRFRN = T

LRP = T

LRLOT = T

LRAS = T

LRSTRT = F

LRLTRJ = T

Figure A.5.- Continued.

INPUT FOR TRAJ-CORR CALCULATION

Q PLANET = 1.0331
 INTERPLANETARY VELOCITY = 3.921E+2
 INTERPLANETARY DENSITY = 2.62E+1
 INTERPLANETARY TEMPERATURE = 1.022E+5
 INTERPLANETARY MAGNETIC FIELD
 MAGNITUDE = 4.42E+1
 X-COMPONENT = -1.74E+1
 Y-COMPONENT = -6.44E+1
 Z-COMPONENT = 4.42E+1
 AZIMUTHAL ANGLE = .33E+1
 POLAR ANGLE = .15E+02

NTRAJ = 37 NMARKT = 4
 (* = POINT TO BE MARKED FOR CROSS REFERENCE)

N	TRAJ	YTRAJ	ZTRAJ	ZTRAJ
(SUN-PLANET COORDINATE SYSTEM)				
1	-32.9711	-0.5431	7.7872	2.0276
2	-35.5371	-0.7050	9.6063	2.0453
3	-37.2131	-0.8461	11.3432	2.0520
4 *	-38.8761	-0.9532	12.9771	2.0571
5	-39.9430	-1.0330	14.5391	2.0614
6	-40.6131	-1.0830	16.0270	2.0650
7	-40.8820	-1.1246	17.4270	2.0676
8	-40.7412	-1.1477	18.7281	2.0693
9 *	-40.2751	-1.1541	19.9221	2.0701
10	-39.6651	-1.1471	21.0091	2.0693
11 *	-38.9612	-1.1271	21.9221	2.0676
12	-38.1251	-1.0940	22.6711	2.0650
13	-37.0571	-1.0471	23.2720	2.0614
14	-35.7211	-0.9871	23.7281	2.0571
15	-34.2121	-0.9130	24.0261	2.0520
16	-32.5221	-0.8254	24.1711	2.0453
17	-30.7350	-0.7251	24.1671	2.0376
18	-28.8512	-0.6121	24.0221	2.0281
19 *	-26.8421	-0.4851	23.7411	2.0164
20	-24.7121	-0.3471	23.3271	2.0020
21	-22.4511	-0.2021	22.7821	1.9850
22	-20.0691	-0.0501	22.1171	1.9650
23	-17.5681	0.1071	21.3471	1.9414
24	-15.0591	0.2511	20.4821	1.9143
25	-12.5431	0.3811	19.5321	1.8826
26	-10.0221	0.4971	18.5071	1.8463
27	-7.4961	0.5991	17.4171	1.8053
28	-4.9651	0.6871	16.2621	1.7600
29	-2.4291	0.7611	15.0421	1.7114
30	0.1011	0.8211	13.7671	1.6600
31	2.6261	0.8671	12.4471	1.6063
32	5.1461	0.8991	11.0821	1.5500
33	7.6611	0.9171	9.6721	1.4914
34	10.1711	0.9211	8.2271	1.4300
35	12.6761	0.9111	6.7571	1.3663
36	15.1761	0.8871	5.2621	1.3000
37	17.6711	0.8501	3.7421	1.2314

VALUES SPECIFIED FOR CONTOUR CALCULATION

14 CONTOUR LEVELS FOR VELOCITY

0.100	0.200	0.300	0.400	0.500	0.600
0.700	0.750	0.800	0.850	0.900	0.950
0.950	0.940				

15 CONTOUR LEVELS FOR DENSITY

0.500	0.600	1.000	1.000	2.000	2.500
3.000	3.500	3.800	4.000	4.200	

16 CONTOUR LEVELS FOR MAGNETIC FIELD STRENGTH

0.450	0.600	0.800	1.000	1.200	1.500
2.000	2.500	3.000	3.500	4.000	5.000
5.000					

Figure A.5.- Continued.

PLUNT BODY CALCULATION

```

ITERATION 1 RMS OF SHOCK SPEED= 1.5177E-2 MAXIMUM SHOCK SPEED= 5.0866E-2 AT J=25
ITERATION 2 RMS OF SHOCK SPEED= 7.5422E-3 MAXIMUM SHOCK SPEED= 1.6263E-2 AT J=23
ITERATION 3 RMS OF SHOCK SPEED= 1.0212E-2 MAXIMUM SHOCK SPEED= 3.6756E-2 AT J=23
ITERATION 4 RMS OF SHOCK SPEED= 1.5333E-2 MAXIMUM SHOCK SPEED= 6.1555E-2 AT J=23
ITERATION 5 RMS OF SHOCK SPEED= 2.1498E-2 MAXIMUM SHOCK SPEED= 9.2467E-2 AT J=23

ITERATION 296 RMS OF SHOCK SPEED= 1.3663E-4 MAXIMUM SHOCK SPEED= 1.2972E-3 AT J=16
ITERATION 297 RMS OF SHOCK SPEED= 1.3117E-4 MAXIMUM SHOCK SPEED= 1.2751E-3 AT J=16
ITERATION 298 RMS OF SHOCK SPEED= 1.2371E-4 MAXIMUM SHOCK SPEED= 1.2411E-3 AT J=13
ITERATION 299 RMS OF SHOCK SPEED= 1.1795E-4 MAXIMUM SHOCK SPEED= 1.2053E-3 AT J=13
ITERATION 300 RMS OF SHOCK SPEED= 1.1147E-4 MAXIMUM SHOCK SPEED= 1.2772E-3 AT J=13

```

FINAL SONIC LINE LOCATION

```

XSL= .5672 RSL= .7745
XSL= .6734 RSL= .8631
XSL= .5437 RSL= .8295
XSL= .5941 RSL= .8323
XSL= .7267 RSL= .8777
XSL= .7211 RSL= .8998
XSL= .7478 RSL= .9230
XSL= .7551 RSL= .9384
XSL= .7743 RSL= .9560
XSL= .7940 RSL= .9697
XSL= .8180 RSL= .9829
XSL= .8401 RSL= .9953
XSL= .86 RSL= 1.0075
XSL= .8892 RSL= 1.0167
XSL= .9153 RSL= 1.0217
XSL= .943 RSL= 1.0232
XSL= .9719 RSL= 1.0239
XSL= 1.0000 RSL= 1.0234
XSL= 1.0281 RSL= .9998

```

**** X BODY IN HT = .4569E+01 RMS JS F 1000 IN HT = .7480E-1 ****

BODY AND FINAL SHOCK SHAPS

J	X(BODY)	Y(BODY)	X(SHOCK)	Y(SHOCK)
2	.9994	.7349	1.3143	.6455
3	.9944	.7146	1.3111	.6306
4	.9856	.6939	1.2904	.6225
5	.9720	.6729	1.2786	.6186
6	.9536	.6509	1.2589	.6190
7	.9314	.6281	1.2376	.6199
8	.9039	.6039	1.2140	.6199
9	.8726	.5789	1.1790	.6157
10	.8372	.5547	1.1419	.6132
11	.7979	.5324	1.1022	.6111
12	.7547	.5129	1.0586	.6112
13	.7077	.4960	1.0107	.6123
14	.6574	.4814	.9596	1.0129
15	.6036	.4688	.9050	1.0126
16	.5468	.4579	.8481	1.0119
17	.4869	.4489	.7895	1.0112
18	.4244	.4417	.7299	1.0114
19	.3592	.4368	.6676	1.0128
20	.2916	.4340	.6017	1.0143
21	.2219	.4334	.5337	1.0139
22	.1509	.4343	.4639	1.0134
23	.0789	.4367	.3937	1.0155
24	-.0000	.4407	.3237	1.0189

Figure A.5.- Continued.

MARKING CALCULATION

STEP NO.	DOWNSTREAM LOCATION	BODY ORIGINATE	SMOCK TERMINATE
1	-0.468	1.140	2.2210
2	-0.495	1.1167	2.2655
3	-0.443	1.1225	2.2700
4	-0.487	1.1273	2.2837
5	-0.245	1.119	2.2825
6	-0.290	1.1354	2.4267
7	-0.153	1.1280	2.4701
8	-0.477	1.1400	2.5131
9	-0.454	1.1444	2.5555
10	-0.329	1.1425	2.6173
11	-0.316	1.1432	2.6583
12	-0.573	1.1436	2.7187
13	-0.780	1.1439	2.7593
14	-0.577	1.1440	2.8073
15	-0.392	1.1441	2.8574
16	-0.375	1.1441	2.9075
17	-1.055	1.1441	2.9851
18	-2.1494	1.1441	3.0422
19	-1.7449	1.1441	3.0907
20	-1.3414	1.1441	3.1392
21	-0.9480	1.1441	3.1877
22	-0.5519	1.1441	3.2353
23	-0.1571	1.1441	3.2823
24	-1.7826	1.1441	3.3291
25	-1.3927	1.1441	3.3779
26	-2.0213	1.1441	3.4267
27	-2.1306	1.1441	3.4745
28	-2.2790	1.1441	3.5215
29	-2.4473	1.1441	3.5676
30	-2.5963	1.1441	3.6140
31	-2.7234	1.1441	3.6593
32	-2.8475	1.1441	3.7046
33	-3.0375	1.1441	3.7497
34	-3.1965	1.1441	3.7944
35	-3.3837	1.1441	3.8376
36	-3.5775	1.1441	3.8817
37	-3.7610	1.1441	3.9257
38	-3.9511	1.1441	3.9697
39	-4.1471	1.1441	4.0143
40	-4.3690	1.1441	4.0582
41	-4.5077	1.1441	4.1024
42	-4.8175	1.1441	4.1465
43	-5.0433	1.1441	4.1917
44	-5.2801	1.1441	4.2369
45	-5.5367	1.1441	4.2821
46	-5.8043	1.1441	4.3273
47	-6.0719	1.1441	4.3725
48	-6.3395	1.1441	4.4177
49	-6.6072	1.1441	4.4629
50	-6.8222	1.1441	4.5076
51	-7.2372	1.1441	4.5522
52	-7.5579	1.1441	4.5977
53	-7.8873	1.1441	4.6422
54	-8.1824	1.1441	4.6877
55	-8.3917	1.1441	4.7322
56	-8.9198	1.1441	4.7777
57	-9.2485	1.1441	4.8222
58	-9.6571	1.1441	4.8677
59	-10.0258	1.1441	4.9122

DETAILED FLOW FIELD OUTPUT

FLOW FIELD VALUES EXTRAPOLATED TO SYMMETRY AXIS, THETA = 180 DEGREE

R	U/F	V/WINF	W/WINF	T/TINF	P/PINF
1	1.0000	0.0000	3.4663	4.0103	13.6710
2	1.0169	0.2740	3.4084	3.9983	13.6278
3	1.0338	0.447	3.4226	3.9946	13.5900
4	1.0507	0.651	3.4341	3.9873	13.5531
5	1.0676	0.753	3.4329	3.9787	13.4578
6	1.0845	0.93	3.4592	3.9567	13.3549
7	1.1014	0.751	3.4931	3.9551	13.2554
8	1.1183	0.444	3.4947	3.9375	13.1303
9	1.1352	0.134	3.444	3.9199	12.9905
10	1.1521	0.121	3.2911	3.9015	12.8178
11	1.1690	0.214	3.2662	3.8765	12.6711
12	1.1859	0.184	3.2393	3.8570	12.4937
13	1.2028	0.238	3.2144	3.8332	12.3361
14	1.2197	0.298	3.1798	3.8162	12.1794
15	1.2366	0.264	3.1475	3.7923	11.9047
16	1.2535	0.284	3.1159	3.7556	11.6932
17	1.2704	0.309	3.0740	3.7244	11.4760
18	1.2873	0.259	3.0410	3.7008	11.2543
19	1.3042	0.313	3.0100	3.6667	11.0300

Figure A.5.- Continued.

FELW FIELD VALUES FROM BLUNT BODY CALCULATION

ANGULAR LOCATION NO. 2, AT THETA = 24.000 DEGREE

I	R/R0	R/R0	Y/R0	VR/VINF	VX/VINF	FELW ANGLE	V/VINF	RW/RW0INF	Y/TINF	P/PINF
1	1.0178	0.340	0.9964	0.150	0.375	44.1063	0.425	3.4261	3.9794	13.6624
2	1.0178	0.355	0.9964	0.231	0.233	44.3068	0.347	3.4119	3.9794	13.6340
3	1.0178	0.411	0.9964	0.247	0.144	48.3113	0.543	3.4144	3.9794	13.5877
4	1.0178	0.367	0.9964	0.356	0.099	48.9320	0.725	3.3940	3.9794	13.5243
5	1.0178	0.379	1.0072	0.221	0.040	43.7745	0.929	3.3433	3.9741	13.4445
6	1.0178	0.370	1.0091	0.213	0.117	41.9714	1.111	3.3589	3.9625	13.3492
7	1.0178	0.364	1.0111	0.217	0.292	39.979	1.314	3.3529	3.9499	13.2390
8	1.0178	0.396	1.0180	0.240	0.470	37.717	1.497	3.3337	3.9357	13.1147
9	1.0178	0.396	1.0240	0.290	0.651	35.7113	1.666	3.3132	3.9167	12.9769
10	1.0178	0.422	1.0318	0.351	0.829	33.7443	1.843	3.2904	3.8961	12.8264
11	1.0178	0.449	1.0409	0.417	0.991	31.8144	2.017	3.2657	3.8779	12.6639
12	1.0178	0.414	1.0457	0.483	1.142	29.9099	2.183	3.2400	3.8562	12.4899
13	1.0234	0.426	1.0526	0.551	1.240	28.1308	2.350	3.2102	3.8331	12.3052
14	1.0234	0.476	1.0596	0.616	1.255	26.4837	2.525	3.1797	3.8087	12.1111
15	1.0234	0.482	1.0665	0.672	1.240	24.9647	2.699	3.1473	3.7829	11.9039
16	1.0234	0.438	1.0734	0.729	1.246	23.4795	2.853	3.1133	3.7557	11.6926
17	1.0272	0.444	1.0774	0.785	1.215	22.0274	3.015	3.0775	3.7274	11.4769
18	1.0299	0.453	1.0823	0.839	1.155	20.6094	3.174	3.0401	3.6977	11.2414
19	1.0321	0.455	1.0873	0.891	1.077	19.2234	3.332	3.0011	3.6669	11.0046

ANGULAR LOCATION NO. 3, AT THETA = 30.000 DEGREE

I	R/R0	R/R0	Y/R0	VR/VINF	VX/VINF	FELW ANGLE	V/VINF	RW/RW0INF	Y/TINF	P/PINF
1	1.0143	0.176	0.9948	0.174	0.307	46.3214	0.354	3.425	4.0914	13.5910
2	1.0144	0.191	0.9949	0.254	0.174	46.4426	0.289	3.3973	4.0914	13.5411
3	1.0144	0.201	0.9949	0.271	0.117	46.5272	0.289	3.3903	4.0782	13.4873
4	1.0143	0.199	1.0087	0.269	0.197	43.4778	0.514	3.3979	3.9693	13.4200
5	1.0185	0.1117	1.0227	0.259	0.345	39.4732	0.769	3.3694	3.9596	13.3393
6	1.0185	0.1135	1.0295	0.317	0.442	36.4369	0.927	3.3557	3.9471	13.2434
7	1.0126	0.1154	1.0366	0.370	0.536	34.4626	1.085	3.3399	3.9338	13.1385
8	1.0147	0.1170	1.0435	0.422	0.610	32.5272	1.243	3.3221	3.9196	13.0190
9	1.0167	0.1186	1.0505	0.470	0.680	30.6332	1.401	3.3022	3.9026	12.8871
10	1.0189	0.1202	1.0575	0.517	0.745	28.7878	1.560	3.2802	3.8840	12.7429
11	1.0178	0.1224	1.0644	0.564	0.804	26.9814	1.717	3.2563	3.8653	12.5868
12	1.0178	0.1242	1.0714	0.609	0.857	25.2175	1.874	3.2305	3.8443	12.4190
13	1.0211	0.1251	1.0784	0.650	0.904	23.4926	2.031	3.2027	3.8217	12.2397
14	1.0229	0.1277	1.0853	0.690	0.949	21.7267	2.188	3.1729	3.7975	12.0493
15	1.0234	0.1295	1.0923	0.723	0.979	20.0060	2.345	3.1414	3.7716	11.8479
16	1.0251	0.1313	1.0993	0.753	0.977	18.3299	2.491	3.1079	3.7440	11.6359
17	1.0273	0.1331	1.1063	0.779	0.941	16.6977	2.636	3.0726	3.7146	11.4136
18	1.0292	0.1349	1.1132	0.804	0.879	15.1094	2.780	3.0356	3.6834	11.1813
19	1.0313	0.1366	1.1201	0.829	0.804	13.5642	2.924	3.0004	3.6503	10.9392

ANGULAR LOCATION NO. 23, AT THETA = 66.000 DEGREE

I	R/R0	R/R0	Y/R0	VR/VINF	VX/VINF	FELW ANGLE	V/VINF	RW/RW0INF	Y/TINF	P/PINF
1	1.0184	0.2427	0.9959	0.199	0.5433	42.2794	0.454	0.9997	1.7562	1.7391
2	1.01424	0.1946	0.9957	0.222	0.412	41.1913	0.481	1.3972	1.8422	2.0213
3	1.0144	0.1935	0.9957	0.239	0.289	41.2987	0.381	1.9989	1.9130	2.2941
4	1.0254	0.2473	0.9957	0.242	0.160	47.651	0.225	1.9950	1.9704	2.5939
5	1.0144	0.1912	0.911	0.340	0.771	37.2554	0.512	1.3876	2.0161	2.7974
6	1.0254	0.2552	0.744	0.240	0.705	39.3890	0.407	1.4745	2.0513	3.0247
7	1.0124	0.1916	0.785	0.282	0.579	41.8133	0.305	1.5570	2.0776	3.2340
8	1.0164	0.2429	0.724	0.266	0.532	41.1555	0.287	1.6353	2.0960	3.4276
9	1.0205	0.2168	0.610	0.246	0.467	39.4333	0.242	1.7197	2.1079	3.6038
10	1.0274	0.2706	0.499	0.264	0.426	36.851	0.224	1.7994	2.1143	3.7642
11	1.0289	0.2444	0.413	0.284	0.354	34.4993	0.202	1.8777	2.1162	3.9193
12	1.0282	0.2784	0.317	0.314	0.272	32.2854	0.187	1.9520	2.1149	4.0800
13	1.0385	0.2723	0.211	0.317	0.245	30.1360	0.185	2.0234	2.1142	4.2463
14	1.0395	0.2762	0.244	0.277	0.240	28.0493	0.185	2.0923	2.1063	4.4206
15	1.0445	0.2401	0.237	0.271	0.241	26.0013	0.186	2.1589	2.1012	4.6092
16	1.0446	0.2439	0.232	0.273	0.244	24.0052	0.186	2.2234	2.0970	4.8048
17	1.0426	0.2479	0.262	0.273	0.245	22.0485	0.186	2.2856	2.0946	5.0007
18	1.0496	0.20917	0.240	0.277	0.246	20.14719	0.186	2.3457	2.0935	5.2000
19	1.0516	0.2156	0.247	0.280	0.249	18.2877	0.187	2.4048	2.0924	5.4000

ANGULAR LOCATION NO. 24, AT THETA = 90.000 DEGREE

I	R/R0	R/R0	Y/R0	VR/VINF	VX/VINF	FELW ANGLE	V/VINF	RW/RW0INF	Y/TINF	P/PINF
1	1.0137	0.117	0.9999	0.1533	0.4722	11.6663	0.660	0.9977	1.6566	1.6818
2	1.0136	0.1216	0.9999	0.1933	0.347	12.9930	0.672	1.3083	1.6737	1.7576
3	1.0216	0.1216	0.9999	0.197	0.247	14.2891	0.554	1.1127	1.8265	2.0257
4	1.0216	0.1915	0.9999	0.224	0.160	16.5517	0.443	1.1127	1.8265	2.0257
5	1.0415	0.1915	0.9999	0.235	0.063	16.1522	0.312	1.3169	1.9523	2.5257
6	1.0415	0.1216	0.9999	0.237	0.267	16.9815	0.224	1.3968	1.9711	2.7533
7	1.0614	0.1216	0.9999	0.235	0.779	17.3213	0.169	1.4922	2.0001	2.9647
8	1.0214	0.1216	0.9999	0.285	0.772	17.7921	0.122	1.5334	2.0268	3.1395
9	1.0113	0.1216	0.9999	0.282	0.773	18.1583	0.094	1.6407	2.0345	3.3390
10	1.0113	0.2763	0.9999	0.283	0.754	18.4659	0.078	1.7425	2.0423	3.5611
11	1.0112	0.2712	0.9999	0.287	0.754	18.7265	0.071	1.8403	2.0492	3.7908
12	1.0112	0.2712	0.9999	0.283	0.741	18.9491	0.072	1.9341	2.0552	4.0261
13	1.0211	0.2711	0.9999	0.269	0.732	19.1395	0.078	2.0234	2.0620	4.2617
14	1.0211	0.2711	0.9999	0.267	0.729	19.3041	0.086	2.1073	2.0687	4.5000
15	1.0411	0.2711	0.9999	0.251	0.721	19.4481	0.094	2.1857	2.0747	4.7406
16	1.0410	0.2710	0.9999	0.277	0.719	19.5944	0.103	2.2586	2.0817	4.9829
17	1.0610	0.2761	0.9999	0.271	0.719	19.6440	0.102	2.3260	2.0890	5.2269
18	1.0809	0.2769	0.9999	0.271	0.712	19.7114	0.097	2.3891	2.0964	5.4716
19	1.0809	0.2809	0.9999	0.249	0.712	19.8400	0.082	2.4503	2.1041	5.7199

Figure A.5.- Continued.

FLOW FIELD VALUES FROM HARPONS CALCULATION

ADDITIONAL AXIAL LOCATION NO. 16 AT X/R = -0.465

T	R/R	V/VINF	W/WINF	FLOW ANGLE	V/VINF	W/WINF	T/TINF	P/PINF
1	1.0100	.9421	.8401	0. 51	.9. 4	.9458	1.0674	1.3151
2	1.0175	.9422	.8409	1.0. 141	.4776	.9422	1.0344	1.6177
3	1.0233	.9423	.8407	1.0. 272	.4519	1.0. 272	1.0772	1.8902
4	1.0291	.9424	.8403	1.0. 403	.4259	1.0174	1.0988	2.1513
5	1.0347	.9425	.8402	1.0. 534	.4004	1.0254	1.0988	2.3925
6	1.0405	.9426	.8401	1.0. 665	.3747	1.0344	1.0257	2.6136
7	1.0463	.9427	.8400	1.0. 796	.3491	1.0434	1.0394	2.8139
8	1.0521	.9428	.8399	1.0. 927	.3234	1.0524	1.0773	2.9943
9	1.0579	.9429	.8398	1.1. 058	.2977	1.0614	1.0976	3.1571
10	1.0637	.9430	.8397	1.1. 189	.2720	1.0704	1.0976	3.3049
11	1.0695	.9431	.8396	1.1. 320	.2463	1.0794	1.0977	3.4324
12	1.0753	.9432	.8395	1.1. 451	.2206	1.0884	1.0978	3.5402
13	1.0811	.9433	.8394	1.1. 582	.1949	1.0974	1.0979	3.6320
14	1.0869	.9434	.8393	1.1. 713	.1692	1.1064	1.0980	3.7128
15	1.0927	.9435	.8392	1.1. 844	.1435	1.1154	1.0981	3.7856
16	1.0985	.9436	.8391	1.1. 975	.1178	1.1244	1.0982	3.8524
17	1.1043	.9437	.8390	1.2. 106	.0921	1.1334	1.0983	3.9152
18	1.1101	.9438	.8389	1.2. 237	.0664	1.1424	1.0984	3.9750
19	1.1159	.9439	.8388	1.2. 368	.0407	1.1514	1.0985	4.0328

ADDITIONAL AXIAL LOCATION NO. 17 AT X/R = -0.495

T	R/R	V/VINF	W/WINF	FLOW ANGLE	V/VINF	W/WINF	T/TINF	P/PINF
1	1.0100	.9421	.8401	0. 51	.9. 4	.9458	1.0674	1.3151
2	1.0175	.9422	.8409	1.0. 141	.4776	.9422	1.0344	1.6177
3	1.0233	.9423	.8407	1.0. 272	.4519	1.0. 272	1.0772	1.8902
4	1.0291	.9424	.8403	1.0. 403	.4259	1.0174	1.0988	2.1513
5	1.0347	.9425	.8402	1.0. 534	.4004	1.0254	1.0988	2.3925
6	1.0405	.9426	.8401	1.0. 665	.3747	1.0344	1.0257	2.6136
7	1.0463	.9427	.8400	1.0. 796	.3491	1.0434	1.0394	2.8139
8	1.0521	.9428	.8399	1.0. 927	.3234	1.0524	1.0773	2.9943
9	1.0579	.9429	.8398	1.1. 058	.2977	1.0614	1.0976	3.1571
10	1.0637	.9430	.8397	1.1. 189	.2720	1.0704	1.0976	3.3049
11	1.0695	.9431	.8396	1.1. 320	.2463	1.0794	1.0977	3.4324
12	1.0753	.9432	.8395	1.1. 451	.2206	1.0884	1.0978	3.5402
13	1.0811	.9433	.8394	1.1. 582	.1949	1.0974	1.0979	3.6320
14	1.0869	.9434	.8393	1.1. 713	.1692	1.1064	1.0980	3.7128
15	1.0927	.9435	.8392	1.1. 844	.1435	1.1154	1.0981	3.7856
16	1.0985	.9436	.8391	1.1. 975	.1178	1.1244	1.0982	3.8524
17	1.1043	.9437	.8390	1.2. 106	.0921	1.1334	1.0983	3.9152
18	1.1101	.9438	.8389	1.2. 237	.0664	1.1424	1.0984	3.9750
19	1.1159	.9439	.8388	1.2. 368	.0407	1.1514	1.0985	4.0328

ADDITIONAL AXIAL LOCATION NO. 18 AT X/R = -0.525

T	R/R	V/VINF	W/WINF	FLOW ANGLE	V/VINF	W/WINF	T/TINF	P/PINF
1	1.0100	.9421	.8401	0. 51	.9. 4	.9458	1.0674	1.3151
2	1.0175	.9422	.8409	1.0. 141	.4776	.9422	1.0344	1.6177
3	1.0233	.9423	.8407	1.0. 272	.4519	1.0. 272	1.0772	1.8902
4	1.0291	.9424	.8403	1.0. 403	.4259	1.0174	1.0988	2.1513
5	1.0347	.9425	.8402	1.0. 534	.4004	1.0254	1.0988	2.3925
6	1.0405	.9426	.8401	1.0. 665	.3747	1.0344	1.0257	2.6136
7	1.0463	.9427	.8400	1.0. 796	.3491	1.0434	1.0394	2.8139
8	1.0521	.9428	.8399	1.0. 927	.3234	1.0524	1.0773	2.9943
9	1.0579	.9429	.8398	1.1. 058	.2977	1.0614	1.0976	3.1571
10	1.0637	.9430	.8397	1.1. 189	.2720	1.0704	1.0976	3.3049
11	1.0695	.9431	.8396	1.1. 320	.2463	1.0794	1.0977	3.4324
12	1.0753	.9432	.8395	1.1. 451	.2206	1.0884	1.0978	3.5402
13	1.0811	.9433	.8394	1.1. 582	.1949	1.0974	1.0979	3.6320
14	1.0869	.9434	.8393	1.1. 713	.1692	1.1064	1.0980	3.7128
15	1.0927	.9435	.8392	1.1. 844	.1435	1.1154	1.0981	3.7856
16	1.0985	.9436	.8391	1.1. 975	.1178	1.1244	1.0982	3.8524
17	1.1043	.9437	.8390	1.2. 106	.0921	1.1334	1.0983	3.9152
18	1.1101	.9438	.8389	1.2. 237	.0664	1.1424	1.0984	3.9750
19	1.1159	.9439	.8388	1.2. 368	.0407	1.1514	1.0985	4.0328

ADDITIONAL AXIAL LOCATION NO. 19 AT X/R = -0.555

T	R/R	V/VINF	W/WINF	FLOW ANGLE	V/VINF	W/WINF	T/TINF	P/PINF
1	1.0100	.9421	.8401	0. 51	.9. 4	.9458	1.0674	1.3151
2	1.0175	.9422	.8409	1.0. 141	.4776	.9422	1.0344	1.6177
3	1.0233	.9423	.8407	1.0. 272	.4519	1.0. 272	1.0772	1.8902
4	1.0291	.9424	.8403	1.0. 403	.4259	1.0174	1.0988	2.1513
5	1.0347	.9425	.8402	1.0. 534	.4004	1.0254	1.0988	2.3925
6	1.0405	.9426	.8401	1.0. 665	.3747	1.0344	1.0257	2.6136
7	1.0463	.9427	.8400	1.0. 796	.3491	1.0434	1.0394	2.8139
8	1.0521	.9428	.8399	1.0. 927	.3234	1.0524	1.0773	2.9943
9	1.0579	.9429	.8398	1.1. 058	.2977	1.0614	1.0976	3.1571
10	1.0637	.9430	.8397	1.1. 189	.2720	1.0704	1.0976	3.3049
11	1.0695	.9431	.8396	1.1. 320	.2463	1.0794	1.0977	3.4324
12	1.0753	.9432	.8395	1.1. 451	.2206	1.0884	1.0978	3.5402
13	1.0811	.9433	.8394	1.1. 582	.1949	1.0974	1.0979	3.6320
14	1.0869	.9434	.8393	1.1. 713	.1692	1.1064	1.0980	3.7128
15	1.0927	.9435	.8392	1.1. 844	.1435	1.1154	1.0981	3.7856
16	1.0985	.9436	.8391	1.1. 975	.1178	1.1244	1.0982	3.8524
17	1.1043	.9437	.8390	1.2. 106	.0921	1.1334	1.0983	3.9152
18	1.1101	.9438	.8389	1.2. 237	.0664	1.1424	1.0984	3.9750
19	1.1159	.9439	.8388	1.2. 368	.0407	1.1514	1.0985	4.0328

Figure A.5.- Continued.

***** STREAMLINE TRAJECTORY CALCULATION *****

49 STREAMLINES CALCULATED

STREAMLINE NO. STARTING AT Y/D = .031+3i, 0/D = .1422
 (CORRESPONDING TO Y/D = 2.0, 0/D = 0.0250, 0/D = .0315)

Y/D	0/D
1.3143	.455
1.2742	.460
1.2341	.464
1.1940	.467
1.1539	.470
1.1138	.473
1.0737	.476
1.0336	.479
1.0135	.480
1.0134	.481
.9733	.482
.9332	.483
.8931	.484
.8530	.485
.8129	.486
.7728	.487
.7327	.488
.6926	.489
.6525	.490
.6124	.491
.5723	.492
.5322	.493
.4921	.494
.4520	.495
.4119	.496
.3718	.497
.3317	.498
.2916	.499
.2515	.500
.2114	.501
.1713	.502
.1312	.503
.0911	.504
.0510	.505
.0109	.506
.0008	.507
.0007	.508
.0006	.509
.0005	.510
.0004	.511
.0003	.512
.0002	.513
.0001	.514
.0000	.515
.0000	.516
.0000	.517
.0000	.518
.0000	.519
.0000	.520
.0000	.521
.0000	.522
.0000	.523
.0000	.524
.0000	.525
.0000	.526
.0000	.527
.0000	.528
.0000	.529
.0000	.530
.0000	.531
.0000	.532
.0000	.533
.0000	.534
.0000	.535
.0000	.536
.0000	.537
.0000	.538
.0000	.539
.0000	.540
.0000	.541
.0000	.542
.0000	.543
.0000	.544
.0000	.545
.0000	.546
.0000	.547
.0000	.548
.0000	.549
.0000	.550
.0000	.551
.0000	.552
.0000	.553
.0000	.554
.0000	.555
.0000	.556
.0000	.557
.0000	.558
.0000	.559
.0000	.560
.0000	.561
.0000	.562
.0000	.563
.0000	.564
.0000	.565
.0000	.566
.0000	.567
.0000	.568
.0000	.569
.0000	.570
.0000	.571
.0000	.572
.0000	.573
.0000	.574
.0000	.575
.0000	.576
.0000	.577
.0000	.578
.0000	.579
.0000	.580
.0000	.581
.0000	.582
.0000	.583
.0000	.584
.0000	.585
.0000	.586
.0000	.587
.0000	.588
.0000	.589
.0000	.590
.0000	.591
.0000	.592
.0000	.593
.0000	.594
.0000	.595
.0000	.596
.0000	.597
.0000	.598
.0000	.599
.0000	.600

Figure A.5.- Continued.

-7.4315	1.1431
-2.4147	1.1433
-2.4133	1.1407
-2.40577	1.1402
-2.773.	1.1424
-2.767	1.1404
-2.4052	1.1407
-2.4050	1.1404
-2.40545	1.1404
-2.7007	1.1407
-2.4035	1.1407
-2.415	1.1403
-2.4054	1.1403
-2.4057	1.1404
-2.4028	1.1404
-2.40775	1.1404
-2.4024	1.1407
-2.4407	1.1473
-2.443	1.1407
-2.4000	1.1403
-2.40143	1.1407
-2.47497	1.1407
-2.4705	1.1407
-2.4704	1.1407
-2.471	1.1407
-2.4011	1.1407
-2.4045	1.1407
-4.4019	1.1407
-4.4071	1.1407
-4.4026	1.1407
-4.4028	1.1407
-4.4053	1.1407
-4.4027	1.1407
-4.4036	1.1407
-4.420	1.1407
-4.4048	1.1407
-4.4042	1.1407
-4.405	1.1407
-4.4051	1.1407
-4.4013	1.1407
-4.4017	1.1407
-4.407	1.1407
-4.4024	1.1407
-4.4027	1.1407
-4.4034	1.1407
-2.401	1.1407
-2.405	1.1407
-2.402	1.1407
-1.404	1.1407
-3.400	1.1407
-2.4013	1.1407
-2.4037	1.1407
-2.4025	1.1407
-2.4010	1.1407
-2.4037	1.1407

STREAMLINE NO.62, STARTING AT YFO. = -7.0543, RFO. = 5.3127

YFO	RFO
-5.0043	5.3129
-5.0007	5.3131
-2.00751	5.3136
-1.00304	5.3137
-1.0019	5.3147
-2.0042	5.3154
-1.0055	5.3157
-2.00367	5.3158

STREAMLINE NO.49, STARTING AT YFO. = -7.4133, RFO. = 5.4382

YFO	RFO
-2.4033	5.4381
-2.4006	5.4401
-2.4016	5.4390
-2.40367	5.4377

Figure A.5.- Continued.

MAGNETIC FIELD COMPONENTS

ANGULAR LOCATION NO. 1, AT THETA = 0.0000 DEGREE

I	PP/R	X/R/INE (PARALLEL)	Y/R/INE (ORPP)	Z/R/INE (IN-PLANE)	W-ANGLE (IN-PLANE)	X/R/INE (NORMAL)	Y/R/INE (RESULTANT)	Z/R/INE (RESULTANT)	W/INE (RESULTANT)
1	1.0000	0.0000	0.0000	0.0000	0.0000	0.0000	0.0000	0.0000	0.0000
2	1.0160	0.1150	12.0040	11.8840	86.9445	3.4184	0.1150	11.8724	0.1558
3	1.0320	0.2300	0.7572	6.6703	89.3558	2.4126	0.2300	6.6613	0.1559
4	1.0480	0.3450	7.1915	7.1192	89.7557	3.3941	0.3450	7.1116	0.1561
5	1.0640	0.4600	0.2000	6.2178	89.5251	3.3829	0.4600	6.2112	0.1566
6	1.0800	0.5750	5.6043	5.6140	89.6914	3.3592	0.5750	5.6038	0.1566
7	1.1116	0.7900	4.1904	5.1392	89.3433	3.3531	0.7900	5.1335	0.1533
8	1.1432	1.0050	4.4736	4.5217	89.0966	3.3347	1.0050	4.4702	0.1524
9	1.1748	1.2200	4.5573	4.5177	89.1335	3.3142	1.1748	4.5174	0.1515
10	1.1921	1.3350	4.3341	4.2928	89.4735	3.2911	1.1921	4.2975	0.1504
11	1.1859	1.3547	4.0190	4.0700	89.7077	3.2662	1.1859	4.0746	0.1493
12	1.1800	1.3733	3.6017	3.8417	89.9362	3.2393	1.1800	3.8464	0.1481
13	1.1740	1.3917	3.1833	3.6178	90.1620	3.2114	1.1740	3.6174	0.1467
14	1.1680	1.4100	2.7647	3.4018	90.3858	3.1798	1.1680	3.4033	0.1453
15	1.1620	1.4286	2.3460	3.1861	90.6087	3.1475	1.1620	3.1891	0.1439
16	1.1560	1.4470	1.9273	3.0226	90.8301	3.1135	1.1560	3.0249	0.1423
17	1.1500	1.4653	1.5086	2.8602	91.0500	3.0790	1.1500	2.8602	0.1407
18	1.1440	1.4835	1.0900	2.7000	91.2680	3.0440	1.1440	2.7000	0.1390
19	1.1380	1.5017	0.6713	2.5425	91.4840	3.0090	1.1380	2.5425	0.1371

ANGULAR LOCATION NO. 2, AT THETA = 2.0000 DEGREE

I	PP/R	X/R/INE (PARALLEL)	Y/R/INE (ORPP)	Z/R/INE (IN-PLANE)	W-ANGLE (IN-PLANE)	X/R/INE (NORMAL)	Y/R/INE (RESULTANT)	Z/R/INE (RESULTANT)	W/INE (RESULTANT)
1	1.0000	0.0000	0.0000	0.0000	0.0000	0.0000	0.0000	0.0000	0.0000
2	1.0170	0.1150	11.7504	11.7504	86.2712	2.1935	0.1150	11.7418	0.2372
3	1.0340	0.2300	6.7063	6.6276	86.1151	2.0053	0.2300	6.6133	0.2288
4	1.0510	0.3450	7.1645	7.1018	86.1420	4.7499	0.2200	7.0907	0.2189
5	1.0680	0.4600	0.2199	6.2177	86.1268	4.6098	0.2100	6.1989	0.2167
6	1.0850	0.5750	5.6043	5.6015	86.1084	4.4658	0.1800	5.5925	0.2039
7	1.1117	0.7900	4.1904	5.1341	86.3768	4.3127	0.2811	4.1256	0.1971
8	1.1387	1.0050	4.4736	4.5171	87.0727	4.1792	0.1750	4.4087	0.1910
9	1.1656	1.2200	4.5573	4.5164	87.7519	4.0561	0.1750	4.4085	0.1854
10	1.1820	1.4350	4.3341	4.2954	87.6674	3.9327	0.1750	4.2773	0.1797
11	1.1880	1.4537	4.0190	4.0758	87.9317	3.8081	0.1750	4.0658	0.1745
12	1.1840	1.4723	3.6017	3.8565	87.9767	3.6774	0.1750	3.8785	0.1695
13	1.1800	1.4910	3.1833	3.6422	87.9830	3.5465	0.1750	3.7331	0.1644
14	1.1760	1.5100	2.7647	3.4348	87.9594	3.4154	0.1750	3.5866	0.1596
15	1.1720	1.5290	2.3460	3.2340	87.9124	3.2837	0.1750	3.4464	0.1549
16	1.1680	1.5480	1.9273	3.0400	87.8401	3.1523	0.1607	3.3370	0.1502
17	1.1640	1.5670	1.5086	2.8527	87.7424	3.0215	0.1500	3.2296	0.1458
18	1.1600	1.5860	1.0900	2.6724	87.6203	2.8912	0.1301	3.1225	0.1415
19	1.1560	1.6050	0.6713	2.4984	87.4737	2.7611	0.1001	3.0155	0.1372

ANGULAR LOCATION NO. 3, AT THETA = 4.0000 DEGREE

I	PP/R	X/R/INE (PARALLEL)	Y/R/INE (ORPP)	Z/R/INE (IN-PLANE)	W-ANGLE (IN-PLANE)	X/R/INE (NORMAL)	Y/R/INE (RESULTANT)	Z/R/INE (RESULTANT)	W/INE (RESULTANT)
1	1.0000	0.0000	0.0000	0.0000	0.0000	0.0000	0.0000	0.0000	0.0000
2	1.0174	0.1150	11.5576	11.4740	84.4470	4.9765	1.1151	11.4099	0.4085
3	1.0348	0.2300	6.7063	6.6112	84.6009	4.3471	0.7910	6.4953	0.3815
4	1.0522	0.3450	7.1645	7.1018	84.7408	4.9959	0.6161	6.9905	0.3147
5	1.0696	0.4600	0.2199	6.2177	84.8686	4.6421	0.5249	6.1333	0.2744
6	1.0870	0.5750	5.6043	5.6015	84.9840	4.2877	0.4713	5.5367	0.2481
7	1.1126	0.7900	4.1904	5.1326	85.2275	4.0977	0.4330	5.0791	0.2284
8	1.1382	1.0050	4.4736	4.7110	85.5926	4.0135	0.4050	4.7594	0.2141
9	1.1638	1.2200	4.5573	4.4782	85.9730	4.0229	0.3941	4.4577	0.2022
10	1.1894	1.4350	4.3341	4.2564	86.3620	4.0955	0.3807	4.2359	0.1918
11	1.2150	1.6500	4.0190	4.0447	86.7597	4.0059	0.3954	4.0203	0.1831
12	1.2406	1.8650	3.6017	3.8444	86.9304	3.8344	0.3405	3.8145	0.1755
13	1.2662	2.0800	3.1833	3.6579	86.9762	3.6848	0.3117	3.6092	0.1684
14	1.2918	2.2950	2.7647	3.4850	86.9981	3.5494	0.3225	3.4055	0.1622
15	1.3174	2.5100	2.3460	3.3269	86.9960	3.4241	0.3131	3.4180	0.1565
16	1.3430	2.7250	1.9273	3.1847	86.9703	3.3059	0.3064	3.3971	0.1511
17	1.3686	2.9400	1.5086	3.0576	86.9220	3.1984	0.3010	3.2001	0.1462
18	1.3942	3.1550	1.0900	2.9453	86.8530	3.0957	0.2961	3.0044	0.1415
19	1.4198	3.3700	0.6713	2.8474	86.7644	2.9968	0.2913	2.8098	0.1376

Figure A.5.- Continued.

7	3.2514	.777	.7913	.777	73.6135	1.441	.2219	.7764	.477
8	3.7614	.831	.7617	.7764	73.3529	1.283	.2317	.7629	.474
9	4.121	.8497	.7509	.7779	73.221	1.184	.2343	.7460	.466
10	4.251	.8726	.7314	.7717	73.051	1.069	.2344	.7321	.458
11	4.304	.8446	.7573	.7825	73.3032	1.1637	.2361	.7463	.4532
12	4.244	.8277	.760	.781	73.2631	1.2150	.2403	.7277	.4516
13	4.0546	1.011	.8517	.8039	71.8173	1.2612	.2417	.8464	.4379
14	4.032	1.1512	.8987	.8434	71.1471	1.3143	.2461	.8903	.421
15	4.277	1.271	.9467	.881	70.363	1.3762	.2529	.9398	.4021
16	4.6627	1.381	.9947	.911	70.321	1.4227	.2637	.9901	.3841
17	4.844	1.427	1.034	1.037	71.651	1.4419	.2629	1.0341	.3856
18	4.813	1.476	1.046	1.079	71.981	1.4514	.2629	1.0408	.3877
19	4.559	1.476	1.024	1.011	71.313	1.4112	.2609	1.0212	.3891

ADDITIONAL AXIAL LOCATION NO.45, AT Y/P = 0.5367									
T	X/Y	R/RINE (PARALLEL)	R/RINE (PERP)	R/RINE (IN-PLANE)	A-ANGLE (IN-PLANE)	R/RINE (NORMAL)	R/RINE (RESULTANT)	R/RINE (RESULTANT)	R/RINE (RESULTANT)
1	1.444	.755							
2	1.3561	.6487	1.0114	1.0852	19.057	1.2337	1.1187	.3712	.4701
3	1.6621	.6788	.9219	.884	56.3486	1.2410	.5341	.3036	.4567
4	1.8721	.7214	.9367	.9488	46.2543	1.2413	.3447	.8907	.4522
5	2.1171	.7477	.9145	.8341	72.0746	1.1015	.2673	.8678	.4513
6	2.324	.7724	.8717	.8480	74.0330	1.0759	.2451	.8590	.4492
7	2.561	.7894	.8313	.8478	74.4117	1.0462	.2219	.8175	.4478
8	2.8391	.8178	.7831	.8174	73.9732	1.0340	.2227	.7752	.4473
9	3.113	.8464	.748	.8131	74.4436	1.0365	.2151	.7399	.4463
10	3.3221	.870	.7087	.8167	74.7746	1.0319	.2152	.7060	.4453
11	3.5641	.8913	.6709	.8119	74.9747	1.0122	.2289	.6702	.4457
12	3.811	1.0229	.6313	.8174	74.761	1.0293	.2406	.6431	.4454
13	4.0441	1.0839	.5717	.8172	72.6543	1.0293	.2751	.6222	.4453
14	4.2621	1.1441	.5097	.8111	71.8379	1.0311	.2903	.6113	.4455
15	4.5221	1.2029	.4601	1.0136	71.3313	.9389	.3191	.6000	.4415
16	4.7741	1.2629	.4111	1.0429	71.3940	.8389	.3384	.5763	.4435
17	4.911	1.313	.3638	1.0167	71.111	1.0272	.3574	.5482	.4432
18	4.241	1.3668	.3165	1.0579	71.3579	.9484	.3774	.5193	.4431
19	4.511	1.4124	.2671	1.0936	70.3851	1.0977	.3933	.4852	.4435

VELOCITY AND TEMPERATURE CONTOURS

14 VELOCITY (TEMPERATURE) CONTOUR LINES FOUND

4 PRINTS IN CONTOUR LINE OF V/VINE = .11%, T/TINE = 3.47%

X/Y	R/P
1.0482	.1142
1.0587	.1149
1.0710	.1151
1.0848	.1153
1.0989	.1155
1.1133	.1157
1.1279	.1159
1.1428	.1161

10 PRINTS IN CONTOUR LINE OF V/VINE = .20%, T/TINE = 3.84%

X/Y	R/P
.9615	.2144
.9787	.2146
.9976	.2148
1.0171	.2150
1.0373	.2152
1.0583	.2154
1.0799	.2156
1.1021	.2158
1.1249	.2160
1.1482	.2162
1.1721	.2164
1.1965	.2166
1.2214	.2168
1.2468	.2170
1.2727	.2172
1.2990	.2174

Figure A.5.- Continued.

MAGNETIC FIELD CONTOURS

11 MAGNETIC FIELD CONTOUR LINES FOUND
 (X-RO COMPONENT ALONG FIELD LINES PARALLEL TO FLOW IN FREESTREAM)

11 POINTS IN CONTOUR LINE OF X/RINE (PARALLEL) = 0.50

X/RD	R/RD
0.9021	0.2963
0.9009	0.1904
1.0712	0.1813
1.0712	0.1861
1.01343	0.1597
1.01592	0.1473
1.01792	0.1169
1.00412	0.1136
1.01101	0.0553
1.01144	0.1385
1.01198	0.1000

11 POINTS IN CONTOUR LINE OF X/RINE (PARALLEL) = 0.51

X/RD	R/RD
0.9067	0.2515
0.9753	0.2598
1.01147	0.1854
1.01123	0.2525
1.01242	0.1481
1.01439	0.2373
1.01043	0.2021
1.01044	0.2021
1.01037	0.1904
1.01171	0.1703
1.01098	0.1245
1.01325	0.1191
1.01468	0.1412
1.01521	0.1134
1.01523	0.1111

12 MAGNETIC FIELD CONTOUR LINES FOUND
 (X-RO COMPONENT ALONG FIELD LINES PERPENDICULAR TO FLOW IN FREESTREAM)

12 POINTS IN CONTOUR LINE OF X/RINE (PERPENDICULAR) = 0.5050

X/RD	R/RD
0.9227	0.3282
0.9648	0.3139
0.9751	0.2614
0.9134	0.1101
0.9301	0.2943
0.9804	0.2114
0.9664	0.2769
0.9274	0.2143
0.9008	0.3044
0.9217	0.2322
0.9191	0.4044
0.9177	0.4571
0.9011	0.4011
1.01164	0.3310
1.01044	0.2590
1.01014	0.2193
1.01055	0.2701
1.01079	0.1102
1.01043	0.1175
1.01053	0.1000

12 POINTS IN CONTOUR LINE OF X/RINE (PERPENDICULAR) = 0.5101

X/RD	R/RD
0.9041	1.01242
0.9721	1.00076
0.9421	0.9732
0.9107	0.9155
0.9740	0.9145
0.9352	0.8763
0.9421	0.8613
0.9050	0.8200
0.9176	0.7754
0.9123	0.7279
0.9013	0.7751
0.9104	0.6094
0.9100	0.6101
0.9100	0.5484
0.9041	0.4669
0.9045	0.4102
1.01174	0.3321
1.01104	0.4110
1.01074	0.3415
1.01072	0.2971
1.01020	0.2174
1.01000	0.1101
1.01000	0.1150
1.01000	0.1000

Figure A.5.- Continued.

DENSITY CONTOURS

7 DENSITY CONTOUR LINES FOUND

25 POINTS IN CONTOUR LINE OF RHO/RADINE = 2.417

Y/R	R/R
.9437	.4512
.9455	.4742
.9201	.4940
.9339	.5111
.9451	.5206
.9428	.5413
.9241	.5549
.9040	.5672
1.0117	.5775
.9223	.5830
1.0471	.5925
1.0469	.5933
1.0599	.5910
1.0732	.5945
1.1132	.5859
1.0463	.5921
1.0664	.5846
1.0227	.4620
1.0242	.4929
1.0394	.4327
1.0488	.4815
1.0576	.5111
1.0262	.2963
1.0287	.5365
1.0032	.5655

94 POINTS IN CONTOUR LINE OF RHO/RADINE = 2.62

Y/R	R/R
.7227	.6523
.7566	.7121
.7575	.7634
.7642	.7761
.7661	.7031
.7571	.6140
.7640	.6443
.7701	.6317
.7702	.6183
.7706	.6219
.7599	.6511
.7571	1.0142
.7635	1.0152
.7633	1.0159
.7538	1.0169
.7480	1.0113
.7614	1.0140
.7366	1.0137
.7595	1.0272
.7546	1.0222
.6588	1.0435
.6687	1.0413
.6517	1.0427
.6281	1.0526
.6452	1.0508
.4757	1.0233

Figure A.5.- Continued.

14 MAGNETIC FIELD CONTOUR LINES FOUND
 (FOR COMPONENT ALONG FIELD LINES NORMAL TO FLOW IN CROSS-STREAM)

16 POINTS IN CONTOUR LINE OF MAXIMUM (NORMAL) = 5.000

X/P	Y/P
1.0142	.0087
1.0310	.0573
1.0475	.791
1.0627	.2115
1.0626	.1117
1.0627	.1177
1.0521	.1955
1.0407	.2543
1.0400	.3543
1.0394	.2611
1.0390	.3311
.0045	.411
.0643	.4703
.0291	.5564
.0880	.5006
.0822	.4146
.0454	.4115
.7061	.7106
.7459	.7724
.6906	.8119
.6955	.8217
.6726	.8719
.6720	.8114
.6179	.8753
.6416	.9690
.6974	.81172

11 POINTS IN CONTOUR LINE OF MAXIMUM (NORMAL) = 5.000

X/P	Y/P
.2511	1.1744
.2053	1.0643
.3792	1.0391
.4454	.72
.5155	.0697
.5352	.0109
.621	.0318
.6441	.2492
.7152	.0412
.7124	.0371
.7647	.7918
.8285	.7374
.8456	.7036
.8640	.6734
.9153	.6574
.9544	.6523
.6651	.5300
.9037	.4646
1.0211	.4142
1.0520	.3613
1.0720	.2573
1.0809	.2211
1.0595	.1921
1.0061	.1193
1.0965	.1157
1.0316	.0811
1.0059	.0391
1.0498	.0401
1.0337	.0361
1.0333	.0361
1.0164	.0317

Figure A.5.- Continued.

TRAJECTORY CALCULATION
 (SOLAR WIND COORDINATE SYSTEM)

TRAJECTORY COORDINATES

R / PLANET = 100

N	TIME	V/R	V/Z	T/R	R/P	V/PLANET	V/PPLANET	V/RPLANET	R/PPLANET
1	-00.970	1.0000	-0.0000	1.0000	4.01195	1.0543	-2.7322	2.0298	4.2494
2	-00.9370	0.9347	-0.0396	1.0421	3.9697	0.9595	-2.9520	2.0492	4.0982
3	-00.9213	0.8460	-0.0740	1.0792	3.9274	0.8398	-3.1841	2.0643	3.9892
4	-00.8700	0.7815	-0.1360	1.1456	3.8641	0.7765	-3.4177	2.0786	3.7814
5	-00.7700	0.6740	-0.2045	1.2335	3.7841	0.6993	-3.6633	2.0798	3.5704
6	-00.6420	0.5519	-0.2696	1.3415	3.6932	0.5859	-3.9177	2.0815	3.4720
7	-00.5700	0.4431	-0.3274	1.4700	3.6000	0.4278	-4.1843	2.0682	3.1710
8	-00.4620	0.3224	-0.3870	1.6170	3.5030	0.3332	-4.4620	2.0499	2.9919
9	-00.4000	0.2140	-0.4470	1.7800	3.4040	0.2187	-4.7500	2.0210	2.8245
10	-00.3600	0.1050	-0.5070	1.9500	3.3040	0.0987	-5.0400	1.9810	2.6666
11	-00.3300	0.0460	-0.5670	2.1200	3.2040	0.0469	-5.3300	1.9320	2.5200
12	-00.3000	0.0000	-0.6270	2.2900	3.1040	0.0199	-5.6200	1.8810	2.3900
13	-00.2800	-0.0100	-0.6870	2.4600	3.0040	-0.0100	-5.9100	1.8280	2.2700
14	-00.2700	-0.0200	-0.7470	2.6300	2.9040	-0.0200	-6.2000	1.7740	2.1600
15	-00.2600	-0.0300	-0.8070	2.8000	2.8040	-0.0300	-6.4900	1.7190	2.0600
16	-00.2500	-0.0400	-0.8670	2.9700	2.7040	-0.0400	-6.7800	1.6640	1.9700
17	-00.2400	-0.0500	-0.9270	3.1400	2.6040	-0.0500	-7.0700	1.6090	1.8900
18	-00.2300	-0.0600	-1.0000	3.3100	2.5040	-0.0600	-7.3600	1.5540	1.8200
19	-00.2200	-0.0700	-1.0700	3.4800	2.4040	-0.0700	-7.6500	1.4990	1.7600
20	-00.2100	-0.0800	-1.1400	3.6500	2.3040	-0.0800	-7.9400	1.4440	1.7000
21	-00.2000	-0.0900	-1.2100	3.8200	2.2040	-0.0900	-8.2300	1.3890	1.6400
22	-00.1900	-0.1000	-1.2800	3.9900	2.1040	-0.1000	-8.5200	1.3340	1.5800
23	-00.1800	-0.1100	-1.3500	4.1600	2.0040	-0.1100	-8.8100	1.2790	1.5200
24	-00.1700	-0.1200	-1.4200	4.3300	1.9040	-0.1200	-9.1000	1.2240	1.4600
25	-00.1600	-0.1300	-1.4900	4.5000	1.8040	-0.1300	-9.3900	1.1690	1.4000
26	-00.1500	-0.1400	-1.5600	4.6700	1.7040	-0.1400	-9.6800	1.1140	1.3400
27	-00.1400	-0.1500	-1.6300	4.8400	1.6040	-0.1500	-9.9700	1.0590	1.2800
28	-00.1300	-0.1600	-1.7000	5.0100	1.5040	-0.1600	-10.2600	1.0040	1.2200
29	-00.1200	-0.1700	-1.7700	5.1800	1.4040	-0.1700	-10.5500	0.9490	1.1600
30	-00.1100	-0.1800	-1.8400	5.3500	1.3040	-0.1800	-10.8400	0.8940	1.1000
31	-00.1000	-0.1900	-1.9100	5.5200	1.2040	-0.1900	-11.1300	0.8390	1.0400
32	-00.0900	-0.2000	-1.9800	5.6900	1.1040	-0.2000	-11.4200	0.7840	0.9800
33	-00.0800	-0.2100	-2.0500	5.8600	1.0040	-0.2100	-11.7100	0.7290	0.9200
34	-00.0700	-0.2200	-2.1200	6.0300	0.9040	-0.2200	-12.0000	0.6740	0.8600
35	-00.0600	-0.2300	-2.1900	6.2000	0.8040	-0.2300	-12.2900	0.6190	0.8000
36	-00.0500	-0.2400	-2.2600	6.3700	0.7040	-0.2400	-12.5800	0.5640	0.7400
37	-00.0400	-0.2500	-2.3300	6.5400	0.6040	-0.2500	-12.8700	0.5090	0.6800

SCALAR FIELD AND MAGNETIC FIELD COMPONENTS ALONG TRAJECTORY
 (SOLAR WIND COORDINATE SYSTEM)

(NON-DIMENSIONALIZED BY INTERPLANETARY VALUES)

N	TIME	V/VINE	V/VZNE	V/VXNE	V/VYNE	PHYSICIAN TEMP/TPHNE	R/VINE	V/VZNE	V/VXNE	V/VYNE	RZ/BINE
1	-00.970	1.0000	0.0000	0.0000	0.0000	1.0000	1.0000	1.0000	1.0000	0.0000	0.0000
2	-00.9370	1.0000	1.0000	0.0000	0.0000	1.0000	1.0000	1.0000	1.0000	0.0000	0.0000
3	-00.9213	1.0000	1.0000	0.0000	0.0000	1.0000	1.0000	1.0000	1.0000	0.0000	0.0000
4	-00.8700	1.0000	1.0000	0.0000	0.0000	1.0000	1.0000	1.0000	1.0000	0.0000	0.0000
5	-00.7700	1.0000	1.0000	0.0000	0.0000	1.0000	1.0000	1.0000	1.0000	0.0000	0.0000
6	-00.6420	1.0000	1.0000	0.0000	0.0000	1.0000	1.0000	1.0000	1.0000	0.0000	0.0000
7	-00.5700	1.0000	1.0000	0.0000	0.0000	1.0000	1.0000	1.0000	1.0000	0.0000	0.0000
8	-00.4620	1.0000	1.0000	0.0000	0.0000	1.0000	1.0000	1.0000	1.0000	0.0000	0.0000
9	-00.4000	1.0000	1.0000	0.0000	0.0000	1.0000	1.0000	1.0000	1.0000	0.0000	0.0000
10	-00.3600	1.0000	1.0000	0.0000	0.0000	1.0000	1.0000	1.0000	1.0000	0.0000	0.0000
11	-00.3300	1.0000	1.0000	0.0000	0.0000	1.0000	1.0000	1.0000	1.0000	0.0000	0.0000
12	-00.3000	1.0000	1.0000	0.0000	0.0000	1.0000	1.0000	1.0000	1.0000	0.0000	0.0000
13	-00.2800	1.0000	1.0000	0.0000	0.0000	1.0000	1.0000	1.0000	1.0000	0.0000	0.0000
14	-00.2700	1.0000	1.0000	0.0000	0.0000	1.0000	1.0000	1.0000	1.0000	0.0000	0.0000
15	-00.2600	1.0000	1.0000	0.0000	0.0000	1.0000	1.0000	1.0000	1.0000	0.0000	0.0000
16	-00.2500	1.0000	1.0000	0.0000	0.0000	1.0000	1.0000	1.0000	1.0000	0.0000	0.0000
17	-00.2400	1.0000	1.0000	0.0000	0.0000	1.0000	1.0000	1.0000	1.0000	0.0000	0.0000
18	-00.2300	1.0000	1.0000	0.0000	0.0000	1.0000	1.0000	1.0000	1.0000	0.0000	0.0000
19	-00.2200	1.0000	1.0000	0.0000	0.0000	1.0000	1.0000	1.0000	1.0000	0.0000	0.0000
20	-00.2100	1.0000	1.0000	0.0000	0.0000	1.0000	1.0000	1.0000	1.0000	0.0000	0.0000
21	-00.2000	1.0000	1.0000	0.0000	0.0000	1.0000	1.0000	1.0000	1.0000	0.0000	0.0000
22	-00.1900	1.0000	1.0000	0.0000	0.0000	1.0000	1.0000	1.0000	1.0000	0.0000	0.0000
23	-00.1800	1.0000	1.0000	0.0000	0.0000	1.0000	1.0000	1.0000	1.0000	0.0000	0.0000
24	-00.1700	1.0000	1.0000	0.0000	0.0000	1.0000	1.0000	1.0000	1.0000	0.0000	0.0000
25	-00.1600	1.0000	1.0000	0.0000	0.0000	1.0000	1.0000	1.0000	1.0000	0.0000	0.0000
26	-00.1500	1.0000	1.0000	0.0000	0.0000	1.0000	1.0000	1.0000	1.0000	0.0000	0.0000
27	-00.1400	1.0000	1.0000	0.0000	0.0000	1.0000	1.0000	1.0000	1.0000	0.0000	0.0000
28	-00.1300	1.0000	1.0000	0.0000	0.0000	1.0000	1.0000	1.0000	1.0000	0.0000	0.0000
29	-00.1200	1.0000	1.0000	0.0000	0.0000	1.0000	1.0000	1.0000	1.0000	0.0000	0.0000
30	-00.1100	1.0000	1.0000	0.0000	0.0000	1.0000	1.0000	1.0000	1.0000	0.0000	0.0000
31	-00.1000	1.0000	1.0000	0.0000	0.0000	1.0000	1.0000	1.0000	1.0000	0.0000	0.0000
32	-00.0900	1.0000	1.0000	0.0000	0.0000	1.0000	1.0000	1.0000	1.0000	0.0000	0.0000
33	-00.0800	1.0000	1.0000	0.0000	0.0000	1.0000	1.0000	1.0000	1.0000	0.0000	0.0000
34	-00.0700	1.0000	1.0000	0.0000	0.0000	1.0000	1.0000	1.0000	1.0000	0.0000	0.0000
35	-00.0600	1.0000	1.0000	0.0000	0.0000	1.0000	1.0000	1.0000	1.0000	0.0000	0.0000
36	-00.0500	1.0000	1.0000	0.0000	0.0000	1.0000	1.0000	1.0000	1.0000	0.0000	0.0000
37	-00.0400	1.0000	1.0000	0.0000	0.0000	1.0000	1.0000	1.0000	1.0000	0.0000	0.0000

Figure A.5.- Continued.

FLOW FIELD AND MAGNETIC FIELD COMPONENTS ALONG TRAJECTORY

(SOLAR WIND COORDINATE SYSTEM)

(DIMENSIONAL, USING INPUT INTERPLANETARY VALUES)

		INTERPLANETARY MACH NUMBER = 3.00				INTERPLANETARY MAGNETIC FIELD					
		RATIO OF SPECIFIC HEATS = 1.6667				MAGNITUDE = .002E+01					
		INTERPLANETARY VELOCITY = 3.920E+02				X-COMPONENT = 1.239E+00					
		INTERPLANETARY DENSITY = 2.000E+01				Y-COMPONENT = 4.726E+00					
		INTERPLANETARY TEMPERATURE = 1.000E+05				Z-COMPONENT = 4.032E-01					
N	TIME	VX	VY	VZ	RHO	TEMP	BY	BZ	BY	BZ	
1	-90.8700	3.920E+02	3.920E+02	0.	0.	2.000E+01	1.020E+05	8.023E+00	1.239E+00	4.726E+00	4.032E-01
2	-89.9370	3.920E+02	3.920E+02	0.	0.	2.020E+01	1.020E+05	8.023E+00	1.239E+00	4.726E+00	4.032E-01
3	-40.2030	3.920E+02	3.920E+02	0.	0.	2.020E+01	1.020E+05	8.023E+00	1.239E+00	4.726E+00	4.032E-01
4	-74.8700	3.920E+02	3.920E+02	0.	0.	2.020E+01	1.020E+05	8.023E+00	1.239E+00	4.726E+00	4.032E-01
5	-70.0630	3.920E+02	3.920E+02	0.	0.	2.020E+01	1.020E+05	8.023E+00	1.239E+00	4.726E+00	4.032E-01
6	-64.2430	3.920E+02	3.920E+02	0.	0.	2.020E+01	1.020E+05	8.023E+00	1.239E+00	4.726E+00	4.032E-01
7	-57.8820	3.920E+02	3.920E+02	0.	0.	2.020E+01	1.020E+05	8.023E+00	1.239E+00	4.726E+00	4.032E-01
8	-51.4020	3.920E+02	3.920E+02	0.	0.	2.020E+01	1.020E+05	8.023E+00	1.239E+00	4.726E+00	4.032E-01
9	-40.7330	3.920E+02	3.920E+02	0.	0.	2.020E+01	1.020E+05	8.023E+00	1.239E+00	4.726E+00	4.032E-01
10	-39.0660	3.920E+02	3.920E+02	0.	0.	2.020E+01	1.020E+05	8.023E+00	1.239E+00	4.726E+00	4.032E-01
11	-30.0620	3.920E+02	3.920E+02	0.	0.	2.020E+01	1.020E+05	8.023E+00	1.239E+00	4.726E+00	4.032E-01
12	-35.9350	3.920E+02	3.920E+02	0.	0.	2.020E+01	1.020E+05	8.023E+00	1.239E+00	4.726E+00	4.032E-01
13	-34.8670	3.920E+02	3.920E+02	0.	0.	2.020E+01	1.020E+05	8.023E+00	1.239E+00	4.726E+00	4.032E-01
14	-32.7350	3.920E+02	3.920E+02	0.	0.	2.020E+01	1.020E+05	8.023E+00	1.239E+00	4.726E+00	4.032E-01
15	-24.0620	3.920E+02	3.920E+02	0.	0.	2.020E+01	1.020E+05	8.023E+00	1.239E+00	4.726E+00	4.032E-01
16	-21.0620	3.920E+02	3.920E+02	0.	0.	2.020E+01	1.020E+05	8.023E+00	1.239E+00	4.726E+00	4.032E-01
17	-16.7330	3.920E+02	3.920E+02	0.	0.	2.020E+01	1.020E+05	8.023E+00	1.239E+00	4.726E+00	4.032E-01
18	-14.0620	3.920E+02	3.920E+02	0.	0.	2.020E+01	1.020E+05	8.023E+00	1.239E+00	4.726E+00	4.032E-01
19	-11.4620	3.920E+02	3.920E+02	0.	0.	2.020E+01	1.020E+05	8.023E+00	1.239E+00	4.726E+00	4.032E-01
20	-8.1220	3.920E+02	3.920E+02	0.	0.	2.020E+01	1.020E+05	8.023E+00	1.239E+00	4.726E+00	4.032E-01
21	-4.9060	3.920E+02	3.920E+02	0.	0.	2.020E+01	1.020E+05	8.023E+00	1.239E+00	4.726E+00	4.032E-01
22	6.0980	3.920E+02	3.920E+02	0.	0.	2.020E+01	1.020E+05	8.023E+00	1.239E+00	4.726E+00	4.032E-01
23	9.4980	3.920E+02	3.920E+02	0.	0.	2.020E+01	1.020E+05	8.023E+00	1.239E+00	4.726E+00	4.032E-01
24	12.9930	3.920E+02	3.920E+02	0.	0.	2.020E+01	1.020E+05	8.023E+00	1.239E+00	4.726E+00	4.032E-01
25	17.3930	3.920E+02	3.920E+02	0.	0.	2.020E+01	1.020E+05	8.023E+00	1.239E+00	4.726E+00	4.032E-01
26	20.1270	3.920E+02	3.920E+02	0.	0.	2.020E+01	1.020E+05	8.023E+00	1.239E+00	4.726E+00	4.032E-01
27	34.4060	3.920E+02	3.920E+02	0.	0.	2.020E+01	1.020E+05	8.023E+00	1.239E+00	4.726E+00	4.032E-01
28	40.0660	3.920E+02	3.920E+02	0.	0.	2.020E+01	1.020E+05	8.023E+00	1.239E+00	4.726E+00	4.032E-01
29	47.2610	3.920E+02	3.920E+02	0.	0.	2.020E+01	1.020E+05	8.023E+00	1.239E+00	4.726E+00	4.032E-01
30	53.8660	3.920E+02	3.920E+02	0.	0.	2.020E+01	1.020E+05	8.023E+00	1.239E+00	4.726E+00	4.032E-01
31	58.0620	3.920E+02	3.920E+02	0.	0.	2.020E+01	1.020E+05	8.023E+00	1.239E+00	4.726E+00	4.032E-01
32	58.9930	3.920E+02	3.920E+02	0.	0.	2.020E+01	1.020E+05	8.023E+00	1.239E+00	4.726E+00	4.032E-01
33	60.0660	3.920E+02	3.920E+02	0.	0.	2.020E+01	1.020E+05	8.023E+00	1.239E+00	4.726E+00	4.032E-01
34	62.1930	3.920E+02	3.920E+02	0.	0.	2.020E+01	1.020E+05	8.023E+00	1.239E+00	4.726E+00	4.032E-01
35	67.5280	3.920E+02	3.920E+02	0.	0.	2.020E+01	1.020E+05	8.023E+00	1.239E+00	4.726E+00	4.032E-01
36	73.9280	3.920E+02	3.920E+02	0.	0.	2.020E+01	1.020E+05	8.023E+00	1.239E+00	4.726E+00	4.032E-01
37	80.3280	3.920E+02	3.920E+02	0.	0.	2.020E+01	1.020E+05	8.023E+00	1.239E+00	4.726E+00	4.032E-01

TRAJECTORY CALCULATION

(SUN-PLANET COORDINATE SYSTEM)

TRAJECTORY COORDINATES

R0/RPLANET = 1.0331

N	TIME	X/RP	Y/RP	Z/RP	R/RP	X/RPLANET	Y/RPLANET	Z/RPLANET	R/RPLANET
1	-90.8700	-.8160	3.6658	1.9621	4.1579	-.8430	3.7870	2.0270	4.2954
2	-89.9370	-.7495	3.4848	1.8796	4.0078	-.7650	3.6630	2.0450	4.1463
3	-40.2030	-.6621	3.2844	1.9960	3.8434	-.6840	3.3930	2.0620	3.9704
4	-74.8700	-.5808	3.0733	2.0667	3.6721	-.6000	3.1770	2.0730	3.7935
5	-70.0630	-.5159	2.9030	2.2125	3.5318	-.5330	2.9990	2.0780	3.6486
6	-64.2430	-.4162	2.6339	2.4125	3.3148	-.4300	2.7210	2.0790	3.4243
7	-57.8820	-.3136	2.3493	2.6309	3.1459	-.3243	2.4270	2.0670	3.1479
8	-51.4020	-.2101	2.0502	1.9776	2.8496	-.2170	2.1180	2.0433	2.9277
9	-43.7350	-.0829	1.5124	1.6982	2.4268	-.0340	1.5620	1.9610	2.5971
10	-39.0660	-.0165	1.4607	1.8806	2.3875	-.0170	1.5090	1.9510	2.4665
11	-30.0620	-.0097	1.3765	1.8712	2.3221	-.0100	1.4220	1.9320	2.3909
12	-35.9350	.0474	1.2400	1.8411	2.2198	.0493	1.2810	1.9020	2.2932
13	-34.8670	.0649	1.1926	1.8256	2.1806	.0670	1.2320	1.8960	2.2527
14	-32.7350	.1329	1.0725	1.7927	2.0891	.1389	1.1080	1.8920	2.1581
15	-24.0620	.2377	.9640	1.6125	1.7083	.2456	.9826	1.8659	1.7647
16	-21.0620	.2859	.8629	1.5191	1.5618	.2954	.8749	1.8693	1.6115
17	-16.7350	.3446	.8071	1.3639	1.3587	.3560	.8090	1.4090	1.4119
18	-14.0620	.3698	.8523	1.2729	1.2739	.3820	.8520	1.3150	1.3160
19	-11.4620	.4017	.9084	1.1132	1.1337	.4150	.8205	1.1500	1.1681
20	-8.1220	.4430	.9148	1.0291	1.0291	.4370	.8470	.9450	1.0990
21	-4.9060	.4279	.8605	.8399	.9334	.4420	.7630	.6630	.9643
22	6.0980	.2991	-1.0007	-.2575	1.0410	.3090	-1.0420	-.2660	1.0754
23	9.4980	.2294	-1.0212	-.5285	1.1499	.2370	-1.0550	-.5460	1.1479
24	12.9930	.1549	-1.0048	-.7794	1.2692	.1600	-1.0380	-.8010	1.3111
25	17.3930	.0329	-.9931	-1.1248	1.4657	-.0340	-.9930	-1.1620	1.5111
26	20.1270	-.2462	-.9815	-1.8266	1.9393	-.2750	-.9830	-1.8870	2.0934
27	34.4060	-.3940	-.9456	-2.0860	2.1441	-.4070	-.9450	-2.1550	2.2150
28	40.0660	-.5430	-.9020	-2.3658	2.3850	-.5610	-.9120	-2.4440	2.4638
29	47.2610	-.6824	-.8409	-2.5846	2.5867	-.7050	-.8660	-2.6720	2.6722
30	53.8660	-.8170	-.8051	-2.8314	2.8330	-.8440	-.8082	-2.9250	2.9266
31	58.0620	-.8809	-.7466	-2.9340	2.9405	-.9160	-.8210	-3.0310	3.0317
32	58.9930	-.9235	-.6604	-2.9979	3.0092	-.9540	-.8660	-3.0970	3.1496
33	60.0660	-.9438	-.6293	-3.0308	3.0458	-.9750	-.8930	-.31310	3.2165
34	62.1930	-.9856	-.5991	-3.0928	3.1135	-1.0180	-.8710	-.33970	3.3094
35	67.5280	-1.0861	-.5237	-3.2399	3.2019	-1.1220	-.8410	-.37140	3.5909
36	73.9280	-1.2013	-.4754	-3.4016	3.4766	-1.2410	-.8730	-.41540	3.7992
37	80.3280	-1.3136	-.4090	-3.5535	3.6679	-1.3570	-.8930	-.46710	3.7992

Figure A.5.- Continued.

FLOW FIELD AND MAGNETIC FIELD COMPONENTS ALONG TRAJECTORY
(GEO-CENTRIC COORDINATE SYSTEM)

(DIMENSIONAL, USING INPUT INTERPLANETARY VALUES)

N	TIME	VX/VE	VY/VE	VZ/VE	VX/VE	VY/VE	TEMP/TREF	BX/BN	BY/BN	BZ/BN
1	-0.4377	0.0000	-0.0000	0.0000	0.0000	0.0000	1.0000	0.0000	-0.0000	0.0000
2	-0.4337	0.0000	-0.0000	0.0000	0.0000	0.0000	1.0000	0.0000	-0.0000	0.0000
3	-0.4297	0.0000	-0.0000	0.0000	0.0000	0.0000	1.0000	0.0000	-0.0000	0.0000
4	-0.4257	0.0000	-0.0000	0.0000	0.0000	0.0000	1.0000	0.0000	-0.0000	0.0000
5	-0.4217	0.0000	-0.0000	0.0000	0.0000	0.0000	1.0000	0.0000	-0.0000	0.0000
6	-0.4177	0.0000	-0.0000	0.0000	0.0000	0.0000	1.0000	0.0000	-0.0000	0.0000
7	-0.4137	0.0000	-0.0000	0.0000	0.0000	0.0000	1.0000	0.0000	-0.0000	0.0000
8	-0.4097	0.0000	-0.0000	0.0000	0.0000	0.0000	1.0000	0.0000	-0.0000	0.0000
9	-0.4057	0.0000	-0.0000	0.0000	0.0000	0.0000	1.0000	0.0000	-0.0000	0.0000
10	-0.4017	0.0000	-0.0000	0.0000	0.0000	0.0000	1.0000	0.0000	-0.0000	0.0000
11	-0.3977	0.0000	-0.0000	0.0000	0.0000	0.0000	1.0000	0.0000	-0.0000	0.0000
12	-0.3937	0.0000	-0.0000	0.0000	0.0000	0.0000	1.0000	0.0000	-0.0000	0.0000
13	-0.3897	0.0000	-0.0000	0.0000	0.0000	0.0000	1.0000	0.0000	-0.0000	0.0000
14	-0.3857	0.0000	-0.0000	0.0000	0.0000	0.0000	1.0000	0.0000	-0.0000	0.0000
15	-0.3817	0.0000	-0.0000	0.0000	0.0000	0.0000	1.0000	0.0000	-0.0000	0.0000
16	-0.3777	0.0000	-0.0000	0.0000	0.0000	0.0000	1.0000	0.0000	-0.0000	0.0000
17	-0.3737	0.0000	-0.0000	0.0000	0.0000	0.0000	1.0000	0.0000	-0.0000	0.0000
18	-0.3697	0.0000	-0.0000	0.0000	0.0000	0.0000	1.0000	0.0000	-0.0000	0.0000
19	-0.3657	0.0000	-0.0000	0.0000	0.0000	0.0000	1.0000	0.0000	-0.0000	0.0000
20	-0.3617	0.0000	-0.0000	0.0000	0.0000	0.0000	1.0000	0.0000	-0.0000	0.0000
21	-0.3577	0.0000	-0.0000	0.0000	0.0000	0.0000	1.0000	0.0000	-0.0000	0.0000
22	-0.3537	0.0000	-0.0000	0.0000	0.0000	0.0000	1.0000	0.0000	-0.0000	0.0000
23	-0.3497	0.0000	-0.0000	0.0000	0.0000	0.0000	1.0000	0.0000	-0.0000	0.0000
24	-0.3457	0.0000	-0.0000	0.0000	0.0000	0.0000	1.0000	0.0000	-0.0000	0.0000
25	-0.3417	0.0000	-0.0000	0.0000	0.0000	0.0000	1.0000	0.0000	-0.0000	0.0000
26	-0.3377	0.0000	-0.0000	0.0000	0.0000	0.0000	1.0000	0.0000	-0.0000	0.0000
27	-0.3337	0.0000	-0.0000	0.0000	0.0000	0.0000	1.0000	0.0000	-0.0000	0.0000
28	-0.3297	0.0000	-0.0000	0.0000	0.0000	0.0000	1.0000	0.0000	-0.0000	0.0000
29	-0.3257	0.0000	-0.0000	0.0000	0.0000	0.0000	1.0000	0.0000	-0.0000	0.0000
30	-0.3217	0.0000	-0.0000	0.0000	0.0000	0.0000	1.0000	0.0000	-0.0000	0.0000
31	-0.3177	0.0000	-0.0000	0.0000	0.0000	0.0000	1.0000	0.0000	-0.0000	0.0000
32	-0.3137	0.0000	-0.0000	0.0000	0.0000	0.0000	1.0000	0.0000	-0.0000	0.0000
33	-0.3097	0.0000	-0.0000	0.0000	0.0000	0.0000	1.0000	0.0000	-0.0000	0.0000
34	-0.3057	0.0000	-0.0000	0.0000	0.0000	0.0000	1.0000	0.0000	-0.0000	0.0000
35	-0.3017	0.0000	-0.0000	0.0000	0.0000	0.0000	1.0000	0.0000	-0.0000	0.0000
36	-0.2977	0.0000	-0.0000	0.0000	0.0000	0.0000	1.0000	0.0000	-0.0000	0.0000
37	-0.2937	0.0000	-0.0000	0.0000	0.0000	0.0000	1.0000	0.0000	-0.0000	0.0000

FLOW FIELD AND MAGNETIC FIELD COMPONENTS ALONG TRAJECTORY
(GEO-CENTRIC COORDINATE SYSTEM)

(DIMENSIONAL, USING INPUT INTERPLANETARY VALUES)

```

INTERPLANETARY MACH NUMBER = 5.0
MAGNETIC FIELD = 6.2E+11
INTERPLANETARY VELOCITY = 3.0E24E+02
TEMPERATURE = 2.0E27E+01
INTERPLANETARY DENSITY = 1.0E-18E+00
AZIMUTHAL ANGLE = 0.0E+00
POLAR ANGLE = 0.0E+00
    
```

N	TIME	VX	VY	VZ	QND	TEMP	BX	BY	BZ	
1	-0.4377	3.0000E+03	-3.0000E+02	2.8237E+01	-1.1028E+00	2.0228E+01	4.8238E+00	-1.7400E+00	-9.6400E+00	4.0000E-01
2	-0.4337	3.0020E+03	-3.0010E+02	2.8257E+01	-1.1028E+00	2.0228E+01	4.8238E+00	-1.7400E+00	-9.6400E+00	4.0000E-01
3	-0.4297	3.0040E+03	-3.0020E+02	2.8277E+01	-1.1028E+00	2.0228E+01	4.8238E+00	-1.7400E+00	-9.6400E+00	4.0000E-01
4	-0.4257	3.0060E+03	-3.0030E+02	2.8297E+01	-1.1028E+00	2.0228E+01	4.8238E+00	-1.7400E+00	-9.6400E+00	4.0000E-01
5	-0.4217	3.0080E+03	-3.0040E+02	2.8317E+01	-1.1028E+00	2.0228E+01	4.8238E+00	-1.7400E+00	-9.6400E+00	4.0000E-01
6	-0.4177	3.0100E+03	-3.0050E+02	2.8337E+01	-1.1028E+00	2.0228E+01	4.8238E+00	-1.7400E+00	-9.6400E+00	4.0000E-01
7	-0.4137	3.0120E+03	-3.0060E+02	2.8357E+01	-1.1028E+00	2.0228E+01	4.8238E+00	-1.7400E+00	-9.6400E+00	4.0000E-01
8	-0.4097	3.0140E+03	-3.0070E+02	2.8377E+01	-1.1028E+00	2.0228E+01	4.8238E+00	-1.7400E+00	-9.6400E+00	4.0000E-01
9	-0.4057	3.0160E+03	-3.0080E+02	2.8397E+01	-1.1028E+00	2.0228E+01	4.8238E+00	-1.7400E+00	-9.6400E+00	4.0000E-01
10	-0.4017	3.0180E+03	-3.0090E+02	2.8417E+01	-1.1028E+00	2.0228E+01	4.8238E+00	-1.7400E+00	-9.6400E+00	4.0000E-01
11	-0.3977	3.0200E+03	-3.0100E+02	2.8437E+01	-1.1028E+00	2.0228E+01	4.8238E+00	-1.7400E+00	-9.6400E+00	4.0000E-01
12	-0.3937	3.0220E+03	-3.0110E+02	2.8457E+01	-1.1028E+00	2.0228E+01	4.8238E+00	-1.7400E+00	-9.6400E+00	4.0000E-01
13	-0.3897	3.0240E+03	-3.0120E+02	2.8477E+01	-1.1028E+00	2.0228E+01	4.8238E+00	-1.7400E+00	-9.6400E+00	4.0000E-01
14	-0.3857	3.0260E+03	-3.0130E+02	2.8497E+01	-1.1028E+00	2.0228E+01	4.8238E+00	-1.7400E+00	-9.6400E+00	4.0000E-01
15	-0.3817	3.0280E+03	-3.0140E+02	2.8517E+01	-1.1028E+00	2.0228E+01	4.8238E+00	-1.7400E+00	-9.6400E+00	4.0000E-01
16	-0.3777	3.0300E+03	-3.0150E+02	2.8537E+01	-1.1028E+00	2.0228E+01	4.8238E+00	-1.7400E+00	-9.6400E+00	4.0000E-01
17	-0.3737	3.0320E+03	-3.0160E+02	2.8557E+01	-1.1028E+00	2.0228E+01	4.8238E+00	-1.7400E+00	-9.6400E+00	4.0000E-01
18	-0.3697	3.0340E+03	-3.0170E+02	2.8577E+01	-1.1028E+00	2.0228E+01	4.8238E+00	-1.7400E+00	-9.6400E+00	4.0000E-01
19	-0.3657	3.0360E+03	-3.0180E+02	2.8597E+01	-1.1028E+00	2.0228E+01	4.8238E+00	-1.7400E+00	-9.6400E+00	4.0000E-01
20	-0.3617	3.0380E+03	-3.0190E+02	2.8617E+01	-1.1028E+00	2.0228E+01	4.8238E+00	-1.7400E+00	-9.6400E+00	4.0000E-01
21	-0.3577	3.0400E+03	-3.0200E+02	2.8637E+01	-1.1028E+00	2.0228E+01	4.8238E+00	-1.7400E+00	-9.6400E+00	4.0000E-01
22	-0.3537	3.0420E+03	-3.0210E+02	2.8657E+01	-1.1028E+00	2.0228E+01	4.8238E+00	-1.7400E+00	-9.6400E+00	4.0000E-01
23	-0.3497	3.0440E+03	-3.0220E+02	2.8677E+01	-1.1028E+00	2.0228E+01	4.8238E+00	-1.7400E+00	-9.6400E+00	4.0000E-01
24	-0.3457	3.0460E+03	-3.0230E+02	2.8697E+01	-1.1028E+00	2.0228E+01	4.8238E+00	-1.7400E+00	-9.6400E+00	4.0000E-01
25	-0.3417	3.0480E+03	-3.0240E+02	2.8717E+01	-1.1028E+00	2.0228E+01	4.8238E+00	-1.7400E+00	-9.6400E+00	4.0000E-01
26	-0.3377	3.0500E+03	-3.0250E+02	2.8737E+01	-1.1028E+00	2.0228E+01	4.8238E+00	-1.7400E+00	-9.6400E+00	4.0000E-01
27	-0.3337	3.0520E+03	-3.0260E+02	2.8757E+01	-1.1028E+00	2.0228E+01	4.8238E+00	-1.7400E+00	-9.6400E+00	4.0000E-01
28	-0.3297	3.0540E+03	-3.0270E+02	2.8777E+01	-1.1028E+00	2.0228E+01	4.8238E+00	-1.7400E+00	-9.6400E+00	4.0000E-01
29	-0.3257	3.0560E+03	-3.0280E+02	2.8797E+01	-1.1028E+00	2.0228E+01	4.8238E+00	-1.7400E+00	-9.6400E+00	4.0000E-01
30	-0.3217	3.0580E+03	-3.0290E+02	2.8817E+01	-1.1028E+00	2.0228E+01	4.8238E+00	-1.7400E+00	-9.6400E+00	4.0000E-01
31	-0.3177	3.0600E+03	-3.0300E+02	2.8837E+01	-1.1028E+00	2.0228E+01	4.8238E+00	-1.7400E+00	-9.6400E+00	4.0000E-01
32	-0.3137	3.0620E+03	-3.0310E+02	2.8857E+01	-1.1028E+00	2.0228E+01	4.8238E+00	-1.7400E+00	-9.6400E+00	4.0000E-01
33	-0.3097	3.0640E+03	-3.0320E+02	2.8877E+01	-1.1028E+00	2.0228E+01	4.8238E+00	-1.7400E+00	-9.6400E+00	4.0000E-01
34	-0.3057	3.0660E+03	-3.0330E+02	2.8897E+01	-1.1028E+00	2.0228E+01	4.8238E+00	-1.7400E+00	-9.6400E+00	4.0000E-01
35	-0.3017	3.0680E+03	-3.0340E+02	2.8917E+01	-1.1028E+00	2.0228E+01	4.8238E+00	-1.7400E+00	-9.6400E+00	4.0000E-01
36	-0.2977	3.0700E+03	-3.0350E+02	2.8937E+01	-1.1028E+00	2.0228E+01	4.8238E+00	-1.7400E+00	-9.6400E+00	4.0000E-01
37	-0.2937	3.0720E+03	-3.0360E+02	2.8957E+01	-1.1028E+00	2.0228E+01	4.8238E+00	-1.7400E+00	-9.6400E+00	4.0000E-01

Figure A.5.- Concluded.

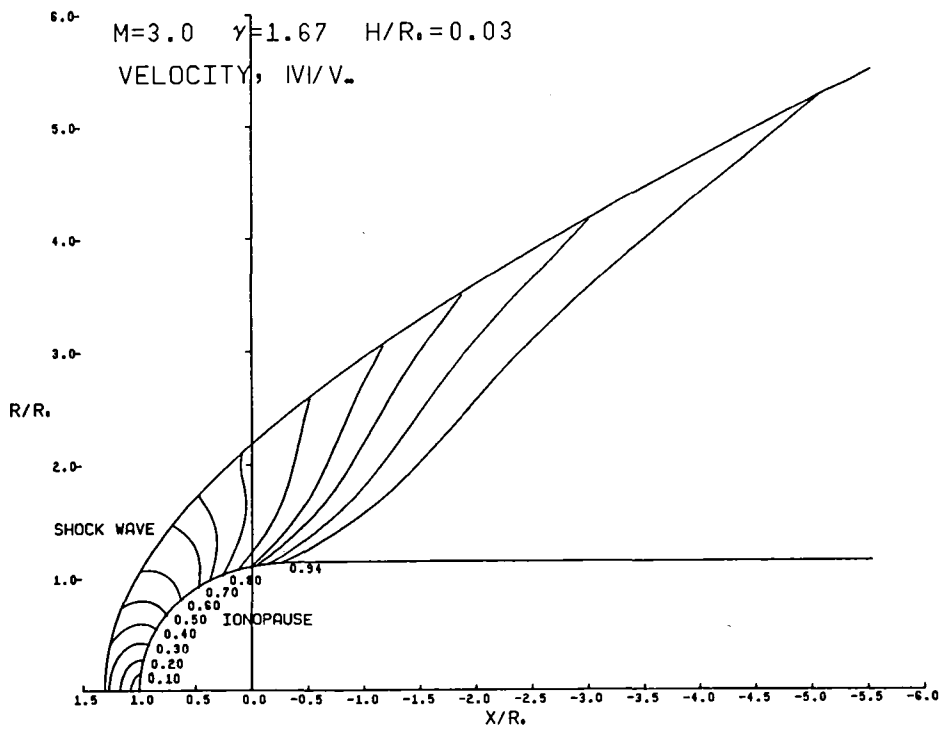
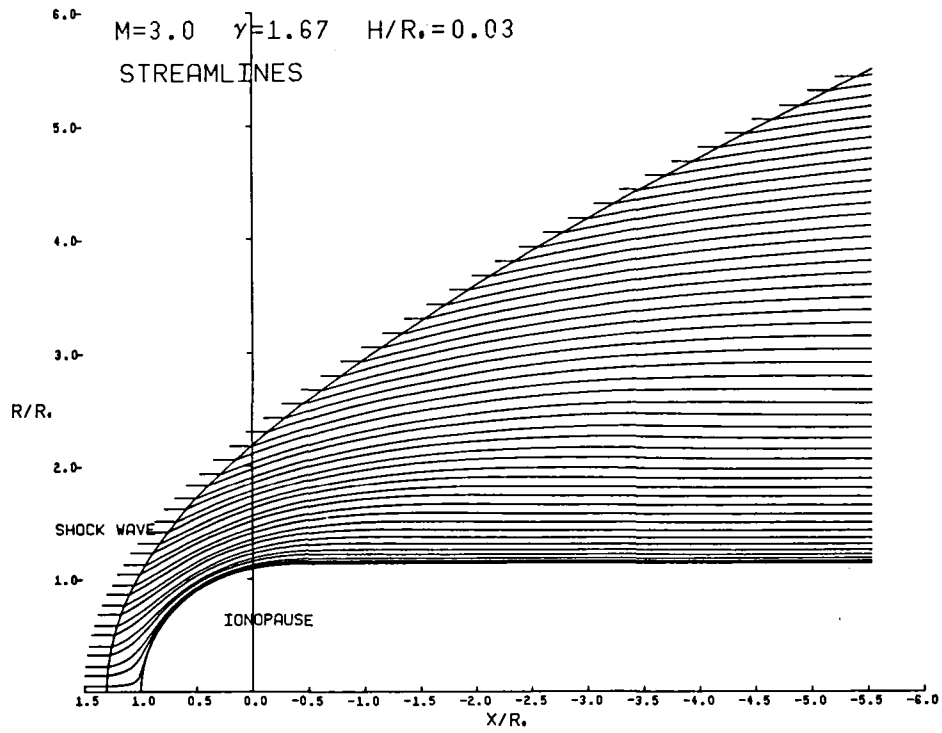


Figure A.6.- Plot output for sample case.

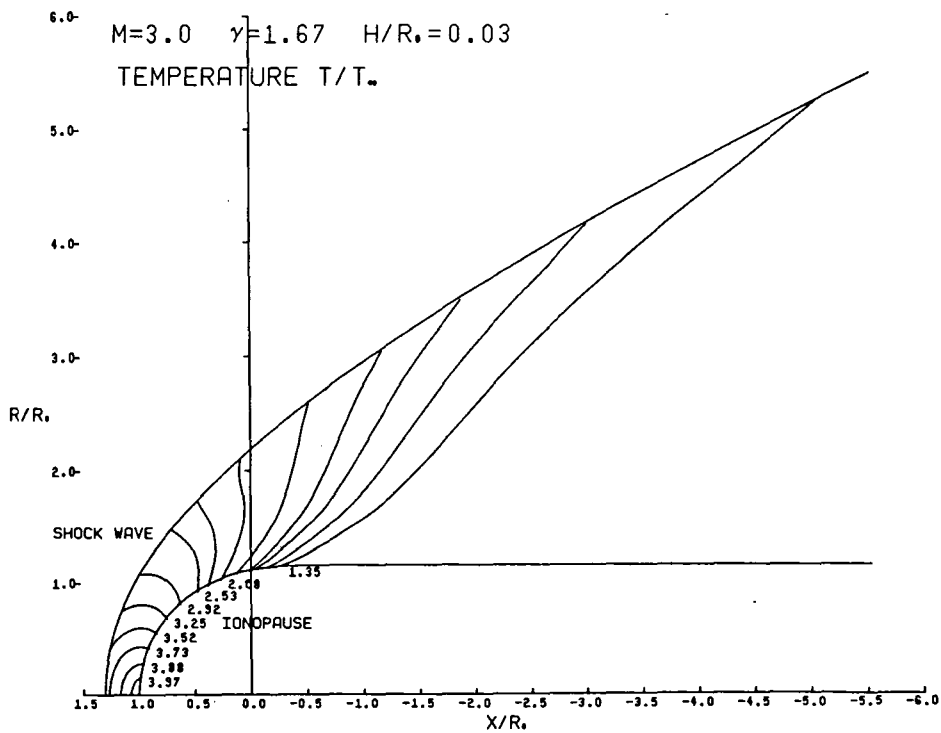
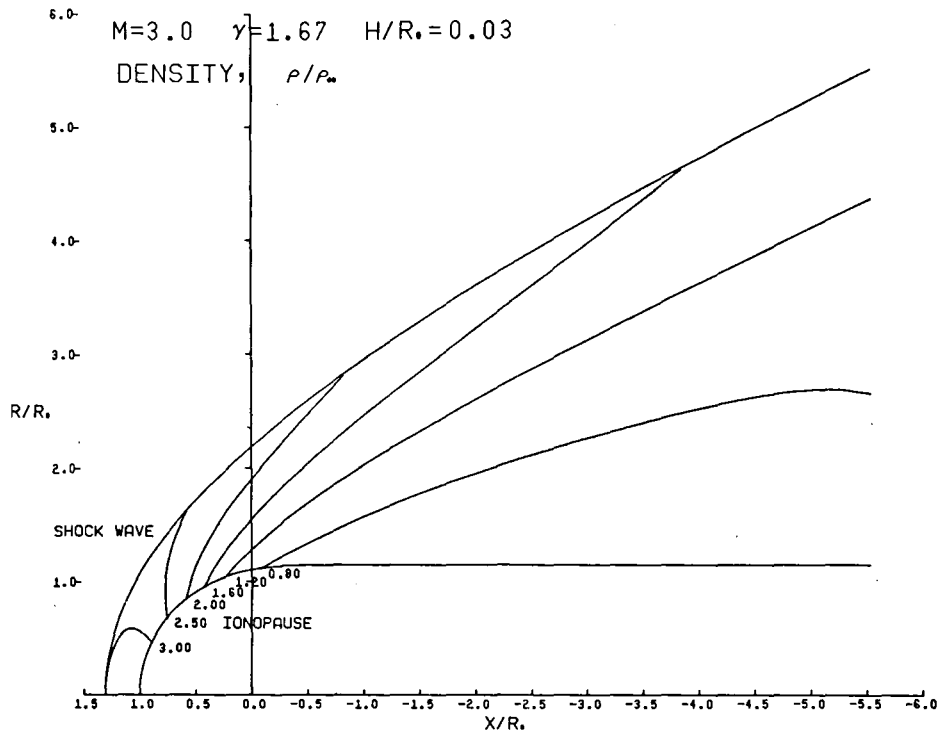


Figure A.6.- Continued

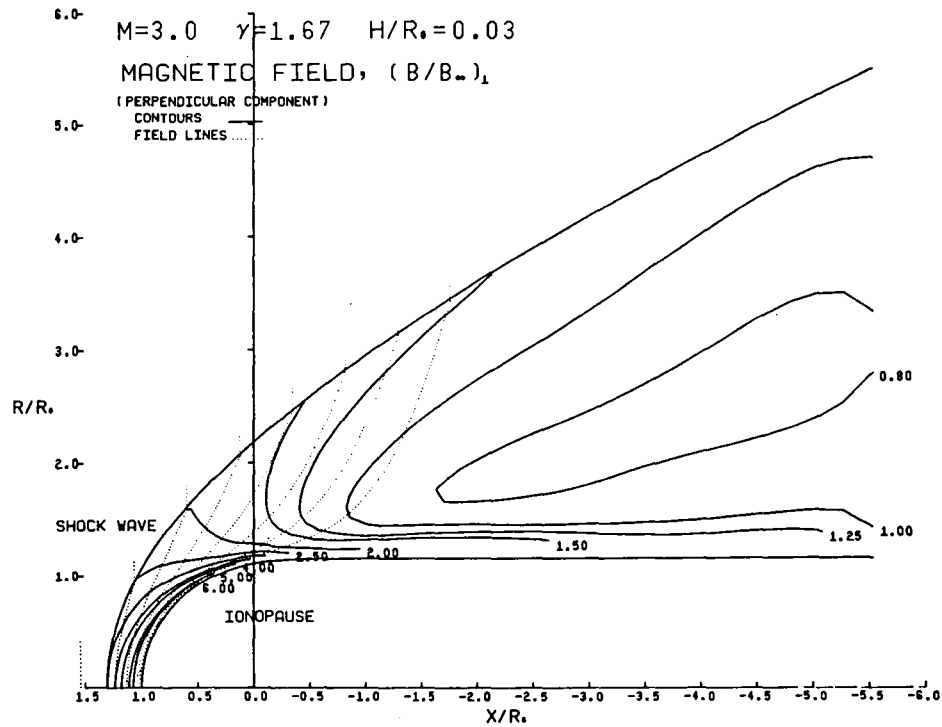
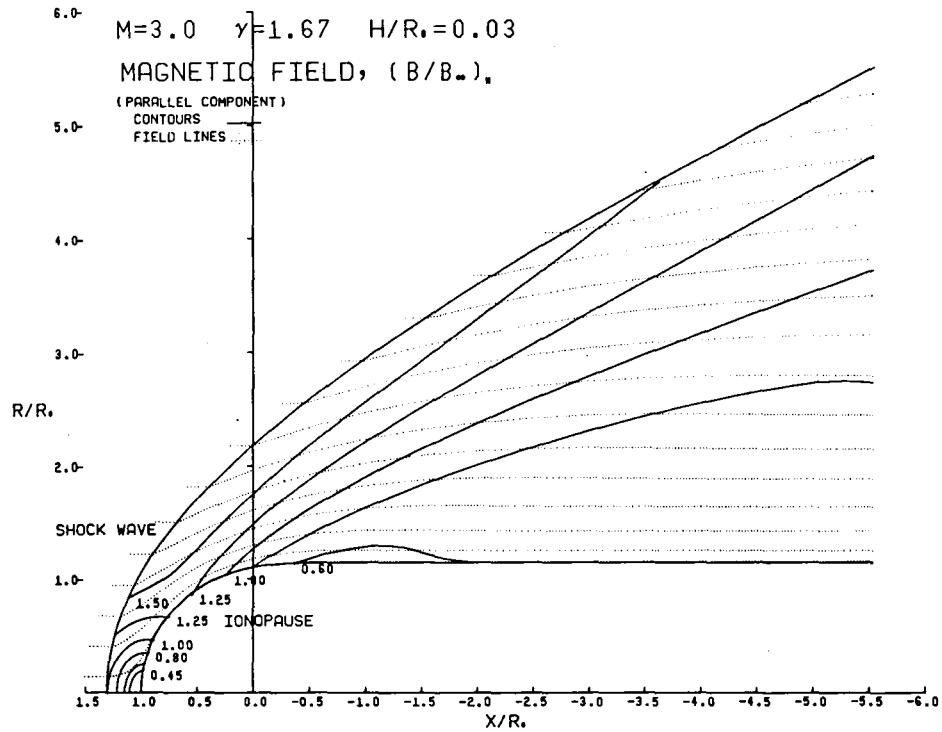


Figure A.6.- Continued

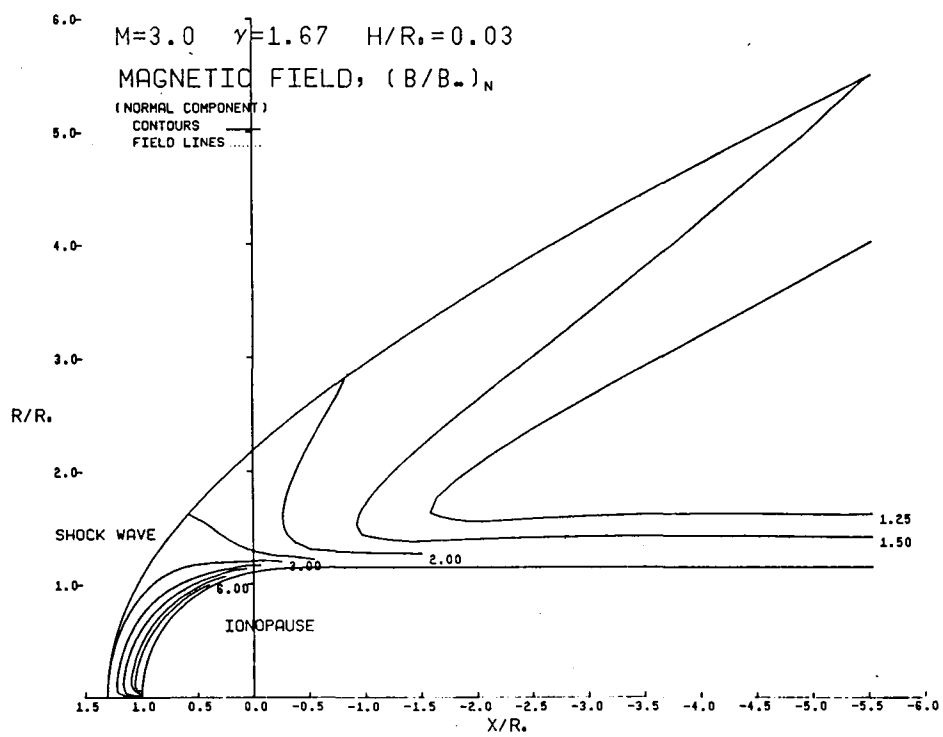
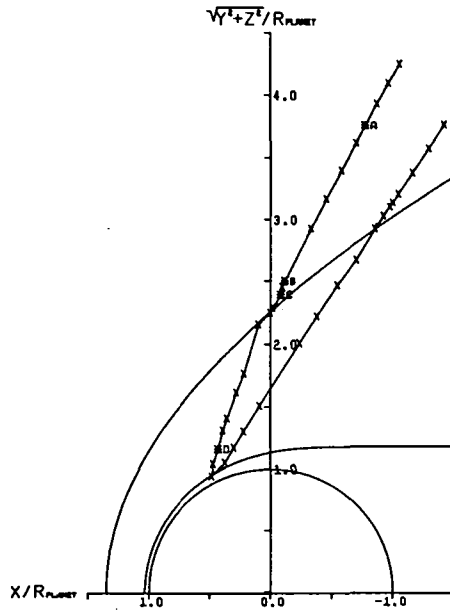
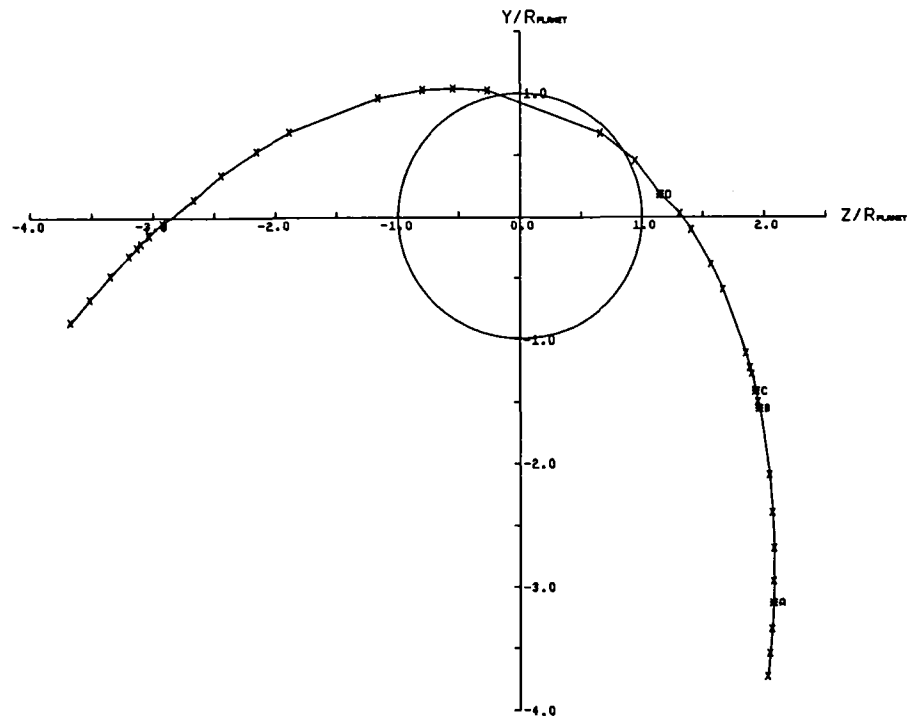


Figure A.6.- Continued



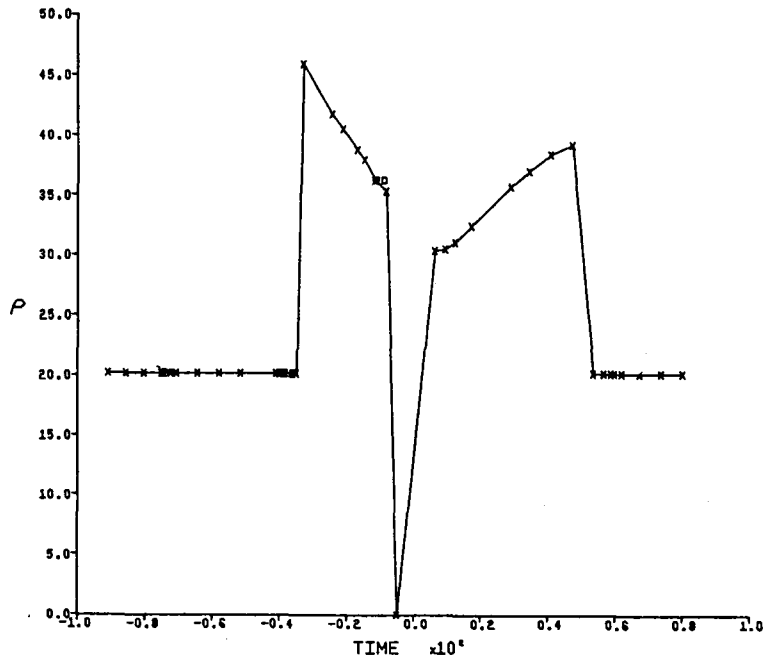
TRAJECTORY
(X-R PROJECTION)



TRAJECTORY
(Y-Z PROJECTION)

Figure A.6.- Continued

DENSITY vs TIME



TEMPERATURE vs TIME

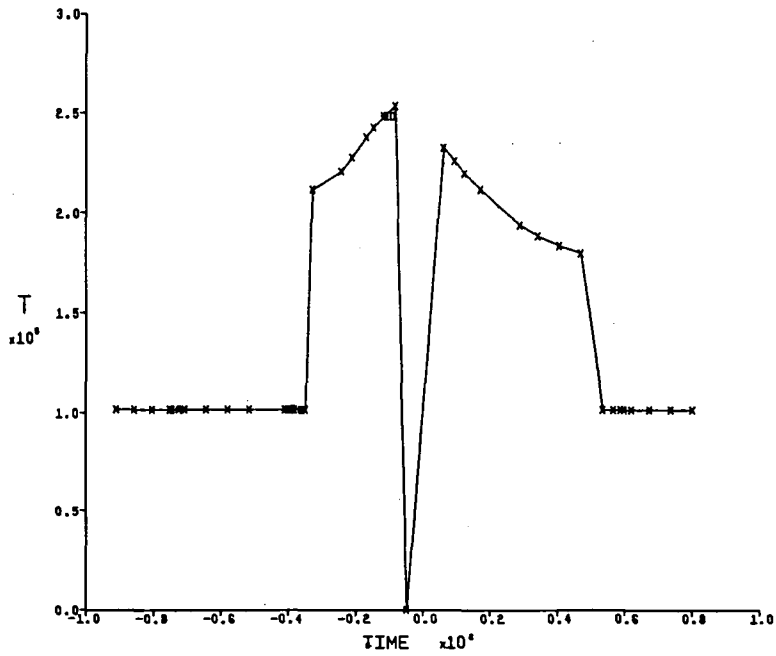


Figure A.6.- Continued.

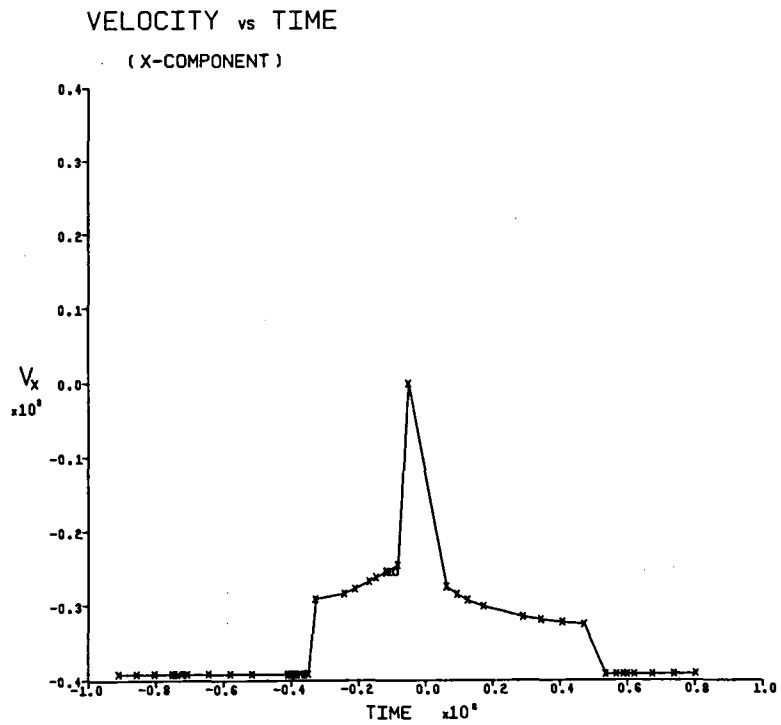
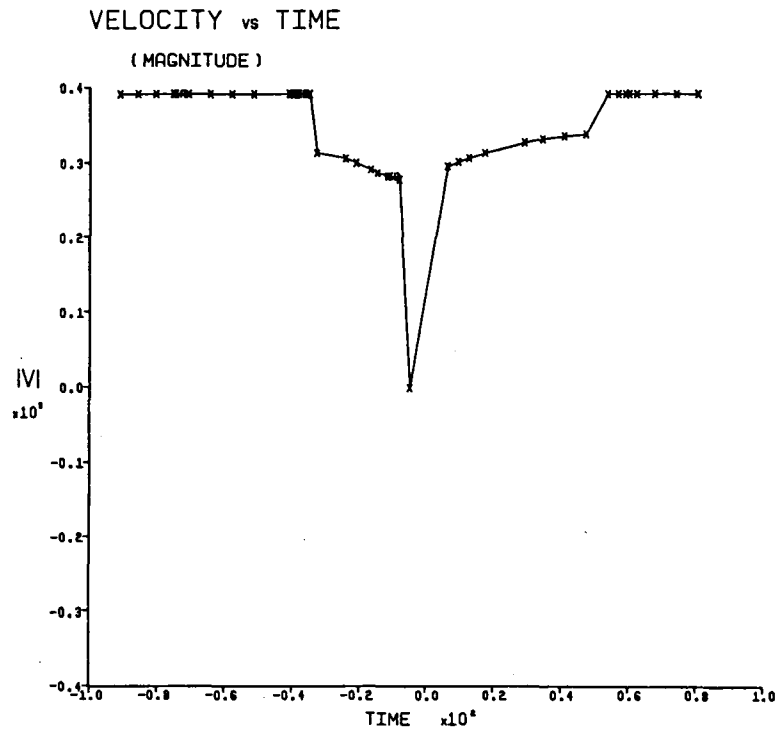


Figure A.6.- Continued

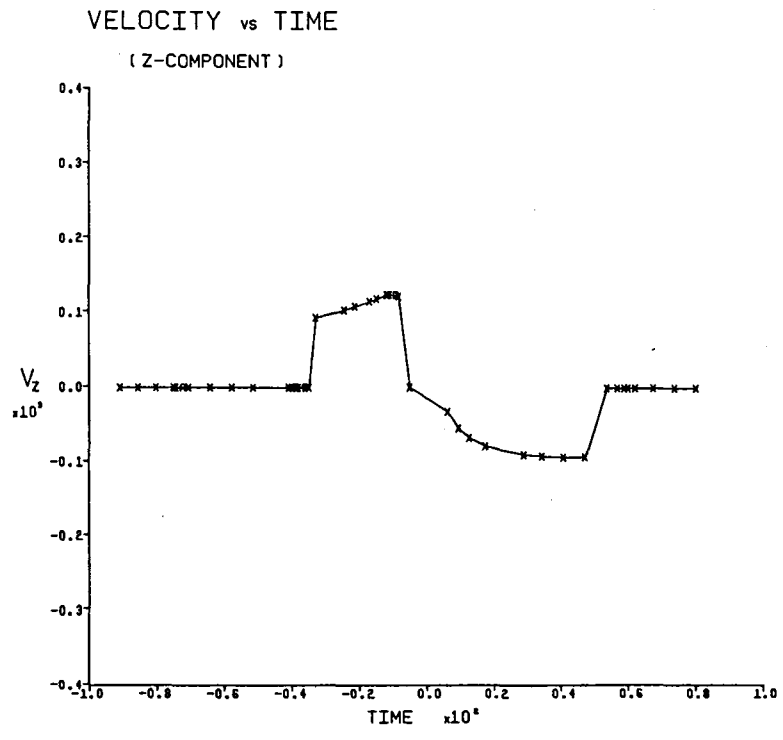
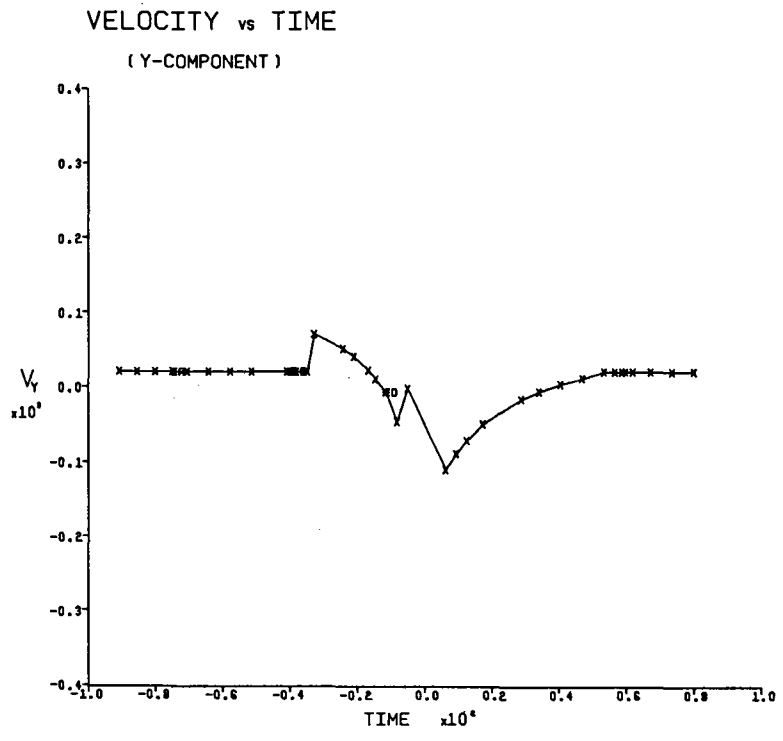


Figure A.6.- Continued.

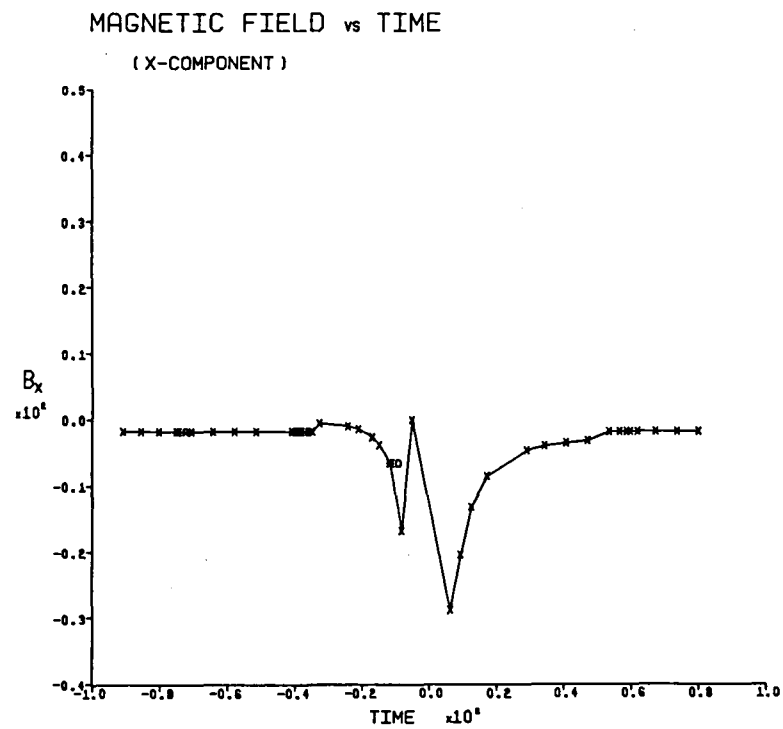
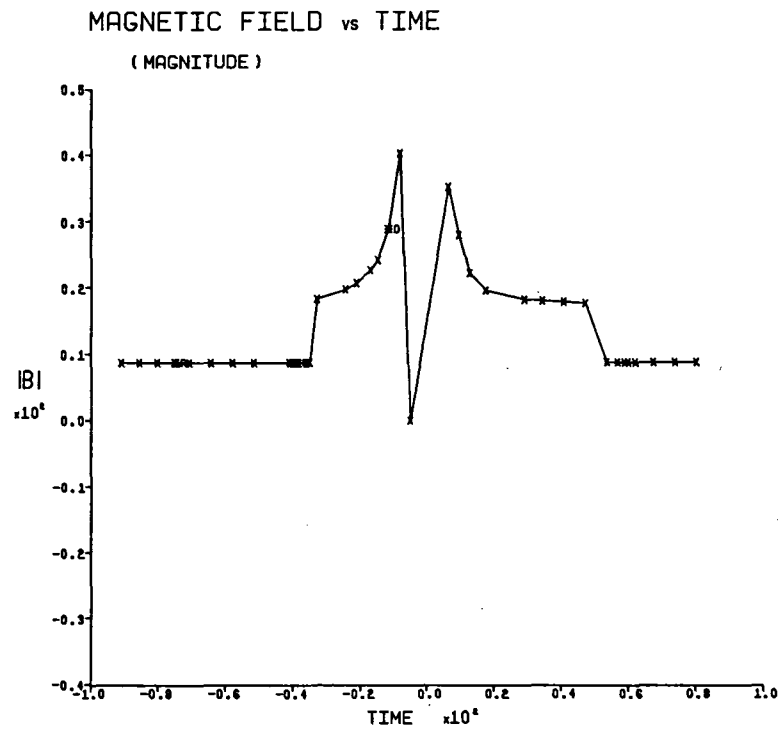


Figure A.6.- Continued.

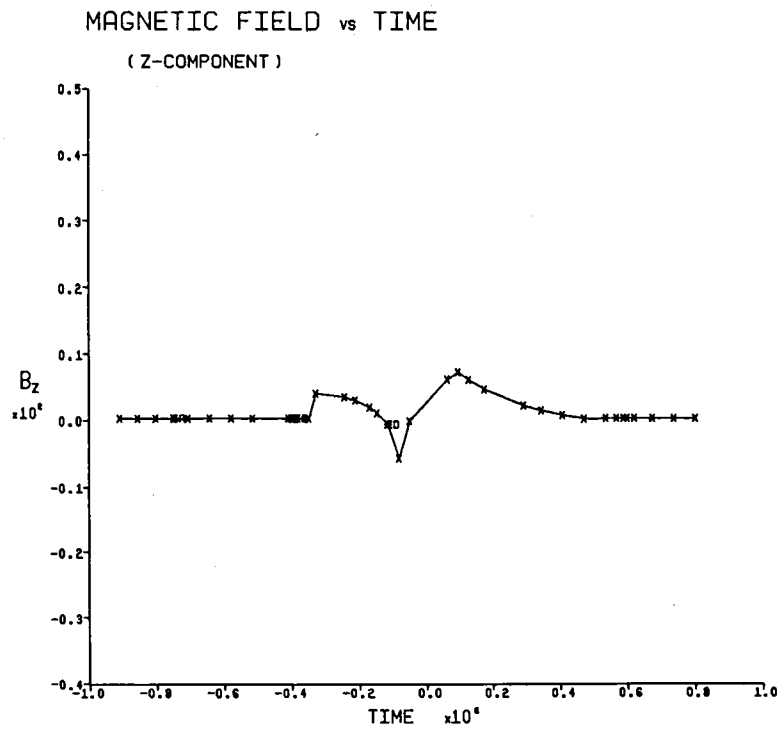
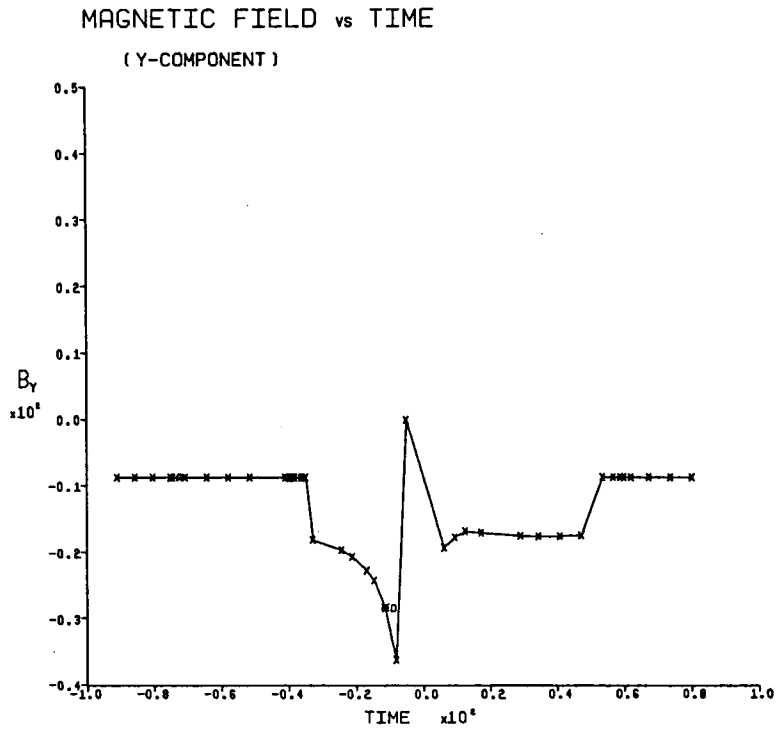


Figure A.6.- Concluded.

APPENDIX B

LISTING OF COMPUTER PROGRAM

```

PROGRAM MAIN (INPUT, OUTPUT, TAPE5=INPUT, TAPE6=OUTPUT,
      TAPE1, TAPE4, TAPE9)
LOGICAL LPRUN, LPPFL, LPRS, LPRCON, LPRR, LPLLOT, LTRAJ, LRSTRT
COMMON //PROPT/ LPRUN, LPPFL, LPRS, LPRCON, LPRR, LPLLOT, LTRAJ, LRSTRT
WRITE(6,200)
CALL ECHINP
NFAI(5,100) NCASE
ND 2: ICASE=1, NCASE
CALL INPUT
IF (LPRUN) GO TO 10
CALL ALJUNT
CALL WPCN
GO TO 15
10 CALL REUN
15 CONTINUE
CALL FLOWST
IF (LPPFL) CALL FLOUT
IF (LPRS) CALL SROUT
CALL SCOP
IF (LPRR) CALL ROUT
CALL CNTUR
IF (LTRAJ) CALL TRAJEC
20 CONTINUE
STOP
END
      MAIN      2
      MAIN      3
      PROPT     4
      MAIN      5
      MAIN      6
      MAIN      7
      MAIN      8
      MAIN      9
      MAIN     10
      MAIN     11
      MAIN     12
      MAIN     13
      MAIN     14
      MAIN     15
      MAIN     16
      MAIN     17
      MAIN     18
      MAIN     19
      MAIN     20
      MAIN     21
      MAIN     22
      MAIN     23
      MAIN     24
      MAIN     25
      MAIN     26
      MAIN     27
      MAIN     28
      MAIN     29
      MAIN     30
      MAIN     31
      MAIN     32
      MAIN     33
      MAIN     34
      MAIN     35
      MAIN     36
      MAIN     37
      MAIN     38
      MAIN     39
      MAIN     40
      MAIN     41
      MAIN     42
      MAIN     43
      MAIN     44
      MAIN     45
      MAIN     46
      MAIN     47
      MAIN     48
      MAIN     49
      MAIN     50
      MAIN     51
      MAIN     52
      MAIN     53
      MAIN     54
      MAIN     55
      MAIN     56
      MAIN     57
      MAIN     58
      MAIN     59
      MAIN     60
      MAIN     61
      MAIN     62
      MAIN     63
      MAIN     64
      MAIN     65
      MAIN     66
      MAIN     67
      MAIN     68
      MAIN     69
      MAIN     70
      MAIN     71
      MAIN     72
      MAIN     73
      MAIN     74
      MAIN     75
      MAIN     76
      MAIN     77
      MAIN     78
      MAIN     79
      MAIN     80
      MAIN     81
      MAIN     82
      MAIN     83
      MAIN     84
      MAIN     85
      MAIN     86
      MAIN     87
      MAIN     88
      MAIN     89
      MAIN     90
      MAIN     91
      MAIN     92
      MAIN     93
      MAIN     94
      MAIN     95
      MAIN     96
      MAIN     97
      MAIN     98
      MAIN     99
      MAIN    100
      ANGEI     2
      ANGEI     3
      ANGEI     4
      ANGEI     5
      ANGEI     6
      ANGEI     7
      ANGEI     8
      ANGEI     9
      ANGEI    10
      ANGEI    11
      ANGEI    12
      ANGEI    13
      ANGEI    14
      ANGEI    15
      ANGEI    16
      ANGEI    17
      ANGEI    18
      ANGEI    19
      ANGEI    20
      ANGEI    21
      ANGEI    22
      ANGEI    23
      ANGEI    24
      ANGEI    25
      ANGEI    26
      ANGEI    27
      ANGEI    28
      ANGEI    29
      ANGEI    30
      ANGEI    31
      ANGEI    32
      ANGEI    33
      ANGEI    34
      ANGEI    35
      ANGEI    36
      ANGEI    37
      ANGEI    38
      ANGEI    39
      ANGEI    40
      ANGEI    41
      ANGEI    42
      ANGEI    43
      ANGEI    44
      ANGEI    45
      ANGEI    46
      ANGEI    47
      ANGEI    48
      ANGEI    49
      ANGEI    50
      ANGEI    51
      ANGEI    52
      ANGEI    53
      ANGEI    54
      ANGEI    55
      ANGEI    56
      ANGEI    57
      ANGEI    58
      ANGEI    59
      ANGEI    60
      ANGEI    61
      ANGEI    62
      ANGEI    63
      ANGEI    64
      ANGEI    65
      ANGEI    66
      ANGEI    67
      ANGEI    68
      ANGEI    69
      ANGEI    70
      ANGEI    71
      ANGEI    72
      ANGEI    73
      ANGEI    74
      ANGEI    75
      ANGEI    76
      ANGEI    77
      ANGEI    78
      ANGEI    79
      ANGEI    80
      ANGEI    81
      ANGEI    82
      ANGEI    83
      ANGEI    84
      ANGEI    85
      ANGEI    86
      ANGEI    87
      ANGEI    88
      ANGEI    89
      ANGEI    90
      ANGEI    91
      ANGEI    92
      ANGEI    93
      ANGEI    94
      ANGEI    95
      ANGEI    96
      ANGEI    97
      ANGEI    98
      ANGEI    99
      ANGEI   100
      ANGEI   101
      ANGEI   102
      ANGEI   103
      ANGEI   104
      ANGEI   105
      ANGEI   106
      ANGEI   107
      ANGEI   108
      ANGEI   109
      ANGEI   110
      ANGEI   111
      ANGEI   112
      ANGEI   113
      ANGEI   114
      ANGEI   115
      ANGEI   116

```

```

43 ELLINF=EL
GAMEL=ANG
RETURN
      ANGEI     33
      ANGEI     34
      ANGEI     35
      ANGEI     36
      ANGEI     37
      ANGEI     38
      ANGEI     39
      ANGEI     40
      ANGEI     41
      ANGEI     42
      ANGEI     43
      ANGEI     44
      ANGEI     45
      ANGEI     46
      ANGEI     47
      ANGEI     48
      ANGEI     49
      ANGEI     50
      ANGEI     51
      ANGEI     52
      ANGEI     53
      ANGEI     54
      ANGEI     55
      ANGEI     56
      ANGEI     57
      ANGEI     58
      ANGEI     59
      ANGEI     60
      ANGEI     61
      ANGEI     62
      ANGEI     63
      ANGEI     64
      ANGEI     65
      ANGEI     66
      ANGEI     67
      ANGEI     68
      ANGEI     69
      ANGEI     70
      ANGEI     71
      ANGEI     72
      ANGEI     73
      ANGEI     74
      ANGEI     75
      ANGEI     76
      ANGEI     77
      ANGEI     78
      ANGEI     79
      ANGEI     80
      ANGEI     81
      ANGEI     82
      ANGEI     83
      ANGEI     84
      ANGEI     85
      ANGEI     86
      ANGEI     87
      ANGEI     88
      ANGEI     89
      ANGEI     90
      ANGEI     91
      ANGEI     92
      ANGEI     93
      ANGEI     94
      ANGEI     95
      ANGEI     96
      ANGEI     97
      ANGEI     98
      ANGEI     99
      ANGEI    100
      ANGEI    101
      ANGEI    102
      ANGEI    103
      ANGEI    104
      ANGEI    105
      ANGEI    106
      ANGEI    107
      ANGEI    108
      ANGEI    109
      ANGEI    110
      ANGEI    111
      ANGEI    112
      ANGEI    113
      ANGEI    114
      ANGEI    115
      ANGEI    116

```

```

SUBROUTINE ANGEI(ELLINF,GAMEL,I,J)
      ANGEI     2
      ANGEI     3
      ANGEI     4
      ANGEI     5
      ANGEI     6
      ANGEI     7
      ANGEI     8
      ANGEI     9
      ANGEI    10
      ANGEI    11
      ANGEI    12
      ANGEI    13
      ANGEI    14
      ANGEI    15
      ANGEI    16
      ANGEI    17
      ANGEI    18
      ANGEI    19
      ANGEI    20
      ANGEI    21
      ANGEI    22
      ANGEI    23
      ANGEI    24
      ANGEI    25
      ANGEI    26
      ANGEI    27
      ANGEI    28
      ANGEI    29
      ANGEI    30
      ANGEI    31
      ANGEI    32
      ANGEI    33
      ANGEI    34
      ANGEI    35
      ANGEI    36
      ANGEI    37
      ANGEI    38
      ANGEI    39
      ANGEI    40
      ANGEI    41
      ANGEI    42
      ANGEI    43
      ANGEI    44
      ANGEI    45
      ANGEI    46
      ANGEI    47
      ANGEI    48
      ANGEI    49
      ANGEI    50
      ANGEI    51
      ANGEI    52
      ANGEI    53
      ANGEI    54
      ANGEI    55
      ANGEI    56
      ANGEI    57
      ANGEI    58
      ANGEI    59
      ANGEI    60
      ANGEI    61
      ANGEI    62
      ANGEI    63
      ANGEI    64
      ANGEI    65
      ANGEI    66
      ANGEI    67
      ANGEI    68
      ANGEI    69
      ANGEI    70
      ANGEI    71
      ANGEI    72
      ANGEI    73
      ANGEI    74
      ANGEI    75
      ANGEI    76
      ANGEI    77
      ANGEI    78
      ANGEI    79
      ANGEI    80
      ANGEI    81
      ANGEI    82
      ANGEI    83
      ANGEI    84
      ANGEI    85
      ANGEI    86
      ANGEI    87
      ANGEI    88
      ANGEI    89
      ANGEI    90
      ANGEI    91
      ANGEI    92
      ANGEI    93
      ANGEI    94
      ANGEI    95
      ANGEI    96
      ANGEI    97
      ANGEI    98
      ANGEI    99
      ANGEI   100
      ANGEI   101
      ANGEI   102
      ANGEI   103
      ANGEI   104
      ANGEI   105
      ANGEI   106
      ANGEI   107
      ANGEI   108
      ANGEI   109
      ANGEI   110
      ANGEI   111
      ANGEI   112
      ANGEI   113
      ANGEI   114
      ANGEI   115
      ANGEI   116

```

```

ELLINF=QUAD(X0,R0,ELO,X,Y)
GAMQ=QUAD(X0,R0,GAM0,X,Y)
RETURN
300 CONTINUE
  IF (SLP2E.LT. 0.0) GO TO 350
  IF (XRF(IST,JJ-1).GT. X) GO TO 300
  JJ=JJ+1
  IF (JJ.LT. N) GO TO 340
C
C *****STREAM BOUNDARY CUTS QUADRILATERAL CONTAINING POINT
C
  IF (XRF(IST+1,JJ-1).LT. XST(IST,1)) GO TO 460
  X0(4)=XRF(IST+1,JJ-1)
  P0(4)=RPF(IST+1,JJ-1)
  ELO(4)=ELRF(IST+1,JJ-1)
  GAMQ(4)=GAMRF(IST+1,JJ-1)
41) IF (IST.GT. NST) GO TO 470
  X0(1)=XRF(IST+1,JJ)
  P0(1)=RPF(IST+1,JJ)
  ELO(1)=ELRF(IST+1,JJ)
  GAMQ(1)=GAMRF(IST+1,JJ)
42) IF (XRF(IST,JJ-1).LT. XST(IST-1,1)) GO TO 490
  X0(3)=XRF(IST,JJ-1)
  P0(3)=RPF(IST,JJ-1)
  ELO(3)=ELRF(IST,JJ-1)
  GAMQ(3)=GAMRF(IST,JJ-1)
450 X0(2)=XRF(IST,NS)
  P0(2)=RPF(IST,NS)
  ELO(2)=ELRF(IST,NS)
  GAMQ(2)=GAMRF(IST,NS)
  ELLINF=QUAD(X0,R0,ELO,X,Y)
  GAMQ=QUAD(X0,R0,GAM0,X,Y)
  RETURN
460 X0(4)=XRF(JJ)
  P0(4)=RPF(JJ)
  ELO(4)=EL
  GAMQ(4)=ANG
  GO TO 420
47) X0(1)=ZPLNT
  CALL ASHKE(X0(1),R0(1),GAM0(1),ELO(1))
  GO TO 430
490 X0(1)=XST(IST-1,1)
  CALL ASHKE(X0(1),R0(1),GAM0(1),ELO(1))
  GO TO 450
C
C *****QUADRILATERAL CONTAINING POINT IS REFLEXIVE
C
52) JJ=JJ-1
  SLOPE=(Y-RPF(IST,JJ-1))/(X-XRF(IST,JJ-1))
  *SLOPE1=(RPF(IST+1,JJ-1)-RPF(IST,JJ-1))
  / (XRF(IST+1,JJ-1)-XRF(IST,JJ-1))
  *SLOPE2=(RPF(IST,JJ)-RPF(IST,JJ-1))/(XRF(IST,JJ)-XRF(IST,JJ-1))
  IF (SLOPE2.LT. SLOPE) GO TO 540
  IF (SLOPE2.GT. SLOPE) GO TO 540
  POINT IS CLOSE TO SHOCK - NEED VALUES ON SHOCK
C
C *****
C
53) X0(1)=XRF(IST+1,JJ)
  CALL ASHKE(X0(1),R0(1),GAM0(1),ELO(1))
  SLOPE=(P0(1)-Y)/(X0(1)-X)
  SLOPE2=(RPF(IST,JJ)-RPF(IST,JJ-1))/(XRF(IST,JJ)-XRF(IST,JJ-1))
  IF (SLOPE2.LT. SLOPE) GO TO 300
54) X0(4)=XRF(JJ)
  P0(4)=RPF(JJ)
  ELO(4)=EL
  GAMQ(4)=ANG
  GO TO 300
56) X0(1)=XST(IST-1,1)
  CALL ASHKE(X0(1),R0(1),GAM0(1),ELO(1))
  GO TO 300
58) N1=N2
60) CONTINUE
C
C *****PROGRAM SHOULD NEVER REACH THIS CONDITION
C
  WRITE(6,1000)
  STOP
100) FORMAT(14,10X,14HERROR IN ANGEL//2X,
  * 35HPROGRAM CAUSE - X PLOT IS TOO LARGE)
  END

```

```

ANGEL 117
ANGEL 118
ANGEL 119
ANGEL 120
ANGEL 121
ANGEL 122
ANGEL 123
ANGEL 124
ANGEL 125
ANGEL 126
ANGEL 127
ANGEL 128
ANGEL 129
ANGEL 130
ANGEL 131
ANGEL 132
ANGEL 133
ANGEL 134
ANGEL 135
ANGEL 136
ANGEL 137
ANGEL 138
ANGEL 139
ANGEL 140
ANGEL 141
ANGEL 142
ANGEL 143
ANGEL 144
ANGEL 145
ANGEL 146
ANGEL 147
ANGEL 148
ANGEL 149
ANGEL 150
ANGEL 151
ANGEL 152
ANGEL 153
ANGEL 154
ANGEL 155
ANGEL 156
ANGEL 157
ANGEL 158
ANGEL 159
ANGEL 160
ANGEL 161
ANGEL 162
ANGEL 163
ANGEL 164
ANGEL 165
ANGEL 166
ANGEL 167
ANGEL 168
ANGEL 169
ANGEL 170
ANGEL 171
ANGEL 172
ANGEL 173
ANGEL 174
ANGEL 175
ANGEL 176
ANGEL 177
ANGEL 178
ANGEL 179
ANGEL 180
ANGEL 181
ANGEL 182
ANGEL 183
ANGEL 184
ANGEL 185
ANGEL 186
ANGEL 187
ANGEL 188
ANGEL 189
ANGEL 190
ANGEL 191
ANGEL 192
ANGEL 193
ANGEL 194
ANGEL 195
ANGEL 196
ANGEL 197
ANGEL 198
C
C *****SUBROUTINE BCOMP
C
THIS SUBROUTINE CALCULATES THE COMPONENTS OF THE MAGNETIC FIELD
PARALLEL, PERPENDICULAR AND NORMAL TO THE FLOW.
C
COMMON /ROUNDS/ XROD(100),YROD(100),XSHK(100),YSHK(100),
* NRMAX,NXMAX,AMACH,GAMMA,HRO,MHIMFY
COMMON /FLOWS/ XC(20,100),YC(20,100),VF(20,100),RHOVF(20,100)
LEVEL 2, RPAPA,RPERR,RPORP,PHAG,RANG
COMMON /RANGES/ RPABA(20,100),RPERP(20,100),RNDRMI(20,100),
* RMAC(20,100),RANG(20,100)
LOGICAL LPERUN,LPRFL,LPRST,LPRCON,LPRN,LPLDT,LTRAJ,LRSTRT
COMMON /RATN/ ANGP,ANGN,RPCON,RCOM(20)
DIMENSION S(100,6),N(100),A(6),XLSO(100),YLSO(100)
DATA V1000,2,0/
C
C *****CALCULATE PERPENDICULAR FIELD LINES
C
  IF (KAPCN.EQL. 0.AND. 0.NOT.LORS .AND. 0.NOT.LTRAJ) RETURN
  CALL RSTP
  CALL RELGAN
C
C *****CALCULATE R/RINF AND EL/ELINF AT EACH GRID POINT, THEN SMOOTH
C *****ALONG CONSTANT-T LINES, USING FIFTH ORDER LEAST SQUARES FIT
C
  NPN=NRMAX-1
  NYN=NYMAX-1
  DO 1, I=2, NXMAX
  *NRN(NRMAX, I)=RINF(NRMAX, I)
  CALL ANGEL(ELLINF,SLOPE,NRMAX, I)
  *RPN(NRMAX, I)=ELINF
  RANG(NRMAX, I)=SLOPEL
  DO 2, J=2, NYN
  *NRN(I, J)=RINF(I, J)
  CALL ANGEL(ELLINF,SLOPEL, I, J)
  *RPN(I, J)=ELINF
  RANG(I, J)=SLOPEL
  *RPN(I, J)=ELINF
  *RANG(I, J)=SLOPEL
1) CONTINUE
  YLSO(I)=0.0
  DO 6, I=2, NYN
  DO 2, J=1, NXN
  *XLSO(J)=XLSO(J)+SQRT((YC(I, J)-YC(I, J))**2
  * +XC(I, J)-X(I, J))**2)
2) CONTINUE
  DO 4, J=1, NXMAX
  *YLSO(J)=RPERP(I, J)
4) CONTINUE
  CALL ELCOFY(NRMAX, S, XLSO, YLSO, V1, P, C, A, IFP)
  DO 5, J=1, NXMAX
  *YLSO(J)=YLSO(J)
  *RPN(I, J)=((R(6)*X+A(5))*R(4)+A(1))*Y+A(2))*Y+A(1)
5) CONTINUE
6) CONTINUE
C
C *****CALCULATE COMPONENTS OF MAGNETIC FIELD - PARALLEL, PERPENDICULAR,
C *****AND NORMAL TO DIRECTION FLOW
C
  DO 7, J=1, NYMAX
  *RPA(1, J)=VF(1, J)*RHOVF(1, J)
  DO 7, I=2, NRMAX
  *RPA(I, J)=VF(I, J)*RHOVF(I, J)
  *RPN(I, J)=RPERP(I, J)*RHOVF(I, J)
  *NRN(I, J)=RNRN(I, J)*RHOVF(I, J)
7) CONTINUE
  RETURN
  END
C
C *****SUBROUTINE RELGAN
C
LEVEL 2, NR, NBF, XRF, RPF, ELRF, GAMRF
COMMON /RVAL/ NR, NBF(51), XRF(51,100), RPF(51,100), ELRF(51,100),
* GAMRF(51,100)
COMMON /NSTRM/ ZPLNT, NZEND, NYADD, NYPLDT
LEVEL 2, XST, YST, NIMST, NST
COMMON /STREAM/ XST(50,152), YST(50,152), NIMST(50), NST
COMMON /SHOCKS/ DRSNV(1,2), DST(50)
DATA PIONZ /1.5707961327/
RELGAN 2
RVAL 3
RVAL 4
RVAL 5
RVAL 6
DRSTRN 2
STREAM 1
STREAM 2
SHOCKS 2
RELGAN 7
RELGAN 8

```



```

2 THIS SUBROUTINE CALCULATES THE MAGNITUDE AND DIRECTION OF
C EL/FIELD AT THE POINTS WHERE THE STREAMLINES INTERSECT THE
C MAGNETIC FIELD LINES WHICH ARE PERPENDICULAR TO THE FLOW
C IN POSTSTREAM
C
C NST(1)=0.5/YST(1,1)
C ND=1+2*NST
C NST(1)=.5/((YST(1,1)+YST(-1,1)))
10 CONTINUE
C
C SET ARRAYS TO FREE STREAM VALUES
C
C NST0=NST+1
C JRFMAX=NRFF(1)
C DO 10 I=1,NST+1
C   IF (NRF(I)) .LT. JRFMAX) GO TO 20
C   JRFMAX=NRFF(I)
30 CONTINUE
C
C DO 2: J=1,JRFMAX
C   DO 2: I=1,NST+1
C     ELRF(I,J)=1.0
C     GAMPF(I,J)=PI*ND
2: CONTINUE
C
C VALUER ALONG FIELD LINES WHICH CROSS STREAM
C
C DO 130 J=1,NNR
C   IF (J .GT. NRFF(1)) GO TO 100
C   D1=COROT((YRF(2,J)-YRF(1,J))**2+RNF(2,J)**2)*.0
C   ELRF(1,J)=D1*DST(1)
C   GAM1=PI*ND
C   NY2=YRF(3,J)-YRF(2,J)
C   NR2=NRFF(3,J)-NRFF(2,J)
C   NZ=COROT((NY2*NY2+NR2*NR2))
C   GAM2=ATAN(DR2/DX2)
C   ELRF(2,J)=D1*D2/(D1+D2)*(DST(2)+DST(1))
C   GAMPF(2,J)=(GAM1*D2+GAM2*D1)/(D1+D2)
C   GO TO 140
130 CONTINUE
C
C D1=COROT((YRF(2,J)-YRF(1,J))**2+RNF(2,J)**2)*.0
C   NY2=YRF(3,J)-YRF(2,J)
C   NR2=NRFF(3,J)-NRFF(2,J)
C   NZ=COROT((NY2*NY2+NR2*NR2))
C   GAM2=ATAN(DR2/DX2)
C   ELRF(2,J)=D1*D2/(D1+D2)*(DST(2)+DST(1))
C   GAMPF(2,J)=(D1*GAM2+D2*GAMPF(2,J-1))/(D1+D2)
C   GO TO 140
140 CONTINUE
C
C DO 110 I=1,3,NST
C   NI=D2
C   GAM1=GAM2
C   IF (NRF(I+1,J)) .LT. YST(I,1)) GO TO 120
C   NY2=YRF(I+1,J)-YRF(I,J)
C   NR2=NRFF(I+1,J)-NRFF(I,J)
C   NZ=COROT((NY2*NY2+NR2*NR2))
C   ELRF(I,J)=D1*D2/(D1+D2)*(DST(I-1)+DST(I))
C   GAM2=ATAN(DR2/DX2)
C   GAMPF(I,J)=(GAM1*D2+GAM2*D1)/(D1+D2)
110 CONTINUE
C
C 120 YS4=YRF(I,1)
C   CALL XCHK(I,ZPLOT,Y1,GAM1,EL1)
C   NY2=YS4-NRF(I,J)
C   NR2=NS4-NRFF(I,J)
C   NZ=COROT((NY2*NY2+NR2*NR2))
C   ELRF(I,J)=D1*(DST(I-1)+DST(I))/(D1+D2)
C   GAMPF(I,J)=(D1*GAM1+D2*GAMPF(I,J-1))/(D1+D2)
130 CONTINUE
C
C JRFMAX=NRFF(3)
C
C VALUER ALONG FIELD LINES WHICH END AT DOWNSTREAM BOUNDARY
C
C N1=N1+1
C DO 10: J=N1,JRFMAX
C   IF (J .GT. NRFF(1)) GO TO 150
C   D1=COROT((YRF(2,J)-YRF(1,J))**2+RNF(2,J)**2)*.0
C   ELRF(1,J)=D1*DST(1)
C   GAM1=PI*ND
C   NY2=YRF(3,J)-YRF(2,J)
C   NR2=NRFF(3,J)-NRFF(2,J)
C   NZ=COROT((NY2*NY2+NR2*NR2))
C   GAM2=ATAN(DR2/DX2)
C   ELRF(2,J)=D1*D2/(D1+D2)*(DST(2)+DST(1))
C   GAMPF(2,J)=(GAM1*D2+GAM2*D1)/(D1+D2)
C   GO TO 140
150: D1=COROT((YRF(2,J)-YRF(1,J))**2+RNF(2,J)-NRFF(2,J-1)**2)*.0

```

```

RELGAN      0
RELGAN      10
RELGAN      11
RELGAN      12
RELGAN      13
RELGAN      14
RELGAN      15
RELGAN      16
RELGAN      17
RELGAN      18
RELGAN      19
RELGAN      20
RELGAN      21
RELGAN      22
RELGAN      23
RELGAN      24
RELGAN      25
RELGAN      26
RELGAN      27
RELGAN      28
RELGAN      29
RELGAN      30
RELGAN      31
RELGAN      32
RELGAN      33
RELGAN      34
RELGAN      35
RELGAN      36
RELGAN      37
RELGAN      38
RELGAN      39
RELGAN      40
RELGAN      41
RELGAN      42
RELGAN      43
RELGAN      44
RELGAN      45
RELGAN      46
RELGAN      47
RELGAN      48
RELGAN      49
RELGAN      50
RELGAN      51
RELGAN      52
RELGAN      53
RELGAN      54
RELGAN      55
RELGAN      56
RELGAN      57
RELGAN      58
RELGAN      59
RELGAN      60
RELGAN      61
RELGAN      62
RELGAN      63
RELGAN      64
RELGAN      65
RELGAN      66
RELGAN      67
RELGAN      68
RELGAN      69
RELGAN      70
RELGAN      71
RELGAN      72
RELGAN      73
RELGAN      74
RELGAN      75
RELGAN      76
RELGAN      77
RELGAN      78
RELGAN      79
RELGAN      80
RELGAN      81
RELGAN      82
RELGAN      83
RELGAN      84
RELGAN      85
RELGAN      86
RELGAN      87
RELGAN      88
RELGAN      89
RELGAN      90
RELGAN      91
RELGAN      92

```

```

NY2=YRF(3,J)-YRF(2,J)
NR2=NRFF(3,J)-NRFF(2,J)
NZ=COROT((NY2*NY2+NR2*NR2))
GAM2=ATAN(DR2/DX2)
ELRF(2,J)=(ELRF(2,J-1)+D1*DST(2))*D2/(D1+D2)
GAMPF(2,J)=(D1*GAM2+D2*GAMPF(2,J-1))/(D1+D2)
160 CONTINUE
C
C DO 170 I=3,NST
C   IF (NRF(I+1)) .LT. J) GO TO 180
C   D1=D2
C   GAM1=GAM2
C   NY2=YRF(I+1,J)-YRF(I,J)
C   NR2=NRFF(I+1,J)-NRFF(I,J)
C   NZ=COROT((NY2*NY2+NR2*NR2))
C   ELRF(I,J)=D1*D2/(D1+D2)*(DST(I-1)+DST(I))
C   GAM2=ATAN(DR2/DX2)
C   GAMPF(I,J)=(GAM1*D2+GAM2*D1)/(D1+D2)
170 CONTINUE
C
C 180 CONTINUE
C   EL1=D1*DST(I-1)
C   EL2=D2*DST(I-1)
C   D1=D1+.0002
C   D2=D2
C   ELRF(I,J)=(EL1*D2+EL2*D1)/(D1+D2)
C   GAMPF(I,J)=(GAM1*D2+GAM2*D1)/(D1+D2)
C   IF (GAMPF(I,J)) .LT. D2) GAMPF(I,J)=D2
190 CONTINUE
C
C EXTAPLATE ALONG STREAMLINES TO LAST GRID LINE
C
C CALL XCHK(ZPLOT,Y1,GAM1,EL1)
C DO 200 I=3,NST+1
C   NY2=YRF(I)
C   NY1=NY2-NRFF(I)
C   IF (NRF(I,N-1)) .LT. YST(I-1,1)) GO TO 220
C   FAC=(ZPLOT-YRF(I,N-1))/(YRF(I,N)-YRF(I,N-1))
C   YRF(I,N)=YST(I-1,MUM)
C   NRFF(I,N)=YST(I-1,MUM)
C   ELRF(I,N)=FAC*ELRF(I,N-1)+(1.0-FAC)*ELRF(I,N-1)
C   GAMPF(I,N)=FAC*GAMPF(I,N-1)+(1.0-FAC)*GAMPF(I,N-1)
C   IF (GAMPF(I,N)) .LT. D2) GAMPF(I,N)=D2
C   NY=N
C   I=I+1
C   GO TO 200
220 NRFF(I,N)=YST(I-1,MUM)
C   YRF(I,N)=YST(I-1,MUM)
C   FAC=(Y1-NRF(I,N+1))/(Y1-NRF(I,N+1))
C   ELRF(I,N)=ELRF(I,N+1)*FAC+(1.0-FAC)*EL1
C   GAMPF(I,N)=GAMPF(I,N+1)*FAC+(1.0-FAC)*GAM1
C   IF (GAMPF(I,N)) .LT. D2) GAMPF(I,N)=D2
230 CONTINUE
C
C RETURN
C END

```

```

RELGAN      93
RELGAN      94
RELGAN      95
RELGAN      96
RELGAN      97
RELGAN      98
RELGAN      99
RELGAN      100
RELGAN      101
RELGAN      102
RELGAN      103
RELGAN      104
RELGAN      105
RELGAN      106
RELGAN      107
RELGAN      108
RELGAN      109
RELGAN      110
RELGAN      111
RELGAN      112
RELGAN      113
RELGAN      114
RELGAN      115
RELGAN      116
RELGAN      117
RELGAN      118
RELGAN      119
RELGAN      120
RELGAN      121
RELGAN      122
RELGAN      123
RELGAN      124
RELGAN      125
RELGAN      126
RELGAN      127
RELGAN      128
RELGAN      129
RELGAN      130
RELGAN      131
RELGAN      132
RELGAN      133
RELGAN      134
RELGAN      135
RELGAN      136
RELGAN      137
RELGAN      138
RELGAN      139
RELGAN      140
RELGAN      141
RELGAN      142
RELGAN      143
RELGAN      144
RELGAN      145
RELGAN      146
RELGAN      147
RELGAN      148
RELGAN      149
RELGAN      150
RELGAN      151
RELGAN      152
RELGAN      153
RELGAN      154
RELGAN      155
RELGAN      156
RELGAN      157
RELGAN      158
RELGAN      159
RELGAN      160
RELGAN      161
RELGAN      162
RELGAN      163
RELGAN      164
RELGAN      165
RELGAN      166
RELGAN      167
RELGAN      168
RELGAN      169
RELGAN      170
RELGAN      171
RELGAN      172
RELGAN      173
RELGAN      174
RELGAN      175
RELGAN      176
RELGAN      177
RELGAN      178
RELGAN      179
RELGAN      180
RELGAN      181
RELGAN      182
RELGAN      183
RELGAN      184
RELGAN      185
RELGAN      186
RELGAN      187
RELGAN      188
RELGAN      189
RELGAN      190
RELGAN      191
RELGAN      192
RELGAN      193
RELGAN      194
RELGAN      195
RELGAN      196
RELGAN      197
RELGAN      198
RELGAN      199
RELGAN      200
RELGAN      201
RELGAN      202
RELGAN      203
RELGAN      204
RELGAN      205
RELGAN      206
RELGAN      207
RELGAN      208
RELGAN      209
RELGAN      210
RELGAN      211
RELGAN      212
RELGAN      213
RELGAN      214
RELGAN      215
RELGAN      216
RELGAN      217
RELGAN      218
RELGAN      219
RELGAN      220
RELGAN      221
RELGAN      222
RELGAN      223
RELGAN      224
RELGAN      225
RELGAN      226
RELGAN      227
RELGAN      228
RELGAN      229
RELGAN      230
RELGAN      231
RELGAN      232
RELGAN      233
RELGAN      234
RELGAN      235
RELGAN      236
RELGAN      237
RELGAN      238
RELGAN      239
RELGAN      240
RELGAN      241
RELGAN      242
RELGAN      243
RELGAN      244
RELGAN      245
RELGAN      246
RELGAN      247
RELGAN      248
RELGAN      249
RELGAN      250
RELGAN      251
RELGAN      252
RELGAN      253
RELGAN      254
RELGAN      255
RELGAN      256
RELGAN      257
RELGAN      258
RELGAN      259
RELGAN      260
RELGAN      261
RELGAN      262
RELGAN      263
RELGAN      264
RELGAN      265
RELGAN      266
RELGAN      267
RELGAN      268
RELGAN      269
RELGAN      270
RELGAN      271
RELGAN      272
RELGAN      273
RELGAN      274
RELGAN      275
RELGAN      276
RELGAN      277
RELGAN      278
RELGAN      279
RELGAN      280
RELGAN      281
RELGAN      282
RELGAN      283
RELGAN      284
RELGAN      285
RELGAN      286
RELGAN      287
RELGAN      288
RELGAN      289
RELGAN      290
RELGAN      291
RELGAN      292
RELGAN      293
RELGAN      294
RELGAN      295
RELGAN      296
RELGAN      297
RELGAN      298
RELGAN      299
RELGAN      300
RELGAN      301
RELGAN      302
RELGAN      303
RELGAN      304
RELGAN      305
RELGAN      306
RELGAN      307
RELGAN      308
RELGAN      309
RELGAN      310
RELGAN      311
RELGAN      312
RELGAN      313
RELGAN      314
RELGAN      315
RELGAN      316
RELGAN      317
RELGAN      318
RELGAN      319
RELGAN      320
RELGAN      321
RELGAN      322
RELGAN      323
RELGAN      324
RELGAN      325
RELGAN      326
RELGAN      327
RELGAN      328
RELGAN      329
RELGAN      330
RELGAN      331
RELGAN      332
RELGAN      333
RELGAN      334
RELGAN      335
RELGAN      336
RELGAN      337
RELGAN      338
RELGAN      339
RELGAN      340
RELGAN      341
RELGAN      342
RELGAN      343
RELGAN      344
RELGAN      345
RELGAN      346
RELGAN      347
RELGAN      348
RELGAN      349
RELGAN      350
RELGAN      351
RELGAN      352
RELGAN      353
RELGAN      354
RELGAN      355
RELGAN      356
RELGAN      357
RELGAN      358
RELGAN      359
RELGAN      360
RELGAN      361
RELGAN      362
RELGAN      363
RELGAN      364
RELGAN      365
RELGAN      366
RELGAN      367
RELGAN      368
RELGAN      369
RELGAN      370
RELGAN      371
RELGAN      372
RELGAN      373
RELGAN      374
RELGAN      375
RELGAN      376
RELGAN      377
RELGAN      378
RELGAN      379
RELGAN      380
RELGAN      381
RELGAN      382
RELGAN      383
RELGAN      384
RELGAN      385
RELGAN      386
RELGAN      387
RELGAN      388
RELGAN      389
RELGAN      390
RELGAN      391
RELGAN      392
RELGAN      393
RELGAN      394
RELGAN      395
RELGAN      396
RELGAN      397
RELGAN      398
RELGAN      399
RELGAN      400
RELGAN      401
RELGAN      402
RELGAN      403
RELGAN      404
RELGAN      405
RELGAN      406
RELGAN      407
RELGAN      408
RELGAN      409
RELGAN      410
RELGAN      411
RELGAN      412
RELGAN      413
RELGAN      414
RELGAN      415
RELGAN      416
RELGAN      417
RELGAN      418
RELGAN      419
RELGAN      420
RELGAN      421
RELGAN      422
RELGAN      423
RELGAN      424
RELGAN      425
RELGAN      426
RELGAN      427
RELGAN      428
RELGAN      429
RELGAN      430
RELGAN      431
RELGAN      432
RELGAN      433
RELGAN      434
RELGAN      435
RELGAN      436
RELGAN      437
RELGAN      438
RELGAN      439
RELGAN      440
RELGAN      441
RELGAN      442
RELGAN      443
RELGAN      444
RELGAN      445
RELGAN      446
RELGAN      447
RELGAN      448
RELGAN      449
RELGAN      450
RELGAN      451
RELGAN      452
RELGAN      453
RELGAN      454
RELGAN      455
RELGAN      456
RELGAN      457
RELGAN      458
RELGAN      459
RELGAN      460
RELGAN      461
RELGAN      462
RELGAN      463
RELGAN      464
RELGAN      465
RELGAN      466
RELGAN      467
RELGAN      468
RELGAN      469
RELGAN      470
RELGAN      471
RELGAN      472
RELGAN      473
RELGAN      474
RELGAN      475
RELGAN      476
RELGAN      477
RELGAN      478
RELGAN      479
RELGAN      480
RELGAN      481
RELGAN      482
RELGAN      483
RELGAN      484
RELGAN      485
RELGAN      486
RELGAN      487
RELGAN      488
RELGAN      489
RELGAN      490
RELGAN      491
RELGAN      492
RELGAN      493
RELGAN      494
RELGAN      495
RELGAN      496
RELGAN      497
RELGAN      498
RELGAN      499
RELGAN      500
RELGAN      501
RELGAN      502
RELGAN      503
RELGAN      504
RELGAN      505
RELGAN      506
RELGAN      507
RELGAN      508
RELGAN      509
RELGAN      510
RELGAN      511
RELGAN      512
RELGAN      513
RELGAN      514
RELGAN      515
RELGAN      516
RELGAN      517
RELGAN      518
RELGAN      519
RELGAN      520
RELGAN      521
RELGAN      522
RELGAN      523
RELGAN      524
RELGAN      525
RELGAN      526
RELGAN      527
RELGAN      528
RELGAN      529
RELGAN      530
RELGAN      531
RELGAN      532
RELGAN      533
RELGAN      534
RELGAN      535
RELGAN      536
RELGAN      537
RELGAN      538
RELGAN      539
RELGAN      540
RELGAN      541
RELGAN      542
RELGAN      543
RELGAN      544
RELGAN      545
RELGAN      546
RELGAN      547
RELGAN      548
RELGAN      549
RELGAN      550
RELGAN      551
RELGAN      552
RELGAN      553
RELGAN      554
RELGAN      555
RELGAN      556
RELGAN      557
RELGAN      558
RELGAN      559
RELGAN      560
RELGAN      561
RELGAN      562
RELGAN      563
RELGAN      564
RELGAN      565
RELGAN      566
RELGAN      567
RELGAN      568
RELGAN      569
RELGAN      570
RELGAN      571
RELGAN      572
RELGAN      573
RELGAN      574
RELGAN      575
RELGAN      576
RELGAN      577
RELGAN      578
RELGAN      579
RELGAN      580
RELGAN      581
RELGAN      582
RELGAN      583
RELGAN      584
RELGAN      585
RELGAN      586
RELGAN      587
RELGAN      588
RELGAN      589
RELGAN      590
RELGAN      591
RELGAN      592
RELGAN      593
RELGAN      594
RELGAN      595
RELGAN      596
RELGAN      597
RELGAN      598
RELGAN      599
RELGAN      600
RELGAN      601
RELGAN      602
RELGAN      603
RELGAN      604
RELGAN      605
RELGAN      606
RELGAN      607
RELGAN      608
RELGAN      609
RELGAN      610
RELGAN      611
RELGAN      612
RELGAN      613
RELGAN      614
RELGAN      615
RELGAN      616
RELGAN      617
RELGAN      618
RELGAN      619
RELGAN      620
RELGAN      621
RELGAN      622
RELGAN      623
RELGAN      624
RELGAN      625
RELGAN      626
RELGAN      627
RELGAN      628
RELGAN      629
RELGAN      630
RELGAN      631
RELGAN      632
RELGAN      633
RELGAN      634
RELGAN      635
RELGAN      636
RELGAN      637
RELGAN      638
RELGAN      639
RELGAN      640
RELGAN      641
RELGAN      642
RELGAN      643
RELGAN      644
RELGAN      645
RELGAN      646
RELGAN      647
RELGAN      648
RELGAN      649
RELGAN      650
RELGAN      651
RELGAN      652
RELGAN      653
RELGAN      654
RELGAN      655
RELGAN      656
RELGAN      657
RELGAN      658
RELGAN      659
RELGAN      660
RELGAN      661
RELGAN      662
RELGAN      663
RELGAN      664
RELGAN      665
RELGAN      666
RELGAN      667
RELGAN      668
RELGAN      669
RELGAN      670
RELGAN      671
RELGAN      672
RELGAN      673
RELGAN      674
RELGAN      675
RELGAN      676
RELGAN      677
RELGAN      678
RELGAN      679
RELGAN      680
RELGAN      681
RELGAN      682
RELGAN      683
RELGAN      684
RELGAN      685
RELGAN      686
RELGAN      687
RELGAN      688
RELGAN      689
RELGAN      690
RELGAN      691
RELGAN      692
RELGAN      693
RELGAN      694
RELGAN      695
RELGAN      696
RELGAN      697
RELGAN      698
RELGAN      699
RELGAN      700
RELGAN      701
RELGAN      702
RELGAN      703
RELGAN      704
RELGAN      705
RELGAN      706
RELGAN      707
RELGAN      708
RELGAN      709
RELGAN      710
RELGAN      711
RELGAN      712
RELGAN      713
RELGAN      714
RELGAN      715
RELGAN      716
RELGAN      717
RELGAN      718
RELGAN      719
RELGAN      720
RELGAN      721
RELGAN      722
RELGAN      723
RELGAN      724
RELGAN      725
RELGAN      726
RELGAN      727
RELGAN      728
RELGAN      729
RELGAN      730
RELGAN      731
RELGAN      732
RELGAN      733
RELGAN      734
RELGAN      735
RELGAN      736
RELGAN      737
RELGAN      738
RELGAN      739
RELGAN      740
RELGAN      741
RELGAN      742
RELGAN      743
RELGAN      744
RELGAN      745
RELGAN      746
RELGAN      747
RELGAN      748
RELGAN      749
RELGAN      750
RELGAN      751
RELGAN      752
RELGAN      753
RELGAN      754
RELGAN      755
RELGAN      756
RELGAN      757
RELGAN      758
RELGAN      759
RELGAN      760
RELGAN      761
RELGAN      762
RELGAN      763
RELGAN      764
RELGAN      765
RELGAN      766
RELGAN      767
RELGAN      768
RELGAN      769
RELGAN      770
RELGAN      771
RELGAN      772
RELGAN      773
RELGAN      774
RELGAN      775
RELGAN      776
RELGAN      777
RELGAN      778
RELGAN      779
RELGAN      780
RELGAN      781
RELGAN      782
RELGAN      783
RELGAN      784
RELGAN      785
RELGAN      786
RELGAN      787
RELGAN      788
RELGAN      789
RELGAN      790
RELGAN      791
RELGAN      792
RELGAN      793
RELGAN      794
RELGAN      795
RELGAN      796
RELGAN      797
RELGAN      798
RELGAN      799
RELGAN      800
RELGAN      801
RELGAN      802
RELGAN      803
RELGAN      804
RELGAN      805
RELGAN      806
RELGAN      807
RELGAN      808
RELGAN      809
RELGAN      810
RELGAN      811
RELGAN      812
RELGAN      813
RELGAN      814
RELGAN      815
RELGAN      816
RELGAN      817
RELGAN      818
RELGAN      819
RELGAN      820
RELGAN      821
RELGAN      822
RELGAN      823
RELGAN      824
RELGAN      825
RELGAN      826
RELGAN      827
RELGAN      828
RELGAN      829
RELGAN      830
RELGAN      831
RELGAN      832
RELGAN      833
RELGAN      834
RELGAN      835
RELGAN      836
RELGAN      837
RELGAN      838
RELGAN      839
RELGAN      840
RELGAN      841
RELGAN      842
RELGAN      843
RELGAN      844
RELGAN      845
RELGAN      846
RELGAN      847
RELGAN      848
RELGAN      849
RELGAN      850
RELGAN      851
RELGAN      852
RELGAN      853
RELGAN      854
RELGAN      855
RELGAN      856
RELGAN      857
RELGAN      858
RELGAN      859
RELGAN      860
RELGAN      861
RELGAN      862
RELGAN      863
RELGAN      864
RELGAN      865
RELGAN      866
RELGAN      867
RELGAN      868
RELGAN      869
RELGAN      870
RELGAN      871
RELGAN      872
RELGAN      873
RELGAN      874
RELGAN      875
RELGAN      876
RELGAN      877
RELGAN      878
RELGAN      879
RELGAN      880
RELGAN      881
RELGAN      882
RELGAN      883
RELGAN      884
RELGAN      885
RELGAN      886
RELGAN      887
RELGAN      888
RELGAN      889
RELGAN      890
RELGAN      891
RELGAN      892
RELGAN      893
RELGAN      894
RELGAN      895
RELGAN      896
RELGAN      897
RELGAN      898
RELGAN      899
RELGAN      900
RELGAN      901
RELGAN      902
RELGAN      903
RELGAN      904
RELGAN      905
RELGAN      906
RELGAN      907
RELGAN      908
RELGAN      909
RELGAN      910
RELGAN      911
RELGAN      912
RELGAN      913
RELGAN      914
RELGAN      915
RELGAN      916
RELGAN      917
RELGAN      918
RELGAN      919
RELGAN      920
RELGAN      921
RELGAN      922
RELGAN      923
RELGAN      924
RELGAN      925
RELGAN      926
RELGAN      927
RELGAN      928
RELGAN      929
RELGAN      930
RELGAN      931
RELGAN      932
RELGAN      933
RELGAN      934
RELGAN      935
RELGAN      936
RELGAN      937
RELGAN      938
RELGAN      939
RELGAN      940
RELGAN      941
RELGAN      942
RELGAN      943
RELGAN      944
RELGAN      945
RELGAN      946
RELGAN      947
RELGAN      948
RELGAN      949
RELGAN      950
RELGAN      951
RELGAN      952
RELGAN      953
RELGAN      954
RELGAN      955
RELGAN      956
RELGAN      957
RELGAN      958
RELGAN      959
RELGAN      960
RELGAN      961
RELGAN      962
RELGAN      963
RELGAN      964
RELGAN      965
RELGAN      966
RELGAN      967
RELGAN      968
RELGAN      969
RELGAN      970
RELGAN      971
RELGAN      972
RELGAN      973
RELGAN      974
RELGAN      975
RELGAN      976
RELGAN      977
RELGAN      978
RELGAN      979
RELGAN      980
RELGAN      981
RELGAN      982
RELGAN      983
RELGAN      984
RELGAN      985
RELGAN      986
RELGAN      987
RELGAN      988
RELGAN      989
RELGAN      990
RELGAN      991
RELGAN      992
RELGAN      993
RELGAN      994
RELGAN      995
RELGAN      996
RELGAN      997
RELGAN      998
RELGAN      999
RELGAN      1000

```



```

RETURN                                95HKL 35
END                                    95HKL 36
                                     DN TLD I=3,N8
                                     TF (YRF(I,J-1)+DSINF ,GT, XST(IM,1)) GO TO 72C
                                     YRF(I,J)=YRF(I,J-1)+DSINF
                                     DRF(I,J)=YST(IM,1)
71J CONTINUE                            C
                                     LOCATE POINTS WITHIN THE MAGNETOSPHERE
72J TOLD=(XST(IM,1)-XRF(I,J-1))
    J=J-1
    VST=1
    IF (IM .GE. NR(LUNT)) GO TO P11
    V2=VF(NRMAX,I)
    GO TO 730
P11 DO P2 J=NR(LUNT),NRMAX
    TF (XST(IM,1) .GT. XC(NRMAX,J)) GO TO P21
    V2=VF(NRMAX,JJ-1)+(VF(NRMAX,J)-VF(NRMAX,JJ-1))
    *(XST(IM,1)-XC(NRMAX,JJ-1))/(XC(NRMAX,J)-XC(NRMAX,JJ-1))
    GO TO 730
P21 CONTINUE
73J V1=V2
    V1=XST(IM,KST+1)
    V1=YST(IM,KST+1)
    V2=V1*PR(X1,Y1)
    DST=SQRT((XST(IM,KST+1)-XST(IM,KST))**2
    *(YST(IM,KST+1)-YST(IM,KST))**2)
    NT=2./DST/(V1+V2)
    A12=V1/J1/NT
    TNEW=TOLD*NT
    TNEW=TOLD*NT
    KST=KST+1
    IF (KST .GE. NUMST(IM)) GO TO 76J
    GO TO 73C
74C J=J+1
    RL=RLT-TOLD
    DELS=V1*NT+0.5*ANT*NT
    YRF(I,J)=XST(IM,KST)+DELS*(XST(IM,KST+1)-XST(IM,KST))/DST
    DRF(I,J)=YST(IM,KST)+DELS*(YST(IM,KST+1)-YST(IM,KST))/DST
    NT=RLT
    TOLD=TOLD-DELT
    GO TO 73C
75J TF (J .GE. JRFMAX) GO TO 76C
    IF (TLD .LT. DELT) GO TO 73J
    J=J+1
    V1=V1*ANT
    DELS=V1*DELT+0.5*ANT*DELT
    XRF(I,J)=XRF(I,J-1)+DELS*(YST(IM,KST)-YST(IM,KST-1))/DST
    DRF(I,J)=DRF(I,J-1)+DELS*(YST(IM,KST)-YST(IM,KST-1))/DST
    NT=DELT
    TOLD=TOLD-DELT
    GO TO 73C
76J CONTINUE
    NRST=J
    TF (J .GT. NMF(I-1)) NMF(I)=NMF(I-1)
76J CONTINUE
    RETURN
    END
                                     SHROUOUTIME AURRL(A,5,8,NR(L),NLAR)
                                     NJRRL 7
                                     USING A SPECIAL TECHNIQUE, THIS ROUTINE SORTS THE REAL
                                     ARRAY S INTO ASCENDING ORDER AND CHANGES
                                     THE ORDER OF ARRAYS A AND B IN A CORRESPONDING
                                     MANNER. K IS THE NUMBER OF DATA POINTS TO
                                     BE SORTED.
                                     C
                                     DIMENSION A(1),S(1),B(1),TLR(1)
                                     NJRRL 14
                                     NJRRL 15
                                     NJRRL 16
                                     NJRRL 17
                                     NJRRL 18
                                     NJRRL 19
                                     NJRRL 20
                                     NJRRL 21
                                     NJRRL 22
                                     TF(K,FO,1) RETURN
                                     K1=K-1
                                     DO I=1, K1
                                     L=I+1
                                     DO JL=J,L,K
                                     TF(S(J),GT,S(I)) GO TO IJC
                                     INTERCHANGE ARRAYS
                                     TEMP=S(I)
                                     S(I)=S(J)
                                     S(J)=TEMP

```

```

S(I)=TEMP
TEMP=4(I)
A(I)=A(I)
A(I)=TEMP
TEMP=4(I)
N(I)=N(I)
N(I)=TEMP
103 CONTINUE
C
RETURN
END
C
SUBROUTINE CHECK(ICM,NXY,KOD2,J,K,NVAL,KOD9)
CHECK 2
CHECK 3
CHECK 4
CHECK 5
CHECK 6
CHECK 7
CHECK 8
CHECK 9
CHECK 10
CHECK 11
CHECK 12
CHECK 13
CHECK 14
CHECK 15
CHECK 16
CHECK 17
CHECK 18
CHECK 19
CHECK 20
CHECK 21
CHECK 22
CHECK 23
CHECK 24
CHECK 25
CHECK 26
CHECK 27
C
SUBROUTINE CONOUT (ACONT,FACT,NHINDX)
CONOUT 2
CONOUT 3
CONOUT 4
CONOUT 5
CONOUT 6
CONOUT 7
CONOUT 8
CONOUT 9
CONOUT 10
CONOUT 11
CONOUT 12
CONOUT 13
CONOUT 14
CONOUT 15
CONOUT 16
CONOUT 17
CONOUT 18
CONOUT 19
CONOUT 20
CONOUT 21
CONOUT 22
CONOUT 23
CONOUT 24
CONOUT 25
CONOUT 26
CONOUT 27
CONOUT 28
CONOUT 29
CONOUT 30
CONOUT 31
CONOUT 32
CONOUT 33
CONOUT 34
CONOUT 35
CONOUT 36
CONOUT 37
CONOUT 38
C
COMMON /TCHECK/ ICHK(4,1),CVAL(3),NAD(3),IPLT
COMMON /PLOT/ CONTX(100),CONTY(100),CVAL(3),NAD(3),IPLT
DIMENSION CONTX(1)
C
DO 1 L=1,NXY
IF(KOD2.NE.ICM(1,L)) GO TO 1
IF(J.NE.ICM(2,L)) GO TO 1
IF(K.NE.ICM(3,L)) GO TO 1
IF(NVAL.EQ.ICM(4,L)) GO TO 2
CONTINUE
KOD9=1
GO TO 3
KOD9=2
RETURN
END
C
SUBROUTINE CONOUT (ACONT,FACT,NHINDX)
CONOUT 2
CONOUT 3
CONOUT 4
CONOUT 5
CONOUT 6
CONOUT 7
CONOUT 8
CONOUT 9
CONOUT 10
CONOUT 11
CONOUT 12
CONOUT 13
CONOUT 14
CONOUT 15
CONOUT 16
CONOUT 17
CONOUT 18
CONOUT 19
CONOUT 20
CONOUT 21
CONOUT 22
CONOUT 23
CONOUT 24
CONOUT 25
CONOUT 26
CONOUT 27
CONOUT 28
CONOUT 29
CONOUT 30
CONOUT 31
CONOUT 32
CONOUT 33
CONOUT 34
CONOUT 35
CONOUT 36
CONOUT 37
CONOUT 38
C
NAD(1)=1
DO 1 N=1,NMAX
NP=NAD(1)+NAD(N)
MCONT=NAD(N)
I=ICM(4,MCONT)
CVAL(1)=ACONT(I)

```



```

244 YSXROD=YS(N-1)+(YS(N)-YS(N-1))*EXROD(J1-XS(N-1))/(XS(N)-XS(N-1))
IF (YSXROD .LT. Y90D(J1)) N1=N
245 CONTINUE
N0=250,NMAX,NM
CALL DDTMEXS(N1),YS(N1),XS(N1+1),YS(N1+1),Z0,3)
25) CONTINUE
22) CONTINUE
RETURN
C
END

```

```

CONTR 101
CONTR 192
CONTR 193
CONTR 194
CONTR 195
CONTR 196
CONTR 197
CONTR 198
CONTR 199
CONTR 200

```

```

SUBROUTINE CONTOUR
CONTR 2
CONTOUR 3
CONTOUR 4
CONTOUR 5
CONTOUR 6
CONTOUR 7
CONTOUR 8
CONTOUR 9
CONTOUR 10
CONTOUR 11
CONTOUR 12
CONTOUR 13
CONTOUR 14
CONTOUR 15
CONTOUR 16
CONTOUR 17
CONTOUR 18
CONTOUR 19
CONTOUR 20
CONTOUR 21
CONTOUR 22
CONTOUR 23
CONTOUR 24
CONTOUR 25
CONTOUR 26
CONTOUR 27
CONTOUR 28
CONTOUR 29
CONTOUR 30
CONTOUR 31
CONTOUR 32
CONTOUR 33
CONTOUR 34
CONTOUR 35
CONTOUR 36
CONTOUR 37
CONTOUR 38
CONTOUR 39
CONTOUR 40
CONTOUR 41
CONTOUR 42
CONTOUR 43
CONTOUR 44
CONTOUR 45
CONTOUR 46
CONTOUR 47
CONTOUR 48
CONTOUR 49
CONTOUR 50
CONTOUR 51
CONTOUR 52
CONTOUR 53
CONTOUR 54
CONTOUR 55
CONTOUR 56
CONTOUR 57
CONTOUR 58
CONTOUR 59
CONTOUR 60
CONTOUR 61
CONTOUR 62
CONTOUR 63
CONTOUR 64
CONTOUR 65

```

```

N0=110,T=2,NRMAX
ASCH(I,J)=BPERP(I,J)
110) CONTINUE
CALL MAP(ASCH,20,CONTX,CONTY,KBCON,2,RCOM,NAD,1000,30,ICM,
* 2,1,NRMAX,NXMAX)
TPLOT=6
IF (LPRCON) CALL COMOUT(ACON,FACT,NHINOV)
IF (LPLLOT) CALL PLOTCH
N0=120,J=1,NXMAX
N0=123,T=2,NRMAX
ASCH(I,J)=ASCH(I,J)
123) CONTINUE
CALL MAP(ASCH,20,CONTX,CONTY,KBCON,2,RCOM,NAD,1000,30,ICM,
* 2,1,NRMAX,NXMAX)
TPLOT=7
IF (LPRCON) CALL COMOUT(BCON,FACT,NHINOV)
IF (LPLLOT) CALL PLOTCH
C
20) CONTINUE
IF (LPLLOT) CALL ENPLT(3,0,0,0)
RETURN
END

```

```

CONTOUR 66
CONTOUR 67
CONTOUR 68
CONTOUR 69
CONTOUR 70
CONTOUR 71
CONTOUR 72
CONTOUR 73
CONTOUR 74
CONTOUR 75
CONTOUR 76
CONTOUR 77
CONTOUR 78
CONTOUR 79
CONTOUR 80
CONTOUR 81
CONTOUR 82
CONTOUR 83
CONTOUR 84
CONTOUR 85
CONTOUR 86
CONTOUR 87

```

```

FUNCTION DRDX(X,Y)
C
C THIS FUNCTION DETERMINES THE SLOPE OF THE STREAMLINE
C AT THE POINT (X,Y)
C
COMMON /RLUNT/ THETA(25),PP(20,23),NRLUNT
COMMON /RNUMDS/ XBON(100),Y90D(100),YSKH(100),YSKH(100),
* NRMAX,NYMAX,AMACH,GAMMA,HRD,NHINOV
LEVEL 2, ANG,DXTH,DSG
COMMON /DRD/ ANG(20,100),DXTM(100),DGT
COMMON /FLOW/ XC(20,100),YC(20,100),VF(20,100),RHO(20,100)
LLOCATING POINT IN ERD
IF (Y .GE. 0.5) GO TO 16
THETA=ATAN2(Y,-Y)*DEG
R=SQRT(Y**2+0.002)
N0=3,J=1,NRLUNT
IF (THETA(J).GT.THETA) GO TO 5
3) CONTINUE
J=NRLUNT
5) J0=J-1
IF (J0.LT.1) JP=1
SLOPE=(THETA-THETA(JR))/DXTM(JR)
P2=PP(1,JR)+ERP(1,JP+1)-PP(1,JP)*SLOPE
R1=R2
R2=PP(I,JP)+ERP(I,JP+1)-PP(I,JP)*SLOPE
IF (R2 .GT. R1) GO TO 8
7) CONTINUE
I=NMAX
I GO TO 21
13) CONTINUE
R=Y
N0=13,J=NRLUNT,NXMAX
IF (XC(J).GT.X) GO TO 15
13) CONTINUE
J=NXMAX
JR=J-1
IF (J0.LT.NRLUNT) JP=NRLUNT
SLOPE=(X-XC(1,JP))/DXTM(JR)
R2=YC(1,JP)+YC(1,JP+1)-YC(1,JP)*SLOPE
N0=17,T=2,NRMAX
R1=R2
R2=YC(I,JP)+YC(I,JP+1)-YC(I,JP)*SLOPE
IF (R2 .GT. R1) GO TO 18
17) CONTINUE
I=NMAX
15) CONTINUE
C
C BIVARIATE LINEAR INTERPOLATION
C
20) CONTINUE
DP1=ANG(I-1,JP)+ANG(I-1,JP+1)-ANG(I-1,JP)*SLOPE
DR2=ANG(I,JP)+ANG(I,JP+1)-ANG(I,JP)*SLOPE
DRDX=DR1+(P2-DR1)*(R-1)/(P2-R1)

```

```

DRDX 2
DRDX 3
DRDX 4
DRDX 5
DRDX 6
DRDX 7
DRDX 8
DRDX 9
DRDX 10
DRDX 11
DRDX 12
DRDX 13
DRDX 14
DRDX 15
DRDX 16
DRDX 17
DRDX 18
DRDX 19
DRDX 20
DRDX 21
DRDX 22
DRDX 23
DRDX 24
DRDX 25
DRDX 26
DRDX 27
DRDX 28
DRDX 29
DRDX 30
DRDX 31
DRDX 32
DRDX 33
DRDX 34
DRDX 35
DRDX 36
DRDX 37
DRDX 38
DRDX 39
DRDX 40
DRDX 41
DRDX 42
DRDX 43
DRDX 44
DRDX 45
DRDX 46
DRDX 47
DRDX 48
DRDX 49
DRDX 50
DRDX 51
DRDX 52
DRDX 53
DRDX 54
DRDX 55
DRDX 56

```

```

RETURN                                DRXK  97
END                                    DRDX  98

SUBROUTINE ECHIMP                      DDX  59
PRINTS INPUT CARDS USED FOR RIM        DRDY  60
DIMENSION CRD(4)                       DRDZ  61
WRITE (6,116)                           DRX  62
CONTINUE                                 DRDY  63
READ (5,116) CRD                         DRDZ  64
IF (EQV(51) 30,20)                       DRX  65
CONTINUE                                 DRDY  66
WRITE (6,101) CRD                         DRDZ  67
EN TO 1P                                  DRX  68
CONTINUE                                 DRDY  69
RETURN 5                                  DRDZ  70
END                                        DRX  71
100 FFORMAT(8,10)                         DRDY  72
101 FFORMAT(12,8,10)                       DRDZ  73
11) FFORMAT(14),40X,35MLISTING OF INPUT CARDS FOR THIS RUN/497,35(14)
1 //))                                     DRX  74
END                                        DRDY  75
                                           DRDZ  76
                                           DRX  77
                                           DRDY  78
                                           DRDZ  79

SUBROUTINE ENTER(KOD2,J,K,NVAL,A1,A2,JM14,M1N,ICM,KOD4,X,Y,MY,
ACNT,ISIZ1)
CONTUR PROGRAMS PAP, WALK, SERCH, ENTER, AND CHECK
WRITTEN BY PEESE SORENSON, NASA-AMES RES. CTR., AUG., 1974.
(MODIFIED VERSION)
ASSUMING THAT A POINT ON A CONTOUR LINE HAS BEEN FOUND,
THIS SUBROUTINE RECORDS THAT POINT IN THE BOOKKEEPING ARRAYS.
COMMON /FLOW/ XC(20,100),YC(20,100),VF(20,100),RHDF(20,100)
DIMENSION ICM(4,1),T(2,1),V(2),ACONT(1)
MYV=MYV+1
IF(MY,GT,ISIZ1) GO TO 1
(ICM(1,MYV)=KOD2
ICM(2,MYV)=J
ICM(3,MYV)=K
ICM(4,MYV)=NVAL
IF ENDPOINTS ARE EQUAL, ENTER MIDPOINT
IF ((A2-A1)/EQ,0.0) GO TO 6
DIF=ACONT(NVAL)-A1)/(A2-A1)
DO TO (2,3),KOD2
DIF=0.5
GO TO (2,3),KOD2
INTERPOLATE FOR CONTOUR POSITION
2 VZ=VC(J,K+1)
YZ=VC(J,K+1)
DO TO 4
3 VZ=XC(I+1,K)
YZ=VC(J+1,K)
4 V1=XC(J,K)
V1=VC(J,K)
V(MYV)=V1+DIF*(V2-V1)
V(NMYV)=V1+DIF*(Y2-Y1)
KMD=1
DO TO 5
WRITE(6,121)
101 FFORMAT(9MLCONTOUR SEARCH ABORTED - TABLE OVERFLOW IN (X,Y)
KMD=2
CONTINUE
RETURN
END

```

```

SUBROUTINE EXTRAP                      EXTRAP  2
THIS ROUTINE CALCULATES EXTRAPOLATED VALUES OF          EXTRAP  3
RHO AND V/I AT POINTS ALONG THE BOUNDARY THETA=9 USING  EXTRAP  4
A LAGRANGIAN INTERPOLATING POLYNOMIAL OVER              EXTRAP  5
THREE UNEQUALLY SPACED POINTS ON EACH RADIAL CURVE.    EXTRAP  6
                                                         EXTRAP  7
COMMON /BLUNT/ THETA(25),RP(20,25),NRBLUNT             EXTRAP  8
COMMON /ROUNDS/ X900(100),Y900(100),XSHK(100),YSHK(100),  EXTRAP  9
* NRMAX,NRMAX,AMACH,GAMMA,MRD,MHINDX                     EXTRAP 10
COMMON /FLOW/ XC(20,100),YC(20,100),VF(20,100),RHDF(20,100)  EXTRAP 11
COMMON /SHOCKS/ DRSDX(100),DST(30)                       EXTRAP 12
                                                         EXTRAP 13
CALCULATE LAGRANGIAN COEFFICIENTS                       EXTRAP 14
TH23=THETA(2)-THETA(3)                                  EXTRAP 15
TH24=THETA(2)-THETA(4)                                  EXTRAP 16
TH34=THETA(3)-THETA(4)                                  EXTRAP 17
E2=THETA(3)*THETA(4)/(TH23*TH24)                        EXTRAP 18
F3=THETA(2)*THETA(4)/(TH23*TH34)                        EXTRAP 19
F4=THETA(2)*THETA(3)/(TH24*TH34)                        EXTRAP 20
                                                         EXTRAP 21
CALCULATE XC, RHO, AND V AT THETA=0.                     EXTRAP 22
AM2=AMCH*AMACH                                           EXTRAP 23
DO 1) I=2,NRMAX                                          EXTRAP 24
YC(I,1)=0.0                                              EXTRAP 25
XC(I,1)=(E2*RP(I,2)+E3*RP(I,3)+E4*RP(I,4))              EXTRAP 26
RP(I,1)=XC(I,1)                                          EXTRAP 27
IF (I,FO,NRMAX) GO TO 10                                 EXTRAP 28
*MF(I,1)=E2*RP(I,2)+E3*RP(I,3)+E4*RP(I,4)              EXTRAP 29
VF(I,1)=E2*VF(I,2)+E3*VF(I,3)+E4*VF(I,4)              EXTRAP 30
IK (VF(I,1) .LT. 0.) VF(I,1)=0.                          EXTRAP 31
1) CONTINUE                                              EXTRAP 32
                                                         EXTRAP 33
CALCULATE EXACT VALUES AT SHOCK WAVE                   EXTRAP 34
*RHDF(NRMAX,1)=(GAMMA+1.0)*AM2/(GAMMA-1.0)*AM2*0.5)    EXTRAP 35
VF(NRMAX,1)=1.0/RHDF(NRMAX,1)                           EXTRAP 36
                                                         EXTRAP 37
EXACT VALUES AT BODY                                   EXTRAP 38
YC(1,1)=0.0                                              EXTRAP 39
YC(1,1)=-1.0                                            EXTRAP 40
*VF(1,1)=0.0                                             EXTRAP 41
*RHDF(1,1)=RHDF(NRMAX,1)/(GAMMA+1.0)**2*AM2*0.5/(2.0*GAMMA+AM2-  EXTRAP 42
* (GAMMA-1.0))**0.5/(GAMMA-1.0))                       EXTRAP 43
*NSOX(1)=9999.0                                          EXTRAP 44
                                                         EXTRAP 45
DEFINE BOUNDARY ARRAYS FOR IONopause/MAGNETopause AND SHOCK  EXTRAP 46
DO 2) J=1,NRMAX                                          EXTRAP 47
VROD(J)=VC(1,J)                                          EXTRAP 48
VROD(J)=VF(1,J)                                          EXTRAP 49
VSHK(J)=XC(NRMAX,J)                                     EXTRAP 50
VSHK(J)=YC(NRMAX,J)                                     EXTRAP 51
2) CONTINUE                                              EXTRAP 52
RETURN                                                  EXTRAP 53
END                                                    EXTRAP 54
                                                         EXTRAP 55
SUBROUTINE FLOUT                                        FLOUT  2
THIS ROUTINE PRINTS THE FLOW FIELD VALUES WHICH WILL BE USED  FLOUT  3
TO CALCULATE THE STREAMLINES AND CONTOURS              FLOUT  4
                                                         FLOUT  5
COMMON /BLUNT/ THETA(25),RP(20,25),NRBLUNT             FLOUT  6
COMMON /ROUNDS/ X900(100),Y900(100),XSHK(100),YSHK(100),  FLOUT  7
* NRMAX,NRMAX,AMACH,GAMMA,MRD,MHINDX                     FLOUT  8
LEVEL 2, ANG,DTM,DEG                                     FLOUT  9
COMMON /DRD/ ANG(23,100),DTM(100),DEG                   FLOUT 10
COMMON /FLOW/ XC(20,100),YC(20,100),VF(20,100),RHDF(20,100)  FLOUT 11
LEVEL 2, VI,VV                                           FLOUT 12
COMMON /VCOMP/ VX(20,100),VY(20,100)                    FLOUT 13
COMMON /ONSTRN/ ZPLOT,NZEND,NZADD,NXPLNT                FLOUT 14
REVERSE SIGN OF XC FOR OUTPUT                            FLOUT 15

```

```

JMAX=N7END+NZADD          FLOWT 16
N0 2 J=1,JMAX            FLOWT 17
N0 2 I=1,NRMAX           FLOWT 18
2 XC(I,J)=XC(I,J)        FLOWT 19
C                               FLOWT 20
C                               FLOWT 21
C                               FLOWT 22
C                               FLOWT 23
C                               FLOWT 24
C                               FLOWT 25
C                               FLOWT 26
C                               FLOWT 27
C                               FLOWT 28
C                               FLOWT 29
C                               FLOWT 30
C                               FLOWT 31
C                               FLOWT 32
C                               FLOWT 33
C                               FLOWT 34
C                               FLOWT 35
C                               FLOWT 36
C                               FLOWT 37
C                               FLOWT 38
C                               FLOWT 39
C                               FLOWT 40
C                               FLOWT 41
C                               FLOWT 42
C                               FLOWT 43
C                               FLOWT 44
C                               FLOWT 45
C                               FLOWT 46
C                               FLOWT 47
C                               FLOWT 48
C                               FLOWT 49
C                               FLOWT 50
C                               FLOWT 51
C                               FLOWT 52
C                               FLOWT 53
C                               FLOWT 54
C                               FLOWT 55
C                               FLOWT 56
C                               FLOWT 57
C                               FLOWT 58
C                               FLOWT 59
C                               FLOWT 60
C                               FLOWT 61
C                               FLOWT 62
C                               FLOWT 63
C                               FLOWT 64
C                               FLOWT 65
C                               FLOWT 66
C                               FLOWT 67
C                               FLOWT 68
C                               FLOWT 69
C                               FLOWT 70
C                               FLOWT 71
C                               FLOWT 72
C                               FLOWT 73
C                               FLOWT 74
C                               FLOWT 75
C                               FLOWT 76
C                               FLOWT 77
C                               FLOWT 78
C                               FLOWT 79
C                               FLOWT 80
C                               FLOWT 81
C                               FLOWT 82
C                               FLOWT 83
C                               FLOWT 84
C                               FLOWT 85
C                               FLOWT 86
C                               FLOWT 87
C                               FLOWT 88
C                               FLOWT 89
C                               FLOWT 90
C                               FLOWT 91
C                               FLOWT 92
C                               FLOWT 93
C                               FLOWT 94
C                               FLOWT 95
C                               FLOWT 96
C                               FLOWT 97
C                               FLOWT 98
C                               FLOWT 99
C                               FLOWT 100

```

```

30) FORMAT(4X,14I,7X,3HR/D,7X,74VR/VINF,5X,74VX/VINF,3X) FLOWT 106
* 10HFLOW ANGLE,5X,6HV/VINF,3X,10HRHO/RHOINF,4X,6HT/TINF,6X, FLOWT 107
* 6HP/PINF) FLOWT 108
31) FORMAT(//33H ADDITIONAL AXIAL LOCATION NO.,I2,14H, AT Y/R =, FLOWT 109
* F8.4F) FLOWT 110
32) FORMAT(4X,14I,7X,3HR/D,6X,74VR/VINF,5X,74VX/VINF,3X) FLOWT 111
* 10HFLOW ANGLE,5X,6HV/VINF,3X,10HRHO/RHOINF,5X,6HT/TINF,6X, FLOWT 112
* 6HP/PINF) FLOWT 113
END FLOWT 114

SUBROUTINE FLOWST FLOWST 2
THIS ROUTINE CALCULATES THE MAGNITUDE AND DIRECTION OF FLOWST 3
THE VELOCITY, THEN CALCULATES THE TRAJECTORY STREAMLINES FLOWST 4
C FLOWST 5
C FLOWST 6
COMMON /RLUNT/ THETA(25),PP(2),Z(25),NRLUNT FLOWST 7
COMMON /RNUMS/ XND(100),YND(100),XSHK(100),YSHK(100), FLOWST 8
* NRMAX,NYMAX,AMACH,GAMMA,HRD,NMINX RNUMS 9
COMMON /DNSTRM/ ZPLOT,NZEND,NZADD,NXPLOT DNSTRM 10
LEVEL 2, ANG,DXTH,DEG DRD 11
COMMON /DRD/ ANG(25,100),DXTH(100),DEG FLOW 12
COMMON /FLOW/ XC(25,100),YC(25,100),VF(25,100),RHOF(25,100) FLOW 13
LEVEL 2, V,VF FLOW 14
LEVEL 2, XST,YST,NUMST,MST STREAM 15
COMMON /STREAM/ XST(50,150),YST(50,150),NUMST(50),MST STREAM 16
LEVEL 2, V,VF VCOMP 17
COMMON /VCOMP/ VX(25,100),VY(25,100) VCOMP 18
DIMENSION W(25),S(25),A(5),AVE(5) FLOWST 19
DATA W/ZC,0,0,0,0 FLOWST 20
CALCULATE VELOCITY AND FLOW ANGLE FROM VELOCITY COMPONENTS FLOWST 21
POLAR COORDINATE REGION FLOWST 17
DEG=ATN(2057735) FLOWST 22
THETA(1)=C,0 FLOWST 23
NYMAX=NYMAX+NZADD FLOWST 24
N0 10 J=2,NRLUNT FLOWST 25
THETA(J)=THETA(J)+DEG FLOWST 26
NYTH(J)=NYTH(J)+THETA(J)-THETA(J-1) FLOWST 27
N0 1, NYMAX FLOWST 28
VF(I,J)=SQRT(VX(I,J)**2+VY(I,J)**2) FLOWST 29
TF (ABS(VX(I,J)) .LT. 1.0E-4) GO TO 5 FLOWST 30
ANG(I,J)=ATN(VY(I,J)/VX(I,J)) FLOWST 31
GO TO 10 FLOWST 32
5 ANG(I,J)=1.0E-4 FLOWST 33
10 CONTINUE FLOWST 34
CYLINDRICAL COORDINATE REGION FLOWST 35
NYI=NRLUNT+1 FLOWST 36
N0 20 I=NYI,NYMAX FLOWST 37
NYTH(J)=XC(I,J)-XC(I,J-1) FLOWST 38
N0 2, I=1,NRMAX FLOWST 39
VF(I,J)=SQRT(VX(I,J)**2+VY(I,J)**2) FLOWST 40
TF (ABS(VX(I,J)) .LT. 1.0E-4) GO TO 10 FLOWST 41
ANG(I,J)=ATN(VY(I,J)/VX(I,J)) FLOWST 42
GO TO 20 FLOWST 43
15 ANG(I,J)=1.0E-4 FLOWST 44
20 CONTINUE FLOWST 45
30) FORMAT(4X,14I,7X,3HR/D,7X,74VR/VINF,5X,74VX/VINF,3X) FLOWST 46
* 10HFLOW ANGLE,5X,6HV/VINF,3X,10HRHO/RHOINF,4X,6HT/TINF,6X, FLOWST 47
* 6HP/PINF) FLOWST 48
31) FORMAT(//33H ADDITIONAL AXIAL LOCATION NO.,I2,14H, AT Y/R =, FLOWST 49
* F8.4F) FLOWST 50
32) FORMAT(4X,14I,7X,3HR/D,6X,74VR/VINF,5X,74VX/VINF,3X) FLOWST 51
* 10HFLOW ANGLE,5X,6HV/VINF,3X,10HRHO/RHOINF,5X,6HT/TINF,6X, FLOWST 52
* 6HP/PINF) FLOWST 53
END FLOWST 54
CALL EXTRAP FLOWST 55
N0 30 I=1,NRMAX FLOWST 56
ANG(I,1)=C,0 FLOWST 57
3) CONTINUE FLOWST 58
C FLOWST 59
C FLOWST 60
C FLOWST 61
C FLOWST 62
C FLOWST 63
C FLOWST 64
C FLOWST 65
C FLOWST 66
C FLOWST 67
C FLOWST 68
C FLOWST 69
C FLOWST 70
C FLOWST 71
C FLOWST 72
C FLOWST 73
C FLOWST 74
C FLOWST 75
C FLOWST 76
C FLOWST 77
C FLOWST 78
C FLOWST 79
C FLOWST 80
C FLOWST 81
C FLOWST 82
C FLOWST 83
C FLOWST 84
C FLOWST 85
C FLOWST 86
C FLOWST 87
C FLOWST 88
C FLOWST 89
C FLOWST 90
C FLOWST 91
C FLOWST 92
C FLOWST 93
C FLOWST 94
C FLOWST 95
C FLOWST 96
C FLOWST 97
C FLOWST 98
C FLOWST 99
C FLOWST 100

```



```

C C C
C
C          CALCULATE STARTING POINTS FOR STREAMLINE CALCULATION
C          USE GRID POINTS ON SHOCK IN WISE REGIM
C          EQUAL Y-SPACING ON SHOCK DOWNSTREAM
C
C          NO 32 J=2,NBLINT
C          YST(1,1)=YC(NRMAX,J)
C          YST(1,2)=YC(NRMAX,J)
32 CONTINUE
C          NST=NRLUNT-1
C          ANNST=1-NST
C          NO 34 K=NRLUNT,NRMAX
C          IF (YCI,K) .GT. ?PLOT) GO TO 35
34 CONTINUE
C          K=NRLUNT
35 YSTC=YC(NRMAX,K)
C          XPLNT=X
C          YSTN=YST(NST,1)
C          DRKT=ANAX,(YSTN-YST(NST-1,1))/(YST-YSTN)/ANOST)
C          X=NRLUNT
C          NO 39 K=NRLUNT,20
C          YSTN=YST(NRST
C          IF (YSTN .GE. YSTF) GO TO 40
C          X=NRLUNT
C          NO 37 I=1,NRMAX
C          IF (YSTN .GT. YC(NRMAX,JX)) GO TO 37
C          YST(NST,1)=YSTN
C          YST(NST,1)=YC(NRMAX,JX-1)+(YC(NRMAX,JX)-YC(NRMAX,JX-1))
C          *(YSTN-YC(NRMAX,JX-1))/(YC(NRMAX,JX)-YC(NRMAX,JX-1))
C          NO TO 39
37 CONTINUE
39 K=J
40 CONTINUE
C          ?PLOT=YCI,X,NPLNT)
C
C          CALCULATE STREAMLINE TRAJECTORIES
C          USING THIRD ORDER MODIFIED EULER INTEGRATION PROCEDURE
C
C          NRMAX=YC(NRMAX,2)*0.2
C          NRMYZ=ANAYI (OWP1,?PLOT*.1)*.E-6)
C          NO 37 I=1,NST
C          YC=YST(I,1)
C          YS=YST(I,2)
C          NRMY=NRMYI
C          IF (YS .GT. 0.0) NRMY=NRMYZ
C          NO 41 N=2,152
C          IF (YS+NRMY .GE.?PLOT) GO TO 47
C          NX=NRMY*.2
C          NO 43 K=1,5
C          NRX1=NRDX(YS,YS)
C          YS1=YS+NRMY*NRX
C          YS=YS1
C          YS=YS1+NX
C          YS=YC+.5*(NRDX1+NRDX(YS,YS1))+NX
C          IF (YS1.LT.0.0 .AND. YS.GT.0.0) NRMY=NRMYZ
43 CONTINUE
C          YST(I,1)=YS
C          YST(I,2)=YS
45 CONTINUE
C          N=252
47 NR=(?PLOT-YS)*.2
C          NO 49 I=1,5
C          NRX1=NRDX(YS,YS)
C          YS1=YS+NRMY*NRX
C          YS=YC+.5*(NRDX1+NRDX(YS,YS1))+NX
49 CONTINUE
C          YST(I,1)=YS
C          YST(I,2)=YS
51 CONTINUE
C          CONVERT ANG ARRAY FROM FLOW FIELD SLOPE TO FLOW ANGLE
C
C          NO 60 J=2,NRMAX
C          NO 60 I=1,NRMAX
C          ANCF(I,J)=ATAN(ANCF(I,J))
6 CONTINUE
C          NRMAX=NPLNT
C          RETURN
C          END
C
C          SUBROUTINE FLSOFY (P,N,X,Y,W,MN1,S1,A,IEP)
C          FLSOFY 2
C          FLSOFY 3
C          FLSOFY 4
C          FLSOFY 5
C          FLSOFY 6
C          FLSOFY 7
C          FLSOFY 8
C          FLSOFY 9
C          FLSOFY 10
C          FLSOFY 11
C          FLSOFY 12
C          FLSOFY 13
C          FLSOFY 14
C          FLSOFY 15
C          FLSOFY 16
C          FLSOFY 17
C          FLSOFY 18
C          FLSOFY 19
C          FLSOFY 20
C          FLSOFY 21
C          FLSOFY 22
C          FLSOFY 23
C          FLSOFY 24
C          FLSOFY 25
C          FLSOFY 26
C          FLSOFY 27
C          FLSOFY 28
C          FLSOFY 29
C          FLSOFY 30
C          FLSOFY 31
C          FLSOFY 32
C          FLSOFY 33
C          FLSOFY 34
C          FLSOFY 35
C          FLSOFY 36
C          FLSOFY 37
C          FLSOFY 38
C          FLSOFY 39
C          FLSOFY 40
C          FLSOFY 41
C          FLSOFY 42
C          FLSOFY 43
C          FLSOFY 44
C          FLSOFY 45
C          FLSOFY 46
C          FLSOFY 47
C          FLSOFY 48
C          FLSOFY 49
C          FLSOFY 50
C          FLSOFY 51
C          FLSOFY 52
C          FLSOFY 53
C          FLSOFY 54
C          FLSOFY 55
C          FLSOFY 56
C          FLSOFY 57
C          FLSOFY 58
C          FLSOFY 59
C          FLSOFY 60
C          FLSOFY 61
C          FLSOFY 62
C          FLSOFY 63
C          FLSOFY 64
C          FLSOFY 65
C          FLSOFY 66
C          FLSOFY 67
C          FLSOFY 68
C          FLSOFY 69
C          FLSOFY 70
C          FLSOFY 71
C          FLSOFY 72
C          FLSOFY 73
C          FLSOFY 74
C          FLSOFY 75
C          FLSOFY 76
C          FLSOFY 77
C          FLSOFY 78
C          FLSOFY 79
C          FLSOFY 80
C          FLSOFY 81
C          FLSOFY 82
C          FLSOFY 83
C          FLSOFY 84
C          FLSOFY 85
C          FLSOFY 86
C          FLSOFY 87
C          FLSOFY 88
C          FLSOFY 89
C          FLSOFY 90
C
C          *****
C          PURPOSE
C          FLSOFY CONSTRUCTS A LEAST SQUARES POLYNOMIAL APPROXIMATION
C          OF SPECIFIED DEGREE TO A GIVEN SET OF DATA POINTS WITH
C          GIVEN WEIGHTS USING ORTHOGONAL POLYNOMIALS.
C          USAGE
C          DIMENSION X(N),Y(N),W(N),S1(MN1,6),A(N+1)
C          CALL FLSOFY (M,N,X,Y,W,MN1,S1,A,IEP)
C          INPUT PARAMETERS
C          N - NUMBER OF DATA POINTS
C          M - DEGREE OF POLYNOMIAL DESIRED, N.L.T.M
C          X - ARRAY OF INDEPENDENT VARIABLES
C          Y - ARRAY OF DEPENDENT VARIABLES
C          W - ARRAY OF POSITIVE WEIGHTS
C          MN1 - ROW DIMENSION OF SCRATCH ARRAY S1, MN1.GE.M
C          S1 - SCRATCH ARRAY
C          IN THE COLUMN DEFINITIONS *LEW,
C          I REFERS TO POLYNOMIAL ORDER
C          J REFERS TO ROW INDEXING WITHIN A COLUMN
C          COL 1 POLYNOMIAL P(I-1), VALUE BY EACH Y(I) THRU 243
C          COEFFICIENT OF EACH X**(J-1) TERM AFTER 243
C          COL 2 POLYNOMIAL P(I), SAME FORM AS COL 1
C          COL 3 ALPHA(I+1), WHERE I=J
C          COL 4 BETA(I), WHERE I=J-1
C          COL 5 S(I), WHERE I=J-1
C          COL 6 SIGMA**2, WHERE I=J-1
C          OUTPUT PARAMETERS
C          A - ARRAY OF COMPUTED COEFFICIENTS
C          A(I) THRU A(M+1) CONTAIN COMPUTED POLYNOMIAL
C          COEFFICIENTS, IN ORDER OF INCREASING DEGREE.
C          TER - ERROR INDICATOR
C          .E0.0 SUCCESS
C          .E0.1 (N.GE.M).OR.(N.LT.0)
C          .E0.2 MN1.LT.M
C          .E0.3 *LEW
C          .E0.4 *M1.LE.0)
C          REFERENCE
C          KEMPNER, G. S., GENERATION AND USE OF ORTHOGONAL
C          POLYNOMIALS FOR DATA-FITTING WITH A DIGITAL COMPUTER,
C          J. SIAM, VOL. 9, NO. 2, (JUNE 1971) PP. 74-84.
C          NOTE - MOST NOTATION AND MOST LOCAL VARIABLE NAMES ARE
C          BASED ON THE REFERENCE. *LEW IS W(I), *M1 IS P(I),
C          *M1 W, *M1 AND *M1 REFER TO THE WEIGHTS ARRAY.
C          *****
C          DIMENSION X(1),Y(1),W(1),S1(MN1,1),A(1)
C          *****
C          *** INITIAL SET-UP ***
C          TEST FOR USER ERRORS
C          I0, TER = 4
C          IF ((N.GE.M).OR.(N.LT.0)) I0=1
C          IF (MN1.LT.M) I0=2
C          IF (M.LT.0) I0=3
C          IF (IEP.NE.4) GO TO 90
C          IF ((S1(1,1).GT.0) .AND. S1(1,2).GT.0) W(1)=SUM(W(1))
C          N1 = N+1
C          S1(1,4)=0.
C          NSO=0.
C          WPP=0.
C          NO 11, J=1,M
C          S1(J,2)=1.
C          S1(J,1)=0.
C          W1 = W(J)
C          IF (M1.LT.0) GO TO 90:
C          WPP = WPP+W1
C          11) NSO = NSO+W1*Y(J)*Y(J)
C          *****
C          *** GENERATE ORTHOGONAL POLYNOMIALS - THRU 90 ***
C          DO 24F I=1,M1
C          WPP=0.
C          WPP=0.
C          COMPUTE (W(I),X(I), AND ONE-GA(I)=(C.F.O(I))
C          NO 2. J=1,M
C          TER=0.5*(S1(J,2)
C          IF (I.LT.M1) WPP=WPP+TER*W(I)*Y(I)*Y(I)
C          2.) WPP=WPP+TER*W(I)
C          S1(I,1)=WPP/WPP
C          DELTA**2(I)=DELTA**2(I-1)-S1(I)**2*W(I,1)
C          NSO=NSO-S1(I,1)*S1(I,1)*WPP
C          SIGMA**2(I)=DELTA**2(I)/(DEGREE OF FREEDOM)
C          SIGMA**2(I)=0
C          NR = N-1
C          FLSOFY 89

```

```

VF (BR,NE,DO) RR = DSQ/RR
SI(T,6) = RR
C      T(M) 240 - CALCULATIONS FOR NEXT I, SKPT WHEN I=N+1
C      ALPHA(I+1)=(XPI(I),XPI(I)/N(I,1)
C      IF (I,GE,N+1) GO TO 240
SI(I,3)=XKPP/UPP
UPP=UPP
UPP=N
BT=SI(I,4)
AL=SI(I,3)
C      P(I+1)=(1-ALPHA(I+1))P(I)-BETA(I)P(I-1)
C      U(I+1)=T+(XPI(I+1),XPI(I+1)), 0(I+1)=U(I+1)+T+1)/U(I,1)
C      DO 230 J=1,M
      TEMP=(J)-AL+SI(J,2)-BT+SI(J,1)
      UPP=UPP+(J)+TEMP+2
      SI(J,1)=SI(J,2)
230 SI(J,2)=TEMP
      SI(I+1,4)=UPP/UPP
240 CONTINUE
C      *** COMPUTE COEFFICIENTS OF SECOND SQUARES POLYNOMIAL
C      A = S(C)P(0)+...+S(N)P(N) ***
C      B(I)=1, P(I)=0, A(INITIAL)=S(C)*P(2)+C(I)
      DO 249 I=1,M1
      A(I)=0
      SI(I,1)=0
31. SI(I,2)=0
      SI(I,2)=0
      A(I)=SI(I,3)
C      SUM I OTH THRU 310 I = ORDER OF POLYNOMIAL FORME)
      DO 310 I=1,M
      AL=SI(I,3)
      BT=SI(I,4)
      T=0
      II = I+1
      FORM P(I+1)=XPI(I)-ALPHA(I+1)P(I)-BETA(I)P(I-1)
      AND ADD TO POLYNOMIAL SUM IN A
      DO 311 I=1,II
      T2=YZ-AL*SI(I,2)-BT*SI(I,1)
      T2=C1(I,2)
      SI(I,1)=SI(I,2)
      SI(I,2)=T2
31. A(I)=A(I)+T2*SI(I,1)
      J=0
90. RETURN
END

SUBROUTINE IJTRAJ(XP,YP,IT,JT,OJ,FLAG)
C      THIS SUBROUTINE LOCATES A TRAJECTORY POINT IN
C      THE COMPUTATIONAL GRID
C      IT,JT IS LOWER LEFT CORNER OF GRID SECTION CONTAINING (XP,YP)
C      COMMON /ALUNT/ THETA(25),PP(2,25),NRLUNT
C      COMMON /RUNDOS/ XADD(100),YADD(100),YCHK(100),YSHK(100),
C      * NMAX,KNAX,KMAX,AMAX,GAMMA,MRO,MHINDX
C      LEVEL 20 ANGD,DXTH,DEG
C      COMMON /DOD/ ANG(2,20),DXT4(100),DEG
C      COMMON /FLTW/ XC(2,100),YC(2,100),XF(2,100),YF(2,100),RHF(20,100)
C      PRINT IS IN POLAR COORDINATE REGION
      IF (YF .GE. DO) GO TO 50
      THA=ATAN2(YF,YP)+DEG
      N=SQRT(YF**2+XF**2)
      DO 1 J=2,NRLUNT
      IF (THETA(J) .GT. THA) GO TO 20
2. CONTINUE
      J=NRLUNT
      JT=J-1
      OJ=(THETA(J)-THA)/DXTH(JT)
      J2=PP(1,JT)*OJ+PP(1,JT+1)*(1.0-OJ)
      IF (YF .LT. J2) GO TO 100
      DO 3 I=2,NMAX
      J2=PP(1,JT)*OJ+PP(1,JT+1)*(1.0-OJ)
      IF (J2 .GT. YF) GO TO 40
3. CONTINUE
      GO TO 150

```

```

FLSOFY  96
FLSOFY  97
FLSOFY  98
FLSOFY  99
FLSOFY 100
FLSOFY 101
FLSOFY 102
FLSOFY 103
FLSOFY 104
FLSOFY 105
FLSOFY 106
FLSOFY 107
FLSOFY 108
FLSOFY 109
FLSOFY 110
FLSOFY 111
FLSOFY 112
FLSOFY 113
FLSOFY 114
FLSOFY 115
FLSOFY 116
FLSOFY 117
FLSOFY 118
FLSOFY 119
FLSOFY 120
FLSOFY 121
FLSOFY 122
FLSOFY 123
FLSOFY 124
FLSOFY 125
FLSOFY 126
FLSOFY 127
FLSOFY 128
FLSOFY 129
FLSOFY 130
FLSOFY 131

```

```

40 IT=I-1
OJ=(P2-R)/(R2-R1)
FLAG=0
RETURN
C      POINT IS IN RECTANGULAR COORDINATE REGION
50 CONTINUE
      NXI=NRLUNT+1
      DO 60 J=NXI,KNMAX
      IF (YC(1,J) .GT. YF) GO TO 70
6. CONTINUE
      J=NRLUNT
70 JT=J-1
      OJ=(YC(1,JT+1)-YF)/DXT4(JT)
      Y2=YC(1,JT)*OJ+YC(1,JT+1)*(1.0-OJ)
      IF (YF .LT. Y2) GO TO 100
      DO 80 I=2,NMAX
      Y1=Y2
      Y2=YC(1,JT)*OJ+YC(1,JT+1)*(1.0-OJ)
      IF (Y2 .GT. YF) GO TO 90
8. CONTINUE
      GO TO 150
90 IT=I-1
      OJ=(Y2-YF)/(Y2-Y1)
      FLAG=1
      RETURN
C      POINT IS INSIDE IONPAUSE
100 CONTINUE
      FLAG=-1
      RETURN
C      POINT IS BEYOND BOV SHOCK
15. CONTINUE
      FLAG=1
      RETURN
END

```

```

IJTRAJ  33
IJTRAJ  34
IJTRAJ  35
IJTRAJ  36
IJTRAJ  37
IJTRAJ  38
IJTRAJ  39
IJTRAJ  40
IJTRAJ  41
IJTRAJ  42
IJTRAJ  43
IJTRAJ  44
IJTRAJ  45
IJTRAJ  46
IJTRAJ  47
IJTRAJ  48
IJTRAJ  49
IJTRAJ  50
IJTRAJ  51
IJTRAJ  52
IJTRAJ  53
IJTRAJ  54
IJTRAJ  55
IJTRAJ  56
IJTRAJ  57
IJTRAJ  58
IJTRAJ  59
IJTRAJ  60
IJTRAJ  61
IJTRAJ  62
IJTRAJ  63
IJTRAJ  64
IJTRAJ  65
IJTRAJ  66
IJTRAJ  67
IJTRAJ  68
IJTRAJ  69
IJTRAJ  70
IJTRAJ  71
IJTRAJ  72
IJTRAJ  73

```

```

SUBROUTINE INPIT
C      THIS ROUTINE READS ALL DATA REQUIRED FOR ONE CASE,
C      EXCEPT FLOW FIELD DATA FOR RERUN
C      INPIT  2
C      INPIT  3
C      INPIT  4
C      INPIT  5
C      INPIT  6
C      COMMON /RTN/ ANGD,ANGN,KKCON,SCON(20)
C      COMMON /CMI/ JMAX,KNAX,JN,KN,XMAC,ALPHA,GAM,GAHI,CH,DT,SMI,DPRT,
C      * CPOFF,NC,NCS,NCC,AA,M,DMEGA,NU,NL,IT,TAU,ITEO,EMT,PTORT,PIFF,
C      * PTIF,ATNF,INP,JC,TM,CIUS,PT,MORN,PMNSZ,NCAS,MPUNCH
C      COMMON /CONIT/ KVCOM,VCOM(20),KPCOM,RCOM(2)
C      COMMON /ALUNT/ THETA(25),PP(2,25),NRLUNT
C      COMMON /RNDSTRM/ 7PLOT,NZERO,NZADD,NXPLOT
C      COMMON /JOE/ ZL1,CF1,CF2,ZLF,ZTRAN,DZTRAN
C      LOGICAL LGRAV
C      COMMON /NRUND/ XX(100),YY(100),N800,LOGRAV
C      COMMON /RUNDOS/ YADD(100),Y500(100),YCHK(100),YSHK(100),
C      * NMAX,KNAX,APACH,GAMMA,MRO,MHINDX
C      LOGICAL LREUM,LPRFL,LPRST,LPRON,LPR,LPLOT,LTRAJ,LRSTRT
C      COMMON /PROPT/ LBERUM,PRFL,LPRST,LPRCON,LPR,LPLTLTRAJ,LRSTRT
C      COMMON /TRAJDAT/ NTRAJ,TRAJ(100),YTRAJ(100),YTRAJ(100),ZTRAJ(100),
C      * YTRAJ(100),XTRAJ(100),YTRAJ(100),ZTRAJ(100),
C      * XTRAJ(100),YTRAJ(100),ZTRAJ(100),
C      * XTRAJ(100),YTRAJ(100),ZTRAJ(100),
C      * XTRAJ(100),YTRAJ(100),ZTRAJ(100)
C      COMMON /MARKPLOT/ MARKPT,MARKT(12)
C      LOGICAL LPLTRJ
C      COMMON /ITOPT/ LPLTRJ,PLMNT,VINF,RMINF,TPINF,8INF
C      LOGICAL LSUM
C      COMMON /SUMDAT/ LSUM,XTRAJS(100),YTRAJS(100),ZTRAJS(100),
C      * XTRAJS(100),AZANG,POLANG,RY1,RY2,RZ1
C      DIMENSION TITLE(8)
C      DIMENSION NK(100)
C      DIMENSION RR(100)
C      EQUIVALENCE (RR(1),YY(1))
C      DATA NMLANK/14 /,MSTAR/140/
C      READ CARD INPUT FOR ONE COMPLETE CALCULATION
C      INPIT  25
C      INPIT  26
C      INPIT  27
C      INPIT  28

```

```

READ(5,110) ANACH,GAPNA,HRO,XCALC,NR,NRLUNT,CM,ITER      INPUT      29
NTPM=NTPM      INPUT      30
READ(5,120) LRRUN,LPRFL,LPRST,LPRCON,LPPR,LPLDT,LTRAJ,LPRSTRT INPUT      31
READ(5,130) XPLDT,ANGP,AMRN,MAXADD,LGRAV      INPUT      32
TF (LPLDT) LPRCON=.TRUE.      INPUT      33
TF (XPLDT) GE. G.0) XPLDT=-1.)      INPUT      34
ZPLDT=XPLDT      INPUT      35
READ(5,140) KVCOM      INPUT      36
IF (KVCOM .GT. 0) READ(5,160) (VCOM(I),I=1,KVCOM)      INPUT      37
READ(5,141) KRCON      INPUT      38
IF (KRCON .GT. 3) READ(5,160) (RCON(I),I=1,KRCON)      INPUT      39
READ(5,142) KRCON      INPUT      40
IF (KRCON .GT. 3) READ(5,160) (RCON(I),I=1,KRCON)      INPUT      41
TF (.NOT. LTRAJ) GO TO 5      INPUT      42
READ(5,170) NTRAJ,(YTRAJ(I),XTRAJ(I),YTRAJ(I),ZTRAJ(I),I=1,NTRAJ) INPUT      43
READ(5,191) (LTRAJ,NPLNT,VINF,RHJINF,TMPINF,ATMF      INPUT      44
READ(5,143) NHARKT      INPUT      45
TF (NHARKT .GT. 0) READ(5,192) (NHARKT(I),I=1,NHARKT)      INPUT      46
READ(5,190) (SIN,ASANG,POLANG,RV1,RV1,RV1)      INPUT      47
TF (LSUM) CALL ROTAT(1)      INPUT      48
5 CONTINUE      INPUT      49
NHTMPC=0      INPUT      50
IF (NHON .GT. 0.0) NHTMPC=1      INPUT      51
IF (I .EQ. UN) GO TO 10      INPUT      52
TF (NHON .LT. .001) READ(5,150) NHND,(XY(I),RR(I),I=1,NHND)      INPUT      53
C      INPUT      54
C      INPUT      55
C      INPUT      56
C      INPUT      57
INITIALIZE DEFAULT PARAMETERS      INPUT      58
TF (XCALC .GE. C.0) XCALC=-1.0      INPUT      59
ZLF=XCALC      INPUT      60
TF (NR .LE. 3) NR=10      INPUT      61
IF (NRLUNT .LE. 0) NRLUNT=24      INPUT      62
TF (CM .LE. 3.0) CM=3.0      INPUT      63
TF (ITER .LE. 3) ITER=300      INPUT      64
TF (MAXADD .LE. 0) MAXADD=0      INPUT      65
JMAX=NRLUNT+MAXADD+1      INPUT      66
NHARKT=NP      INPUT      67
NHARKT=NR      INPUT      68
NTPM=NTPM+1      INPUT      69
NTRAJ=NTRAJ+1      INPUT      70
VINF=ANACH      INPUT      71
CAM=GAPNA      INPUT      72
C      INPUT      73
C      INPUT      74
C      INPUT      75
WRITE OUT INPUT AND DEFAULT VALUES TO BE USED      INPUT      76
10 CONTINUE      INPUT      77
WRITE(6,20) TITLE      INPUT      78
TF (LGRAV) RETURN      INPUT      79
WRITE(6,210) ANACH,GAPNA      INPUT      80
WRITE(6) NRLUNT,NR,ANACH,GAPNA,ATMP      INPUT      81
TF (NTPM) 14,16,18      INPUT      82
24 WRITE(6,214) NHND,(XY(I),RR(I),I=1,NHND)      INPUT      83
WRITE(6) NHND,(XY(I),RR(I),I=1,NHND)      INPUT      84
GO TO 2.      INPUT      85
25 WRITE(6,216)      INPUT      86
GO TO 20      INPUT      87
26 WRITE(6,218) GO TO 10      INPUT      88
WRITE(6,219) HORN      INPUT      89
GO TO 25      INPUT      90
27 WRITE(6,219) HORN      INPUT      91
28 CONTINUE      INPUT      92
WRITE(6,222) NR,NRLUNT,MAXADD,CM,ITER,XCALC      INPUT      93
WRITE(6,230) XPLDT      INPUT      94
TF (LSUM) GO TO 17      INPUT      95
WRITE(6,231) ANGP,ANGN      INPUT      96
17 CONTINUE      INPUT      97
WRITE(6,235) LRRUN,LPRFL,LPRST,LPRCON,LPPR,LPLDT,LTRAJ,LPRSTRT INPUT      98
TF (.NOT. LTRAJ) GO TO 29      INPUT      99
RCR=1.;RPLNT      INPUT      100
WRITE(6,260) LPLTRAJ,RCR,VINF,RHJINF,TMPINF      INPUT      101
TF (LSUM) WRITE (6,269) (TMP,RV1,RV1,RV1,ASANG,POLANG      INPUT      102
WRITE(6,253) NTRAJ,NHARKT      INPUT      103
GO TO 2. N=1,NTRAJ      INPUT      104
NH(N)=NRLANK      INPUT      105
TF (NHARKT .LE. 0) GO TO 24      INPUT      106
DO 22 I=1,NHARKT      INPUT      107
NHARKT(I)      INPUT      108
22 NH(N)=NHARKT      INPUT      109
24 CONTINUE      INPUT      110
WRITE (6,268)      INPUT      111
WRITE (6,267) (N,NK(N),YTRAJ(N),XTRAJ(N),YTRAJ(N),ZTRAJ(N),      INPUT      112
N=1,NTRAJ)      INPUT      113
25 CONTINUE      INPUT      114
WRITE(6,240)      INPUT      115
WRITE(6,242) KVCOM      INPUT      116
TF (KVCOM .GT. 0) WRITE(6,250) (VCOM(I),I=1,KVCOM)      INPUT      117
WRITE(6,244) KRCON      INPUT      118
TF (KRCON .GT. 0) WRITE(6,250) (RCON(I),I=1,KRCON)      INPUT      119
WRITE(6,246) KRCON      INPUT      120
TF (KRCON .GT. 0) WRITE(6,250) (RCON(I),I=1,KRCON)      INPUT      121
ATMP=.01745329232      INPUT      122
ANGP=ANGPDTOR      INPUT      123
ANGN=ANGNDTOR      INPUT      124
RETURN      INPUT      125
C      INPUT      126
100. FORMAT(A10)      INPUT      127
110. FORMAT(F10.0,2E11,7F10.0,1I0)      INPUT      128
120. FORMAT(L10)      INPUT      129
130. FORMAT (3F10.0,1D,1I0)      INPUT      130
140. FORMAT(I10)      INPUT      131
150. FORMAT(I10,12F10.0)      INPUT      132
160. FORMAT(F10.0)      INPUT      133
170. FORMAT(I10,14F10.0)      INPUT      134
180. FORMAT(I10)      INPUT      135
190. FORMAT(I10,5F10.0)      INPUT      136
200. FORMAT(1H//25X,PA,1//25X,15HINPUT VARIABLES/25X,15(14H)) INPUT      137
210. FORMAT(//20X,25HINTERPLANETARY MACH NO. =F6.2      INPUT      138
*      INPUT      139
* //2. X,21H5SPECIFIC HEAT RATIO =F6.1)      INPUT      140
214. FORMAT(//23X,46HOBSTACLE GEOMETRY: USER-SUPPLIED COORDINATES --      INPUT      141
*      INPUT      142
* 14,7H POINTS//33H,34F7.0,11X,34F7.0)      INPUT      143
* (3E, F6.4,6X, F6.1)      INPUT      144
215. FORMAT(//23X,42HOBSTACLE GEOMETRY: DEFAULT MAGNETOPAUSE COORDINAT,      INPUT      145
*      INPUT      146
* 21HES = EQUATORIAL TRACE)      INPUT      147
214. FORMAT(//23X,42HOBSTACLE GEOMETRY: DEFAULT IONOPAUSE SHAPE,      INPUT      148
*      INPUT      149
* 7,30X,36HFOR CONSTANT SCALE HEIGHT WITH N/RJ=F6.2)      INPUT      150
210. FORMAT(//23X,42HOBSTACLE GEOMETRY: DEFAULT IONOPAUSE SHAPE,      INPUT      151
*      INPUT      152
* 7,39X,314NHM GRAVITATIONAL VARIATION Tn      INPUT      153
*      INPUT      154
* 7,39X,194SCALE HEIGHT, N/RJ=F6.2)      INPUT      155
220. FORMAT(//23X,37HPARAMETERS FOR ALUNT BODY CALCULATION//      INPUT      156
*      INPUT      157
* 35X,284ND. OF PARTIAL MESH POINTS =I4)      INPUT      158
*      INPUT      159
* 25X,234ND. OF ANGULAR MESH POINTS =I4)      INPUT      160
*      INPUT      161
* 25X,274ND. OF ADDITIONAL POINTS IN)      INPUT      162
*      INPUT      163
* 35X,184NRLUNT BODY MESH =I4)      INPUT      164
*      INPUT      165
* 25X,144NDUPANT NUMBER,13X,1H=F6.2)      INPUT      166
*      INPUT      167
* 25X,174ND. OF ITERATIONS,10X,1H=I4)      INPUT      168
*      INPUT      169
* //23X,42HINTERNAL DOWNSTREAM LOCATION FOR PLOTTING =      INPUT      170
*      INPUT      171
* 7H,CALCULATION,19D=F6.2)      INPUT      172
230. FORMAT(//2. X,47HINTERNAL DOWNSTREAM LOCATION FOR PLOTTING,17D=      INPUT      173
*      INPUT      174
* F6.2)      INPUT      175
231. FORMAT(//23X,53HUSER SPECIFIED DEVIATION IN SOLAR-WIND COORDINATES      INPUT      176
*      INPUT      177
* //23X,47HOF MAGNETIC FIELD SYMMETRY-PLANE COMPONENT FROM,      INPUT      178
*      INPUT      179
* //20X,17H FLOW DIRECTION =F7.2,8H DEGREES      INPUT      180
*      INPUT      181
* //23X,50HUSER SPECIFIED DEVIATION IN SOLAR-WIND COORDINATES      INPUT      182
*      INPUT      183
* //23X,50HOF MAGNETIC FIELD FROM MAGNETIC SYMMETRY PLANE =,      INPUT      184
*      INPUT      185
* F7.2,14 DEGREES)      INPUT      186
235. FORMAT(//23X,84HRRUN =L2//23X,84HPRFL =L2//20X,84HPRST =L2,      INPUT      187
*      INPUT      188
* //23X,84HPRCON =L2//23X,84HPPR =L2//23X,84HPLDT =L2,      INPUT      189
*      INPUT      190
* //23X,84HLTRAJ =L2//23X,84HLRSTRT =L2)      INPUT      191
240. FORMAT(14I//45X,40HVALUES SPECIFIED FOR CONTOUR CALCULATION/      INPUT      192
*      INPUT      193
* 45X,40(1H=))      INPUT      194
242. FORMAT(//20X,12,29H CONTOUR LEVELS FOR VLOCITY)      INPUT      195
244. FORMAT(//20X,12,29H CONTOUR LEVELS FOR DENSITY)      INPUT      196
246. FORMAT(//23X,12,44H CONTOUR LEVELS FOR MAGNETIC FIELD STRENGTH)      INPUT      197
250. FORMAT(10I,6F10.0)      INPUT      198
260. FORMAT(20X,84HPLTRAJ =L2/      INPUT      199
*      INPUT      200
* 14I//25X,32HINPUT FOR TRAJECTORY CALCULATION/      INPUT      201
*      INPUT      202
* 50X,32(14=)///      INPUT      203
*      INPUT      204
* //20X,34HRO/PLANET =F6.4,6/      INPUT      205
*      INPUT      206
* //20X,34HINTERPLANETARY VELOCITY =L2E11.2/      INPUT      207
*      INPUT      208
* //23X,34HINTERPLANETARY DENSITY =F11.3/      INPUT      209
*      INPUT      210
* //23X,34HINTERPLANETARY TEMPERATURE =F11.3/      INPUT      211
*      INPUT      212
* //23X,34HINTERPLANETARY MAGNETIC FIELD =      INPUT      213
*      INPUT      214
* //23X,74HTRAJ =I6,15,84HMARKT =I3)      INPUT      215
*      INPUT      216
* 30X,45H( = POINT TO BE MARKED FOR CROSS REFERENCE)///      INPUT      217
*      INPUT      218
* 28X,144X,9X,54HTRAJ,8X,54HTRAJ,7X,54HTRAJ,7X,54HTRAJ//      INPUT      219
267. FORMAT(25X,14,1X,A1,3X,F10.0,3X,F6.4,2(4Y,6,41))      INPUT      220
265. FORMAT(44X,30H(SUN-PLANE) COORDINATE SYSTEM)      INPUT      221
269. FORMAT(35X,14H MAGNITUDE =E11.3      INPUT      222
*      INPUT      223
* //35X,144X-COMPONENT =E11.3      INPUT      224
*      INPUT      225
* //35X,144X-COMPONENT =E11.3      INPUT      226
*      INPUT      227
* //20X,29HAZIMUTHAL ANGLE =E11.3/      INPUT      228
*      INPUT      229
* //20X,29HPOLAR ANGLE =E11.3)      INPUT      230
END      INPUT      231

```

```

SUBROUTINE LABEL
THIS ROUTINE ELIMINATES OVERLAP IN PLOTTING A
SET OF CONTOUR LABELS.
COMMON /LABLE/ YLAB(30),YLAB(30),CV(30),NCL,ITL(30),MLA9
COMMON /SCALE/ XSF,YSF,XMAX,YMAX,XLNGTH,YLNGTH
COPY THE ARRAY YLAB INTO ASCENDING ORDER. CHANGE
THE ORDER OF XLAB AND CV TO CORRESPOND.
CALL MURKLE(LAB,YLAB,CV,NCL,ILA,MLA9)
FIND FIRST LABEL FROM SORTED ARRAY THAT IS ABOVE X-AXIS.
DO 5 K=1,NCL
  IF(YLAB(K).LT.0.) GO TO 5
  KMIN=K
  GO TO 10
5 CONTINUE
NO LABELS FOUND ABOVE X-AXIS. MAD SET OF CONTOUR VALUES
SPECIFIED. STOP PROGRAM.
WRITE(6,2)
2) FORMATE (14,1)M*****1)X,4MUMBLE TO LABEL CONTOUR LINES REC
IANSF OF OVERLAP,10)IC*****
STOP
1) ITL(1)=KMIN
MLA=1
IF(NCL.EQ.1) RETURN
EXAMINE ALL LABELS BEYOND LABEL KMIN FOR OVERLAP.
K=2
KMIN=KMIN+1
DO 15 I=KMIN,NCL
  IF(YLAB(I).LT.YLAB(KMIN)+.1/YSF.AND.XLAB(I).LT.XLAB(KMIN))
  1 0.4/YSF) GO TO 15
SAVE ARRAY INDEY FOR LABEL TO BE PLOTTED.
KMIN=I
ILN(I)=I
YLAB=K
K=K+1
15 CONTINUE
ENSURE THAT THE LAST LABEL IS PLOTTED.
ITL(NCL)=NCL
RETURN
END

```

```

LABEL 2
LABEL 3
LABEL 4
LABEL 5
LABEL 6
LABEL 7
LABEL 8
LABEL 9
LABEL 10
LABEL 11
LABEL 12
LABEL 13
LABEL 14
LABEL 15
LABEL 16
LABEL 17
LABEL 18
LABEL 19
LABEL 20
LABEL 21
LABEL 22
LABEL 23
LABEL 24
LABEL 25
LABEL 26
LABEL 27
LABEL 28
LABEL 29
LABEL 30
LABEL 31
LABEL 32
LABEL 33
LABEL 34
LABEL 35
LABEL 36
LABEL 37
LABEL 38
LABEL 39
LABEL 40
LABEL 41
LABEL 42
LABEL 43
LABEL 44
LABEL 45
LABEL 46
LABEL 47
LABEL 48
LABEL 49
LABEL 50
LABEL 51
LABEL 52
LABEL 53
LABEL 54
LABEL 55
LABEL 56
LABEL 57
LABEL 58

```

```

SUBROUTINE MAP (A,JMIN,X,Y,MLIN,KOD,ACONT,MAD,ISIZ1,ISIZ2,ICM,
JMIN,KMIN,JMAX,KMAX)
CONTOUR PROGRAMS MAP, WALK, SEARCH, ENTER, AND CHECK
WRITTEN BY REESE SOMERSON, NASA-GMEX PDS, CTR., AUG., 1974.
(MODIFIED VERSION)
THIS SUBROUTINE AND THOSE WHICH IT CALLS PREPARE DATA
FOR CONTOUR PLOTTING.
CALLING PARAMETERS:
A TWO-DIMENSIONAL ARRAY TO BE CONTOUR PLOTTED.
JMIN FIRST-POSITION DIMENSION-SIZE OF A.
X,Y ARRAYS TO CONTAIN CONTOUR LINE DATA UPON RETURN.
EACH PAIR OF X(I) AND Y(I) REPRESENTS A POINT ON A
CONTOUR LINE.
MLIN IS THE NUMBER OF CONSTANT-A CONTOUR LEVELS.
KOD =1 IF CONTOUR LEVELS ARE TO BE COMPUTED INTERNALLY
BY LINEARLY INTERPOLATING BETWEEN THE MAXIMUM AND
MINIMUM VALUES OF A.
=2 IF CONTOUR LEVELS ARE TO BE GIVEN BY THE USER.

```

```

ACONT ARRAY OF CONTOUR LEVELS. SCRATCH IF KOD=1.
IF KOD=2, ACONT MUST BE FILLED WITH MONOTONICALLY
INCREASING CONTOUR LEVELS. SHOULD BE DIMENSIONED
AT LEAST MLIN.
MAD IT SHOULD BE RECOGNIZED THAT MANY CONTOUR LINES
MIGHT RESULT FROM EACH CONTOUR LEVEL.
UPON RETURN, MAD(I) IS THE TOTAL NUMBER OF CONTOUR
LINES. ALL THE LINES ARE RUN-TOGETHER, HEAD TO TAIL
IN ARRAYS X AND Y. THE FIRST LINE STARTS AT X(I)
AND Y(I) AND ENDS AT X(I) AND Y(I) FOR I=MAD(I)-1.
THE N-TH CONTOUR LINE STARTS AT X(I) AND Y(I) FOR
I=MAD(I) AND ENDS AT X(I) AND Y(I) FOR I=MAD(I)+1.
MAD(I) FOR M.GE.2 IS THE STARTING INDEX IN X AND Y
OF THE N-TH CONTOUR LINE.
ISIZ1 DIMENSION SIZE OF X AND Y.
ISIZ2 DIMENSION SIZE OF MAD. IT IS DIFFICULT TO SAY
HOW LARGE X, Y, AND MAD SHOULD BE DIMENSIONED.
THIS DEPENDS ON THE DIMENSION SIZE OF ARRAY A,
THE VALUE OF MLIN, AND THE DEGREE OF ECCENTRICITY
OF THE SURFACE REPRESENTED BY ARRAY A. ERROR MESSAGES
WILL RESULT IF THESE ARRAYS ARE TOO SMALL.
ICM AN ARRAY TO BE USED AS SCRATCH BY THE CONTOUR PROGRAMS.
IT SHOULD HAVE AT LEAST 4*ISIZ1 CELLS.
JMIN,KMIN,JMAX,KMAX IT IS RECOGNIZED THAT ONE MIGHT
WISH TO CONTOUR PLOT AN ARRAY A FOR SUBSCRIPTS
STARTING AT SOME VALUE LARGER THAN 1. THIS SUBROUTINE
WILL PROCESS ARRAY A(J,K) FOR JMIN,LE,J,LE,JMAX,
AND KMIN,LE,K,LE,KMAX. JMIN, KMIN, JMAX, AND KMAX
ARE THE LIMITS ON THE SUBSCRIPTS. JMIN AND KMIN MAY
BE 1.
DIMENSION A(1),X(1),Y(1),ACONT(1),MAD(1),ICM(4*1)
INDEX(J,K)=J+(K-1)*JMIN
FIND JMAX AND JMIN
I=INDEX(JMIN,KMIN)
JMAX=I(1)
KMIN=KMAX
DO 1 J=JMIN,JMAX
  I=INDEX(J,K)
  YLAB(I)
  IF(YLAB(I).GT.0.)
  3 JMAX=J
  GO TO 2
  IF(YLAB(I).GT.0.)
  4 JMIN=J
  CONTINUE
FIND ACONT BY LINEARLY INTERPOLATING
GO TO (5,6),KOD
IF(JMAX=JMIN)/FLOAT(MLIN+1)
DO 7 M=1,MLIN
  ACONT(M)=JMIN+FLOAT(M)*DIF
  MMIN=J
  MMAX=JMIN
  GO TO *
CHECK ACONT IF GIVEN BY USER
MMIN=J
MMAX=MMAX+1
IF(MMIN.GT.MLIN) GO TO 9
IF(JMIN.GT.ACNT(MMIN)) GO TO 10
MMAX=MLIN+1
MMAX=MMAX-1
IF(MMAX.LT.1) GO TO 9
IF(JMAX.LT.ACNT(MMAX)) GO TO 11
IF(MMIN.GT.MMAX) GO TO 9
IF (MMIN.EQ.MMAX) GO TO 12
MST=MMIN+1
DO 13 N=MST,MMAX
  IF(ACONT(N).LE.ACNT(MIN-1)) GO TO 9
CONTINUE
PART 1: GO AROUND THE BOUNDARY LOOKING FOR LINES WHICH
INTERSECT THE BOUNDARY.
MAD(1)=0
J=JMIN
K=KMIN

```

```

MAP 24
MAP 25
MAP 26
MAP 27
MAP 28
MAP 29
MAP 30
MAP 31
MAP 32
MAP 33
MAP 34
MAP 35
MAP 36
MAP 37
MAP 38
MAP 39
MAP 40
MAP 41
MAP 42
MAP 43
MAP 44
MAP 45
MAP 46
MAP 47
MAP 48
MAP 49
MAP 50
MAP 51
MAP 52
MAP 53
MAP 54
MAP 55
MAP 56
MAP 57
MAP 58
MAP 59
MAP 60
MAP 61
MAP 62
MAP 63
MAP 64
MAP 65
MAP 66
MAP 67
MAP 68
MAP 69
MAP 70
MAP 71
MAP 72
MAP 73
MAP 74
MAP 75
MAP 76
MAP 77
MAP 78
MAP 79
MAP 80
MAP 81
MAP 82
MAP 83
MAP 84
MAP 85
MAP 86
MAP 87
MAP 88
MAP 89
MAP 90
MAP 91
MAP 92
MAP 93
MAP 94
MAP 95
MAP 96
MAP 97
MAP 98
MAP 99
MAP 100
MAP 101
MAP 102
MAP 103
MAP 104
MAP 105
MAP 106
MAP 107

```

```

NINT=2*(JMAX-JMIN)+2*(KMAX-KMIN)
KOD7=2
KOD2=1
KOD1=1
I=INDEX(JMIN,KMIN)
A=AL(I)
MXY=C
C
DO 25 N=1,NINT
GO TO (7,22,23,24),KOD7
C
C ORIENTATION 1: UPWARDS
21 J=J-1
I=INDEX(J,K)
IF(J.GE.JMIN) GO TO 25
J=J+1
I=INDEX(J,K+1)
KOD7=2
KOD2=1
GO TO 25
C
C ORIENTATION 2: TO THE RIGHT
22 K=K+1
I=INDEX(J,K+1)
IF(K.LT.KMAX) GO TO 25
I=INDEX(J+1,K)
KOD7=1
KOD2=2
GO TO 25
C
C ORIENTATION 3: DOWNWARD
23 J=J+1
I=INDEX(J+1,K)
IF(J.LT.JMAX) GO TO 25
K=K-1
I=INDEX(J,K)
KOD7=4
KOD2=1
GO TO 25
C
C ORIENTATION 4: TO THE LEFT
24 K=K-1
I=INDEX(J,K)
IF(K.GE.KMIN) GO TO 25
K=K+1
J=J-1
I=INDEX(J,K)
KOD7=1
KOD2=2
C
C FIND A4 AND A5
25 A4=A4
A5=A5(I)
IF(A4-A5)26,26,27
26 A4=A4
A5=A5
GO TO 24
27 A4=A4
A5=A5
C
C CHECK TO SEE IF A CONTOUR LINE PASSES THROUGH THE INTERVAL
UNDER CONSIDERATION.
28 KOD8=1
DO 29 NVAL=NMIN,MPAX
VAL=ACONT(NVAL)
GO TO (37,30),KOD8
37 IF(IVAL.LT.A4) GO TO 29
KOD8=2
IF(IVAL.GT.A4) GO TO 23
C
C CHECK TO SEE IF THE CONTOUR LINE POINT JUST FOUND IS A
NEW ONE, OR THE TAIL END OF ONE ALREADY FOUND.
CALL CHECK(ICHK,MXY,KOD2,J,K,NVAL,KOD9)
IF(KOD9.EQ.2) GO TO 29
C
C DETERMINE A1 AND A2
IF(KOD7.EQ.1.OR.KOD7.EQ.4) GO TO 32
A2=A1
A1=A4
GO TO 33
32 A2=A4
A1=A4
C
C ENTER IN THE TABLE THE POINT JUST FOUND.
33 NDUH=NAD(I)+1

```

MAP 100
MAP 109
MAP 110
MAP 111
MAP 112
MAP 113
MAP 114
MAP 115
MAP 116
MAP 117
MAP 118
MAP 119
MAP 120
MAP 121
MAP 122
MAP 123
MAP 124
MAP 125
MAP 126
MAP 127
MAP 128
MAP 129
MAP 130
MAP 131
MAP 132
MAP 133
MAP 134
MAP 135
MAP 136
MAP 137
MAP 138
MAP 139
MAP 140
MAP 141
MAP 142
MAP 143
MAP 144
MAP 145
MAP 146
MAP 147
MAP 148
MAP 149
MAP 150
MAP 151
MAP 152
MAP 153
MAP 154
MAP 155
MAP 156
MAP 157
MAP 158
MAP 159
MAP 160
MAP 161
MAP 162
MAP 163
MAP 164
MAP 165
MAP 166
MAP 167
MAP 168
MAP 169
MAP 170
MAP 171
MAP 172
MAP 173
MAP 174
MAP 175
MAP 176
MAP 177
MAP 178
MAP 179
MAP 180
MAP 181
MAP 182
MAP 183
MAP 184
MAP 185
MAP 186
MAP 187
MAP 188
MAP 189
MAP 190
MAP 191

```

YFENDJH.GY.ISI72) GO TO 35
NAD(I)=NDUH
CALL ENTER(KOD2,J,K,NVAL,A1,A2,JMIN,KMIN,IC4K,KOD4,X,Y,MXY,ACONT,
* ISI71)
IF(KOD4.EQ.2) GO TO 70
NAD(NDUH)=MXY
C
C NOW FOLLOW UP THIS LEAD, WALK THE LENGTH OF THE LINE.
KOD5=KOD7
KOD6=2
JS=J
KS=K
36 CALL WALK(KOD5,JS,KS,A,JDIM,IC4K,JMIN,JMAX,KMIN,KMAX,KOD4,MXY,
* ACONT,KOD6,X,Y,NVAL,ISI71)
IF(KOD4.EQ.2) GO TO 70
IF(KOD5.GT.0) GO TO 36
C
29 CONTINUE
20 CONTINUE
C
C PART 2: SCAN THE WHOLE FIELD FOR LINES THAT DON'T INTERSECT
THE BOUNDARY
JE=JMAX-1
KE=KMAX-1
DO 40 J=JMIN,JE
DO 40 K=KMIN,KE
I=INDEX(JMIN,K)
A2=A(I)
DO 40 J=JMIN,JE
A1=A2
DO 44 KOD2=1,2
GO TO (41,42),KOD2
41 IF(J.E>JMIN) GO TO 46
I=INDEX(J,K+1)
A2=A(I)
GO TO 43
42 I=INDEX(J+1,K)
A2=A(I)
IF(K.EQ.KMIN) GO TO 44
CONTINUE
C
C FIND A4 AND A5
YF(A1-A2)45,45,46
45 A4=A2
A5=A1
GO TO 47
46 A4=A1
A5=A2
C
C CHECK TO SEE IF A CONTOUR LINE PASSES THROUGH THE INTERVAL
UNDER CONSIDERATION.
47 KOD8=1
DO 48 NVAL=NMIN,MPAX
VAL=ACONT(NVAL)
GO TO (49,50),KOD8
49 IF(IVAL.LT.A4) GO TO 48
KOD8=2
YF(IVAL.GT.A4) GO TO 44
C
C WE HAVE FOUND A POINT ON A CONTOUR LINE. CHECK TO SEE IF
IT IS A NEW ONE, OR IF WE HAVE ALREADY DONE THIS LINE.
CALL CHECK(ICHK,MXY,KOD2,J,K,NVAL,KOD9)
IF(KOD9.EQ.2) GO TO 44
C
C WE HAVE A POINT. ENTER IT IN THE TABLE.
NDUH=NAD(I)+1
YFENDJH.GY.ISI72) GO TO 35
NAD(I)=NDUH
CALL ENTER(KOD2,J,K,NVAL,A1,A2,JMIN,KMIN,IC4K,KOD4,X,Y,MXY,ACONT,
* ISI71)
IF(KOD4.EQ.2) GO TO 70
NAD(NDUH)=MXY
C
C NOW WALK THE LENGTH OF THE LINE.
KOD5=KOD2
KOD6=2
MXYST=MXY
JS=J
KS=K
56 CALL WALK(KOD5,JS,KS,A,JDIM,IC4K,JMIN,JMAX,KMIN,KMAX,KOD4,MXY,
* ACONT,KOD6,X,Y,NVAL,ISI71)
IF(KOD4.EQ.2) GO TO 70
IF(KOD5.GT.0) GO TO 56
C

```

MAP 192
MAP 193
MAP 194
MAP 195
MAP 196
MAP 197
MAP 198
MAP 199
MAP 200
MAP 201
MAP 202
MAP 203
MAP 204
MAP 205
MAP 206
MAP 207
MAP 208
MAP 209
MAP 210
MAP 211
MAP 212
MAP 213
MAP 214
MAP 215
MAP 216
MAP 217
MAP 218
MAP 219
MAP 220
MAP 221
MAP 222
MAP 223
MAP 224
MAP 225
MAP 226
MAP 227
MAP 228
MAP 229
MAP 230
MAP 231
MAP 232
MAP 233
MAP 234
MAP 235
MAP 236
MAP 237
MAP 238
MAP 239
MAP 240
MAP 241
MAP 242
MAP 243
MAP 244
MAP 245
MAP 246
MAP 247
MAP 248
MAP 249
MAP 250
MAP 251
MAP 252
MAP 253
MAP 254
MAP 255
MAP 256
MAP 257
MAP 258
MAP 259
MAP 260
MAP 261
MAP 262
MAP 263
MAP 264
MAP 265
MAP 266
MAP 267
MAP 268
MAP 269
MAP 270
MAP 271
MAP 272
MAP 273
MAP 274
MAP 275

```

C      IF THIS LINE IS A CLOSED CURVE, CLOSE IT BY ENTERING FIRST
C      POINT AGAIN.
DIST=SQRT((X(NKYST)-X(NXY))**2+(Y(NKYST)-Y(NXY))**2)
IF(MIN(ST,1,42) GT 4) GO TO 4*
NXY=NXY+1
IFENDY=ST,ISIZ1) GO TO 60
Y(NXY)=Y(NKYST)
Y(NXY)=Y(NKYST)
TCMK(1,NXY)=TCMK(1,NKYST)
TCMK(2,NXY)=TCMK(2,NKYST)
TCMK(3,NXY)=TCMK(3,NKYST)
TCMK(4,NXY)=TCMK(4,NKYST)
C
44 CONTINUE
45 CONTINUE
46 CONTINUE
C      ENTER END OF LAST LINE IN BOOKKEEPING ARRAYS.
NXY=NXY+1
NMIN=NMIN+1) GO TO 35
IFENDY=ST,ISIZ2) GO TO 35
NAD(NMIN)=NXY
GO TO 34
C
C      WRITE "GOOD" MESSAGES.
35 WRITE(4,100)
100 FORMAT(47H1) CONTOUR SEARCH ADOPTED - TABLE OVERFLOW IN MAP)
NAD(1)=ISIZ2)
GO TO 34
C
C      WRITE(4,133)
103 FORMAT(1M,5X,5(1,4),2X,2L) EXECUTION TERMINATED, 2Y,5(1,4) //
* 11,44) ARRAY OF CONTOUR VALUES IMPROPERLY SPECIFIED)
STOP
C
60 WRITE(6,104)
GO TO 7)
104 FORMAT(A4H) CONTOUR SEARCH ADOPTED - TABLE OVERFLOW IN (X,Y)
C
34 RETURN
END

```

```

MAP 276
MAP 277
MAP 278
MAP 279
MAP 280
MAP 281
MAP 282
MAP 283
MAP 284
MAP 285
MAP 286
MAP 287
MAP 288
MAP 289
MAP 290
MAP 291
MAP 292
MAP 293
MAP 294
MAP 295
MAP 296
MAP 297
MAP 298
MAP 299
MAP 300
MAP 301
MAP 302
MAP 303
MAP 304
MAP 305
MAP 306
MAP 307
MAP 308
MAP 309
MAP 310
MAP 311
MAP 312
MAP 313
MAP 314
MAP 315
MAP 316

```

```

C      TPLOT = 4 FOR TEMPERATURE PLOT PLOTCH 11
C      TPLOT = 5 FOR PARALLEL B-FIELD COMPONENT PLOT PLOTCH 12
C      TPLOT = 5 FOR PERPENDICULAR B-FIELD COMPONENT PLOT PLOTCH 13
C      TPLOT = 7 FOR NORMAL B-FIELD COMPONENT PLOT PLOTCH 14
C      PLOTCH 15
COMMON /PLOT/ CONTX(100),CONTY(100),CVAL(10),MAD(10),IPLT
COMMON /BOUNDS/ XBD(100),YBD(100),YSK(100),YSK(100),
* NMAX, NMIN, AMACH, GAMMA, HND, NHINDY
COMMON /SCALE/ XSF, YSF, XMAX, YMAX, XLNGTH, YLNGTH
C
PLOT STREAMLINES PLOTCH 19
THE FIRST CALL TO PLOT INITIALIZES THE PLOT. PLOTCH 20
SCALE FACTORS ARE EQUAL TO 1. PLOTCH 21
SUBROUTINE SETUP ESTABLISHES PERMANENT PLOT ORIGIN, PLOTCH 22
SUBROUTINE ROUND DRAWS AND LABELS SHOCK WAVES, PLANET, PLOTCH 23
AND MAGNETOSPHERE (TROOP=0) OR IONOSPHERE PLOTCH 24
(TROOP=1) BOUNDARY. PLOTCH 25
PLOTCH 26
PLOTCH 27
PLOTCH 28
PLOTCH 29
IF(IPLT,ME,3) GO TO 10 PLOTCH 30
CALL DASH(1,2,3,4,5,6,7,8,9,10) PLOTCH 31
CALL PLOT(3,0,-12,0,-3) PLOTCH 32
CALL SETUP(IPLT,AMACH,GAMMA,NHINDY) PLOTCH 33
CALL ROUND PLOTCH 34
CALL CONTOUR PLOTCH 35
CALL PLOT(XMAX,0,0,-3) PLOTCH 36
CALL RESET PLOTCH 37
CALL PLOT(2,0,0,-3) PLOTCH 38
RETURN PLOTCH 39
C
C      DRAW CONTOUR PLOTS PLOTCH 40
C
1) CONTINUE PLOTCH 41
CALL PLOT(2,0,-12,0,-3) PLOTCH 42
CALL SETUP(IPLT,AMACH,GAMMA,NHINDY) PLOTCH 43
CALL ROUND PLOTCH 44
CALL CONTOUR PLOTCH 45
CALL PLOT(XMAX,0,0,-3) PLOTCH 46
CALL RESET PLOTCH 47
CALL PLOT(2,0,0,-3) PLOTCH 48
IF(IPLT,ME,1) GO TO 2) PLOTCH 49
RETURN PLOTCH 50
C
C      CHANGE VELOCITY CONTOUR VALUES TO TEMPERATURE PLOTCH 51
C
2) IPLT=4 PLOTCH 52
FACT=1.5*(GAMMA-1.0)*AMACH*AMACH PLOTCH 53
NVAL=NMIN(1) PLOTCH 54
DO 25 I=NVAL PLOTCH 55
CVAL(I)=1.0*FACT*(1.0-CVAL(I)**2) PLOTCH 56
25 CONTINUE PLOTCH 57
GO TO 1) PLOTCH 58
END PLOTCH 59
C
SUBROUTINE PLOTFB PLOTFB 2
C THIS SUBROUTINE CONTROLS THE DRAWING OF THE TIME HISTORY PLOTS PLOTFB 3
OF VELOCITY, TEMPERATURE, DENSITY, AND MAGNETIC FIELD PLOTFB 4
PLOTFB 5
COMMON /TRJDAT/ NTRAJ,TTTRAJ(100),XTRAJ(100),YTRAJ(100),ZTRAJ(100), PLOTFB 6
* VTRAJ(1,1),VTRAJ(100),YTRAJ(100),VTRAJ(100),VTRAJ(100), PLOTFB 7
* XTRAJ(100),XTRAJ(100),YTRAJ(100),YTRAJ(100),RDTTRAJ(1,1), PLOTFB 8
* ZTRAJ(100), ZTRAJ(100) PLOTFB 9
LOGICAL LPLTRJ PLOTFB 10
COMMON /TRPNT/ LPLTRJ,RPPLNT,VINF,PHOINF,THOINF,BINF PLOTFB 11
DATA PLTST/7.0/, TLNGTH/P.0/ PLOTFB 12
DATA NSYN/4X /, ISYN/1/ PLOTFB 13
C
CALCULATE SETUP PARAMETERS FOR TIME AXIS PLOTFB 14
NTAXIS=0 PLOTFB 15
CALL TAXIS(TIMESF,TOFFST,TLNGTH,NTAXIS) PLOTFB 16
PLOT V VS TIME PLOTFB 17
CALL TAXIS(TIMESF,TOFFST,TLNGTH,NTAXIS) PLOTFB 18
CALL VAXIS(VSF,VOFFST,VINF,PLTSE,1) PLOTFB 19
CALL SCALE(TIMESF,VSF,1) PLOTFB 20
PLOTFB 21

```

```

CALL OFFST(TOFFST,VOFFST,1)
CALL VECTOR(TTRAJ,VTRAJ,MTRAJ,1,ISYN,MSYM)
CALL MKPLT(TTRAJ,VTRAJ,TIMESF,VSF)
CALL RESET
CALL PLOT(PLTSE,0,0,-3)
C
C
C
PLOT VY VS TIME
CALL TAXIS(TIMESF,TOFFST,TLNGTH,NTAXIS)
CALL VAXIS(VSF,VOFFST,VINF,PLTSE,11)
CALL SCALF(TIMESF,VSF,1)
CALL OFFST(TOFFST,VOFFST,1)
CALL VECTOR(TTRAJ,VTRAJ,MTRAJ,1,ISYN,MSYM)
CALL MKPLT(TTRAJ,VTRAJ,TIMESF,VSF)
CALL RESET
CALL PLOT(PLTSE,0,0,-3)
C
C
C
PLOT VV VS TIME
CALL TAXIS(TIMESF,TOFFST,TLNGTH,NTAXIS)
CALL VAXIS(VSF,VOFFST,VINF,PLTSE,12)
CALL SCALF(TIMESF,VSF,1)
CALL OFFST(TOFFST,VOFFST,1)
CALL VECTOR(TTRAJ,VTRAJ,MTRAJ,1,ISYN,MSYM)
CALL MKPLT(TTRAJ,VTRAJ,TIMESF,VSF)
CALL RESET
CALL PLOT(PLTSE,0,0,-3)
C
C
C
PLOT VZ VS TIME
CALL TAXIS(TIMESF,TOFFST,TLNGTH,NTAXIS)
CALL VAXIS(VSF,VOFFST,VINF,PLTSE,13)
CALL SCALF(TIMESF,VSF,1)
CALL OFFST(TOFFST,VOFFST,1)
CALL VECTOR(TTRAJ,VTRAJ,MTRAJ,1,ISYN,MSYM)
CALL MKPLT(TTRAJ,VTRAJ,TIMESF,VSF)
CALL RESET
CALL PLOT(PLTSE,0,0,-3)
C
C
C
PLOT TEMPERATURE VS TIME
CALL TAXIS(TIMESF,TOFFST,TLNGTH,NTAXIS)
CALL VAXIS(VSF,VOFFST,VINF,PLTSE,20)
CALL SCALF(TIMESF,VSF,1)
CALL OFFST(TOFFST,VOFFST,1)
CALL VECTOR(TTRAJ,VTRAJ,MTRAJ,1,ISYN,MSYM)
CALL MKPLT(TTRAJ,VTRAJ,TIMESF,VSF)
CALL RESET
CALL PLOT(PLTSE,0,0,-3)
C
C
C
PLOT DENSITY VS TIME
CALL TAXIS(TIMESF,TOFFST,TLNGTH,NTAXIS)
CALL VAXIS(VSF,VOFFST,VINF,PLTSE,30)
CALL SCALF(TIMESF,VSF,1)
CALL OFFST(TOFFST,VOFFST,1)
CALL VECTOR(TTRAJ,VTRAJ,MTRAJ,1,ISYN,MSYM)
CALL MKPLT(TTRAJ,VTRAJ,TIMESF,VSF)
CALL RESET
CALL PLOT(PLTSE,0,0,-3)
C
C
C
PLOT R VS TIME
CALL TAXIS(TIMESF,TOFFST,TLNGTH,NTAXIS)
CALL VAXIS(VSF,VOFFST,VINF,PLTSE,40)
CALL SCALF(TIMESF,VSF,1)
CALL OFFST(TOFFST,VOFFST,1)
CALL VECTOR(TTRAJ,VTRAJ,MTRAJ,1,ISYN,MSYM)
CALL MKPLT(TTRAJ,VTRAJ,TIMESF,VSF)
CALL RESET
CALL PLOT(PLTSE,0,0,-3)
C
C
C
PLOT RX VS TIME
CALL TAXIS(TIMESF,TOFFST,TLNGTH,NTAXIS)
CALL VAXIS(VSF,VOFFST,VINF,PLTSE,41)
CALL SCALF(TIMESF,VSF,1)
CALL OFFST(TOFFST,VOFFST,1)
CALL VECTOR(TTRAJ,VTRAJ,MTRAJ,1,ISYN,MSYM)
CALL MKPLT(TTRAJ,VTRAJ,TIMESF,VSF)
CALL RESET
CALL PLOT(PLTSE,0,0,-3)
C
C
C
PLOT RY VS TIME
CALL TAXIS(TIMESF,TOFFST,TLNGTH,NTAXIS)
CALL VAXIS(VSF,VOFFST,VINF,PLTSE,42)
CALL SCALF(TIMESF,VSF,1)
CALL OFFST(TOFFST,VOFFST,1)
CALL VECTOR(TTRAJ,VTRAJ,MTRAJ,1,ISYN,MSYM)
CALL MKPLT(TTRAJ,VTRAJ,TIMESF,VSF)
CALL RESET
CALL PLOT(PLTSE,0,0,-3)
C
C
C
PLOT AZ VS TIME
CALL TAXIS(TIMESF,TOFFST,TLNGTH,NTAXIS)
CALL VAXIS(VSF,VOFFST,VINF,PLTSE,43)
CALL SCALF(TIMESF,VSF,1)
CALL OFFST(TOFFST,VOFFST,1)
CALL VECTOR(TTRAJ,VTRAJ,MTRAJ,1,ISYN,MSYM)
CALL MKPLT(TTRAJ,VTRAJ,TIMESF,VSF)
CALL RESET
CALL PLOT(PLTSE,0,0,-3)
CALL ENPLT(3,0,0,0)
C
C
C
SUBROUTINE PLOTTP
C
C
C
THIS SUBROUTINE PLOTS (X,R) AND (Y,Z) PROJECTIONS OF THE
TRAJECTORY, WHERE R=SQRT(Y**2+Z**2), USING THE SAME SCALE FACTOR
FOR BOTH PLOTS.
CERTAIN POINTS ARE FLAGGED TO PERMIT CROSS-REFERENCING
WITH THE PLOTS OF FLOW FIELD AND MAGNETIC FIELD DATA
C
COMMON /PLTTP/ XTHAX,XTMIN,YTHAX,YTMIN,ZTHAX,ZTMIN,RTMAX
COMMON /ROUNDS/ XROUND(10),YROUND(10),ZROUND(10),
* XTHAX,XTHMIN,XTMIN,XTHAX,XTHMIN,XTHAX,XTHMIN,RTMAX
COMMON /TRAJDAT/ NTRAJ,TTRAJ(100),XTRAJ(100),YTRAJ(100),
* ZTRAJ(100),VTRAJ(100),VYTRAJ(100),VZTRAJ(100),
* RTTRAJ(100)
COMMON /TRAJ(100)/ XTRAJ(100),YTRAJ(100),ZTRAJ(100),
* VTRAJ(100),VYTRAJ(100),VZTRAJ(100),
* RTTRAJ(100)
LOGICAL LPLTRJ
COMMON /TRPTP/ LPLTRJ,PLNT,VINF,RTINF,T*INF,BTNC
C
DIMENSION TITLX(2),TITLY(2)
DATA PTONE/1.57096327/
DATA PLTSE/0.0/
DATA TITLX/10HTRAJECTORY/
DATA TITLY/10HY-Z PROJECTIONS/
DATA TITLX/10HX-R PROJECTIONS/
C
ESTABLISH PLOT ROUNDS
RNDSE=1.0/PLNT
XTHAX=.0C
YTHAX=.0C
YTHMIN=.0C
ZTHAX=.0C
ZTHMIN=.0C
RTMAX=.0C
DO 70 N=1,MTRAJ
IF (XTRAJ(N).GT.XTHAX) XTHAX=XTRAJ(N)
IF (YTRAJ(N).GT.YTHAX) YTHAX=YTRAJ(N)
IF (YTRAJ(N).LT.YTHMIN) YTHMIN=YTRAJ(N)
IF (ZTRAJ(N).GT.ZTHAX) ZTHAX=ZTRAJ(N)
IF (ZTRAJ(N).LT.ZTHMIN) ZTHMIN=ZTRAJ(N)
IF (RTTRAJ(N).GT.RTMAX) RTMAX=RTTRAJ(N)
70 CONTINUE
RTMAX=AMAX1(XTHAX,RNDSE,1.5)
YTHIN=AMIN1(YTHMIN,RNDSE,-1.5)
YTHAX=MAX1(YTHAX,RNDSE,1.5)
YTHIN=MIN1(YTHIN,RNDSE,-1.5)
YTHAX=MAX1(YTHAX,RNDSE,1.5)
ZTHIN=AMIN1(ZTHMIN,RNDSE,-1.5)
ZTHAX=MAX1(ZTHAX,RNDSE,2.0)
XTHAX=.5*AMIN1(2.0,XTHAX,.000)
YTHIN=.5*AMIN1(2.0,YTHIN,-.000)
YTHAX=.5*AMIN1(2.0,YTHAX,.000)
YTHIN=.5*AMIN1(2.0,YTHIN,-.000)
PLOTTP 2
PLOTTP 3
PLOTTP 4
PLOTTP 5
PLOTTP 6
PLOTTP 7
PLOTTP 8
PLOTTP 9
PLOTTP 10
PLOTTP 11
PLOTTP 12
PLOTTP 13
PLOTTP 14
PLOTTP 15
PLOTTP 16
PLOTTP 17
PLOTTP 18
PLOTTP 19
PLOTTP 20
PLOTTP 21
PLOTTP 22
PLOTTP 23
PLOTTP 24
PLOTTP 25
PLOTTP 26
PLOTTP 27
PLOTTP 28
PLOTTP 29
PLOTTP 30
PLOTTP 31
PLOTTP 32
PLOTTP 33
PLOTTP 34
PLOTTP 35
PLOTTP 36
PLOTTP 37
PLOTTP 38
PLOTTP 39
PLOTTP 40
PLOTTP 41
PLOTTP 42
PLOTTP 43
PLOTTP 44
PLOTTP 45
PLOTTP 46
PLOTTP 47
PLOTTP 48
PLOTTP 49
PLOTTP 50
PLOTTP 51
PLOTTP 52

```

```

YTMX=0.5*INT(2.0*ZTMX+.000)      PLOTT  53
YTMN=0.5*INT(2.0*ZTMN+.000)      PLOTT  54
OTMAX=0.5*INT(2.0*RTMAX+.000)    PLOTT  55
C      COMPUTE SCALE FACTOR      PLOTT  56
C      PLOTT  57
C      YTSIZE=YTMX-YTMN          PLOTT  58
TSF=PLYS7F/ANX1(YTSIZE,RTMAX)    PLOTT  59
YSPRO=TSF*PROSE                   PLOTT  60
CALL PLNT(4,0,-12,0,-3)           PLOTT  61
C      (Y,Z) PROJECTION          PLOTT  62
C      PLOTT  63
C      DRAW AXES USING SUBROUTINE AXIS PLOTT  64
C      PLOTT  65
C      PLOTT  66
C      CALL PLNT(0,0,1.5-YTMN*TSF,-3) PLOTT  67
NTC=INT(2*(ZTMX-ZTMN)+1,0)        PLOTT  68
CALL AXIS(0,0,0,0,14,1,ZTMX-ZTMN+NTC,1,0,0) PLOTT  70
CALL PLNT(-ZTMN*TSF,YTMN*TSF,-3)  PLOTT  71
NTC=INT(2*(YTSIZE+1,0))           PLOTT  72
CALL AXIS(0,0,0,0,14,0,YTSIZE*TSF,-NTC,2,PI*92) PLOTT  73
CALL PLNT(0,0,-YTMN*TSF,-3)      PLOTT  74
C      LABEL AND ANNOTATE Z-AXIS (HORIZONTAL) PLOTT  75
C      PLOTT  76
C      CALL SCALF(TSF,TSF,1)       PLOTT  77
YCH=1.5/TSF                       PLOTT  78
YCM=INT(YTMN)                     PLOTT  80
OYCH=1.0                          PLOTT  91
100 CONTINUE                      PLOTT  82
CALL MXPPLT(ZCH,YCH,0,0,-0.1,7,CH,1) PLOTT  93
ZCH=ZCH+OYCH                     PLOTT  94
IF (ZCH.LE.ZTMX) GO TO 100        PLOTT  95
ZCH=ZTMX+.2/TSF                  PLOTT  97
YCM=.5/TSF                        PLOTT  98
CALL CHAR(ZCH,YCH,0,0,14,3M/R,3)  PLOTT  99
ZCH=ZCH+.42/TSF                  PLOTT  90
CALL CHAR(ZCH,YCH,0,0,06,6HPLANET,6) PLOTT  92
C      LABEL AND ANNOTATE Y-AXIS (VERTICAL) PLOTT  93
C      PLOTT  94
YCM=INT(YTMN)                    PLOTT  95
OYCM=.35/TSF                     PLOTT  96
110 CONTINUE                     PLOTT  97
IF (YCM.NE.0,0) CALL MXPPLT(ZCH,YCM-.05/TSF,0,0,0,1,CH,1) PLOTT  98
YCM=YCM+OYCM                     PLOTT  99
IF (YCM.LE.YTMX) GO TO 110       PLOTT 100
YCM=.7/TSF                       PLOTT 101
YCH=YTMX+.2/TSF                  PLOTT 102
CALL CHAR(ZCH,YCH,0,0,14,3M/R,3)  PLOTT 103
IF (RPLNT .LE. C.0) GO TO 120    PLOTT 104
YCM=YCM+.42/TSF                  PLOTT 105
CALL CHAR(ZCH,YCH,0,0,06,6HPLANET,6) PLOTT 106
C      DRAW PLANET AND LABEL PLOT  PLOTT 107
C      PLOTT 108
C      CALL ELIPSE(1,0,0,0,1,0,1,0,0,0,0,0,0,0,0,0,3) PLOTT 109
120 CONTINUE                     PLOTT 110
YCM=.5*(ZTMX+ZTMN)-1.0/TSF       PLOTT 111
YCH=YTMN-.3/TSF                  PLOTT 112
CALL CHAR(ZCH,YCH,0,0,2,TITLE1,10) PLOTT 113
YCM=YCM+.06/TSF                  PLOTT 114
YCH=YCM+.03/TSF                  PLOTT 115
CALL CHAR(ZCH,YCH,0,0,0,12,TITLE7,16) PLOTT 116
C      DRAW (Y,Z) PROJECTION      PLOTT 117
C      PLOTT 118
C      YTMX=YTMX*ORPLNT          PLOTT 119
YTMN=YTMN*ORPLNT                 PLOTT 120
CALL PLNT(0,0,0,0,3)             PLOTT 121
CALL SCALF(TSF,TSF,1)            PLOTT 122
CALL VECTOR(ZTRAJ,YTRAJ,NTRAJ,1,1,14) PLOTT 123
CALL MXPPLT(ZTRAJ,YTRAJ,TSF,TSF) PLOTT 124
CALL PLNT(ZTMX,YTMN,-3)         PLOTT 125
CALL RESET                       PLOTT 126
C      (X,R) PROJECTION          PLOTT 127
C      PLOTT 128
C      PLOTT 129
C      PLOTT 130
C      PLOTT 131
C      DRAW, LABEL, AND ANNOTATE X-AXIS (HORIZONTAL) PLOTT 132
C      PLOTT 133
C      PLOTT 134
NTC=INT(2.0*(XTMX-XTMN)+1,0)    PLOTT 135
YCH=C.0                          PLOTT 136
IF (YTSIZE=RTMAX,GE,1,0) YCH=0.5 PLOTT 137
CALL PLNT(4,0,YCH,-3)           PLOTT 138
CALL AXIS(0,0,0,0,14,-1,(XTMX-XTMN)+TSF,-NTC,1,0,0) PLOTT 139
CALL PLNT(-XTMN*TSF,0,0,-3)    PLOTT 140
CALL SCALF(TSF,TSF,1)          PLOTT 141
YCM=.15/TSF                     PLOTT 142
YCM=INT(XTMN)                   PLOTT 143
OYCM=1.0                        PLOTT 144
200 CONTINUE                    PLOTT 145
CALL MXPPLT(XCH,RCH,0,0,-0.1,-YCM,1) PLOTT 146
XCH=XCH+OYCM                   PLOTT 147
IF (XCH.LE.XTMX) GO TO 200     PLOTT 148
XCM=XTMN-.9/TSF                 PLOTT 149
YCM=.25/TSF                     PLOTT 150
CALL CHAR(XCH,RCH,0,0,14,3M/R,3) PLOTT 151
XCM=XCM+.42/TSF                 PLOTT 152
CALL CHAR(XCH,RCH,0,0,06,6HPLANET,6) PLOTT 153
C      DRAW, LABEL, AND ANNOTATE R-AXIS (VERTICAL) PLOTT 154
C      PLOTT 155
C      PLOTT 156
NTC=INT(2.0*RTMX+1,0)           PLOTT 157
CALL AXIS(0,0,0,0,14,0,RTMX*TSF,-NTC,2,PI*92) PLOTT 158
RCH=1.0                          PLOTT 159
ORCH=1.0                         PLOTT 160
YCM=.75/TSF                     PLOTT 161
210 CONTINUE                    PLOTT 162
CALL MXPPLT(XCH,RCH-.05/TSF,0,0,0,1,RCH,1) PLOTT 163
RCH=RCH+ORCH                    PLOTT 164
IF (RCH.LE.RTMX) GO TO 210     PLOTT 165
YCM=.0.9/TSF                    PLOTT 166
YCM=RTMX+.1/TSF                 PLOTT 167
CALL MATH(XCH,RCH,.26/TSF,C.0,21) PLOTT 168
XCH=XCH+.16/TSF                 PLOTT 169
CALL PLNT(XCH,.55/TSF,RCH+.20/TSF,2) PLOTT 170
CALL CHAR(XCH,RCH,0,0,14,1M,1)  PLOTT 171
CALL CHAR(XCH,.14/TSF,RCH+.11/TSF,C.0,06,14Z,1) PLOTT 172
YCH=XCH+.2/TSF                  PLOTT 173
CALL CHAR(XCH,RCH,0,0,14,2M,7,2) PLOTT 174
CALL CHAR(XCH,.28/TSF,RCH+.11/TSF,0,0,06,14Z,1) PLOTT 175
YCM=YCM+.35/TSF                 PLOTT 176
CALL CHAR(XCH,RCH,0,0,14,2M/R,2) PLOTT 177
IF (RPLNT .LE. C.0) GO TO 215   PLOTT 178
YCM=YCM+.28/TSF                 PLOTT 179
CALL CHAR(XCH,RCH,0,0,06,6HPLANET,6) PLOTT 180
C      DRAW PLANET AND IDHOPAUSE, AND LABEL PLOT PLOTT 181
C      PLOTT 182
C      CALL ELIPSE(1,0,0,0,1,0,1,0,0,0,0,0,0,0,0,0,3) PLOTT 183
215 CONTINUE                    PLOTT 184
XTMN=XTMN*ORPLNT                PLOTT 185
YTMX=YTMX*ORPLNT                PLOTT 186
RTMX=RTMX*ORPLNT                PLOTT 187
CALL PLNT(0,0,0,0,3)            PLOTT 188
CALL SCALF(TSF,TSF,1)          PLOTT 189
DO 22 I=1,NKMAX                  PLOTT 190
IF (XND(I).GT.YTMX) GO TO 230   PLOTT 191
IF (YSD(I).GT.RTMX) GO TO 230   PLOTT 192
NRODY=I                          PLOTT 193
220 CONTINUE                    PLOTT 194
230 CONTINUE                    PLOTT 195
DO 24 J=1,NYMAX                  PLOTT 196
IF (YSH(J).GT.XTMX) GO TO 250   PLOTT 197
IF (YSH(J).GT.RTMX) GO TO 250   PLOTT 198
NSHOK=J                          PLOTT 199
240 CONTINUE                    PLOTT 200
250 CONTINUE                    PLOTT 201
CALL VECTOR(XBOD,YBOD,NRODY,1,1,14) PLOTT 202
YCM=.5*(XTMN+XTMX)-1.0/TSFRO    PLOTT 203
RCH=.0.7/TSFRO                  PLOTT 204
CALL CHAR(XCH,RCH,0,0,0,2,TITLE1,10) PLOTT 205
YCM=XCM+.04/TSFRO               PLOTT 206
RCH=RCH+.03/TSFRO              PLOTT 207
CALL CHAR(XCH,RCH,0,0,0,12,TITLEX,16) PLOTT 208
C      DRAW (X,R) PROJECTION      PLOTT 209
C      PLOTT 210
C      PLOTT 211
CALL VECTOR(XTRAJ,RTRAJ,NTRAJ,1,1,14) PLOTT 212
CALL MXPPLT(XTRAJ,RTRAJ,TSF,TSF) PLOTT 213
CALL PLNT(XTMX,0,0,-3)          PLOTT 214
CALL RESET                      PLOTT 215
RETURN                          PLOTT 216
END                              PLOTT 217

```



```

SUBROUTINE SERCH(J,K,KOD2,A,JDTH,ICM,KRY,KOD3,NVAL,A1,A2,ACONT)  SERCH  2
CONTOUT PROGRAMS MAP, WALK, SERCH, ENTER, AND CHECK          SERCH  3
WRITTEN BY REESE SORENSON, NASA-AMES RES. CTR., AUG., 1974.  SERCH  4
(MODIFIED VERSION)                                           SERCH  5
                                                                SERCH  6
THIS SUBROUTINE CHECKS WHETHER A CONTOUR LINE AT LEVEL NVAL  SERCH  7
PASSES THROUGH AN INTERVAL HAVING INDICES J,K AT ITS      SERCH  8
LEFT(KOD2=2) OR RIGHT(KOD2=1) POINT.                        SERCH  9
                                                                SERCH 10
DIMENSION A(1),ACONT(1),ICM(6,1)                            SERCH 11
IPEV(J,K)=J+K-1+JDTH                                        SERCH 12
                                                                SERCH 13
GO TO (1,2),KOD2                                           SERCH 14
I=IPEV(J,K)                                                 SERCH 15
I=I-1                                                         SERCH 16
GO TO 1                                                       SERCH 17
I=IPEV(J,K)                                                 SERCH 18
I2=A(I)                                                       SERCH 19
I=IPEV(J,K)                                                 SERCH 20
A1=A(I)                                                       SERCH 21
                                                                SERCH 22
VF(A1-A2)/5,5                                              SERCH 23
A4=A2                                                         SERCH 24
A1=A1                                                         SERCH 25
GO TO A                                                       SERCH 26
A4=A1                                                         SERCH 27
A1=A2                                                         SERCH 28
                                                                SERCH 29
VAL=ACONT(NVAL)                                             SERCH 30
IF(VAL.LT.A1) GO TO 12                                       SERCH 31
VF(VAL,GT.A4) GO TO 12                                       SERCH 32
                                                                SERCH 33
CALL CHECK(ICM,KRY,KOD2,J,K,NVAL,KOD3)                     SERCH 34
IF(KOD3.EQ.2) GO TO 12                                       SERCH 35
                                                                SERCH 36
KOD3=1                                                       SERCH 37
GO TO 20                                                       SERCH 38
KOD3=3                                                         SERCH 39
RETURN                                                       SERCH 40
END                                                           SERCH 42

```

```

SUBROUTINE SETUP(IPLDT,THACH,SAM,INDVY)                      SETUP  2
THIS ROUTINE ESTABLISHES PLOT ORIGIN, DRAWS                SETUP  3
AND LABELS AXES, AND WRITES TITLE.                         SETUP  4
HCC PLOT SUBROUTINES USED ARE                              SETUP  5
PLOT,AXIS,HUMPLT,CHAR,SCALE,                               SETUP  6
GREEK,MATH,PLTLN,OTLNL.                                    SETUP  7
                                                                SETUP  8
DIMENSION TITLE3(2),TITLE4(2)                               SETUP  9
DIMENSION TITLE5(2),TITLE6(3),TITLE7(2),TITLE8(4)         SETUP 10
DIMENSION TITLEF(2)                                         SETUP 11
COMMON /SCALE/ XSF,YSF,YMAX,YMAX,YLNSTH,YLNSTH            SETUP 12
DATA PZ/1.57079633/                                         SETUP 13
DATA TITLE1,TITLE2/04VELOCITY,,ANDENSTY,/                 SETUP 14
DATA TITLE3(1),TITLE3(2)/10MSTREAMLINE,1MS/               SETUP 15
DATA TITLE4(1),TITLE4(2)/10TEMPERATURE,14E/               SETUP 16
DATA TITLE5(1),TITLE5(2)/10HORIZONTAL SL,10HCOMPONENT//    SETUP 17
DATA TITLE6(1),TITLE6(2),TITLE6(3)/10HPERPENDIC,10HILAR COMP, SETUP 18
SHMENT//                                                    SETUP 19
DATA TITLE7(1),TITLE7(2)/10NORMAL CO,10MOMENT//           SETUP 20
DATA TITLE8(1),TITLE8(2)/10MAGNETIC F,5MFLD,/             SETUP 21
DATA TITLEF/9MCONTOURS/,TITLEF(1),TITLEF(2)/10FIELD LINE,1MS/ SETUP 22
                                                                SETUP 23
SET ORIGIN AT LEFT END OF X-AXIS                            SETUP 24
                                                                SETUP 25
CALL PLOT(0,,1,0,-3)                                        SETUP 26
XS=YSF                                                       SETUP 27
YS=YSF                                                       SETUP 28
CALL SCALFXS,YS,1)                                          SETUP 29
                                                                SETUP 30
DRAW AND LABEL X-AXIS. NOTE THAT SUBROUTINE AXIS          SETUP 31
REQUIRES PARAMETERS IN INCHES, NOT USER UNITS.           SETUP 32
                                                                SETUP 33
NTC=INT(2.001XMAX+1.5)+1.0)                                SETUP 34
CALL AXYS(0.0,0.0,1M,,0,YLNSTH,-NTC,1,0,0)                 SETUP 35
                                                                SETUP 36
SET PERMANENT ORIGIN AT X=0                                  SETUP 37
                                                                SETUP 38
                                                                SETUP 39

```

```

CALL PLOT(1.5,0.0,-3)                                       SETUP  40
XS=YSF                                                       SETUP  41
YS=YSF                                                       SETUP  42
CALL SCALFXS,YS,1)                                          SETUP  43
                                                                SETUP  44
DRAW Y-AXIS                                                 SETUP  45
                                                                SETUP  46
NTC=INT(YMAX)+1                                             SETUP  47
CALL AXYS(0.0,0.0,1M,,0,YLNSTH,-NTC,2,PIZ)                 SETUP  48
                                                                SETUP  49
LABEL Y-AXIS                                                SETUP  50
                                                                SETUP  51
YCM=-.4/YSF                                                  SETUP  52
YCM=0.5XMAX-.75-.21/XSF                                     SETUP  53
IF (IENDY.EQ.1) GO TO 2                                       SETUP  54
CALL CHAR(YCM,YCM,0.0,0.14,3MV/0,3)                         SETUP  55
GO TO 3                                                       SETUP  56
2 CALL CHAR(YCM,YCM,0.0,0.14,3MV/0,3)                         SETUP  57
YCM=YCM+.42/XSF                                             SETUP  58
CALL CHAR(YCM,YCM,0.0,0.05,1M,1)                             SETUP  59
3 CONTINUE                                                  SETUP  60
                                                                SETUP  61
ANNOTATE Y-AXIS - NOTE ANNOTATION IS POSITIVE LEFT.       SETUP  62
                                                                SETUP  63
YV=-.15/YSF                                                 SETUP  64
YV=0                                                         SETUP  65
YV=-1.5                                                      SETUP  66
5 DELY=PI*AT(YV)*0.5                                         SETUP  67
YDX=XV*DELX                                                 SETUP  68
CALL HUMPLT(YDX,YV,0.0,-0.1,-YDX,1)                          SETUP  69
IF(YV)                                                       SETUP  70
IF(YVX.LT.XMAX) GO TO 5                                       SETUP  71
                                                                SETUP  72
ANNOTATE Y-AXIS AT SIDE EDGE OF PLOT                       SETUP  73
                                                                SETUP  74
YV=0.0                                                       SETUP  75
10 YV=YV+.2,C                                               SETUP  76
YCM=-1.5+.25/XSF                                           SETUP  77
CALL HUMPLT(YCM,YV-.05/YSF,0.0,-0.1,YV,1)                   SETUP  78
YVTC=YCM+.16/XSF                                           SETUP  79
CALL CHAR(YVTC,YV-.05/YSF,0.0,0.09,1M,-1)                   SETUP  80
IF(YV.LT.YMAX) GO TO 10                                       SETUP  81
                                                                SETUP  82
LABEL Y-AXIS.                                              SETUP  83
                                                                SETUP  84
YCM=-1.5-.05/XSF                                           SETUP  85
YCM=INT(YMAX-1.0)*0.5+.05-.07/YSF                          SETUP  86
IF (IENDY.EQ.1) GO TO 12                                       SETUP  87
CALL CHAR(YCM,YCM,0.0,0.14,3MV/0,3)                         SETUP  88
GO TO 13                                                       SETUP  89
2 CALL CHAR(YCM,YCM,0.0,0.14,3MV/0,3)                         SETUP  90
YCM=YCM+.42/XSF                                             SETUP  91
CALL CHAR(YCM,YCM,0.0,0.05,1M,1)                             SETUP  92
13 CONTINUE                                                  SETUP  93
                                                                SETUP  94
DRAW TITLE. IPLOT DETERMINES WHICH TITLE                   SETUP  95
SHOULD BE DRAWN.                                           SETUP  96
                                                                SETUP  97
YCM=YMAX-.05/YSF                                            SETUP  98
YCM=-1.5+.45/XSF                                           SETUP  99
IF(IPLDT.EQ.2) GO TO 15                                       SETUP 100
IF(IPLDT.EQ.3) GO TO 20                                       SETUP 101
IF (IPLDT.EQ.4) GO TO 14                                       SETUP 102
IF (IPLDT.EQ.4) GO TO 21                                       SETUP 103
                                                                SETUP 104
VELOCITY PLOT                                              SETUP 105
                                                                SETUP 106
CALL CHAR(YCM,YCM,0.0,0.20,TITLE1,9)                         SETUP 107
YCM=YCM+.2/XSF                                              SETUP 108
CALL PLTLN(YCM,YCM,YCM,YCM+.2/YSF)                           SETUP 109
CALL CHAR(YCM+.05/XSF,YCM,0.0,0.2,1MV,1)                     SETUP 110
YCM=YCM+.25/YSF                                             SETUP 111
CALL PLTLN(YCM,YCM,YCM+.2/YSF)                               SETUP 112
CALL CHAR(YCM+.05/XSF,YCM,0.0,0.2,2MV,2)                     SETUP 113
CALL MATH(XCM+.4/XSF,YCM-.05/YSF,.15/YSF,0.0,0,15)          SETUP 114
GO TO 25                                                       SETUP 115
                                                                SETUP 116
TEMPERATURE PLOT                                           SETUP 117
                                                                SETUP 118
14 CONTINUE                                                  SETUP 119
CALL CHAR(YCM,YCM,0.0,0.20,TITLEF,11)                       SETUP 120
YCM=YCM+.24/XSF                                             SETUP 121
CALL CHAR(YCM,YCM,0.0,0.2,3MV/7,3)                           SETUP 122
CALL MATH(XCM+.55/XSF,YCM-.05/YSF,.15/YSF,0.0,0,15)          SETUP 123

```

```

C      GO TO 25
C      DENSITY PLOT
C      19 CONTINUE
C      CALL CHAR(XC4,YC4,G,0.2,TITLE2,9)
C      YC4=YC4+2/XSF
C      CALL GREK(XC4,YC4,2,0.0,17)
C      CALL CHAR(XC4+2/XSF,YC4,0.0,0.1,11)
C      CALL GREK(XC4+2/XSF,YC4,2,0.0,17)
C      CALL MATHE(XC4,49/XSF,YC4,0.5/YSF,13/XSF,0.0,13)
C      GO TO 25
C      STREAMLINES PLOT
C      2. CONTINUE
C      CALL CHAR(XC4,YC4,G,0.2,TITLE3,11)
C      GO TO 25
C      MAGNETIC FIELD PLOTS
C      2. CONTINUE
C      CALL CHAR(XC4,YC4,G,0.2,TITLE5,15)
C      YC4=YC4+2/XSF
C      CALL CHAR(XC4,YC4,0.0,0.2,4M(8)/B,4)
C      CALL MATHE(XC4,75/XSF,YC4,0.05/YSF,15/XSF,0.0,15)
C      CALL CHAR(XC4+0.9/XSF,YC4,0.0,0.2,14,11)
C      IF (PLMT.EQ.0) GO TO 22
C      IF (PLMT.EQ.7) GO TO 24
C      CALL CHAR(XC4,2/XSF,YC4,0.05/YSF,1.5709,0.1,14,11)
C      YC4=1.5+0.4/YSF
C      YC4=YC4+1/YSF
C      CALL CHAR(XC4,YC4,0.0,0.1,0,TITLE5,22)
C      GO TO 23
C      22 CALL CHAR(XC4+1.15/XSF,YC4,0.05/YSF,3.1416,0.1,14,11)
C      YC4=1.5+0.4/YSF
C      YC4=YC4+1/YSF
C      CALL CHAR(XC4,YC4,0.0,0.1,0,TITLE5,25)
C      GO TO 23
C      24 CALL CHAR(XC4+1.15/XSF,YC4,0.05/YSF,3.0,0.1,14,11)
C      YC4=1.5+0.4/YSF
C      YC4=YC4+1/YSF
C      CALL CHAR(XC4,YC4,0.0,0.1,0,TITLE7,20)
C      YC4=YC4+1.3/YSF
C      YC4=1.5+0.6/XSF
C      CALL CHAR(XC4,YC4,0.0,0.1,0,TITLEC,8)
C      CALL PLT(M(XC4+1.1/XSF,YC4+1.5/XSF,YC4)
C      YC4=YC4+1.5/YSF
C      CALL CHAR(XC4,YC4,0.0,0.1,0,TITLEF,11)
C      CALL PLT(M(XC4+1.15/XSF,YC4+1.0/XSF,YC4,2,0.0)
C      19. DRAW EACH NUMBER (N) AND RATIO OF SPECIFIC
C      HEATS (GAMMA).
C      25 CONTINUE
C      YC4=YC4+3/YSF
C      YC4=1.5+0.4/XSF
C      CALL CHAR(XC4,YC4,0.1,0.2,24M,2)
C      CALL MIMPLT(XC4,4/XSF,YC4,0.0,0.2,TM(X4,2)
C      YC4=YC4+1.4/XSF
C      CALL GREK(XC4,YC4,2,0.0,3)
C      CALL CHAR(XC4+2/XSF,YC4,0.0,0.2,14,11)
C      CALL MIMPLT(XC4,4/XSF,YC4,0.0,0.2,6A,2)
C      RETURN
C      END
C      SUBROUTINE SF(CALC(XSH,XSK,NTMAX)
C      THIS ROUTINE DETERMINES SCALE FACTORS AND TYPE OF PLOT.
C      COMMON /SCALE/ XSF,YSF,YMAX,YMAX,YLNGTH,YLNGTH
C      DIMENSION XSH(1),YSHK(1)
C      DATA YSIZE/8.0/
C      CALCULATE XMAX AND YMAX BASED ON LAST POINT OF SHOCK WAVE.
C      XMAX=AIMT(XSH(NTMAX))+0.5
C      YMAX=AIMT(YSHK(NTMAX))
C      YMAX=XMAX+.5
C      YMAX=AIMT(YSHK(NTMAX))+1.0

```

```

SETUP 124
SETUP 125
SETUP 126
SETUP 127
SETUP 128
SETUP 129
SETUP 130
SETUP 131
SETUP 132
SETUP 133
SETUP 134
SETUP 135
SETUP 136
SETUP 137
SETUP 138
SETUP 139
SETUP 140
SETUP 141
SETUP 142
SETUP 143
SETUP 144
SETUP 145
SETUP 146
SETUP 147
SETUP 148
SETUP 149
SETUP 150
SETUP 151
SETUP 152
SETUP 153
SETUP 154
SETUP 155
SETUP 156
SETUP 157
SETUP 158
SETUP 159
SETUP 160
SETUP 161
SETUP 162
SETUP 163
SETUP 164
SETUP 165
SETUP 166
SETUP 167
SETUP 168
SETUP 169
SETUP 170
SETUP 171
SETUP 172
SETUP 173
SETUP 174
SETUP 175
SETUP 176
SETUP 177
SETUP 178
SETUP 179
SETUP 180
SETUP 181
SETUP 182
SETUP 183
SETUP 184
SETUP 185
SETUP 186
SETUP 187
SETUP 188
SETUP 189

```

```

IF(YMAX.LT.3.0)YMAX=3.0
IF(XMAX.LT.0.5) XMAX=0.5
C      PLY PLOT SIZE IN Y-DIRECTION
C      ADJUST SCALE FACTORS FOR EQUAL X AND Y SCALE FACTORS
C      YLNGTH=YSTY
C      YSF=YLNGTH/YMAX
C      YSF=YSF
C      YLNGTH=YSF*(XMAX+1.5)
C      RETURN
C      END
C      SUBROUTINE SF(OFF(LF,FIN,PLTZE,PSF,PDEFST,NA,NTICK,AMTN,ANEL,
C      * PDEL)
C      THIS SUBROUTINE CALCULATES THE PARAMETERS REQUIRED TO DRAW THE
C      VERTICAL AXIS OF THE TRAJECTORY DATA PLOTS
C      LF = 1 VELOCITY
C      = 2 TEMPERATURE
C      = 3 DENSITY
C      = 4 MAGNETIC FIELD
C      COMMON /TRJDAT/ NTRAJ,ITRAJ(100),XTRAJ(100),YTRAJ(100),ZTRAJ(100),
C      * VTRAJ(100),VXTRAJ(100),VYTRAJ(100),VZTRAJ(100),TMPTJ(100),
C      * NTRAJ(100),XNTRAJ(100),YNTRAJ(100),ZNTRAJ(100),
C      * RTJ(100)
C      GO TO (100,200,300,400),LF
C      VELOCITY
C      10. FMIN=0.0
C      DO 11 I=1,NTRAJ
C      IF (VXTRAJ(I).LT. FMIN) FMIN=VXTRAJ(I)
C      11. CONTINUE
C      IF (VYTRAJ(I).LT. FMIN) FMIN=VYTRAJ(I)
C      12. CONTINUE
C      DO 13 I=1,NTRAJ
C      IF (VZTRAJ(I).LT. FMIN) FMIN=VZTRAJ(I)
C      13. CONTINUE
C      FMIN=FMIN*PIF
C      FMAX=FINF
C      GO TO 700
C      TEMPERATURE
C      20. FMIN=0.0
C      FMAX=0.0
C      DO 21 I=1,NTRAJ
C      IF (TMPTJ(I).GT. FMAX) FMAX=TMPTJ(I)
C      21. CONTINUE
C      FMAX=FMAX*PIF
C      GO TO 730
C      DENSITY
C      30. FMIN=0.0
C      FMAX=0.0
C      DO 31 I=1,NTRAJ
C      IF (RTJ(I).GT. FMAX) FMAX=RTJ(I)
C      31. CONTINUE
C      FMAX=FMAX*PIF
C      GO TO 730
C      MAGNETIC FIELD STRENGTH
C      40. FMIN=0.0
C      FMAX=0.0
C      DO 41 I=1,NTRAJ
C      IF (XNTRAJ(I).LT. FMIN) FMIN=XNTRAJ(I)
C      41. CONTINUE
C      DO 42 I=1,NTRAJ
C      IF (YNTRAJ(I).LT. FMIN) FMIN=YNTRAJ(I)
C      42. CONTINUE
C      DO 43 I=1,NTRAJ
C      IF (ZNTRAJ(I).LT. FMIN) FMIN=ZNTRAJ(I)
C      43. CONTINUE
C      DO 44 I=1,NTRAJ

```

```

SFCALC 15
SFCALC 16
SFCALC 17
SFCALC 18
SFCALC 19
SFCALC 20
SFCALC 21
SFCALC 22
SFCALC 23
SFCALC 24
SFCALC 25
SFCALC 26
SFCALC 27
SFCALC 28
SFCALC 29
SFCALC 30
SFCALC 31
SFCALC 32
SFCALC 33
SFCALC 34
SFCALC 35
SFCALC 36
SFCALC 37
SFCALC 38
SFCALC 39
SFCALC 40
SFCALC 41
SFCALC 42
SFCALC 43
SFCALC 44
SFCALC 45
SFCALC 46
SFCALC 47
SFCALC 48
SFCALC 49
SFCALC 50
SFCALC 51
SFCALC 52
SFCALC 53
SFCALC 54
SFCALC 55
SFCALC 56
SFCALC 57
SFCALC 58
SFCALC 59
SFCALC 60
SFCALC 61
SFCALC 62
SFCALC 63
SFCALC 64
SFCALC 65
SFCALC 66

```



```

      9ZTRAJ(N)=SANGH
100 CONTINUE
      OUTPUT TRAJECTORY INFORMATION, AND CREATE PLOTS IF REQUIRED
      CALL TROUT
      IF (.NOT. LPLTRJ) GO TO 290
      CALL PLNTFF
      CALL PLNTF
203 CONTINUE
      RETURN
      END

SUBROUTINE TROUT
      THIS SUBROUTINE PRINTS THE TRAJECTORY COORDINATES AND THE
      FLOW FIELD AND MAGNETIC FIELD COMPONENTS ALONG THE TRAJECTORY
      AS TABLES WITH TIME AS THE REFERENCE QUANTITY
      COMMON /RIN/ ANCP,ANGN,KACON,ACONIZ0
      COMMON /RNUMDS/ X500(100),Y500(100),X5M(100),Y5M(100),
      * NRMAX,NVMAX,AMACH,GAMMA,MRD,WHIMDZ
      LOGICAL LPERIM,LPRFL,LPRST,LPRCON,LPRB,LPLNT,LTRAJ,LRSTRT
      COMMON /RPRPT/ LRERUN,LPRFL,LPRST,LPRCON,LPRB,LPLNT,LTRAJ,LRSTRT
      COMMON /RSDAT/ NTRAJ,ZTRAJ(100),XTRAJ(100),YTRAJ(100),ZTRAJ(100),
      * VTRAJ(100),VXTRAJ(100),VYTRAJ(100),VZTRAJ(100),TMPTRAJ(100),
      * RTRAJ(100),RTRAJ(100),BYTRAJ(100),RZTRAJ(100),ROTTRAJ(100),
      * RTRAJ(100)
      LOGICAL LPLTRJ
      COMMON /RTRPT/ LPLTRJ,RPLMT,VINF,RHOINF,TMPINF,RINF
      LOGICAL LLSUM
      COMMON /SUMDAT/ LSUM,XTRAJ(100),YTRAJ(100),ZTRAJ(100),
      * RTRAJ(100),AZANG,POLANG,XYL,NYL,RZL
      DIMENSION VXTRAJ(100),VYTRAJ(100),VZTRAJ(100),RTRAJ(100),
      * BYTRAJ(100),RZTRAJ(100)
      WRITE COORDINATES (X,Y,Z,R) AS A FUNCTION OF TIME,
      IN UNITS OF BOTH R0 AND RPLANET
      RNOSE=1.0
      IF (RPLMT .GT. 0.0) RNOSE=1.0/RPLMT
      WRITE (6,1000)
      WRITE (6,1001)
      WRITE (6,1100) RNOSE
      WRITE (6,1200)
      DO 20 N=1,NTRAJ
      XPLNT=XTRAJ(N)*RNOSE
      YPLNT=YTRAJ(N)*RNOSE
      ZPLNT=ZTRAJ(N)*RNOSE
      RPLNT=RTRAJ(N)*RNOSE
      RTPLNT=XTRAJ(N)*RNOSE
      XT=XTRAJ(N)
      WRITE (6,2200) N,ZTRAJ(N),XT,YTRAJ(N),ZTRAJ(N),RTRAJ(N),XPLNT,
      * YPLNT,ZPLNT,RTPLNT
21. CONTINUE
      WRITE OUT FLOW FIELD AND MAGNETIC FIELD COMPONENTS
      NON-DIMENSIONAL WITH RESPECT TO FREE STREAM
      WRITE (6,1300)
      WRITE (6,1301)
      WRITE (6,1400)
      WRITE (6,1500)
      DO 40 N=1,NTRAJ
      WRITE (6,2100) N,ZTRAJ(N),VTRAJ(N),VXTRAJ(N),VYTRAJ(N),VZTRAJ(N),
      * ROTRAJ(N),TMPTRAJ(N),BTRAJ(N),RTRAJ(N),BYTRAJ(N),RZTRAJ(N)
40 CONTINUE
      WRITE OUT FLOW FIELD AND MAGNETIC FIELD COMPONENTS
      DIMENSIONALIZE BY INPUT FREE STREAM VALUES
      SANGH=SYM(ANGH)
      CANGH=COS(ANGH)
      SANGP=SM(ANGP)
      CANGP=COS(ANGP)
      X0=RTINF*CANGH*CANGP
      Y0=RINF*CANGH*SANGP
      Z0=RTINF*SANGH
      WRITE (6,1300)
      WRITE (6,1001)
      WRITE (6,1600)

```

```

TRAJEC 119
TRAJEC 116
TRAJEC 117
TRAJEC 118
TRAJEC 119
TRAJEC 120
TRAJEC 121
TRAJEC 122
TRAJEC 123
TRAJEC 124
TRAJEC 125
TRAJFC 126

```

```

      WRITE (6,1700) AMACH,GAMMA,RINF,VINF,X0,RHOINF,Y0,TMPINF,Z0
      WRITE (6,1800)
      DO 60 N=1,NTRAJ
      VDIM=VTRAJ(N)*VINF
      VYDIM=VYTRAJ(N)*VINF
      VZDIM=VZTRAJ(N)*VINF
      RHODIM=RHOINF
      TMPDIM=TMPTRAJ(N)*TMPINF
      RDTM=RTRAJ(N)*RINF
      RYDIM=RTRAJ(N)*RINF
      RZDIM=RTRAJ(N)*RINF
      WRITE (6,2200) N,ZTRAJ(N),VDIM,VXDIM,VYDIM,VZDIM,RHODIM,TMPDIM,
      * RDTM,RYDIM,RZDIM
63 CONTINUE
      IF (LSUM) GO TO 70
      RETURN
      TRANSFORM OUTPUT QUANTITIES TO SUN-PLANET COORDINATE SYSTEM
71. CONTINUE
      DO 75 N=1,NTRAJ
      XTRAJ(N)=XTRAJ(N)*RPLNT
      YTRAJ(N)=YTRAJ(N)*RPLNT
      ZTRAJ(N)=ZTRAJ(N)*RPLNT
75 CONTINUE
      TEMPA7=AZANG*.01745329
      TEMPNL=POLANG*.01745329
      SA7=SM(TEMPA7)
      CPAL=COS(TEMPL)
      CPOL=COS(TEPNL)
      DO 80 N=1,NTRAJ
      RTRAJ(N)=RTRAJ(N)*RPLNT
      VXTRAJ(N)=SA7*CPOL*XTRAJ(N)+CA7*VYTRAJ(N)+CAZ*SPOL*VZTRAJ(N)
      VYTRAJ(N)=SAZ*CPOL*YTRAJ(N)-CA7*VXTRAJ(N)+CAZ*SPOL*VZTRAJ(N)
      VZTRAJ(N)=-SPOL*VZTRAJ(N)+CPOL*VZTRAJ(N)
      RTRAJ(N)=-CA7*CPOL*XTRAJ(N)-SA7*VYTRAJ(N)-CAZ*SPOL*VZTRAJ(N)
      *YTRAJ(N)+SAZ*CPOL*YTRAJ(N)-CA7*VXTRAJ(N)+CAZ*SPOL*VZTRAJ(N)
      *RTRAJ(N)+SPOL*VZTRAJ(N)+CPOL*VZTRAJ(N)
81 CONTINUE
      XNS=-CA7*CPOL*X0-CAZ*Y0-CAZ*SPOL*Z0
      YNS=SA7*CPOL*X0+CAZ*Y0+SAZ*SPOL*Z0
      ZNS=-SPOL*X0+CPOL*Z0
      WRITE COORDINATES (X,Y,Z,R) AS A FUNCTION OF TIME
      IN UNITS OF BOTH R0 AND RPLANET
      WRITE (6,1300)
      WRITE (6,1302)
      WRITE (6,1400) RNOSE
      WRITE (6,1200)
      DO 90 N=1,NTRAJ
      XPLNT=XTRAJ(N)*RNOSE
      YPLNT=YTRAJ(N)*RNOSE
      ZPLNT=ZTRAJ(N)*RNOSE
      RPLNT=RTRAJ(N)*RNOSE
      RTPLNT=XTRAJ(N)*RNOSE
      XT=XTRAJ(N)
      WRITE (6,2200) N,ZTRAJ(N),XT,YTRAJ(N),ZTRAJ(N),RTRAJ(N),XPLNT,
      * YPLNT,ZPLNT,RTPLNT
91 CONTINUE
      WRITE FLOW FIELD AND MAGNETIC FIELD COMPONENTS
      NON-DIMENSIONALIZED WITH RESPECT TO FREESTREAM
      WRITE (6,1300)
      WRITE (6,1002)
      WRITE (6,1400)
      WRITE (6,1500)
      DO 95 N=1,NTRAJ
      WRITE (6,2100) N,ZTRAJ(N),VTRAJ(N),VXTRAJ(N),VYTRAJ(N),VZTRAJ(N),
      * ROTRAJ(N),TMPTRAJ(N),BTRAJ(N),RTRAJ(N),BYTRAJ(N),RZTRAJ(N),
      * VTRAJ(N),BTRAJ(N)
95 CONTINUE
      WRITE FLOW FIELD AND MAGNETIC FIELD COMPONENTS
      DIMENSIONALIZED BY INPUT FREESTREAM VALUES
      WRITE (6,1300)
      WRITE (6,1002)
      WRITE (6,1600)
      WRITE (6,1700) AMACH,GAMMA,RINF,VINF,X0,RHOINF,Y0,TMPINF,Z0
      WRITE (6,1701) AZANG,POLANG

```

```

TROUT 61
TROUT 62
TROUT 63
TROUT 64
TROUT 65
TROUT 66
TROUT 67
TROUT 68
TROUT 69
TROUT 70
TROUT 71
TROUT 72
TROUT 73
TROUT 74
TROUT 75
TROUT 76
TROUT 77
TROUT 78
TROUT 79
TROUT 80
TROUT 81
TROUT 82
TROUT 83
TROUT 84
TROUT 85
TROUT 86
TROUT 87
TROUT 88
TROUT 89
TROUT 90
TROUT 91
TROUT 92
TROUT 93
TROUT 94
TROUT 95
TROUT 96
TROUT 97
TROUT 98
TROUT 99
TROUT 100
TROUT 101
TROUT 102
TROUT 103
TROUT 104
TROUT 105
TROUT 106
TROUT 107
TROUT 108
TROUT 109
TROUT 110
TROUT 111
TROUT 112
TROUT 113
TROUT 114
TROUT 115
TROUT 116
TROUT 117
TROUT 118
TROUT 119
TROUT 120
TROUT 121
TROUT 122
TROUT 123
TROUT 124
TROUT 125
TROUT 126
TROUT 127
TROUT 128
TROUT 129
TROUT 130
TROUT 131
TROUT 132
TROUT 133
TROUT 134
TROUT 135
TROUT 136
TROUT 137
TROUT 138
TROUT 139
TROUT 140
TROUT 141
TROUT 142
TROUT 143
TROUT 144

```



```

FUNCTION VINTERP(X,Y)
C THIS FUNCTION INTERPOLATES FOR V AT (X,Y) FROM THE GRID VALUES
C
C COMMON /RLUNT/ THETA(25),PP(22,25),NRLUNT
C COMMON /ROUNDS/ X3DD(100),Y3DD(100),V3MK(100),Y3MK(100),
C N3MAX,N3MAX,AMACH,GAMMA,NR0,NMINDX
C COMMON /FLOW/ XC(2,100),YC(2,100),VF(2,100),RHF(2,100)
DATA DCR/57.29578/
VF(X,CT,CC) GO TO 100
TMST=ATANI=VF(X)0020
DO 10 NT=NRLUNT
VF(THET,LT,THETA(NT)) GO TO 20
10 CONTINUE
20 P=SQRT(X0X+Y0Y)
VF(THET,LT,THETA(NT)-THET)/(THETA(NT)-THETA(NT-1))
PP1=DTHE*V(1,NT-1)+(1.0-J-DTHE)*V(1,NT)
NR=NR0-NR0*P
PP2=DTHE*V(NR,NT-1)+(1.0-DTHE)*V(NR,NT)
VF(LT,PP2) GO TO 40
PP1=PP2
30 CONTINUE
40 NR=(PP2-NR)/(PP2-PP1)
VINTD=(DTHE*V(NR-1,NT-1)+(1.0-DTHE)*V(NR,NT))+(1.0-NR)
* (NT*V(NR,NT-1)+(1.0-DTHE)*V(NR,NT))+(1.0-NR)
* V(NR)
100 DO 100 NT=NRLUNT, N3MAX
VF(LT,VF(1,NT)) GO TO 120
100 CONTINUE
NT=N3MAX
120 THET=VF(1,NT)-X/(XC(1,NT)-XC(1,NT-1))
PP1=DTHE*V(1,NT-1)+(1.0-DTHE)*V(1,NT)
DO 100 NR=NR0,N3MAX
PP2=DTHE*V(NR,NT-1)+(1.0-DTHE)*V(NR,NT)
VF(LT,PP2) GO TO 40
PP1=PP2
130 CONTINUE
RETURN
END

```

VINTDP	2	KK(2)=K-1		WALK	40
VINTDP	3	KK(3)=K-1		WALK	41
VINTDP	4	KK(1)=1		WALK	42
VINTDP	5	KK(2)=2		WALK	43
RLUNT	6	KK(3)=1		WALK	44
ROUNDS	7	GO TO 14		WALK	45
RLIMDC	8			WALK	46
FLOW	9			WALK	47
VINTDP	10	ORIENTATION 41 TO THE LEFT		WALK	48
VINTDP	11	JJ(1)=J-1		WALK	49
VINTDP	12	JJ(2)=J-1		WALK	50
VINTDP	13	JJ(3)=J-1		WALK	51
VINTDP	14	KK(1)=K		WALK	52
VINTDP	15	KK(2)=K+1		WALK	53
VINTDP	16	KK(3)=K		WALK	54
VINTDP	17	KK(2)=1		WALK	55
VINTDP	18	KK(3)=2		WALK	56
VINTDP	19			WALK	57
VINTDP	20	SEARCH THE 3 POSSIBLE DIRECTIONS.		WALK	58
VINTDP	21	DO 17 N=1,3		WALK	59
VINTDP	22	CALL SEARCH(JJ(N),KK(N),K2(N),A,JOIN,TCHK,NYV,K3(N),NVAL,A1(N),		WALK	60
VINTDP	23	AZ(N),ACONT)		WALK	61
VINTDP	24			WALK	62
VINTDP	25	K35=K3(1)+K3(2)+K3(3)		WALK	63
VINTDP	26	IF(K35=11),2,19		WALK	64
VINTDP	27			WALK	65
VINTDP	28	BRANCH POINT		WALK	66
VINTDP	29	VF(K3(KND5),NE,1) GO TO 9		WALK	67
VINTDP	30	K6=KND6		WALK	68
VINTDP	31	GO TO 4		WALK	69
VINTDP	32			WALK	70
VINTDP	33	ONE IS ONE OUT. FIND WHERE OUT.		WALK	71
VINTDP	34	DO 3 N=1,3		WALK	72
VINTDP	35	VF(K3(N),EQ,1) GO TO 4		WALK	73
VINTDP	36	CONTINUE		WALK	74
VINTDP	37			WALK	75
VINTDP	38	RECORD THE POINT		WALK	76
VINTDP	39	CALL PINTERP(K1(K6),JJ(K6),KK(K6),NVAL,A1(K6),A2(K6),JMIN,KMIN,TCHK,		WALK	77
VINTDP	40	KND4,X,Y,NYV,ACONT,TS7I)		WALK	78
VINTDP	41			WALK	79
VINTDP	42			WALK	80
VINTDP	43	RESET J AND K		WALK	81
VINTDP	44	J=JJ(K4)		WALK	82
VINTDP	45	K=KK(K4)		WALK	83
VINTDP	46			WALK	84
VINTDP	47	SEE IF WE'RE AT A BOUNDARY. IF SO, QUIT.		WALK	85
VINTDP	48	VF(J,CT,DMIN) GO TO 23		WALK	86
VINTDP	49	GO TO (76,9,26,23),KND5		WALK	87
VINTDP	50	VF(J,LT,DMAX) GO TO 19		WALK	88
VINTDP	51	GO TO (74,25,26,19),KND5		WALK	89
VINTDP	52	VF(K5,EQ,1) GO TO 1		WALK	90
VINTDP	53	GO TO 10		WALK	91
VINTDP	54	VF(K6,EQ,2) GO TO 1		WALK	92
VINTDP	55	GO TO 19		WALK	93
VINTDP	56	VF(K4,EQ,1) GO TO 1		WALK	94
VINTDP	57			WALK	95
VINTDP	58	IF(K5,CT,KMIN) GO TO 27		WALK	96
VINTDP	59	GO TO (8,30,29,28),KND5		WALK	97
VINTDP	60	VF(K,LT,NMAX) GO TO 8		WALK	98
VINTDP	61	GO TO (29,28,9,20),KND5		WALK	99
VINTDP	62	VF(K5,EQ,1) GO TO 1		WALK	100
VINTDP	63	GO TO 4		WALK	101
VINTDP	64	VF(K5,EQ,2) GO TO 1		WALK	102
VINTDP	65	GO TO 4		WALK	103
VINTDP	66	VF(K6,EQ,3) GO TO 1		WALK	104
VINTDP	67			WALK	105
VINTDP	68	PREPARE FOR NEXT STEP		WALK	106
VINTDP	69	KND4=K6		WALK	107
VINTDP	70	KND5=KND5+K6-2		WALK	108
VINTDP	71	VF(KND5,CT,4) KND5=KND5-4		WALK	109
VINTDP	72	VF(KND5,LT,1) KND5=KND5+4		WALK	110
VINTDP	73	GO TO 31		WALK	111
VINTDP	74			WALK	112
VINTDP	75	CONTINUE		WALK	113
VINTDP	76	KND5=0		WALK	114
VINTDP	77	RETURN		WALK	115
VINTDP	78	END		WALK	116

SUBROUTINE ARMATX(J,K,I)
COMMON/CDRL/JMAX,KMAX,JM,KN,KNACH,ALPHA,GAM,GAMPL,CM,DT,SBU,IPRT,
CDNDR,NCA,NCB,CCC,AA,B,OREGA,MU,NL,IT,TAU,ITCR,ENT,PTORT,PTMF,
ARMATY 2
CDML 2
CDML 3

```

4
5
6
7
8
9
10
11
12
13
14
15
16
17
18
19
20
21
22
23
24
25
26
27
28
29
30
31
32
33
34
35
36
37
38
39
40
41
42
43
44
45
46
47
48
49
50
51
52
53
54
55
56
57
58
59
60
61
62
63
64
65
66
67
68
69
70
71
72
73
74
75
76
77
78
79
80
81
82
83
84
85
86
87
88
89
90
91
92
93
94
95
96
97
98
99
100
101
102
103
104
105
106
107
108
109
110
111
112
113
114
115
116
117
118
119
120
121
122
123
124
125
126
127
128
129
130
131
132
133
134
135
136
137
138
139
140
141
142
143
144
145
146
147
148
149
150
151
152
153
154
155
156
157
158
159
160
161
162
163
164
165
166
167
168
169
170
171
172
173
174
175
176
177
178
179
180
181
182
183
184
185
186
187
188
189
190
191
192
193
194
195
196
197
198
199
200
201
202
203
204
205
206
207
208
209
210
211
212
213
214
215
216
217
218
219
220
221
222
223
224
225
226
227
228
229
230
231
232
233
234
235
236
237
238
239
240
241
242
243
244
245
246
247
248
249
250
251
252
253
254
255
256
257
258
259
260
261
262
263
264
265
266
267
268
269
270
271
272
273
274
275
276
277
278
279
280
281
282
283
284
285
286
287
288
289
290
291
292
293
294
295
296
297
298
299
300
301
302
303
304
305
306
307
308
309
310
311
312
313
314
315
316
317
318
319
320
321
322
323
324
325
326
327
328
329
330
331
332
333
334
335
336
337
338
339
340
341
342
343
344
345
346
347
348
349
350
351
352
353
354
355
356
357
358
359
360
361
362
363
364
365
366
367
368
369
370
371
372
373
374
375
376
377
378
379
380
381
382
383
384
385
386
387
388
389
390
391
392
393
394
395
396
397
398
399
400
401
402
403
404
405
406
407
408
409
410
411
412
413
414
415
416
417
418
419
420
421
422
423
424
425
426
427
428
429
430
431
432
433
434
435
436
437
438
439
440
441
442
443
444
445
446
447
448
449
450
451
452
453
454
455
456
457
458
459
460
461
462
463
464
465
466
467
468
469
470
471
472
473
474
475
476
477
478
479
480
481
482
483
484
485
486
487
488
489
490
491
492
493
494
495
496
497
498
499
500
501
502
503
504
505
506
507
508
509
510
511
512
513
514
515
516
517
518
519
520
521
522
523
524
525
526
527
528
529
530
531
532
533
534
535
536
537
538
539
540
541
542
543
544
545
546
547
548
549
550
551
552
553
554
555
556
557
558
559
560
561
562
563
564
565
566
567
568
569
570
571
572
573
574
575
576
577
578
579
580
581
582
583
584
585
586
587
588
589
590
591
592
593
594
595
596
597
598
599
600
601
602
603
604
605
606
607
608
609
610
611
612
613
614
615
616
617
618
619
620
621
622
623
624
625
626
627
628
629
630
631
632
633
634
635
636
637
638
639
640
641
642
643
644
645
646
647
648
649
650
651
652
653
654
655
656
657
658
659
660
661
662
663
664
665
666
667
668
669
670
671
672
673
674
675
676
677
678
679
680
681
682
683
684
685
686
687
688
689
690
691
692
693
694
695
696
697
698
699
700
701
702
703
704
705
706
707
708
709
710
711
712
713
714
715
716
717
718
719
720
721
722
723
724
725
726
727
728
729
730
731
732
733
734
735
736
737
738
739
740
741
742
743
744
745
746
747
748
749
750
751
752
753
754
755
756
757
758
759
760
761
762
763
764
765
766
767
768
769
770
771
772
773
774
775
776
777
778
779
780
781
782
783
784
785
786
787
788
789
790
791
792
793
794
795
796
797
798
799
800
801
802
803
804
805
806
807
808
809
810
811
812
813
814
815
816
817
818
819
820
821
822
823
824
825
826
827
828
829
830
831
832
833
834
835
836
837
838
839
840
841
842
843
844
845
846
847
848
849
850
851
852
853
854
855
856
857
858
859
860
861
862
863
864
865
866
867
868
869
870
871
872
873
874
875
876
877
878
879
880
881
882
883
884
885
886
887
888
889
890
891
892
893
894
895
896
897
898
899
900
901
902
903
904
905
906
907
908
909
910
911
912
913
914
915
916
917
918
919
920
921
922
923
924
925
926
927
928
929
930
931
932
933
934
935
936
937
938
939
940
941
942
943
944
945
946
947
948
949
950
951
952
953
954
955
956
957
958
959
960
961
962
963
964
965
966
967
968
969
970
971
972
973
974
975
976
977
978
979
980
981
982
983
984
985
986
987
988
989
990
991
992
993
994
995
996
997
998
999
1000

```



```

P5=(2.0*GAN*XY-GAMM1)/GAMP1*PINF          INITIA 53
P6=GAMP1*XX/(GAMM1*XX*2.0)*PINF           INITIA 54
P5=(1.0-2.0*PTE-1.0)/GAMM1*FXMACH*21*OINF INITIA 55
V5=2.0*PXY-1.0)*COS(SANG)/GAMM1*XMACH*2*SMISANG)*OINF INITIA 56
TF(J,GT,2) GO TO 3                          INITIA 57
Y1=(2.0*GAN*XMACH*2-GAMM1)/(GAN+1.0)      INITIA 58
Y2=(GAN+1.0)*XMACH*2/(GAMM1*XMACH*2+2.0)  INITIA 59
P1=X1*PINF                                  INITIA 60
P1=X2*PINF                                  INITIA 61
ENTP1/P1**GAN                               INITIA 52
X=(1.0*FX1)**(1.0/GAMM1)*(0.5*(GAN+1.0)*YHAC*2)**(GAN/GAMM1)*PINF INITIA 63
X=(1.0*Y*5*GAMM1*XMACH*2                   INITIA 64
*PTORT*XY*PINF/RINF                        INITIA 65
3 CONTINUE                                    INITIA 66
PB=PINF*(1*PT/PINF-1.0)*(1.0-1.0*2*SIN(THET)**2+0.12*SIN(THET)**4)+ INITIA 67
1.0)                                          INITIA 68
RR=(PR/ENT)**(1.0/GAM)                     INITIA 69
OR=SORT(2.0*GAN/GAMM1*AS(PTORT-PB/RR))     INITIA 70
YY=PI*0.5*THET                              INITIA 71
JH=OR*OR*NS(VY)                              INITIA 72
VR=OR*SM(YV)                                INITIA 73
ZKH=KMAX-1                                  INITIA 74
DO 2 K=1,KMAX                                INITIA 75
YV=FLOAT(K-1)/ZKH                           INITIA 76
PPRESS=PV*YV*(PS-PB)                       INITIA 77
RMD=PV*YV*(RS-RB)                          INITIA 78
VVEL=UR*YV*(US-UR)                         INITIA 79
VT=L.0/PI*YV*(VS-VB)                       INITIA 80
O(J,K,1)=RMD*DI                             INITIA 81
O(J,K,2)=RMD*VVEL*DI                       INITIA 82
O(J,K,3)=PPRESS*GAM1+RMD*(VVEL**2+VVEL**3)*0.5*DI INITIA 83
2 O(J,K,4)=PPRESS*GAM1+RMD*(VVEL**2+VVEL**3)*0.5*DI INITIA 84
C...REFLECT METRICS AND DEPENDENT VARIABLES ABOUT PLANE OF SYMMETRY INITIA 85
DO 4 K=1,KMAX                                INITIA 87
DD=(1.0)*JCS                                INITIA 88
DD=(4.0)*JCS                                INITIA 89
O(1,K)=O(2,K)*DD                            INITIA 90
YEX(1,K,1)=-XEX(2,K,1)                    INITIA 91
YEX(1,K,1)=XEX(2,K,1)                      INITIA 92
XEX(1,K,2)=XEX(2,K,2)                      INITIA 93
XEX(1,K,2)=-XEX(2,K,2)                     INITIA 94
DO 3 N=1,4                                  INITIA 95
O(1,K,N)=O(2,K,N)*DD                       INITIA 96
O(1,K,3)=-O(2,K,3)*DD                      INITIA 97
RETURN                                       INITIA 98
END                                          INITIA 99

SUBROUTINE INTEGR                            INTEGR 2
COMMON/COM1/JMAX,KMAX,JM,KH,XMACH,ALPHA,GAM,GAMM1,CN,DT,SMU,TPRT, COM1 2
> CHORD,NCA,NCC,NCC,AA,4,OMEGA,NU,ML,IT,TAU,ITER,ENT,PTORT,PINF, COM1 3
<OINF,OINF,CINF,JCS,TP,CLUS,PT,HORN,RNOSE,NCASE,NPUNCH COM1 4
LEVEL 2,0,EF,S,G,AB COM1 5
COMMON /COM3/ Q(40,20,4),EF(40,4),S(40,20,4),G(4),AR(4,4) COM3 2
LEVEL 2, A, R, C, MD COM3 3
COMMON /COM4/ A(40,4,4),R(40,4,4),C(40,4,4),MD(40,4,4) COM4 2
DO 1 K=1,KMAX                                LBLTRA 4
C...LOAD BLOCK N MATRIX EVALUATED AT N TH LEVEL F70 ALL J INTO MD ARRAY LBLTRA 7
CALL AMATX(J,K,I)                            LBLTRA 9
DO 1 M=1,4                                    LBLTRA 9
DO 1 L=1,4                                    LBLTRA 10
1 MD(J,L,M)=A(L,M)                          LBLTRA 11
C...FILL OFF-DIAGONAL AND DIAGONAL ELEMENTS BASED ON A 2-ND ORDER LBLTRA 12
C...CENTRAL DIFFERENCE                      LBLTRA 13
DO 2 J=2,JM                                LBLTRA 14
DO 2 M=1,4                                    LBLTRA 15
DO 3 L=1,4                                    LBLTRA 16
A(J,L,M)=MD(J-L,L,M)*M                     LBLTRA 17
A(J,L,M)=0.0                                LBLTRA 18
3 C(J,L,M)=M*(J+1,L,M)*M                    LBLTRA 19
C...FILL FORCING FUNCTION FROM S ARRAY      LBLTRA 20
FF(J,M)=S(J,K,M)                            LBLTRA 21
C...SET R ON THE DIAGONAL REPRESENTING THE IDENTITY MATRIX TO ONE LBLTRA 22
2 R(J,M,M)=1.0                              LBLTRA 23
RETURN                                       LBLTRA 24
END                                          LBLTRA 25

SUBROUTINE LBLTRA(J)                         LBLTRA 2
COMMON/COM1/JMAX,KMAX,JM,KH,XMACH,ALPHA,GAM,GAMM1,CN,DT,SMU,TPRT, COM1 2
> CHORD,NCA,NCC,NCC,AA,4,OMEGA,NU,ML,IT,TAU,ITER,ENT,PTORT,PINF, COM1 3
<OINF,OINF,CINF,JCS,TP,CLUS,PT,HORN,RNOSE,NCASE,NPUNCH COM1 4
LEVEL 2,0,EF,S,G,AB COM1 5
COMMON /COM3/ Q(40,20,4),EF(40,4),S(40,20,4),G(4),AR(4,4) COM3 2
LEVEL 2, A, R, C, MD COM3 3
COMMON /COM4/ A(40,4,4),R(40,4,4),C(40,4,4),MD(40,4,4) COM4 2
DO 1 K=1,KMAX                                LBLTRA 4
C...LOAD BLOCK N MATRIX EVALUATED AT N TH LEVEL F70 ALL K INTO MD ARRAY LBLTRA 7
CALL AMATX(J,K,2)                          LBLTRA 9
DO 1 M=1,4                                    LBLTRA 9
DO 1 L=1,4                                    LBLTRA 9
1 MD(K,L,M)=A(L,M)                          LBLTRA 10
C...FILL OFF-DIAGONAL AND DIAGONAL ELEMENTS BASED ON A 2-ND ORDER LBLTRA 12
C...CENTRAL DIFFERENCE                      LBLTRA 13
DO 2 K=2,KH                                LBLTRA 14
DO 2 M=1,4                                    LBLTRA 15
DO 3 L=1,4                                    LBLTRA 16
A(K,L,M)=MD(K-L,L,M)*M                     LBLTRA 17
A(K,L,M)=0.0                                LBLTRA 18
3 C(K,L,M)=M*(K+1,L,M)*M                    LBLTRA 19
C...FILL FORCING FUNCTION FROM S ARRAY      LBLTRA 20
FF(M,M)=S(J,K,M)                            LBLTRA 21
C...SET R ON THE DIAGONAL REPRESENTING THE IDENTITY MATRIX TO ONE LBLTRA 22
2 R(K,M,M)=1.0                              LBLTRA 23
RETURN                                       LBLTRA 24
END                                          LBLTRA 25

SUBROUTINE LUDEC(A)                          LUDEC 2
DIMENSION A(4,4)                            LUDEC 3
REAL L11,L21,L22,L31,L32,L33,L41,L42,L43,L44 LUDEC 4
COMMON /LUD/ L11,L21,L22,L31,L32,L33,L41,L42,L43,L44,V1,V2,V3,V4, LUDEC 5
* U12,U13,U14,U23,U24,U34 LUDEC 6
C SUBROUTINE COMPUTES L-U DECOMPOSITION ELEMENTS LUDEC 9
L11 = A(1,1) LUDEC 6
V1 = 1./L11 LUDEC 7

```

```

U12 = V10A(1,2)
U13 = V10A(1,3)
U14 = V10A(1,4)
L21 = A(2,1)
L22 = A(2,2) - L21*U12
V2 = 1./L22
U23 = ( A(2,3) - L21*U13 ) / V2
U24 = ( A(2,4) - L21*U14 ) / V2
L31 = A(3,1)
L32 = A(3,2) - L31*U12
L33 = A(3,3) - L31*U13 - L32*U23
V3 = 1./L33
U34 = ( A(3,4) - L31*U14 - L32*U24 ) / V3
L41 = A(4,1)
L42 = A(4,2) - L41*U12
L43 = A(4,3) - L41*U13 - L42*U23
L44 = A(4,4) - L41*U14 - L42*U24 - L43*U34
V4 = 1./L44
*ETURN
END

LUMEC 0
LUDEC 0
LUDEC 10
LUDEC 11
LUDEC 12
LUDEC 13
LUDEC 14
LUDEC 15
LUDEC 16
LUDEC 17
LUDEC 18
LUDEC 19
LUDEC 20
LUDEC 21
LUDEC 22
LUDEC 23
LUDEC 24
LUDEC 25
LUDEC 26
LUDEC 27

SURMUTHE NOLPTS 2
COMMON/COM1/JMAX,KMAX,JN,KN,KNACH,ALPHA,GAM,GAM1,CN,DT,SMU,IPRT,
> CMORD,MCA,NCB,MCC,AA,OMEGA,MU,ML,IT,TAU,ITER,ENT,PTORT,PINF,
> CINF,CINF,CJCS,TH,CLUS,PT,HORN,RNDSE,NCASF,NPUNCA
LEVEL 2,0,Y,XET,KEY,KEYD
COMMON /COM2/ X(40,20),Y(40,20),XET(40,20,2),KEY(40,20,2),
* XE(40,20,2),D(40,20)
LEVEL 2,0,EF,5,6,8
COMMON /COM3/ Q(40,20,6),EF(40,4),S(60,20,4),G(4),AR(4,4)
DIMENSION XL(40),CON(6)
GO TO (3,2,3,4,5),L
1 CONTINUE
C...JHPUT FLOWFIELD DATA
RMS=0.0
PERP=0.0
HTIME=GAM/SMU*(CINF/PTORT+CINF**2+0.5
WRITE(6,111)
DO 12 J=1,KMAX
DO 6 J=1,JMAX
EN=Q(J,K,4)*D(I,J,K)
RMO=Q(J,K,1)*D(I,J,K)
H=Q(I,J,2)/Q(J,K,1)
V=Q(I,J,3)/Q(J,K,1)
HT=GAM/SMU*(RMO/HTIME+V*(U0U+V0V))
SS=SQRT(GAM**2/RMO)
PERP=4*S*(HT-HTIME)*100.0/HTIME
IF(PERP.GT.PERRMX) PERRMX=PERP
RMC=RMC+PERP**2
5 SL(J)=SQRT(U0U+V0V)/SS
CONTINUE
DO 11 J=1,JMAX
TF(SL(J),LE,1,C,AND,SL(J-1),RE,1,0),OP,(SL(J),6F,1,2),AND,SL(J-1)
*LE,1,C) TO 12
GO TO 11
12 JSL=J
JSLM=JSL-1
CDEF=(1.0-SL(JSLM))/(SL(JSL)-SL(JSLM))
XSL=Y(JSLM,K)*CDEF+(X(JSL,K)-X(JSLM,K))
YSL=Y(JSLM,K)*CDEF+(Y(JSL,K)-Y(JSLM,K))
XSL1=XSL
YSL1=YSL
WRITE(6,113) XSL,YSL
11 CONTINUE
2 CONTINUE
RMS=SQRT(RMS**2+PERP**2)
WRITE(6,107) PERRMX,RMS
*ETURN
2 CONTINUE
C...JHPUT E AND F CONSERVATIVE VARIABLES
WRITE(6,133)
DO 7 K=1,KMAX
WRITE(6,134) K
DO 7 J=1,JMAX
CALL EFCOM(J,K,1)
DO 8 N=1,4
8 FOM(N)=G(N)
CALL EFCOM(J,K,2)
DO 9 M=1,4
9 COM(M)=G(M)
7 WRITE(6,135) J,(COM(N),N=1,8)
RETURN
3 CONTINUE
RETURN
4 CONTINUE
WRITE(6,139)
WRITE(6,139) ((J,K,X(J,K),Y(J,K),(XET(J,K,T),KEY(J,K,T),KEY(J,K,T))
> I=1,21),J,K,K=1,KMAX),J=1,JMAX)
RETURN
5 CONTINUE

```

```

RETURN
03 FORMAT(1H0,3X,32M<<< CONSERVATIVE VARIABLES >>>)
104 FORMAT(30K0,1Z/4X,1HJ,6X,2HE1,10X,2HE2,10X,2HE3,10X,2HE4,10X,
> 2HF,10X,2HF2,10X,2HF3,10X,2HF4)
105 CONTINUE,IF(EL2,4)
107 FORMAT(7H0<<<< X ERROR IN HY =>E12,4,3X,22HRMS OF X ERROR IN XT
> E12,4,3X >>>)
108 FORMAT(1H1,3X,1HJ,4X,2H4,8X,1HX,11X,1HY,10X,4HX1-T,8X,4HX1-X,8X,
> 4HX1-Y,7X,5HETA-T,7X,5HETA-X,7X,5HETA-Y,8X,1HJ)
109 FORMAT(2IS,0F12,6)
110 FORMAT(5H,7SL=,F7,4,3X,4HRSL=,F7,4)
111 FORMAT(/26H FINAL SONIC LINE LOCATION/)
END

```

```

OUTPUT 67
OUTPUT 68
OUTPUT 69
OUTPUT 70
OUTPUT 71
OUTPUT 72
OUTPUT 73
OUTPUT 74
OUTPUT 75
OUTPUT 76
OUTPUT 77
OUTPUT 78
OUTPUT 79

```

```

4 VX(I,J)=V(J,1,3)-V(J-1,3)*0.5
PX(I,1)=PX(I,2)
UY(I,1)=UY(I,2)
VX(I,1)=VX(I,2)
*XI(JMAX)=(3.0*P(JMAX,3)-4.0*P(JM,3)+P(JM,3))*0.5
UXI(JMAX)=(3.0*U(JMAX,3)-4.0*U(JM,3)+U(JM,3))*0.5
VXI(JMAX)=(3.0*V(JMAX,3)-4.0*V(JM,3)+V(JM,3))*0.5
DN 5 3=J, JMAX
PETA(I,1)=3.0*P(J,3)-4.0*P(J,2)+P(J,1)*0.5
UETA(I,1)=3.0*U(J,3)-4.0*U(J,2)+U(J,1)*0.5
VETA(I,1)=3.0*V(J,3)-4.0*V(J,2)+V(J,1)*0.5
TF(J,EO,1,CR,JEQ,JMAX) GO TO 5
P(J,7)=P(J+1,3)+P(J-1,3)-2.0*P(J,3)
5 CONTINUE
P(I,2)=P(I,2)
P(JMAX,2)=3.0
NO 2 3=J, JMAX
K=JMAX
C...DETERMINE SHOCK ANGLE DELTA=ARCTAN(-ETAY/ETAX) J,KMAX
DELTA=ATAN(-XEY(J,K,2)/XEX(J,K,2))
SN=STN(DELTA)
CO=COS(DELTA)
UIY=OSIN(CO)
HNA=XEY(J,K,1)+U(J,3)*XEY(J,K,1)+V(J,3)*XEY(J,K,1)
VNA=XEY(J,K,2)+U(J,3)*XEY(J,K,2)+V(J,3)*XEY(J,K,2)
CR=COS(P(J,3))
PTAI=HNA*P(XI(J,1)-VNA*PETA(I,1)-CRS*U(XI(J,1)+XEY(J,K,1)+
> VX(I,1)*XEY(J,K,1)+HETA(I,1)*XEY(J,K,2)+VETA(I,1)*XEY(J,K,2)+
> IV(J,3)/V(J,K,1)*FLOAT(JCS))
P2=P(J,3)+PTAU*DT*0.2+0.1*P(J,2)
TF(J,EO, JMAX)P2=2.0*P(JM,3)-P(JM-1,3)
IF(P2,LE,3.0) GO TO 6
7=GAMMA*U
HNA=OSIN(P2,5/GAMMA/P2/PINF+2+GAMMA))
OS=CTHETAXX=UIT
PA=P(J,3)
PB=P(J,3)
HNA=U(J,3)
VNA=V(J,3)
SN=PA/GAMMA*1.0,5*ORR*(UOR+2+VOR+2)
U2T=2.0*(1.0-XHX+2)*CINF/(GAMMA*0.01*XHX)+UIT
V2T=VNF*(P2/PINF+GAMMA/7)/(1.0+GAMMA/7*P2/PINF)
H2=HNF*OS*P2-U2T*CO
R2=OTNF*OS*PD-U2T*CO
E2=P2/GAMMA*0.5*P2*(U2+2+V2+2)
C...COMPUTE CONSERVATIVE VARIABLES AT SHOCK
K=KMAX
NT=1.0/OT(J,K)
O(J,K,1)=R2*NT
O(J,K,2)=R2*H2*DI
O(J,K,3)=R2*V2*DI
O(J,K,4)=E2*NT
C...DETERMINE ANGLE OF XI=CONST LINE WITH X-AXIS
K=KMAX
TF(AS(XEY(J,K,1))-0.037001) 7,7,0
7 THEY=1.5779633
GO TO 9
9 CONTINUE
THEY=ATAN(XEY(J,K,1)/XEY(J,K,1))
J=CONTINUE
C...COMPUTE SHOCK SPEED IN X AND Y DIRECTIONS
ETA=THEY-DELTA
OS=OS/COS(ETA)
TF(AS(OS)) .GE. AS(OSEM))JOS=J
IF(AS(OS)) .GE. AS(OSEM))OSEM=OSE
PMS=OS+OSE**2
KTY=OS*OS*(HETA)
VST=OSE*OS*(HETA)
THETA=THEY+ST.29578
DELTA=THEY+ST.29578
FTA=ETA+ST.29578
C...PROPAGATE SHOCK
V(J,K)=X(J,K)+XST*DT
V(J,K)=Y(J,K)+YST*DT
C...ADJUST OTHER GRID POINTS
NO 2 3=J, K
ZFAC=FLOAT(K-1)/ZKN
X(J,K)=X(J,KMAX)-X(J,1)*ZKFAC+X(J,1)
Y(J,K)=Y(J,KMAX)-Y(J,1)*ZKFAC+Y(J,1)
2 CONTINUE
1 CONTINUE
PMS=5*DT*(PMS/float(JMAX))
WRITE(6,12) IT,PMS,OSEM,JOS
RETURN

```

```

SHOCK 25
SHOCK 26
SHOCK 27
SHOCK 28
SHOCK 29
SHOCK 30
SHOCK 31
SHOCK 32
SHOCK 33
SHOCK 34
SHOCK 35
SHOCK 36
SHOCK 37
SHOCK 38
SHOCK 39
SHOCK 40
SHOCK 41
SHOCK 42
SHOCK 43
SHOCK 44
SHOCK 45
SHOCK 46
SHOCK 47
SHOCK 48
SHOCK 49
SHOCK 50
SHOCK 51
SHOCK 52
SHOCK 53
SHOCK 54
SHOCK 55
SHOCK 56
SHOCK 57
SHOCK 58
SHOCK 59
SHOCK 60
SHOCK 61
SHOCK 62
SHOCK 63
SHOCK 64
SHOCK 65
SHOCK 66
SHOCK 67
SHOCK 68
SHOCK 69
SHOCK 70
SHOCK 71
SHOCK 72
SHOCK 73
SHOCK 74
SHOCK 75
SHOCK 76
SHOCK 77
SHOCK 78
SHOCK 79
SHOCK 80
SHOCK 81
SHOCK 82
SHOCK 83
SHOCK 84
SHOCK 85
SHOCK 86
SHOCK 87
SHOCK 88
SHOCK 89
SHOCK 90
SHOCK 91
SHOCK 92
SHOCK 93
SHOCK 94
SHOCK 95
SHOCK 96
SHOCK 97
SHOCK 98
SHOCK 99
SHOCK 100
SHOCK 101
SHOCK 102
SHOCK 103
SHOCK 104
SHOCK 105
SHOCK 106
SHOCK 107
SHOCK 108

```



```

5 CONTINUE
WRITE(6,103) J,P2,P(J,3),PTAU
STOP
102 FORMAT(10H ITERATION:1,4X,10HRMS OF SHOCK SPEED=,1PE11,4,X,
* ZCMXMINUR SHOCK SPEED=,E11,4,6H AT J=,I2)
103 FORMAT(10H,41MNEGATIVE PRESSURE DETECTED BY SHOCK AT J=,I2/
* 3X,3HPD=,1PE10,3,3X,3HPD=,3Y,E10,3,3X,5HPD=,E10,3)
END

SUBROUTINE XIEYAD (IFLAG)
COMMON /COM1 /JMAX,KMAX,3M,KH,KHACH,ALPHA,GAM,GAMH1,CM,DT,SMU,EPDT,
* CNDRO,NCI,MCB,MC,AB,MO,OMEGA,NU,NL,VT,YAU,ITER,ENT,P,TORT,PIHF,
* QINF,QINF,CMF,JCS,TM,CIUS,PT,HORN,RNISE,MCASE,NPUNCH
LEVEL 2,X,Y,XET,XYE,XYD
COMMON /COM2 /X(40,20),Y(40,20),XET(40,20,2),YET(40,20,2),
* XEY(40,20,2),D(40,20)
LEVEL 3,0,EF,S,C,AB
COMMON /COM3 /O(40,20,4),EF(4,4),S(4,2),Z(4),R(4),AN(4,4)
DO 11 K=1,KMAX
DO 11 J=1,JMAX
YET(J,K,1)=0.0
YET(J,K,2)=0.0
11 CONTINUE
JMH=1
KMH=1
C...COMPUTE X-YI AND Y-XI; DXI AND DELTA = 1
DO 1 K=1,KMAX
DO 2 J=2,JH
YET(J,K,2)=X(J,1,K)-X(J-1,K)100.5
2 YET(J,K,2)=(-1.0*(X(J,1,K)+X(J-1,K))0.5
YET(J,K,2)=(-1.0*(X(J,1,K)+X(J-1,K))0.5
YET(J,K,2)=(-1.0*(X(J,1,K)+X(J-1,K))0.5
YET(J,K,2)=(-1.0*(X(J,1,K)+X(J-1,K))0.5
YET(J,K,2)=(-1.0*(X(J,1,K)+X(J-1,K))0.5
1 YET(J,K,2)=(-1.0*(X(J,1,K)+X(J-1,K))0.5
C...COMPUTE X-ETA AND Y-ETA
DO 3 J=1,JMAX
DO 4 K=2,KH
YET(J,K,1)=X(J,K,1)-X(J,K-1)100.5
4 YET(J,K,1)=Y(J,K,1)-Y(J,K-1)100.5
YET(J,1,1)=(-3.0*(X(J,1)+4.0*(X(J,2)-X(J,3))100.5
YET(J,KMAX,1)=(-3.0*(X(J,KMAX)+4.0*(X(J,K)+X(J,K+1))100.5
YET(J,1,1)=(-3.0*(Y(J,1)+4.0*(Y(J,2)-Y(J,3))100.5
3 YET(J,KMAX,1)=(-3.0*(Y(J,KMAX)+4.0*(Y(J,K)+Y(J,K+1))100.5
C...COMPUTE XT-Y, YI-Y, ETA-Y, AND ETA-Y
DO 5 K=1,KMAX
DO 5 J=1,JMAX
DT=1.0/(X(J,K,1)+X(J,K,2))-XET(J,K,1)+YET(J,K,2)
DT=DT
IF(IFLAG.EQ.0) GO TO 7
C...ADJUST CONSERVATIVE VARIABLES BASED ON NEW MESH
DO 6 M=1,4
O(J,K,M)=O(J,K,M)*DT
7 CONTINUE
C...THE GEOMETRIC JACOBIAN IS DEFINED HERE AND STORED IN THE D ARRAY
Y(J,K)=DT
YET(J,K,1)=XET(J,K,1)*DT
YET(J,K,1)=XET(J,K,1)*DT
YET(J,K,2)=XET(J,K,2)*DT
5 YET(J,K,2)=XET(J,K,2)*DT
C...REFLECT METRICS AND DEPENDENT VARIABLES ABOUT PLANE OF SYMMETRY
IF(IFLAG.EQ.0) GO TO 8
DO 9 K=1,KMAX
DO 9 M=1,3
Y(1,M)=O(1,M)*DD
Y(1,K,1)=XET(2,K,1)
Y(1,K,1)=XET(2,K,1)
Y(1,K,2)=XET(2,K,2)
Y(1,K,2)=XET(2,K,2)
DO 10 M=1,4
O(1,K,M)=O(2,K,M)*DD
9 O(1,K,3)=O(2,K,3)*DD
8 CONTINUE
RETURN
END

```

```

SHOCK 100
*FNCI 110
SHOCK 111
SHOCK 112
SHOCK 113
SHOCK 114
SHOCK 115
SHOCK 116
XIEYAD 2
COM1 3
COM2 3
COM3 4
COM2 2
COM2 2
COM2 2
COM3 2
COM3 2
COM3 3
XIEYAD 6
XIEYAD 7
XIEYAD 9
XIEYAD 9
XIEYAD 10
XIEYAD 11
XIEYAD 12
XIEYAD 13
XIEYAD 14
XIEYAD 15
XIEYAD 16
XIEYAD 17
XIEYAD 18
XIEYAD 19
XIEYAD 20
XIEYAD 21
XIEYAD 22
XIEYAD 23
XIEYAD 24
XIEYAD 25
XIEYAD 26
XIEYAD 27
XIEYAD 28
XIEYAD 29
XIEYAD 30
XIEYAD 31
XIEYAD 32
XIEYAD 33
XIEYAD 34
XIEYAD 35
XIEYAD 36
XIEYAD 37
XIEYAD 38
XIEYAD 39
XIEYAD 40
XIEYAD 41
XIEYAD 42
XIEYAD 43
XIEYAD 44
XIEYAD 45
XIEYAD 46
XIEYAD 47
XIEYAD 48
XIEYAD 49
XIEYAD 50
XIEYAD 51
XIEYAD 52
XIEYAD 53
XIEYAD 54
XIEYAD 55
XIEYAD 56
XIEYAD 57
XIEYAD 58
XIEYAD 59
XIEYAD 60
XIEYAD 61

```

```

COMMON /INVAR/RK,ETA(41),PHI(41),DTIL(41),DTILE(41),PETA,TP(24)
COMMON /JDEF/ZL,CF1,CF2,ZLFL,TRAM,DZTRAM
LEVEL 2, RM,PS,U,V,W,ROR,ROBZ,VINF,VINF,RORPH,RB,PSZ,PSPH,DTOPH,
* ACT,DTDZ,DTDR,ACT,ICNST,GAM,CONST,NREGON,RS,RST,PSPHI,RST,PSZT,
* PSMIT
COMMON /PVARR/ RHO(24,41), P(24,41), U(24,41), V(24,41), W(24,41),
* ROR(41), ROBZ(41), VINF(41), VINF(41),
* RORPH(41), PH(41), PHZ(41), RAPH(41),
* DTOPH(24,41), DCT(41), DTDZ(24,41),DTDR(41), ACT(41),
* ICNST(50), GAM(20), CONST(50),NREGON, PS(41),
* SZ(41), PSMI(41), PST(41), PSZT(41), PSMIT(41)
COMMON /SVARR/ Z, PHI, DT, DZ, DP, DP, DT, DT,
* ZEND, PT, ALPHA, GAMMA, SIGMA, XHACH, TAPE1,
* TAPE2, DISK1, ALPH, DISK2, SIGM, NPHNT, DDT,
* DZDPH, ZH, TEND, TMLD, TWH, TML,
* TTM, PZ, PZ, NPHI, NIT, KPHI, NITER,
* NPH1, NPH11, NPH12, NPH13, NPH14, NPH15, NPH16,
* NT, NT1, NT2, NT3, NPHI, NCOM, RADI,
* PHIF, METHOD, LAG, NSC, PINF, RHOIN, JINF,
* QINF,GASCON,NREAL,NPUNCH
COMMON /DNSTRM/ ZPLOT,ZTEND,ZTADD,NXPLOT
CALL SETDAT
CALL RCOMB(O,PHI,PHI,7,RA,R*7,PSPH,TPNT)
SIGMA=ATAN(CF2)*57.29578
ICNST(41)=0
CALL INITA
IF (7,ACT, ZEND) GO TO 10
MTEP=ICOM-MTEMO
WRITE(6,61)
STOP=MTE-1
CALL ANRHYM(2)
DO 6 M=1,MITER
ICNST(5)=JUDI
C...COMPUTE AUTOMATIC STEPSIZE
IF (MTEP.EQ. 1) GO TO 3
IF (MTEP.DTIL,ICNST(49),NREGON) GO TO 5
3 CALL STEPFM
IF (MTEP.EQ. 1.0) GO TO 5
MTEP=STEPSE
MTEP=DT*DT
OZDPH=DT/DETA
5 CONTINUE
CALL DIFFR
C...WRITE DATA FOR REFIN ON TAPES
CALL DOUTPR
IF (7,ACT, ZEND) GO TO 10
CONTINUE
10 CONTINUE
C...ALL DATA REQUIRED FOR REFIN OF THIS CASE IS NOW ON TAPES
END FILE 0
RETURN
610 FORMAT(1H//54X,20HARCHING CALCULATION/54Y,2C(1H//)
* 2Y,4HSTEP NO.,4X,10HDOWNSTREAM LOCATION,4Y,13HRODY OPINATE,
* 5X,14HSHOCK ORINATE)
ENH
*JABROUTINE BNDRYK(1)
COMMON/ENTRO/S(41),7AS,ZFLD,ITORT,ITPOT,MCASE,NTDSM
RNDVHM 2
ENTRO 2
LEVEL 2, RM,PS,U,V,W,ROR,ROBZ,VINF,VINF,RORPH,RB,PSZ,PSPH,DTOPH,
* ACT,DTDZ,DTDR,ACT,ICNST,GAM,CONST,NREGON,RS,RST,PSPHI,RST,PSZT,
* PSMIT
PVARR 3
PVARR 4
PVARR 5
COMMON /PVARR/ RHO(24,41), P(24,41), U(24,41), V(24,41), W(24,41),
* ROR(41), ROBZ(41), VINF(41), VINF(41),
* RORPH(41), PH(41), PHZ(41), RAPH(41),
* DTOPH(24,41), DCT(41), DTDZ(24,41),DTDR(41), ACT(41),
* ICNST(50), GAM(20), CONST(50),NREGON, PS(41),
* SZ(41), PSMI(41), PST(41), PSZT(41), PSMIT(41)
PVARR 6
PVARR 7
PVARR 8
PVARR 9
PVARR 10
COMMON /SVARR/ Z, PHI, DT, DZ, DP, DP, DT, DT,
* ZEND, PT, ALPHA, GAMMA, SIGMA, XHACH, TAPE1,
* TAPE2, DISK1, ALPH, DISK2, SIGM, NPHNT, DDT,
* DZDPH, ZH, TEND, TMLD, TWH, TML,
* TTM, PZ, PZ, NPHI, NIT, KPHI, NITER,
* NPH1, NPH11, NPH12, NPH13, NPH14, NPH15, NPH16,
* NT, NT1, NT2, NT3, NPHI, NCOM, RADI,
* PHIF, METHOD, LAG, NSC, PINF, RHOIN, JINF,
* QINF,GASCON,NREAL,NPUNCH
SVARR 2
SVARR 3
SVARR 4
SVARR 5
SVARR 6
SVARR 7
SVARR 8
SVARR 9
SVARR 10

```

```

IDVARR 2
JOE 2
PVARR 3
PVARR 4
PVARR 5
PVARR 6
PVARR 7
PVARR 8
PVARR 9
PVARR 10
SVARR 2
SVARR 3
SVARR 4
SVARR 5
SVARR 6
SVARR 7
SVARR 8
SVARR 9
SVARR 10
DNSTRM 2
HARCH 8
HARCH 9
HARCH 10
HARCH 11
HARCH 12
HARCH 13
HARCH 14
HARCH 15
HARCH 16
HARCH 17
HARCH 18
HARCH 19
HARCH 20
HARCH 21
HARCH 22
HARCH 23
HARCH 24
HARCH 25
HARCH 26
HARCH 27
HARCH 28
HARCH 29
HARCH 30
HARCH 31
HARCH 32
HARCH 33
HARCH 34
HARCH 35
HARCH 36
HARCH 37
HARCH 38
HARCH 39
HARCH 40
HARCH 41
HARCH 42
HARCH 43
HARCH 44
HARCH 45

```

SUBROUTINE HARCH

HARCH 2

```

DTMENSTON PK13(41),PK14(41),PK21(41),PK22(41),PK23(41)
LOGICAL ITZND
ARSTN(A)=ASIN(A)
GM TN (10,10,11),K1
10 CONTINUE
C..WEAK OR SMALL ANGLE CORRECTIONS (USES WRANDTL-MEYER RELATIONS)
DO 9 K=3,NPHI
PK4=1./DSORT(RBZ(K)**2+1.D+(RAPH(K)/RA(K))**2)
PK1=-R7(K)**4
PK2=PK4
PK3=-RPH(K)/RRE(K)*PK4
ITZND=.FALSE.
QSO=U(3,K)**2+V(3,K)**2+W(3,K)**2
IF(P(3,K).GE.P(0)) GO TO 4
C..NEGATIVE SURFACE PRESSURE
ICHECK=1
Y=1.C-7
IF (K .EQ. 3) WRITE(6,1L2) X,P(3,K),RHQ(3,K),U(3,K),V(3,K)
P(3,K)=PI*MF(1.-Q,5/GAMMA)
RHO(3,K)=(P(3,K)/S(K))**1./G/GAMMA
Q3K=SQRT(1.-P(3,K)/RHQ(3,K))
U(3,K)=U(3,K)*Q3K/QSO**0.5
V(3,K)=V(3,K)*Q3K/QSO**0.5
W(3,K)=W(3,K)*Q3K/QSO**0.5
QSO=Q3K**2
4 CONTINUE
TF(RHNS,K) .GE. 0.01G TO 5
ICHECK=2
Y=1.C-7
IF (K .EQ. 3) WRITE(6,10C) X,P(3,K),RHQ(3,K),U(3,K),V(3,K)
RHO(3,K)=(P(3,K)/S(K))**1./G/GAMMA
Q3K=SQRT(1.-P(3,K)/RHQ(3,K))
U(3,K)=U(3,K)*Q3K/QSO**0.5
V(3,K)=V(3,K)*Q3K/QSO**0.5
W(3,K)=W(3,K)*Q3K/QSO**0.5
5 CONTINUE
PK5=DSORT(QSO)
PK6=(PK1**3+PK2**3+PK3**3+PK5**3)/PK5
PK7=4051N(PK6)
PK8=GAM(1)*P(3,K)/RHQ(3,K)
PK9=PK5**0.2/PK8
PK10=PK9-1.0
TF(PK10.LT. 0.01G TO 6
ICHECK=3
Y=1.C-7
TF (K .EQ. 3) WRITE(6,10C) X,P(3,K),RHQ(3,K),U(3,K),V(3,K)
PK10=0.5
PK9=1.5
PK8=PK5**0.2/PK9
RHO(3,K)=GAM(1)*P(3,K)/PK8
Q3K=SQRT(1.-P(3,K)/RHQ(3,K))
U(3,K)=U(3,K)*Q3K/QSO**0.5
V(3,K)=V(3,K)*Q3K/QSO**0.5
W(3,K)=W(3,K)*Q3K/QSO**0.5
6 CONTINUE
PK11=GAMMA*PK9/DSORT(PK10)
PK12=GAMMA*PK9*((GAMMA+1.C)*PK9**2-4.C*PK10)/(4.C*PK10**2)
PK13(K)=P(3,K)/(1.-PK11*PK7+PK12*PK7**2)
EACTOR=0.5*GAMMA*PK9/(PK10**0.5)
TERM1=(GAMMA+1.0)*PK9**0.76/0
TERM2=-19.*0.76*GAMMA**2.2*GAMMA**2)*PK9**0.76/0
TERM3= 5.0*(GAMMA+1.0)*PK9**0.2/3.0
TERM4=4.0/3.0-2.0*PK9
COEFF3=FACTOR*(TERM1+TERM2+TERM3+TERM4)
PTEST=PK13(K)-P(3,K)+COEFF3*PK7**3
TF (ABS(PTEST).LT.A95(6.011)GO TO 123
Y=1 .SOFT(PK0)
CALL PHTURN(X1,PK7,P20,MTTS,GAMMA)
P7MIE = P(3,K)*P2P1
PTEST = P7MIE
123 CONTINUE
PK13(K)=PTEST
PK14(K)=(PK13(K)/S(K))**1./G/GAMMA
PK15=DSORT(1.-PK13(K)/PK14(K))
PK16=PK6**0.5*PK4
PK17=U(3,K)*PK16**R7(K)
PK18=V(3,K)*PK16**16
PK19=U(3,K)*PK16**RPH(K)/RRE(K)
PK20=SQRT(PK17**2+PK18**2+PK19**2)
PK24=PK15/PK20
PK21(K)=PK24*PK17
PK22(K)=PK24*PK18
PK23(K)=PK24*PK19
CONTINUE
11 CONTINUE

```

ENDRYM	6
ENDRYM	7
ENDRYM	8
ENDRYM	9
ENDRYM	10
ENDRYM	11
ENDRYM	12
ENDRYM	13
ENDRYM	14
ENDRYM	15
ENDRYM	16
ENDRYM	17
ENDRYM	18
ENDRYM	19
ENDRYM	20
ENDRYM	21
ENDRYM	22
ENDRYM	23
ENDRYM	24
ENDRYM	25
ENDRYM	26
ENDRYM	27
ENDRYM	28
ENDRYM	29
ENDRYM	30
ENDRYM	31
ENDRYM	32
ENDRYM	33
ENDRYM	34
ENDRYM	35
ENDRYM	36
ENDRYM	37
ENDRYM	38
ENDRYM	39
ENDRYM	40
ENDRYM	41
ENDRYM	42
ENDRYM	43
ENDRYM	44
ENDRYM	45
ENDRYM	46
ENDRYM	47
ENDRYM	48
ENDRYM	49
ENDRYM	50
ENDRYM	51
ENDRYM	52
ENDRYM	53
ENDRYM	54
ENDRYM	55
ENDRYM	56
ENDRYM	57
ENDRYM	58
ENDRYM	59
ENDRYM	60
ENDRYM	61
ENDRYM	62
ENDRYM	63
ENDRYM	64
ENDRYM	65
ENDRYM	66
ENDRYM	67
ENDRYM	68
ENDRYM	69
ENDRYM	70
ENDRYM	71
ENDRYM	72
ENDRYM	73
ENDRYM	74
ENDRYM	75
ENDRYM	76
ENDRYM	77
ENDRYM	78
ENDRYM	79
ENDRYM	80
ENDRYM	81
ENDRYM	82
ENDRYM	83
ENDRYM	84
ENDRYM	85
ENDRYM	86
ENDRYM	87
ENDRYM	88
ENDRYM	89
ENDRYM	90

```

C..RESPT BODY VARIABLES TO THOSE CALCULATED BY ABBETS SCHEME
DO 12 N=3,NPHI
P(3,K)=PK23(K)
RHO(3,K)=PK14(K)
U(3,K)=PK21(K)
V(3,K)=PK22(K)
W(3,K)=PK23(K)
12 CONTINUE
GM TN 21
18 CONTINUE
C
C..APPLY REFLECTION PRINCIPLE AT PLANES OF SYMMETRY
C
DO 1 K=1,2
M=6-K
L=NPHI+K
N=NPHI-K
DO 1 J=3,NTZ
P(M,J)=P(HI(J),M)
RHO(J)=RHO(J),M)
P(J,K)=P(J,M)
P(J,L)=P(J,N)
U(J,K)=U(J,M)
U(J,L)=U(J,N)
V(J,K)=V(J,M)
V(J,L)=V(J,N)
W(J,K)=W(J,M)
W(J,L)=W(J,N)
W(J,3)=0
U(J,NHI)=0.0
1 CONTINUE
21 CONTINUE
1. : FORMATE(24,4) NEGATIVE PRESSURE OR DENSITY ON BODY DETECTED BY
* 114NDRY AT X=F7.3/3X,3499,PE1,3,3X,54P40*,E10.3,3X,
* 44VVV=E10.3,3X,44VVB=E10.3)
PETHN
END
DIFFR 91
ENDRYM 92
ENDRYM 93
ENDRYM 94
ENDRYM 95
ENDRYM 96
ENDRYM 97
ENDRYM 98
ENDRYM 99
ENDRYM 100
ENDRYM 101
ENDRYM 102
ENDRYM 103
ENDRYM 104
ENDRYM 105
ENDRYM 106
ENDRYM 107
ENDRYM 108
ENDRYM 109
ENDRYM 110
ENDRYM 111
ENDRYM 112
ENDRYM 113
ENDRYM 114
ENDRYM 115
ENDRYM 116
ENDRYM 117
ENDRYM 118
ENDRYM 119
ENDRYM 120
ENDRYM 121
ENDRYM 122
ENDRYM 123
ENDRYM 124
ENDRYM 125
ENDRYM 126
ENDRYM 127
DIFFR 2
DIFFR 3
DIFFR 4
DIFFR 5
DIFFR 6
DIFFR 7
DIFFR 8
DIFFR 9
DIFFR 10
DIFFR 11
DIFFR 12
DIFFR 13
DIFFR 14
DIFFR 15
DIFFR 16
DIFFR 17
DIFFR 18
DIFFR 19
DIFFR 20
DIFFR 21
DIFFR 22
DIFFR 23
DIFFR 24
DIFFR 25
DIFFR 26

```

```

C..CALCULATES GEOMETRIC FACTORS BASED ON NEW BODY AND SHOCK GEOMETRY    DIFFR 27
CALL GEOM(1)                                                                DIFFR 28
C..APPLIES PLANE OF SYMMETRY BOUNDARY CONDITIONS                          DIFFR 29
CALL NBOUND(2)                                                              DIFFR 30
C..FORM INTERMEDIATE CONSERVATIVE VARIABLES AT ALL POINTS                DIFFR 31
CALL ICOND(1)                                                                DIFFR 32
DO 3 J=3,NPHI                                                                DIFFR 33
  DO 3 K=3,NTZ                                                                DIFFR 34
    K=KPHI                                                                    DIFFR 35
  C..DISSIPATION FUNCTION                                                  DIFFR 36
  DISS=0.0                                                                    DIFFR 37
  IF (CONST(4).NE.C.0) .OR. CONST(5).NE.C.0) CALL DISSPH(N,J,K,DISS)    DIFFR 38
  TF(J,EO,3) GO TO 9                                                         DIFFR 39
  TF(J,EO,NTZ) GO TO 5                                                       DIFFR 40
C..CORRECTOR IN FIELD                                                    DIFFR 41
ETEMP(N,J,K)=C.5*(E0(N,J,K)+ETEMP(N,J,K)-(I707*(FO(N,J,K)
+FO(N,J,K-1)+OZDPH*(GO(N,J,K)-GO(N,J,K-1))+OZ*HO(N,J,K))+DISS)
  GO TO 9                                                                      DIFFR 42
C..CORRECTOR AT SHOCK                                                    DIFFR 43
ETEMP(N,J,K)=0.5*(ETEMP(N,J,K)+E0(N,J,K)-(I707*(FO(N,J,K)
+FO(N,J,K-1)+OZDPH*(GO(N,J,K)-GO(N,J,K-1))+OZ*HO(N,J,K))+DISS)
  GO TO 9                                                                      DIFFR 44
C..CORRECTOR AT BODY                                                     DIFFR 45
ETEMP(N,J,K)=C.5*(ETEMP(N,J,K)+E0(N,J,K)-(I707*(FO(N,J,K)+FO(N,J,K
+OZDPH*(GO(N,J,K)-GO(N,J,K-1))+OZ*HO(N,J,K))+DISS)
  GO TO 9                                                                      DIFFR 46
C..DECLINE CONSERVATIVE VARIABLES                                        DIFFR 47
CALL ICOND(2)                                                                DIFFR 48
C..CALCULATE CONNECTED SHOCK VALUES                                    DIFFR 49
CALL SHOCK(2)                                                                DIFFR 50
C..CALCULATES GEOMETRIC FACTORS BASED ON OLD BODY AND NEW SHOCK GEOMETRY DIFFR 51
CALL GEOM(2)                                                                DIFFR 52
C..RESPTS BODY VARIABLES                                                DIFFR 53
CALL NBOUND(1)                                                              DIFFR 54
C..APPLIES PLANE OF SYMMETRY BOUNDARY CONDITIONS                          DIFFR 55
CALL NBOUND(2)                                                              DIFFR 56
END                                                                            DIFFR 57
DIFFR 58

SUBROUTINE DISSPH(N,J,K,DISS)
LEVEL 2,ETEMP,E0,EO,GO,HO
COMMON /CVAR8/ ETEMP(4,24,41), E0(4,24,41),
  FO(4,24,41), GE(4,24,41), M(4,24,41)
COMMON /TVAR8/ AK,ETA(41),PHI(41),DTIL(41),DTILE(41),DETA,TP(24)
LEVEL 2, P40,P,U,V,W,ROA,RDZ,VINF,VINF,RRPH,RA,RZ,RRPH,OTOP,4
ACT,DTD,DTDR,ACT,ICONST,GAM,CONST,NREGON,RS,RSZ,RSPHI,PS,PSZ,
  RSPT
  PSPT
COMMON /SVAR8/ RHO(24,41), P(24,41), U(24,41), V(24,41), W(24,41),
  ROZ(41), ROZ(41), VINF(41), VINF(41), RRPH(41)
  RRPH(41), ACT(41), OTDZ(24,41), OTDR(41), ACT(41),
  ICONST(50), GAM(20), CONST(50), NREGON, RS(41),
  RSZ(41), RSPHI(41), PST(41), RSZT(41), PSPT(41)
COMMON /SVAR8/TZ, PHT, DT, DPHT, ZINT,
  ZEND, PI, ALPHA, GAMMA, SIGMA, XHACH, TAPP1,
  TAPP2, DISK1, ALPHA, DISK2, SIGM, NPHNT, DZPT,
  OTOPH, ZH, THUD, THLO, TRU, THL, TYM,
  TYM, RZ, RZ, NPHI, NIT, NPHI, NITER,
  NPHI, NPHI1, NPHI2, NPHI3, NPHM1, NPHM2, NPHM3,
  NT, NT1, NT2, NT3, PHIF, NCOME, RADI,
  PHF, METHOD, LAG, MNC, PINE, RMJIN, UINF,
  OTNF,GASCON,NREAL,NPUNCH
  DIFFR 2
  CVAR8 3
  CVAR8 4
  CVAR8 3
  IOVAR8 2
  VVAR8 2
  VVAR8 3
  VVAR8 4
  VVAR8 5
  VVAR8 6
  VVAR8 7
  VVAR8 8
  VVAR8 9
  VVAR8 10
  VVAR8 2
  VVAR8 3
  VVAR8 4
  VVAR8 5
  VVAR8 6
  VVAR8 7
  VVAR8 8
  VVAR8 9
  VVAR8 10
  VVAR8 11
  VVAR8 12
  VVAR8 13
  DISSPH 14
  DISSPH 15
  DISSPH 16
  DISSPH 17
  DISSPH 18
  DISSPH 19
  DISSPH 20
  DISSPH 21

```

```

5 JD=J
5 DISSPH=CONST(4)*E0.J1*(E0(N,JD+2,K)+E0(N,JD+2,K)-4.0*(E0(N,JD+1,K)
+E0(N,JD-1,K))+6.0*(E0(N,JD,K)))
GO TO 3
21 CONTINUE
IF(J.GE. 4 .AND. J.LE. NT1)GO TO 33
IF(J.LT. 4)GO TO 70
JD=NT
70 GO TO 60
70 JD=4
60 GO TO 60
50 DISSPH=CONST(4)*E0.J1*(E0(N,JD+1,K)+E0(N,JD-1,K))-0.25*(E0(N,JD,K))
60 GO TO 2
1 DISSPH=0.0
C
C..... CONST(5) < 0 = LAX DAMPING
C..... CONST(5) = 0 = NO DAMPING
C..... CONST(5) > 0 = 4TH ORDER DAMPING
C
2 IF(CONST(5))31,1,23
C..DISSIPATION TERM IN THE MERIDIANAL DIRECTION
CONTINUE
TFK .GE. 4 .AND. K .LE. NPHI1 GO TO 80
TFK .LT. 4 GO TO 100
K=NPHI1
GO TO 9.
11. K=4
  GO TO 90
  K=N
  DIFFR 22
  DIFFR 23
  DIFFR 24
  DIFFR 25
  DIFFR 26
  DIFFR 27
  DIFFR 28
  DIFFR 29
  DIFFR 30
  DIFFR 31
  DIFFR 32
  DIFFR 33
  DIFFR 34
  DIFFR 35
  DIFFR 36
  DIFFR 37
  DIFFR 38
  DIFFR 39
  DIFFR 40
  DIFFR 41
  DIFFR 42
  DIFFR 43
  DIFFR 44
  DIFFR 45
  DIFFR 46
  DIFFR 47
  DIFFR 48
  DIFFR 49
  DIFFR 50
  DIFFR 51
  DIFFR 52
  DIFFR 53
  DIFFR 54
  DIFFR 55
  DIFFR 56
  DIFFR 57
  DIFFR 58
  DIFFR 59
  DIFFR 60
  DIFFR 61
  DIFFR 62
  DIFFR 63
  DIFFR 64
  DIFFR 65
  DIFFR 66
  DIFFR 67
  DIFFR 68
  DIFFR 69
  DIFFR 70
  DIFFR 71

SUBROUTINE EIGENP
COMMON/CLUSTR/R, XI(24), TXI(24), TXIT(24)
COMMON /TVAR8/ AK,ETA(41),PHI(41),DTIL(41),DTILE(41),DETA,TP(24)
LEVEL 2, P40,P,U,V,W,ROA,RDZ,VINF,VINF,RRPH,RA,RZ,RRPH,OTOP,4
ACT,DTD,DTDR,ACT,ICONST,GAM,CONST,NREGON,RS,RSZ,RSPHI,PS,PSZ,
  RSPT,PSPT
COMMON /SVAR8/ RHO(24,41), P(24,41), U(24,41), V(24,41), W(24,41),
  ROZ(41), ROZ(41), VINF(41), VINF(41), RRPH(41)
  RRPH(41), ACT(41), OTDZ(24,41), OTDR(41), ACT(41),
  ICONST(50), GAM(20), CONST(50), NREGON, RS(41),
  RSZ(41), RSPHI(41), PST(41), RSZT(41), PSPT(41)
COMMON /SVAR8/TZ, PHT, DT, DPHT, ZINT,
  ZEND, PI, ALPHA, GAMMA, SIGMA, XHACH, TAPP1,
  TAPP2, DISK1, ALPHA, DISK2, SIGM, NPHNT, DZPT,
  OTOPH, ZH, THUD, THLO, TRU, THL, TYM,
  TYM, RZ, RZ, NPHI, NIT, NPHI, NITER,
  NPHI, NPHI1, NPHI2, NPHI3, NPHM1, NPHM2, NPHM3,
  NT, NT1, NT2, NT3, PHIF, NCOME, RADI,
  PHF, METHOD, LAG, MNC, PINE, RMJIN, UINF,
  OTNF,GASCON,NREAL,NPUNCH
  EIGENP 2
  CLUSTR 2
  IOVAR8 2
  VVAR8 2
  VVAR8 3
  VVAR8 4
  VVAR8 5
  VVAR8 6
  VVAR8 7
  VVAR8 8
  VVAR8 9
  VVAR8 10
  VVAR8 11
  VVAR8 12
  VVAR8 13
  VVAR8 14
  VVAR8 15
  VVAR8 16
  VVAR8 17
  VVAR8 18
  VVAR8 19
  VVAR8 20
  VVAR8 21
  EIGENP 7
  EIGENP 8
  EIGENP 9
  EIGENP 10
  EIGENP 11
  EIGENP 12
  EIGENP 13
  EIGENP 14

```

```

C2=GAM(1)*P(J,K)/R4D(J,K)
TF(C2) 17,17,18
17 CONTINUE
C2=C2
18 CONTINUE
P=50*PI/21
R=DT9*H(J,K)+(R0B(K)-R0(K))/R
O1=(V(J,K)+W(J,K))/R0(J,K)
R001=U(J,K)*O2+O1*(V(J,K)+W(J,K))/R**2-C2*(1,0,0)**O2
19 CONTINUE
R001=-R001
T=J-2
TF (M ,EO, 3) WRITE(6,103) I
CONTINUE
O2=C*SORTI(G001)
O3=U(J,K)**2-C2
SIGR1=(O1+O2)/O3
SIGR2=(O1-O2)/O3
R002=H(J,K)**2+O2*(J,K)**2-C2
IF(G002) 21,21,22
21 CONTINUE
R002=-R002
T=J-2
TF (M ,EO, 3) WRITE(6,104) I
CONTINUE
O4=U(J,K)*W(J,K)
O5=C*SORTI(G002)
SIGR3=(O4+O5)/O3**O2IL(K)
SIGR4=(O4-O5)/O3**O2IL(K)
C.....COMPUTE LOCAL T AND PHI EIGENVALUES
SIG1=ANG*((O7O2(J,K)+SIGB1*DTOR(K))*TRT(J))
SIG2=ANG*((O7O2(J,K)+SIGB2*DTOR(K))*TRT(J))
SIG12=AMAX1(SIG1,SIG2)
SIG3=AMIN1(SIG1)
SIG4=AMIN1(SIG2)
SIG34=AMAX1(SIG3,SIG4)
TF(SIG12.LE.SIG12M) GO TO 2
C.....LOCATE MAXIMUM U-W EIGENVALUE
JMAX1=J
KMAX1=K
SIG12=SIG12
ICNST(11)=JMAX1
ICNST(12)=KMAX1
CONTINUE
2 TF(SIG34.LE.SIG34M) GO TO 3
C.....LOCATE MAXIMUM U-W EIGENVALUE
JMAX2=J
KMAX2=K
ICNST(13)=JMAX2
ICNST(14)=KMAX2
SIG34=SIG34
CONTINUE
3 CONTINUE
1 CONTINUE
C.....COMPUTE STEP SIZE BASED ON MAXIMUM EIGENVALUE
O712=DT*CONST(9)/SIG12M
O734=DT*CONST(9)/SIG34M
TF(O712.GV.O734) GO TO 4
O712=CONST(9)/SIG12M
O7=O712*DT
O7D04=O7/DETA
ICNST(13)=1.5*ICNST(13)
ICNST(14)=1.5*ICNST(14)
GO TO 5
4 CONTINUE
O7D04=CONST(9)/SIG34M
O7=O7D04*DETA
ICNST(11)=1.0*ICNST(11)
ICNST(12)=1.0*ICNST(12)
CONTINUE
5 RETURN
1,3 *****ALPHANEUTRAL SIGMA-BAR-1 IN EIGEN INDICATES *
* 194548SONIC FLOW AT I=12)
1,4 *****ALPHANEUTRAL SIGMA-BAR-2 IN EIGEN INDICATES *
* 194548SONIC FLOW AT I=12)
END

```

```

SUBROUTINE GEOM(RMOSE,ANG,RZ,DRDZ,ZSTA,M,P00,MMAX)
DIMENSION ZSTA(200),DRDZ(200),RZ(200)

```

```

EIGENN 15
EIGENN 16
EIGENN 17
EIGENN 18
EIGENN 19
EIGENN 20
EIGENN 21
EIGENN 22
EIGENN 23
EIGENN 24
EIGENN 25
EIGENN 26
EIGENN 27
EIGENN 28
EIGENN 29
EIGENN 30
EIGENN 31
EIGENN 32
EIGENN 33
EIGENN 34
EIGENN 35
EIGENN 36
EIGENN 37
EIGENN 38
EIGENN 39
EIGENN 40
EIGENN 41
EIGENN 42
EIGENN 43
EIGENN 44
EIGENN 45
EIGENN 46
EIGENN 47
EIGENN 48
EIGENN 49
EIGENN 50
EIGENN 51
EIGENN 52
EIGENN 53
EIGENN 54
EIGENN 55
EIGENN 56
EIGENN 57
EIGENN 58
EIGENN 59
EIGENN 60
EIGENN 61
EIGENN 62
EIGENN 63
EIGENN 64
EIGENN 65
EIGENN 66
EIGENN 67
EIGENN 68
EIGENN 69
EIGENN 70
EIGENN 71
EIGENN 72
EIGENN 73
EIGENN 74
EIGENN 75
EIGENN 76
EIGENN 77
EIGENN 78
EIGENN 79
EIGENN 80
EIGENN 81
EIGENN 82
EIGENN 83
EIGENN 84
EIGENN 85
EIGENN 86
EIGENN 87
EIGENN 88
EIGENN 89
EIGENN 90
EIGENN 91

```

```

GEOM 2
GEOM 3

```

```

LOGICAL LGRAV
COMMON/NU80D/XX(100),YY(100),NU80D,LGRAV
C
C.....FUNCTION DEFINITIONS
C
E(A)=EXP(-ABS(A-RMOSE)/M)
F(A,B)=50*PI*(SIN(2*PI*B)-2*SORT(E(A)-E(A)**2))/(E(A)-SIN(A)**2)
G(A,B)=ABS(A*(A**6*SIN(B)*COS(B)+SORT(A**6-1.1)/(A**6+COS(B)**2-
* 1.1)
H(A,B)=C*D1+RMOSE*SORT(D*(1-D1))/(D-R00)
G(A,B)=EXP(-ABS(1.-1./A)/M)
C
C.....M =E0, 0.3 ; IONOSPHERE FOR ANOMAGNETIC PLANET
C.....M =E0, 0.0 ; EQUATORIAL PLANE FOR A MAGNETIC PLANET
C
TF(M ,EO, 0.0)GO TO 10
TF(M ,LT,0.0) GO TO 20
TF (M ,LT, 0.01) GO TO 30
C
C.....THIS DETERMINES THE BODY SHAPE OF A MAGNETIC PLANET
C
C
TMAX=210
PI=3.1415926535898
RADI=180./PI
DELTA=ANG/RADI/PLDAT(TMAX)
THETA=PI/2.
RJ=RMOSE
TF (ICRAV) GO TO 40
C
C.....PERFORM AN INTEGRATION FROM 0 TO 170 DEGREES
C
ZSTA(1)=0.0
O7(1)=R07
THETA1=THETA
O7O7(1)=RPI,THETA1/R1
J=0
TMAX1=TMAX-1
O7 5 I=1,TMAX1
C.....PREDICTOR
O7=PI*DELTA+O7(1),THETA1)
THETA1=THETA+DELTA
C.....CORRECTOR
O7O7(1)=O7,DELTA+O7(1),THETA1)+O7(1),THETA1)
O7O7(1)=O7,THETA1)
O7=0
THETA1=THETA
ZSTA(J)=R*DCOS(THETA)
O7(J)=R*OSIN(THETA)
O7O7(J)=(DRDTH*OSIN(THETA)+R*DCOS(THETA))/
* (-DRDTH*DCOS(THETA)+R*OSIN(THETA))
J=J+1
5 CONTINUE
NMAX=J-1
*ETURN
C
C USE CYLINDRICAL BODY FOR M/RD <LT, 0.01
C
3) ZSTA(1)=1.0
ZSTA(2)=1.05*G
O7(1)=R00
O7(2)=R00
O7O7(1)=0.0
O7O7(2)=0.0
NMAX=2
RETURN
C
C.....THIS DETERMINES THE BODY SHAPE OF A MAGNETIC PLANET
C
C
J=1
ANG=ANG+90.
TMAX=350
PI=3.1415926535898
RADI=180./PI
DELTA=ANG/RADI/PLDAT(TMAX+1)
THETA=PI/2.
RJ=RMOSE
C
C.....PERFORM AN INTEGRATION FROM 90 TO 260 DEGREES
C
O7 15 T=1,TMAX
C.....PREDICTOR

```

```

NU80D 2
NU80D 3
GEOM 4
GEOM 5
GEOM 6
GEOM 7
GEOM 8
GEOM 9
GEOM 10
GEOM 11
GEOM 12
GEOM 13
GEOM 14
GEOM 15
GEOM 16
GEOM 17
GEOM 18
GEOM 19
GEOM 20
GEOM 21
GEOM 22
GEOM 23
GEOM 24
GEOM 25
GEOM 26
GEOM 27
GEOM 28
GEOM 29
GEOM 30
GEOM 31
GEOM 32
GEOM 33
GEOM 34
GEOM 35
GEOM 36
GEOM 37
GEOM 38
GEOM 39
GEOM 40
GEOM 41
GEOM 42
GEOM 43
GEOM 44
GEOM 45
GEOM 46
GEOM 47
GEOM 48
GEOM 49
GEOM 50
GEOM 51
GEOM 52
GEOM 53
GEOM 54
GEOM 55
GEOM 56
GEOM 57
GEOM 58
GEOM 59
GEOM 60
GEOM 61
GEOM 62
GEOM 63
GEOM 64
GEOM 65
GEOM 66
GEOM 67
GEOM 68
GEOM 69
GEOM 70
GEOM 71
GEOM 72
GEOM 73
GEOM 74
GEOM 75
GEOM 76
GEOM 77
GEOM 78
GEOM 79
GEOM 80
GEOM 81
GEOM 82
GEOM 83
GEOM 84
GEOM 85
GEOM 86

```

```

      THETA1=THETA
      *R1=AC1*TA*G(R1,THETA1)
      THETA2=THETA+DELTA
C.....CORRECTOR
      *R1=0.5*DELTA*(G(PI),THETA1)+G(R,THETA))
      DRDT=6(R,THETA)
      R1=R
      IF (THETA .LT. PI) GO TO 15
      YSTA(J)=-R*SIN(THETA)
      Y7(J)=-R*COS(THETA)
      DRDZ(J)=(-DRDT*GOS(THETA)+R*SIN(THETA))/
      (-DRDT*SIN(THETA)-R*COS(THETA))
15
      J=J+1
      CONTINUE
      NMAX=J-1
      RETURN
C
C.....BODY SHAPE TABLE SUPPLIED BY USER
C
20
      CONTINUE
      J=1
      DX2=C*H
      DR2=C*J
      NRODM=NROD-1
      DO 25 I=1,NRODM
      DX1=DX2
      DR1=DR2
      DX2=XX(I+1)-XX(I)
      DR2=YY(I+1)-YY(I)
      Y7(I)=Y7(I)+G(T,9,0) GO TO 29
      YSTA(I)=-XX(I)
      Y7(J)=YY(I)
      Y1=SORT(DR1*DR1+DX1*DX1)
      Y2=SORT(DR2*DR2+DX2*DX2)
      DRDZ(J)=-DR1*DR2/(DX1*DR2+DX2*(DR1+DR2))
      I=J+1
25
      CONTINUE
      YSTA(J)=-YX(NROD)
      Y7(J)=YY(NROD)
      DRDZ(J)=-DR2*(2.*C*DX2+DX1)/DX2-DR1*DX2/DY1/(DX1+DX2)
      NMAX=J
      RETURN
40
      CONTINUE
      YSTA(1)=0.0
      R7(1)=R0
      THETA1=THETA
      A1=C*(R1,4)
      DRDZ(1)=-F2(R1,1,C*J,L,A1)/R0
      I=2
      NMAX1=NMAX-1
      DO 50 I=1,NMAX1
      AS=C*(N(THETA))
      AC=COS(THETA)
C.....CORRECTOR
      A1=C*(R1,4)
      K=0
      DRX=F2(R1,AS,AC,A1)
      IF (DRX.LT.0.0) DRX=2.*R0*AS*AC
      *R1=DRX+DELTA
      THETA2=THETA+DELTA
      AS1=C*(N(THETA))
      AC1=COS(THETA)
C.....CORRECTOR
45
      CONTINUE
      A1=C*(R1,4)
      DRX=F2(R1,AS1,AC1,A1)
      IF (DRX.LT.0.0) DRX=2.*R0*AS1*AC1
      *R1=DRX+DELTA
      *R1=5*DRX+DELTA
      K=K+1
      IF (K.LT.5) GO TO 45
      YSTA(1)=-R0*AC1
      Y7(1)=-R0*AS1
      DRDZ(1)=-R0*AC1*AS1*SLOPE1/(R0*AS1-AC1*SLOPE)
      R1=R
      J=J+1
      CONTINUE
      NMAX=J-1
      RETURN
      END
      GEOM 87
      GEOM 88
      GEOM 89
      GEOM 90
      GEOM 91
      GEOM 92
      GEOM 93
      GEOM 94
      GEOM 95
      GEOM 96
      GEOM 97
      GEOM 98
      GEOM 99
      GEOM 100
      GEOM 101
      GEOM 102
      GEOM 103
      GEOM 104
      GEOM 105
      GEOM 106
      GEOM 107
      GEOM 108
      GEOM 109
      GEOM 110
      GEOM 111
      GEOM 112
      GEOM 113
      GEOM 114
      GEOM 115
      GEOM 116
      GEOM 117
      GEOM 118
      GEOM 119
      GEOM 120
      GEOM 121
      GEOM 122
      GEOM 123
      GEOM 124
      GEOM 125
      GEOM 126
      GEOM 127
      GEOM 128
      GEOM 129
      GEOM 130
      GEOM 131
      GEOM 132
      GEOM 133
      GEOM 134
      GEOM 135
      GEOM 136
      GEOM 137
      GEOM 138
      GEOM 139
      GEOM 140
      GEOM 141
      GEOM 142
      GEOM 143
      GEOM 144
      GEOM 145
      GEOM 146
      GEOM 147
      GEOM 148
      GEOM 149
      GEOM 150
      GEOM 151
      GEOM 152
      GEOM 153
      GEOM 154
      GEOM 155
      GEOM 156
      GEOM 157
      GEOM 158
      GEOM 159
      GEOM 160
      GEOM 161
      GEOM 162
      GEOM 163
      GEOM 164
      GEOM 165
      GEOM 166
      SUBROUTINE GEOM1(K5)
      COMMON /CLUSTER/RJ,XTI(24),TXIT(24)
      COMMON /IDVAR/RK,ETA(41),PHIP(41),DTIL(41),DETA,TP(24)
      LEVEL 2, PNO,P,PU,V,ROD,ROZ,VINF,VINF,ROBP4,R0,R97,RBPH,DTOP4,
      * ACT,DTOT,OTDR,ACT,ICNST,GAM,CONST,NREGON,RS,RS7,RSPHI,RS7,RS7T,
      * RSPHIT
      COMMON /PVARS/ RHO(24,41), P(24,41), U(24,41), V(24,41), W(24,41),
      * ROR(41), * ROZ(41), * VINF(41), * VINF(41),
      * RORPH(41), * RB(41), * RZ(41), * RBPH(41),
      * DTOPH(24,41), ACT(41), DTOT(24,41),DTOR(41), ACT(41),
      * ICNST(50), GAM(20), CONST(50), NREGON, RS(41),
      * RS7(41), * RSPHI(41), * RS7T(41), * RSPHIT(41)
      COMMON /SVAR8/T,Z, * PHI, * DT, * DZ, * DPHI, * ZMT, *
      * ZENO, * PI, * ALPHA, * GAMMA, * SIGMA, * XFACH, * TAPE1,
      * TAPE2, * DISK1, * ALPH, * DISK2, * SIG, * NPHNT, * DZOT,
      * DTOPH, * ZM, * TWD, * TMLD, * TWM, * TML, * TTM,
      * TTL, * RZ, * RZ, * NIPHI, * MIT, * KPHI, * NITER,
      * NPHI, * NPHI1, * NPHI2, * NPHI3, * NPHM1, * NPHM2, * NPHM3,
      * NT, * NT1, * NT2, * NT3, * PHIF, * MONE, * RADT,
      * PHIF, * METHOD, * LAG, * NSC, * PINF, * RHOIN, * UINF,
      * OINF, * GASCOM, * NREAL, * NPUNCH
      PRINT=ICNST(14)
      TFI(K5,FO,2) GO TO 12
      CALL GEOM3(I,PHIP,NPHI,Z,PS,RSZ,ROBP,IPRNT)
12
      CONTINUE
      CALL GEOM2(K5)
      DO 1 J=3,NTZ
      Y=Y(I,J)
      DO 2 K=2,NPHI1
      *PHI=PHI(K)
      A=-PRZ(K)-T*(ROZ(K)-ROZ(K))
      B=-RPH(K)-T*(ROPH(K)-ROPH(K))
      C=ROD(K)-RA(K)
      D=-ROR(K)-RZ(K)
      E=-ROBP(K)-ROBP(K)
      OTOT(J,K)=A/C
      OTOPH(J,K)=B/C
      OTOR(K)=D/C
      ACT(K)=D/C
      ACT(K)=E/C
      R=COT(A*(K))
      X=PS*(PHI)
      Y=-R*COS(PHI)
2
      CONTINUE
1
      CONTINUE
      RETURN
      END
      GEOM1 2
      GEOM1 2
      GEOM1 2
      GEOM1 3
      GEOM1 4
      GEOM1 5
      GEOM1 6
      GEOM1 7
      GEOM1 8
      GEOM1 9
      GEOM1 10
      GEOM1 11
      GEOM1 12
      GEOM1 13
      GEOM1 14
      GEOM1 15
      GEOM1 16
      GEOM1 17
      GEOM1 18
      GEOM1 19
      GEOM1 20
      GEOM1 21
      GEOM1 22
      GEOM1 23
      GEOM1 24
      GEOM1 25
      GEOM1 26
      GEOM1 27
      GEOM1 28
      GEOM1 29
      GEOM1 30
      GEOM1 31
      GEOM1 32
      SUBROUTINE GEOM2(K3)
      COMMON /IDVAR/RK,ETA(41),PHIP(41),DTIL(41),NTILE(41),DETA,TP(24)
      LEVEL 2, PNO,P,PU,V,ROD,ROZ,VINF,VINF,ROBP4,R0,R97,RBPH,DTOP4,
      * ACT,DTOT,OTDR,ACT,ICNST,GAM,CONST,NREGON,RS,RS7,RSPHI,RS7,RS7T,
      * RSPHIT
      COMMON /PVARS/ RHO(24,41), P(24,41), U(24,41), V(24,41), W(24,41),
      * ROR(41), * ROZ(41), * VINF(41), * VINF(41),
      * RORPH(41), * RB(41), * RZ(41), * RBPH(41),
      * DTOPH(24,41), ACT(41), DTOT(24,41),DTOR(41), ACT(41),
      * ICNST(50), GAM(20), CONST(50), NREGON, RS(41),
      * RS7(41), * RSPHI(41), * RS7T(41), * RSPHIT(41)
      COMMON /SVAR8/T,Z, * PHI, * DT, * DZ, * DPHI, * ZMT, *
      * ZENO, * PI, * ALPHA, * GAMMA, * SIGMA, * XFACH, * TAPE1,
      * TAPE2, * DISK1, * ALPH, * DISK2, * SIG, * NPHNT, * DZOT,
      * DTOPH, * ZM, * TWD, * TMLD, * TWM, * TML, * TTM,
      * TTL, * RZ, * RZ, * NIPHI, * MIT, * KPHI, * NITER,
      * NPHI, * NPHI1, * NPHI2, * NPHI3, * NPHM1, * NPHM2, * NPHM3,
      * NT, * NT1, * NT2, * NT3, * PHIF, * MONE, * RADT,
      * PHIF, * METHOD, * LAG, * NSC, * PINF, * RHOIN, * UINF,
      * OINF, * GASCOM, * NREAL, * NPUNCH
      DO 1 K=1,NPHI2
      PHI=PHI(K)
      GO TO (3,2),K3
2
      CONTINUE
      ROR(K)=OS(K)
      ROZ(K)=RSZ(K)
      RORPH(K)=RSPHIT(K)
      GO TO 4
3
      CONTINUE
      ROR(K)=RST(K)
      ROZ(K)=RSZT(K)
      ROBP(K)=RSPHIT(K)
      GEOM2 2
      GEOM2 2
      GEOM2 2
      GEOM2 3
      GEOM2 4
      GEOM2 5
      GEOM2 6
      GEOM2 7
      GEOM2 8
      GEOM2 9
      GEOM2 10
      GEOM2 11
      GEOM2 12
      GEOM2 13
      GEOM2 14
      GEOM2 15
      GEOM2 16
      GEOM2 17

```

```

4 CONTINUE
1 CONTINUE
RETURN
END
GEOM2 18
GEOM2 19
GEOM2 20
GEOM2 21

SUBROUTINE GEOM3(K7,PHI,MPHI,Z,RB,R7,RP4,IPRNT)
COMMON/JOE/ZL1,CF1,CF2,ZLF,ZTRAN,DZTRAN
COMMON/TRANSF/AMACH,GAMF,KM2,PLINF,PIINF,V1INF,P9L(20,3),
* RH90(20,3),U90(20,3),V90(20,3),W90(20,3),R590(3),
* PSZ90(3),RSPH90(3),HRO,R90,XINIT
LEVEL ? , P9,RBPH,RBZ
DIMENSION R(41),RPH(41),PRZ(41),PHIF(41)
DIMENSION ZSTA(200),DRDZ(200),PZ(200)
C
C.....CONSTANTS
C
TF(K7,NE,1) GO TO 1
CF2=1.5
AMG=9.5
NST=1
M=HRD
RHOSE=1.
CALL GEOMIRHOSE,AMG,RZ,DRDZ,ZSTA,H,R90,MMAY)
MMAY1=MMAY-1
RETURN
C
C.....FIND CORRECT Z INTERVAL
C
1 CONTINUE
N=NST
TF (7,LT,ZSTA(NST)) GO TO 22
DO 18 N=NST,MMAY1
TF (7,LT,ZSTA(N+1)) GO TO 20
19 CONTINUE
N=MMAY1
20 CONTINUE
22 CONTINUE
* QDDY=PZ(N)+(RZ(N+1)-RZ(N))/(ZSTA(N+1)-ZSTA(N))*(7-ZSTA(N))
* QDDY7=DRDZ(N)+(DRDZ(N+1)-DRDZ(N))/(ZSTA(N+1)-ZSTA(N))*(7-ZSTA(N))
RRODP4=0.0
DO 30 K=3,MPHI
R(K)=QDDY
RPH(K)=RRODPH
RPH(K)=RRODPY
30 CONTINUE
DO 36 K=1,2
M=K
I=MPHI+K
N=MPHI-K
R(K)=R(I)
R(I)=R(N)
R(K)=R(I)
R(I)=R(N)
RPH(K)=RPH(I)
RPH(I)=RPH(N)
RPH(K)=RPH(I)
RPH(I)=RPH(N)
36 CONTINUE
RETURN
END
GEOM3 2
JTE 2
TRANSF 2
TRANSF 3
TRANSF 4
GEOM3 5
GEOM3 6
GEOM3 7
GEOM3 8
GEOM3 9
GEOM3 10
GEOM3 11
GEOM3 12
GEOM3 13
GEOM3 14
GEOM3 15
GEOM3 16
GEOM3 17
GEOM3 18
GEOM3 19
GEOM3 20
GEOM3 21
GEOM3 22
GEOM3 23
GEOM3 24
GEOM3 25
GEOM3 26
GEOM3 27
GEOM3 28
GEOM3 29
GEOM3 30
GEOM3 31
GEOM3 32
GEOM3 33
GEOM3 34
GEOM3 35
GEOM3 36
GEOM3 37
GEOM3 38
GEOM3 39
GEOM3 40
GEOM3 41
GEOM3 42
GEOM3 43
GEOM3 44
GEOM3 45
GEOM3 46
GEOM3 47
GEOM3 48
GEOM3 49
GEOM3 50
GEOM3 51
GEOM3 52
GEOM3 53

```

```

SUBROUTINE INITA
COMMON/CLUSTER/J,XI(24),YXI(24),XIT(24)
COMMON/ENTR/N(541),Z0S,ZFLO,ITPRTS,ITPRTF,MCASE,NTOSOS
COMMON /DVARB/ARK,ETA(41),PHIF(41),DTILE(41),DTILE(41),DETA,TP(24)
COMMON/JOE/ZL1,CF1,CF2,ZLF,ZTRAN,DZTRAN
LEVEL ? , RHO,P9,U90,V90,W90,RBZ,VINF,VTNF,RORPH4,R8,R97,RP4,OTDP4,
* RCT,NTZ,DTDR,ACT,ICONST,GAM,CONST,MREGON,R5,R57,PSPHI,RST,PSZT,
* RSPHT
COMMON /PVARR/ RHO(24,41), PEZ4(41), U(24,41), V(24,41), W(24,41),
* RPH(41), RBZ(41), VINF(41), VINF(41),
* RORPH(41), R(41), R8(41), R97(41), RPH(41),
* DTOPH(24,41), BCT(41), DTDZ(24,41), DTOR(41), ACT(41),
* ICONST(SO), GAM(20), CONST(SO), MREGON, RS(41),
* RST(41), RSPHI(41), RST(41), RST(41), RSPHT(41)
COMMON/SVARR/IZ, PHI, DT, OZ, DPHI, ZIMT,
* ZEND, PI
INITA 2
CLUSTR 2
ENTRO 2
INVARB ?
JOE ?
PVARR 3
PVARR 3
PVARR 4
PVARR 5
PVARR 6
PVARR 7
PVARR 8
PVARR 9
PVARR 10
PVARR 10
SVARR 2
SVARR 3

```

```

* TAPE2 , DISK1 , ALPH , DISK2 , SIGN , NPPMT , DZOT ,
* DZOPH , ZN , THWD , THLD , TRW , TML , TTHW ,
* TTL , RZ , BZ , NIPHI , NIT , KPHI , NITER ,
* NPHI , NPHI1 , NPHI2 , NPHI3 , NPHI4 , NPHI5 , NPHI6 , NPHI7 ,
* NT , NT1 , NT2 , NT3 , PHIFD , NCON , RADT ,
* PHIF , METHOD , LAG , MRC , PTNC , RHOIN , UINF ,
* QINF,GASCON,MREAL,NPUNCH
COMMON /TRANSF/ AMACH,GAMF,KM2,PLINF,PIINF,V1INF,P90(20,3),
* RH90(20,3),U90(20,3),V90(20,3),W90(20,3),R590(3),
* PSZ90(3),RSPH90(3),HRO,R90,XINIT
* P5790(3),RSPH90(3),HRO,R90,XINIT
RADI=57.29578
* P3=14159265
* INT=XINIT
* P7MT
ZEND=ZLF
ALPHA=J.O
NIPHI=?
NIT=KMZ
YMACH=AMACH
GAMMA=GAMF
ALPH=ALPHA/RADI
SIGMA=SICMA/RADI
PHIF=PI,*/RADI
NPHI=NPHI+3
NPHI1=NPHI+1
NPHI2=NPHI+2
NPHI1=NPHI-1
NPHI2=NPHI-2
NT=NT+2
NT1=NT+1
NT2=NT+2
ICNST(1)=1
ICNST(101)=1
TPNT=ICNST(4)
IF (ICNST(48),NE,1) ICNST(5)=0
LAG=1
DETA=PHIF/FLJAT(NTPHI)
RPHI=DETA
DT=1./FLOAT(NT-1)
RZ=OTPH*DT
OTDPH=DT/DETA
GAM(1)=(GAMMA-1.0)*0.5
GAM(2)=GAM(1)*GAMMA
C..MERIDIONAL CLUSTERING
PHIF=J.O
PK=0.7
PJ=0.3
TF(RK,EO,0,0) GO TO 15
YQ=0.5/RK*ALOG((1.0)+(EXP(RK)-1.0)*PHIF/1*G.O1)
* ((1.0-(1.0-EXP(-RK))*PHIFD/103.01)
* YQ=YQ/(RK*PHIFD/RADI)
15 CONTINUE
DO 35 IT=2,MPHI1
ZI=IT-3
ETA(IT)=ZT*DETA
TF(RK,GT,0,0) GO TO 43
PHIF(IT)=ETA(IT)
DTILE(IT)=1.0
DTILE(IT)=DT*G
DTILE(IT)=DT*G
GO TO 35
CONTINUE
Y3=RK*(ETA(IT)/PI-YC)
SMETA=STNH(Y3)
PHETA=COSH(Y3)
PHIF(IT)=PHIFD/RADI*(1.0+SMETA/Y3)
DTILE(IT)=Y3*PHETA/CHETA
DTILE(IT)=Y3*PHETA/CHETA**2
CONTINUE
PHIF(2)=PHIF(4)
PHI(NPHI1)=PHI(NPHI1)
DTILE(2)=DTILE(4)
DTILE(NPHI1)=DTILE(NPHI1)
DTILE(2)=DTILE(4)
DTILE(NPHI1)=DTILE(NPHI1)
DTILE(3)=G
DTILE(NPHI1)=G
C..RADIAL CLUSTERING
SINH=SIMH(RJ)
DO 36 IT=1,NTZ
ZT=IT-5
TP(IT)=ZT*OT
IF(RJ,EO,0,0) GO TO 41
DT=RJ*TP(IT)

```



```

16 10000 73
17 10000 74
18 10000 75
19 10000 76
20 10000 77
21 10000 78
22 10000 79
23 10000 80
24 10000 81
25 10000 82
26 10000 83
27 10000 84
28 10000 85
29 10000 86
30 10000 87
31 10000 88
32 10000 89
33 10000 90
34 10000 91
35 10000 92
36 10000 93
37 10000 94
38 10000 95
39 10000 96
40 10000 97
41 10000 98
42 10000 99
43 10000 100
44 10000 101
45 10000 102
46 10000 103
47 10000 104
48 10000 105
49 10000 106
50 10000 107
51 10000 108
52 10000 109
53 10000 110
54 10000 111
55 10000 112
56 10000 113
57 10000 114
58 10000 115
59 10000 116
60 10000 117
61 10000 118
62 10000 119
63 10000 120
64 10000 121
65 10000 122
66 10000 123
67 10000 124
68 10000 125

```

```

FACT=0.5*YFACH*XMACH*(GAMMA-1.0)
FACD=(FACT+1.0)*((1.0/(GAMMA-1.0))
FACV=SQRT((FACT+1.0)/FACT)
MZADD=M*ADD*1
K7=M*END*7*ADD
ZC=M
WRITE(6,60) MZADD,ZC,R(3),R3(3)
DRSDX(K7)=R3(3)
WRITE(9) MZADD,Z,DRSDX(K7)
DO 20 J=3,NTZ
  Y=X(I,J)
  Y=Y*(Z**3)-R(3)+R3(3)
  JZ=J-2
  VC(I,J,KZ)=Z
  VC(I,J,K7)=Y
  VY(J,KZ)=U(I,J)*FACV
  VY(J,K7)=V(I,J)*FACV
  RHOF(J,KZ)=RHOF(J,3)*FACD
  WRITE(9) J,V,VC(I,J,KZ),VY(J,KZ),RHOF(J,K7)
20 CONTINUE
RETURN
6.7. FORMAT(2X,I3,3(10X,F10.4))
END

```

```

SUBROUTINE OUTPTH
COMMON/CLUSTER/PJ,YI(24),XII(24),XIII(24)
COMMON /RHS TRM/ ZPLDT,MFEND,MFADD,MFPLMT
COMMON /FVARA/RK,ETA(41),PHI(41),DTIL(41),DTILE(41),DETA,TP(24)
LEVEL 2, 940,P,U,V,W,RDR,DRZ,VINC,VINC,RDRPH,R,RZ,RDRP,OTDPH,
* RCT,OTDT,OTDR,ACT,ICNST,GAM,CONST,NREGON,R5,RSZ,RSPI,OST,PSY,
* RSPHT
COMMON /PVARA/ RMO(24,41), P(24,41), U(24,41), V(24,41), W(24,41),
* DR(41) , DR7(41) , VINF(41) , VINF(41) ,
* DRPH(41) , DR(41) , R7(41) , RPH(41) ,
* YTH(24,41) , RCT(41) , OTZ(24,41),OTDR(41) , ACT(41) ,
* ICNST(50) , GAM(20) , NREGON , RS(41) ,
* RST(41) , RSPHT(41) , RST(41) , RST(41) , RSPHT(41)
COMMON /SHOCKS/ DRSDX(103),NST(53)
COMMON/SVARA/Z, Z , PHI , DT , NZ , DPHI , ZTNT ,
* ZEND , PT , ALPHA , GAMMA , SIGMA , XNACH , TAPE1 ,
* TAPE2 , DISK1 , ALPH , DISK2 , SIGM , NPHRT , DTDT ,
* DZDPH , ZH , THWD , TMLD , TMW , TML , TTMW ,
* TTM , RZ , RZ , NIPHI , NIT , NPHI , NITER ,
* NPHI , NPH1 , NPH2 , NPH3 , NPH4 , NPH5 , NPH6 ,
* NT , NTL , NT2 , NT3 , NTHZ , NCONE , RADT ,
* NPHI , METHODD , LAG , NRC , NINC , RMOIN , UTMF ,
* NINF , GASCON , NREAL , NPUNCH
COMMON /FLOW/ VC(20,100),V(20,100),VF(20,100),RHOF(20,100)
LEVEL 7, VX,VY
COMMON/VCONP/ VX(20,100),VY(20,100)
OUTPTH 2
CLUSTP 2
DRSTPH 2
TVARA 2
PVARA 3
SVARA 4
PVARA 5
PVARA 6
PVARA 7
PVARA 8
PVARA 9
PVARA 10
PVARA 11
PVARA 12
PVARA 13
PVARA 14
PVARA 15
PVARA 16
PVARA 17
PVARA 18
PVARA 19
PVARA 20
PVARA 21
PVARA 22
PVARA 23
PVARA 24
PVARA 25
PVARA 26
PVARA 27
PVARA 28
PVARA 29
PVARA 30
PVARA 31
PVARA 32
PVARA 33
PVARA 34
PVARA 35
PVARA 36
PVARA 37
PVARA 38
PVARA 39
PVARA 40
PVARA 41
PVARA 42
PVARA 43
PVARA 44
PVARA 45
PVARA 46
PVARA 47
PVARA 48
PVARA 49
PVARA 50
PVARA 51
PVARA 52
PVARA 53
PVARA 54
PVARA 55
PVARA 56
PVARA 57
PVARA 58
PVARA 59
PVARA 60
PVARA 61
PVARA 62
PVARA 63
PVARA 64
PVARA 65
PVARA 66
PVARA 67
PVARA 68
PVARA 69
PVARA 70
PVARA 71
PVARA 72
PVARA 73
PVARA 74
PVARA 75
PVARA 76
PVARA 77
PVARA 78
PVARA 79
PVARA 80
PVARA 81
PVARA 82
PVARA 83
PVARA 84
PVARA 85
PVARA 86
PVARA 87
PVARA 88
PVARA 89
PVARA 90
PVARA 91
PVARA 92
PVARA 93
PVARA 94
PVARA 95
PVARA 96
PVARA 97
PVARA 98
PVARA 99
PVARA 100
PVARA 101
PVARA 102
PVARA 103
PVARA 104
PVARA 105
PVARA 106
PVARA 107
PVARA 108
PVARA 109
PVARA 110
PVARA 111
PVARA 112
PVARA 113
PVARA 114
PVARA 115
PVARA 116
PVARA 117
PVARA 118
PVARA 119
PVARA 120
PVARA 121
PVARA 122
PVARA 123
PVARA 124
PVARA 125
PVARA 126
PVARA 127
PVARA 128
PVARA 129
PVARA 130
PVARA 131
PVARA 132
PVARA 133
PVARA 134
PVARA 135
PVARA 136
PVARA 137
PVARA 138
PVARA 139
PVARA 140
PVARA 141
PVARA 142
PVARA 143
PVARA 144
PVARA 145
PVARA 146
PVARA 147
PVARA 148
PVARA 149
PVARA 150
PVARA 151
PVARA 152
PVARA 153
PVARA 154
PVARA 155
PVARA 156
PVARA 157
PVARA 158
PVARA 159
PVARA 160
PVARA 161
PVARA 162
PVARA 163
PVARA 164
PVARA 165
PVARA 166
PVARA 167
PVARA 168
PVARA 169
PVARA 170
PVARA 171
PVARA 172
PVARA 173
PVARA 174
PVARA 175
PVARA 176
PVARA 177
PVARA 178
PVARA 179
PVARA 180
PVARA 181
PVARA 182
PVARA 183
PVARA 184
PVARA 185
PVARA 186
PVARA 187
PVARA 188
PVARA 189
PVARA 190
PVARA 191
PVARA 192
PVARA 193
PVARA 194
PVARA 195
PVARA 196
PVARA 197
PVARA 198
PVARA 199
PVARA 200
PVARA 201
PVARA 202
PVARA 203
PVARA 204
PVARA 205
PVARA 206
PVARA 207
PVARA 208
PVARA 209
PVARA 210
PVARA 211
PVARA 212
PVARA 213
PVARA 214
PVARA 215
PVARA 216
PVARA 217
PVARA 218
PVARA 219
PVARA 220
PVARA 221
PVARA 222
PVARA 223
PVARA 224
PVARA 225
PVARA 226
PVARA 227
PVARA 228
PVARA 229
PVARA 230
PVARA 231
PVARA 232
PVARA 233
PVARA 234
PVARA 235
PVARA 236
PVARA 237
PVARA 238
PVARA 239
PVARA 240
PVARA 241
PVARA 242
PVARA 243
PVARA 244
PVARA 245
PVARA 246
PVARA 247
PVARA 248
PVARA 249
PVARA 250
PVARA 251
PVARA 252
PVARA 253
PVARA 254
PVARA 255
PVARA 256
PVARA 257
PVARA 258
PVARA 259
PVARA 260
PVARA 261
PVARA 262
PVARA 263
PVARA 264
PVARA 265
PVARA 266
PVARA 267
PVARA 268
PVARA 269
PVARA 270
PVARA 271
PVARA 272
PVARA 273
PVARA 274
PVARA 275
PVARA 276
PVARA 277
PVARA 278
PVARA 279
PVARA 280
PVARA 281
PVARA 282
PVARA 283
PVARA 284
PVARA 285
PVARA 286
PVARA 287
PVARA 288
PVARA 289
PVARA 290
PVARA 291
PVARA 292
PVARA 293
PVARA 294
PVARA 295
PVARA 296
PVARA 297
PVARA 298
PVARA 299
PVARA 300

```

```

SUBROUTINE PHTUPH(M1,ONU,P201,MITS,GAMMA)
REAL M1,M2,M
XNU(M) = ATAN(SQRT(COS(M)-1.)) / SQRT(-ATAN(SQRT(COS(M)-1.))
XNU(M) = SQRT(M-1.)/(1.+(G-1.)/2.+(M-1.))
C=GAMMA
C = (C-1.)/(G+1.)
SOPTC = SOPT(C)
CPC = 3.14159
XNU1 = XNU(M)
XNU2 = XNU1*DNH
M = M
M1 = M1*20
MITS = 1
M2 = M - (XNU1(M)-XNU2)/XNU1(M)
TE (M) ,GT, 100.0) GO TO 20
TE (M) ,LT, EPS) GO TO 30
M = M
2 CONTINUE
M2 = 100.0
WRITE(6,11)
30 CONTINUE
P201 = ((1.-(G-1.)/2.+(M1-1.)/(1.+(G-1.)/2.+(M2-1.)))/(G+(G-1.))
RETURN
1 FORMAT(10X,47H - - - ADDY TURN STOPPED AT M2 = 100.0 - - -)
END
OUTPTH 2
SHOCKM 2
CVARA 2
CVARA 3
CVARA 4
CVARA 5
CVARA 6
CVARA 7
CVARA 8
CVARA 9
CVARA 10
CVARA 11
CVARA 12
CVARA 13
CVARA 14
CVARA 15
CVARA 16
CVARA 17
CVARA 18
CVARA 19
CVARA 20
CVARA 21
CVARA 22
CVARA 23
CVARA 24
CVARA 25
CVARA 26
CVARA 27
CVARA 28
CVARA 29
CVARA 30
CVARA 31
CVARA 32
CVARA 33
CVARA 34
CVARA 35
CVARA 36
CVARA 37
CVARA 38
CVARA 39
CVARA 40
CVARA 41
CVARA 42
CVARA 43
CVARA 44
CVARA 45
CVARA 46
CVARA 47
CVARA 48
CVARA 49
CVARA 50
CVARA 51
CVARA 52
CVARA 53
CVARA 54
CVARA 55
CVARA 56
CVARA 57
CVARA 58
CVARA 59
CVARA 60
CVARA 61
CVARA 62
CVARA 63
CVARA 64
CVARA 65
CVARA 66
CVARA 67
CVARA 68
CVARA 69
CVARA 70
CVARA 71
CVARA 72
CVARA 73
CVARA 74
CVARA 75
CVARA 76
CVARA 77
CVARA 78
CVARA 79
CVARA 80
CVARA 81
CVARA 82
CVARA 83
CVARA 84
CVARA 85
CVARA 86
CVARA 87
CVARA 88
CVARA 89
CVARA 90
CVARA 91
CVARA 92
CVARA 93
CVARA 94
CVARA 95
CVARA 96
CVARA 97
CVARA 98
CVARA 99
CVARA 100
CVARA 101
CVARA 102
CVARA 103
CVARA 104
CVARA 105
CVARA 106
CVARA 107
CVARA 108
CVARA 109
CVARA 110
CVARA 111
CVARA 112
CVARA 113
CVARA 114
CVARA 115
CVARA 116
CVARA 117
CVARA 118
CVARA 119
CVARA 120
CVARA 121
CVARA 122
CVARA 123
CVARA 124
CVARA 125
CVARA 126
CVARA 127
CVARA 128
CVARA 129
CVARA 130
CVARA 131
CVARA 132
CVARA 133
CVARA 134
CVARA 135
CVARA 136
CVARA 137
CVARA 138
CVARA 139
CVARA 140
CVARA 141
CVARA 142
CVARA 143
CVARA 144
CVARA 145
CVARA 146
CVARA 147
CVARA 148
CVARA 149
CVARA 150
CVARA 151
CVARA 152
CVARA 153
CVARA 154
CVARA 155
CVARA 156
CVARA 157
CVARA 158
CVARA 159
CVARA 160
CVARA 161
CVARA 162
CVARA 163
CVARA 164
CVARA 165
CVARA 166
CVARA 167
CVARA 168
CVARA 169
CVARA 170
CVARA 171
CVARA 172
CVARA 173
CVARA 174
CVARA 175
CVARA 176
CVARA 177
CVARA 178
CVARA 179
CVARA 180
CVARA 181
CVARA 182
CVARA 183
CVARA 184
CVARA 185
CVARA 186
CVARA 187
CVARA 188
CVARA 189
CVARA 190
CVARA 191
CVARA 192
CVARA 193
CVARA 194
CVARA 195
CVARA 196
CVARA 197
CVARA 198
CVARA 199
CVARA 200

```



```

DRSDZ(A,B,C,D)=UINF+C+A*SORT(D*(1.+D*B)+C*C)/D
RHOS(A)=(-GRATIO/PI+GRATIOA)
ANAP(A,B,C,D,E,F)=(-1.+ASS(-UINF+D+A-R*E)/(D*D+1.+E*E)+F)
US(A,B,C)=A-C*B
VS(A,B)=A*B
WS(A,B,C)=A-B*C
GAMM1=GAMMA+1.
GAMM2=GAMMA-1.
CPAYTO=GAMM1/GAMM1
GAMM3=GAMM1/GAMMA
C1=0.5*GAMM1*PI*INF/RHOIN
C2=0.5*GAMM1*GOC1
DO TO (1,2),K4
1
CONTINUE
C..SNOCK CORRECTOR
DO 3 K=3,NPHI
  PST(K)=PST(K)+DZ*RSZ(K)
  DO 4 K=1,2
    M=6-K
    I=NPHT+K
    N=NPHT-K
    PST(K)=PST(K)
    PST(I)=PST(I)
  4
  CONTINUE
  DO 5 K=3,NPHI
    RSPHIT(K)=(RST(K+1)-RST(K-1))/(2.0*DETA)*DTIL(K)
    PS=PINTZ,K
    PSRAT=PS/PI*INF
    UIT=UITLD(PSRAT)
    RHAT=RHOS(PSRAT)
    PS1=PST(K)
    RSPH=RSPHIT(K)
    RSPH=RSPH/RS1
    FACT1=VINFK(K)-VINFK(K)*RSPHR
    FACT2=UINF+UINF-UIT*UIT
    IF(FACT2.LT.0.)UIT=-UIT
    RST1=RSZ(UIT,RSPHR,FACT1,FACT2)
    RST1(K)=RST1
    ANART=ANAP(VINFK(K),VINFK(K),PSZ1,RSPHR,RHRAT)
    UST=US(UINF,ANART,RSZ1)
    VST=VS(VINF(K),ANART)
    WST=WS(VINF(K),ANART,RSPHR)
    IF (NREAL.EQ.0) ROST=RHRAT*RHOTIN
    RHO(INT2,K)=ROST
    WINT2,K=UST
    WINT2,K=VST
    WINT2,K=WST
  5
  CONTINUE
  DO 6 K=1,2
    M=6-K
    I=NPHT+K
    N=NPHT-K
    RST(K)=RST(K)
    RST(I)=RST(I)
  6
  CONTINUE
  RETURN
C..SNOCK CORRECTOR
DO 8 K=3,NPHI
  RST(K)=RST(K)+.5*(RSZ(K)+RSZ(K)+DZ)
  DO 9 K=1,2
    M=6-K
    I=NPHT+K
    N=NPHT-K
    RST(K)=RST(K)
    RST(I)=RST(I)
  9
  CONTINUE
  DO 10 K=3,NPHI
    RSPHIT(K)=(RST(K+1)-RST(K-1))/(2.0*DETA)*DTIL(K)
    PS=PINTZ,K
    PSRAT=PS/PI*INF
    UIT=UITLD(PSRAT)
    RHAT=RHOS(PSRAT)
    RST1=RST(K)
    RSPH=RSPHIT(K)
    RSPH=RSPH/RS1
    FACT1=VINFK(K)-VINFK(K)*RSPHR
    FACT2=UINF+UINF-UIT*UIT
    IF(FACT2.LT.0.)UIT=-UIT
    RST1=DRSDZ(UIT,RSPHR,FACT1,FACT2)
    RST(K)=RST1
    ANART=ANAP(VINFK(K),VINFK(K),PSZ1,RSPHR,RHRAT)

```

SNOCK 9
 SNOCK 10
 SNOCK 11
 SNOCK 12
 SNOCK 13
 SNOCK 14
 SNOCK 15
 SNOCK 16
 SNOCK 17
 SNOCK 18
 SNOCK 19
 SNOCK 20
 SNOCK 21
 SNOCK 22
 SNOCK 23
 SNOCK 24
 SNOCK 25
 SNOCK 26
 SNOCK 27
 SNOCK 28
 SNOCK 29
 SNOCK 30
 SNOCK 31
 SNOCK 32
 SNOCK 33
 SNOCK 34
 SNOCK 35
 SNOCK 36
 SNOCK 37
 SNOCK 38
 SNOCK 39
 SNOCK 40
 SNOCK 41
 SNOCK 42
 SNOCK 43
 SNOCK 44
 SNOCK 45
 SNOCK 46
 SNOCK 47
 SNOCK 48
 SNOCK 49
 SNOCK 50
 SNOCK 51
 SNOCK 52
 SNOCK 53
 SNOCK 54
 SNOCK 55
 SNOCK 56
 SNOCK 57
 SNOCK 58
 SNOCK 59
 SNOCK 60
 SNOCK 61
 SNOCK 62
 SNOCK 63
 SNOCK 64
 SNOCK 65
 SNOCK 66
 SNOCK 67
 SNOCK 68
 SNOCK 69
 SNOCK 70
 SNOCK 71
 SNOCK 72
 SNOCK 73
 SNOCK 74
 SNOCK 75
 SNOCK 76
 SNOCK 77
 SNOCK 78
 SNOCK 79
 SNOCK 80
 SNOCK 81
 SNOCK 82
 SNOCK 83
 SNOCK 84
 SNOCK 85
 SNOCK 86
 SNOCK 87
 SNOCK 88
 SNOCK 89
 SNOCK 90
 SNOCK 91
 SNOCK 92

```

USF=US(UINF,ANART,RSZ1)
VSF=VS(VINF(K),ANART)
WSF=WS(VINF(K),ANART,RSPHR)
IF (NREAL.EQ.0) ROSF=RHRAT*RHOTIN
RHO(INT2,K)=ROSF
WINT2,K=UST
WINT2,K=VST
WINT2,K=WST
CONTINUE
DO 11 K=1,2
  M=6-K
  I=NPHT+K
  N=NPHT-K
  RSZ(K)=RSZ(K)
  RSZ(I)=RSZ(I)
  RSPHIT(K)=RSPHIT(K)
  RSPHIT(I)=RSPHIT(I)
11
CONTINUE
RETURN
END
SUBROUTINE SETDAT
COMMON/CLUSTR/RJ,XTI(24),XTI(24),XTI(24)
LEVEL 2,ETE*P,ED*P,GO*MD
COMMON /CVARB/ ETEMP(4,24,41), E(4,24,41),
  * Q(4,24,41) , GD(4,24,41) , HD(4,24,41)
COMMON/INTD/S(41),ZBS,ZFLD,ITPR78,ITPR7F,NCASE,MTDSDS
COMMON /IDVARS/RK,ETA(41),PHI(41),DTIL(41),DTILE(41),DETA,TP(24)
COMMON/IDE/TL,CF2,CF2,ZL,FZ,TRAM,OTRAM
LEVEL 3, *H0,P,U,V,W,ROH,RORT,VINF,UTNF,RORPH,RSZ,RRPH,DTDPH,
  * BT,DTDP,OTDR,ACT,ICONST,GAM,CONST,NREGON,RS,RSZ,RSPHIT,PSZT,
  * RSPHIT
COMMON /PVARS/ RMO(24,41),PIZ(41),U(24,41),V(24,41),W(24,41),
  * ROR(41) , RORZ(41) , VINF(41) , WINF(41) ,
  * RORPH(41) , RORZ(41) , RPH(41) , RPHZ(41) , RRRPH(41) ,
  * DTDPH(24,41) , BCT(41) , DTDP(24,41) , RTDR(41) , ACT(41) ,
  * ICONST(5C) , GAM(2D) , CONST(5D) , NREGON , RS(41) ,
  * PSZ(41) , RSPHIT(41) , RST(41) , RSTZ(41) , RSPHIT(41)
COMMON/SVARS/OT,PHI,DT,DZ,DPHI,ZINT,
  * TEND , PI , ALPHA , GAMMA , SIGMA , XMAC , TAPE1 ,
  * TAPE2 , DISK1 , ALPH , DISF2 , SIGM , NPHY , DZDT ,
  * RZPHN , ZH , THUD , TMLD , TRM , TML , TTMW ,
  * TTHL , RZ , RZ , RPH1 , RPH2 , RPH3 , RPH4 , RPH5 , RPH6 ,
  * RPH7 , RPH8 , RPH9 , RPH10 , RPH11 , RPH12 , RPH13 , RPH14 , RPH15 , RPH16 ,
  * RPH17 , RPH18 , RPH19 , RPH20 , RPH21 , RPH22 , RPH23 , RPH24 ,
  * RPH25 , RPH26 , RPH27 , RPH28 , RPH29 , RPH30 , RPH31 , RPH32 , RPH33 , RPH34 ,
  * RPH35 , RPH36 , RPH37 , RPH38 , RPH39 , RPH40 , RPH41 , RPH42 , RPH43 , RPH44 , RPH45 ,
  * RPH46 , RPH47 , RPH48 , RPH49 , RPH50 , RPH51 , RPH52 , RPH53 , RPH54 , RPH55 , RPH56 ,
  * RPH57 , RPH58 , RPH59 , RPH60 , RPH61 , RPH62 , RPH63 , RPH64 , RPH65 , RPH66 , RPH67 , RPH68 , RPH69 , RPH70 ,
  * RPH71 , RPH72 , RPH73 , RPH74 , RPH75 , RPH76 , RPH77 , RPH78 , RPH79 , RPH80 , RPH81 , RPH82 , RPH83 , RPH84 , RPH85 , RPH86 , RPH87 , RPH88 , RPH89 , RPH90 ,
  * RPH91 , RPH92 , RPH93 , RPH94 , RPH95 , RPH96 , RPH97 , RPH98 , RPH99 , RPH100
*INF,GASCON,NREAL,NPUNCH
C
C
C
TTTTALISE ARRAYS
ICONST(1)=0
ICONST(2)=2
ICONST(3)=0
ICONST(4)=1
DO 1 I=5,52
  ICONST(I)=0
1
CONTINUE
MRC=1
RETHID=2
NPHIT=0
DZDT=0.0
CONTINUE
DO 2 I=1,24
  GAM(I)=0.0
2
CONTINUE
DO 3 I=1,50
  CONST(I)=0.0
3
CONTINUE
DO 4 I=1,24
  TP(I)=0.0
4
CONTINUE
DO 5 I=1,41
  OR(I)=0.0
  ROR(I)=0.0
  VINF(I)=0.0
  WINF(I)=0.0
  RORPH(I)=0.0
  RORZ(I)=0.0
  RPH(I)=0.0
  RPHZ(I)=0.0
  RRRPH(I)=0.0

```

SNOCK 98
 SNOCK 99
 SNOCK 100
 SNOCK 101
 SNOCK 102
 SNOCK 103
 SNOCK 104
 SNOCK 105
 SNOCK 106
 SNOCK 107
 SNOCK 108
 SNOCK 109
 SNOCK 110
 SNOCK 111
 SNOCK 112

SETDAT 2
 CLUSTR 2
 CVARB 2
 CVARB 3
 CVARB 4
 ENTRD 2
 IDVARS 2
 JOE 2
 PVARS 2
 PVARS 3
 PVARS 4
 PVARS 5
 PVARS 6
 PVARS 7
 PVARS 8
 PVARS 9
 PVARS 10
 SVARS 2
 SVARS 3
 SVARS 4
 SVARS 5
 SVARS 6
 SVARS 7
 SVARS 8
 SVARS 9
 SVARS 10
 SETDAT 10
 SETDAT 11
 SETDAT 12
 SETDAT 13
 SETDAT 14
 SETDAT 15
 SETDAT 16
 SETDAT 17
 SETDAT 18
 SETDAT 19
 SETDAT 20
 SETDAT 21
 SETDAT 22
 SETDAT 23
 SETDAT 24
 SETDAT 25
 SETDAT 26
 SETDAT 27
 SETDAT 28
 SETDAT 29
 SETDAT 30
 SETDAT 31
 SETDAT 32
 SETDAT 33
 SETDAT 34
 SETDAT 35
 SETDAT 36
 SETDAT 37
 SETDAT 38
 SETDAT 39
 SETDAT 40
 SETDAT 41
 SETDAT 42

```

ACT(I)=0.0
DTR(I)=0.0
ACT(I)=0.0
RS(I)=0.0
RSZ(I)=0.0
*SPHT(I)=0.0
RST(I)=0.0
RST(I)=0.0
RSPHT(I)=0.0
ETA(I)=0.0
PHI(I)=0.0
DTIL(I)=0.0
DTILE(I)=0.0
DO 11 J=1,24
RMD(J,T)=0.0
R(J,I)=0.0
U(J,T)=0.0
V(J,T)=0.0
W(J,I)=0.0
DTOPH(J,I)=0.0
DTDZ(J,I)=0.0
11 CONTINUE
RETURN
END

```

```

SETDAT 43
SETDAT 44
SETDAT 45
SETDAT 46
SETDAT 47
SETDAT 48
SETDAT 49
SETDAT 50
SETDAT 51
SETDAT 52
SETDAT 53
SETDAT 54
SETDAT 55
SETDAT 56
SETDAT 57
SETDAT 58
SETDAT 59
SETDAT 60
SETDAT 61
SETDAT 62
SETDAT 63
SETDAT 64
SETDAT 65
SETDAT 66

```

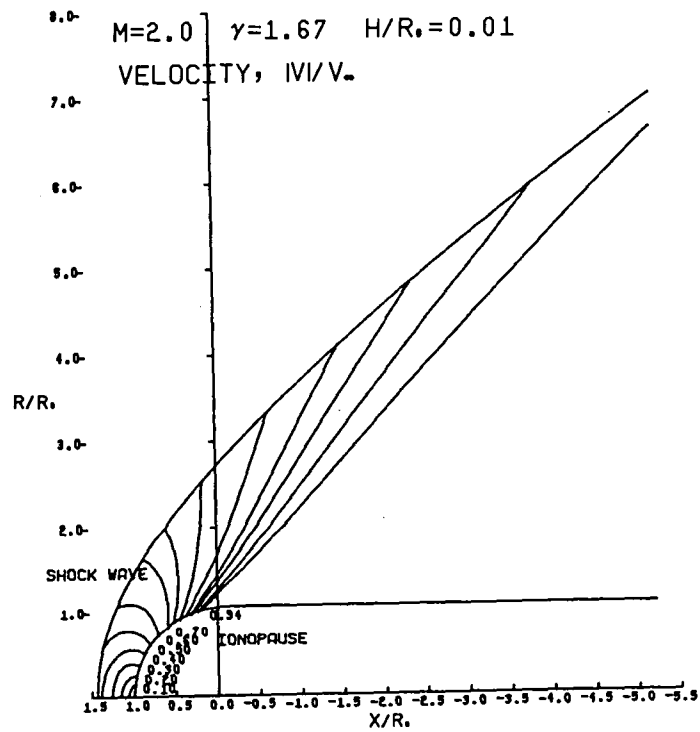
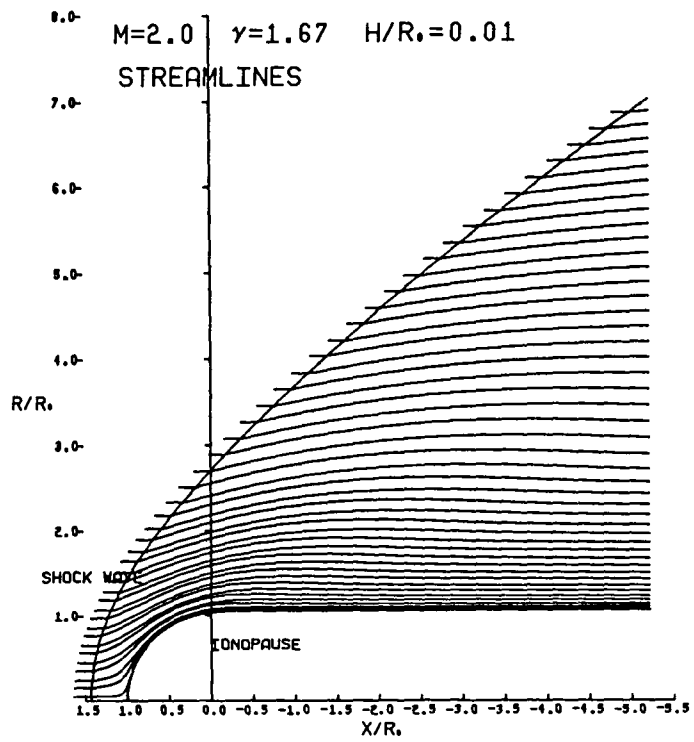
This Page Intentionally Left Blank

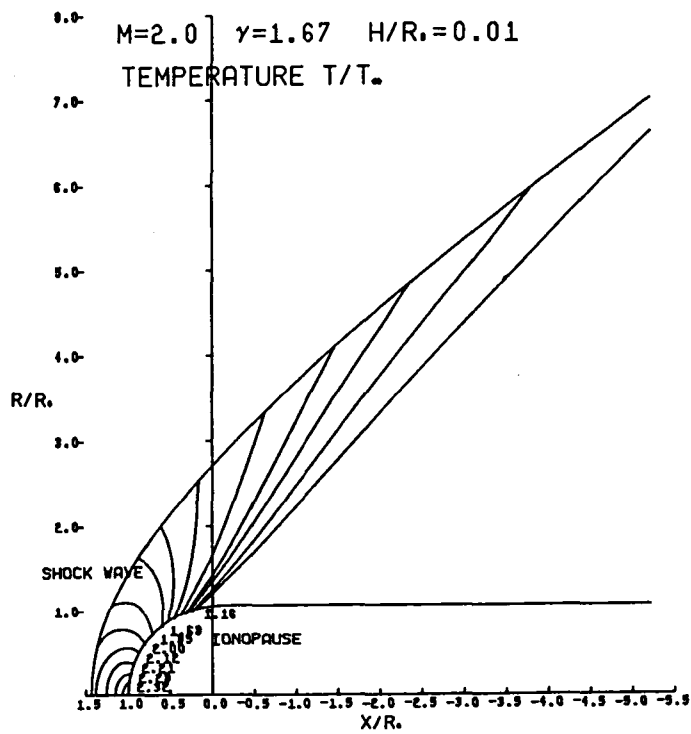
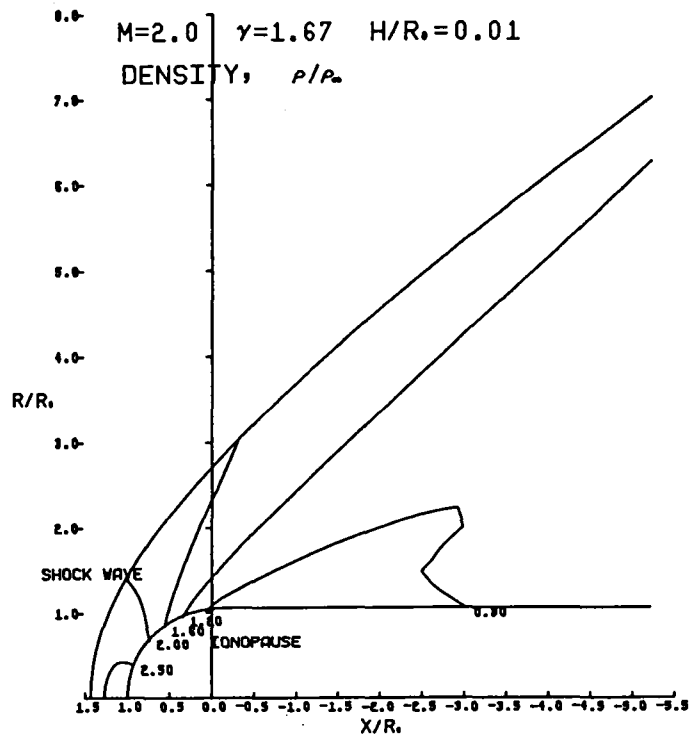
APPENDIX C

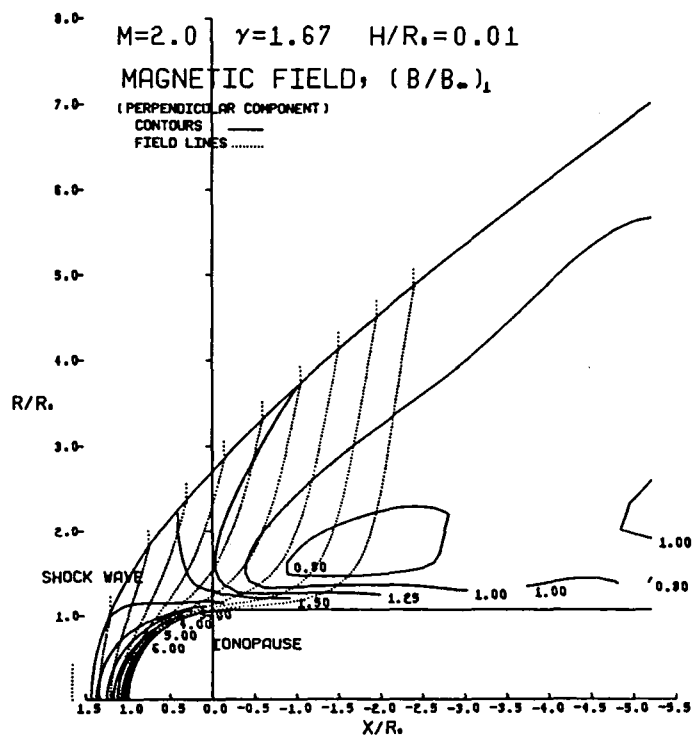
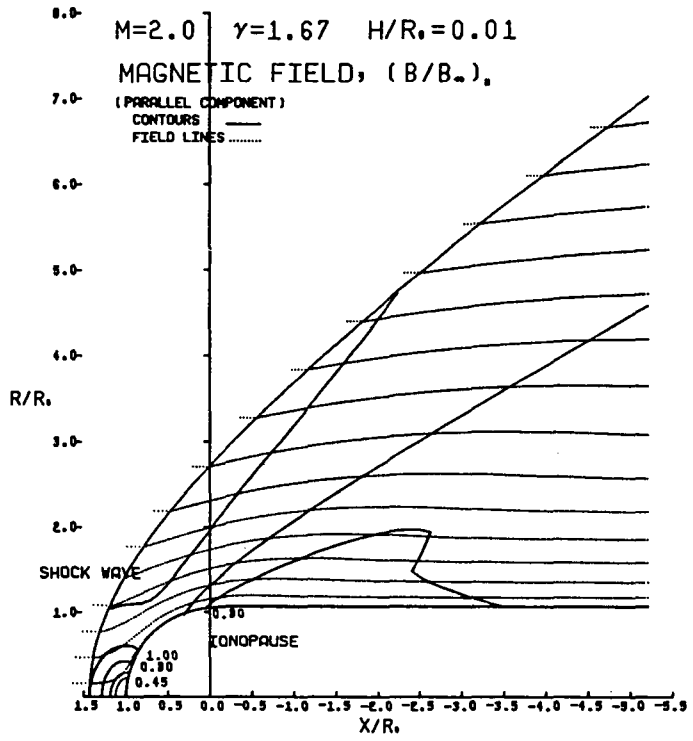
CATALOG OF TEST CASES

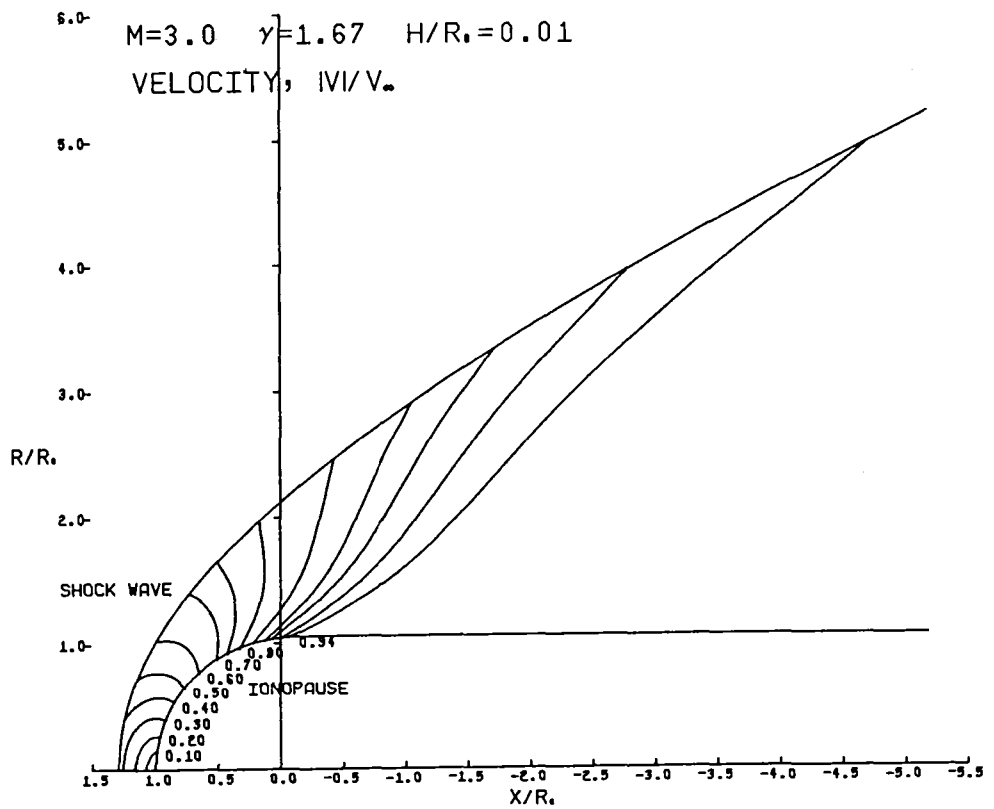
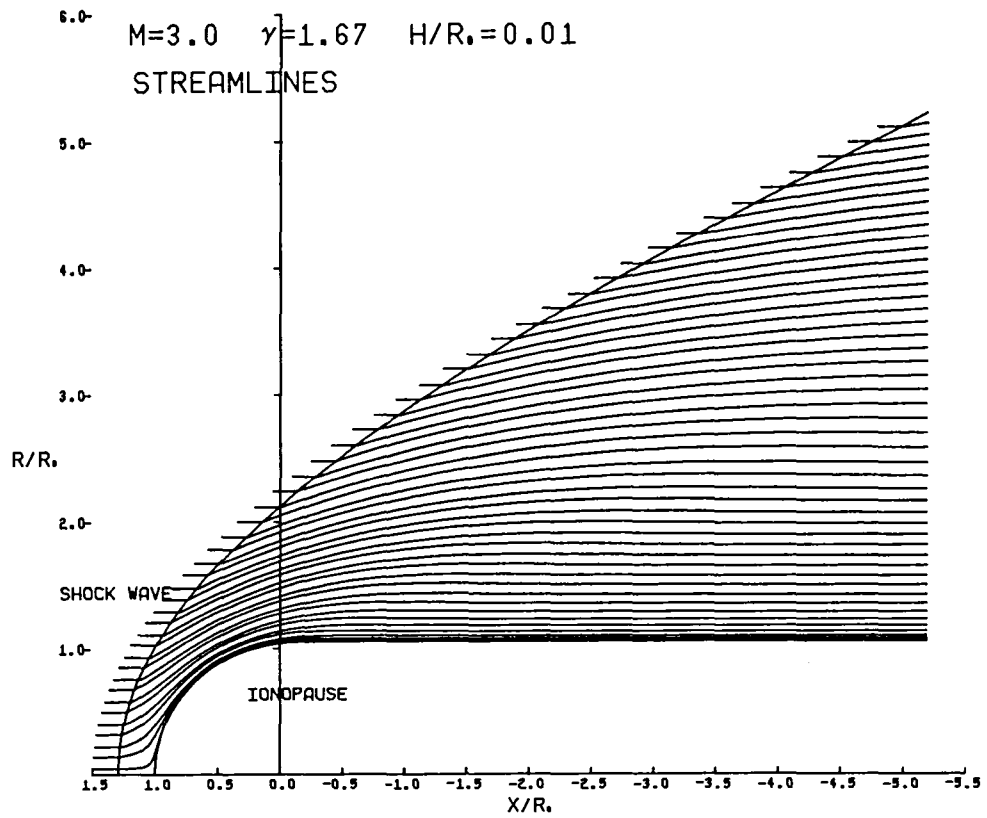
Catalog page number index for plasma streamline, velocity magnitude, density, temperature, and unit magnetic-field maps for various solar-wind flows past planetary ionopauses

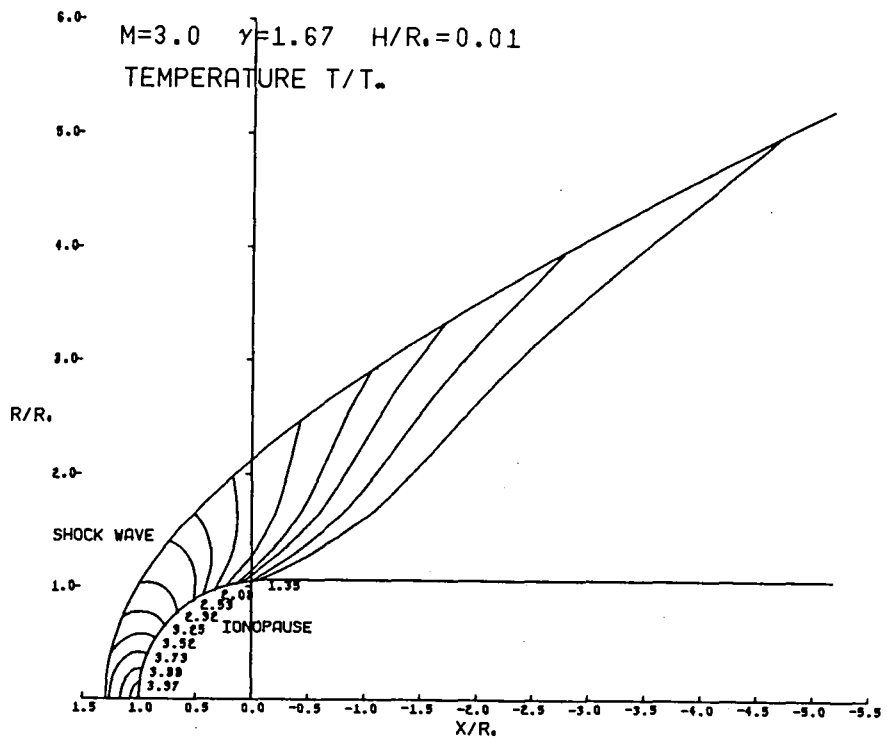
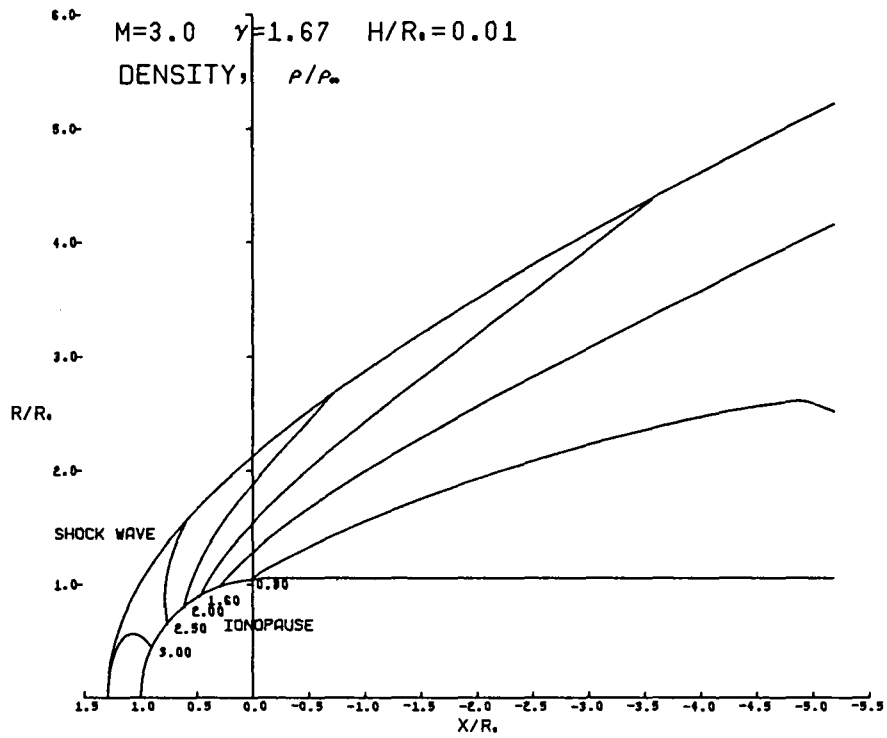
H/R_{\odot}	M_{∞}	γ	(Page No.) Streamlines	(Page No.) Velocity magnitude $ v /v_{\infty}$	(Page No.) Density ρ/ρ_{∞}	(Page No.) Temperature T/T_{∞}	(Page No.) Parallel magnetic field $(B /B_{\infty})_{\parallel}$	(Page No.) Perpendicular magnetic field $(B /B_{\infty})_{\perp}$	
.01 ↓ ↓ ↓ ↓ ↓ ↓ ↓ ↓ ↓ ↓ ↓ ↓ ↓ ↓ ↓	2.0	5/3 ↓ ↓ ↓ ↓ ↓ ↓ ↓ ↓ ↓ ↓ ↓ ↓ ↓ ↓ ↓	179	179	180	180	181	181	
	3.0		182	182	183	183	184	184	
	5.0		185	185	186	186	187	187	
	8.0		188	188	189	189	190	190	
	12.0		191	191	192	192	193	193	
	25.0		194	194	195	195	196	196	
	.10		2.0	197	197	198	198	199	199
			3.0	200	200	201	201	202	202
			5.0	203	203	204	204	205	205
	8.0		206	206	207	207	208	208	208
			12.0	209	209	210	210	211	211
			25.0	212	212	213	213	214	214
	.25		2.0	215	215	216	216	217	217
			3.0	218	218	219	219	220	220
			5.0	221	221	222	222	223	223
8.0		224	224	225	225	226	226		
12.0		227	227	228	228	229	229		
25.0	230	230	231	231	232	232			
\bar{H}/R_{\odot}	M_{∞}	γ	Streamlines	$ v /v_{\infty}$	ρ/ρ_{∞}	T/T_{∞}	$(B /B_{\infty})_{\parallel}$	$(B /B_{\infty})_{\perp}$	
.10 ↓ ↓ ↓ ↓ ↓ ↓ ↓ ↓ ↓ ↓ ↓ ↓ ↓ ↓ ↓	2.0	5/3 ↓ ↓ ↓ ↓ ↓ ↓ ↓ ↓ ↓ ↓ ↓ ↓ ↓ ↓ ↓	233	233	234	234	235	235	
	3.0		236	236	237	237	238	238	
	5.0		239	239	240	240	241	241	
	8.0		242	242	243	243	244	244	
	12.0		245	245	246	246	247	247	
	25.0		248	248	249	249	250	250	
	.20		2.0	251	251	252	252	253	253
			3.0	254	254	255	255	256	256
			5.0	257	257	258	258	259	259
	8.0		260	260	261	261	262	262	262
			12.0	263	263	264	264	265	265
			25.0	266	266	267	267	268	268
	.25		2.0	269	269	270	270	271	271
			3.0	272	272	273	273	274	274
			5.0	275	275	276	276	277	277
8.0		278	278	279	279	280	280		
12.0		281	281	282	282	283	283		
25.0	284	284	285	285	286	286			

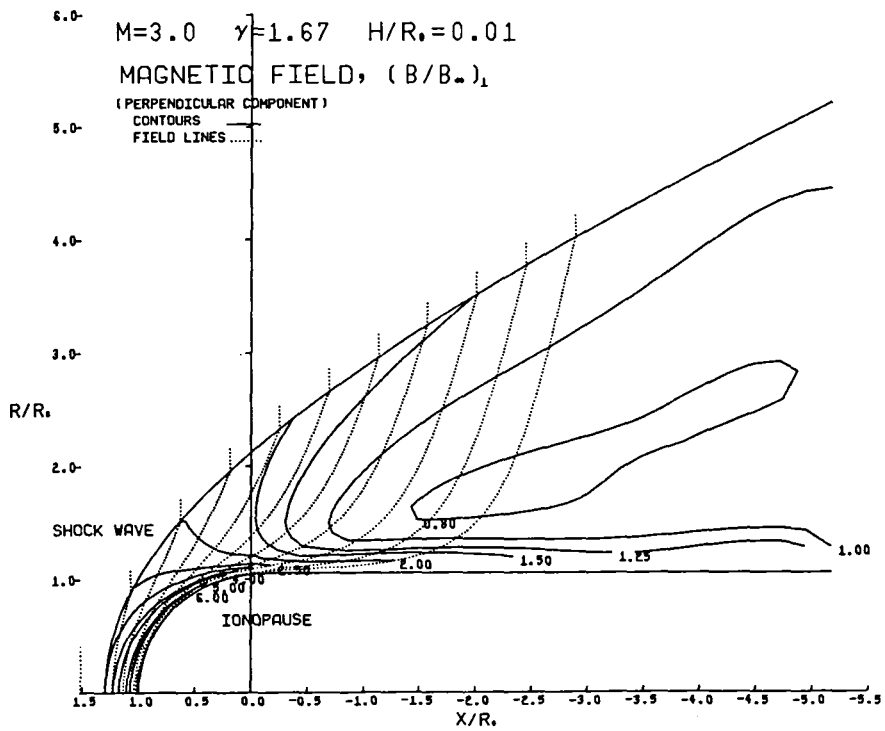
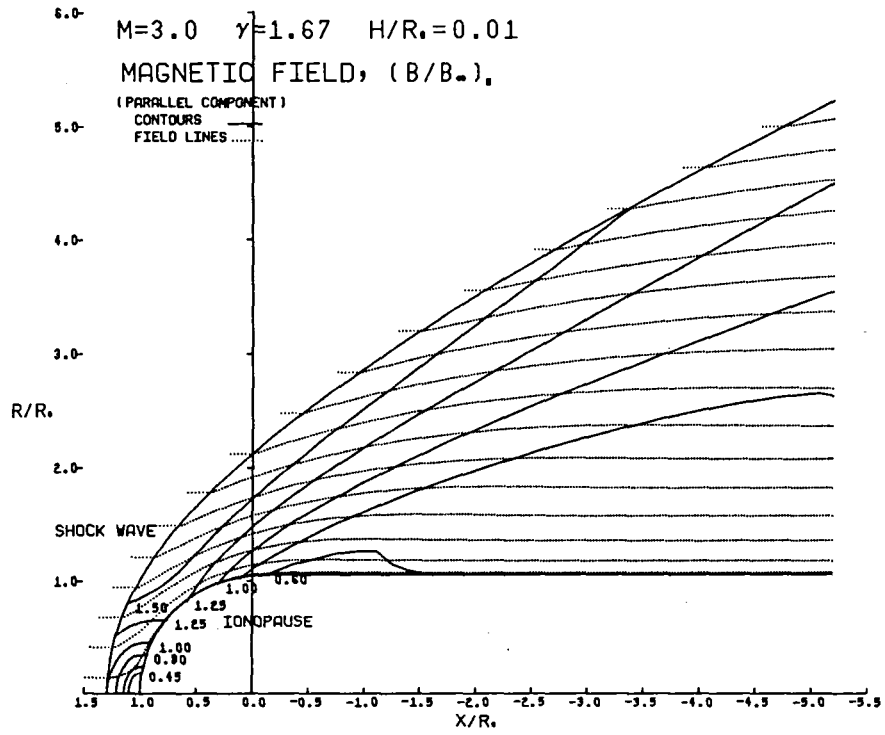


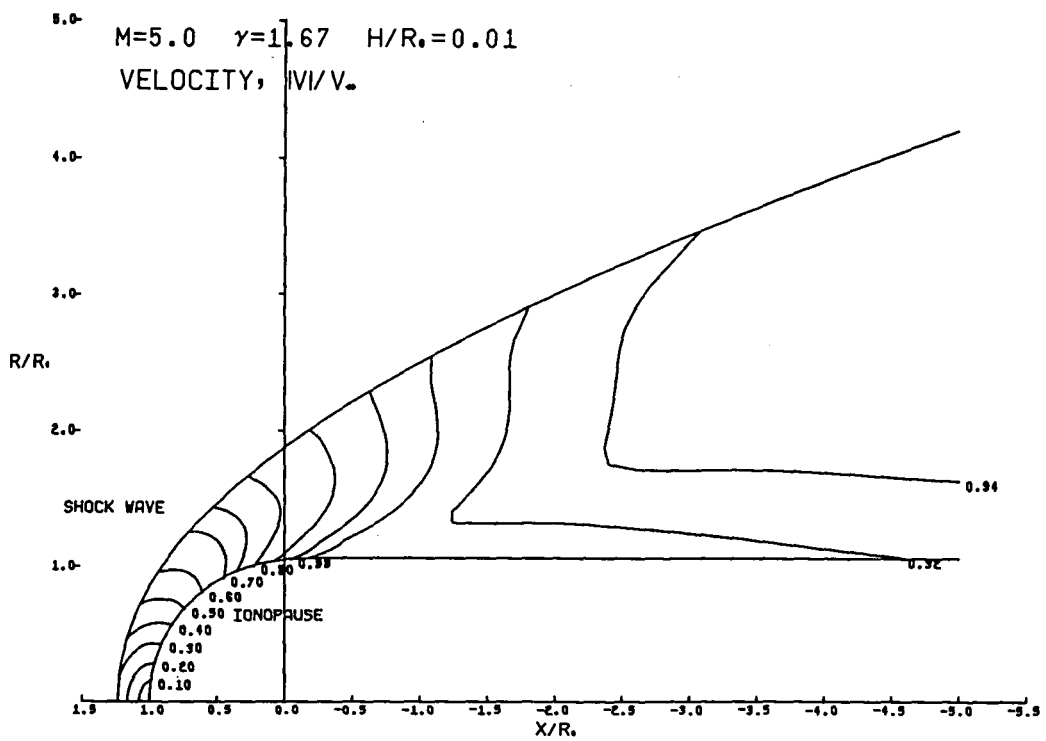
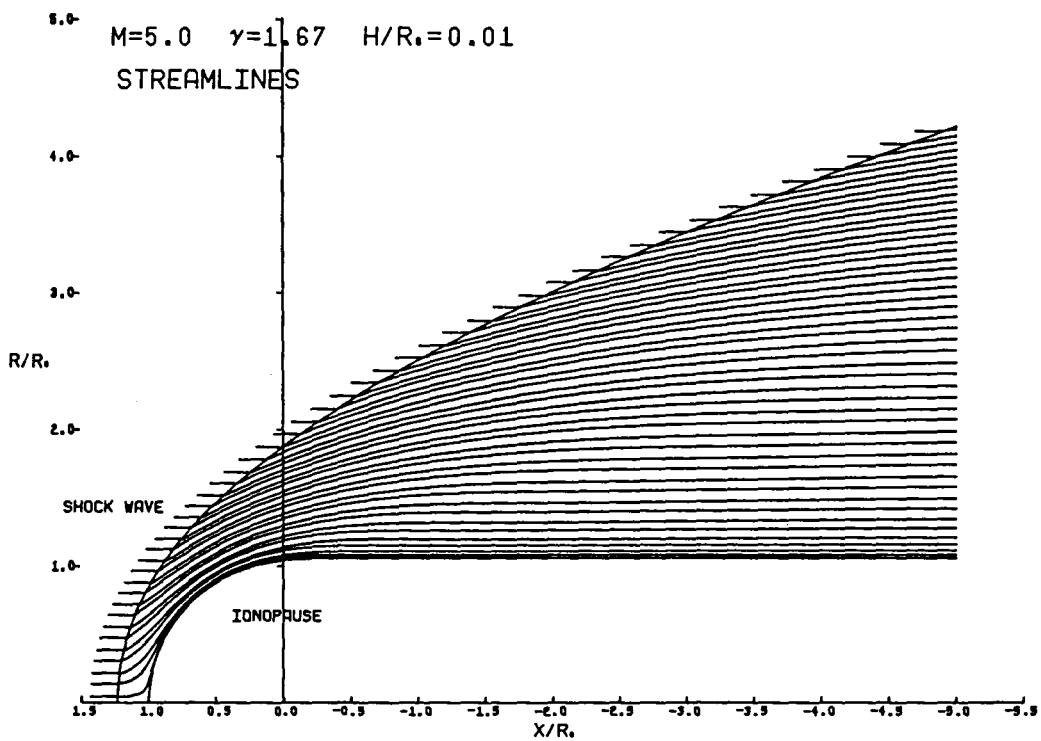


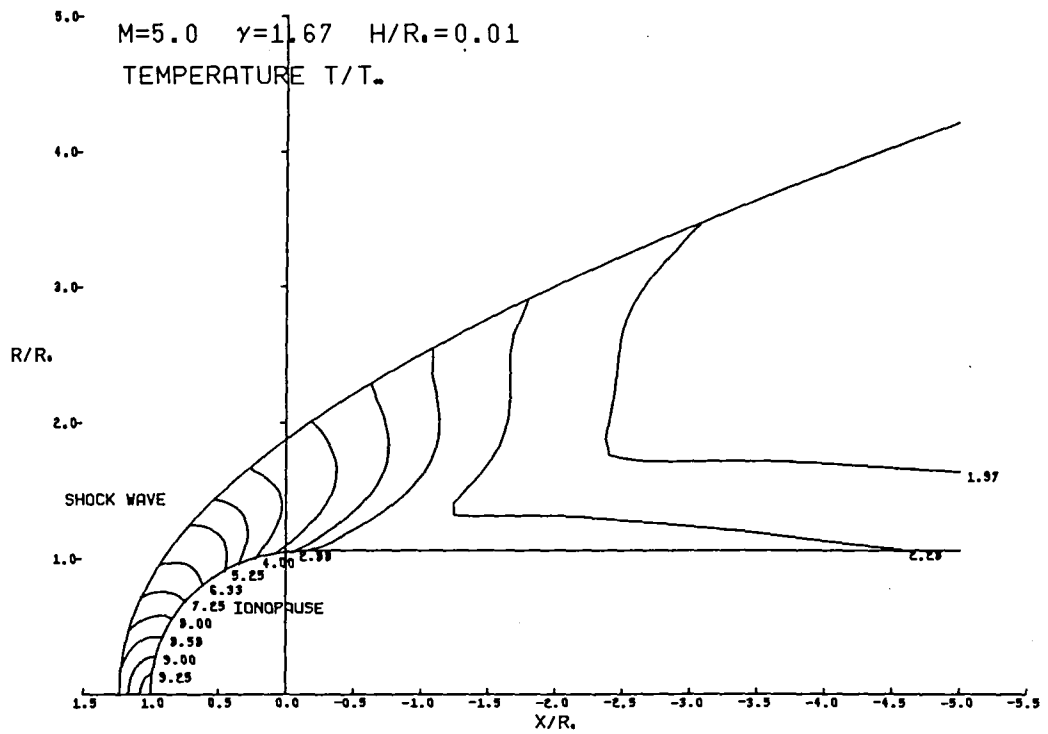
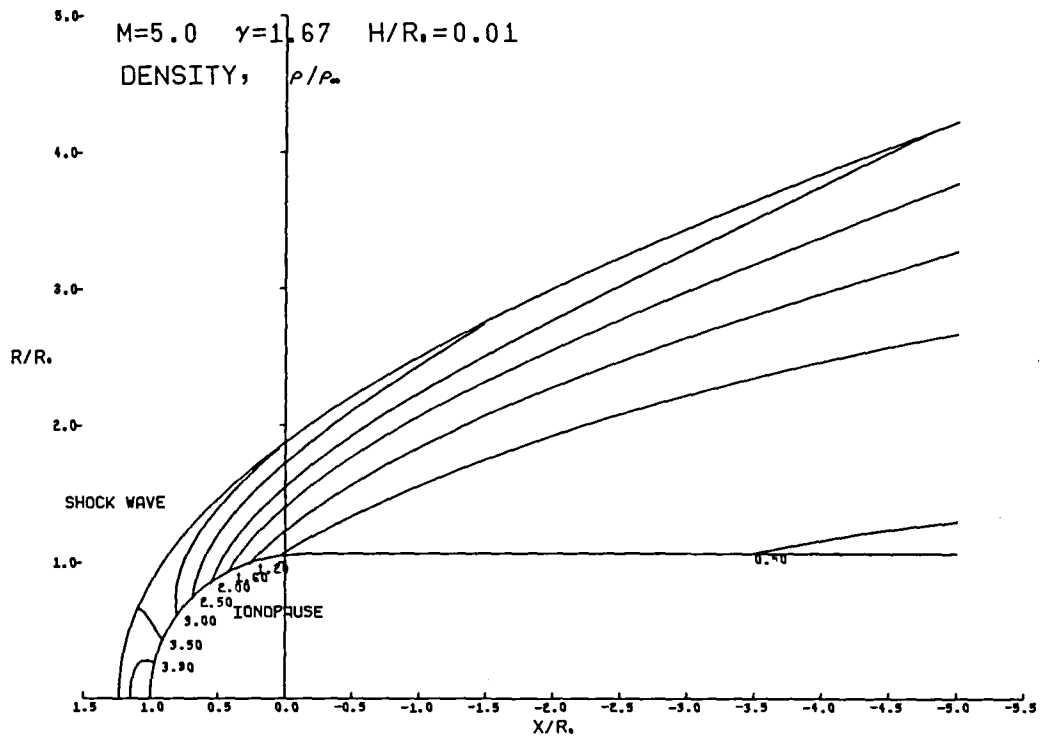


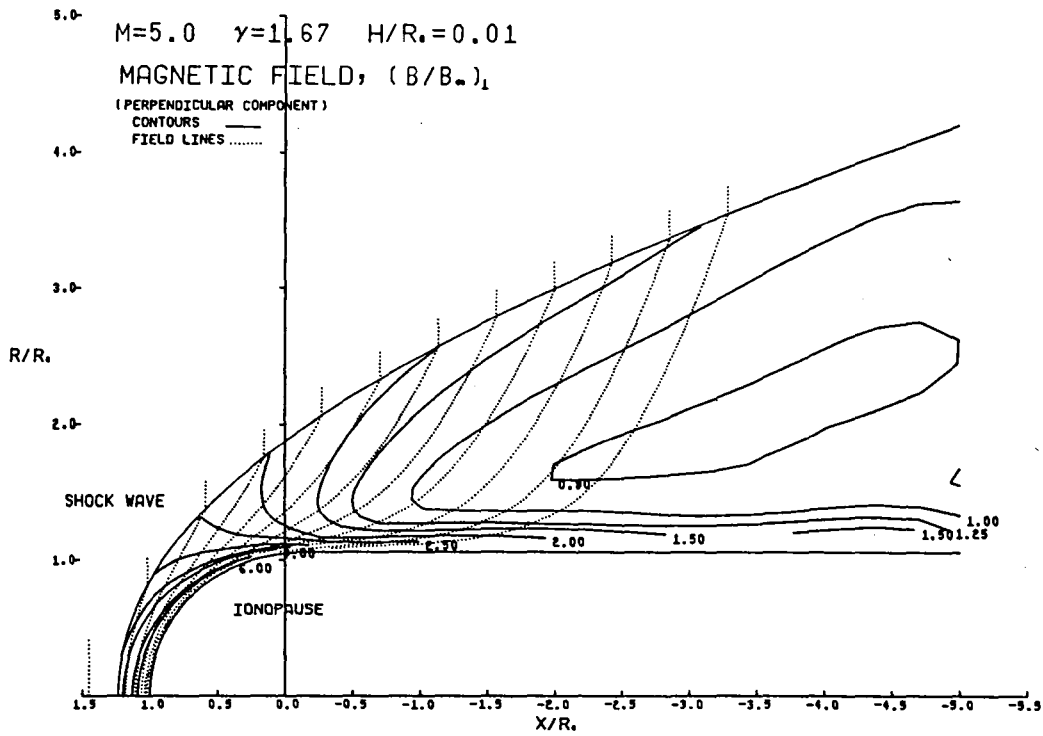
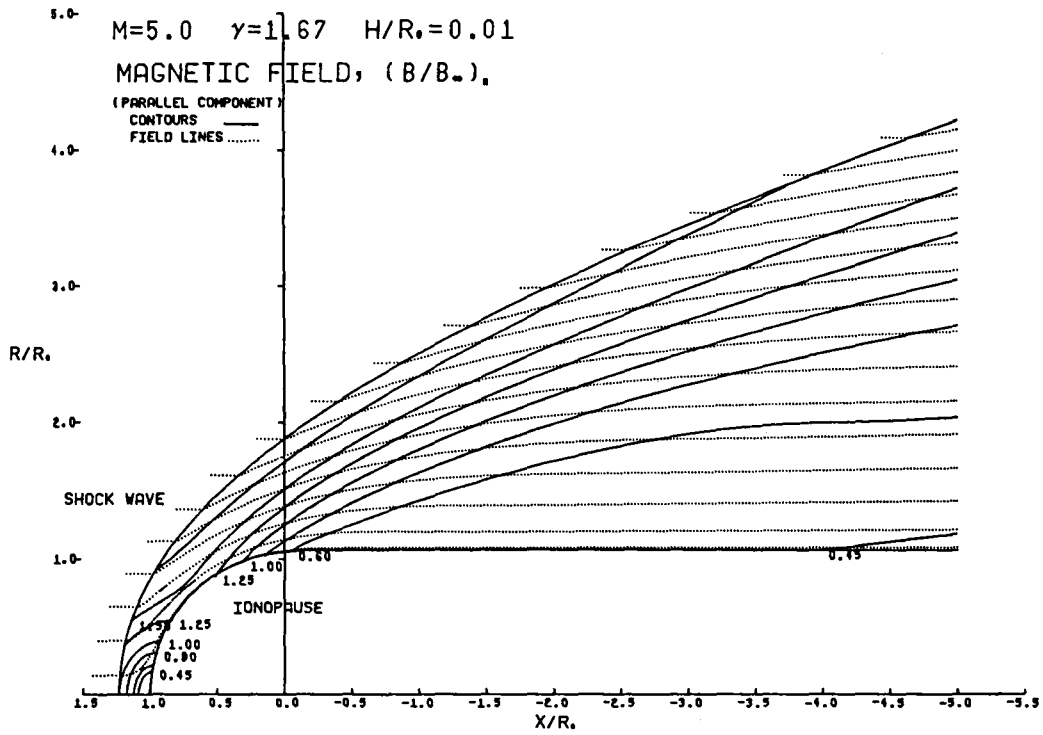


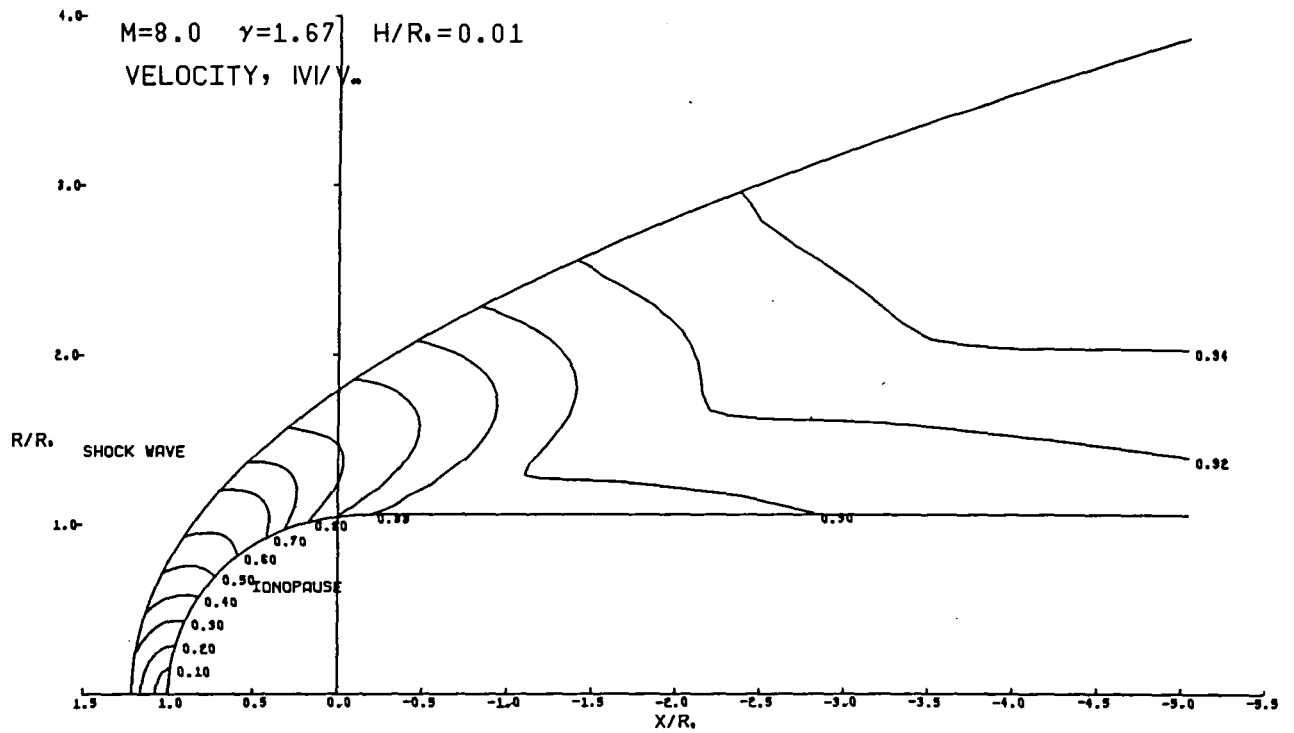
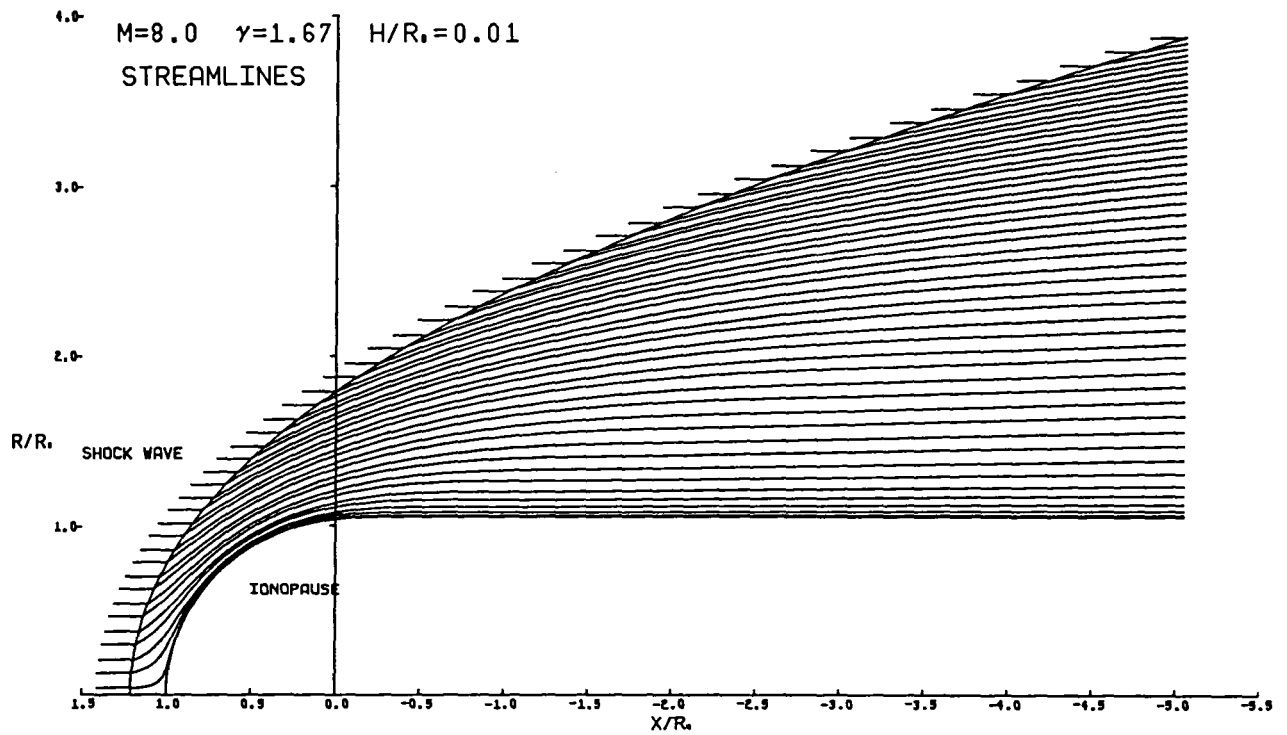


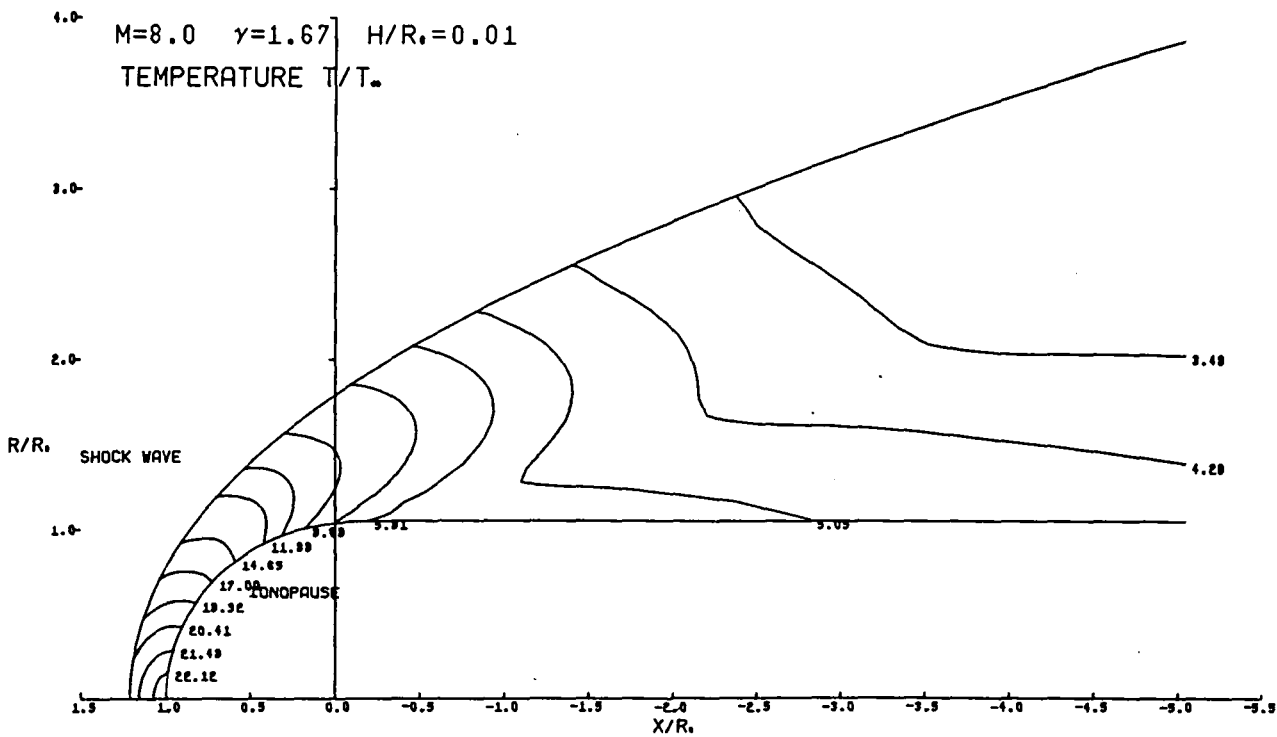
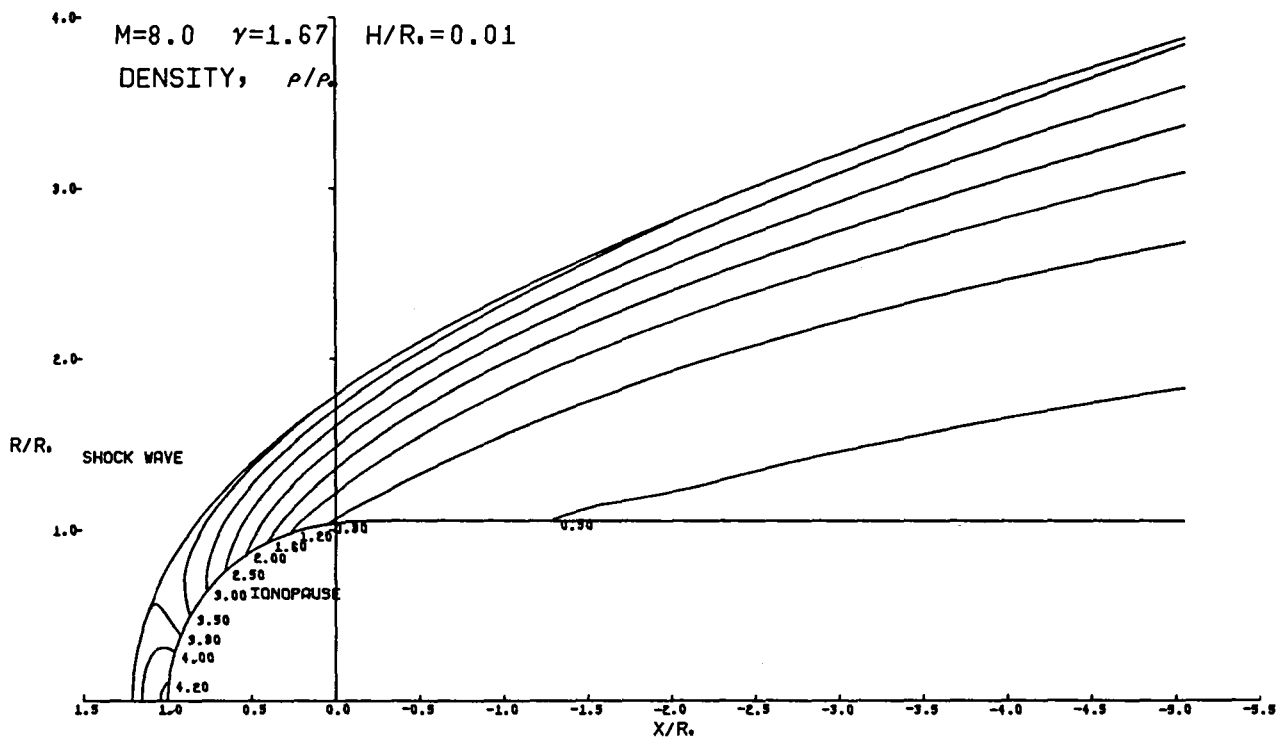


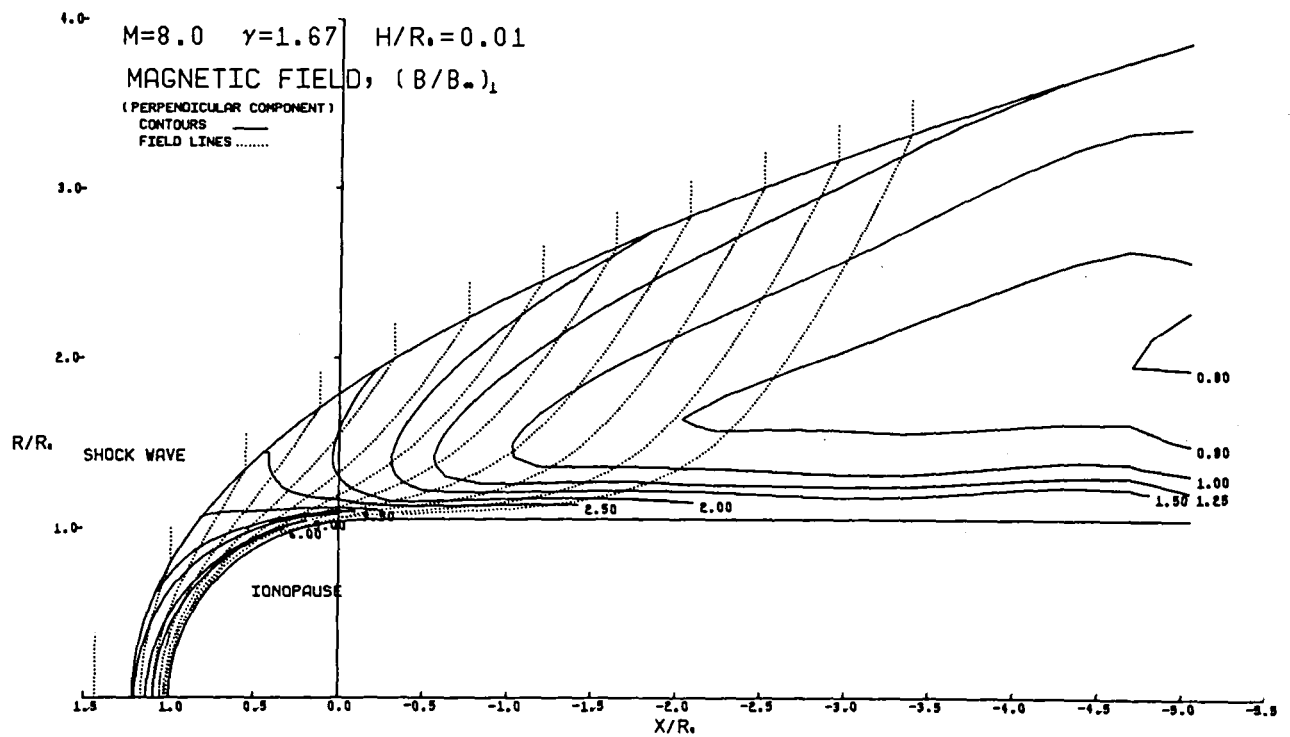
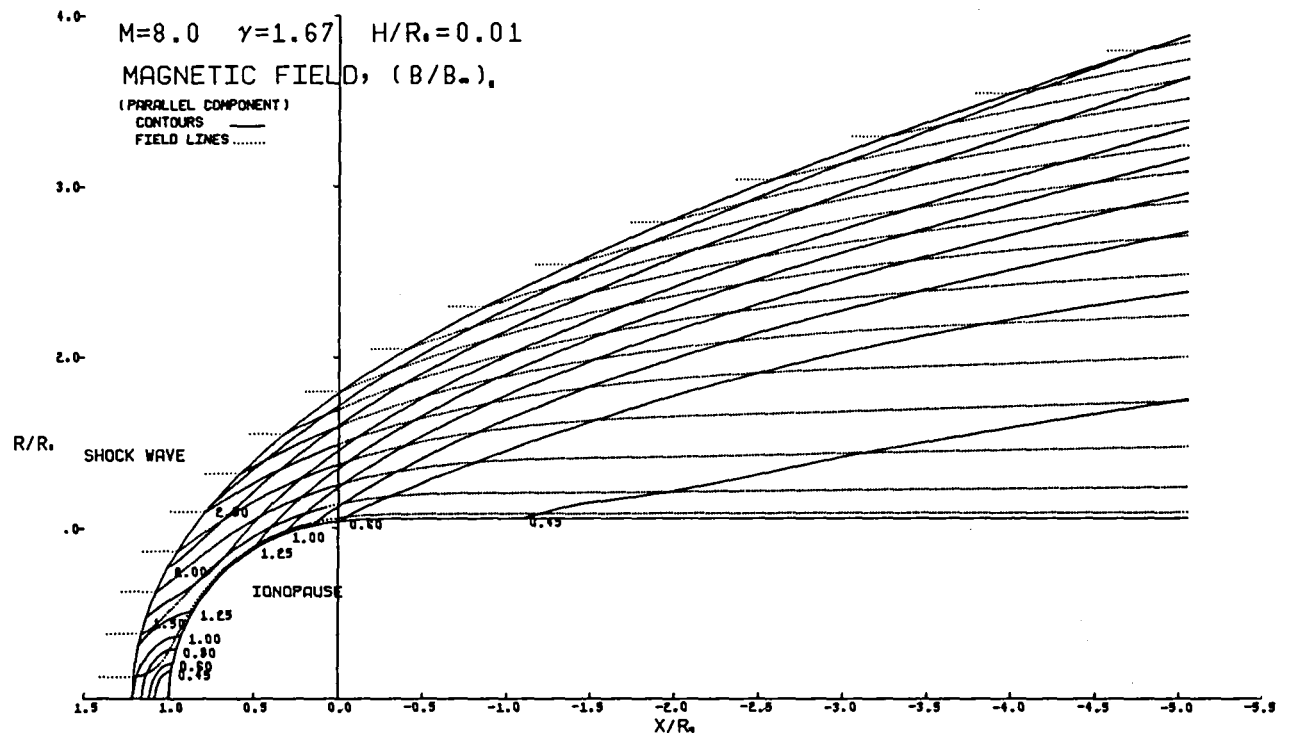


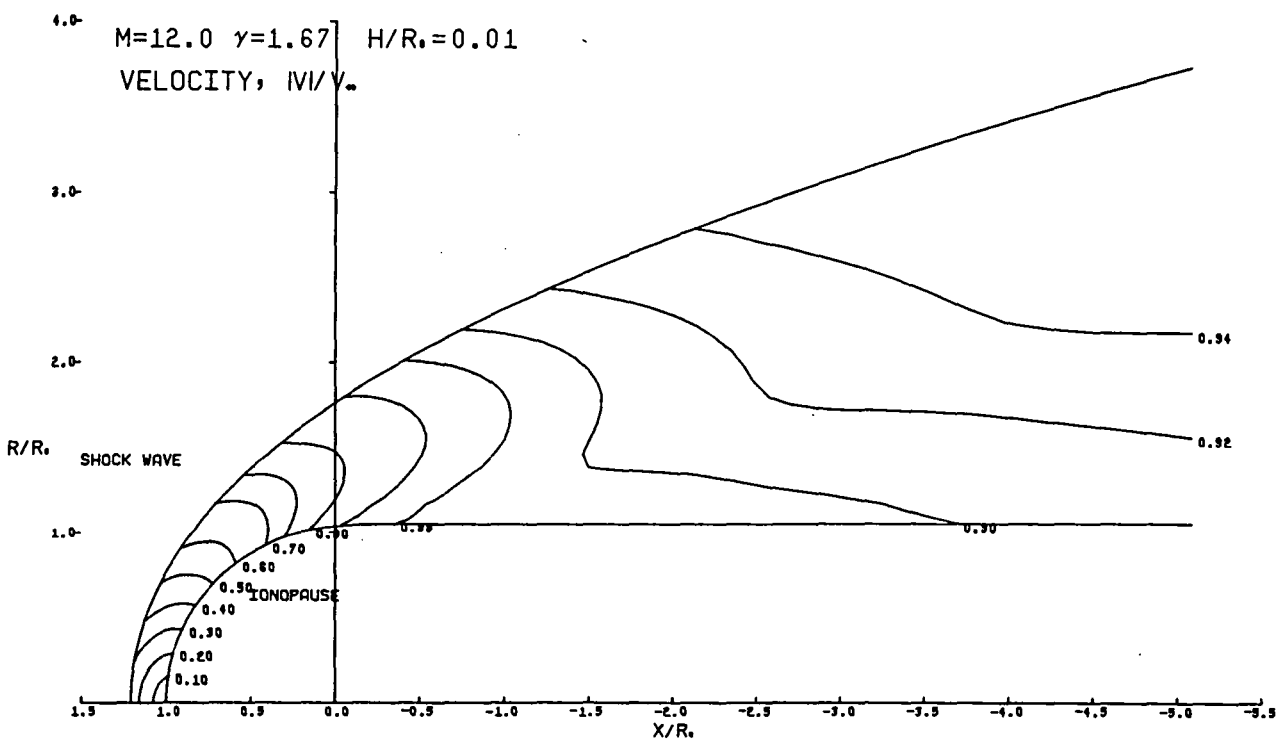
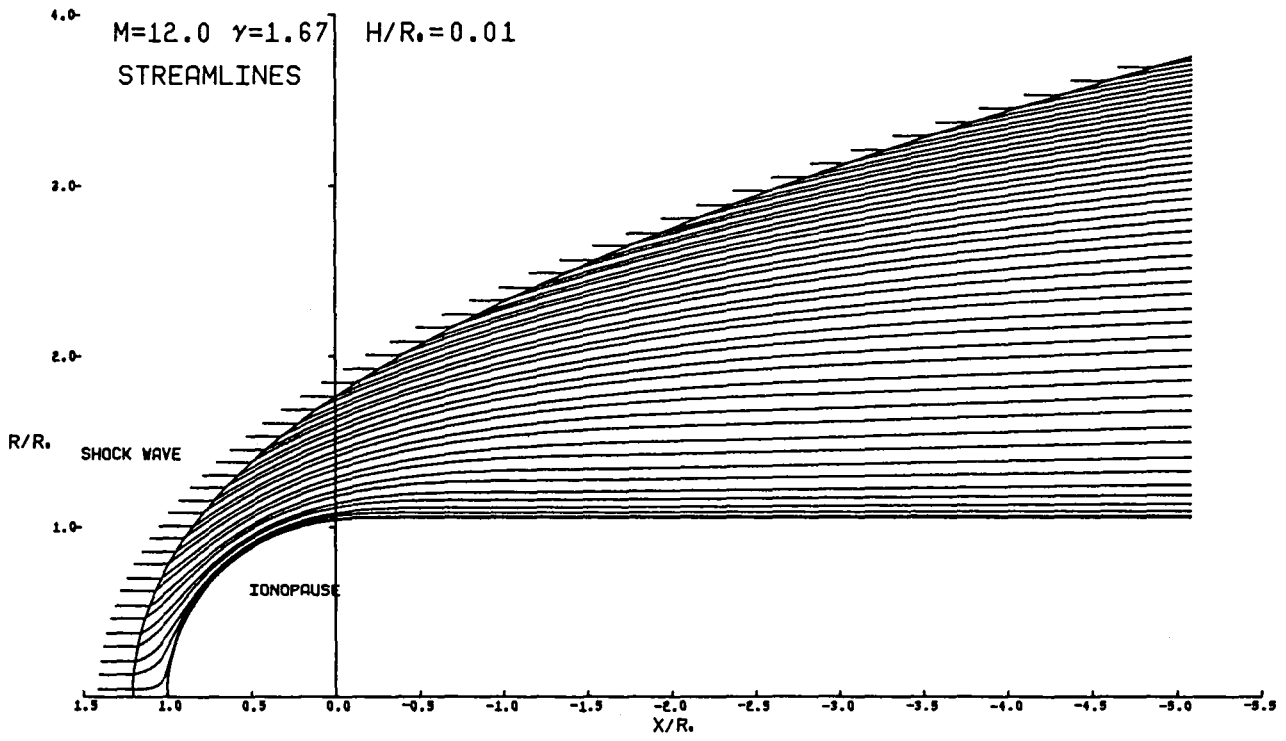


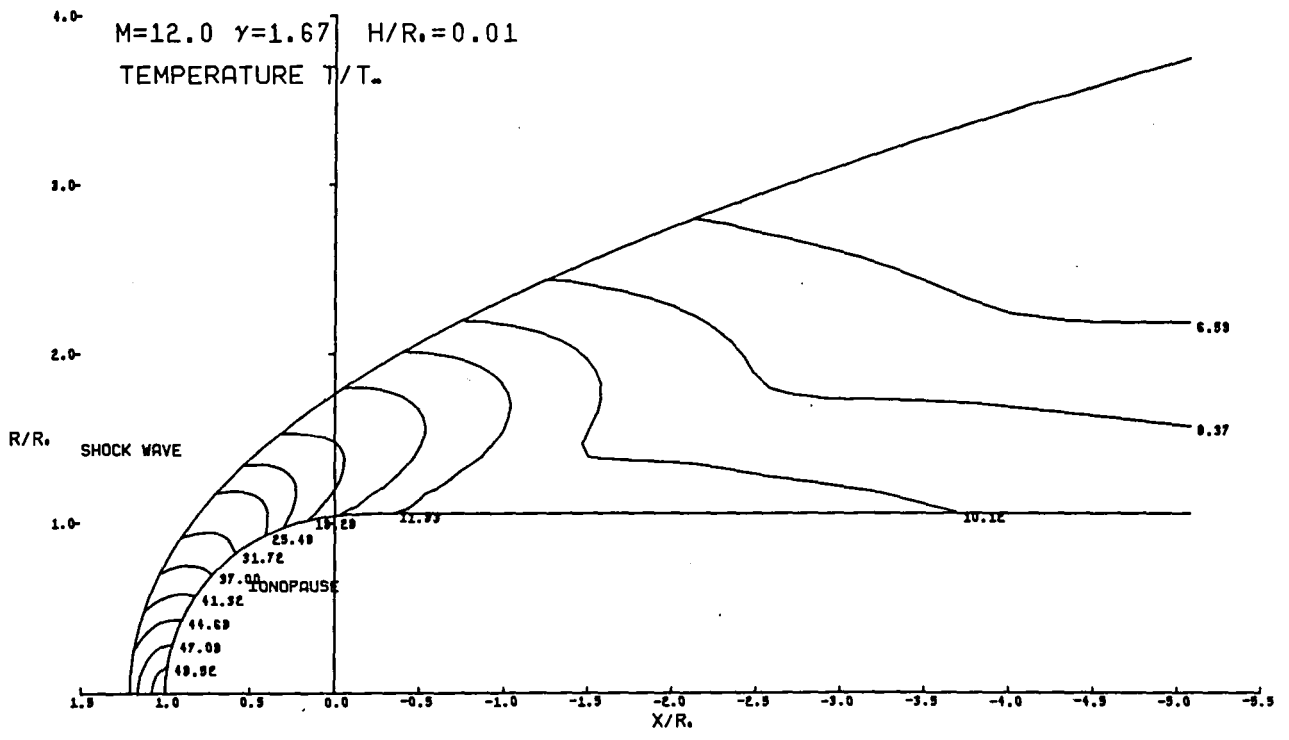
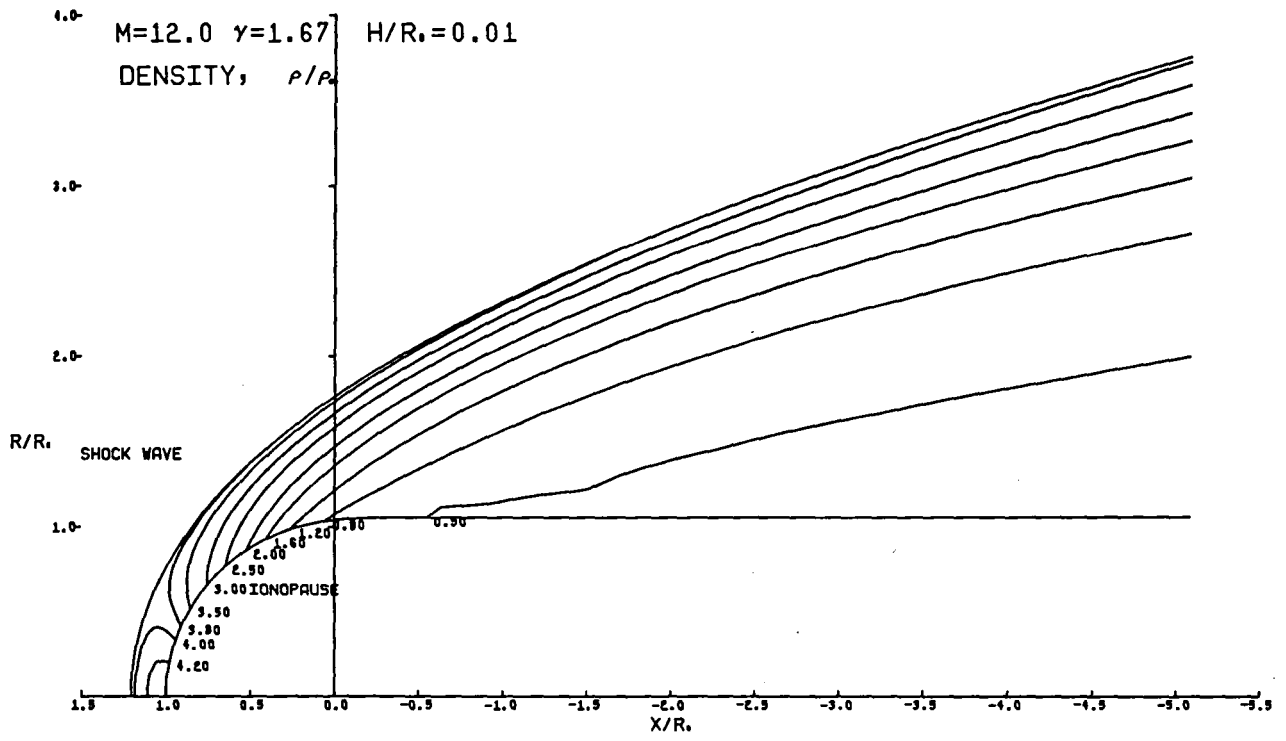


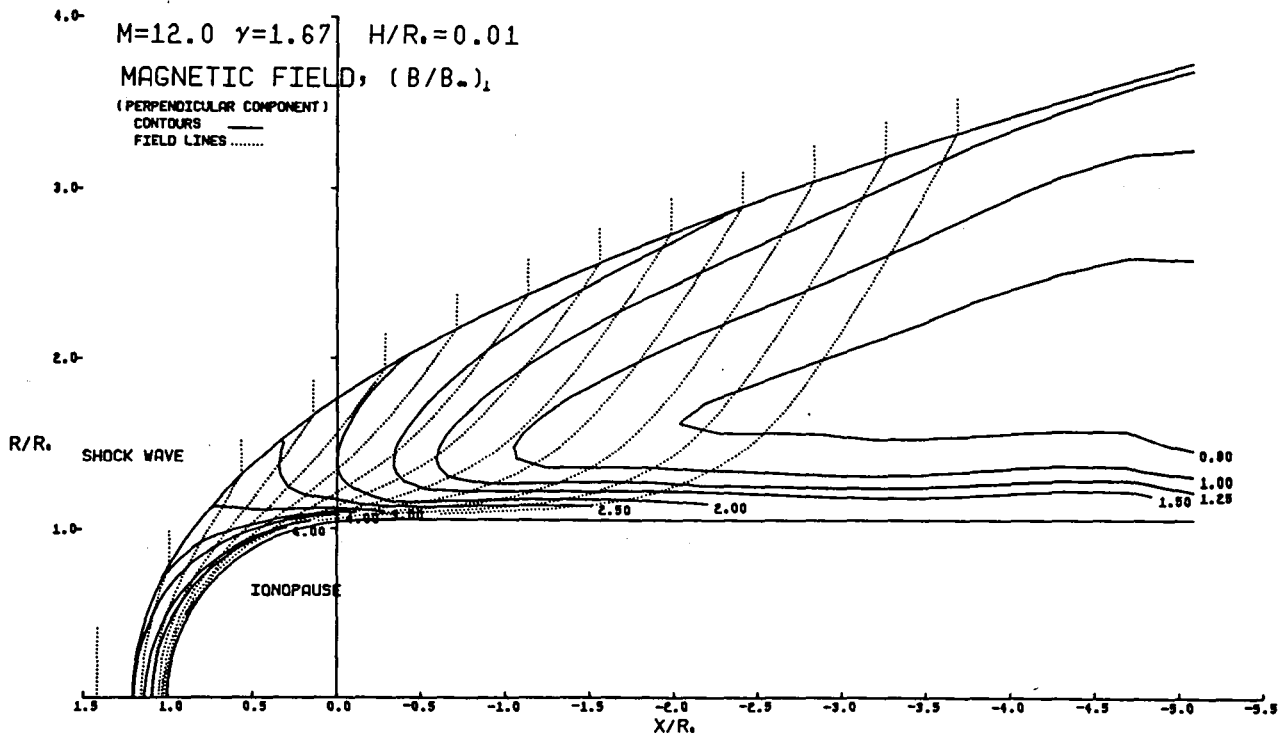
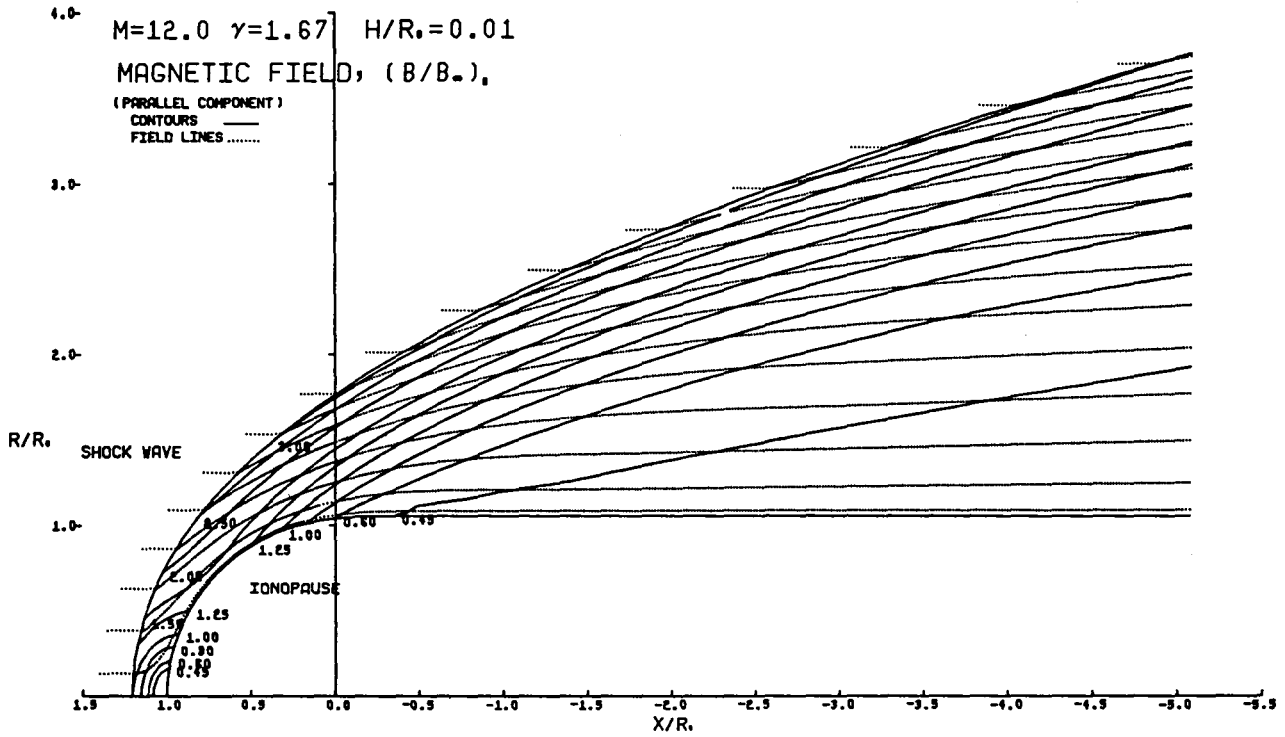


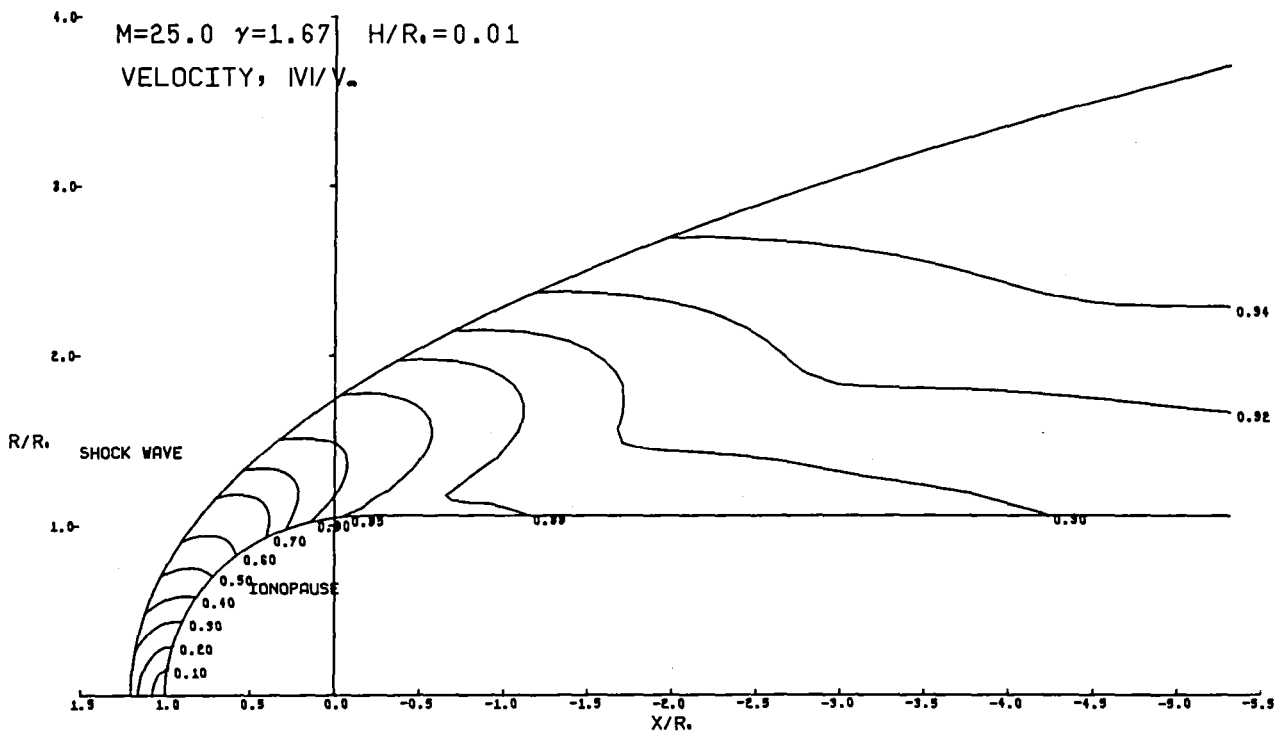
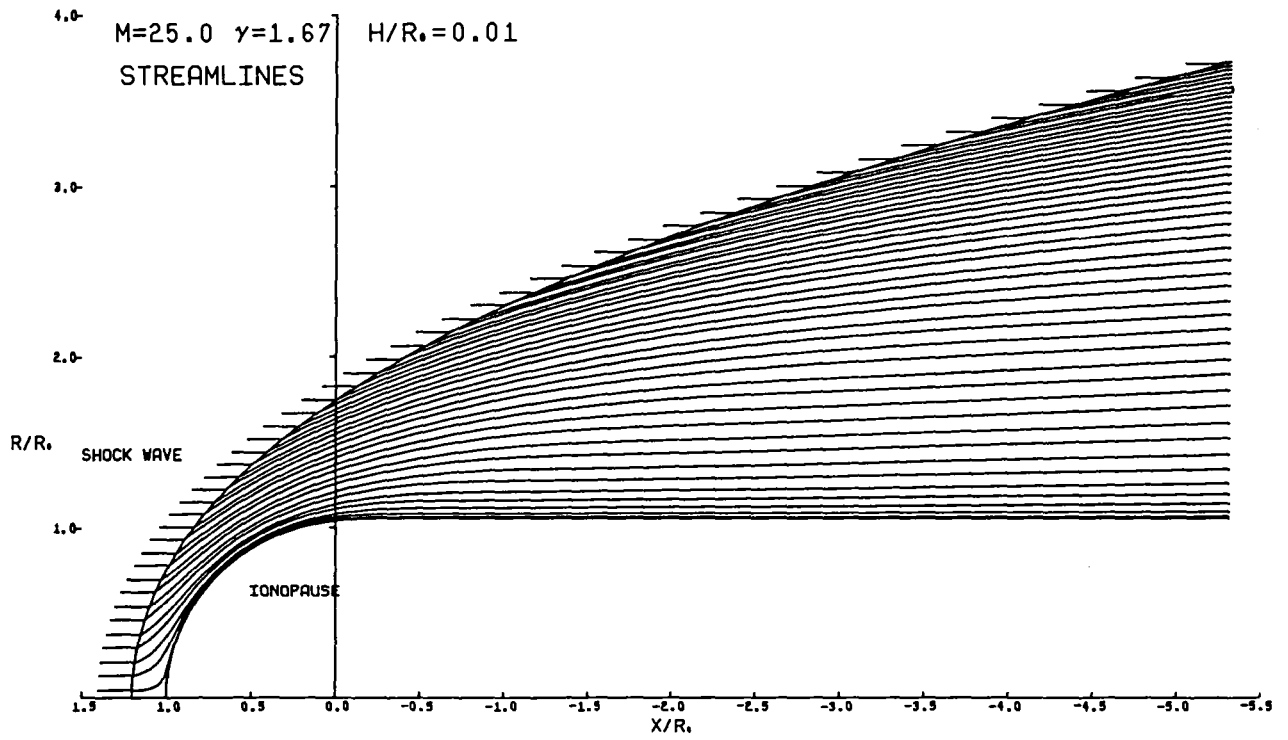


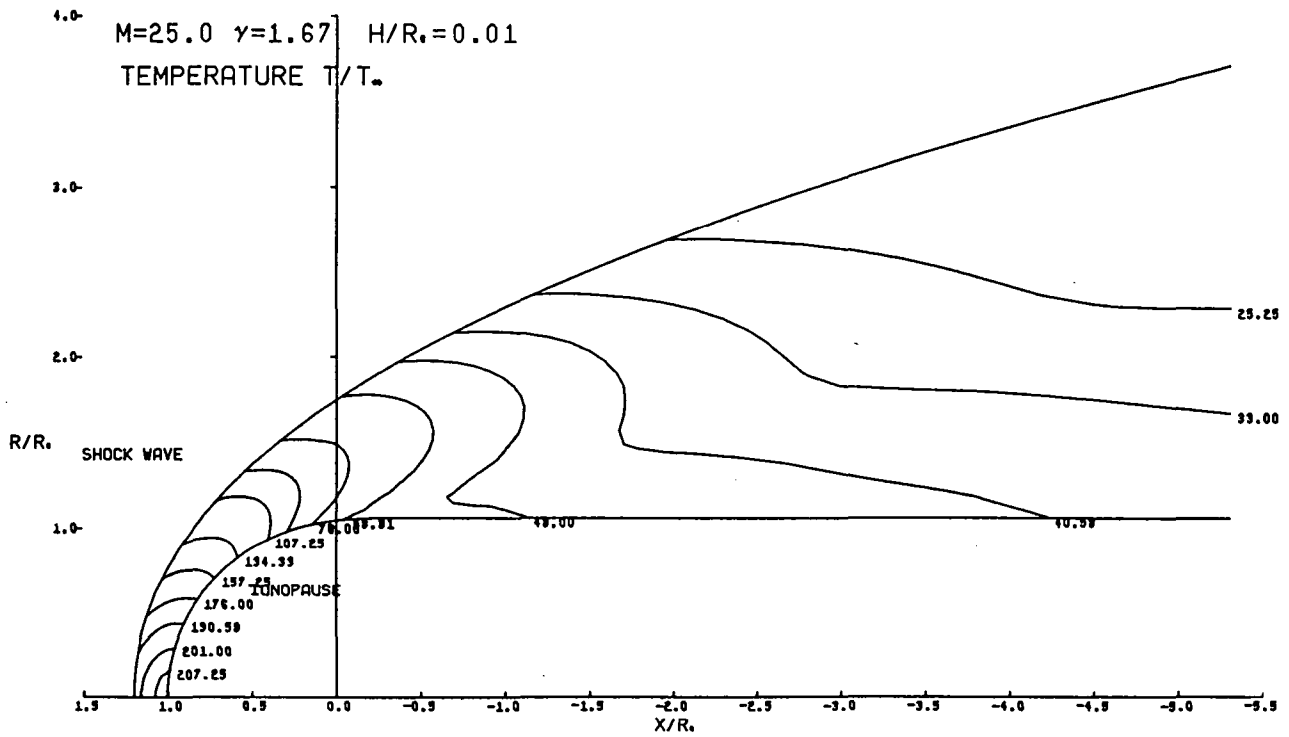
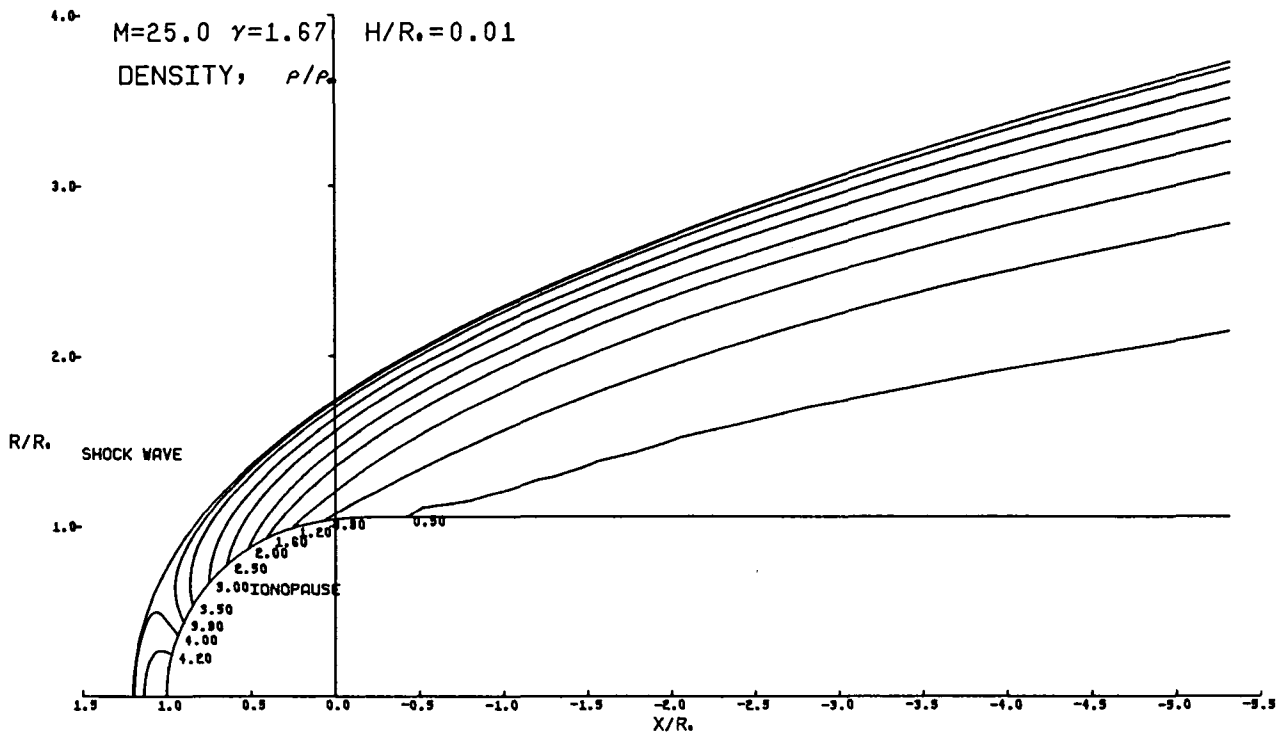


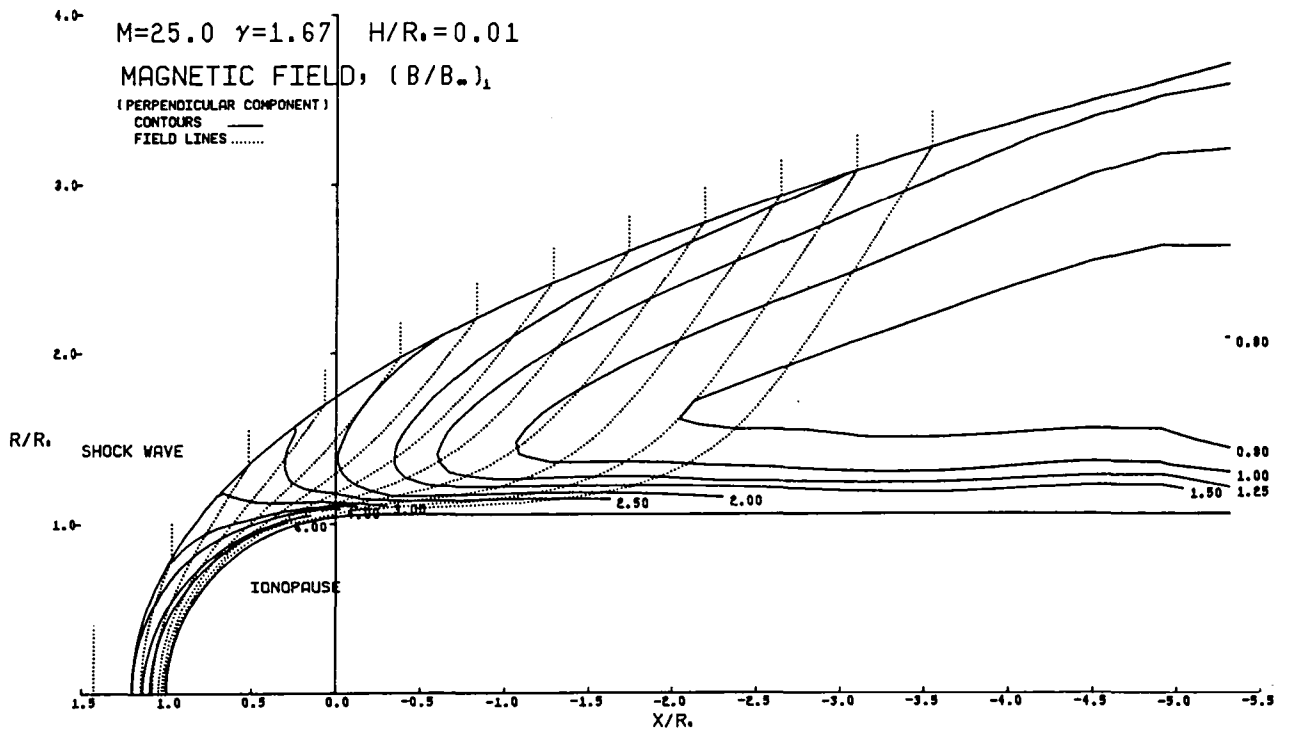
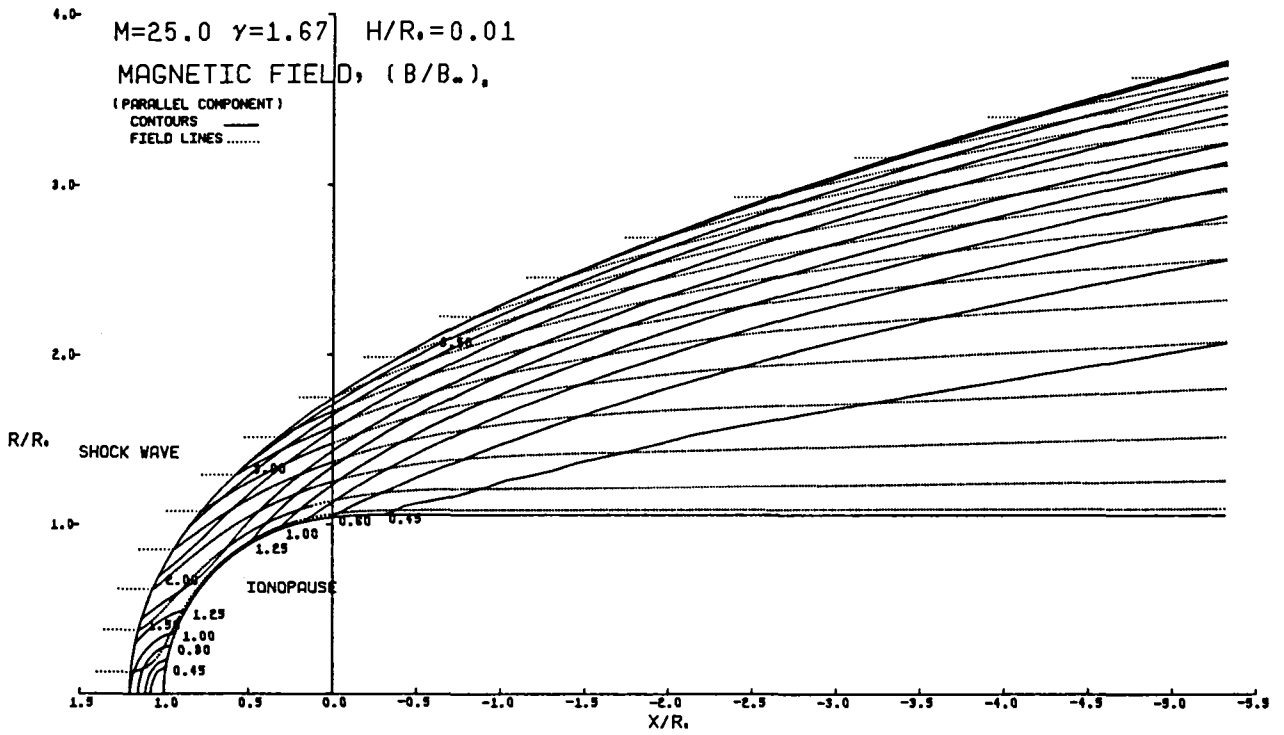


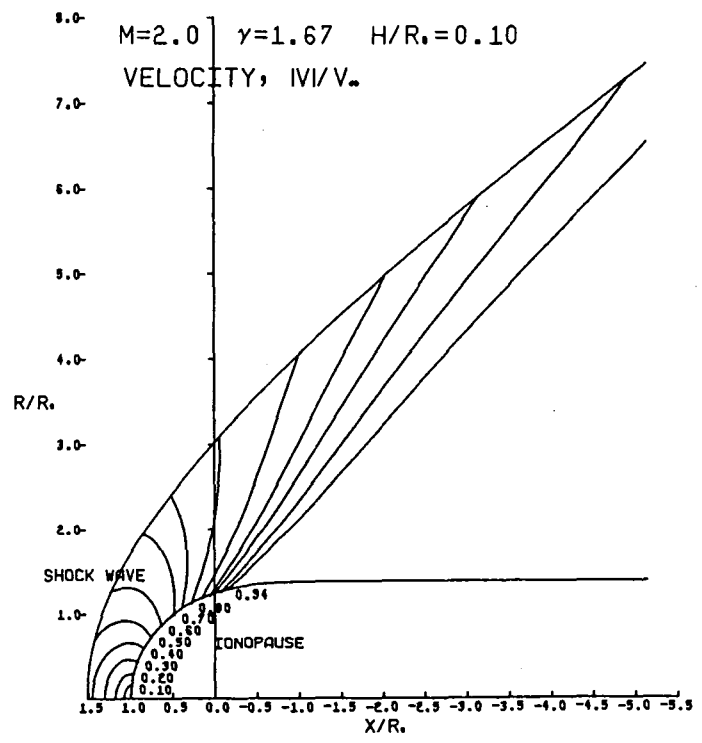
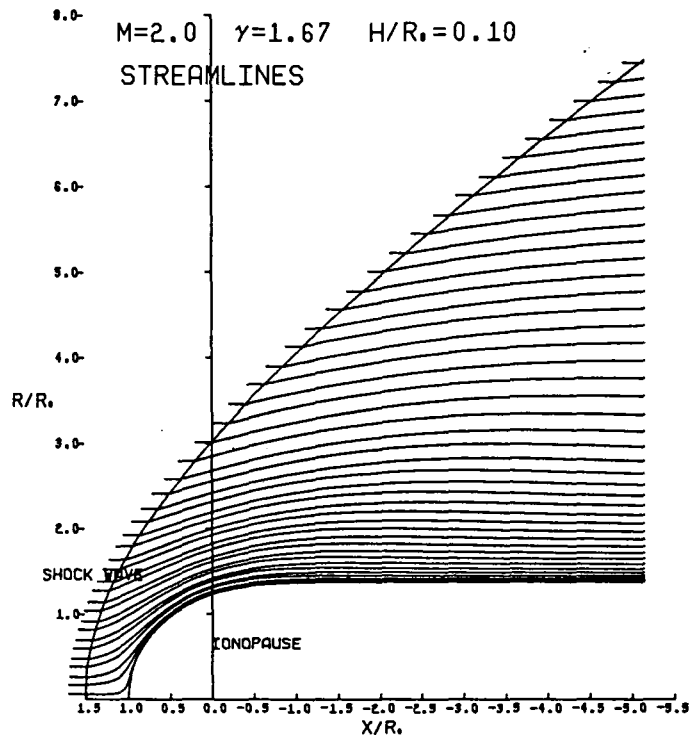


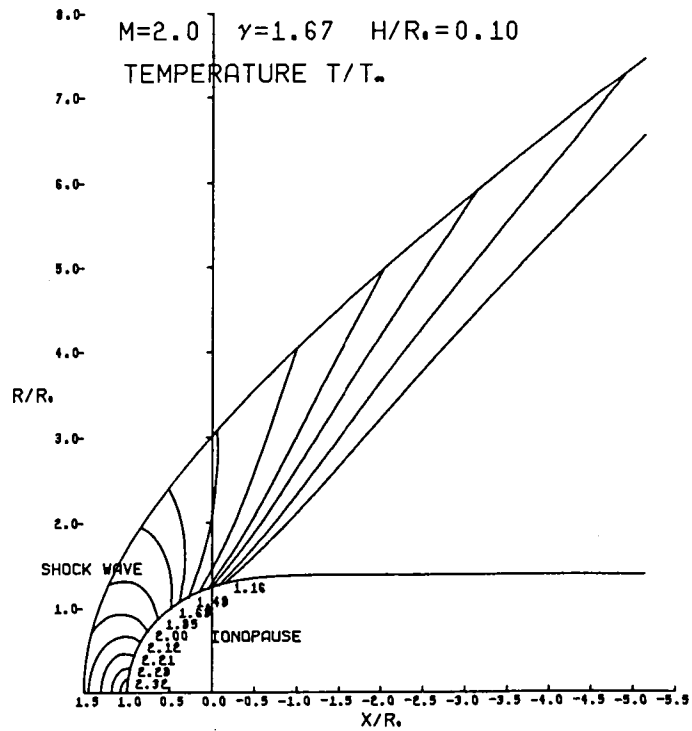
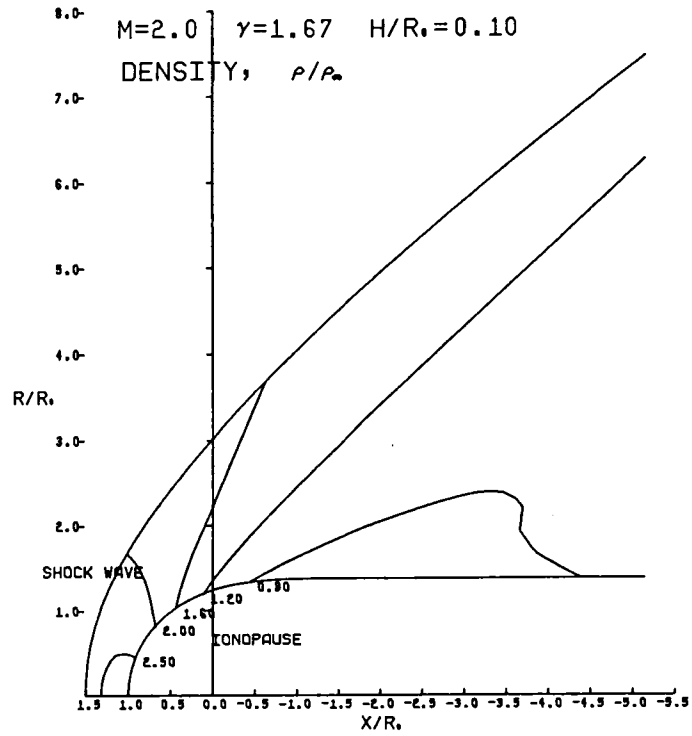


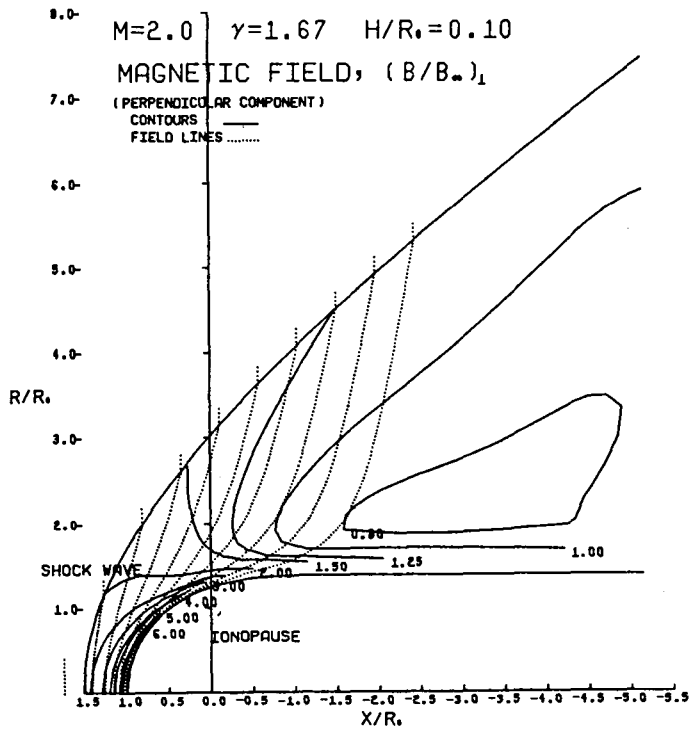
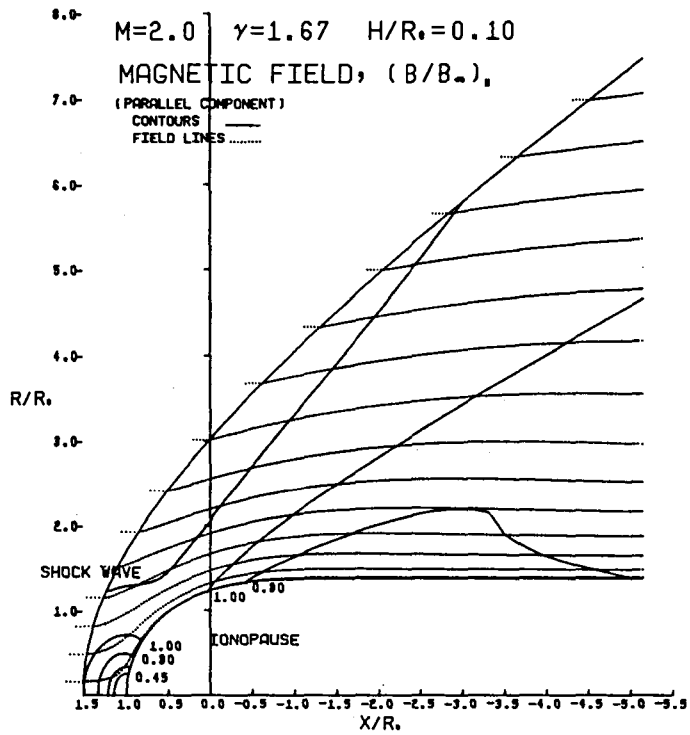


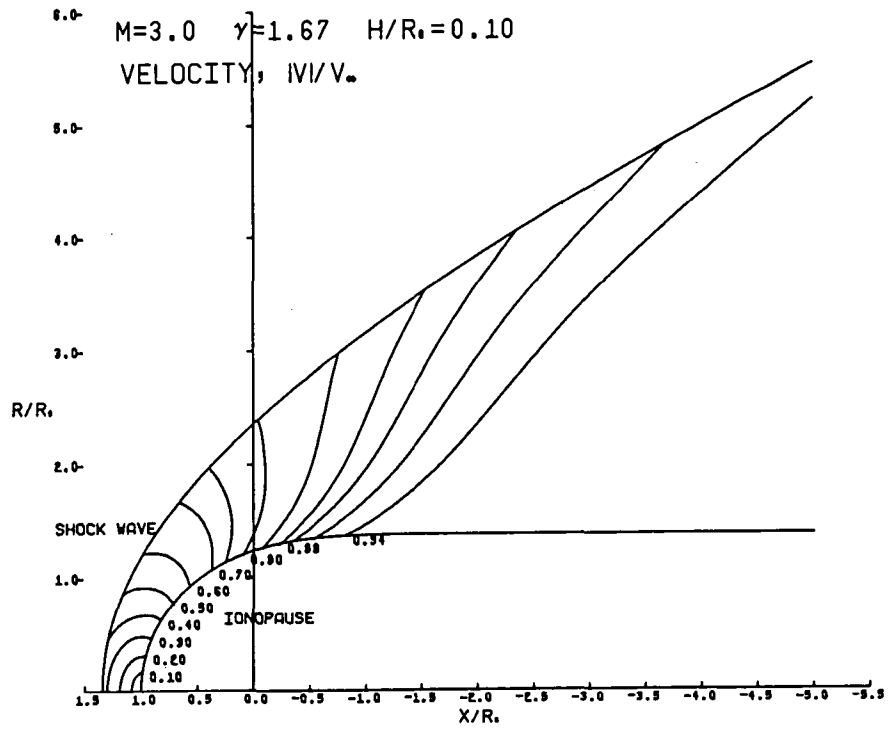
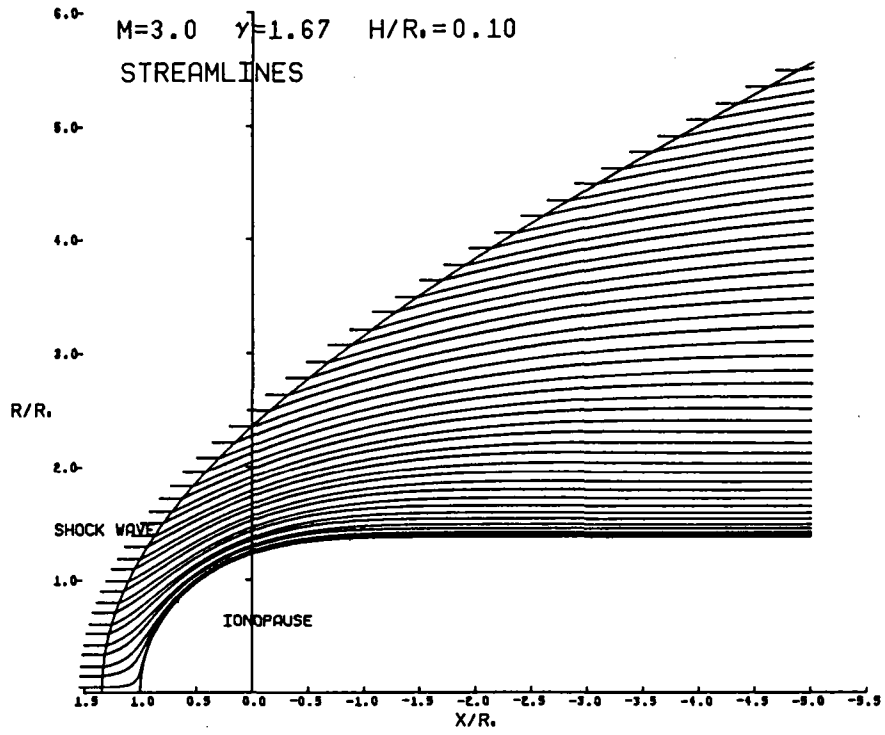


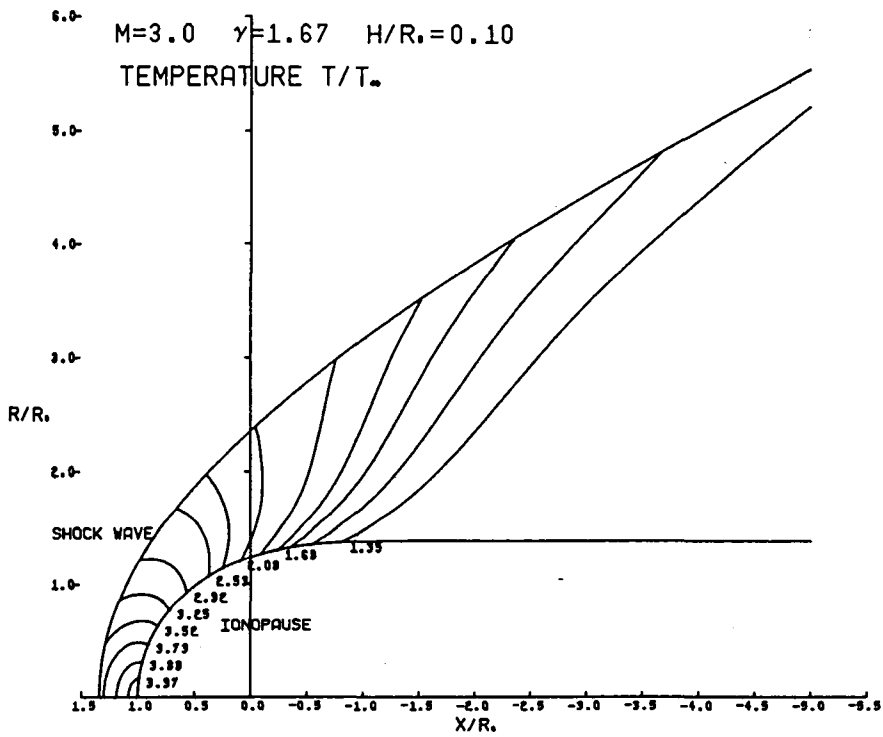
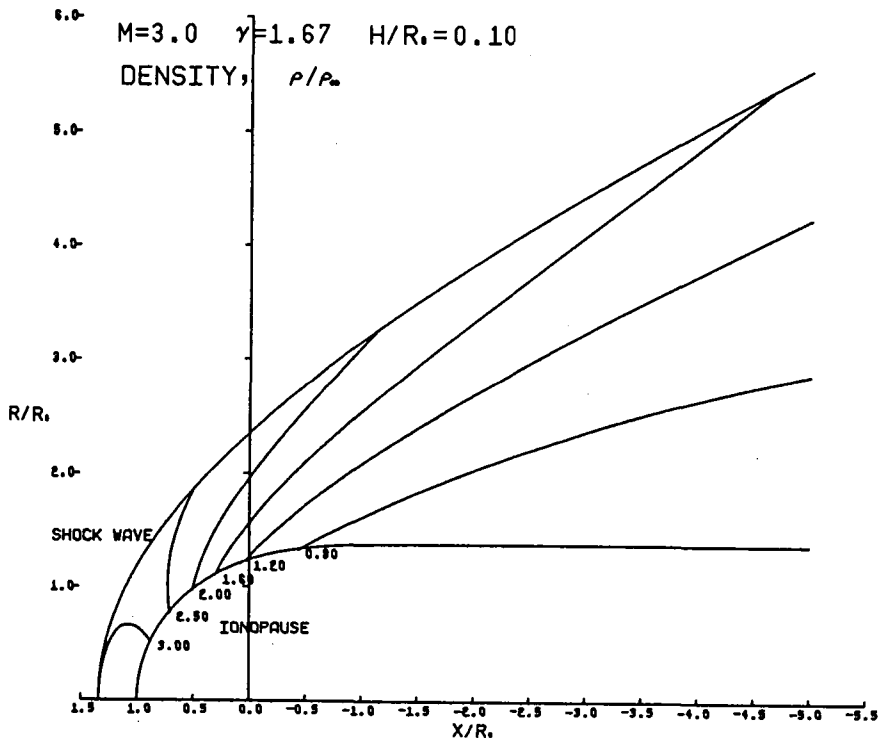


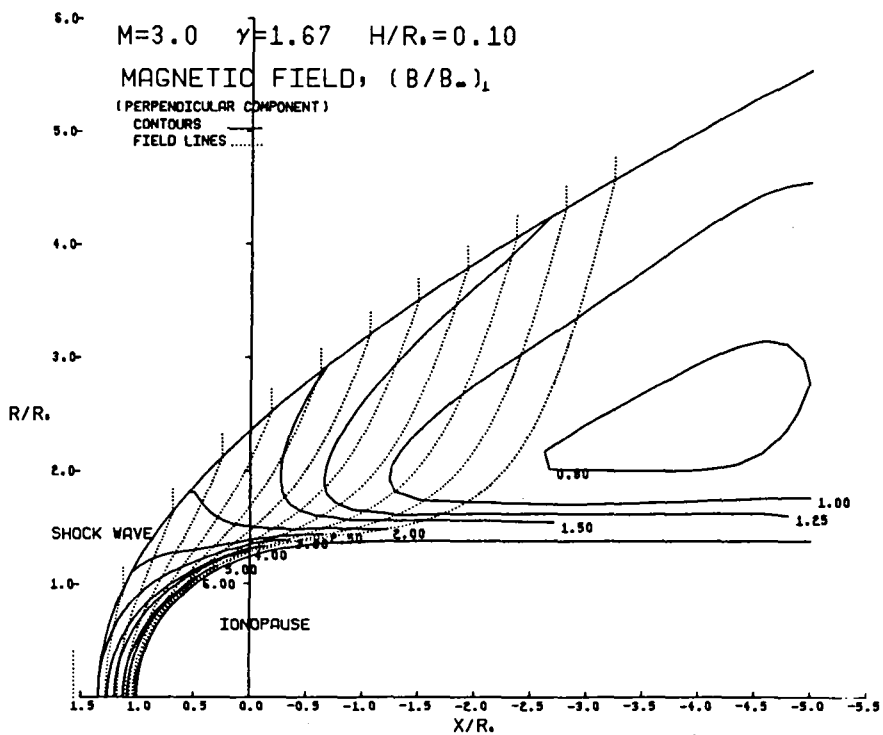
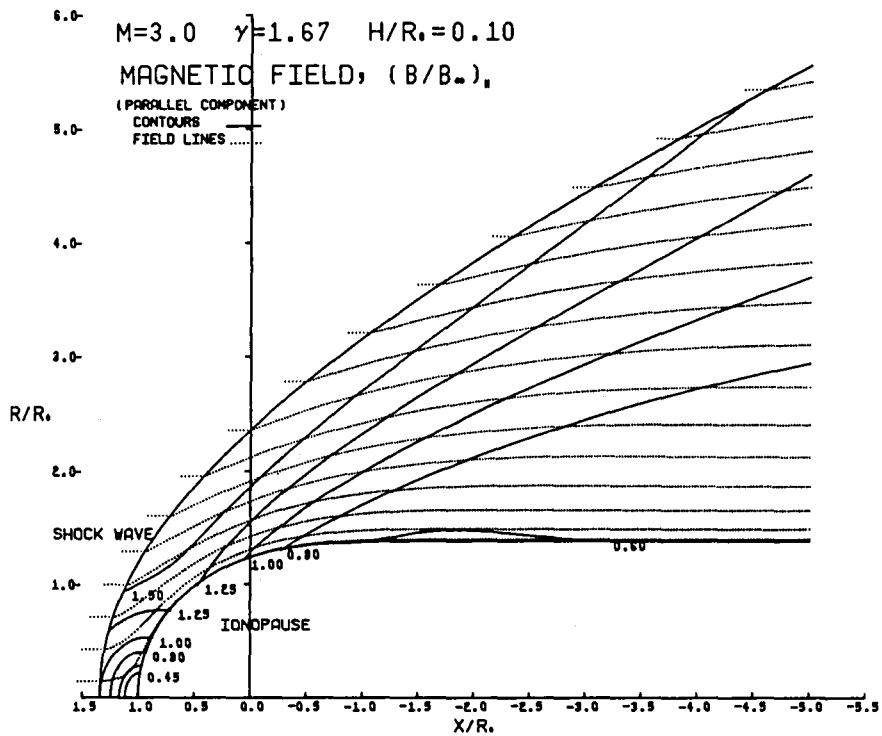


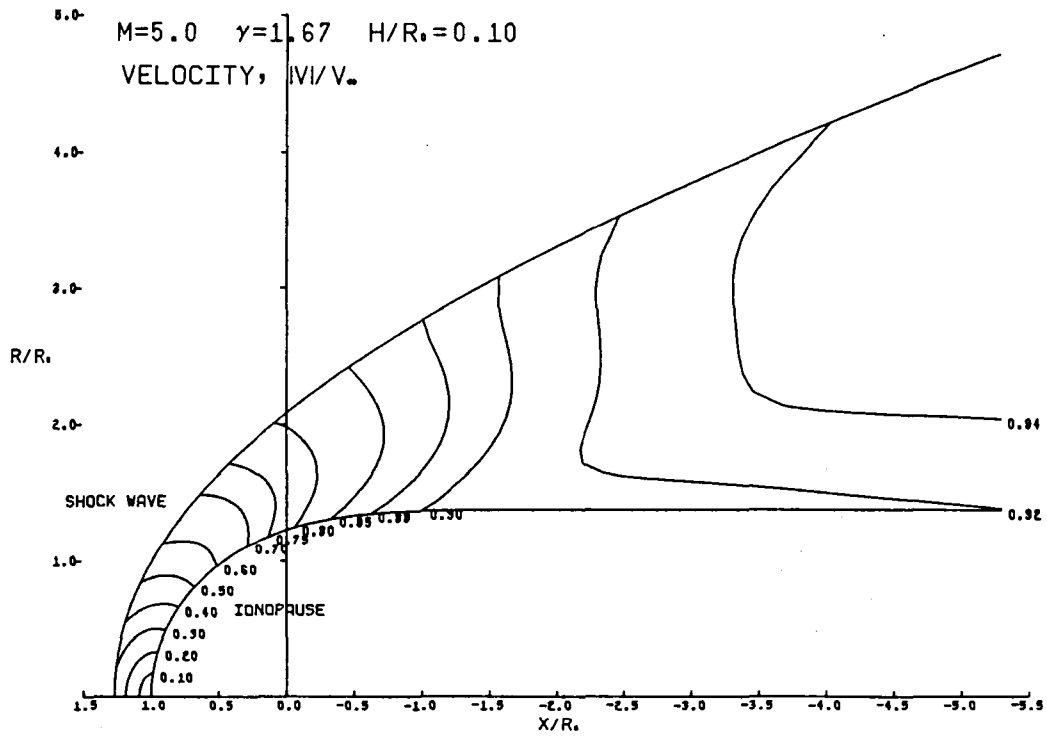
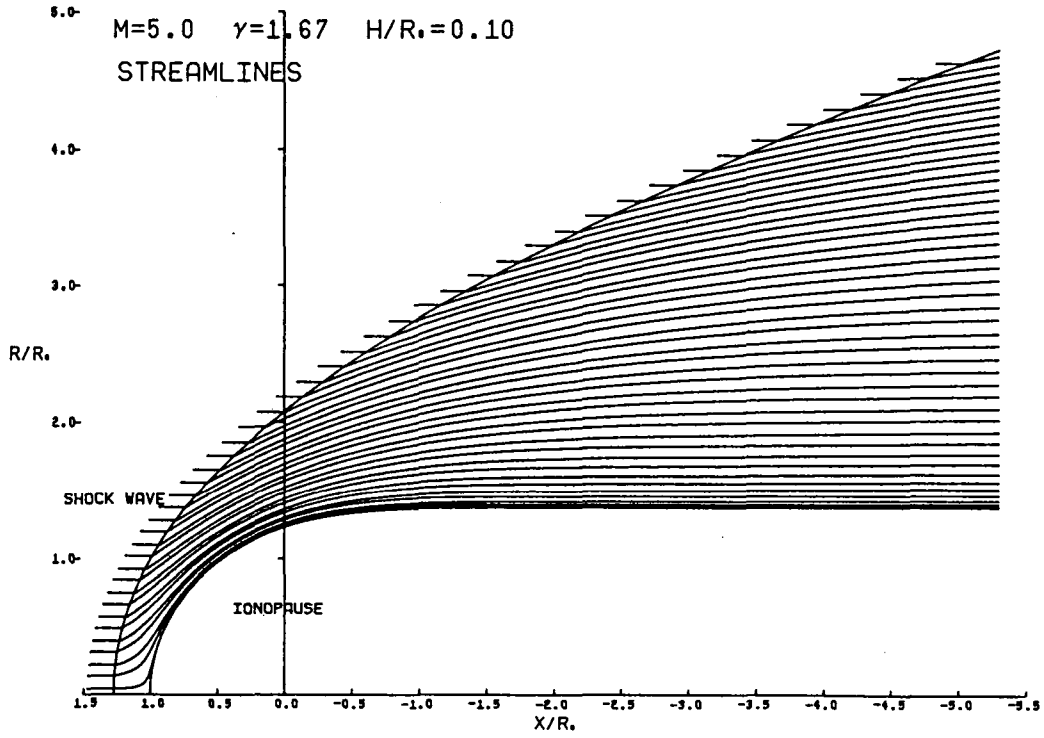


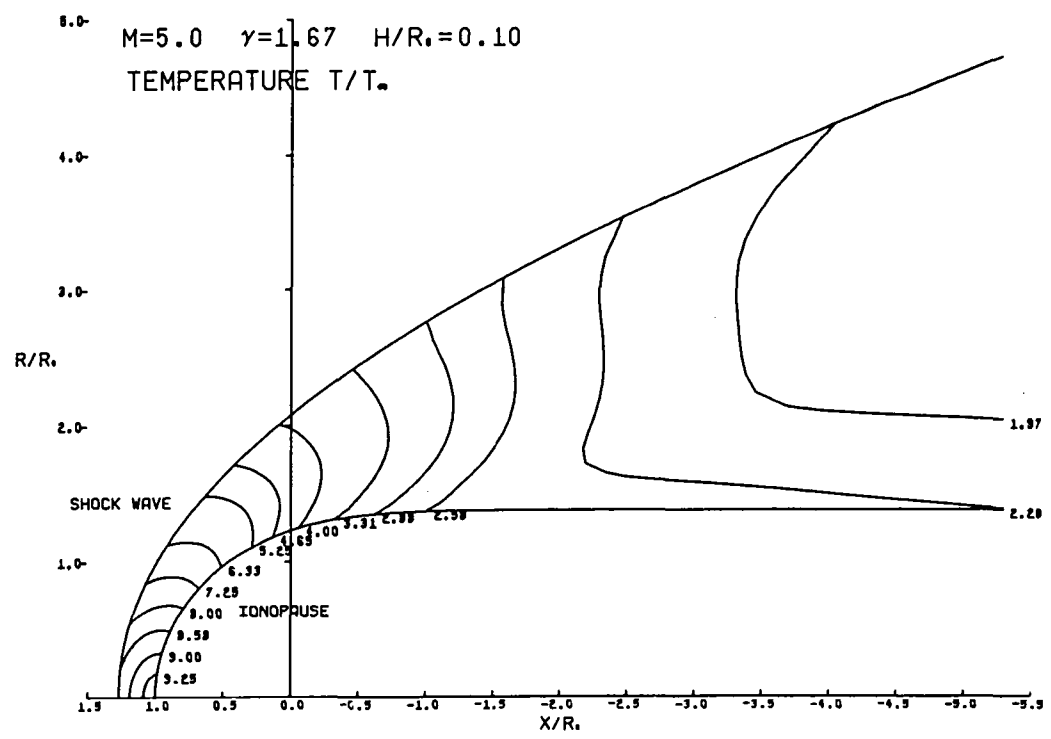
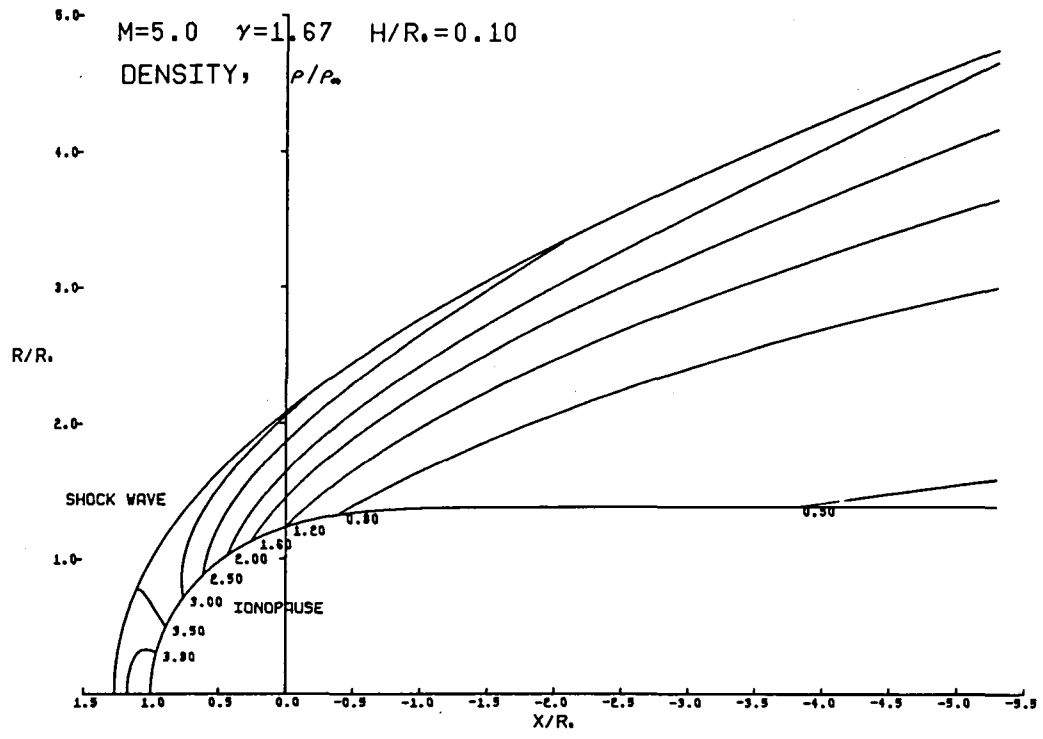


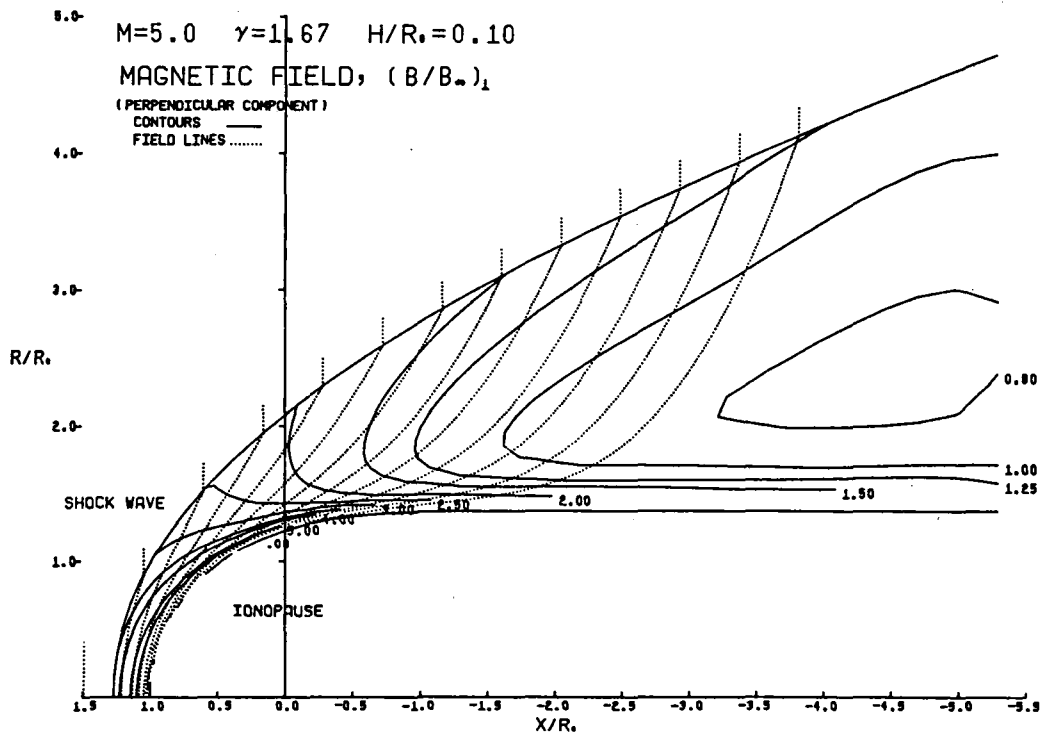
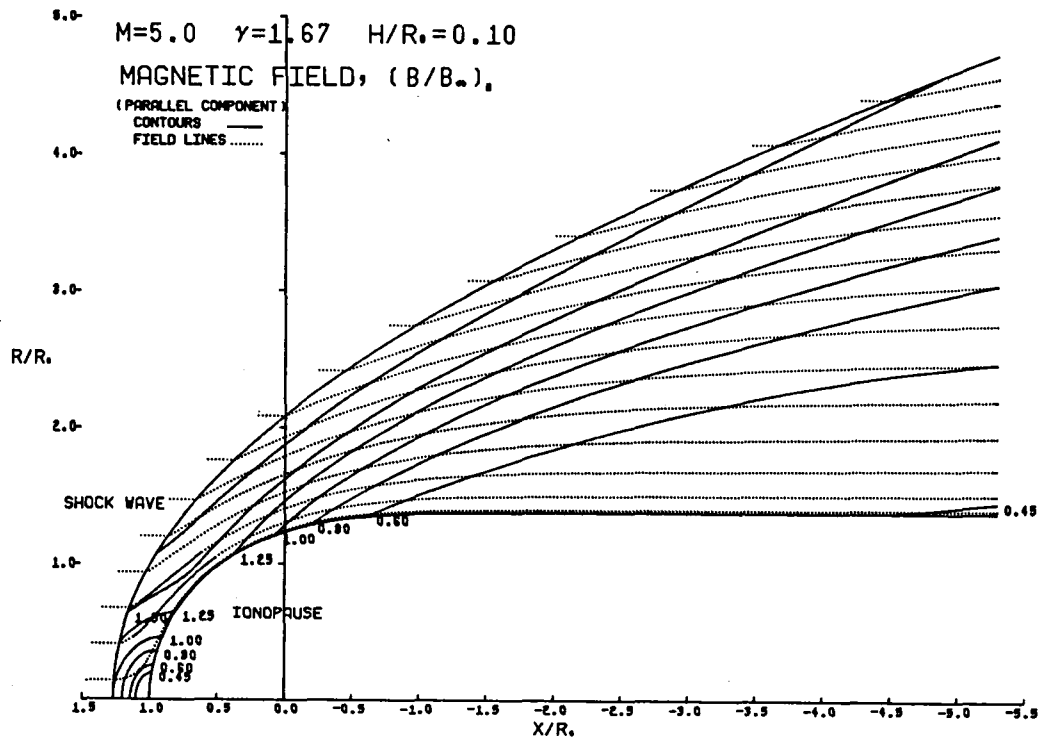


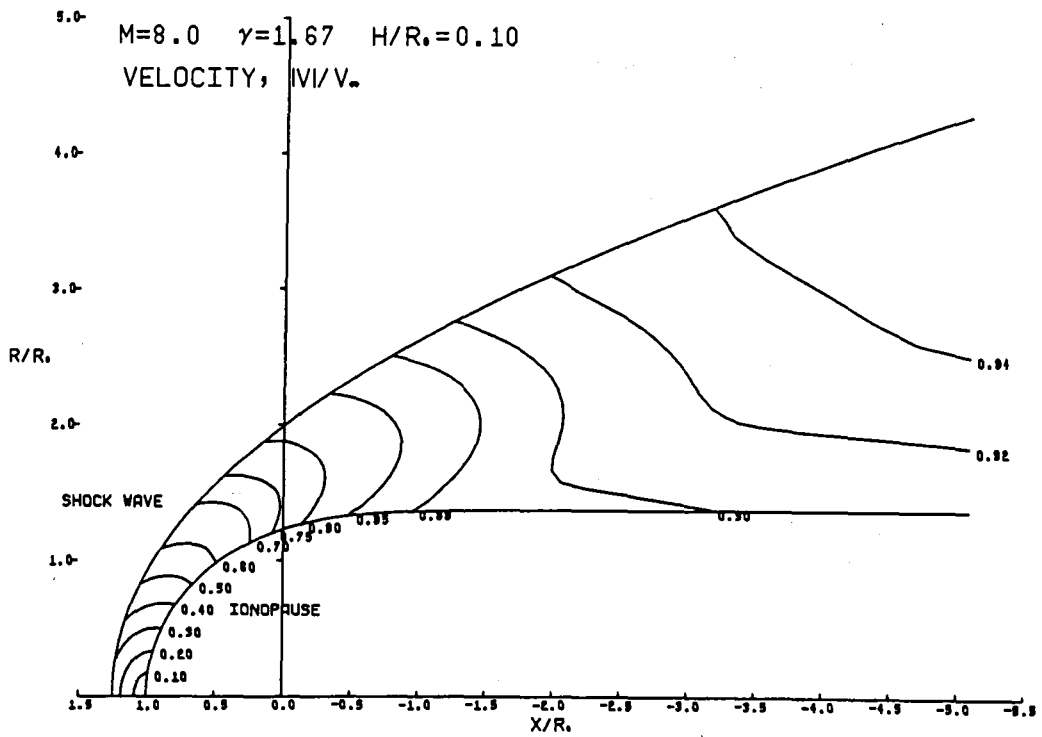
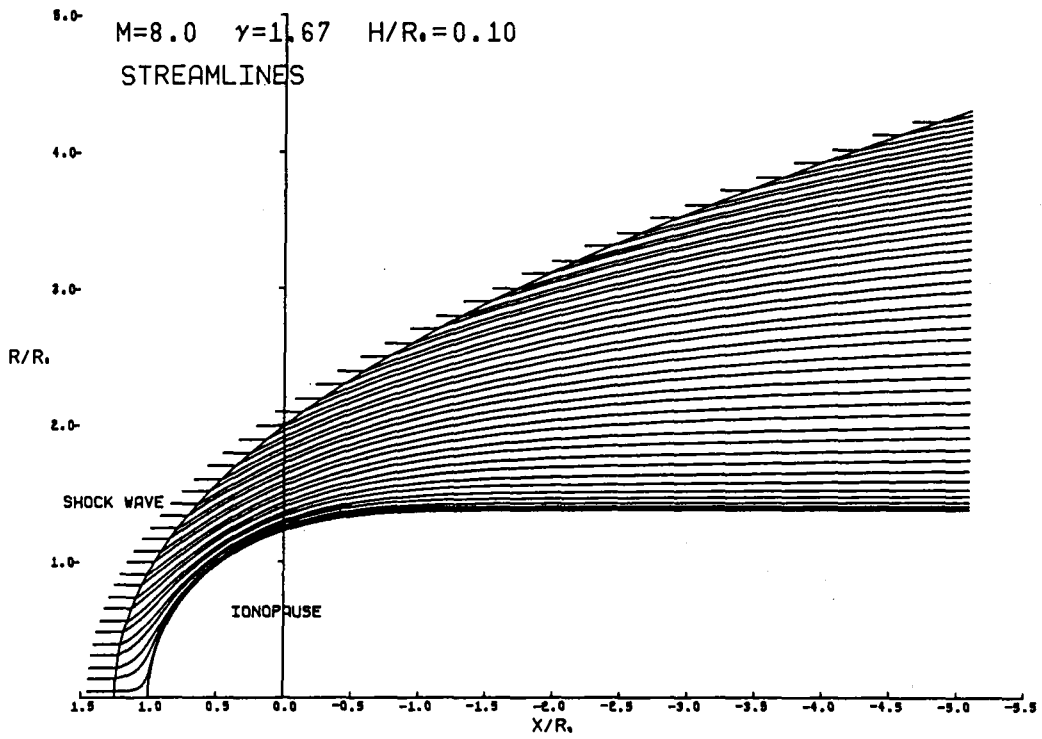


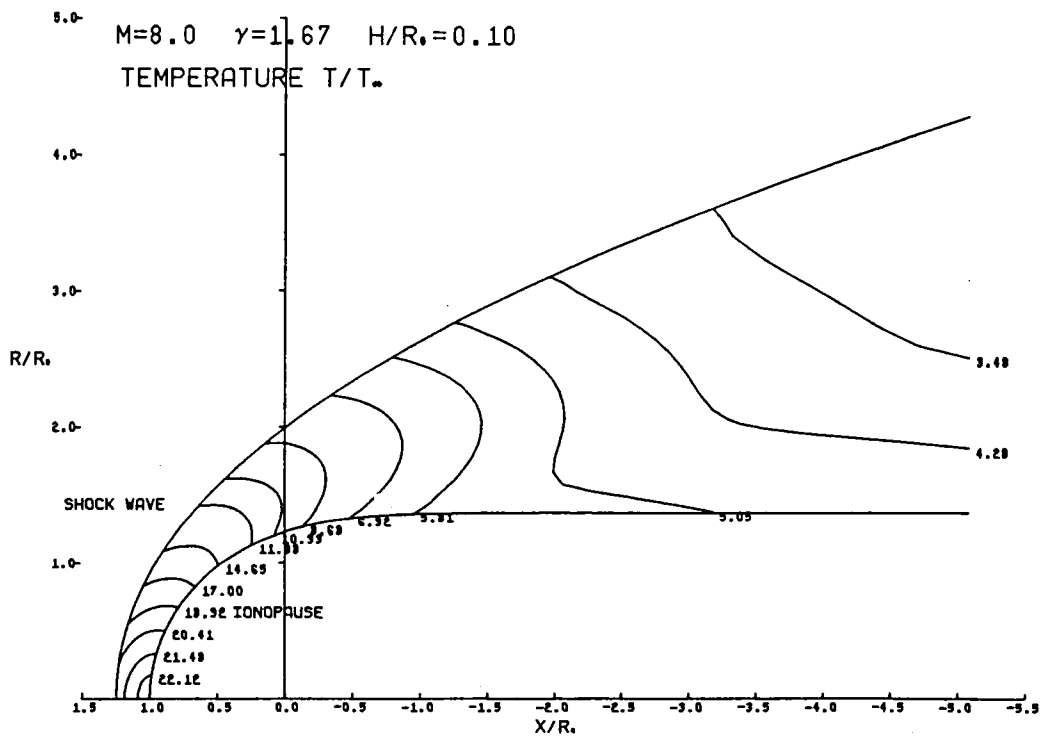
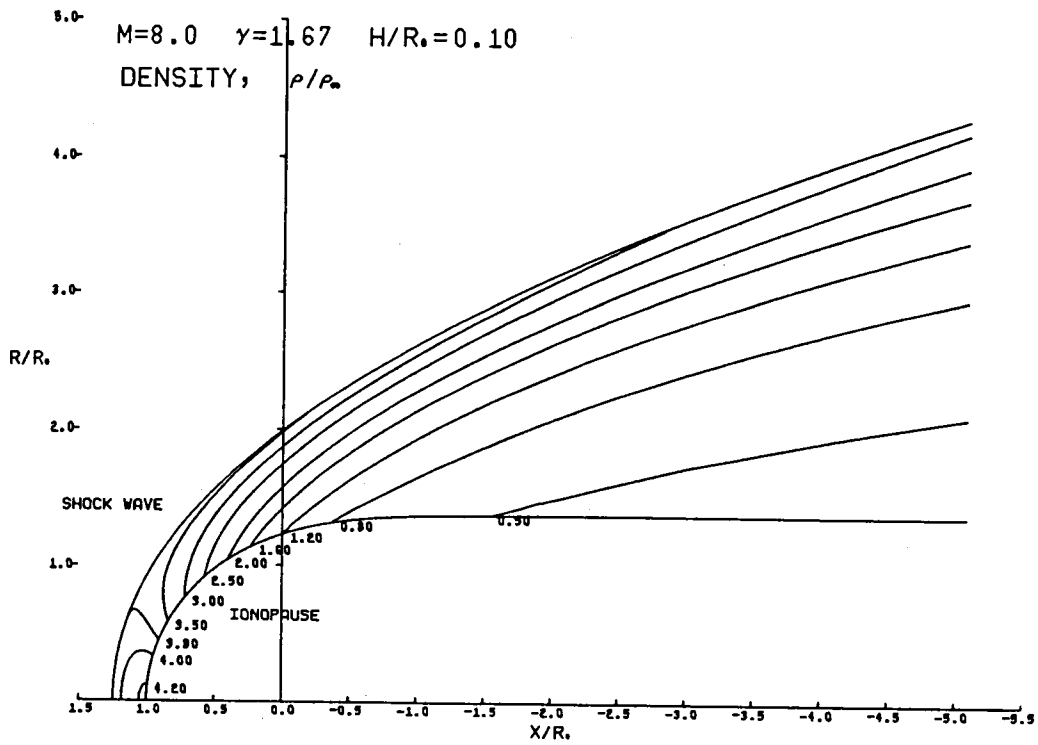


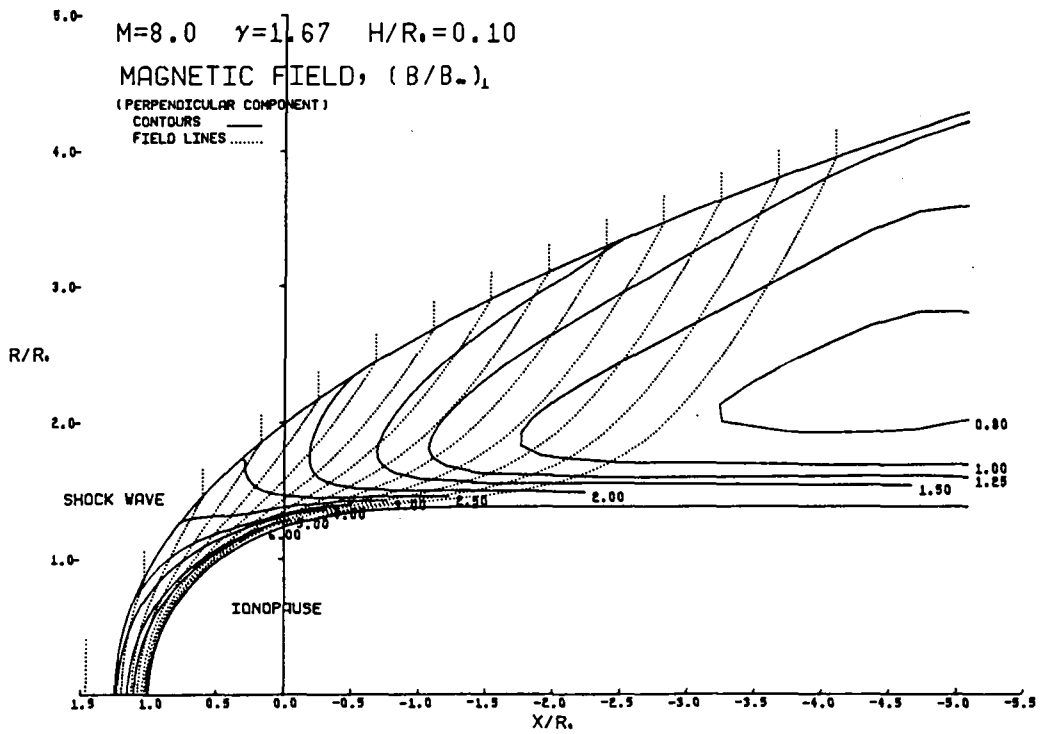
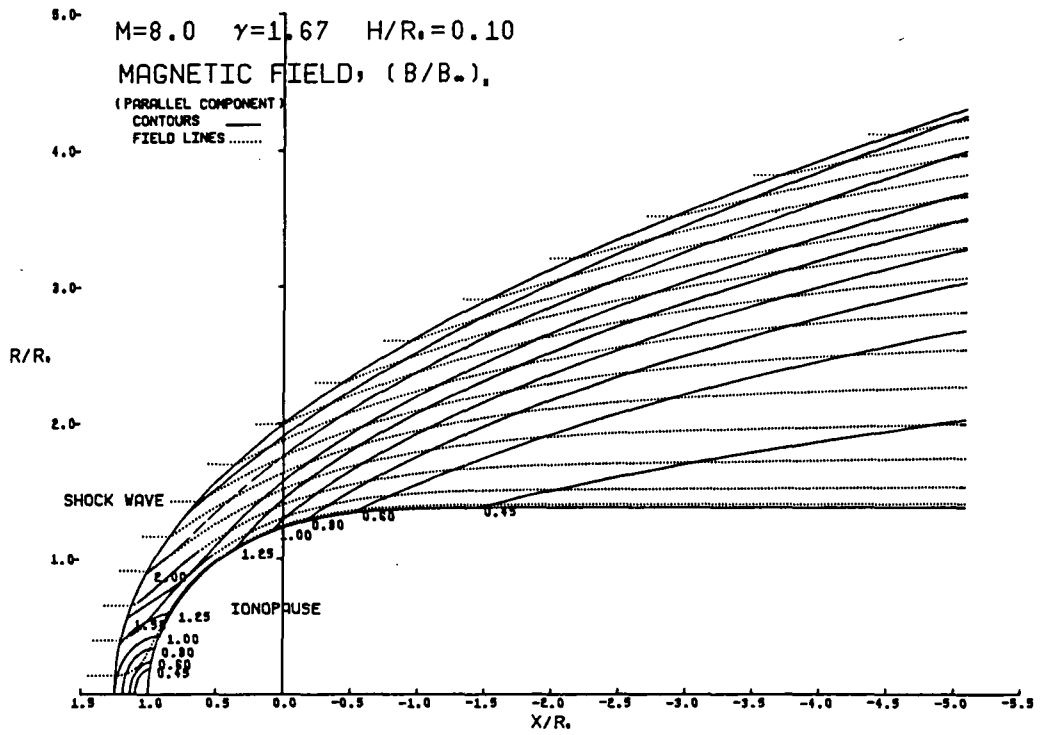


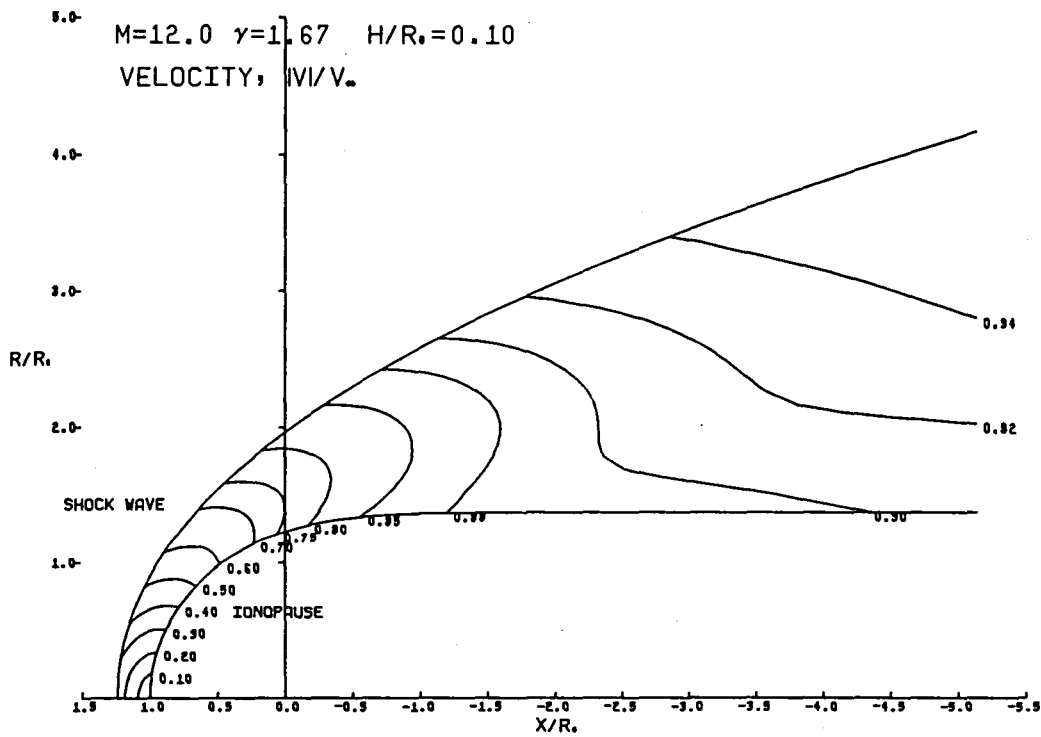
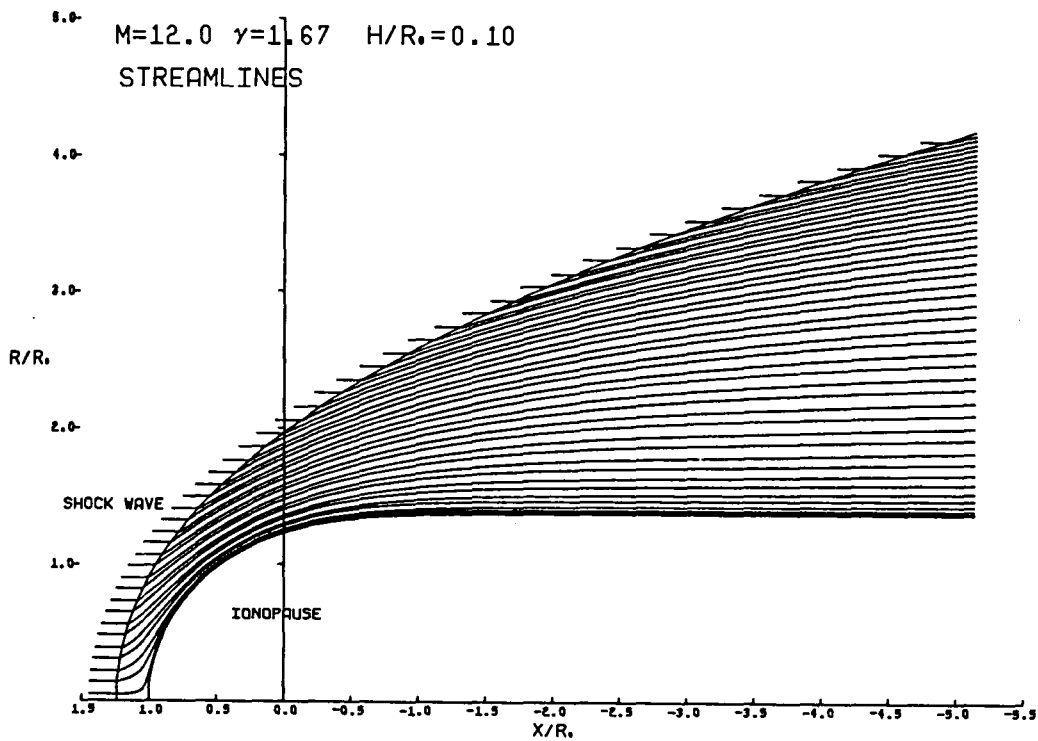


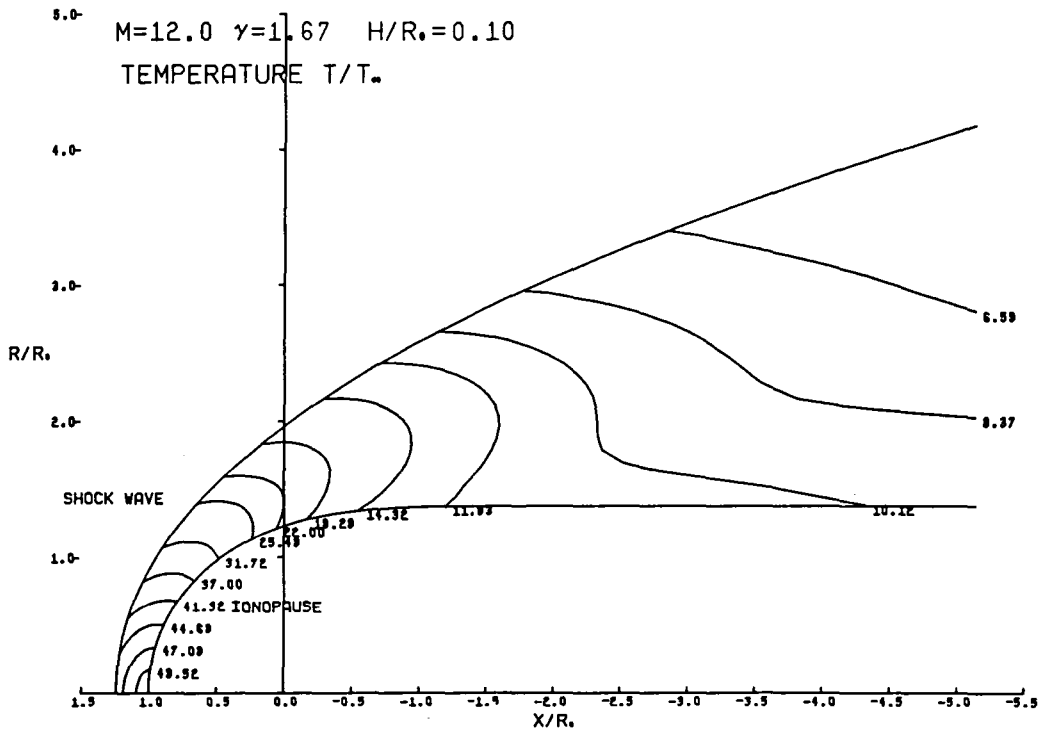
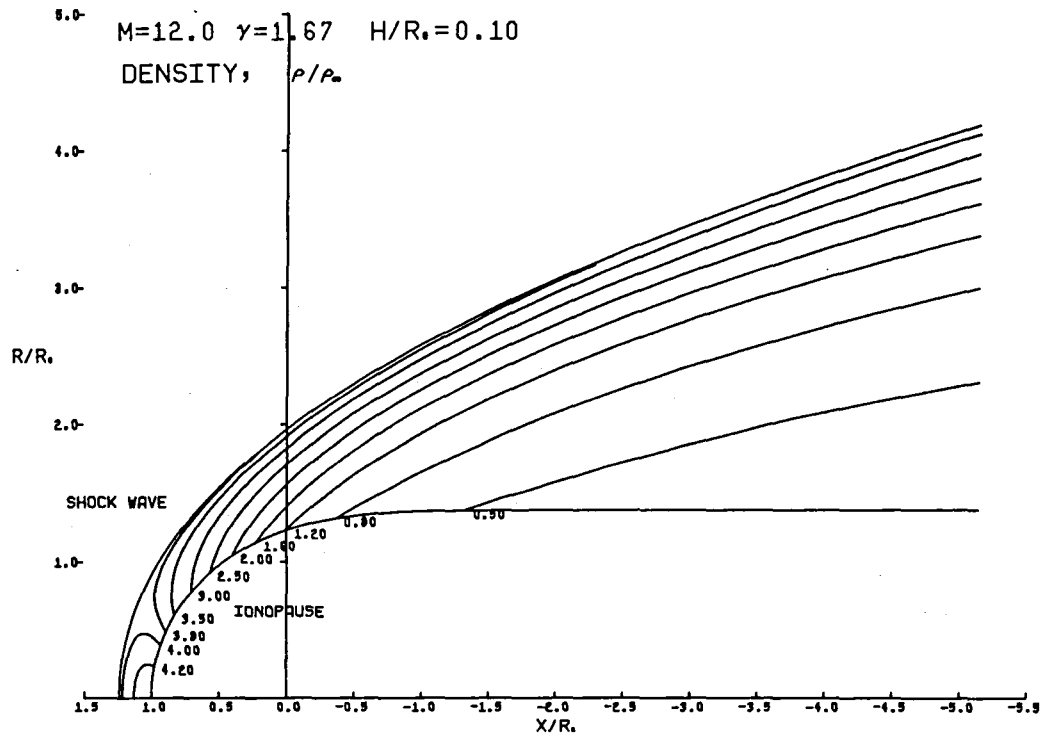


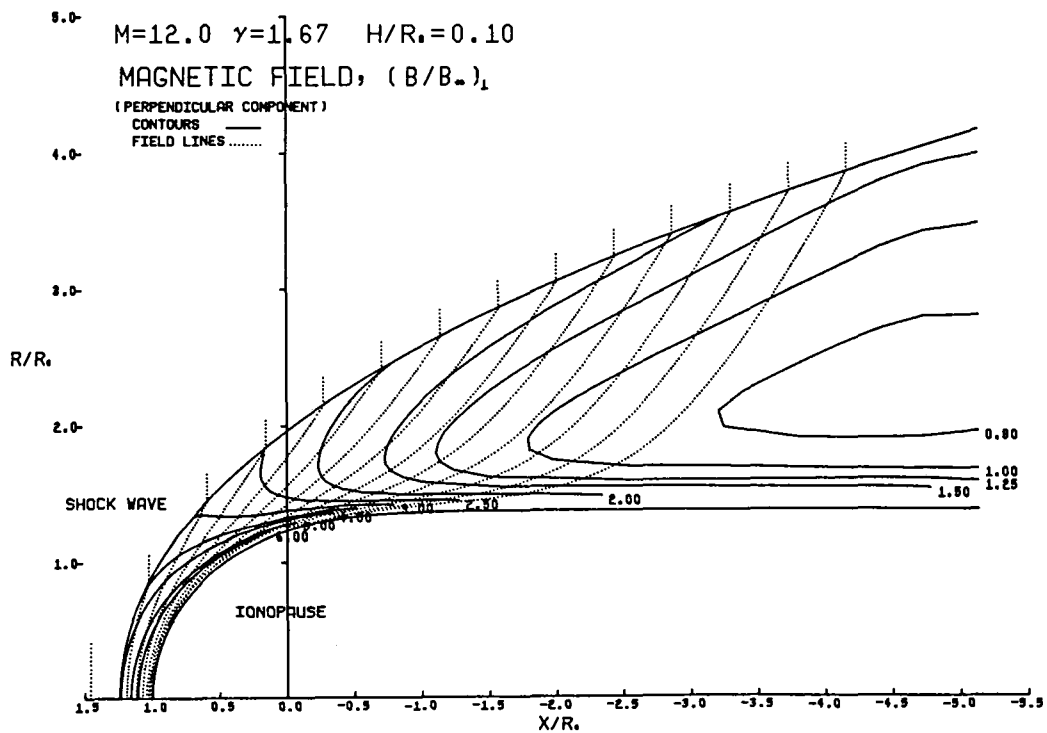
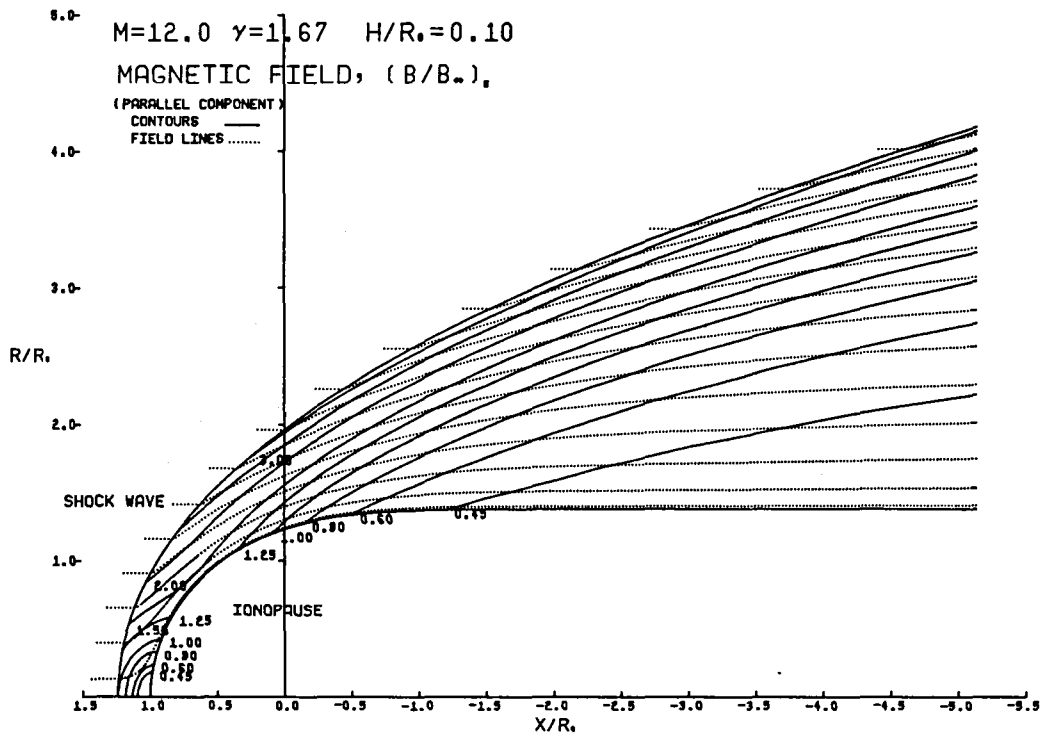


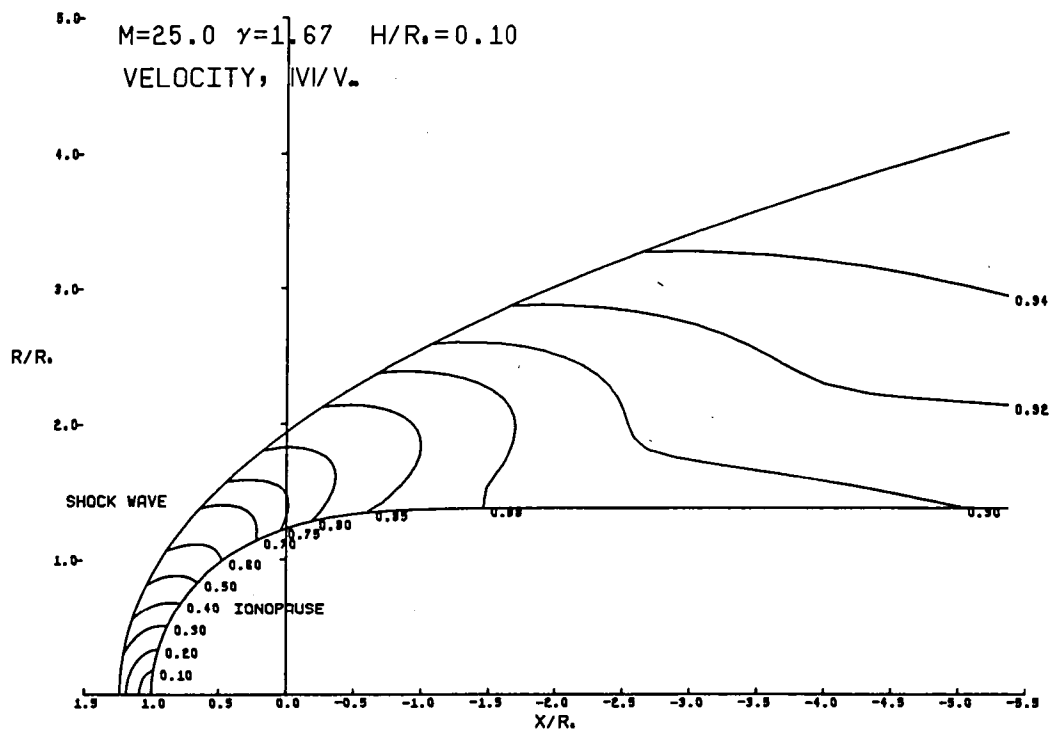
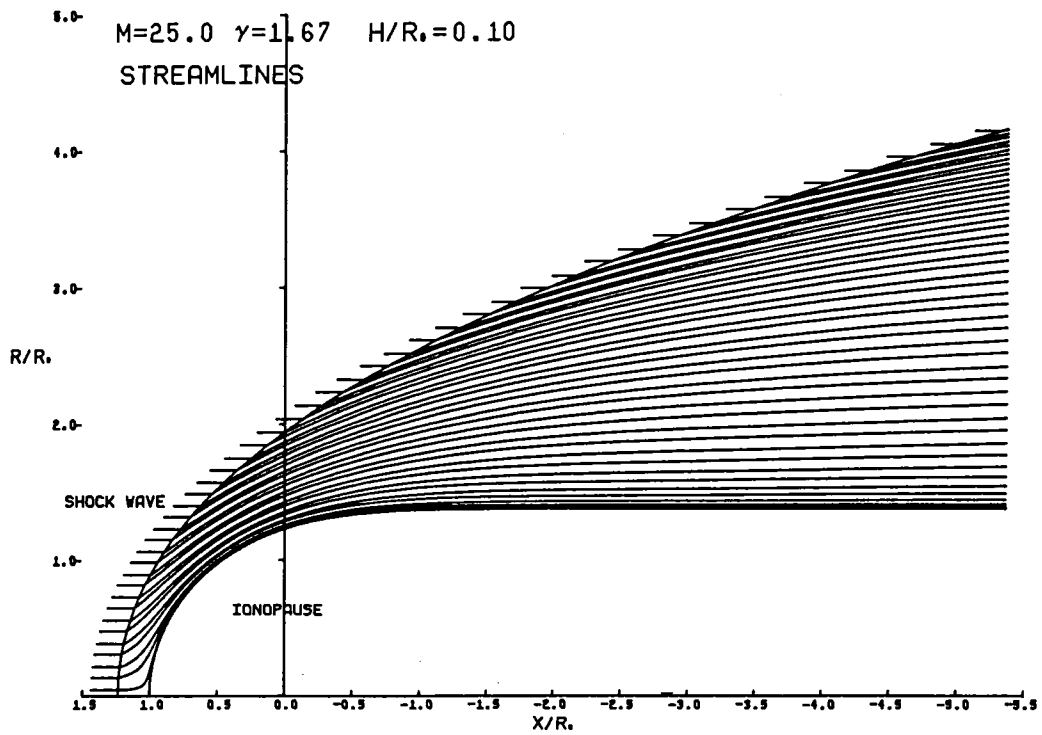


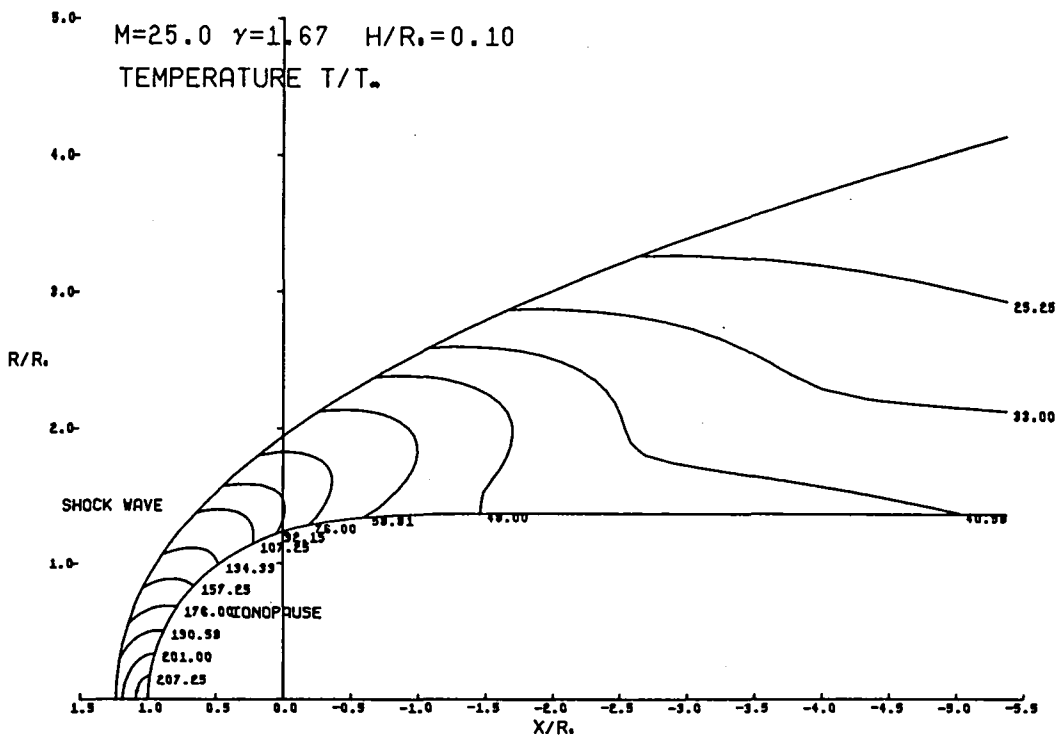
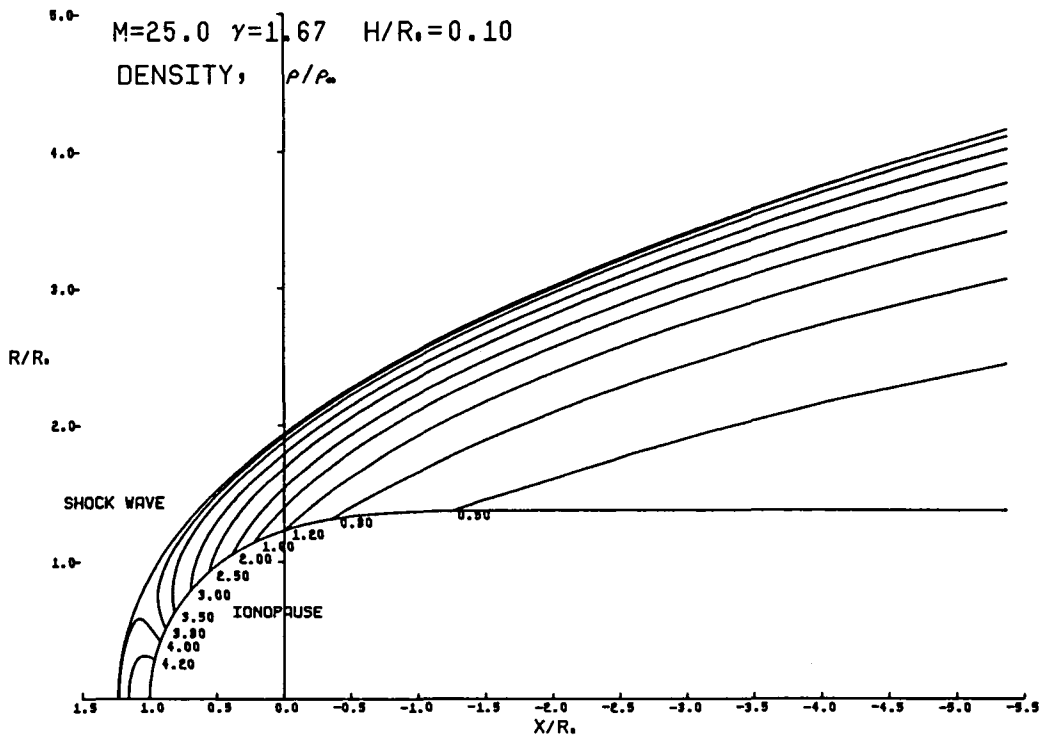


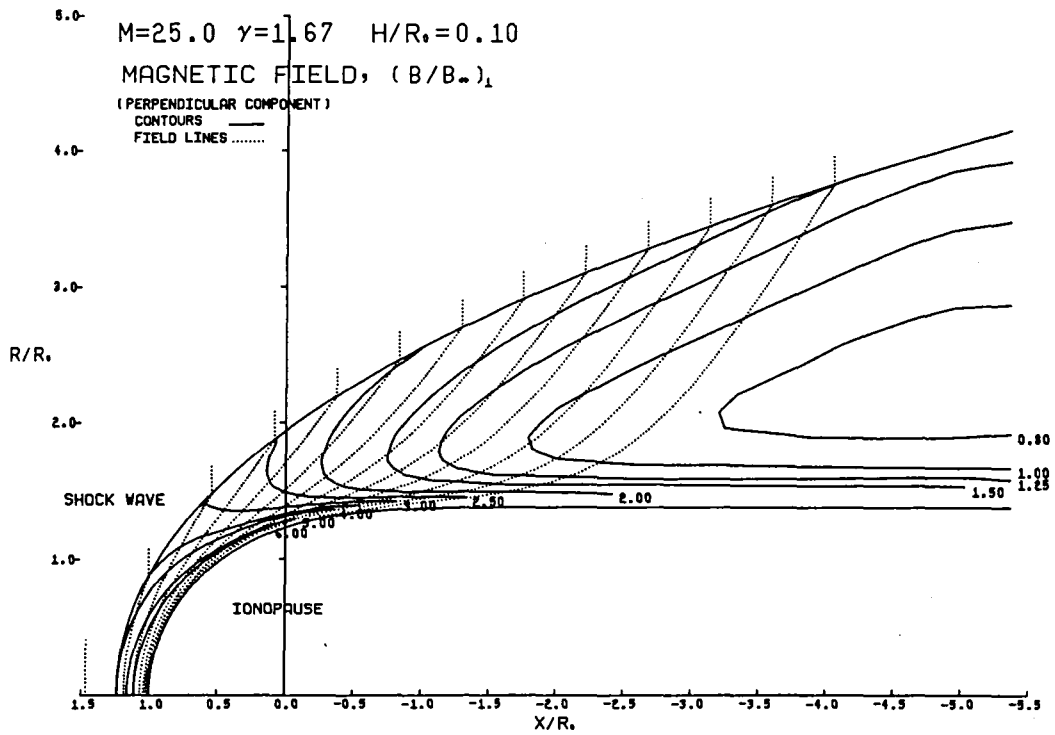
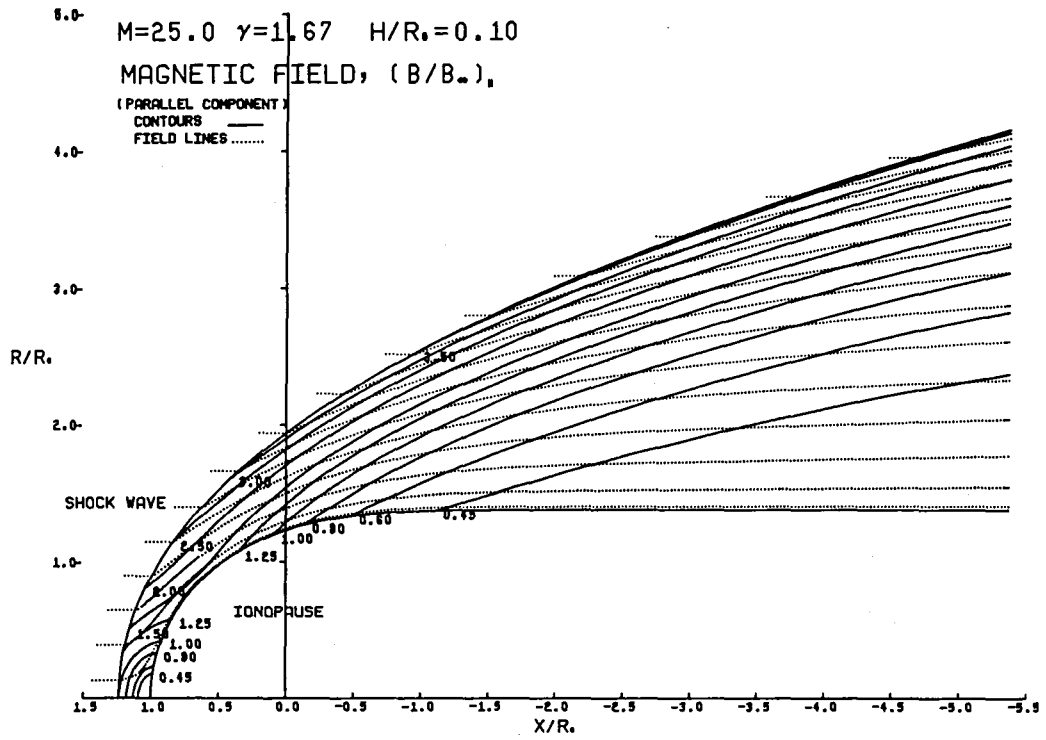


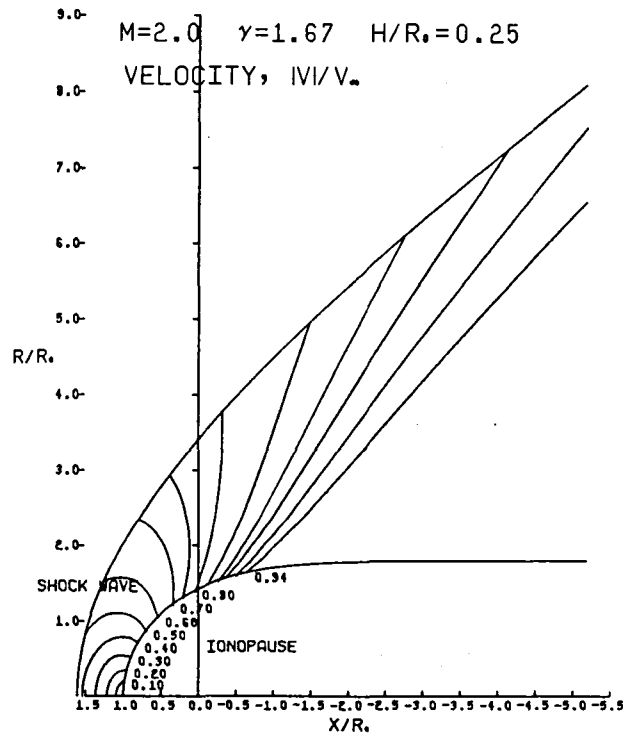
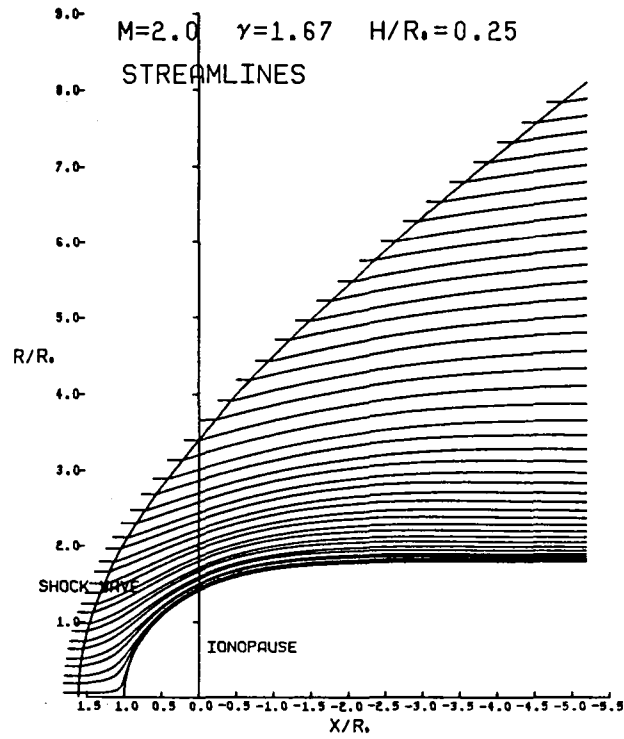


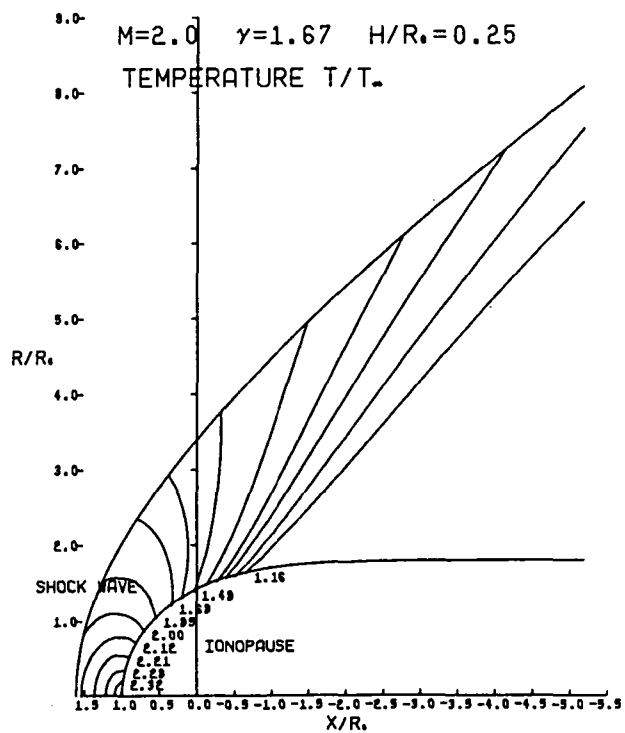
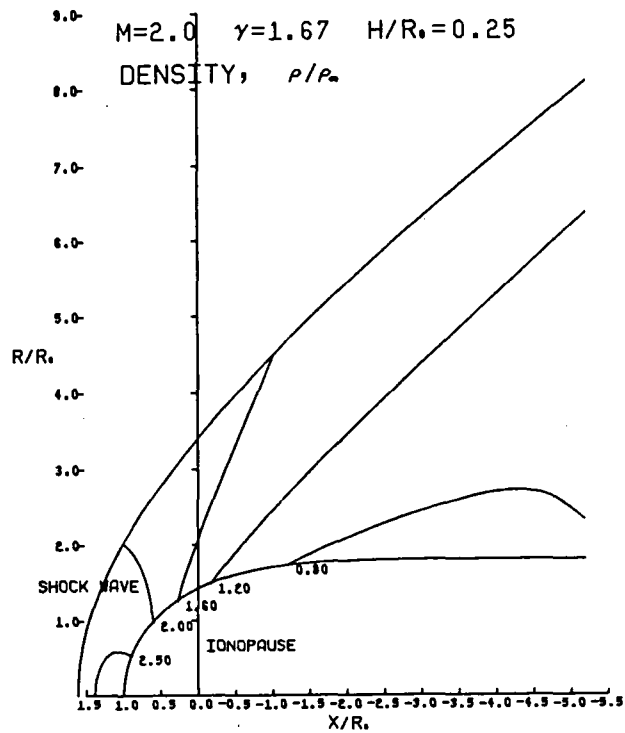


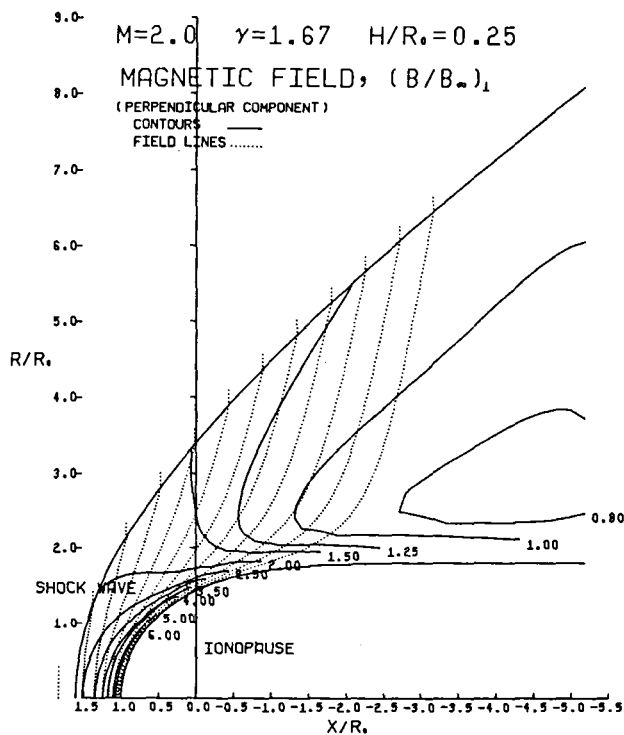
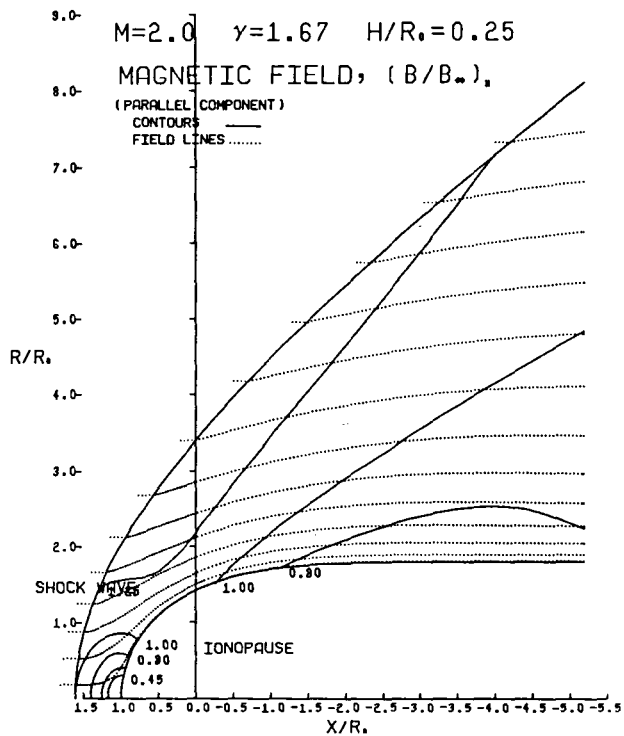


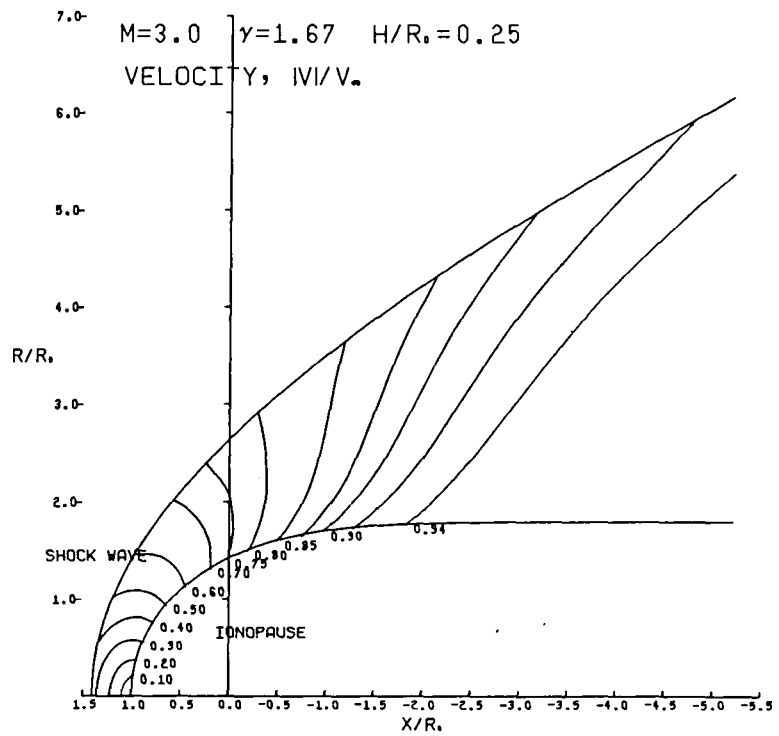
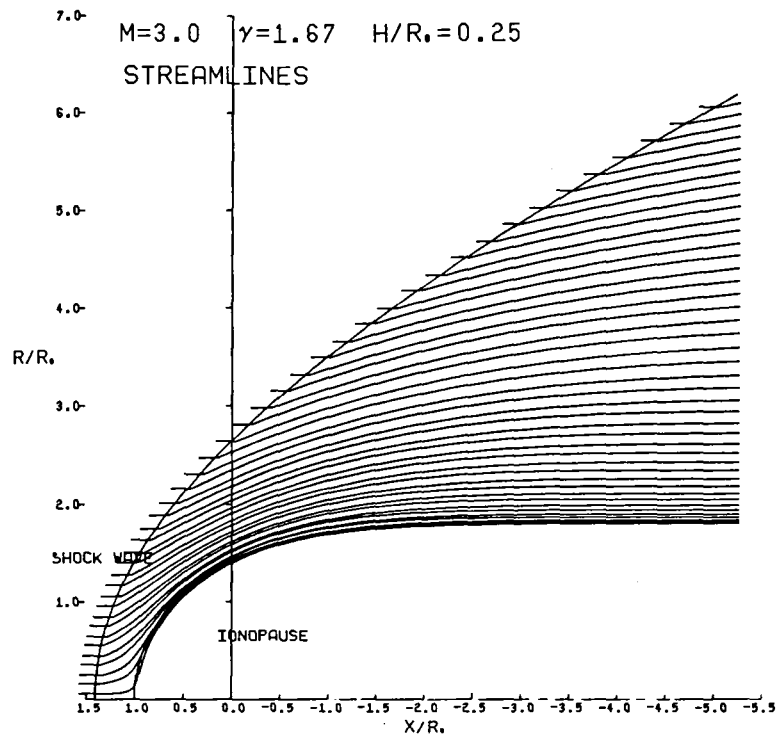


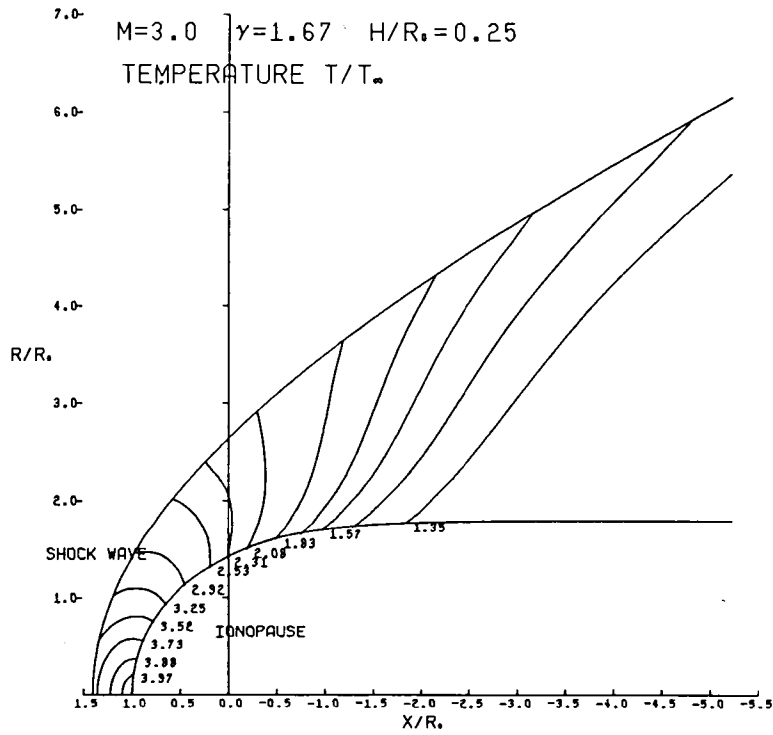
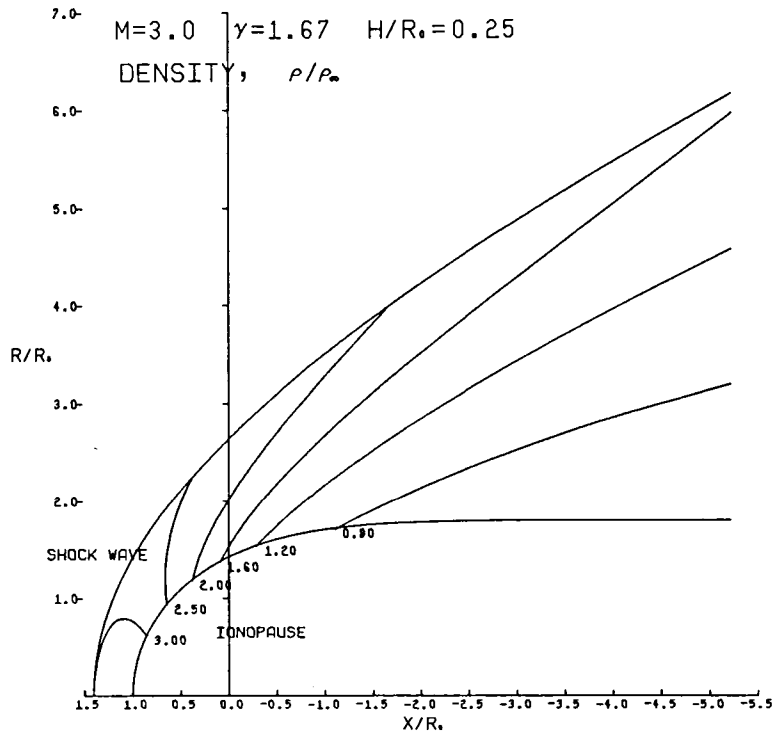


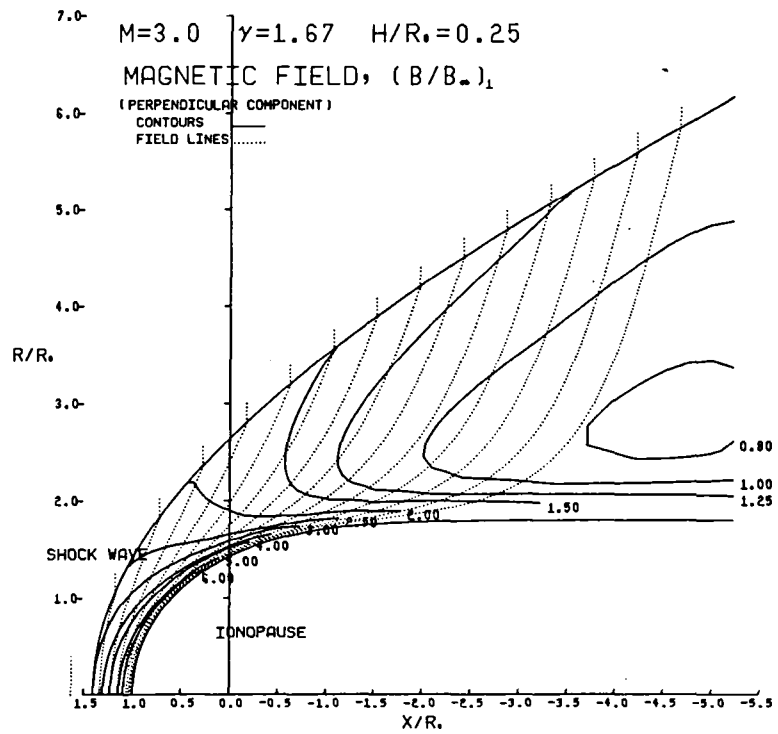
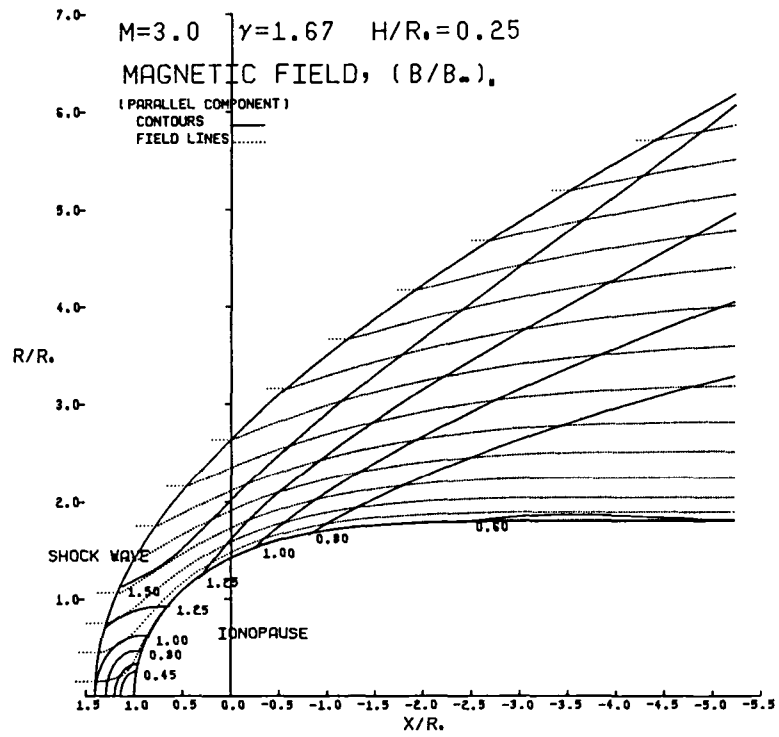


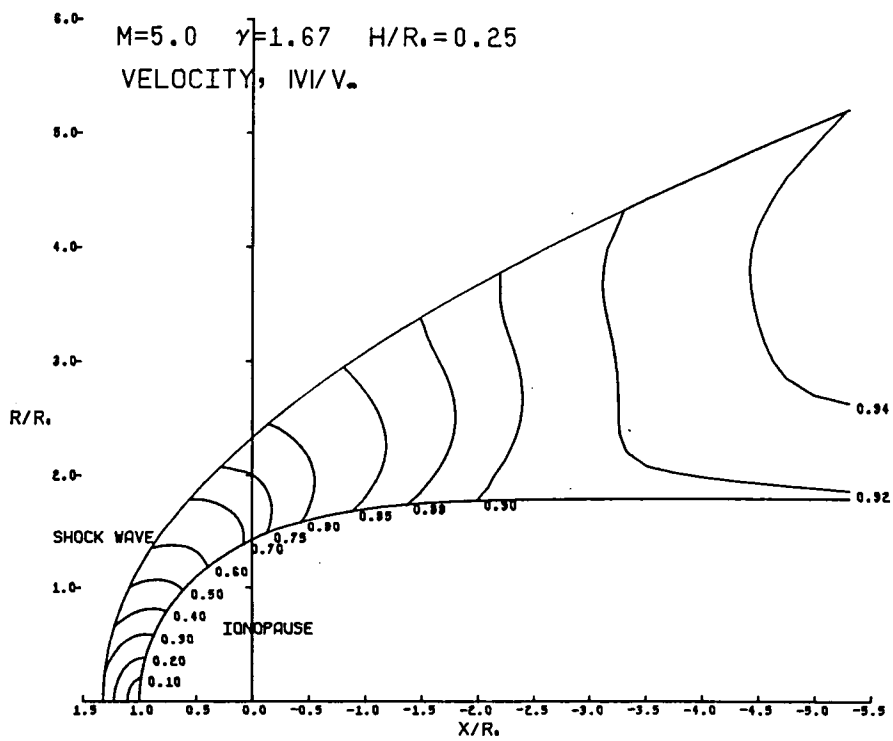
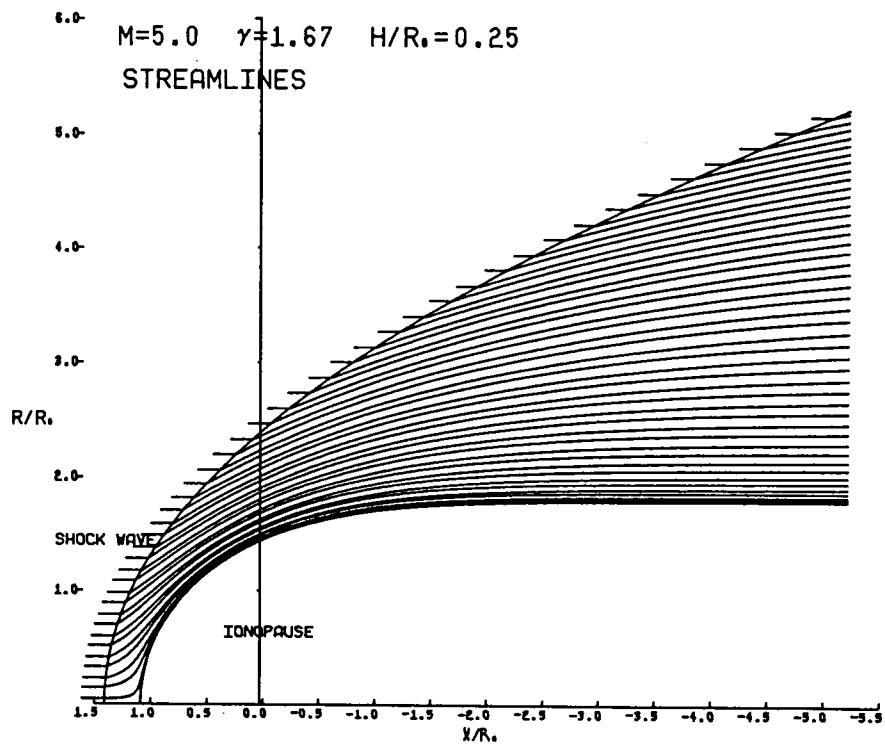


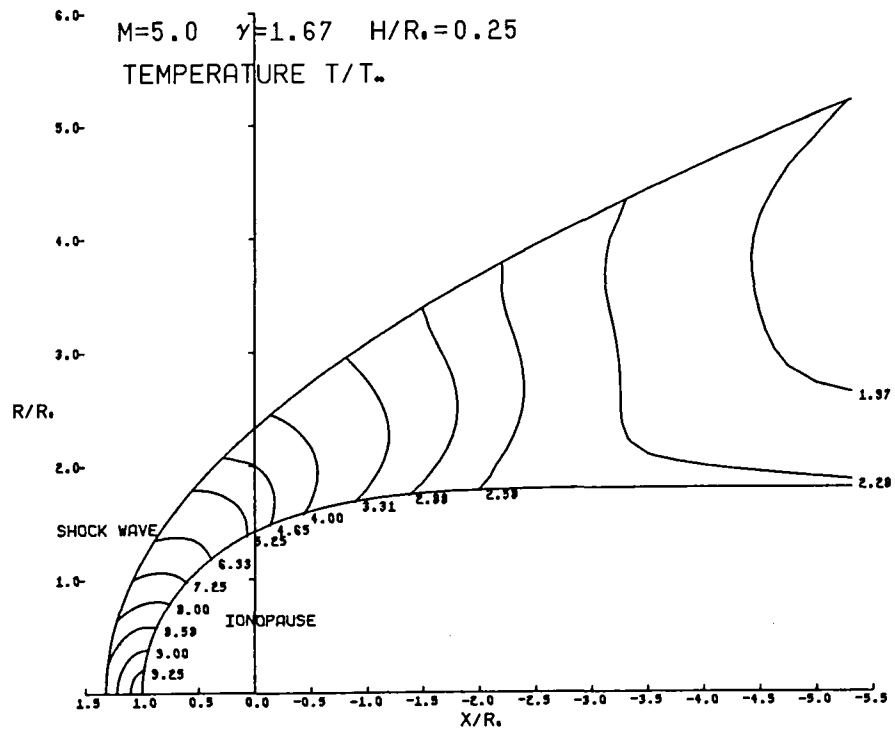
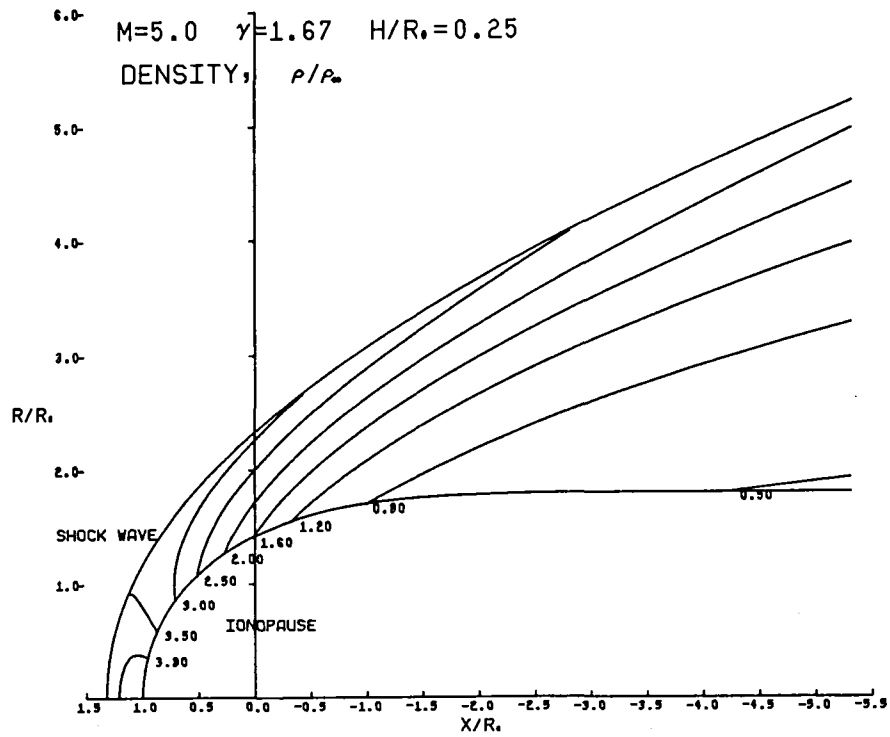


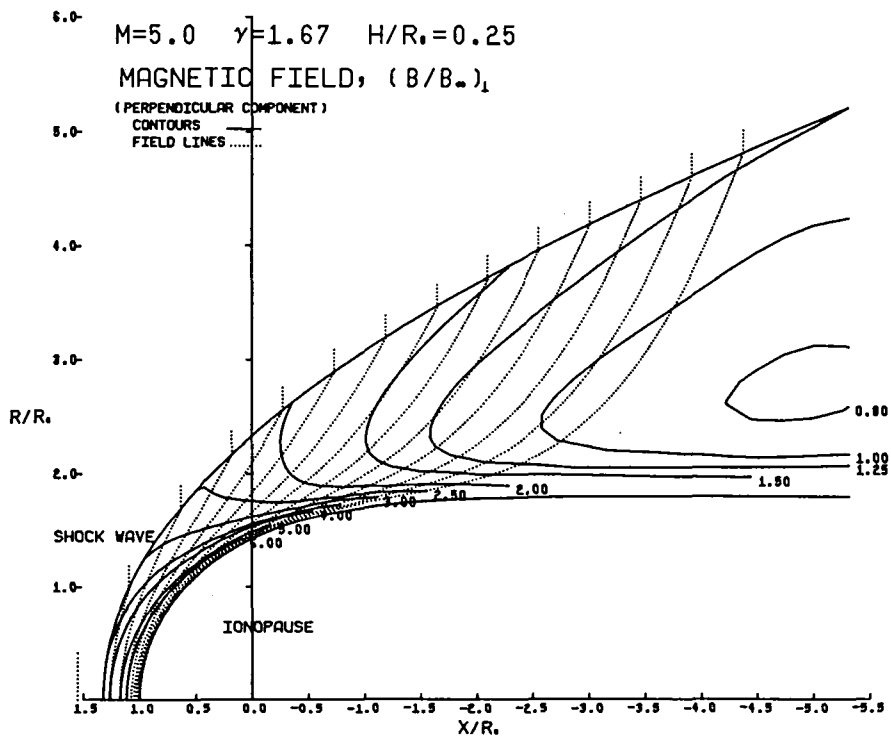
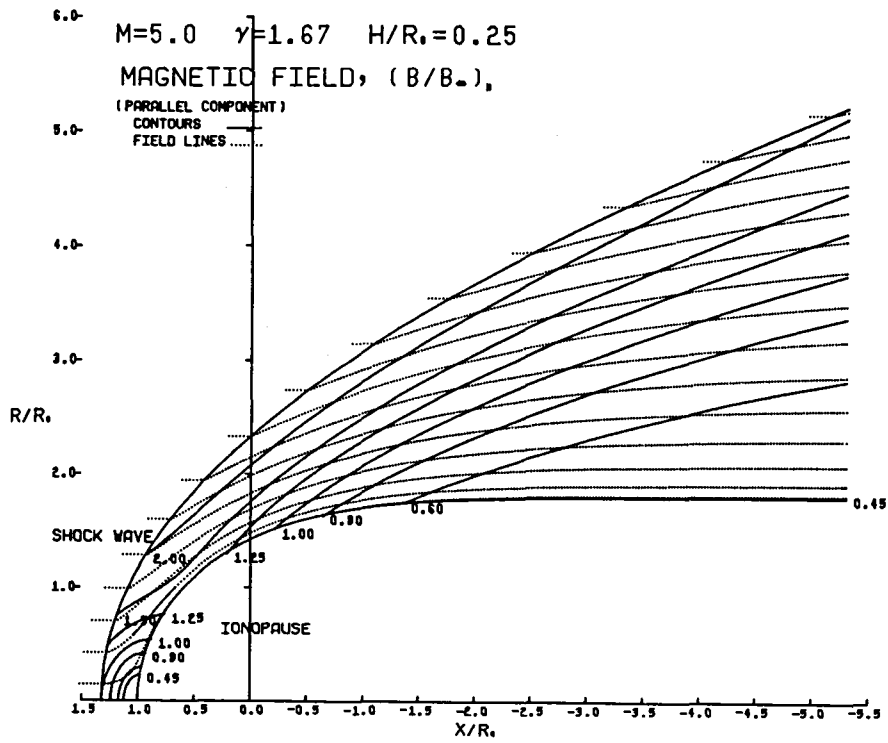


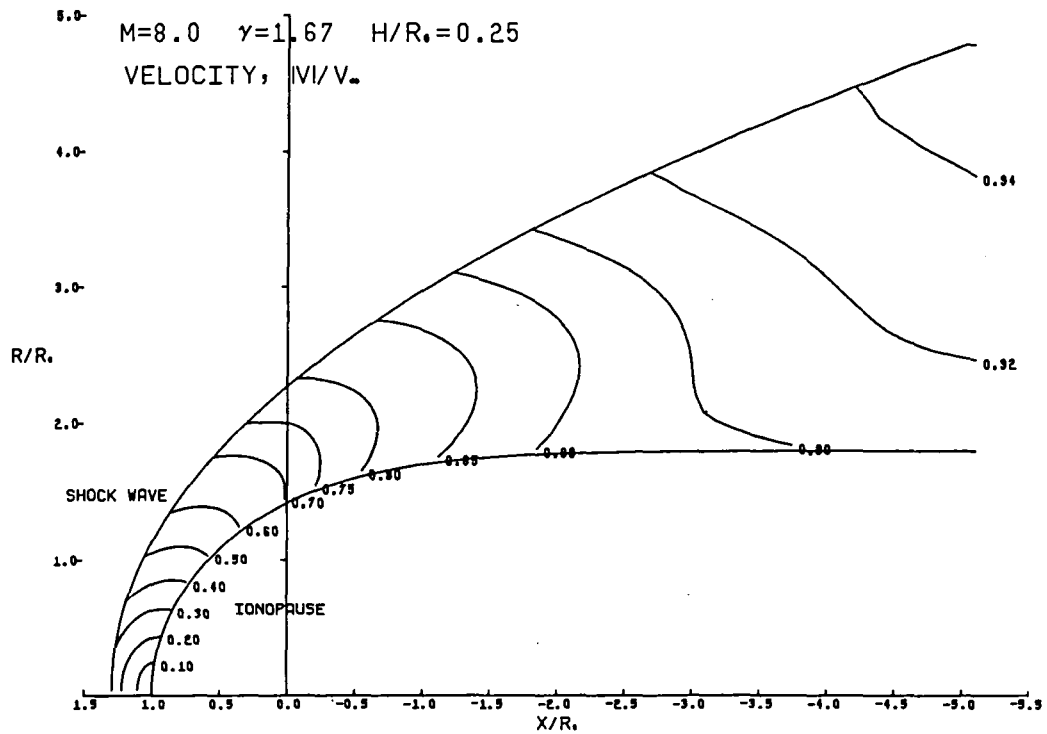
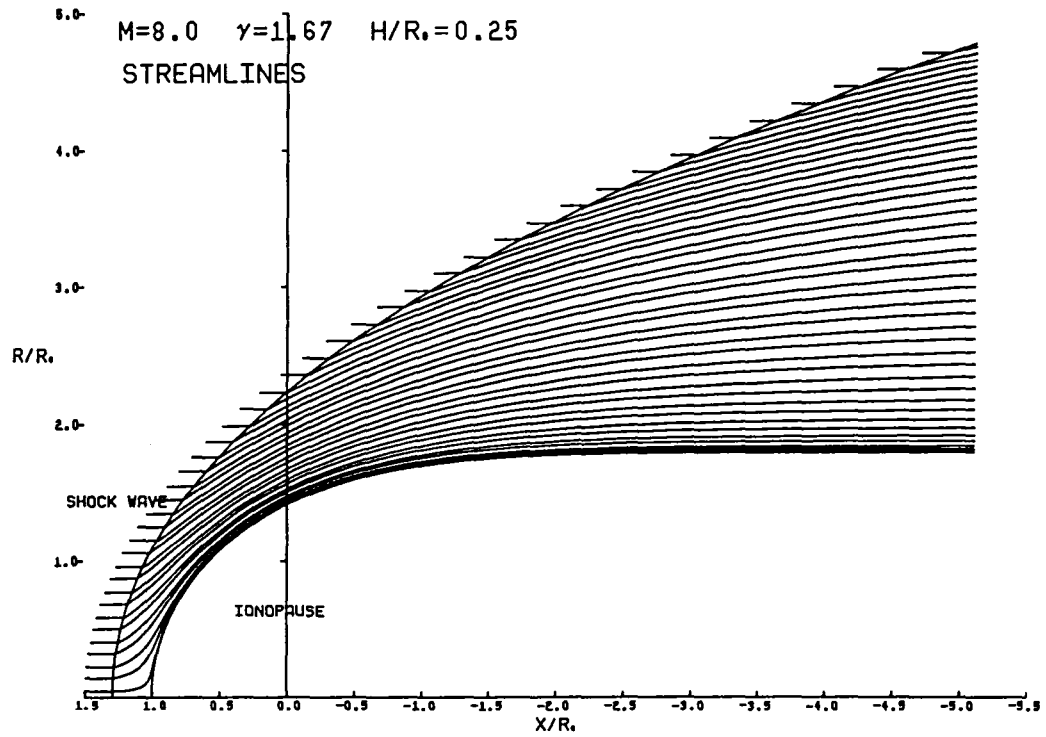


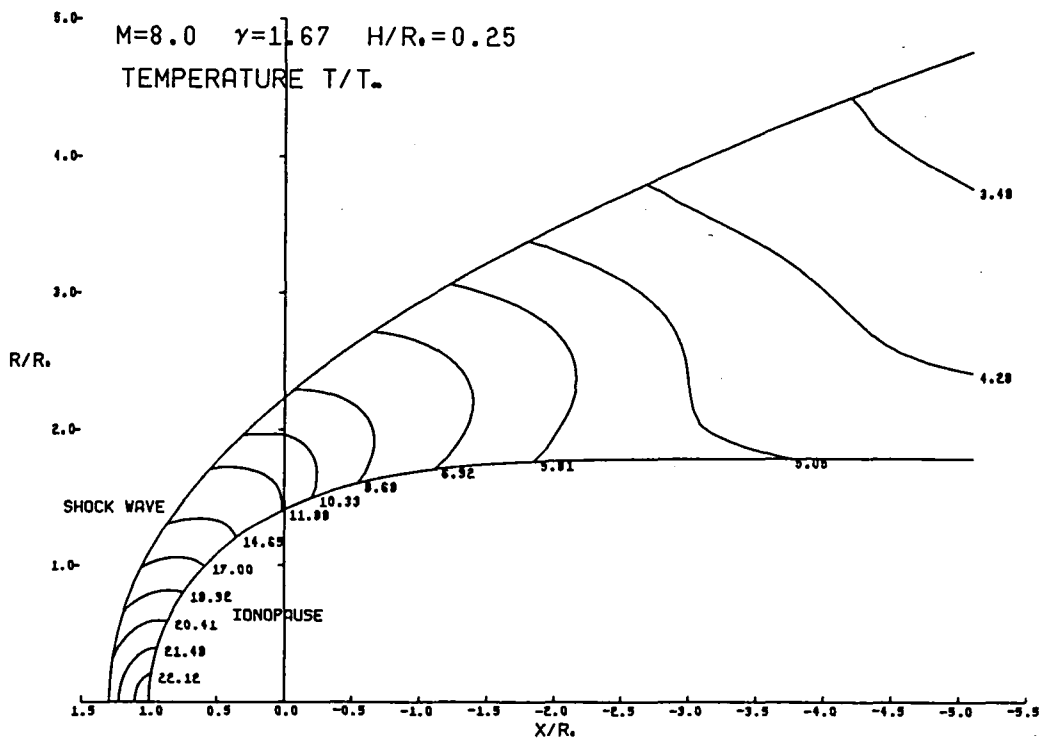
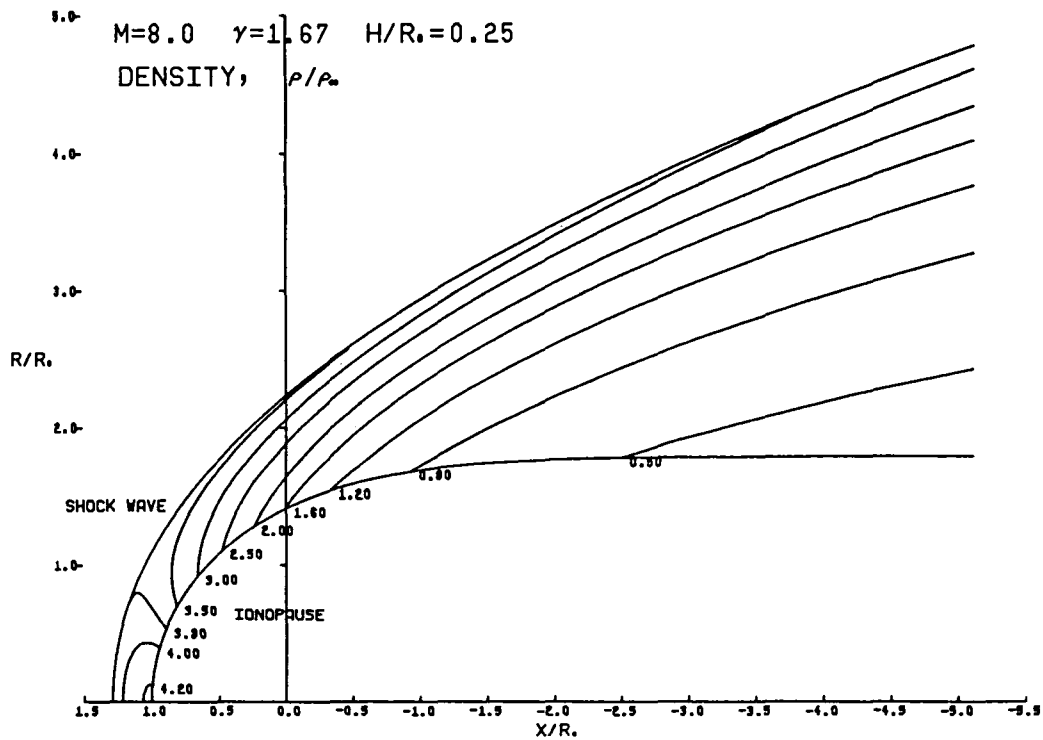


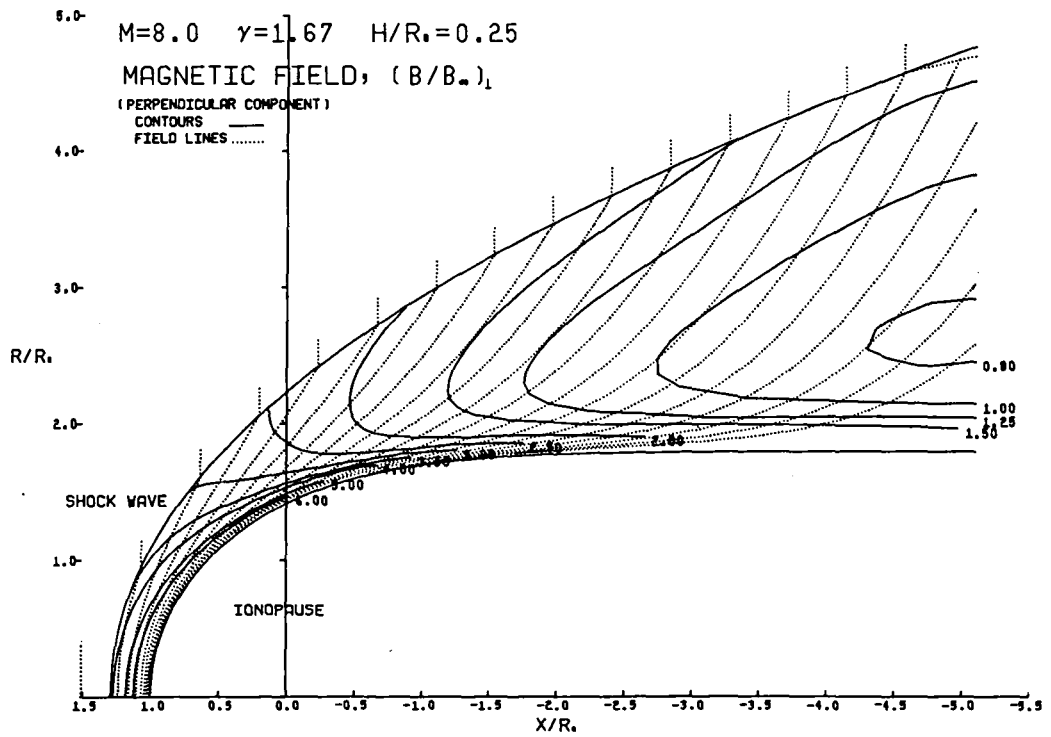
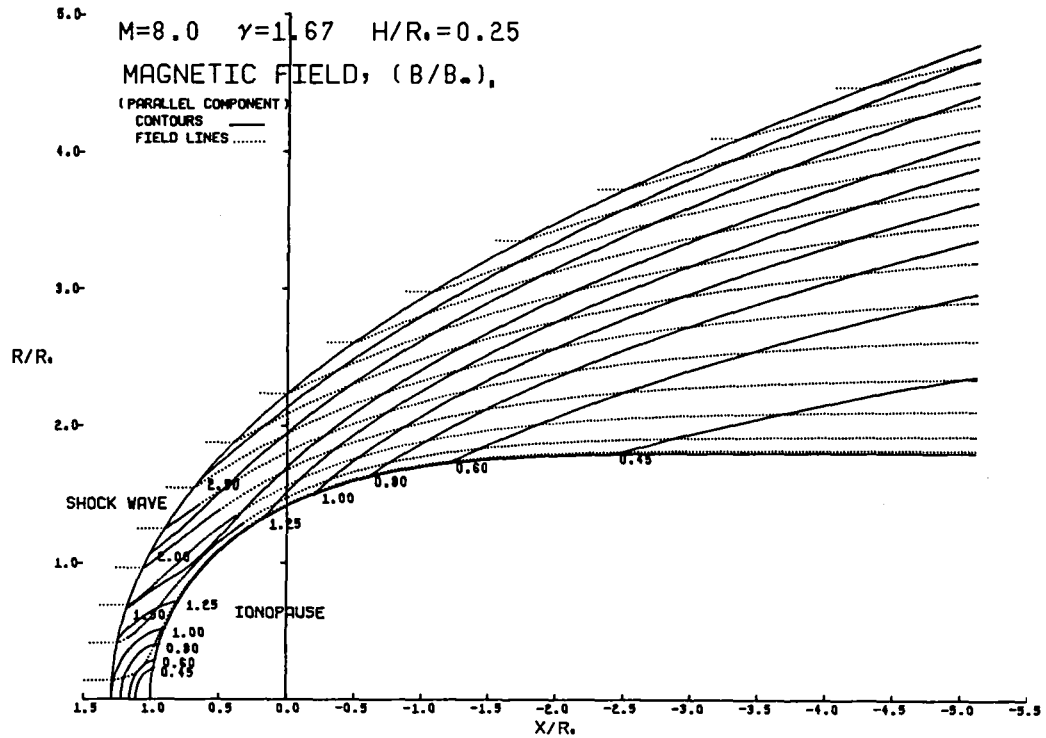


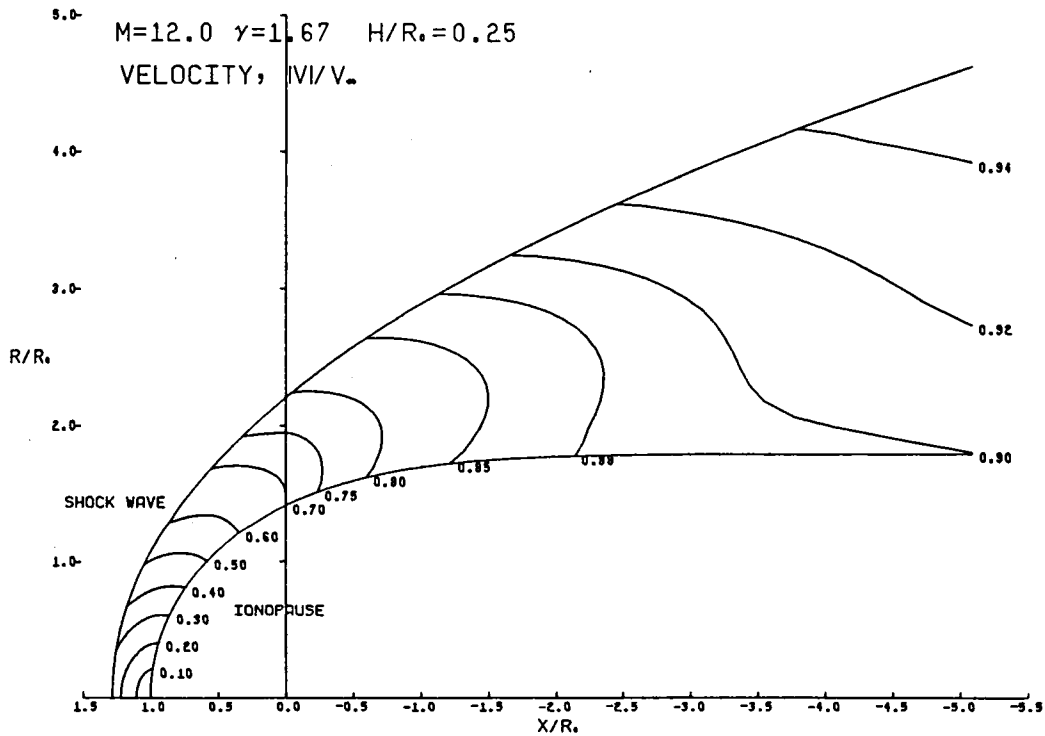
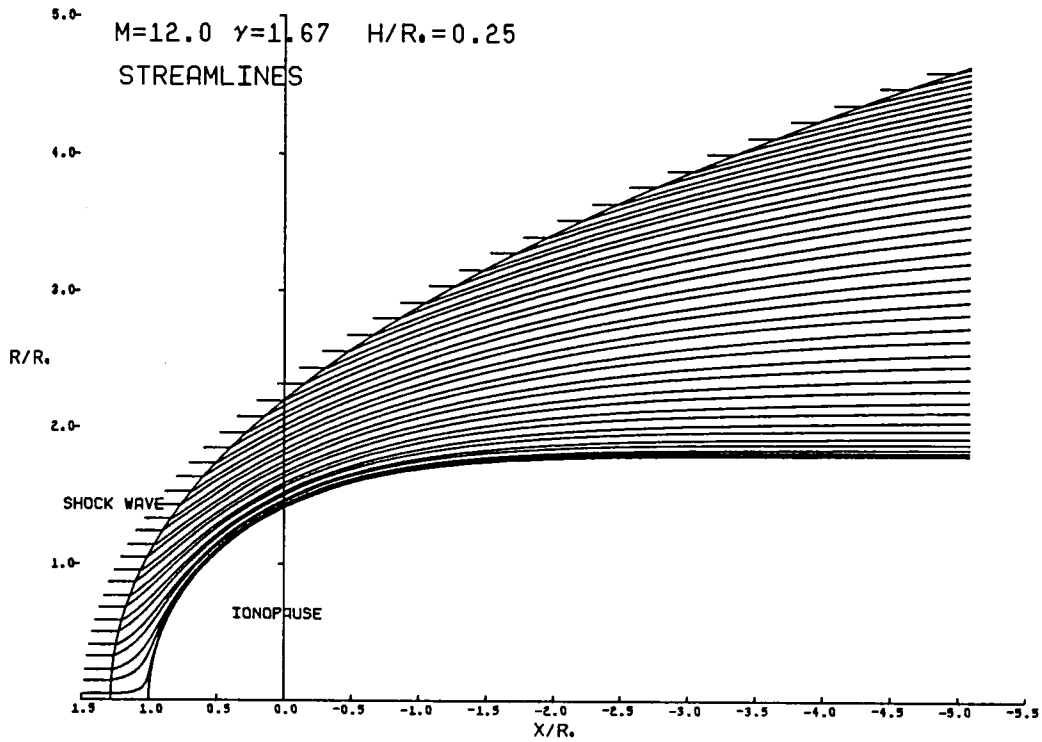


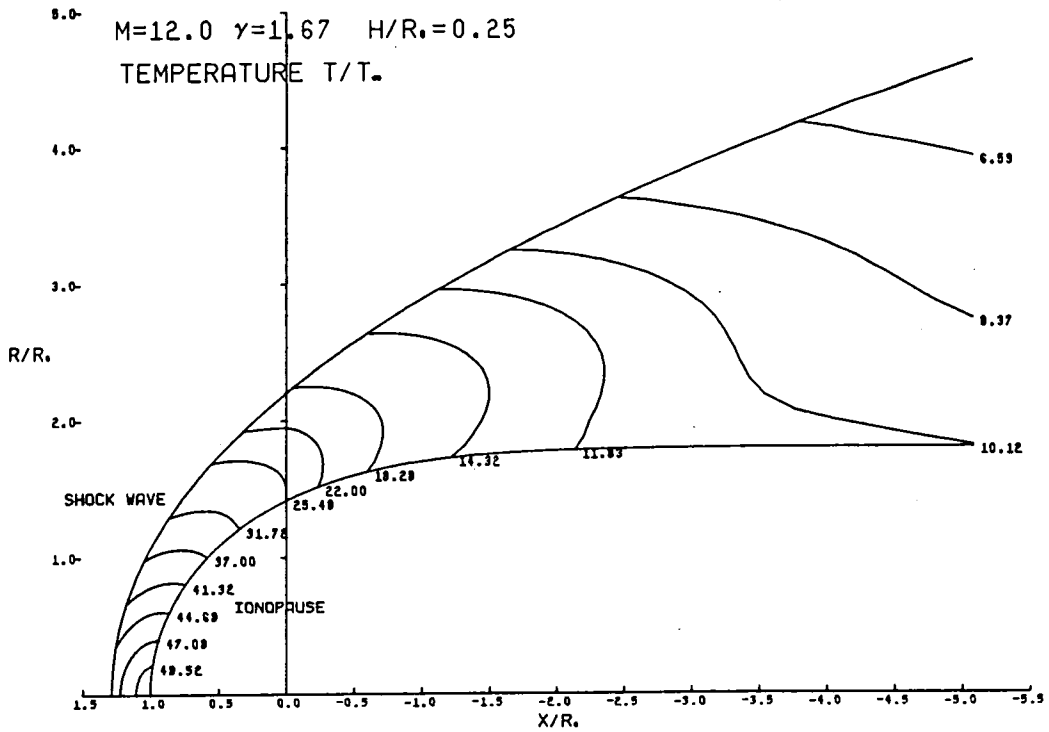
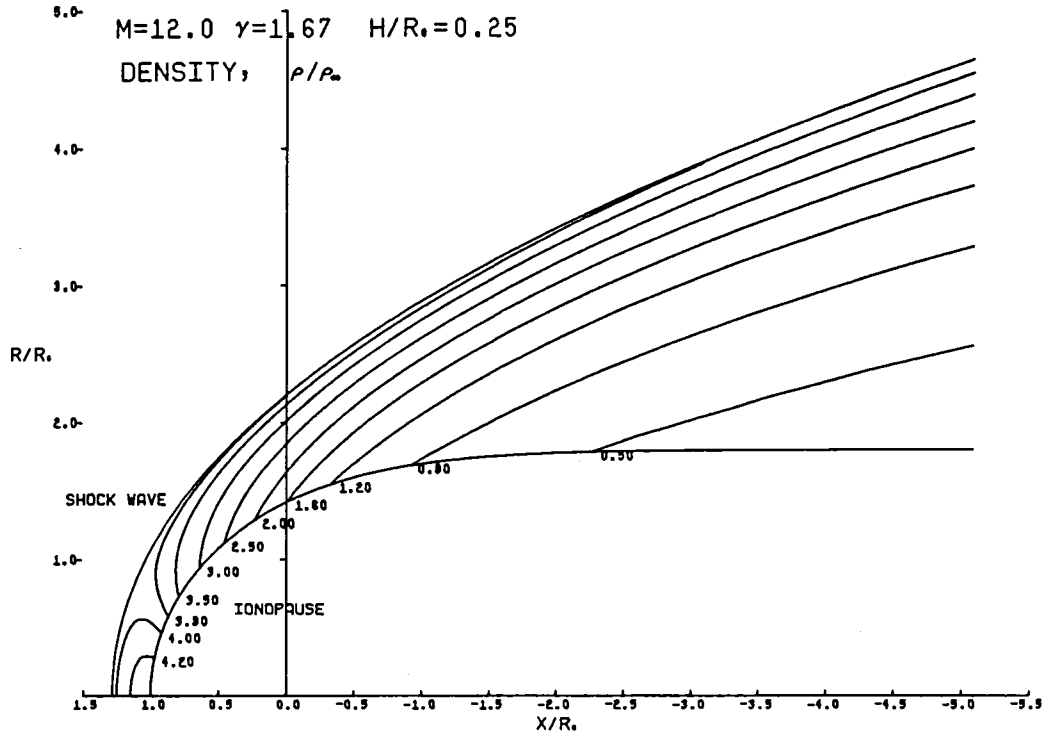


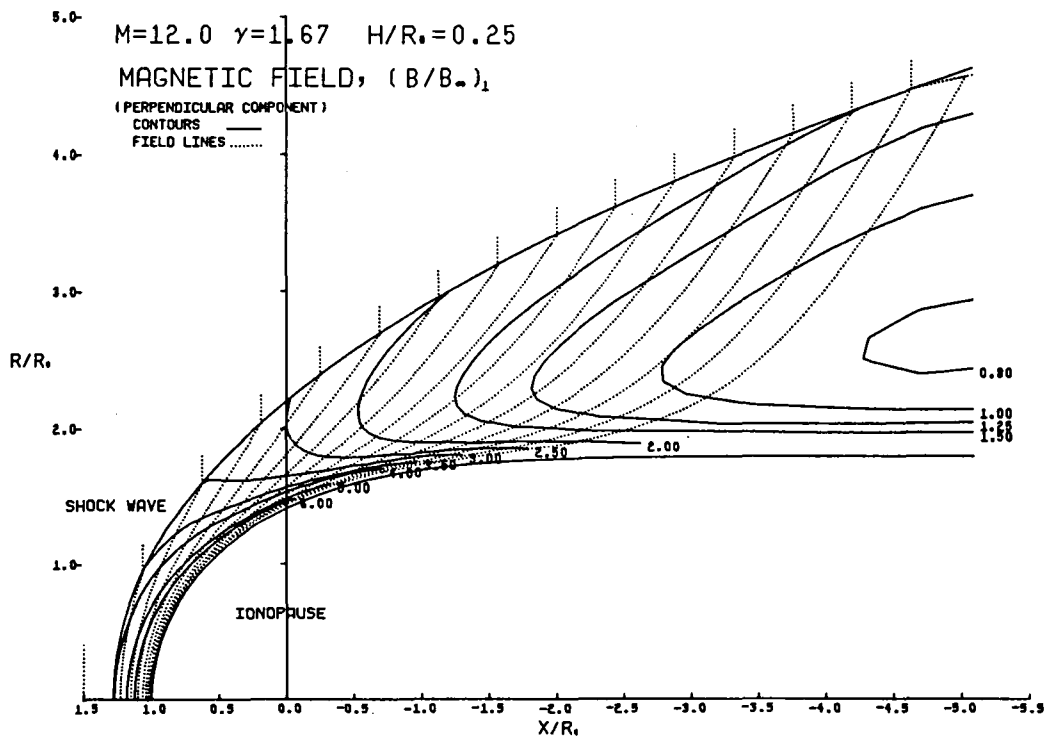
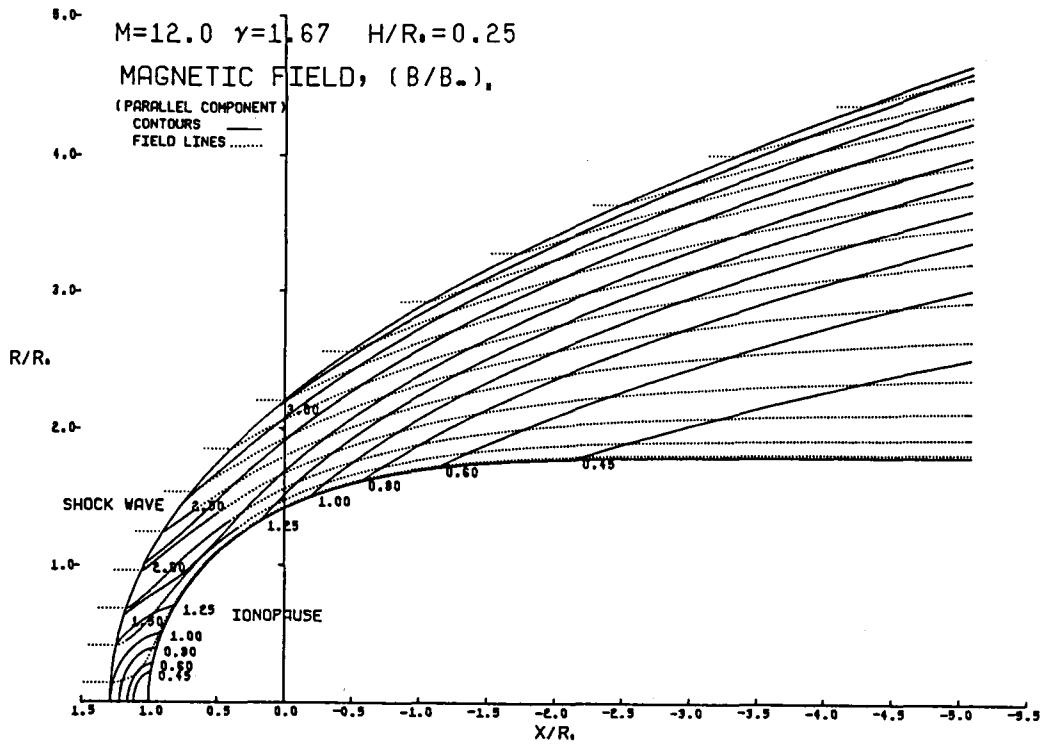


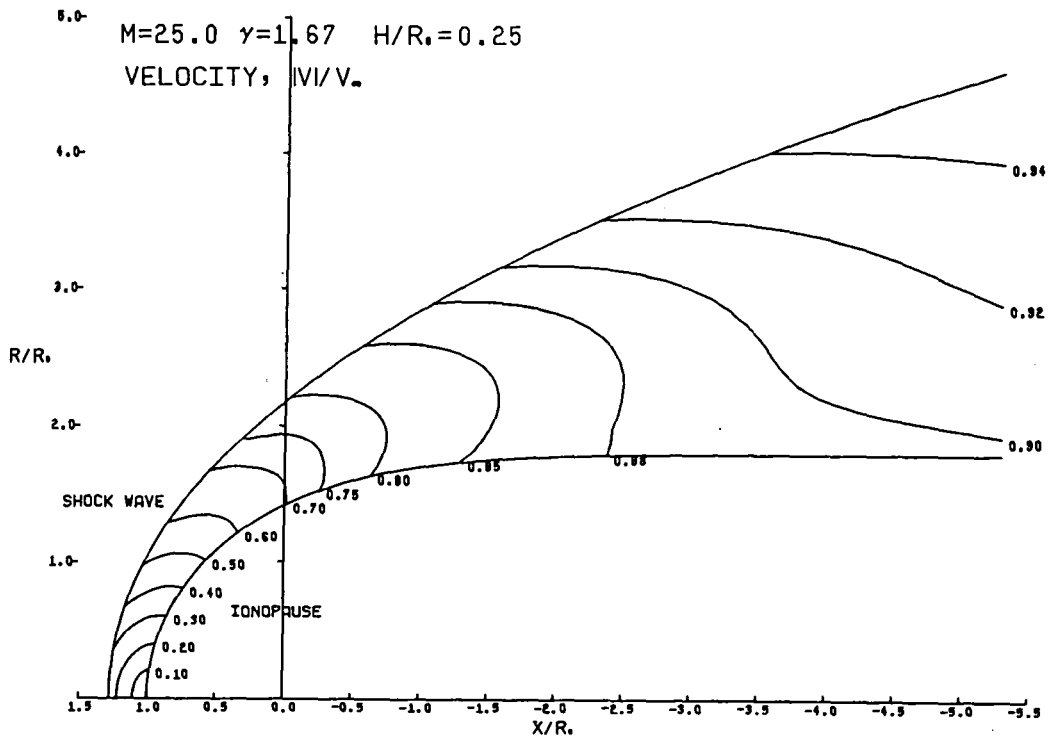
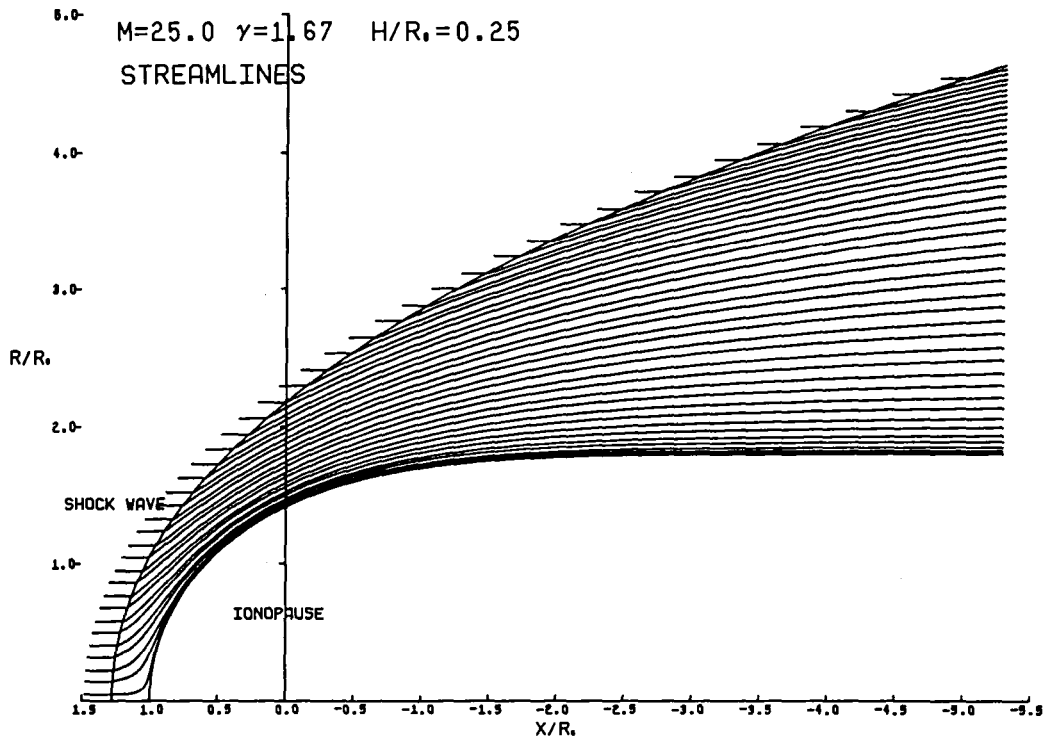


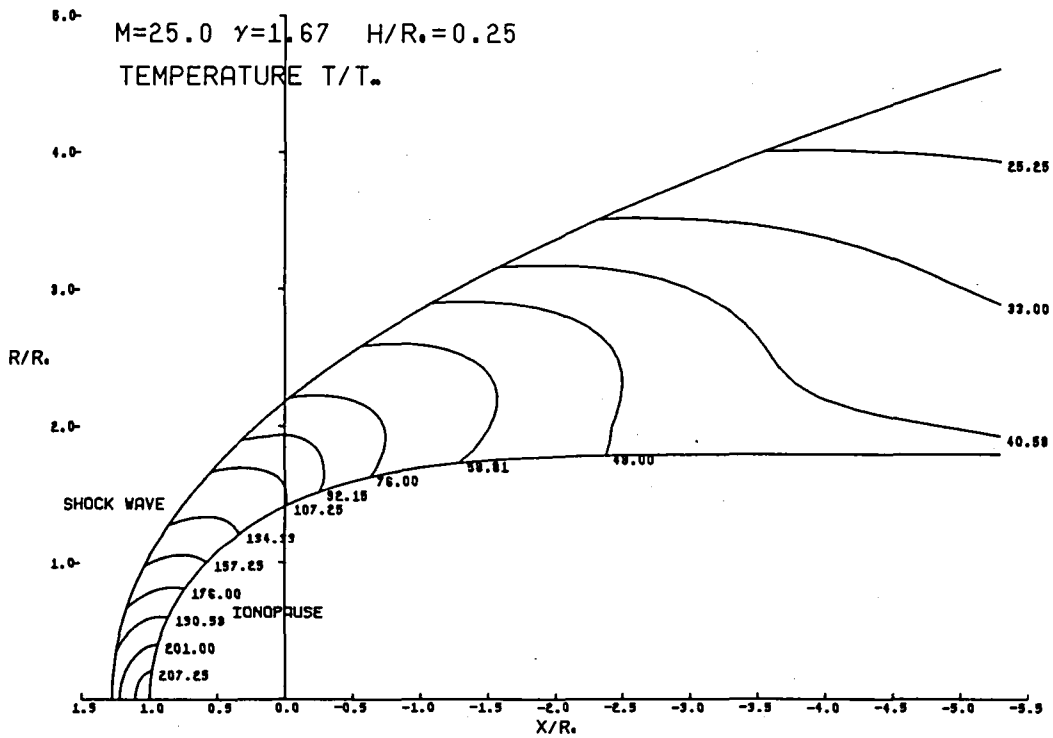
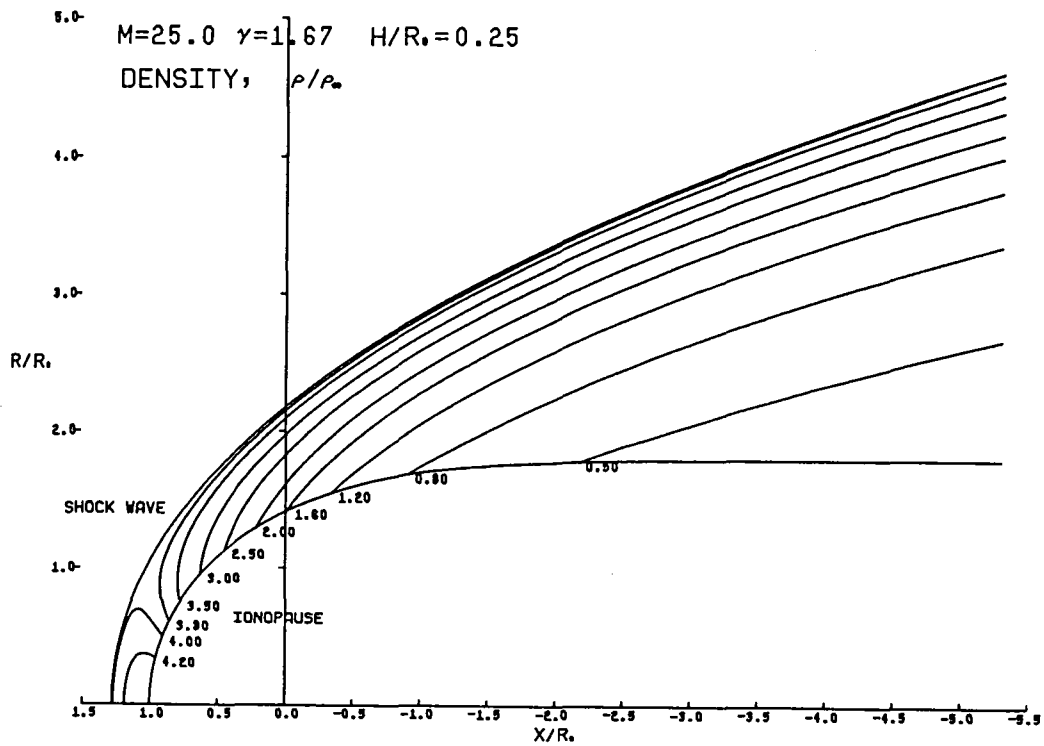


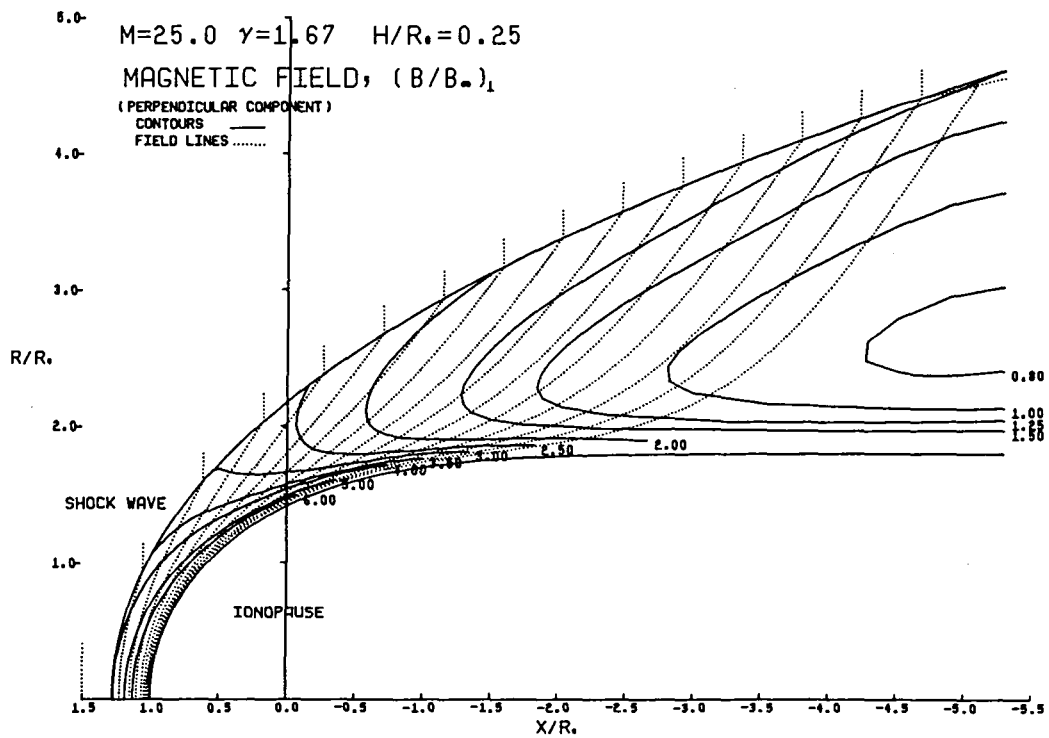
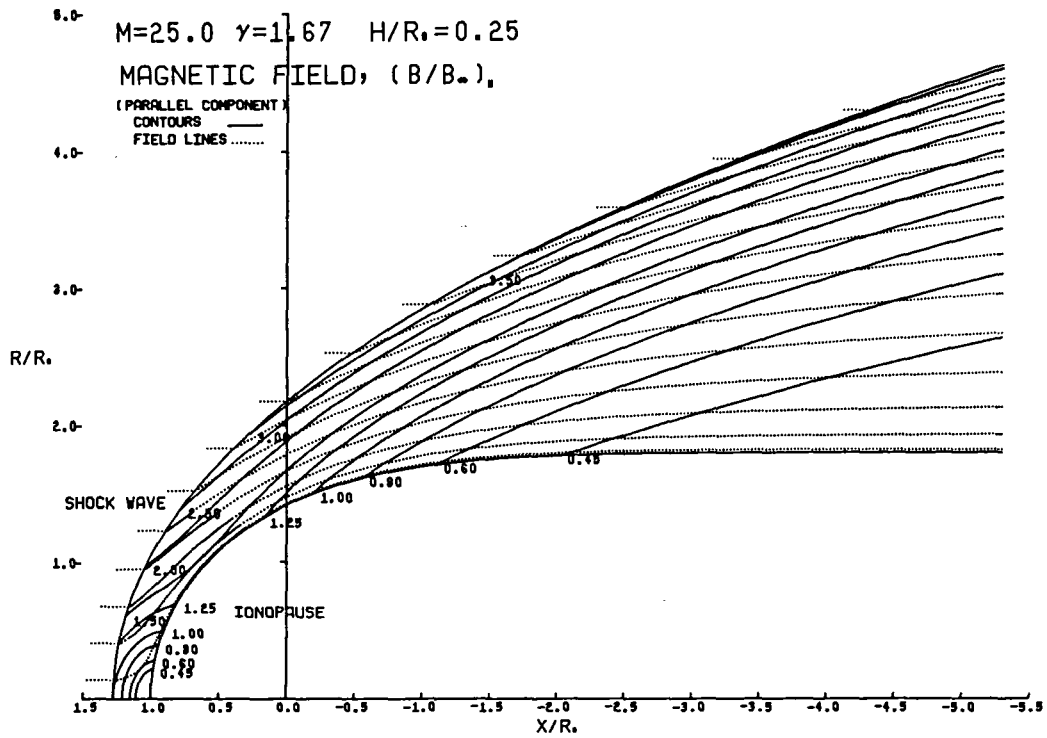


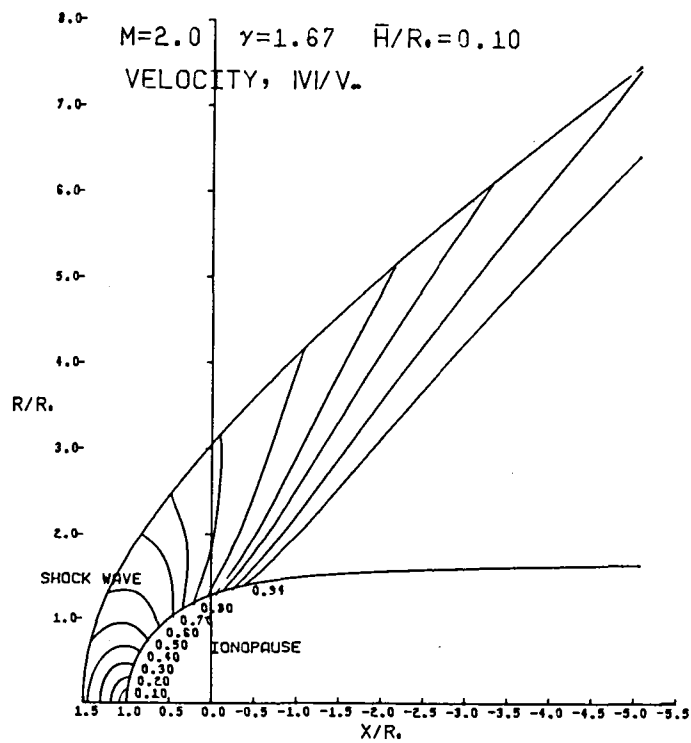
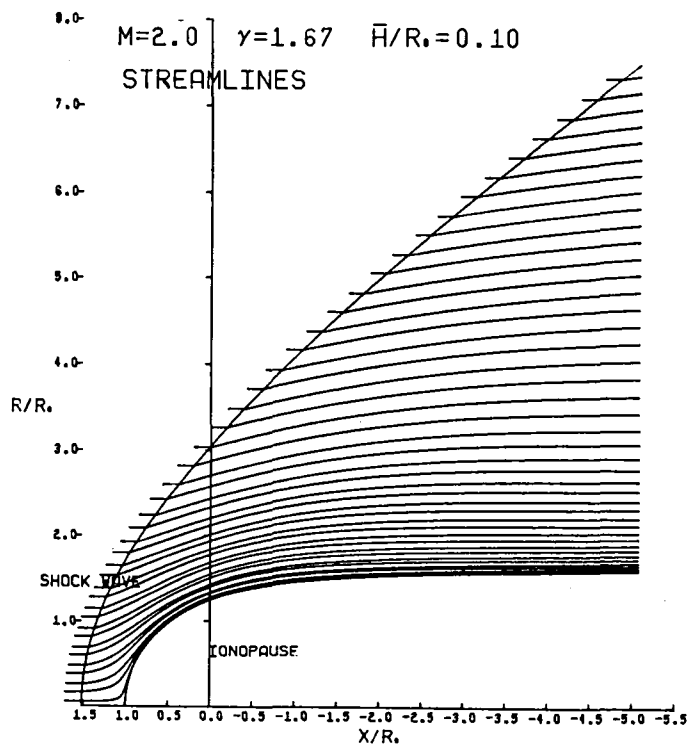


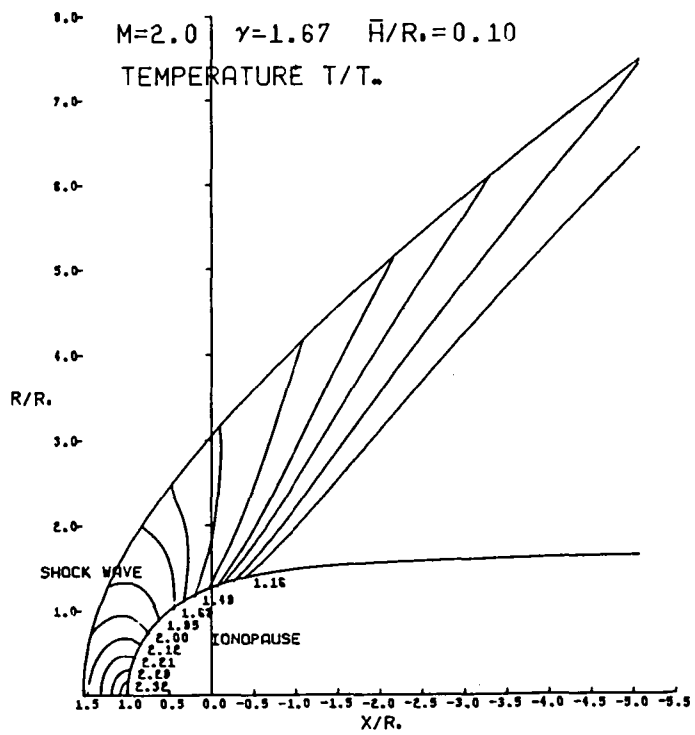
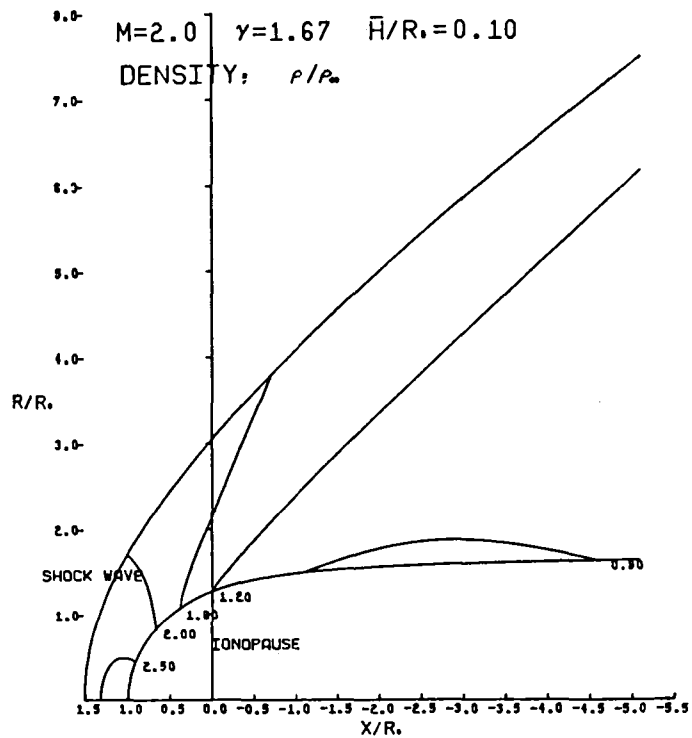


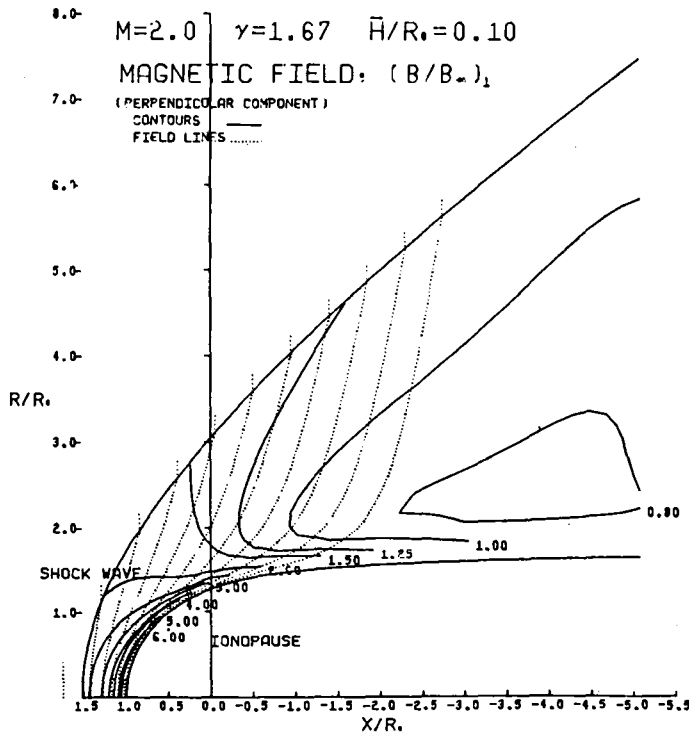
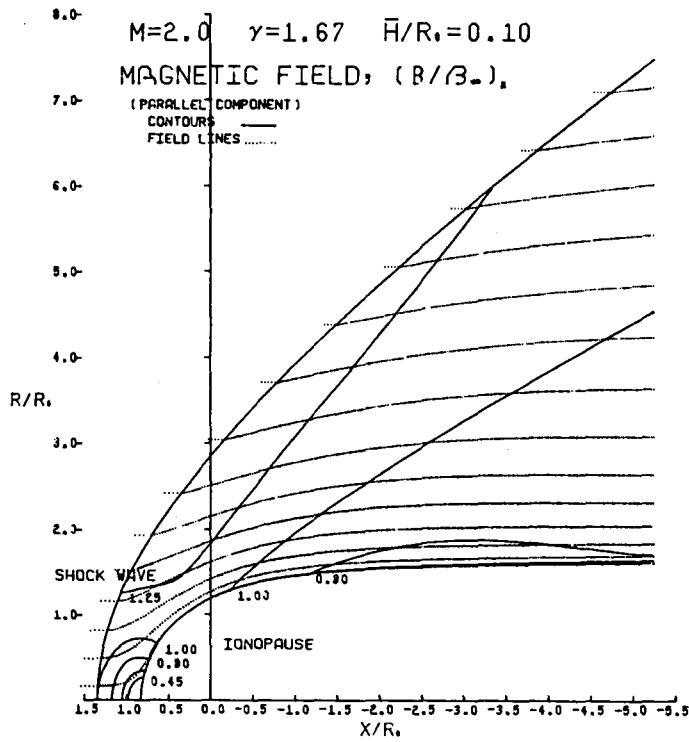


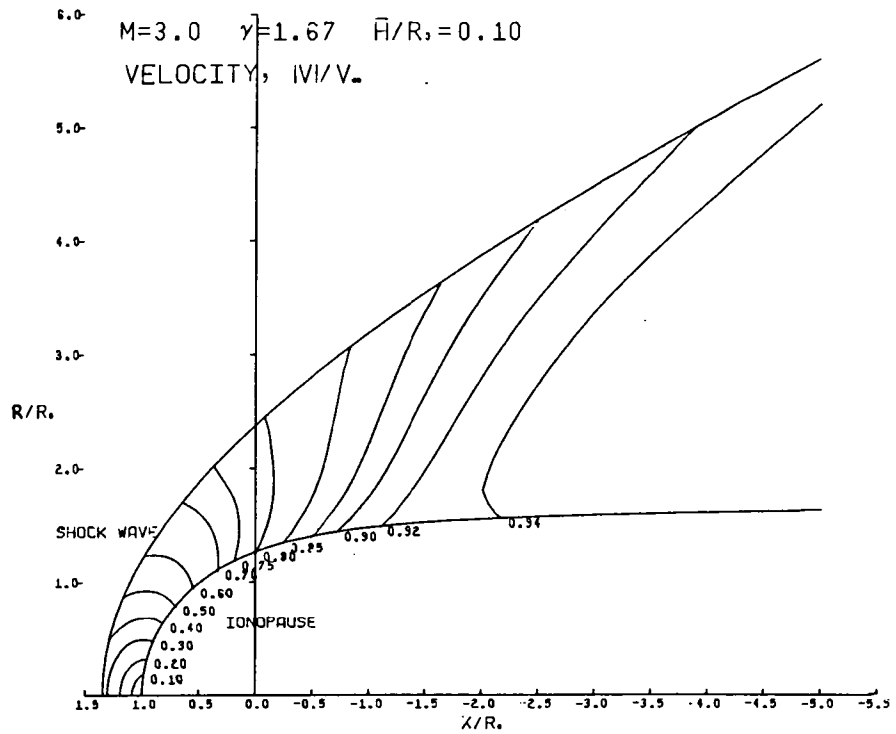
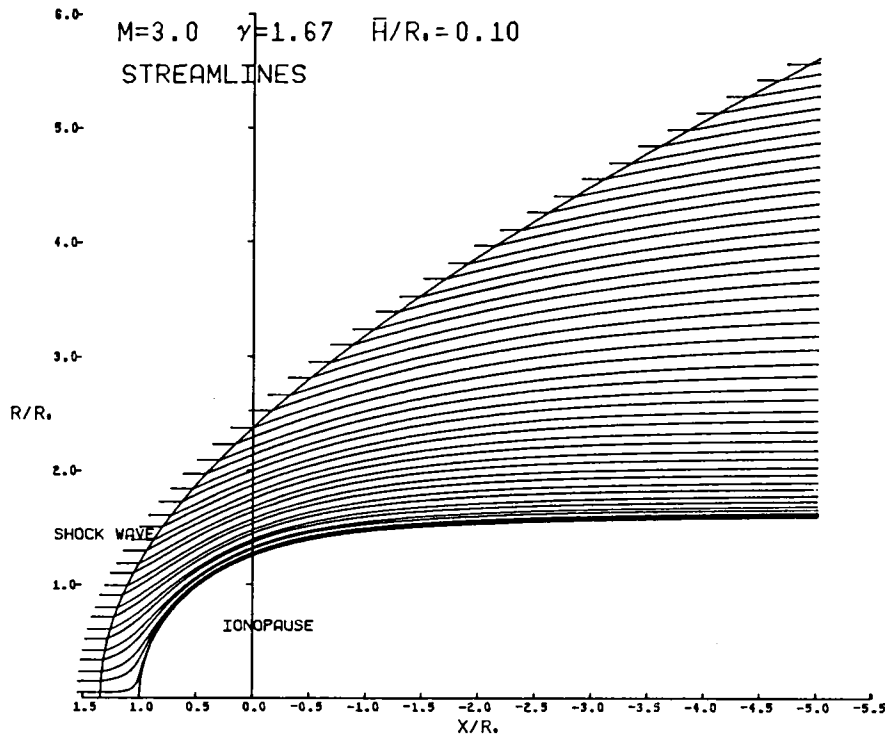


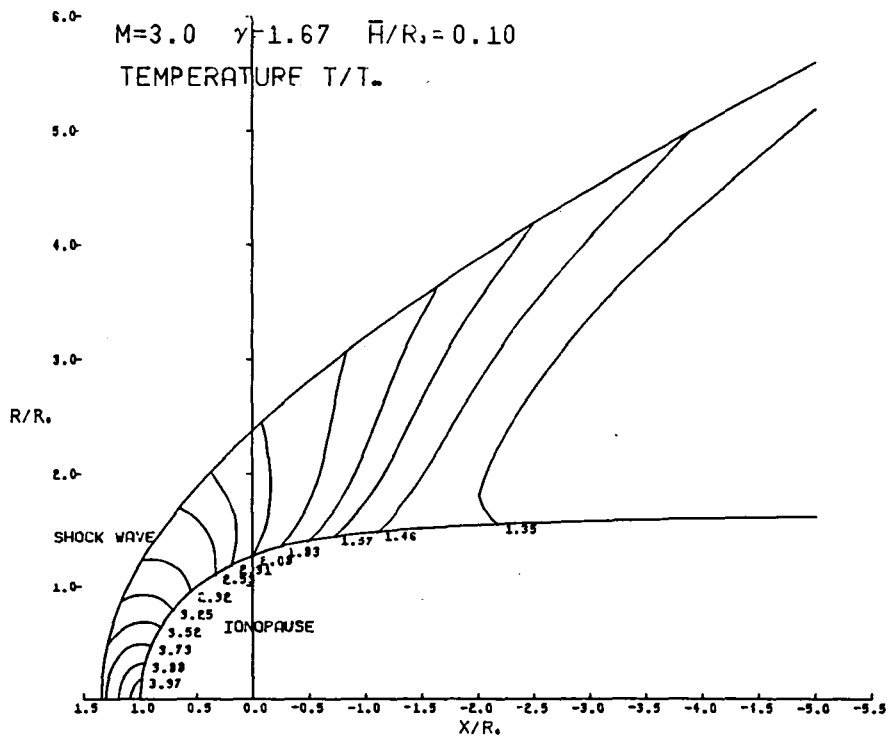
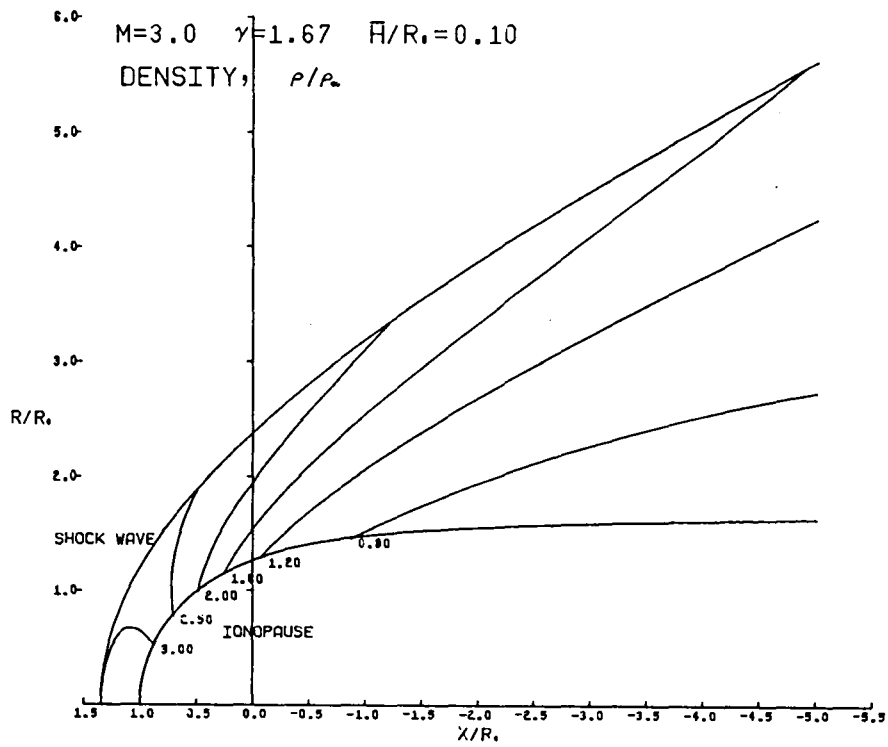


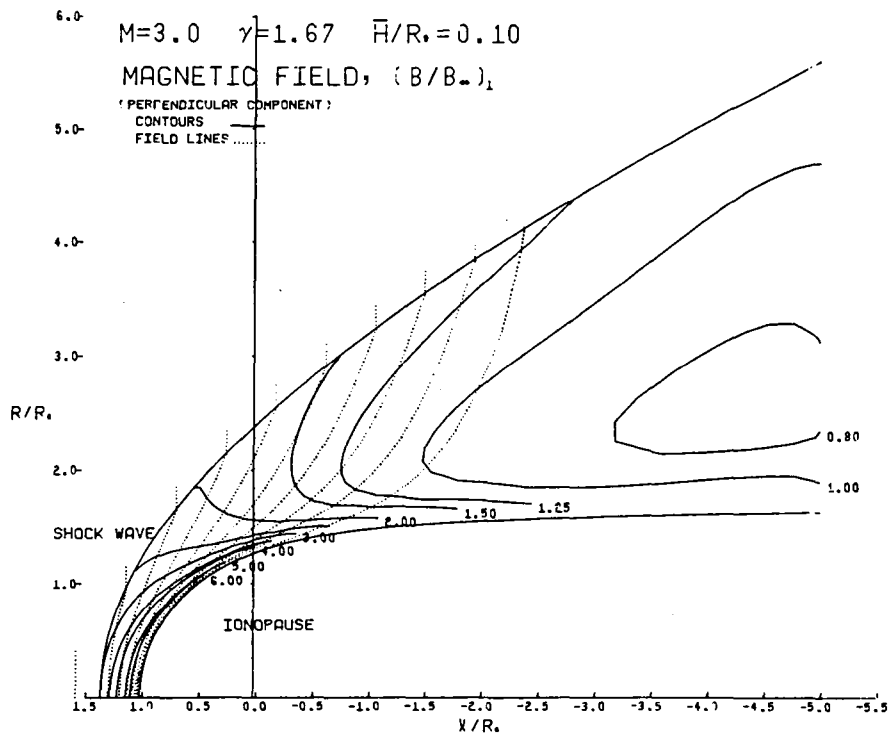
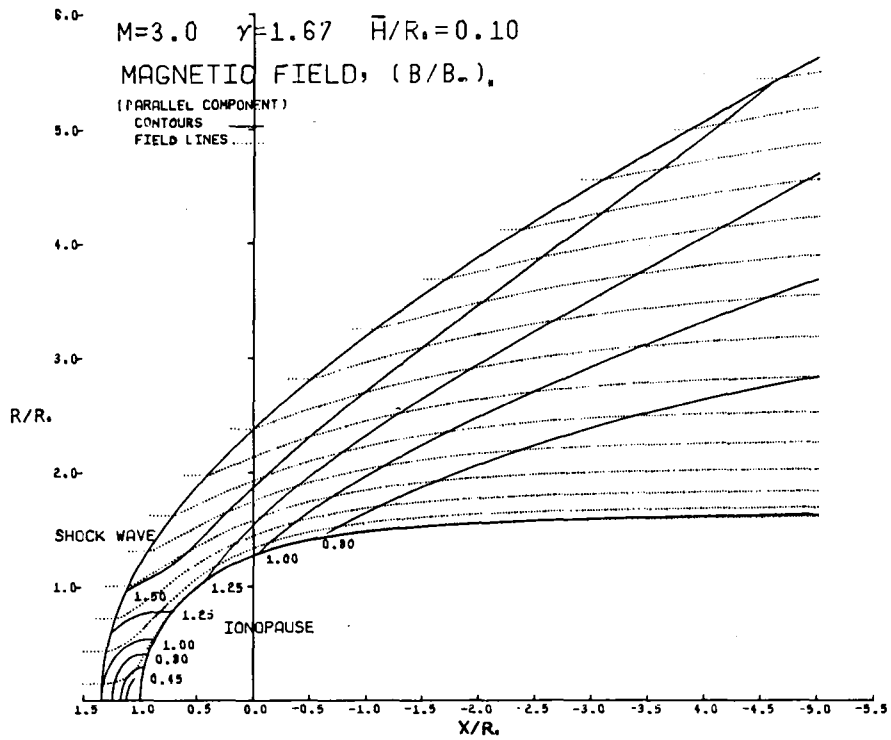


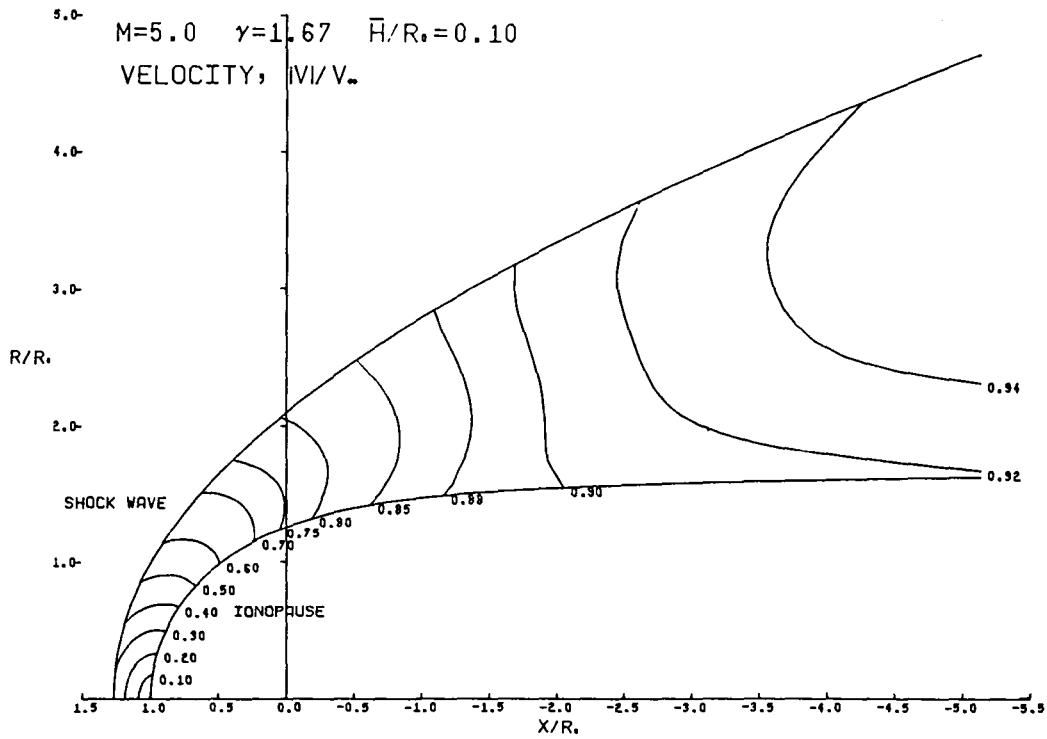
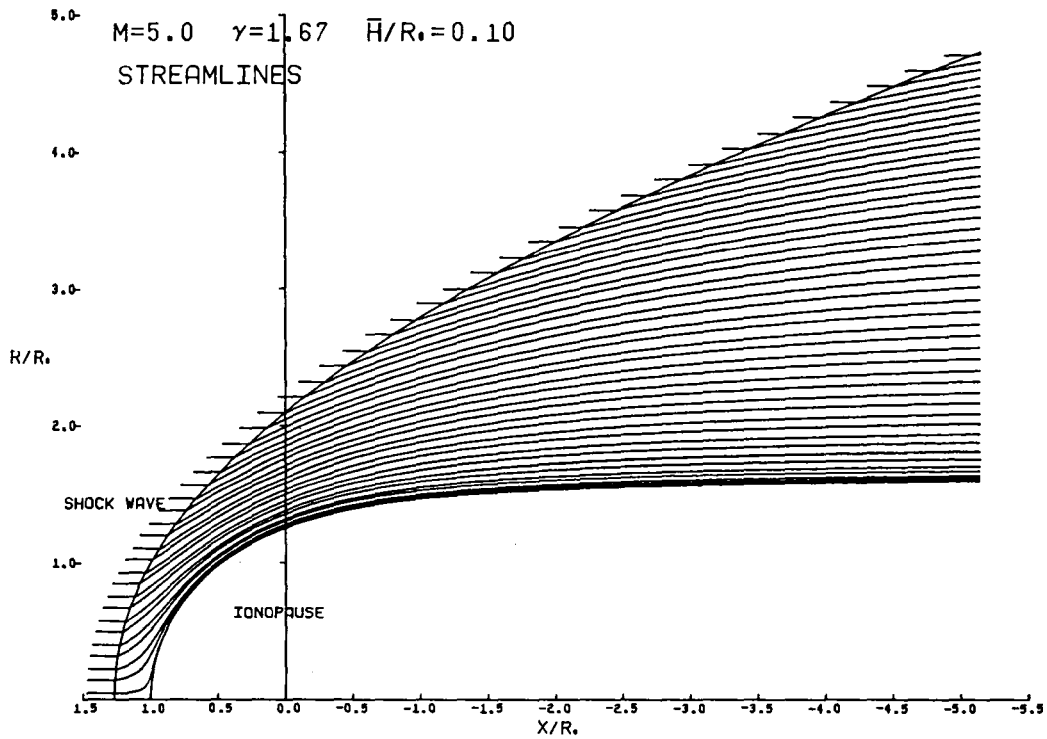


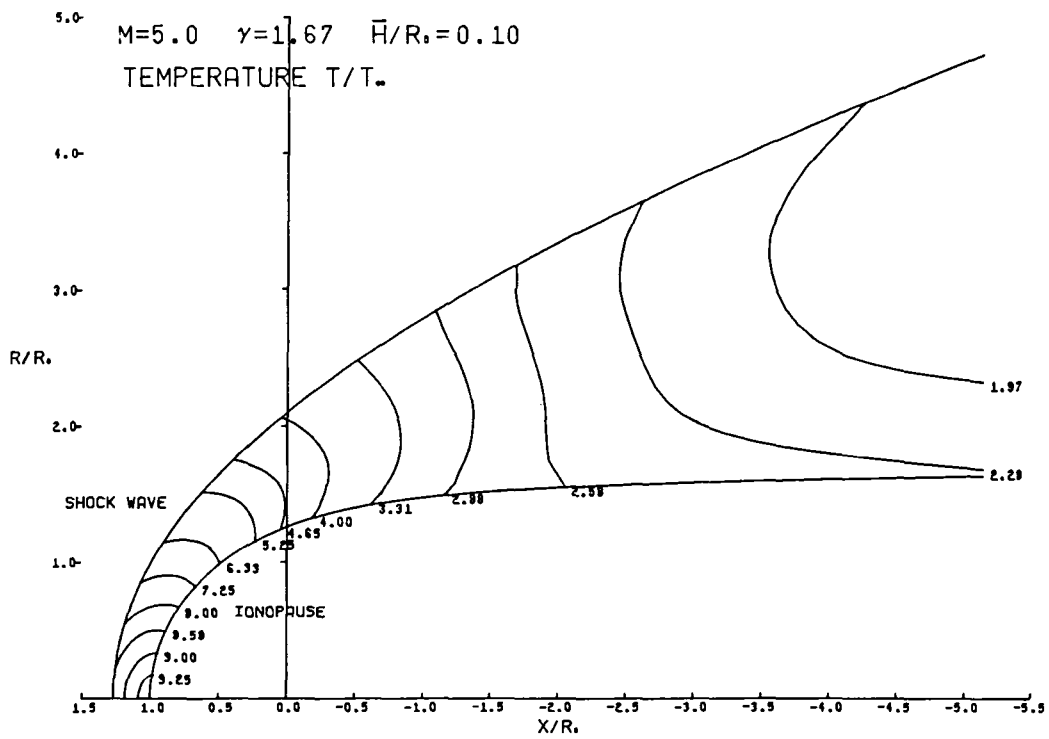
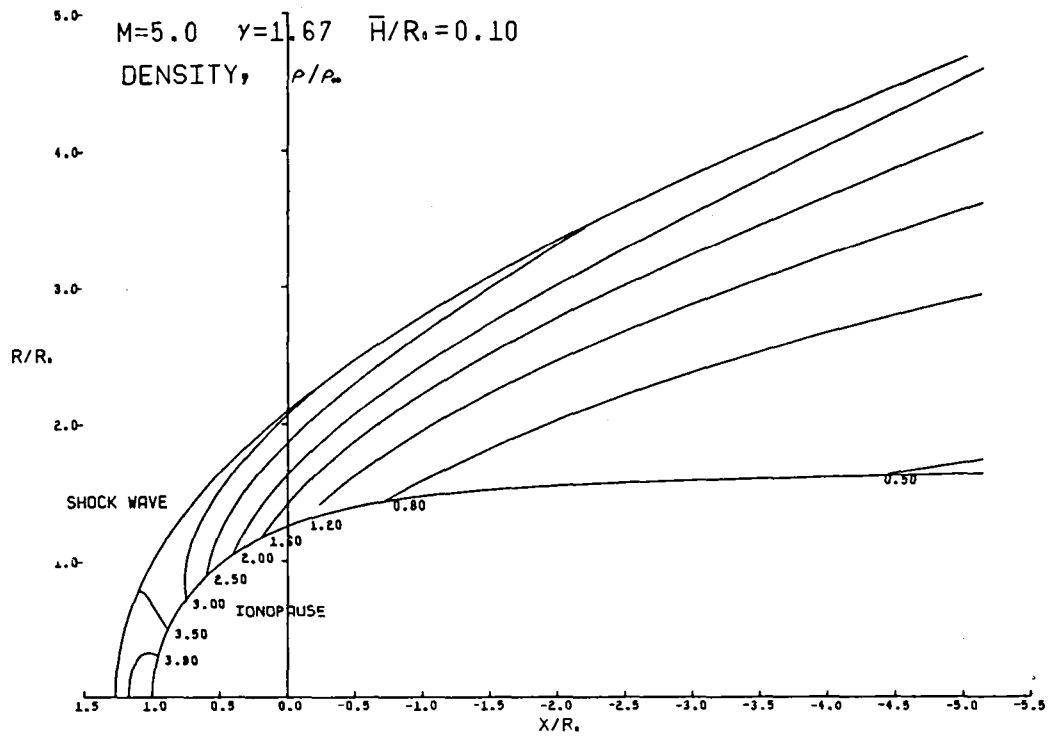


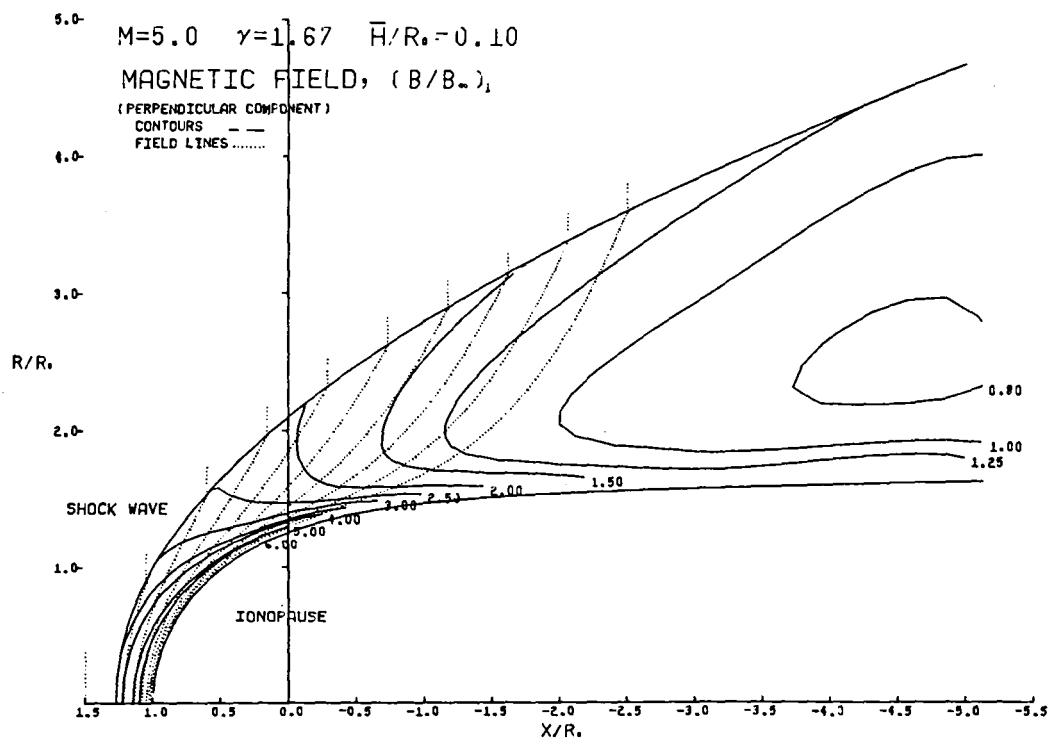
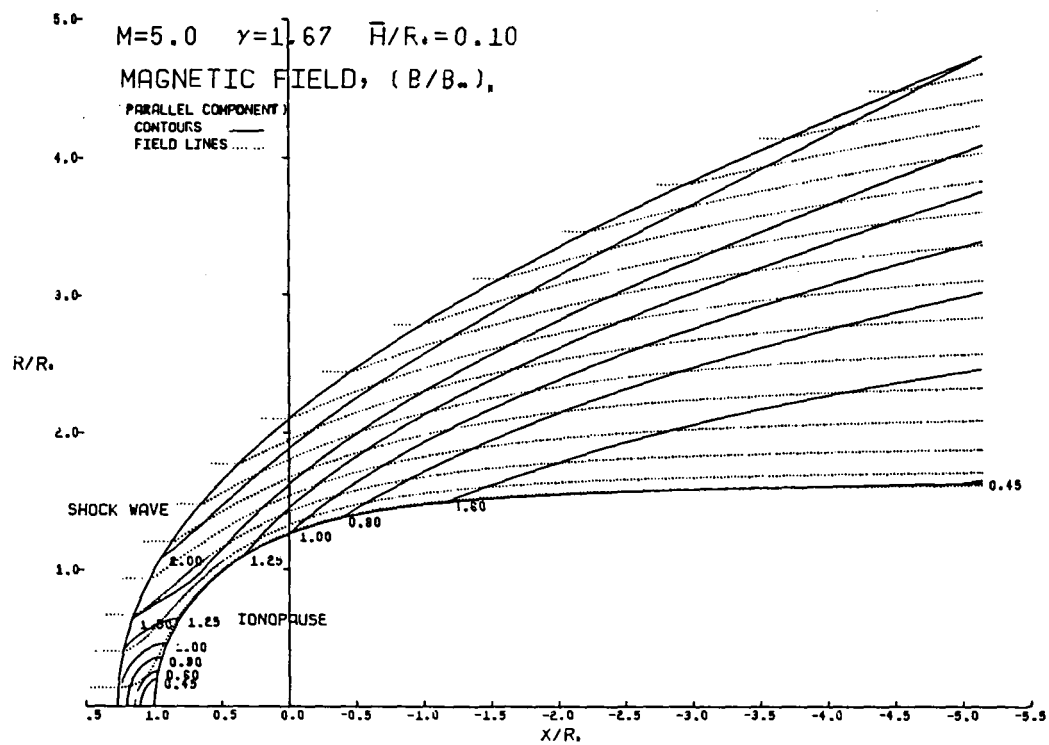


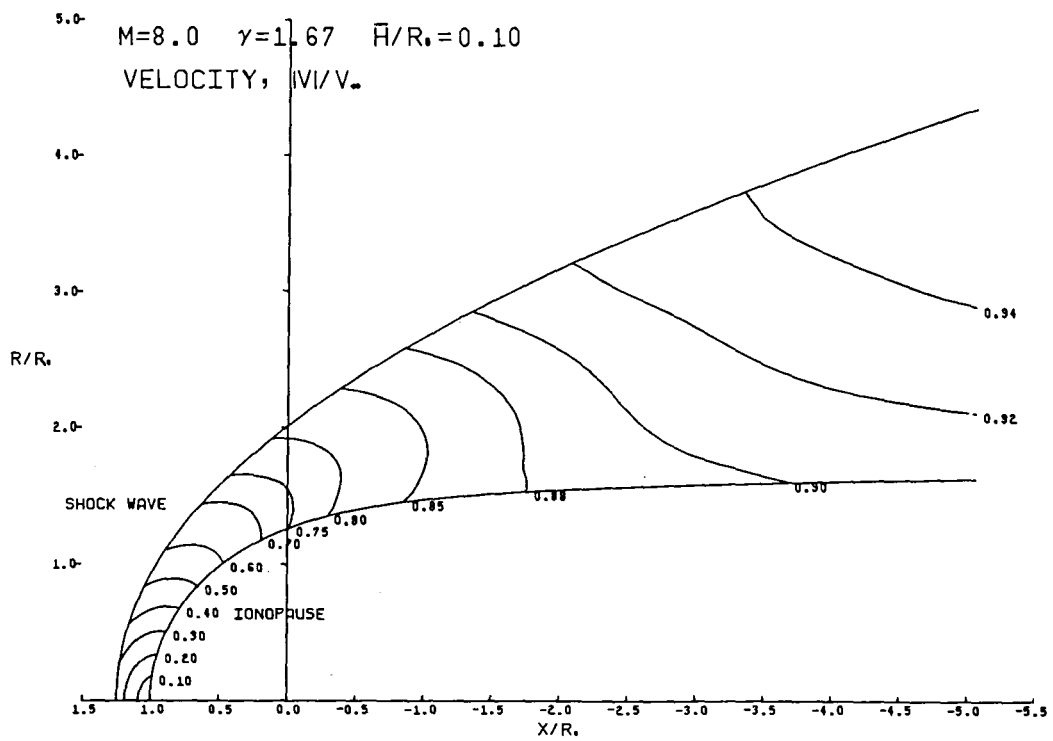
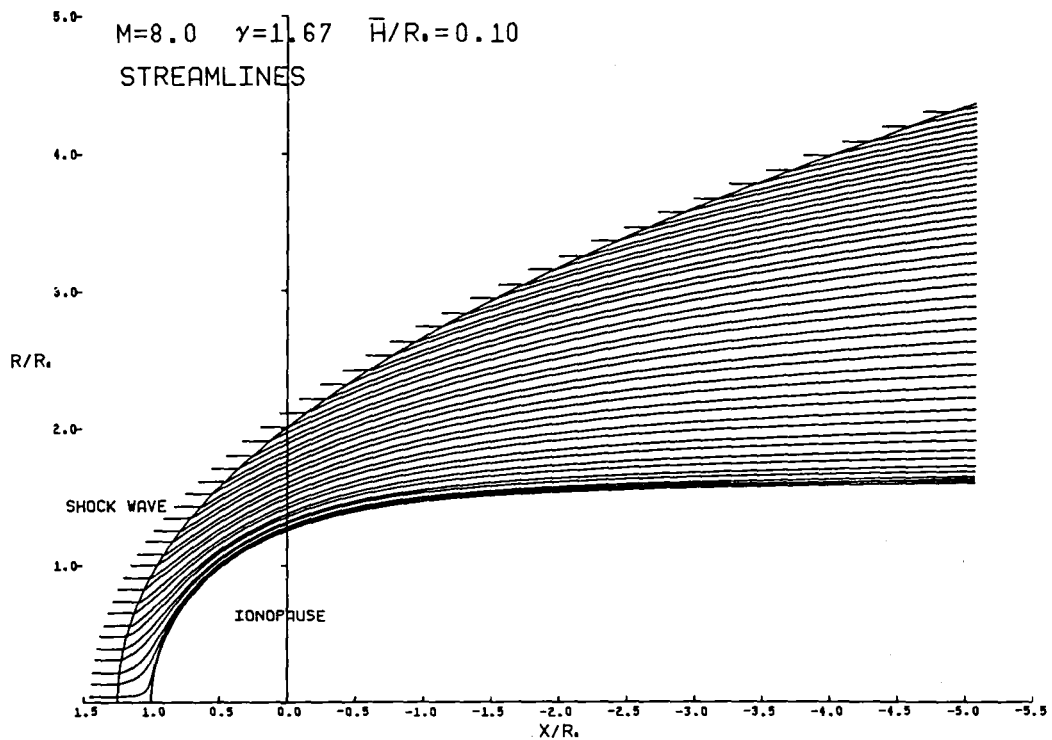


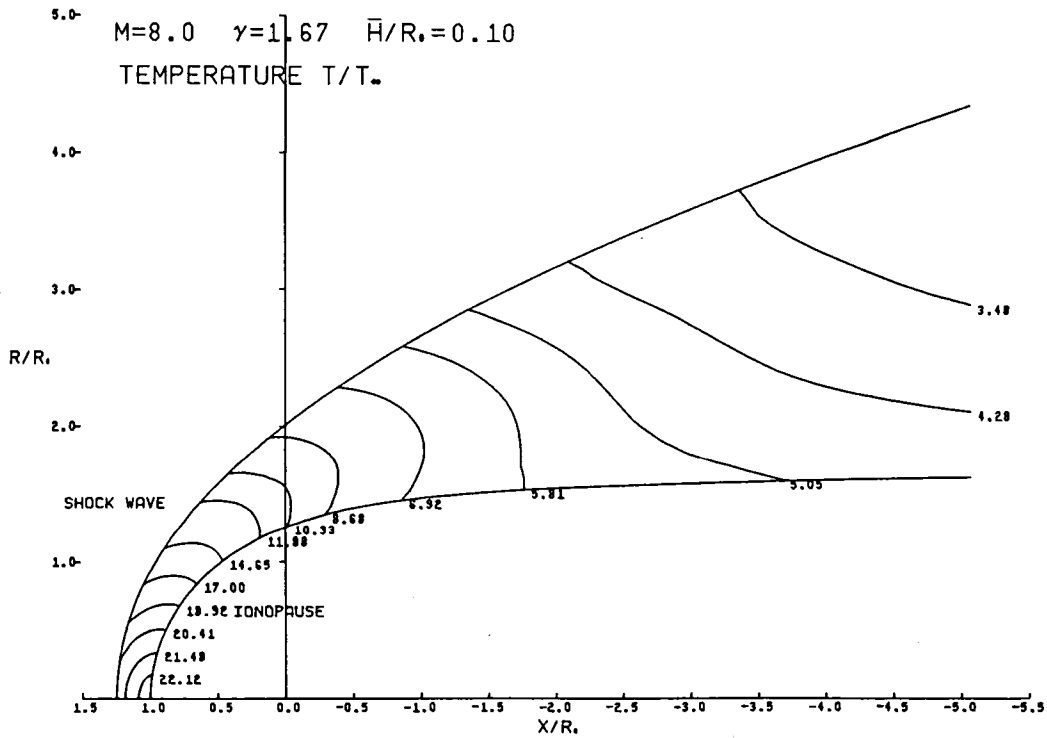
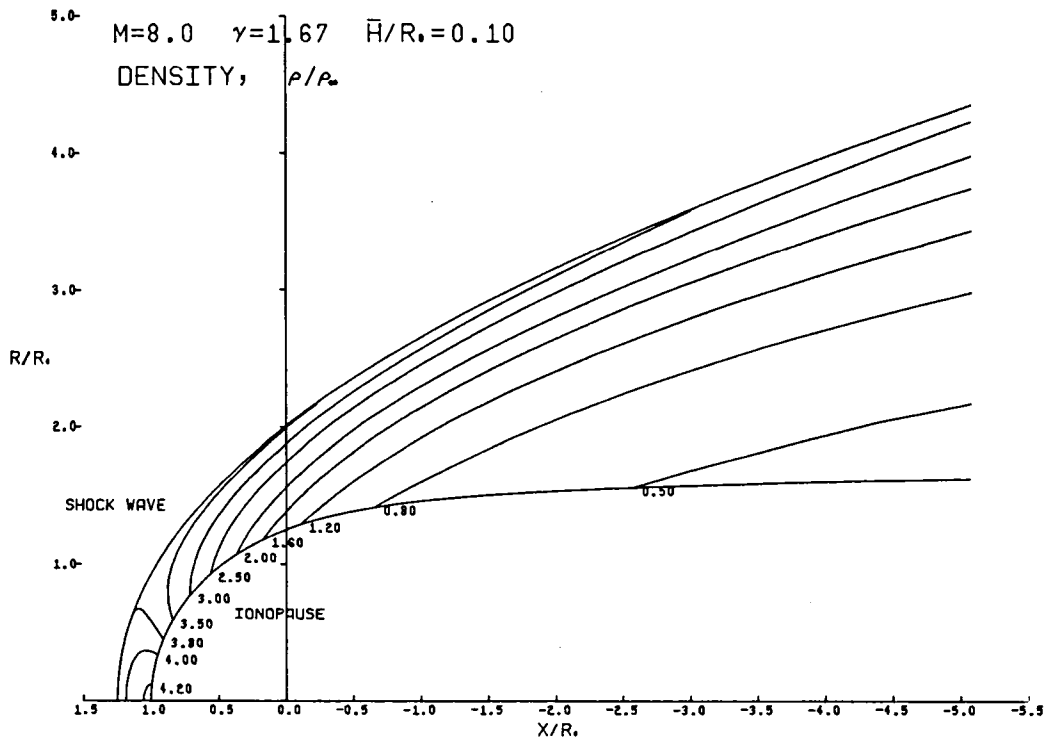


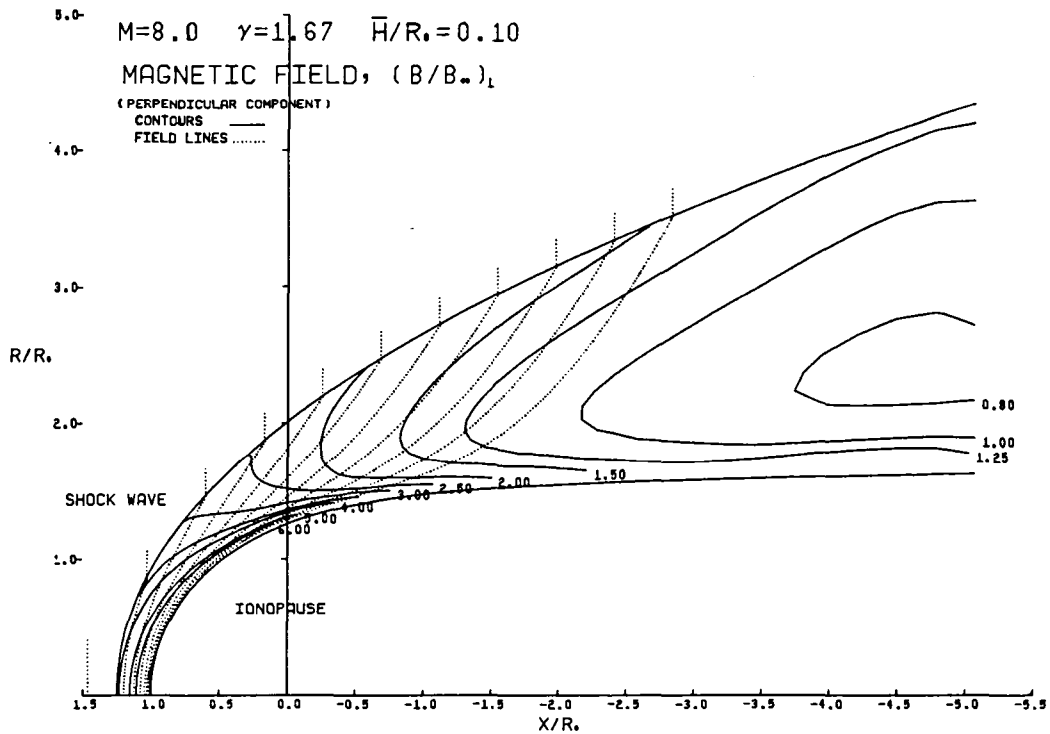
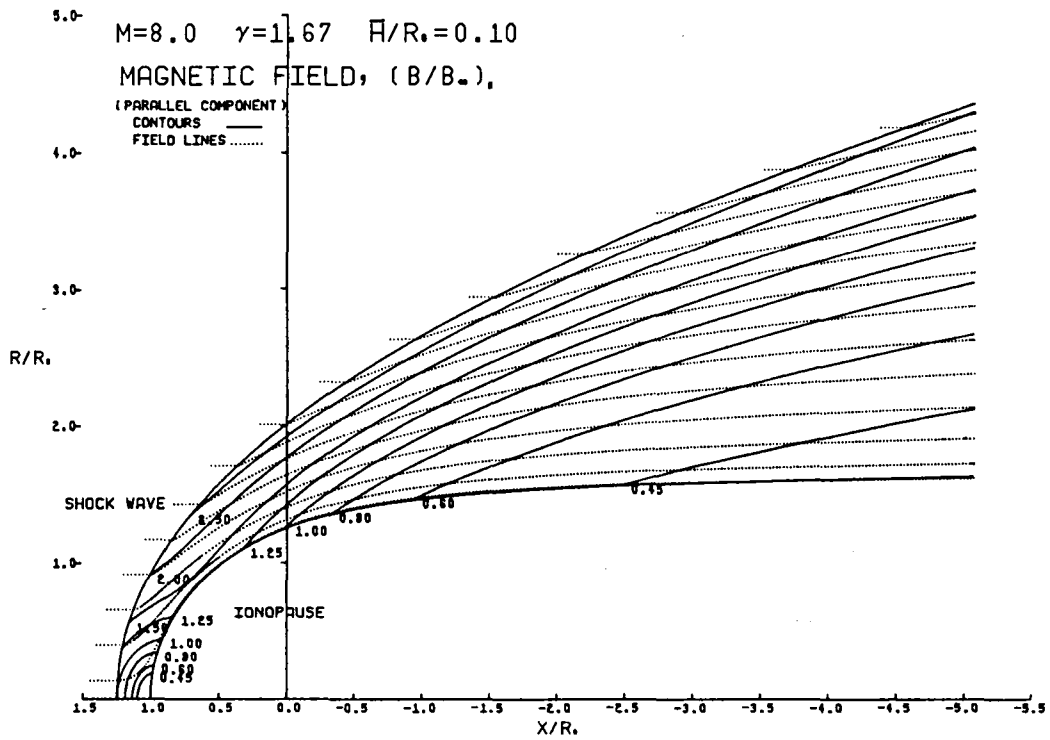


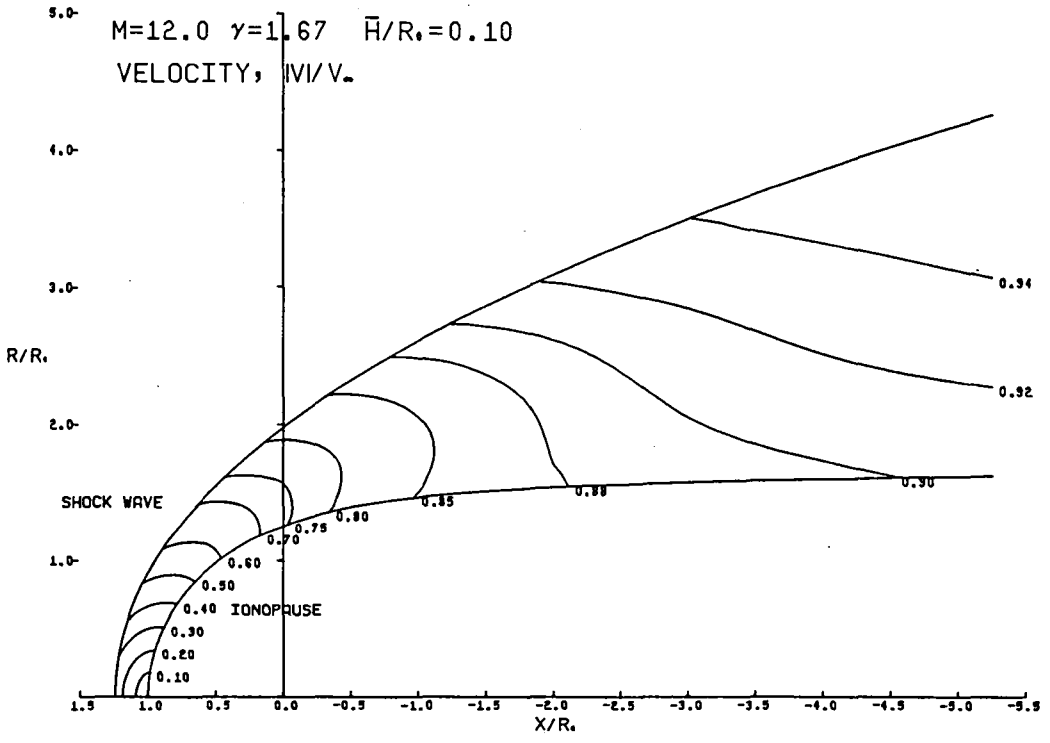
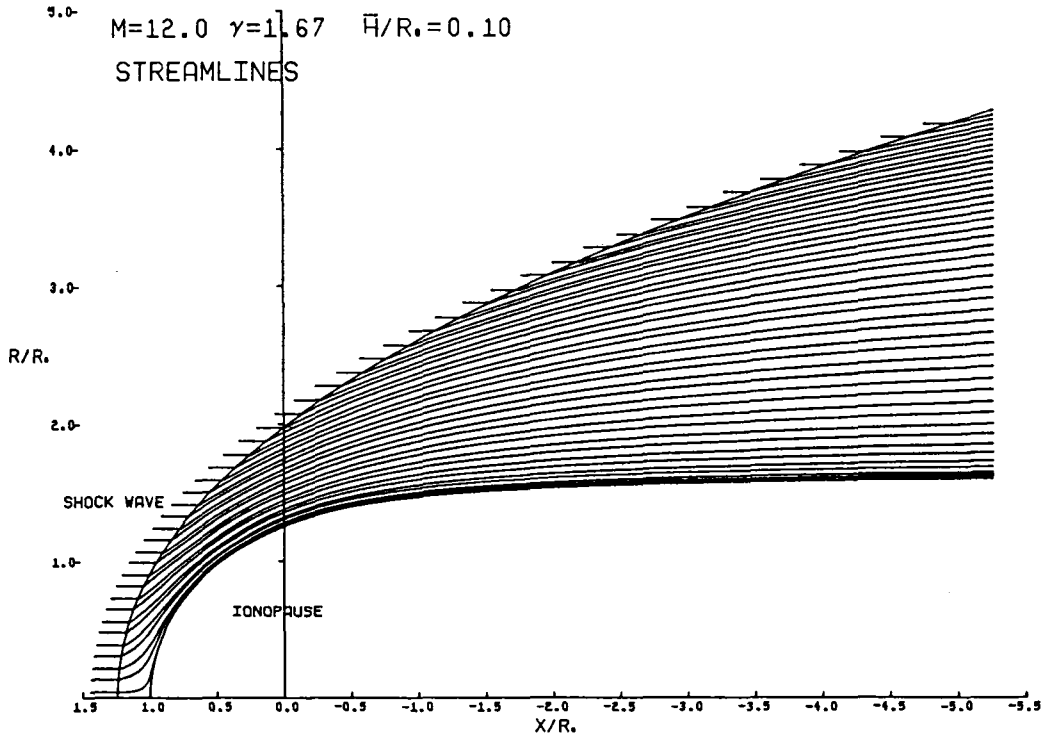


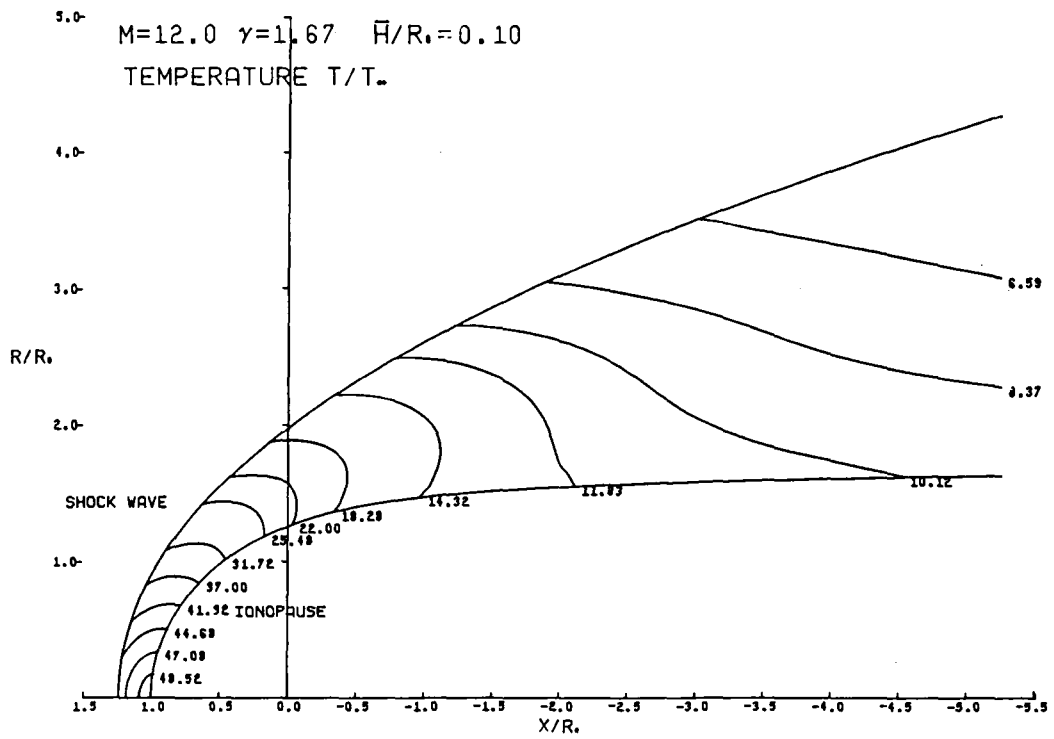
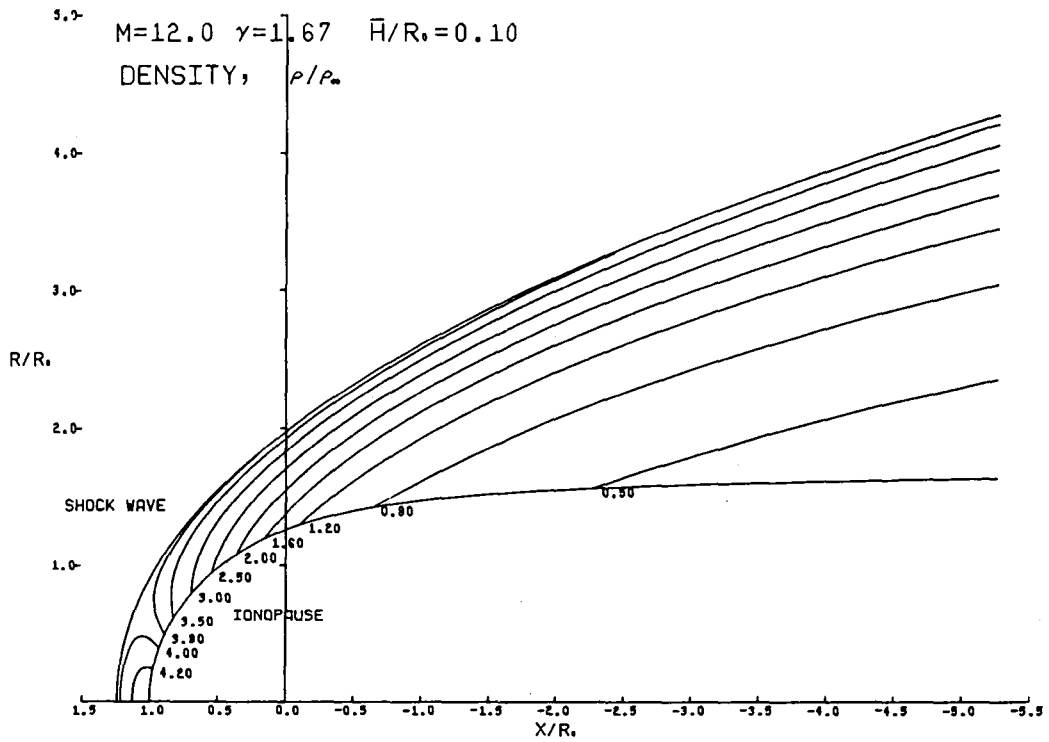


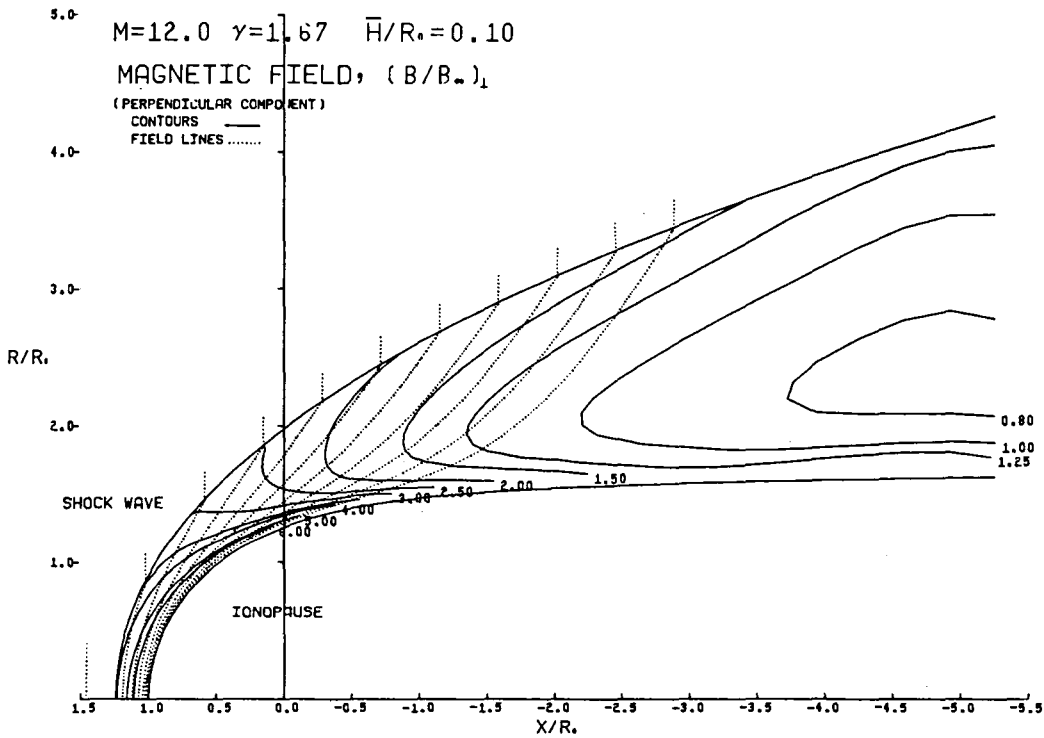
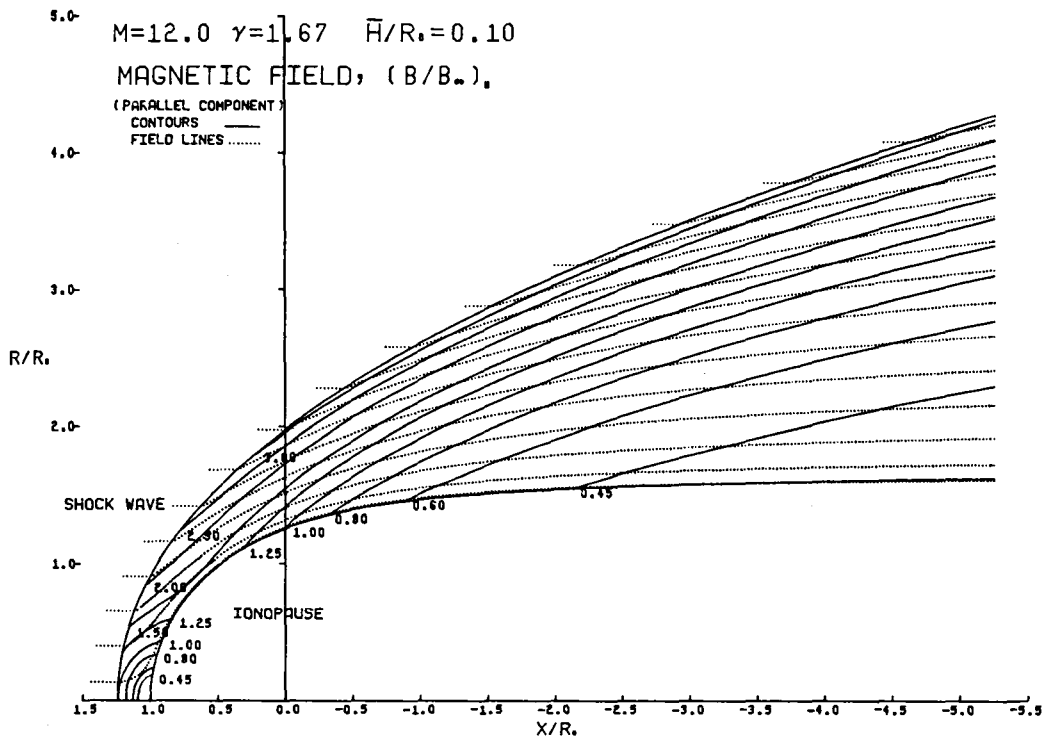


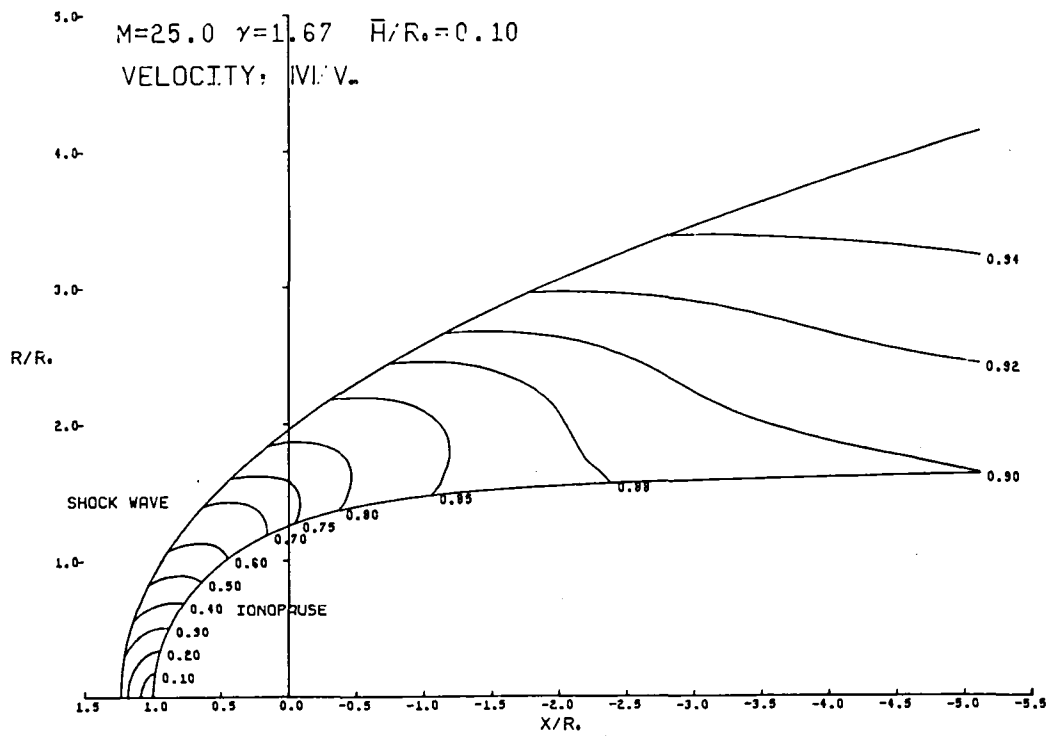
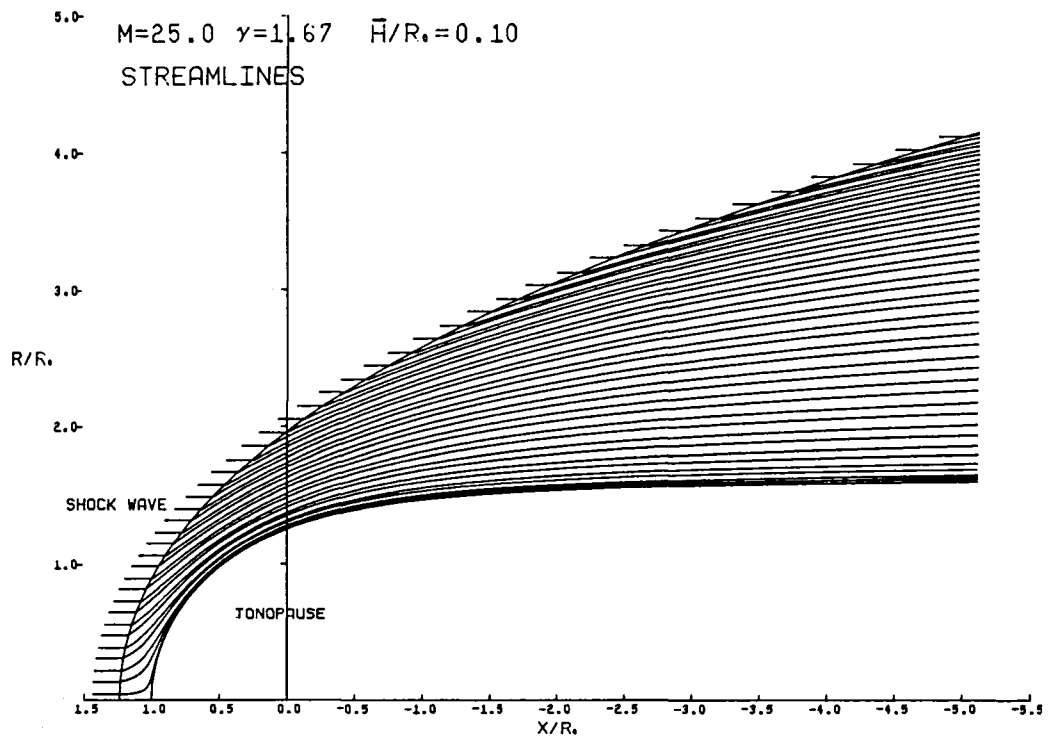


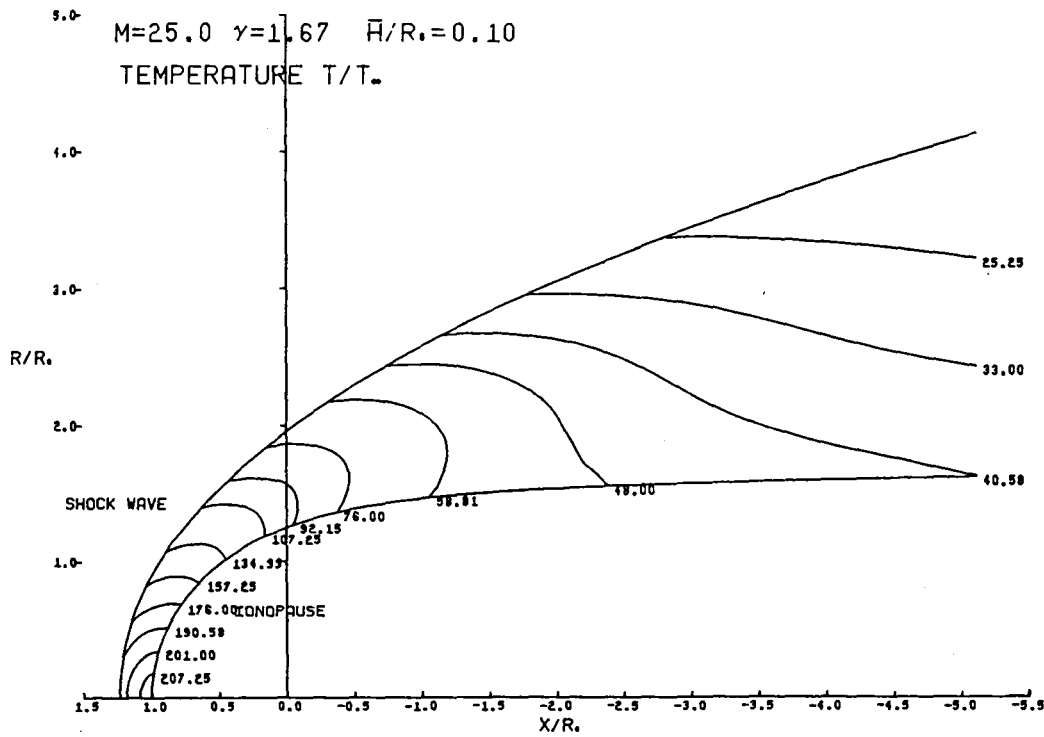
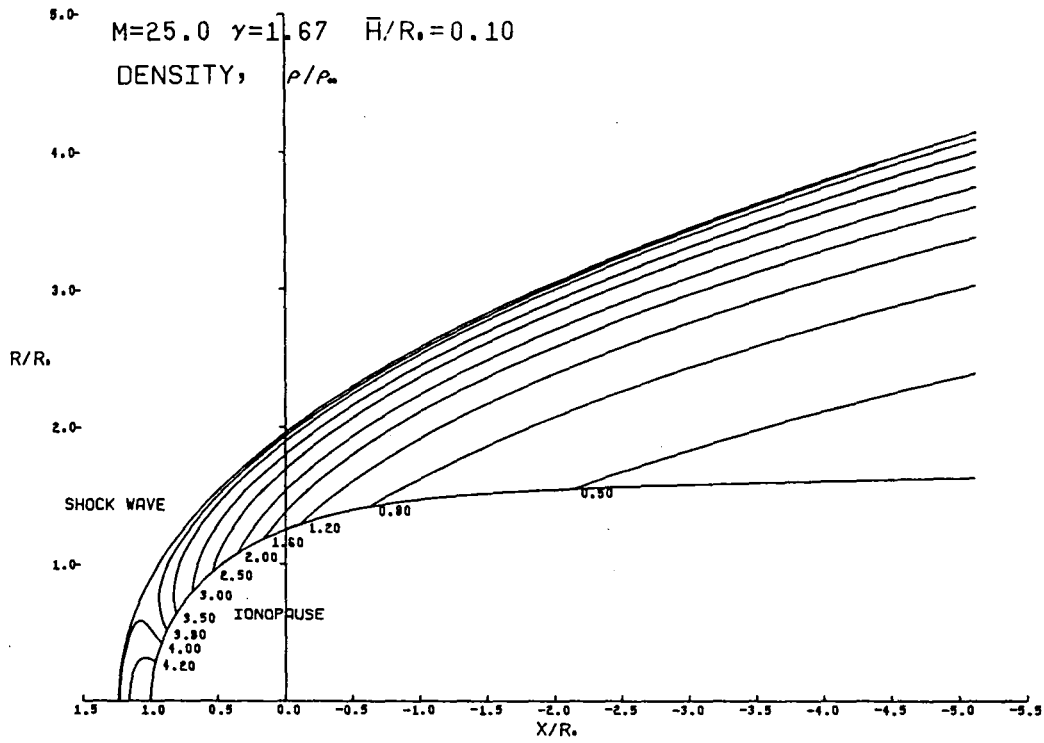


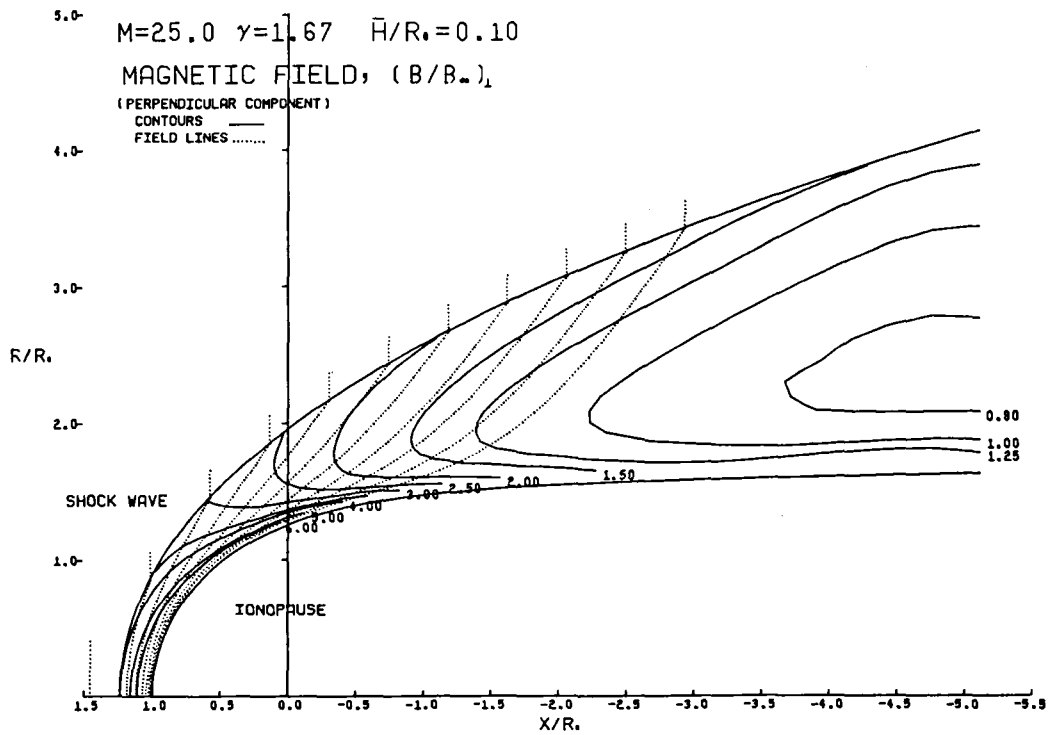
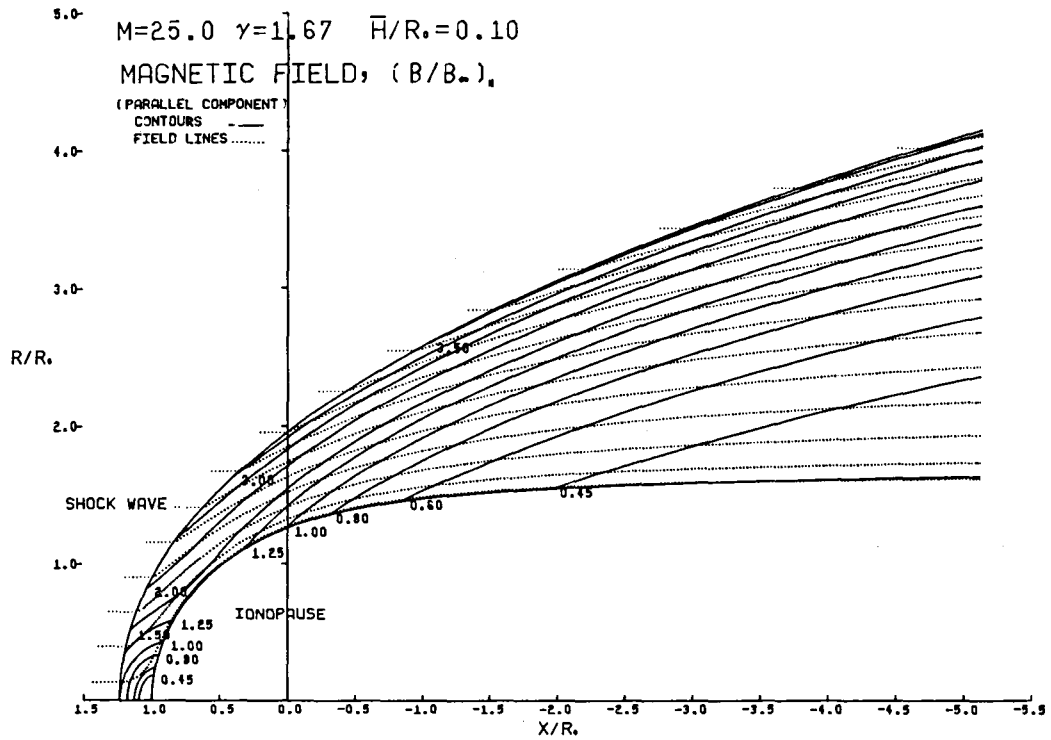


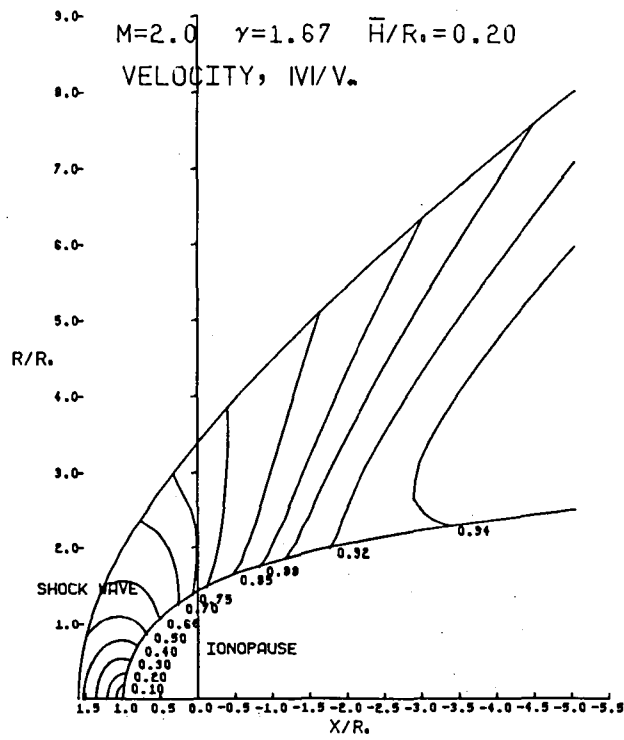
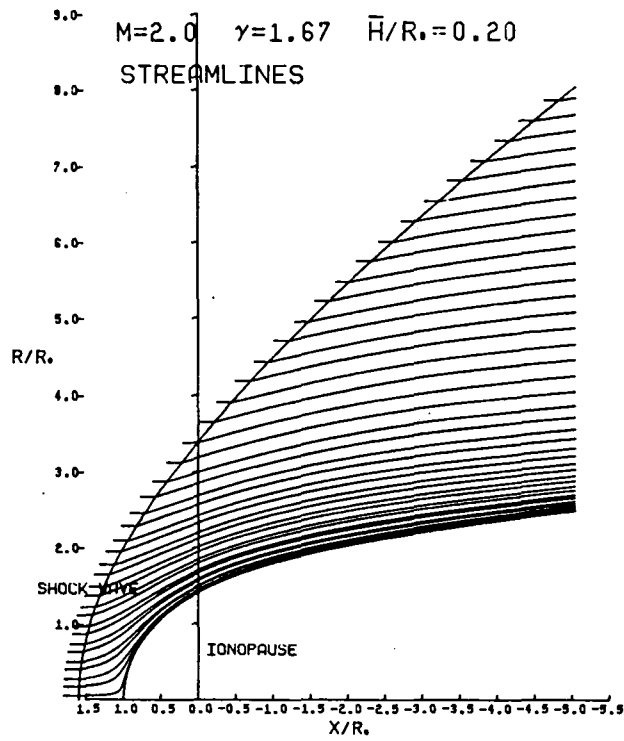


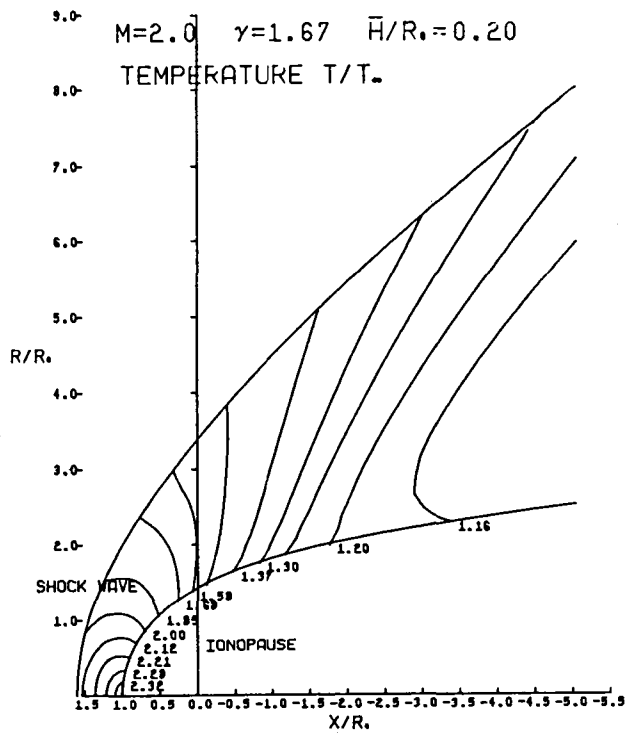
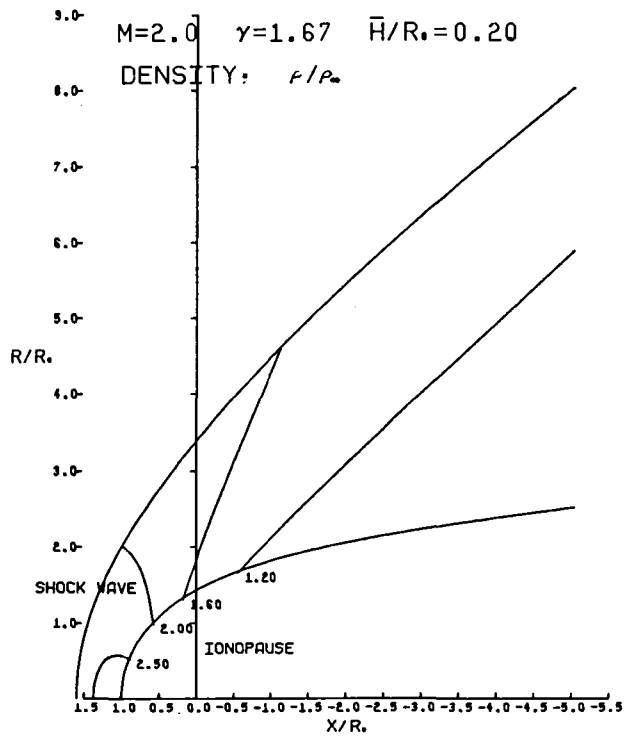


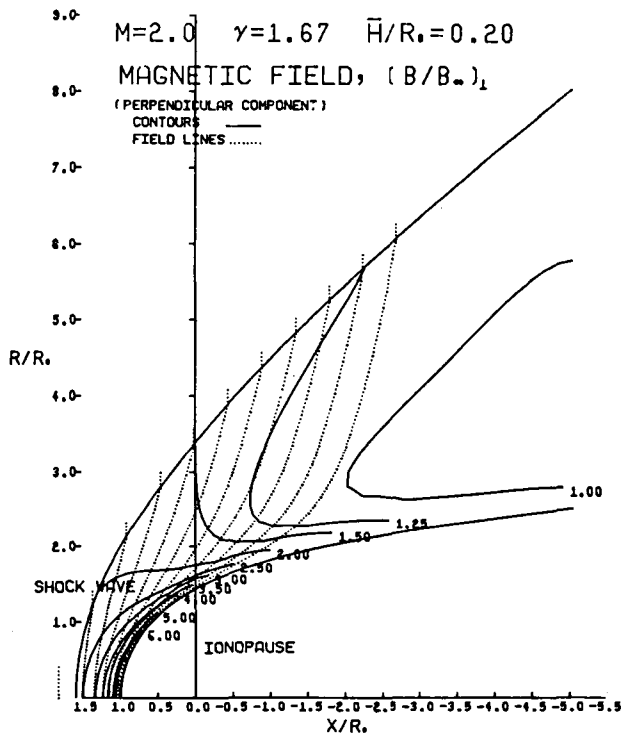
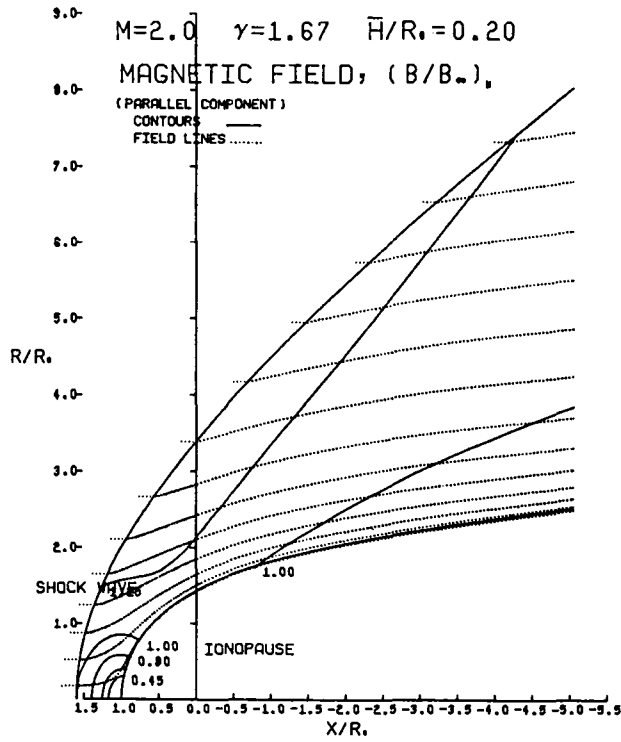


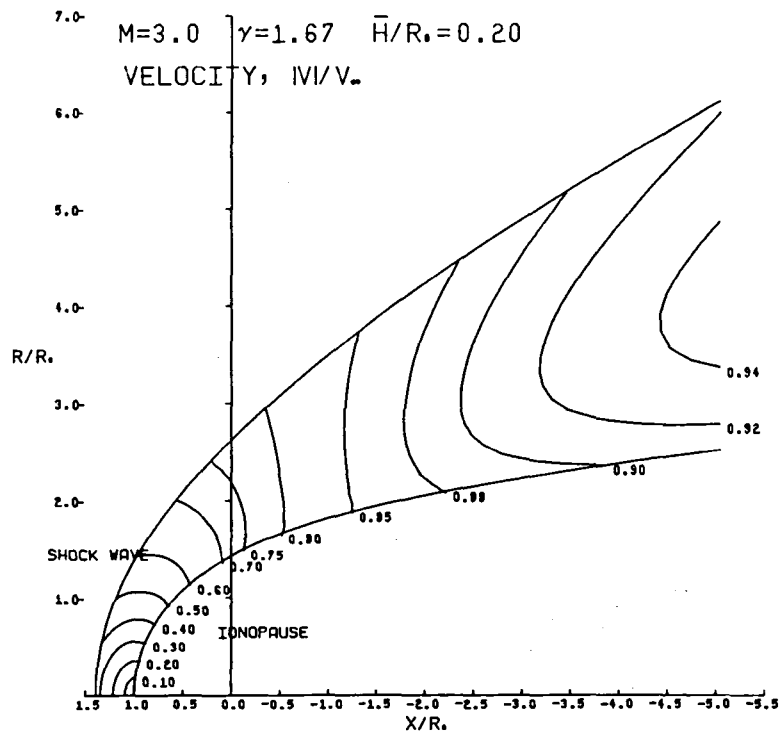
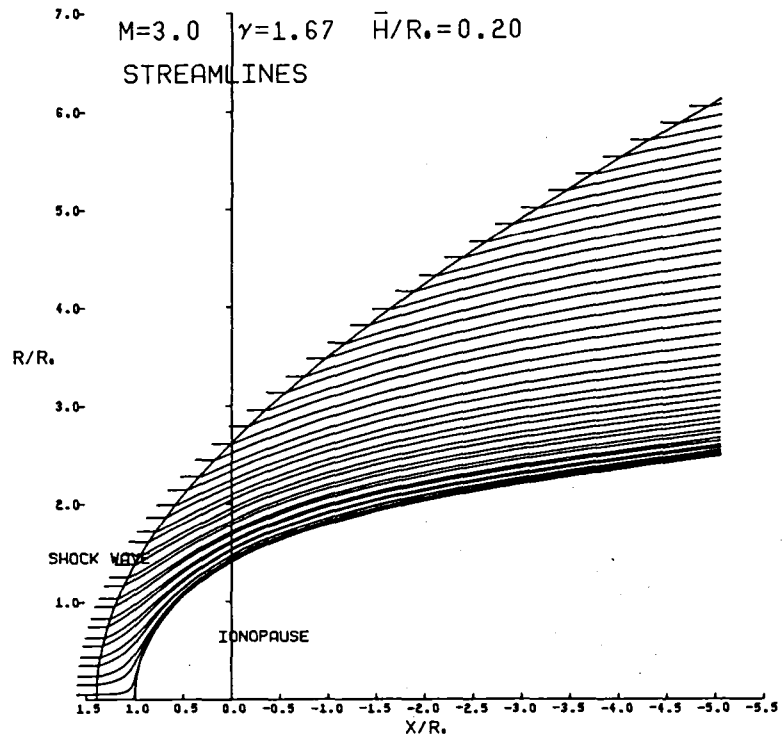


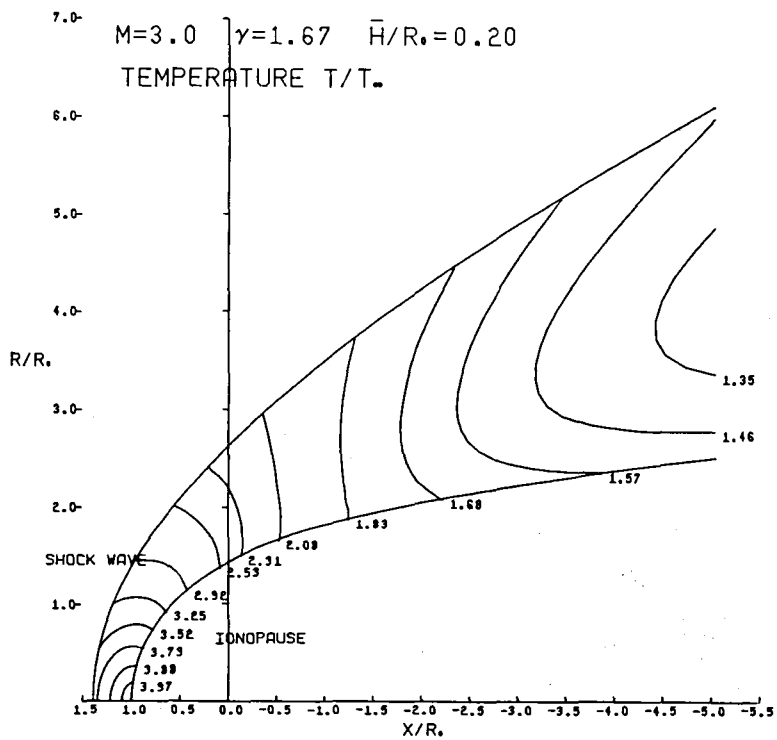
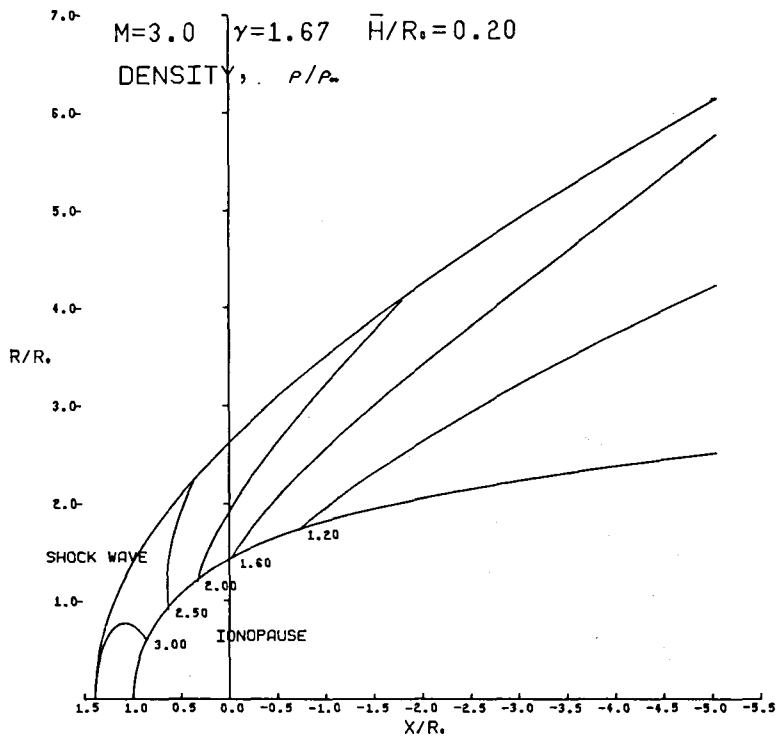


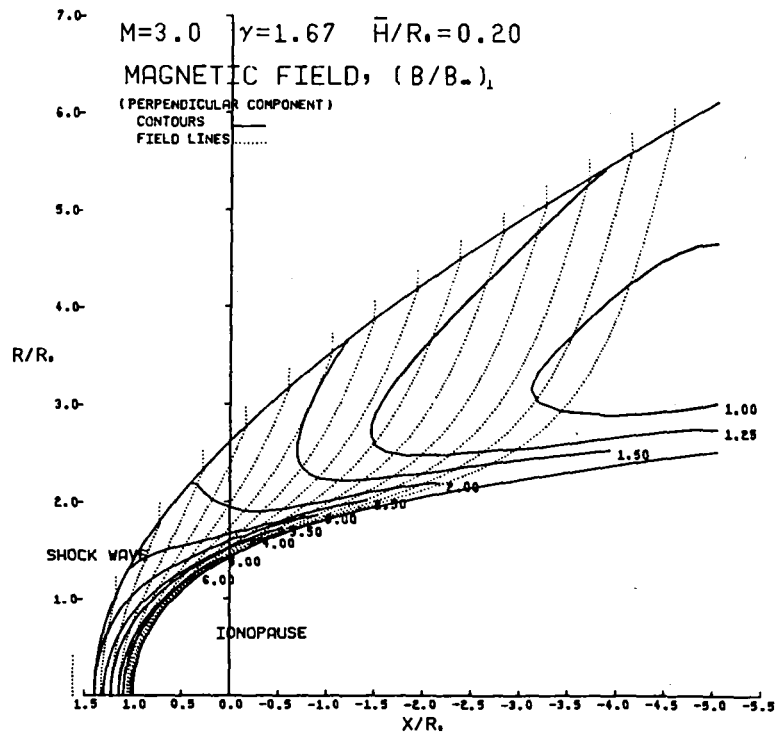
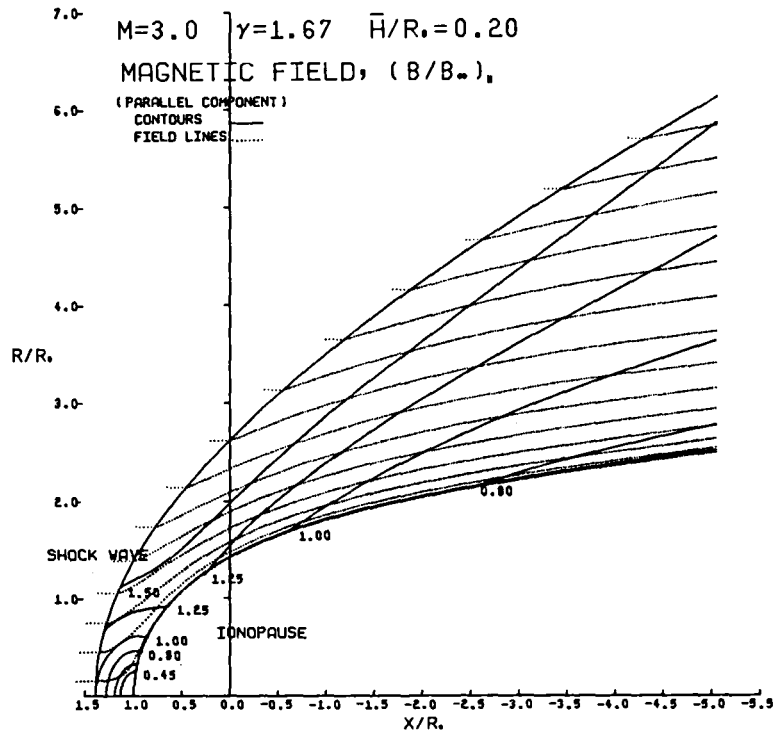


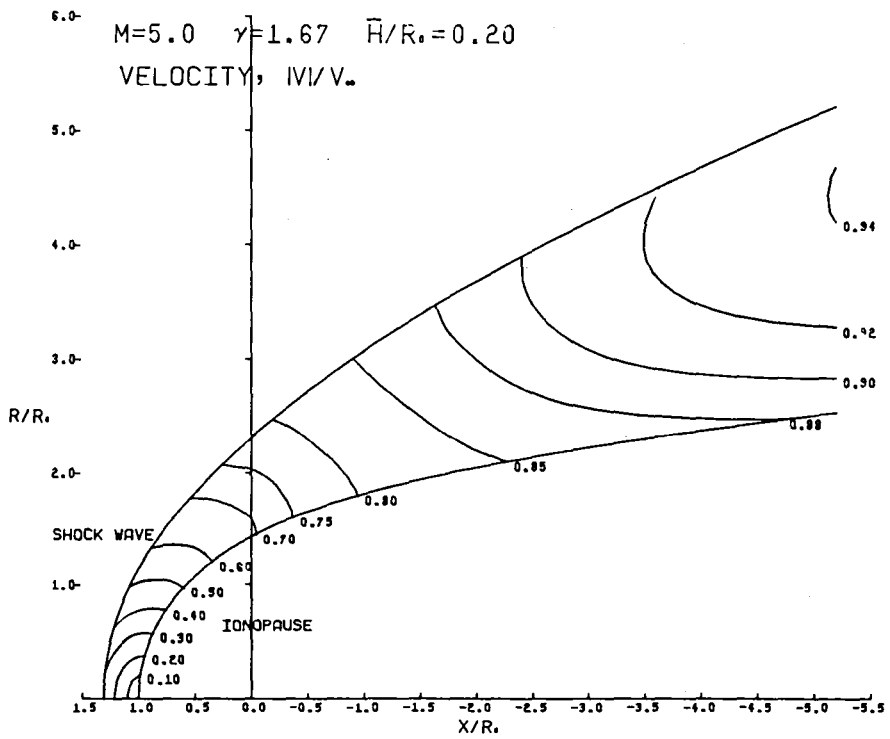
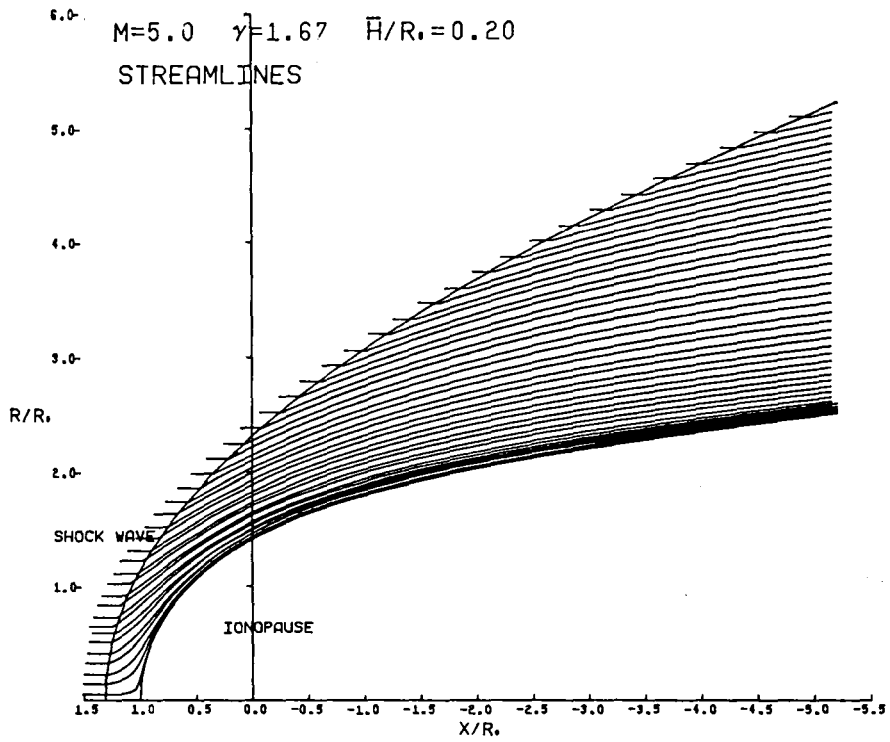


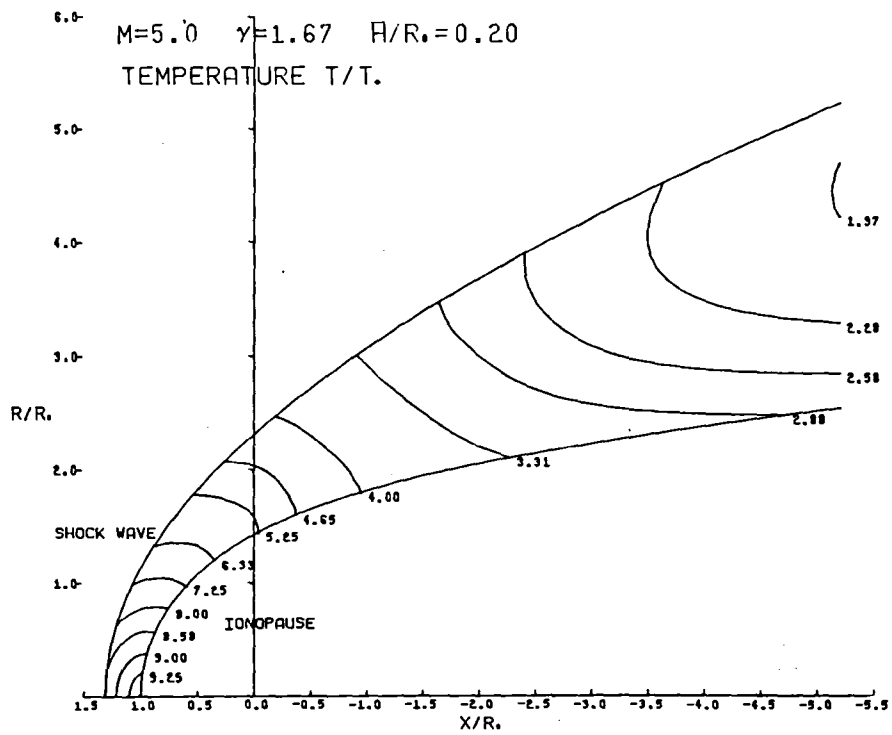
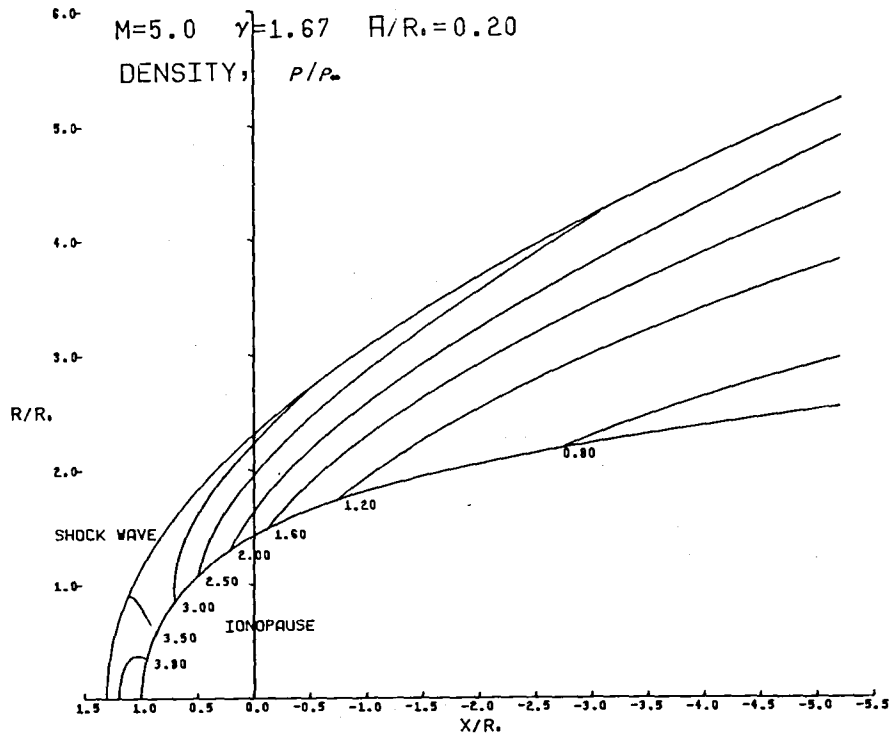


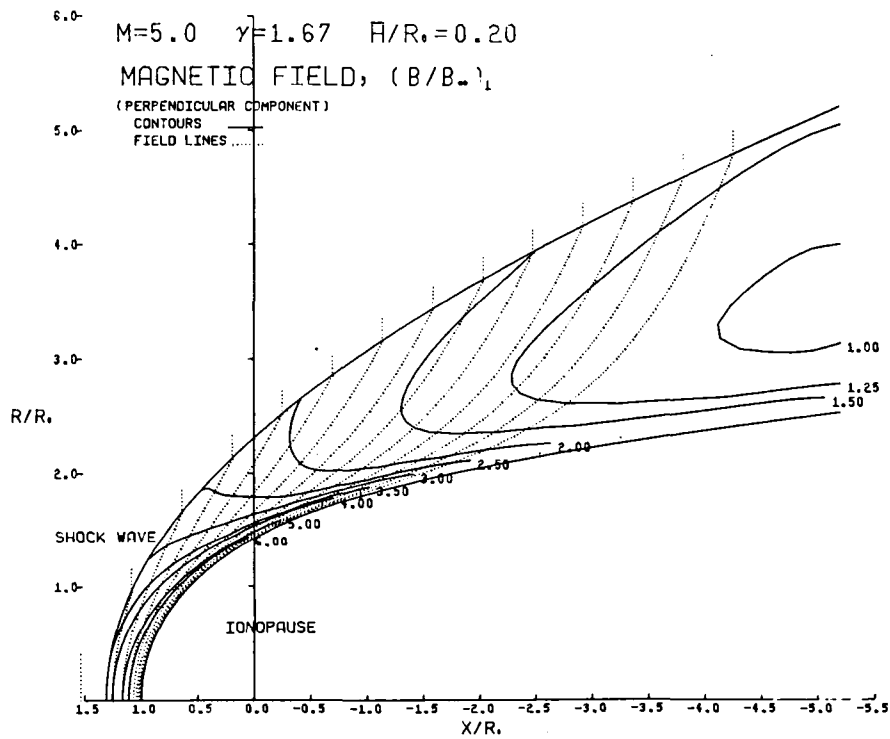
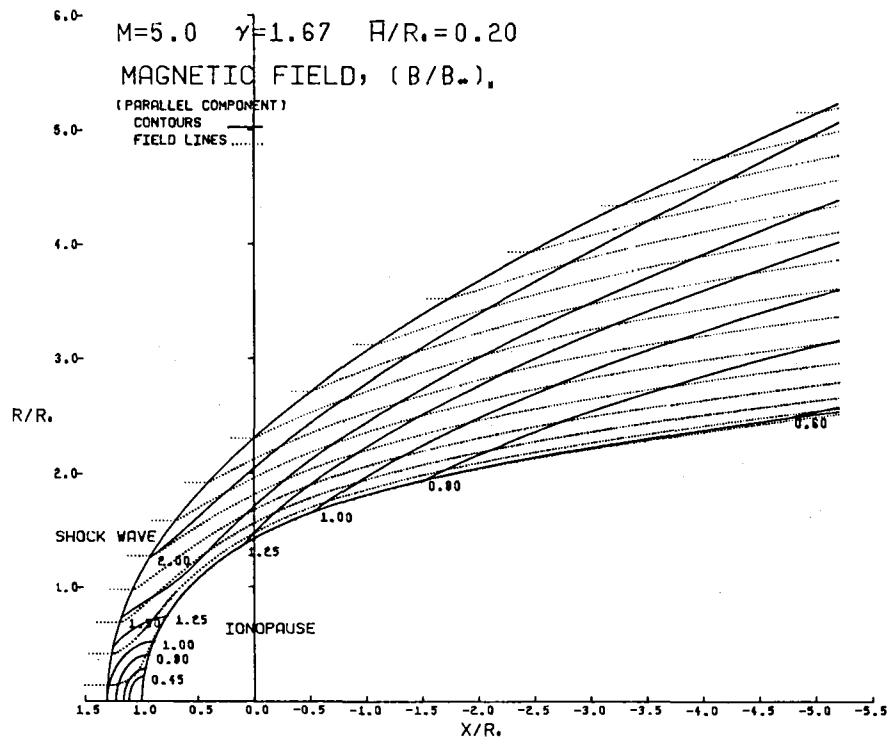


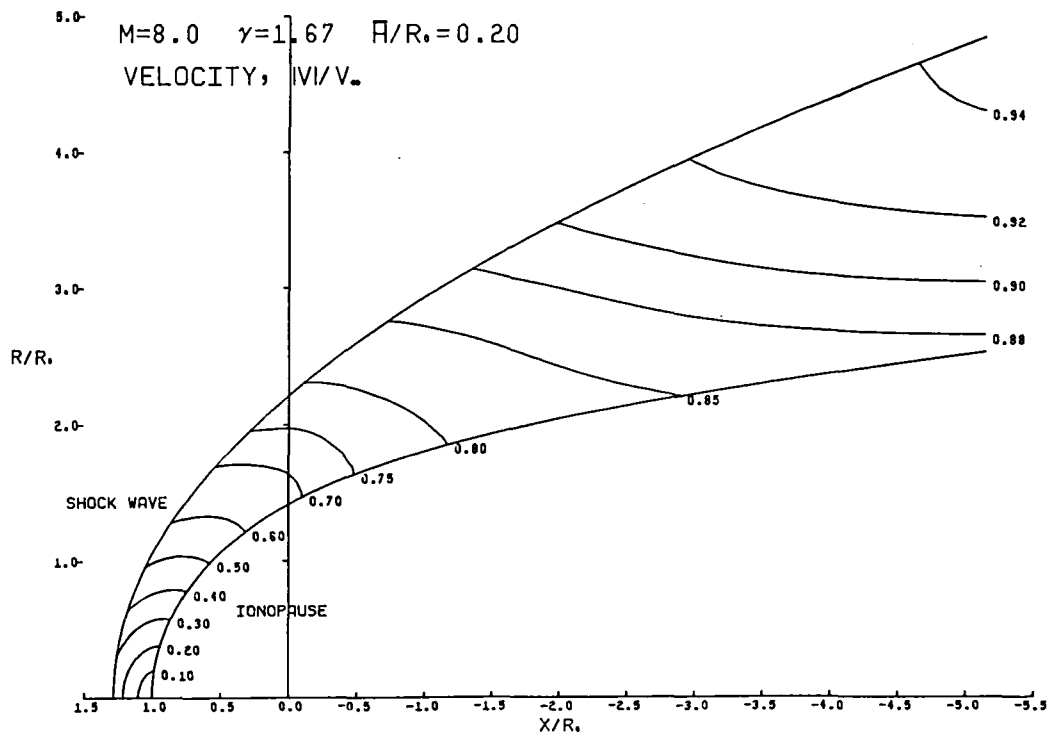
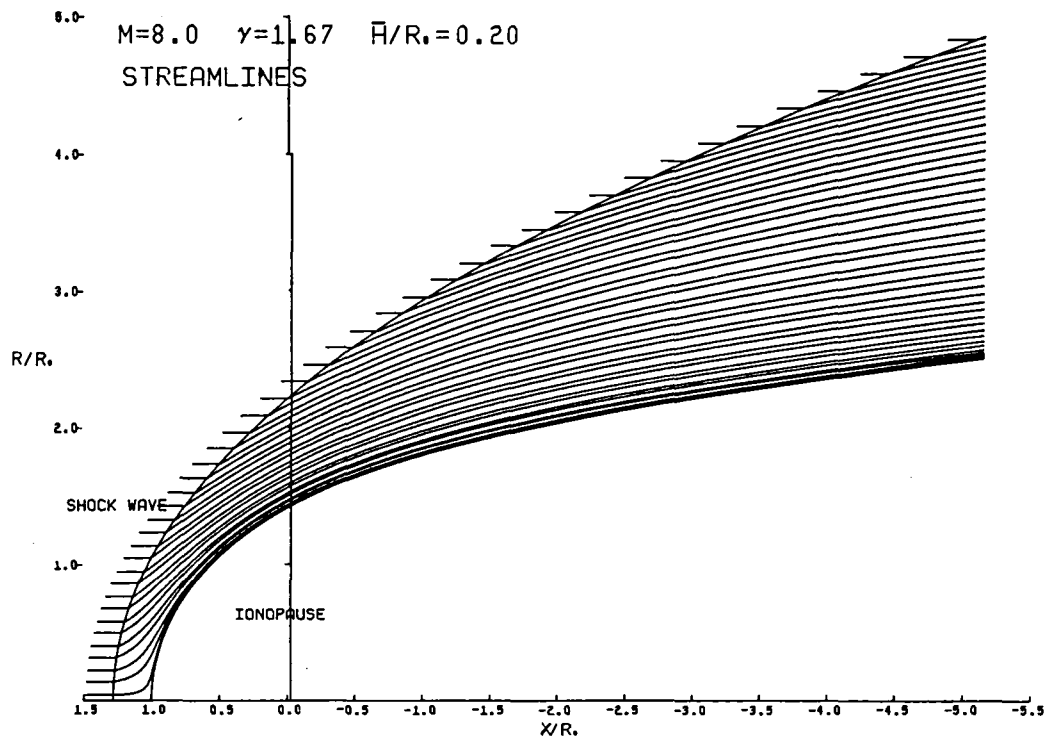


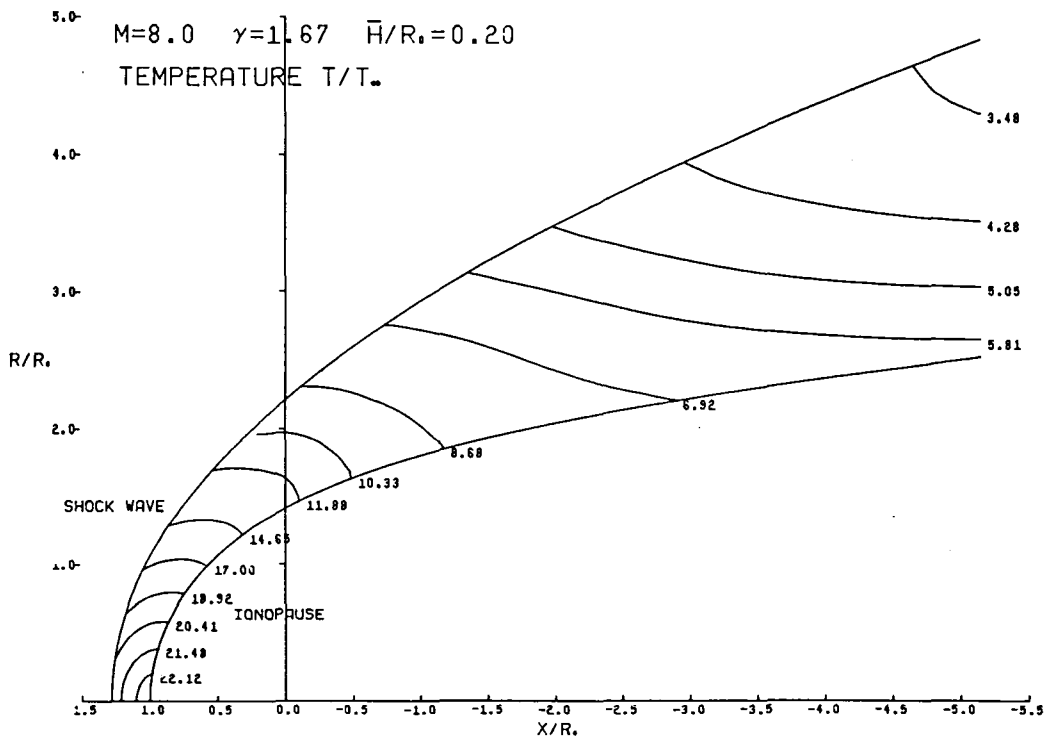
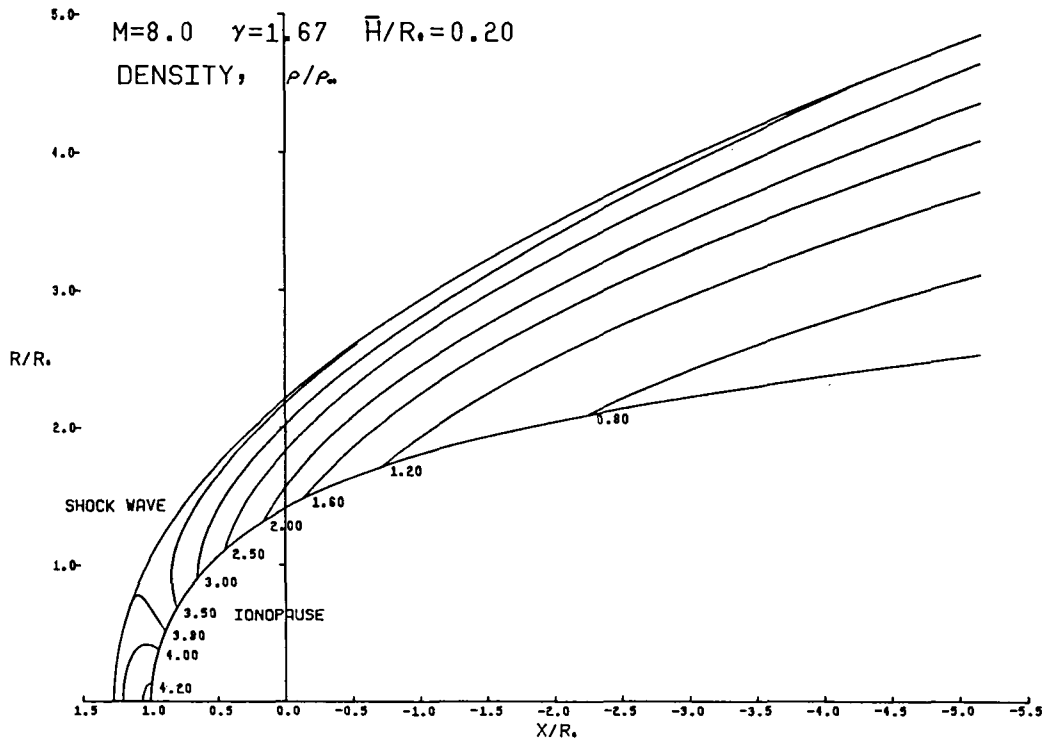


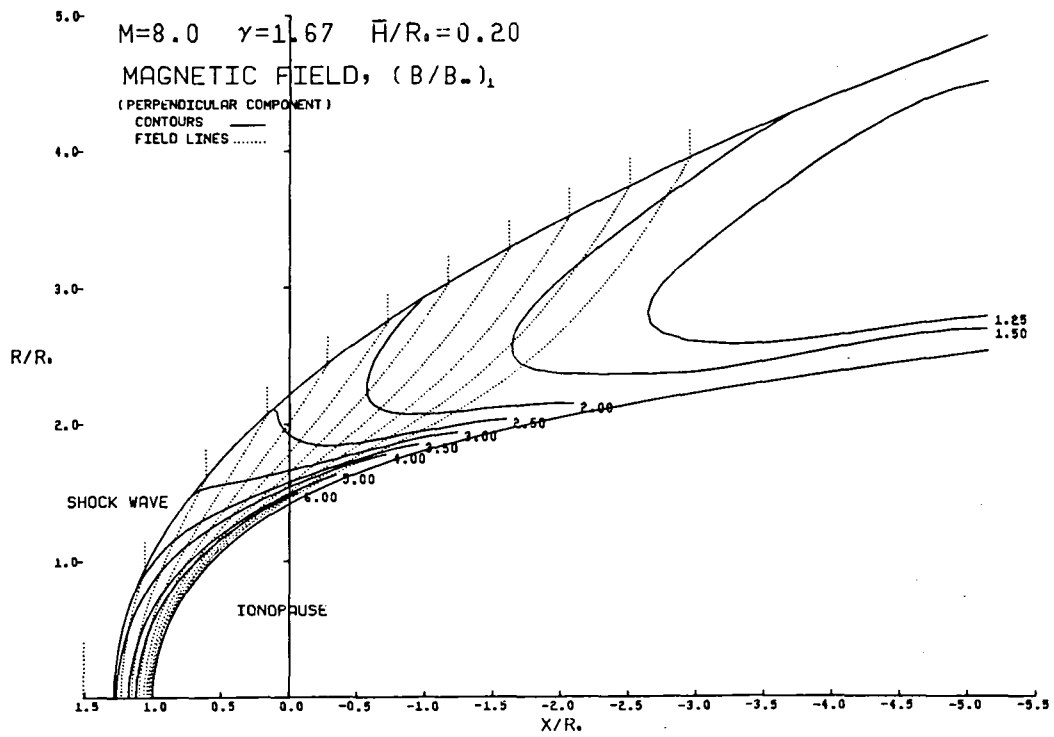
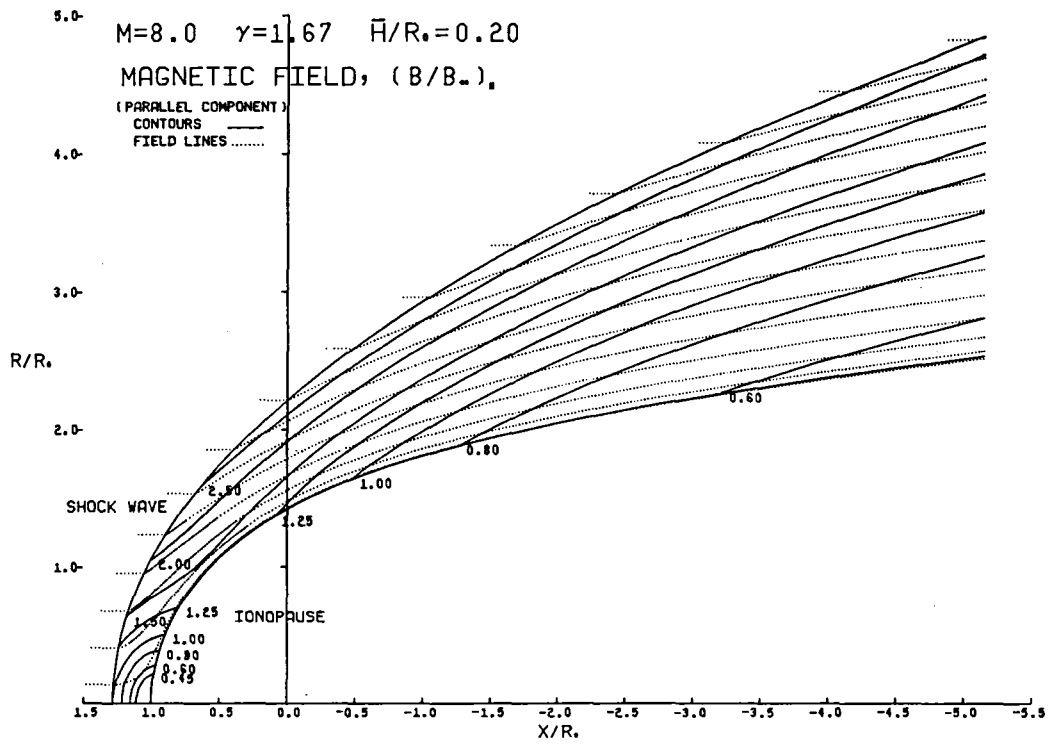


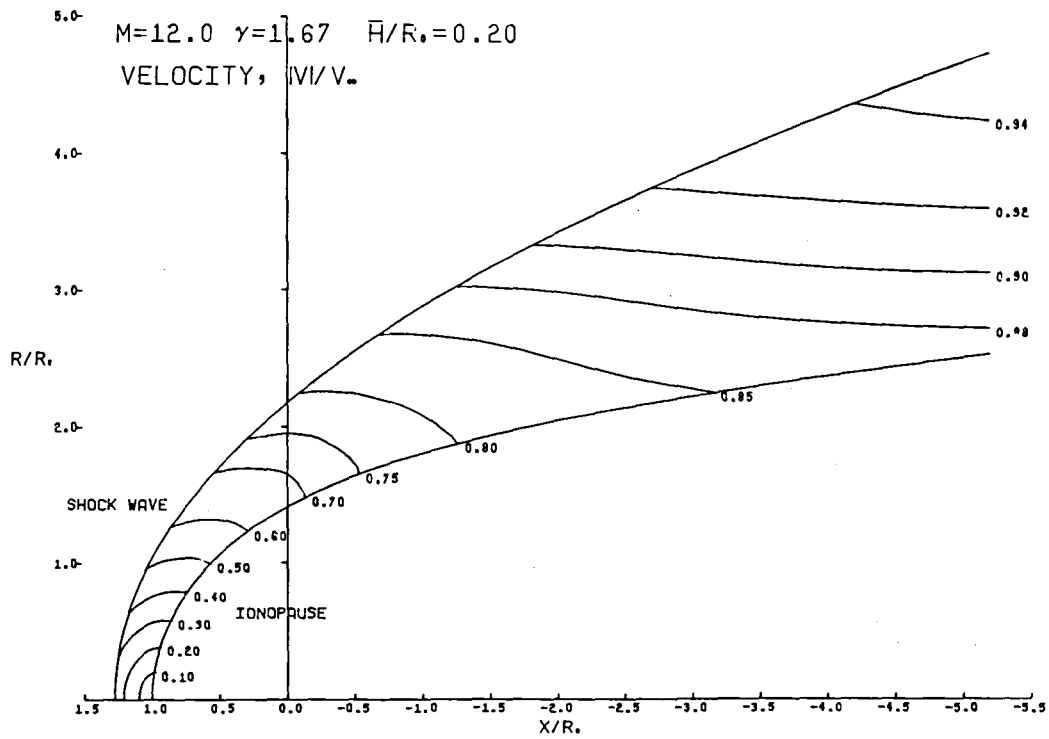
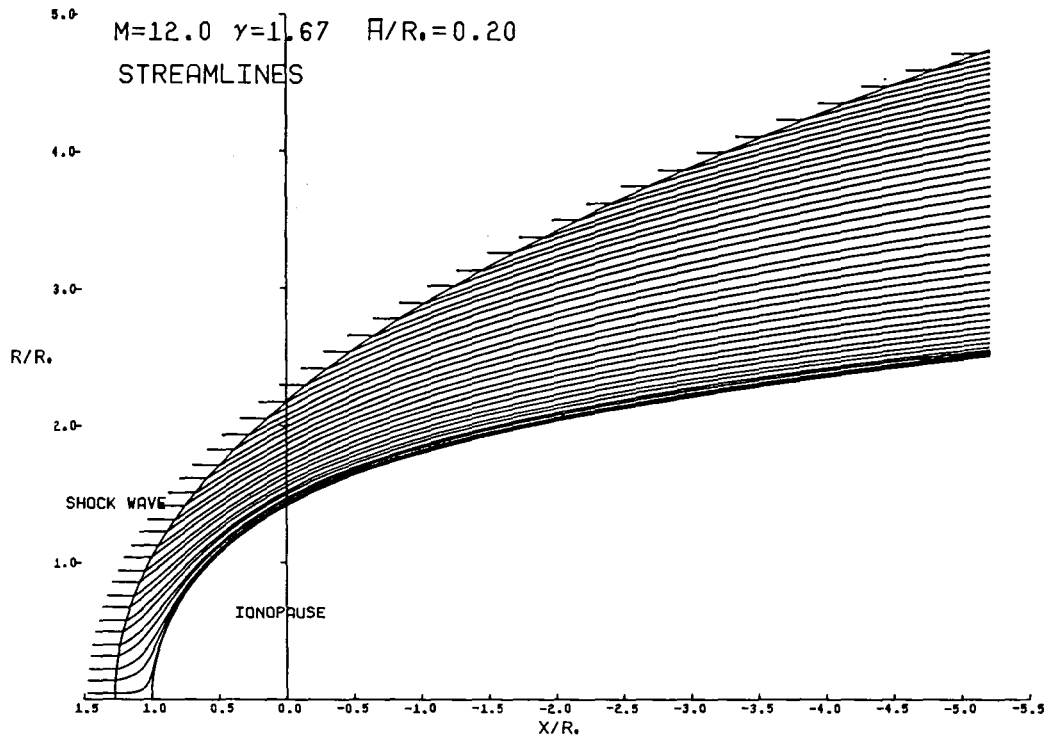


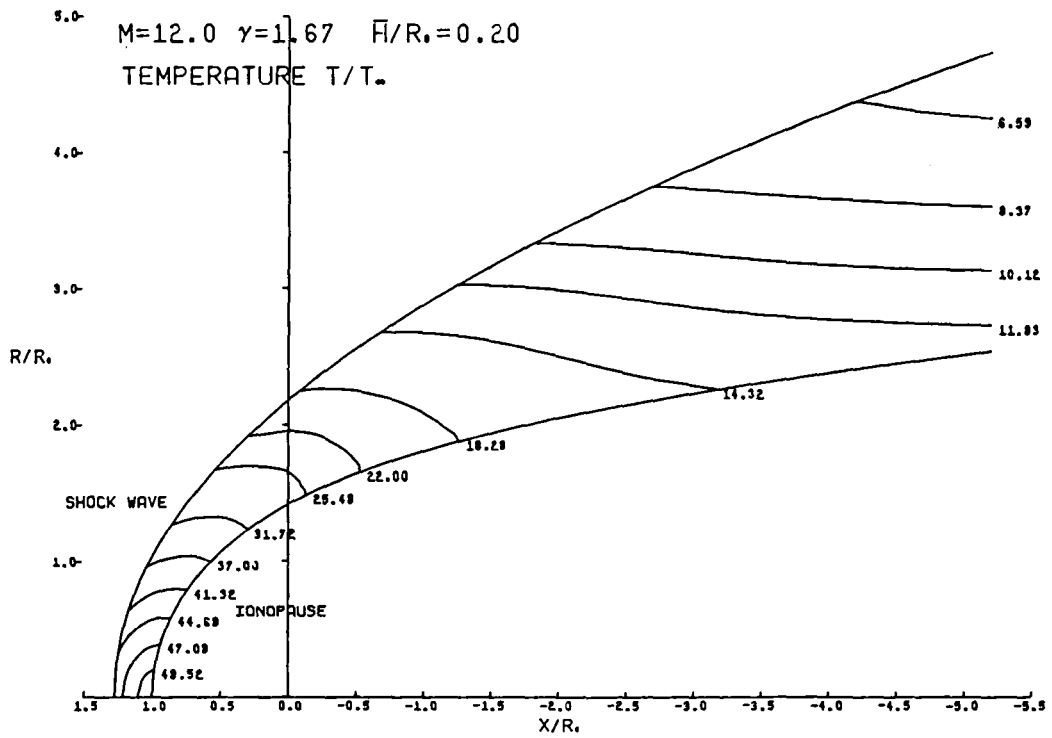
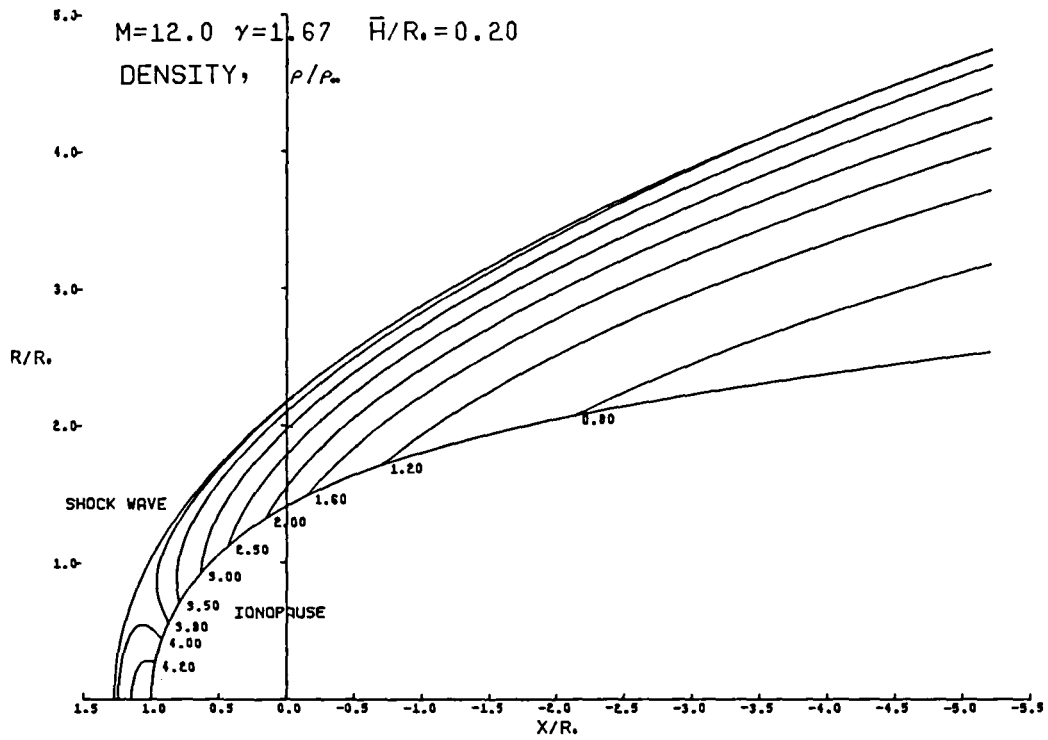


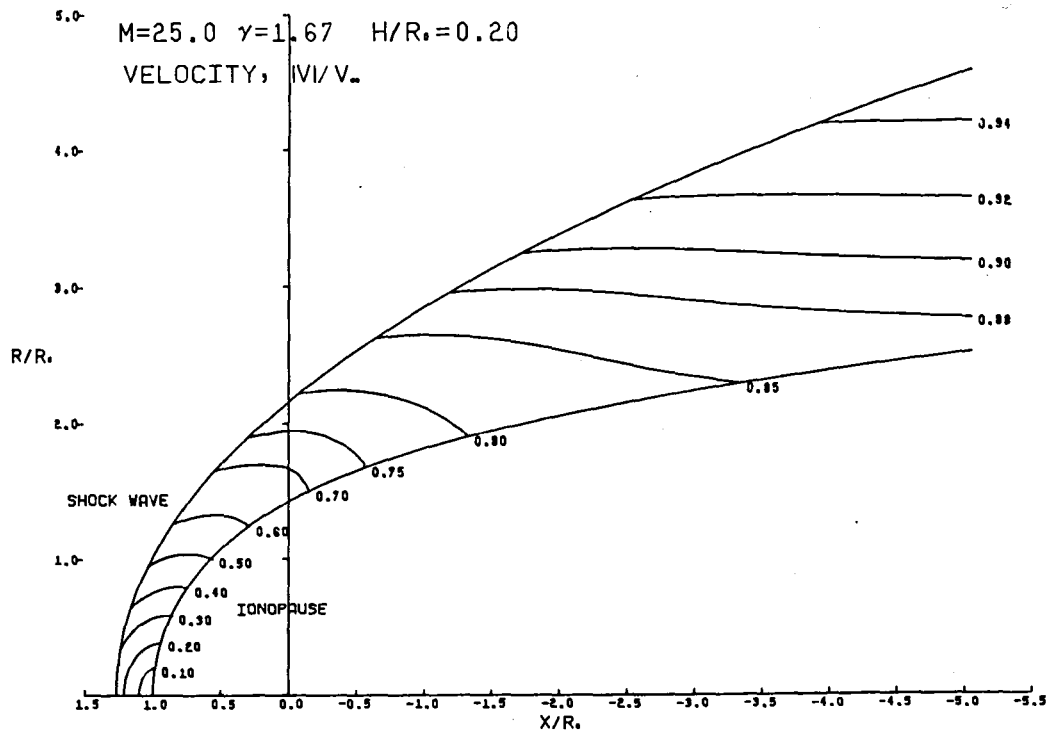
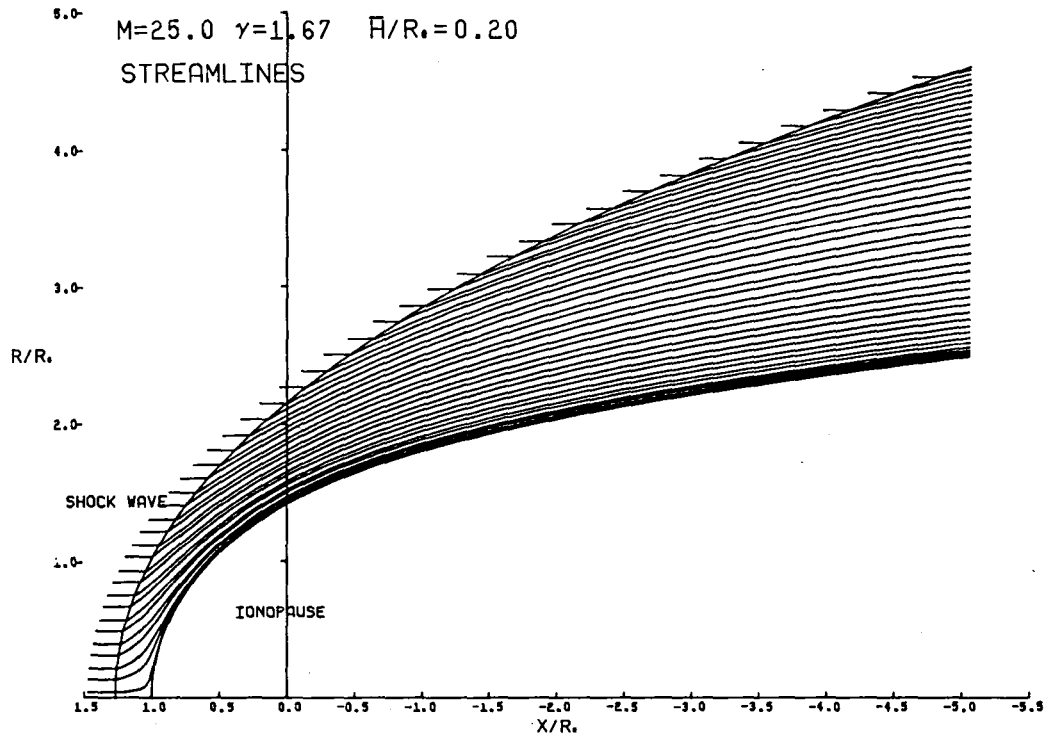


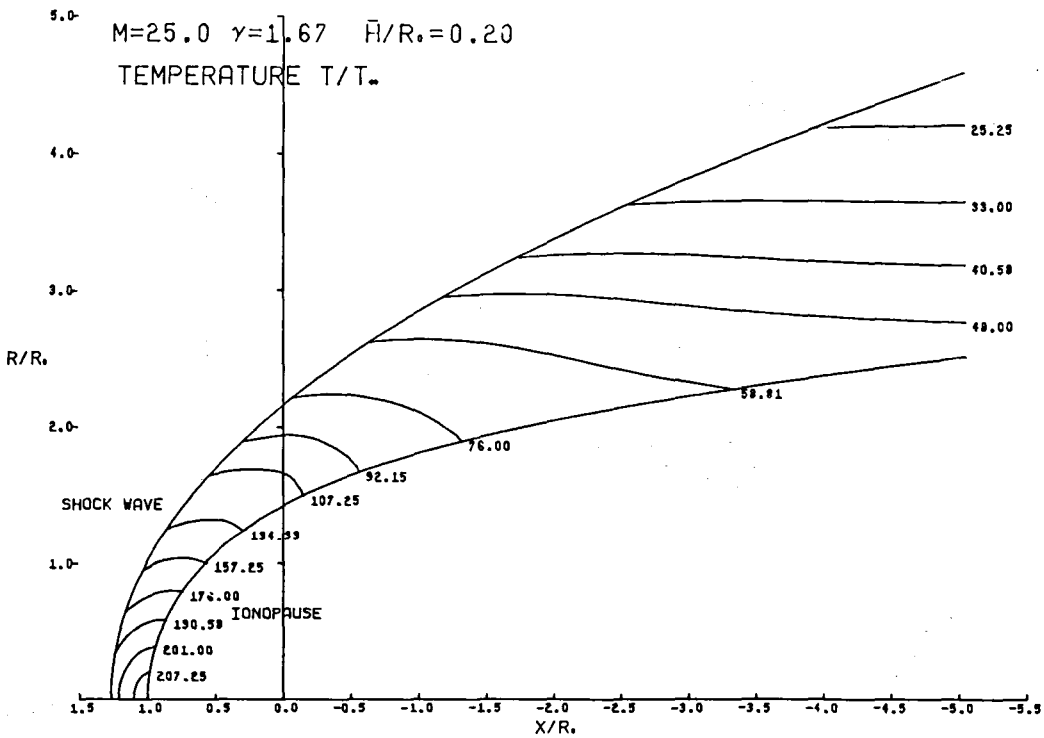
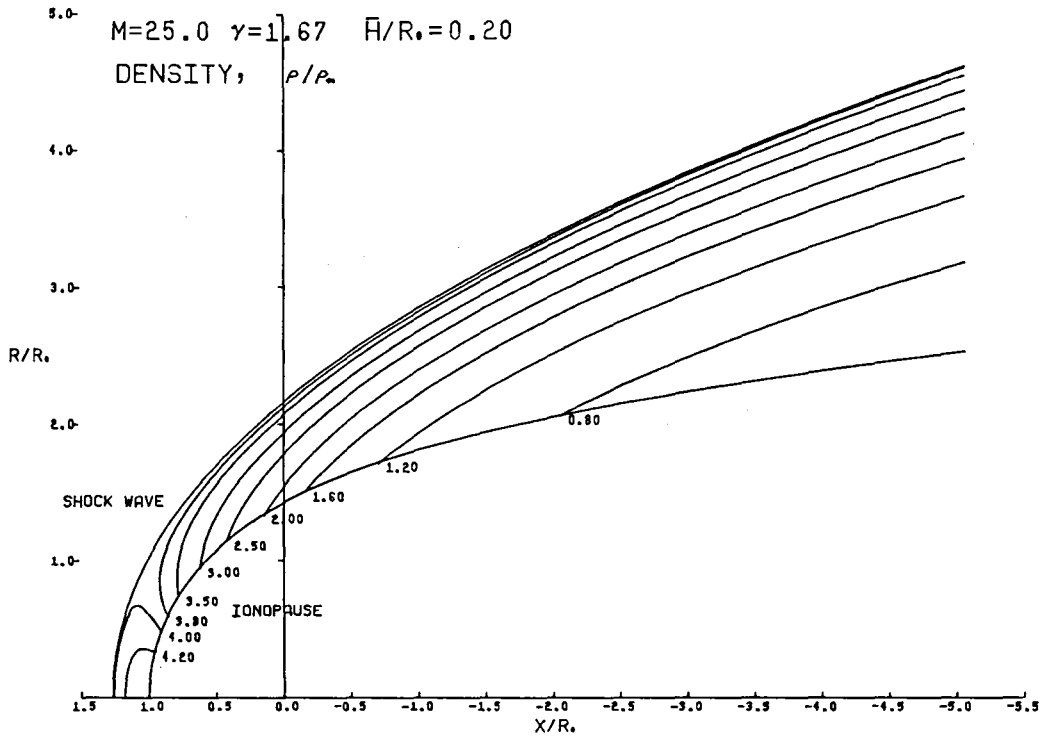


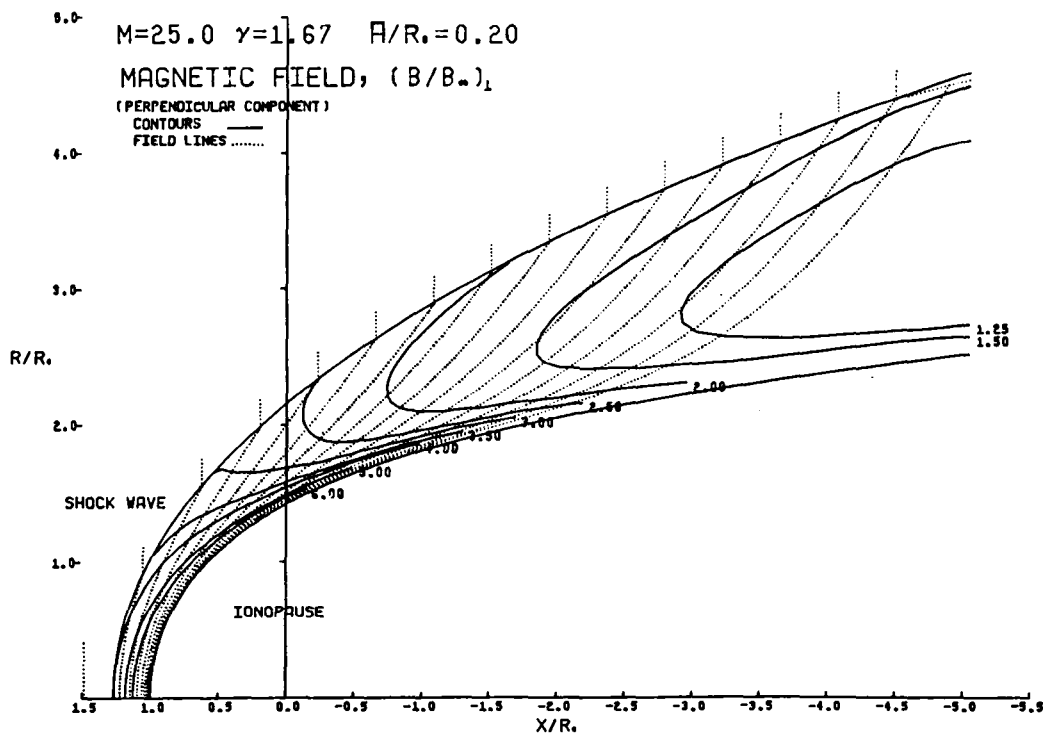
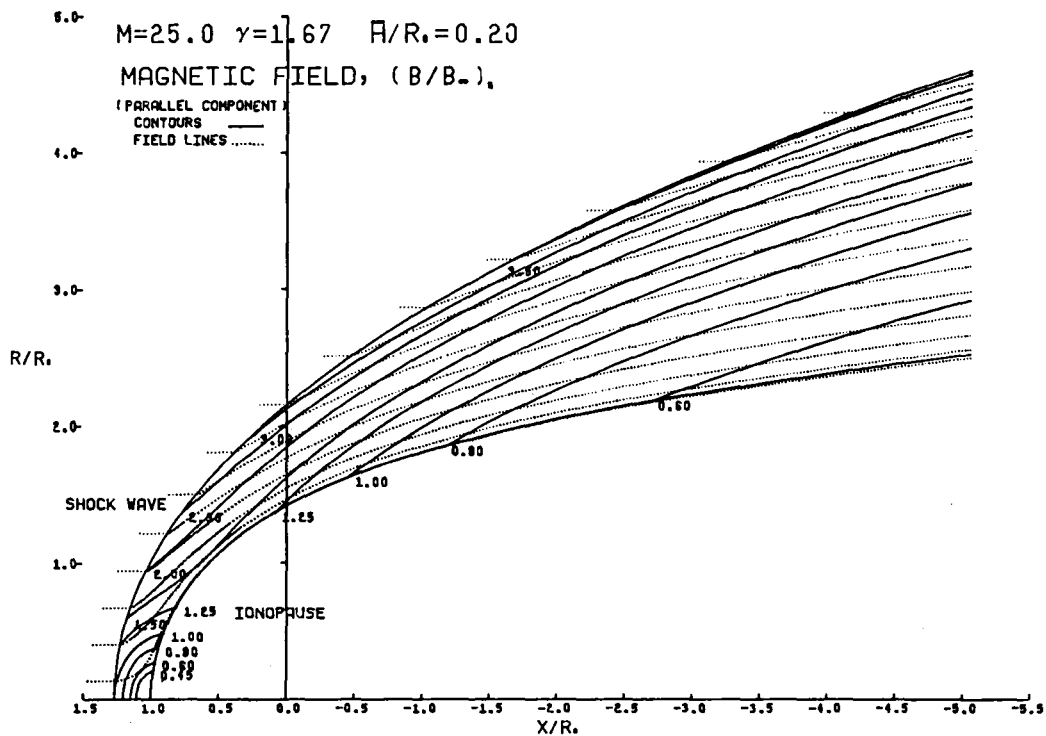


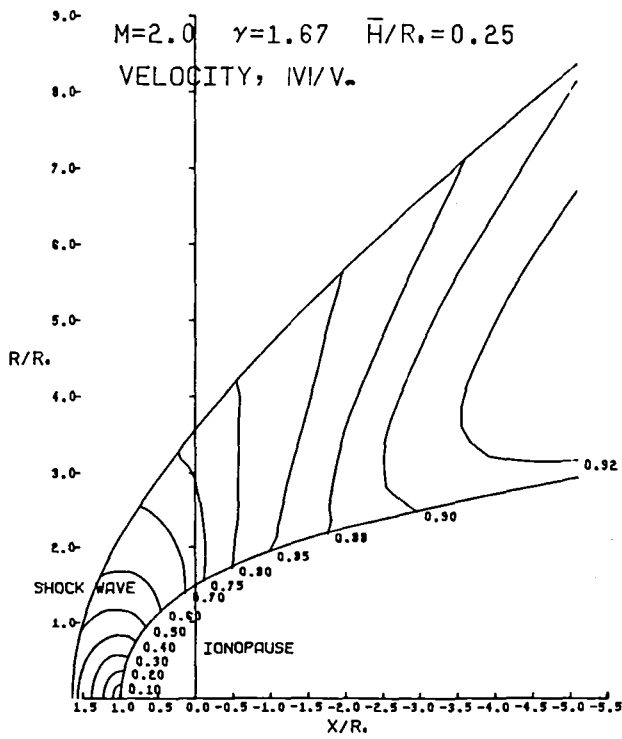
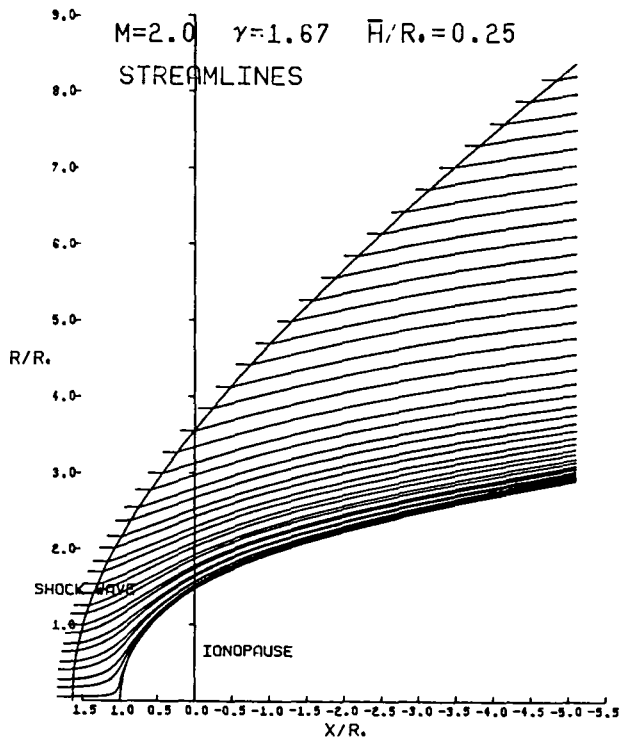


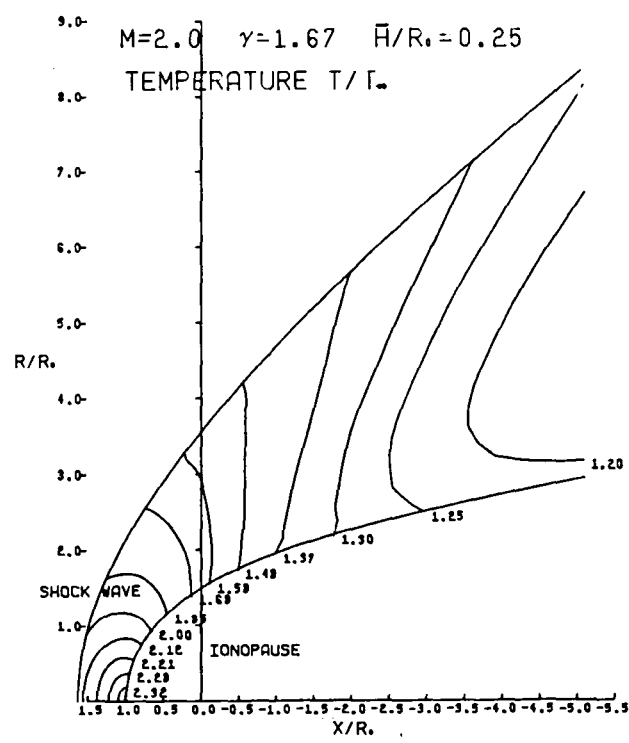
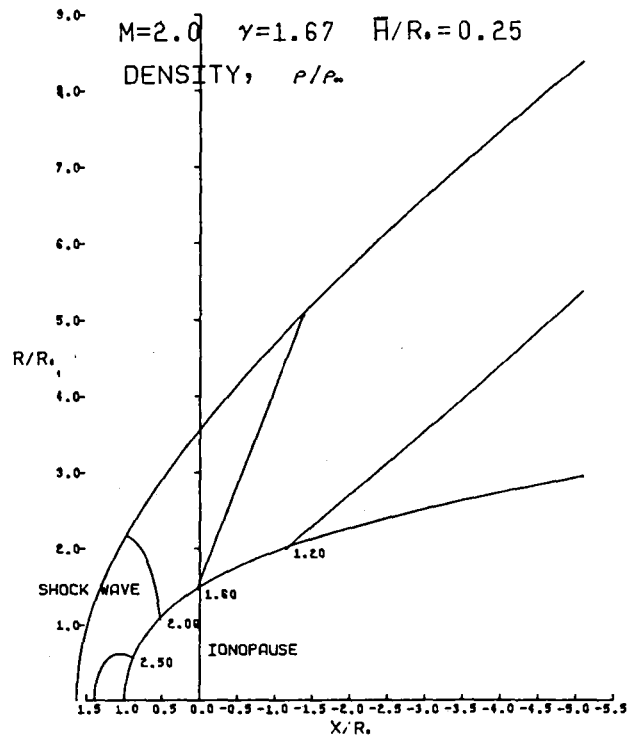


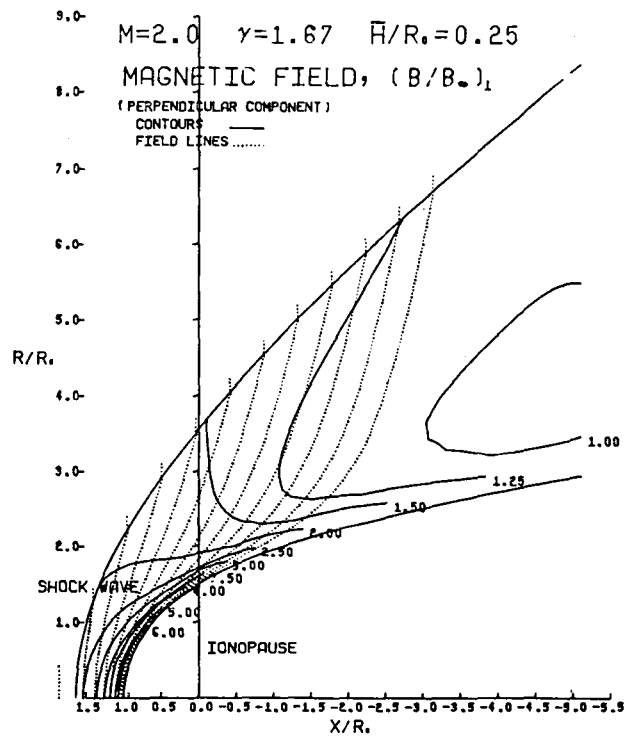
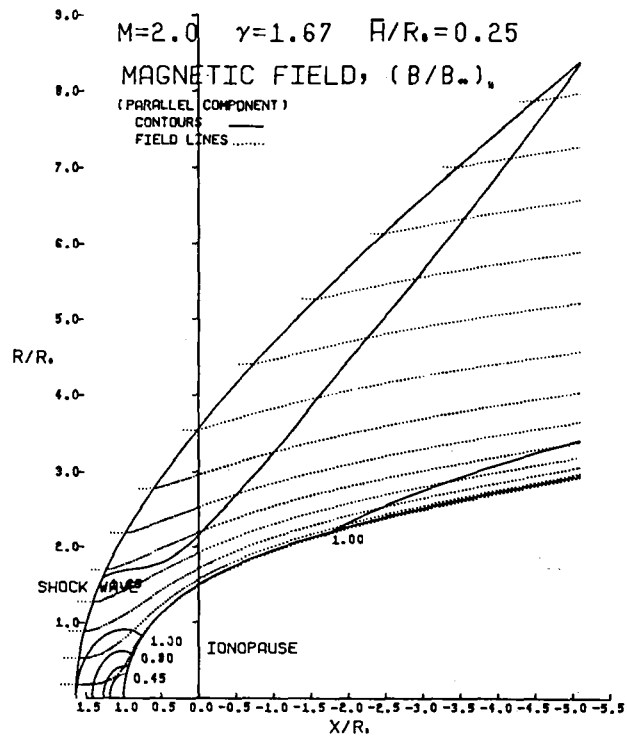


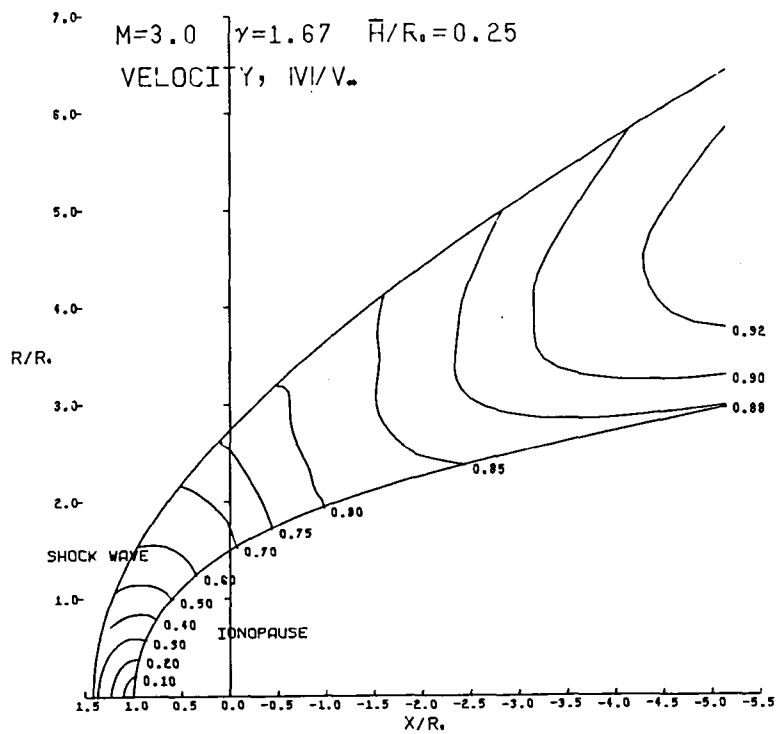
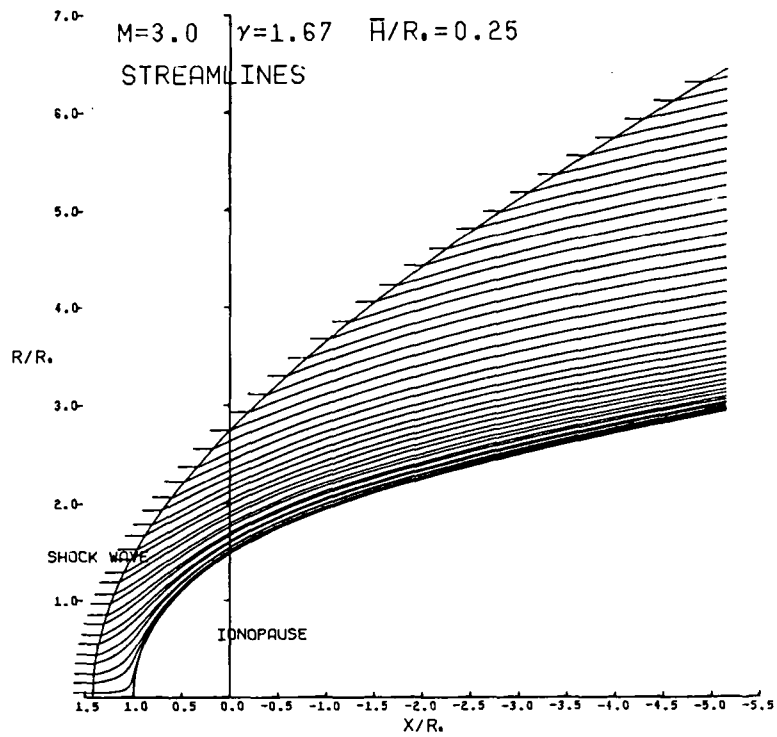


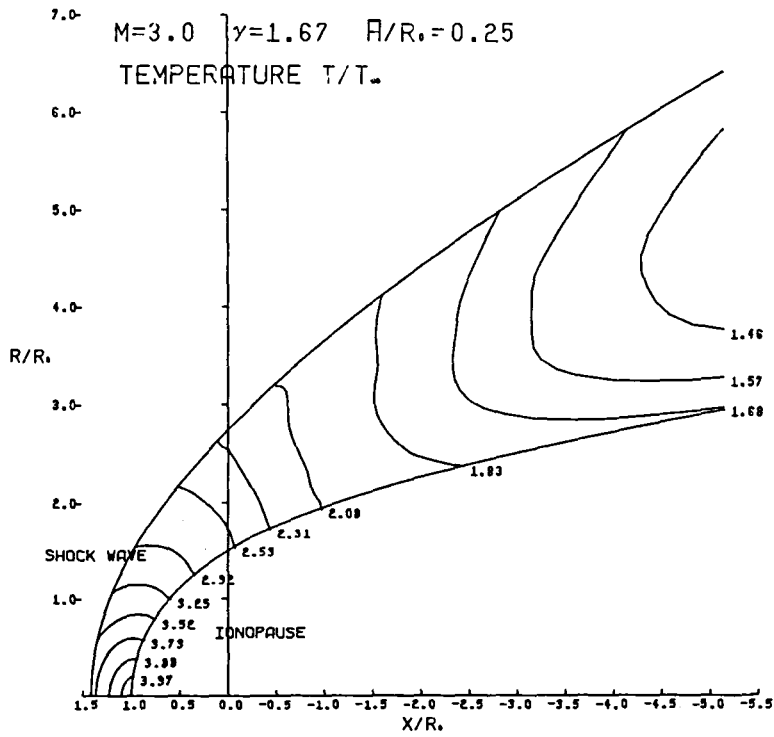
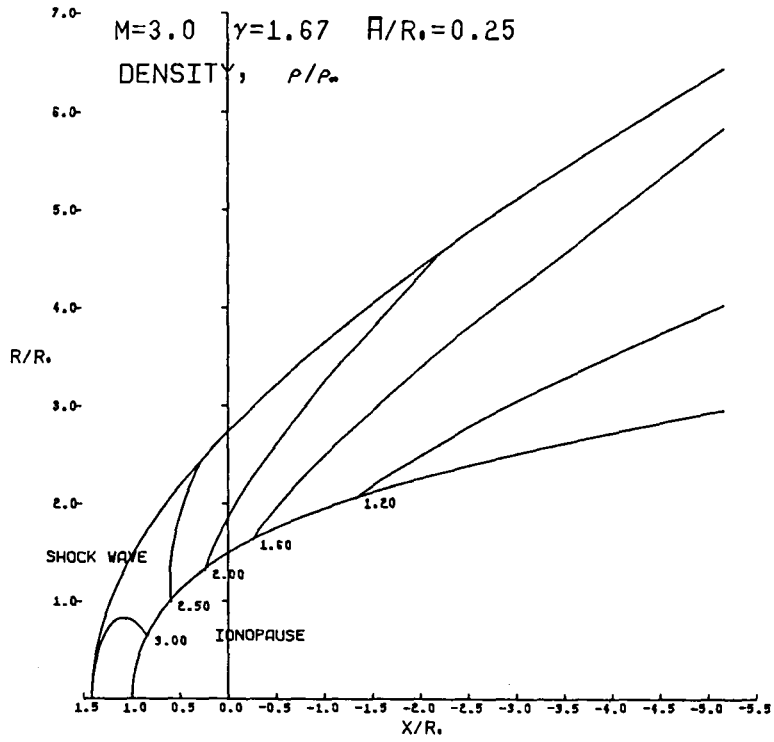


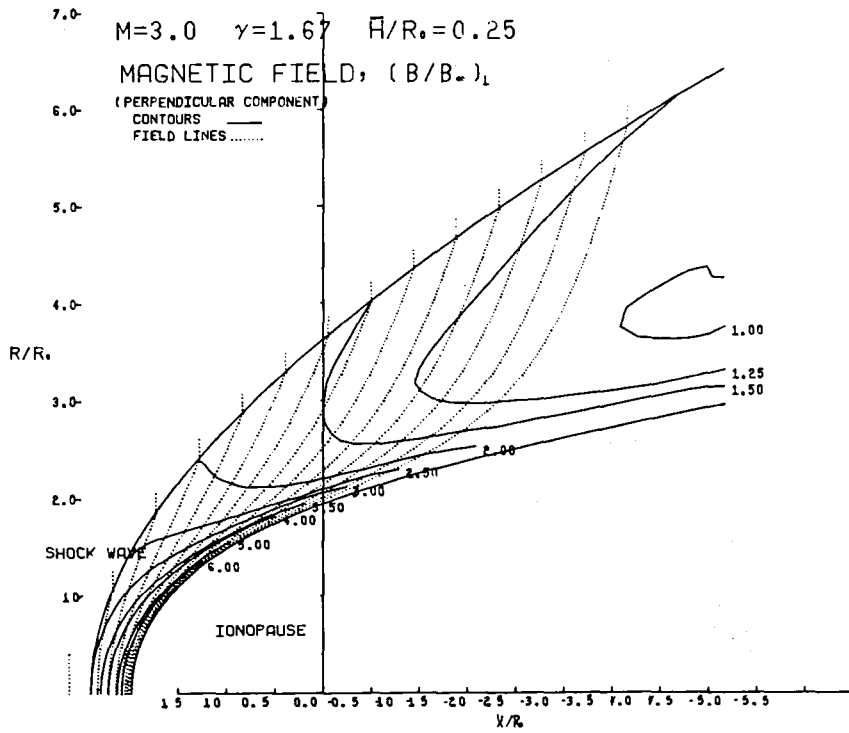
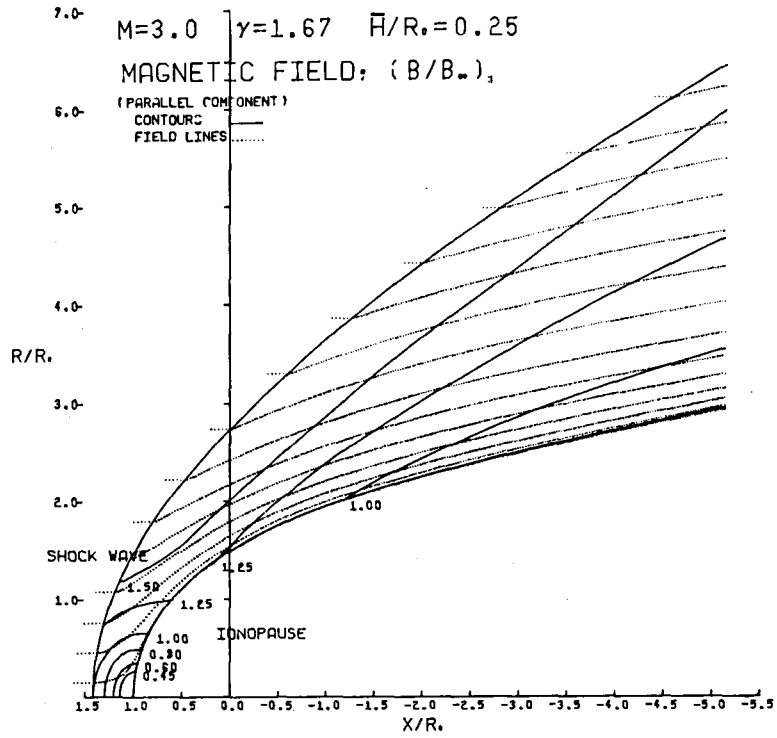


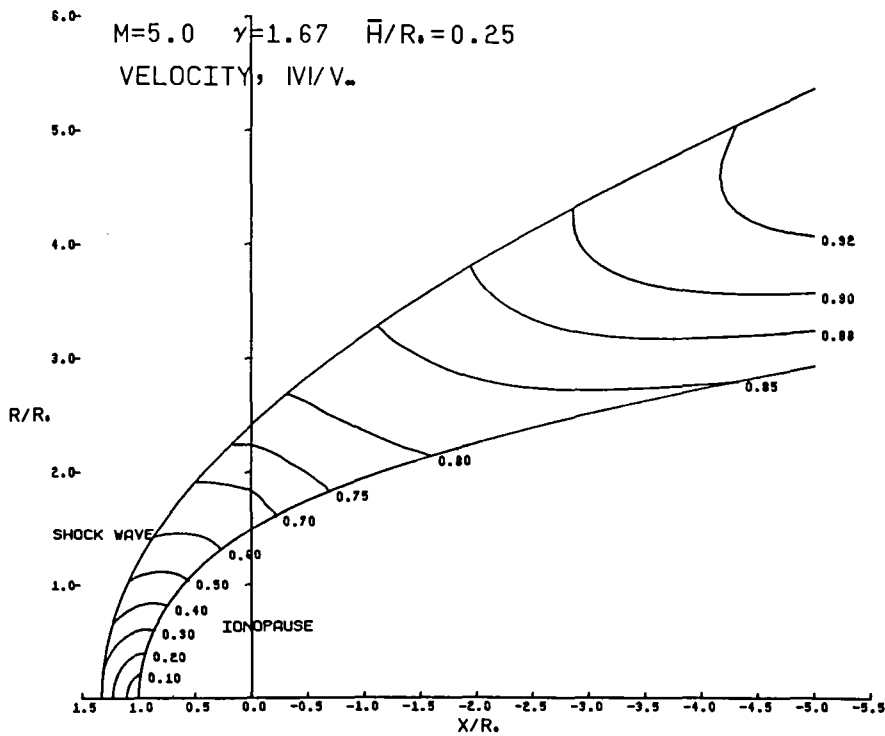
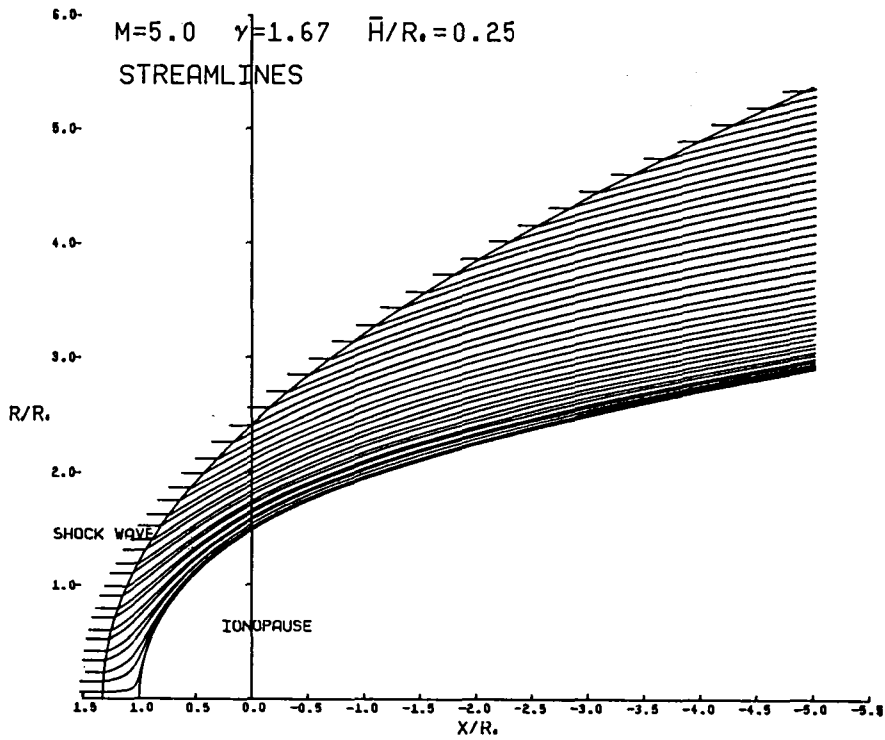


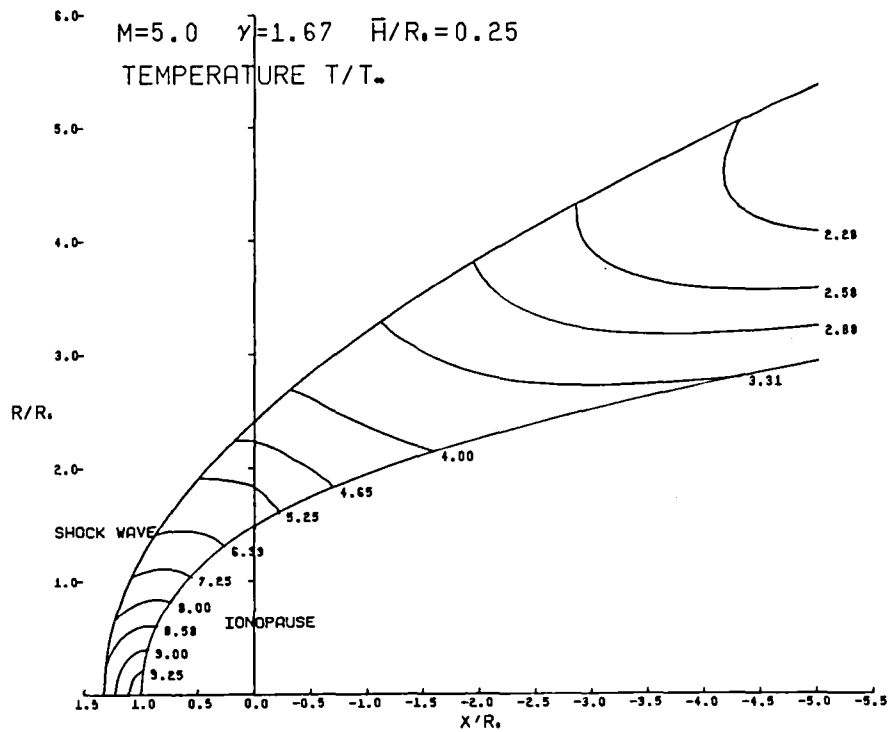
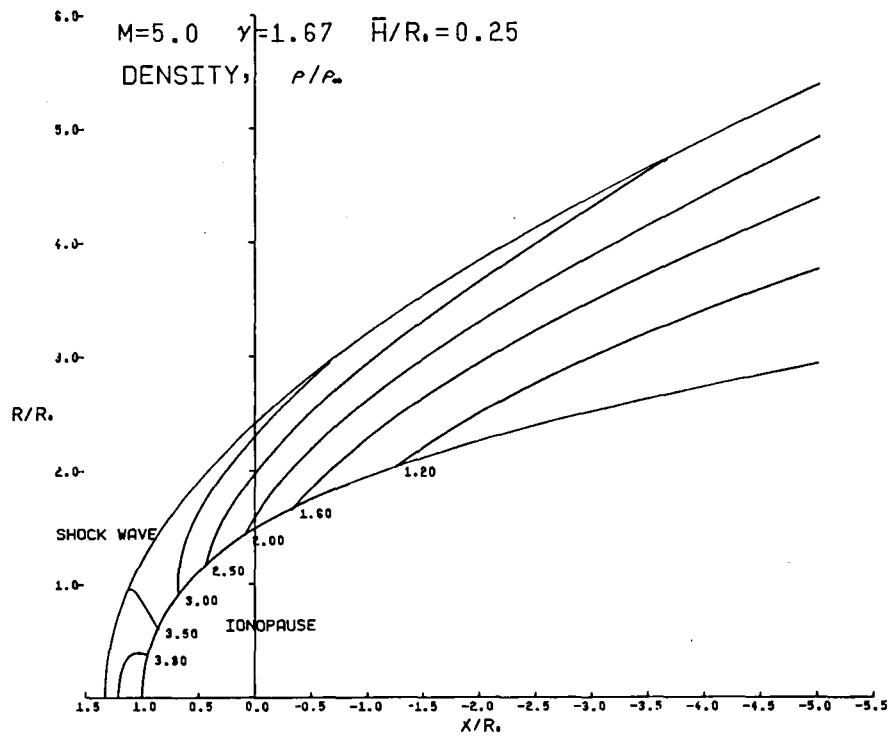


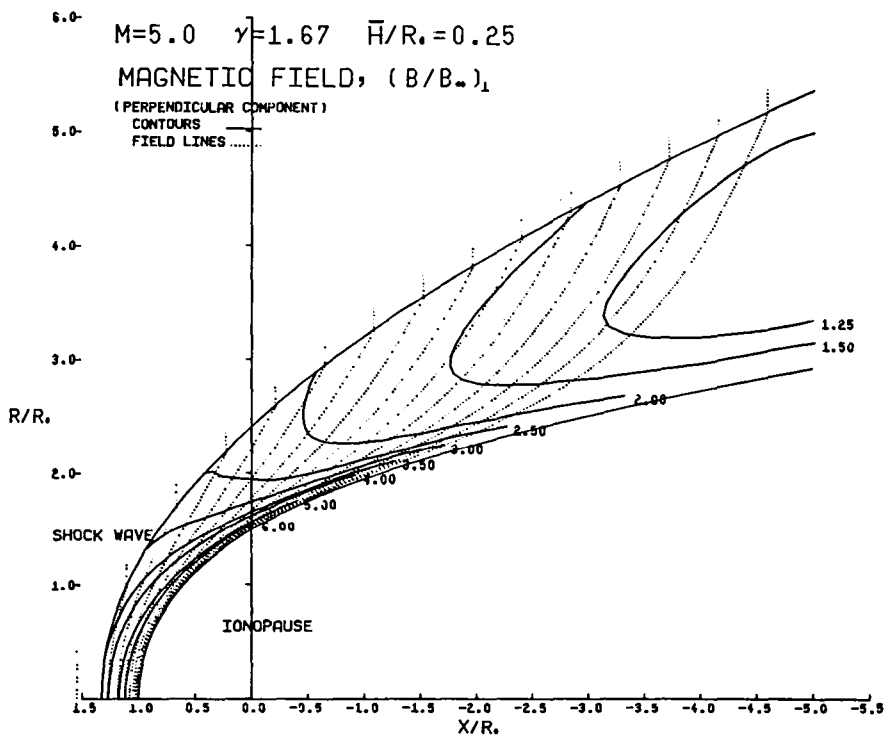
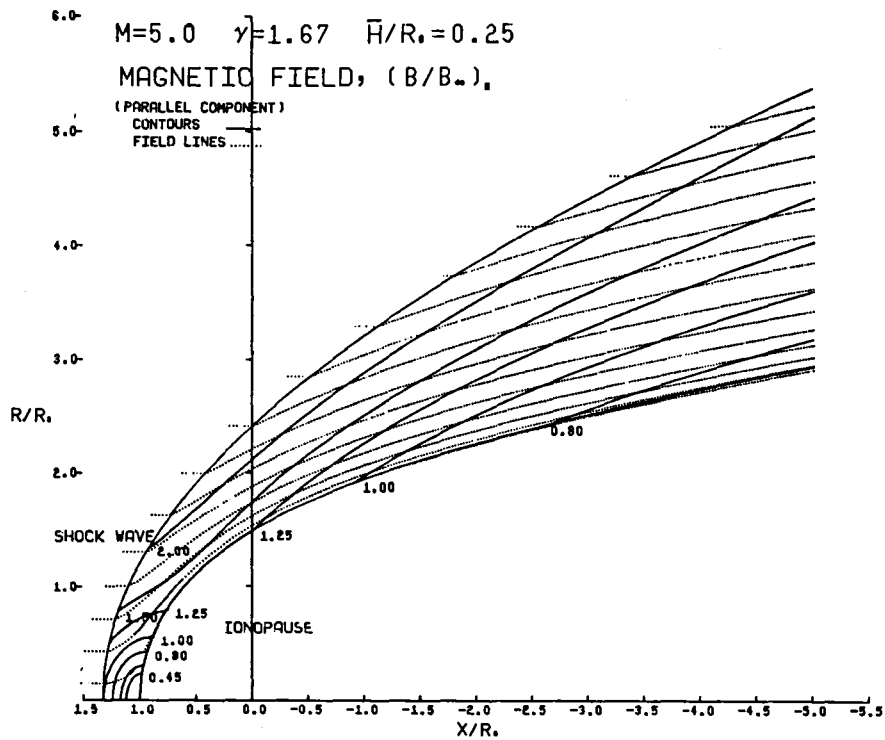


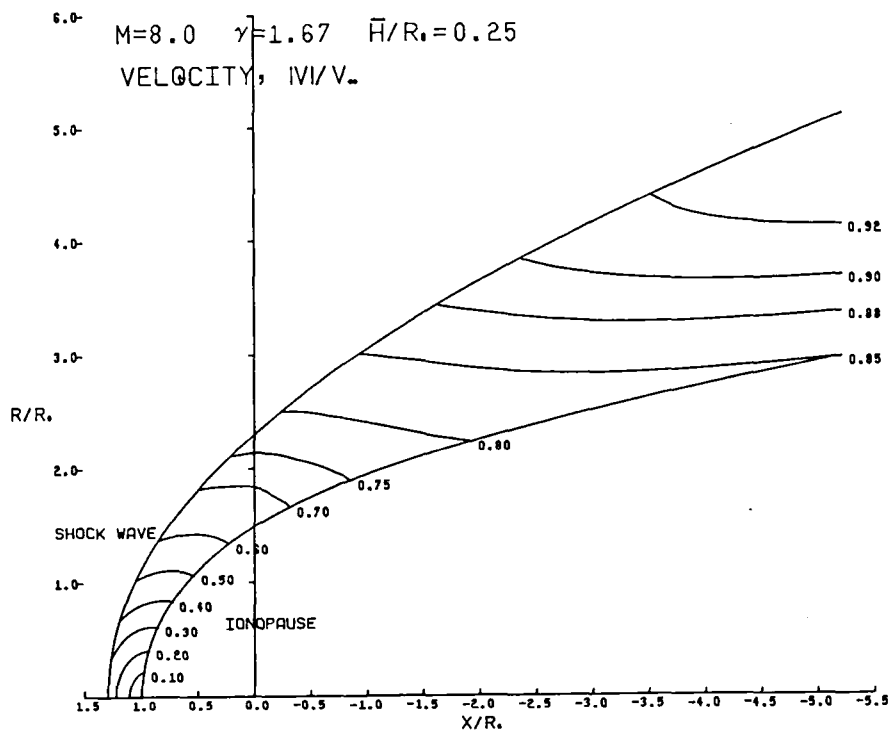
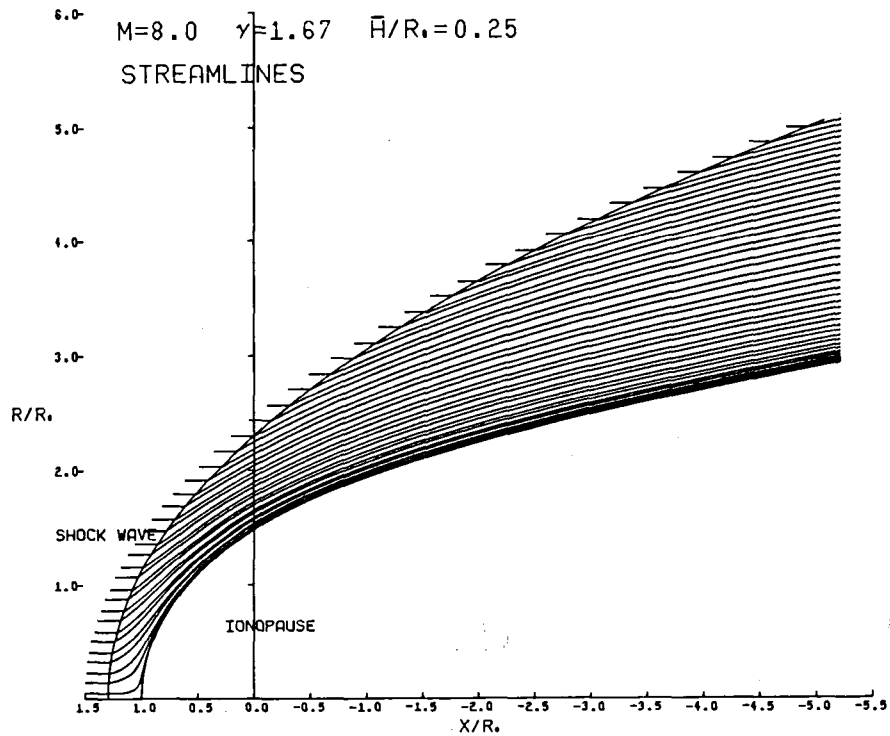


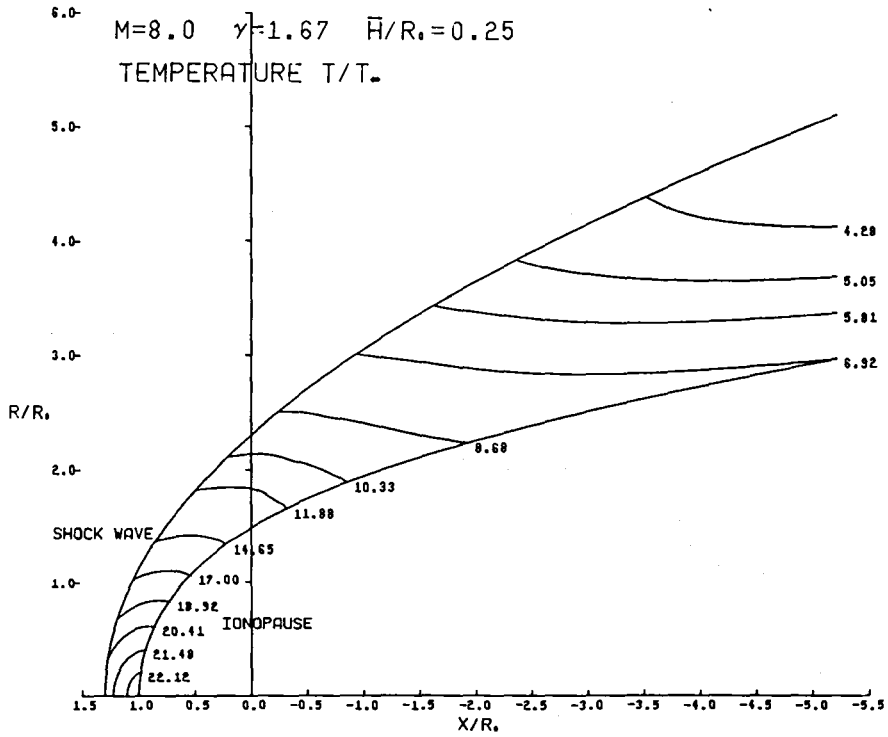
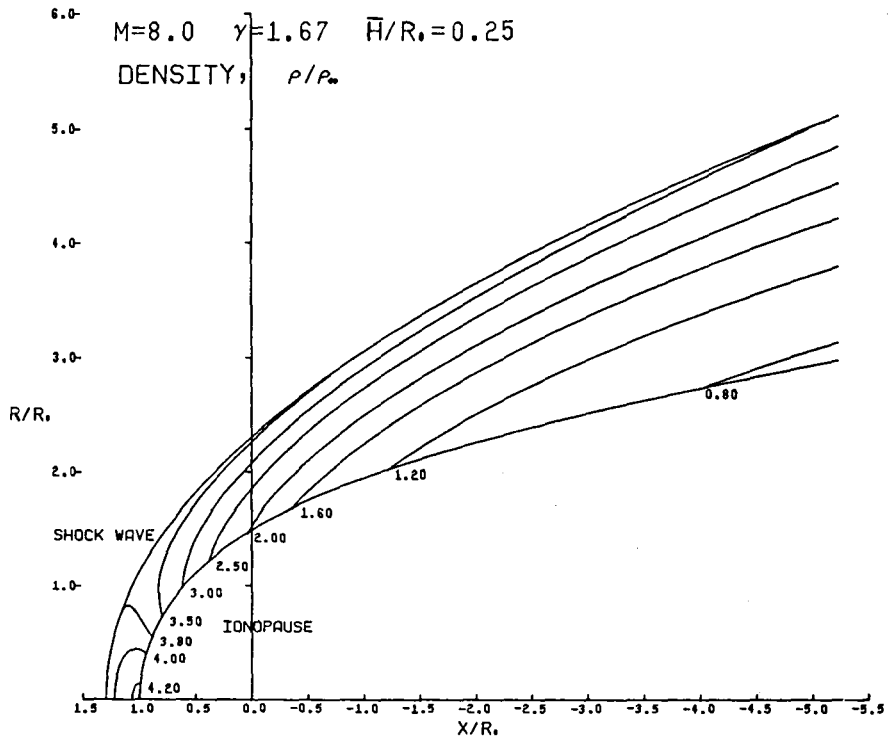


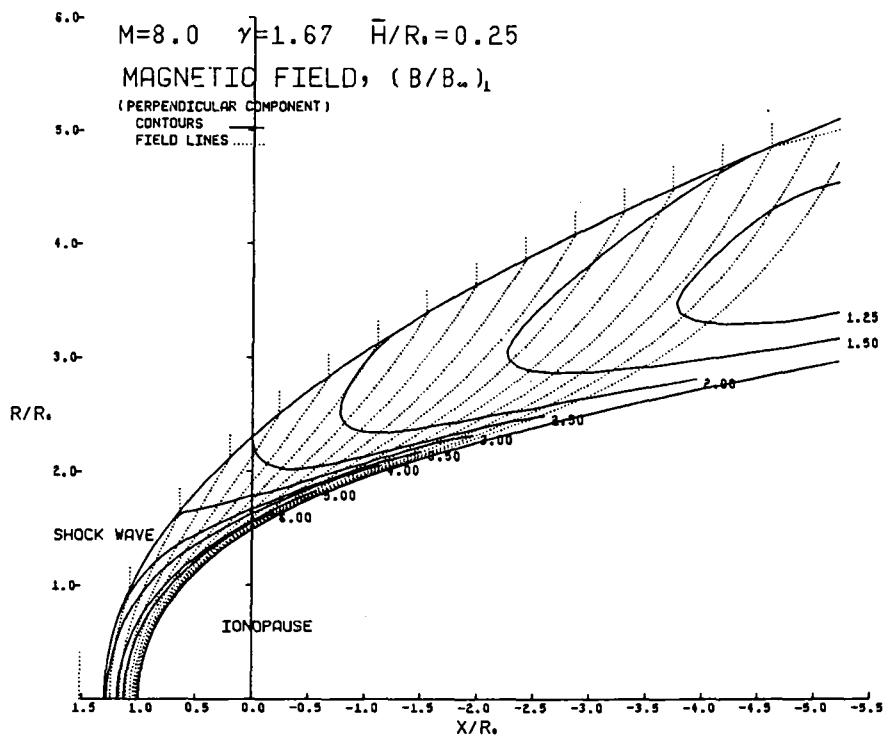
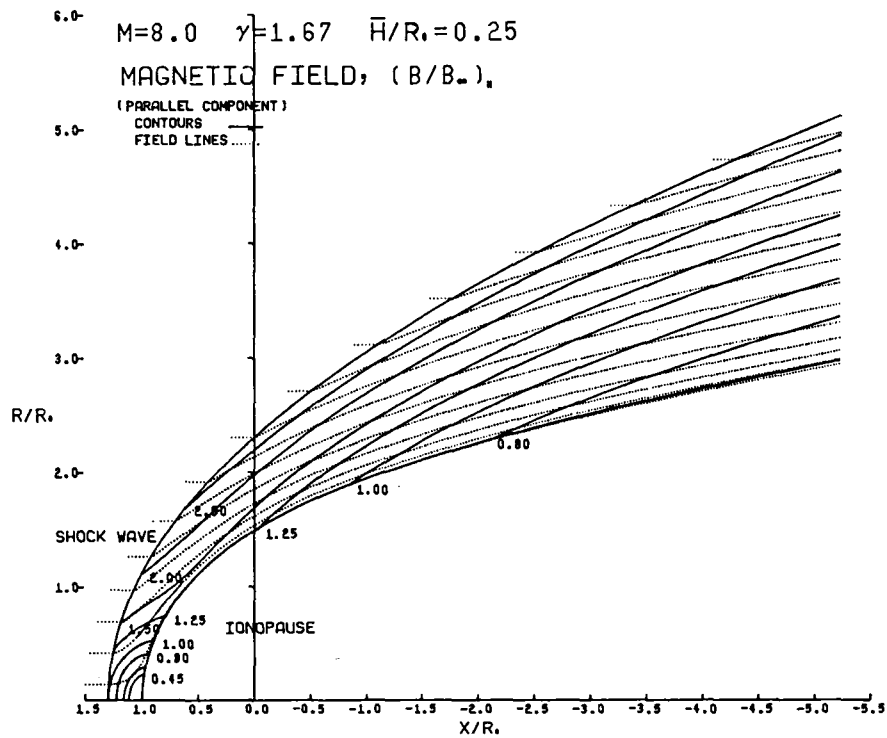


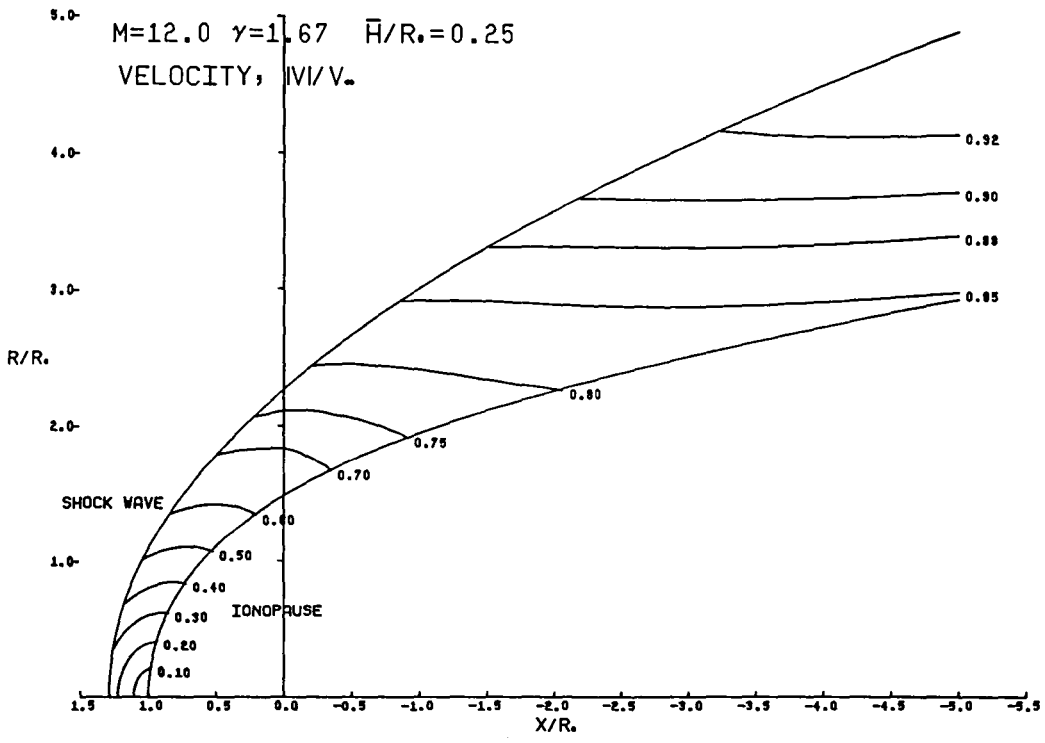
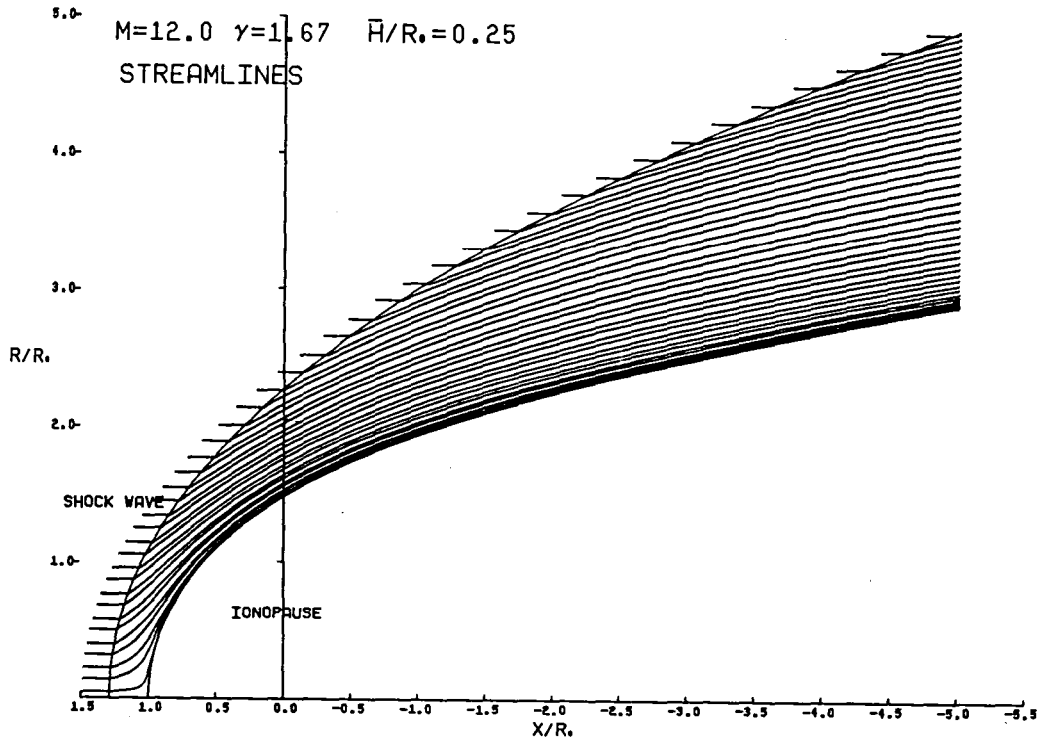


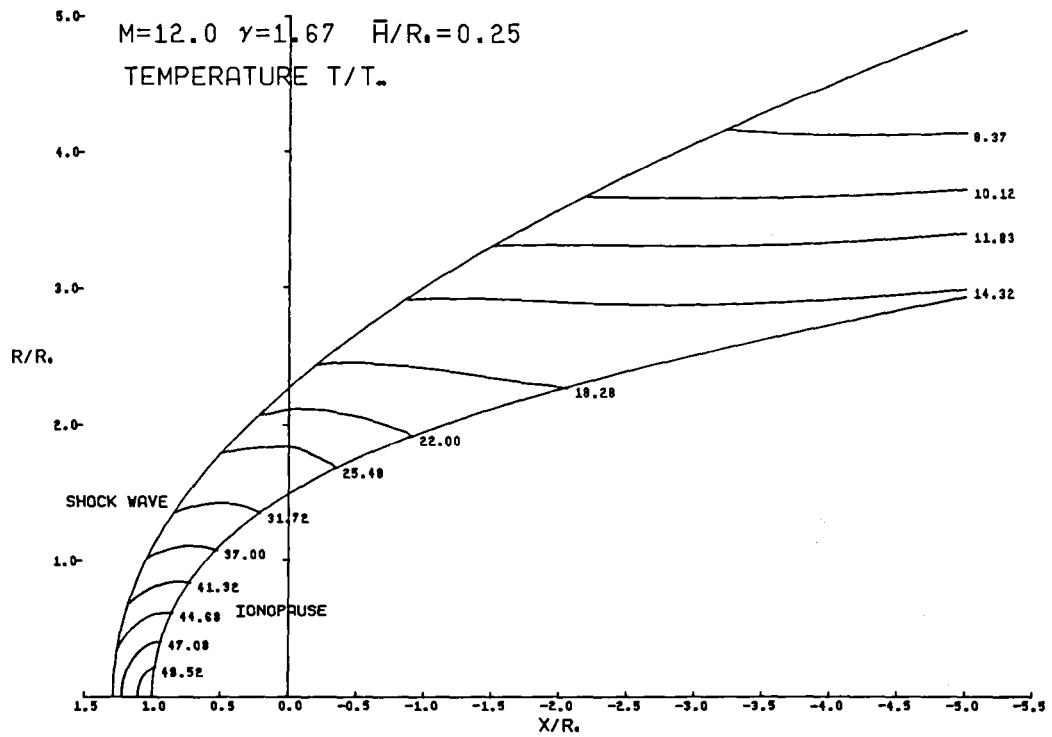
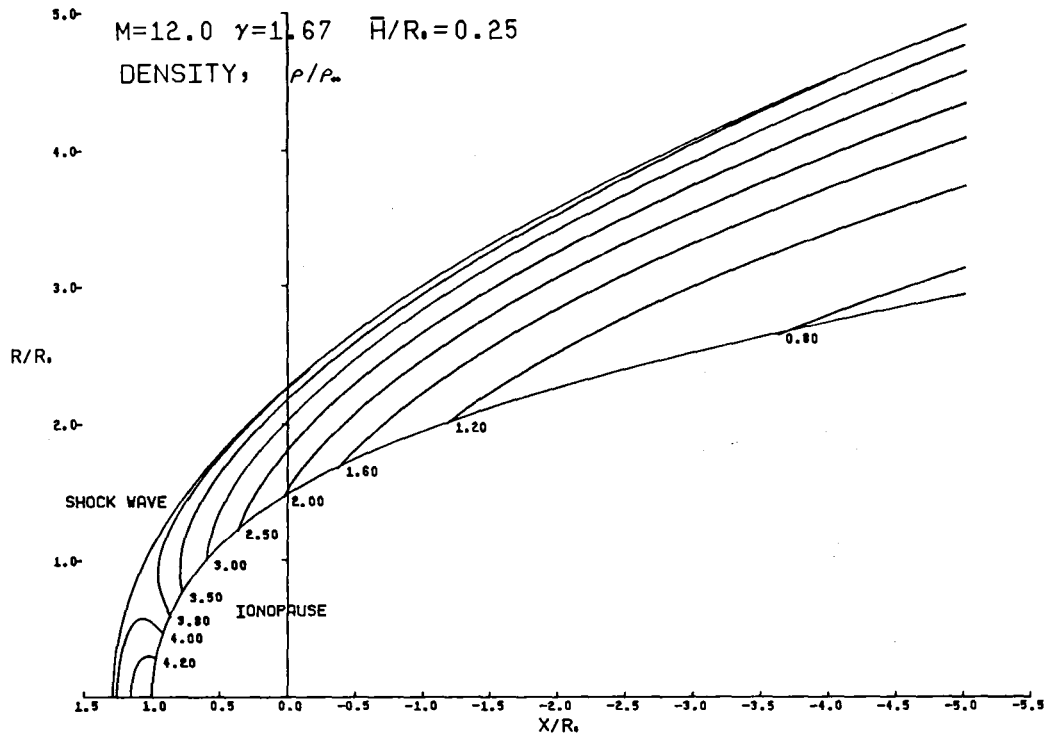


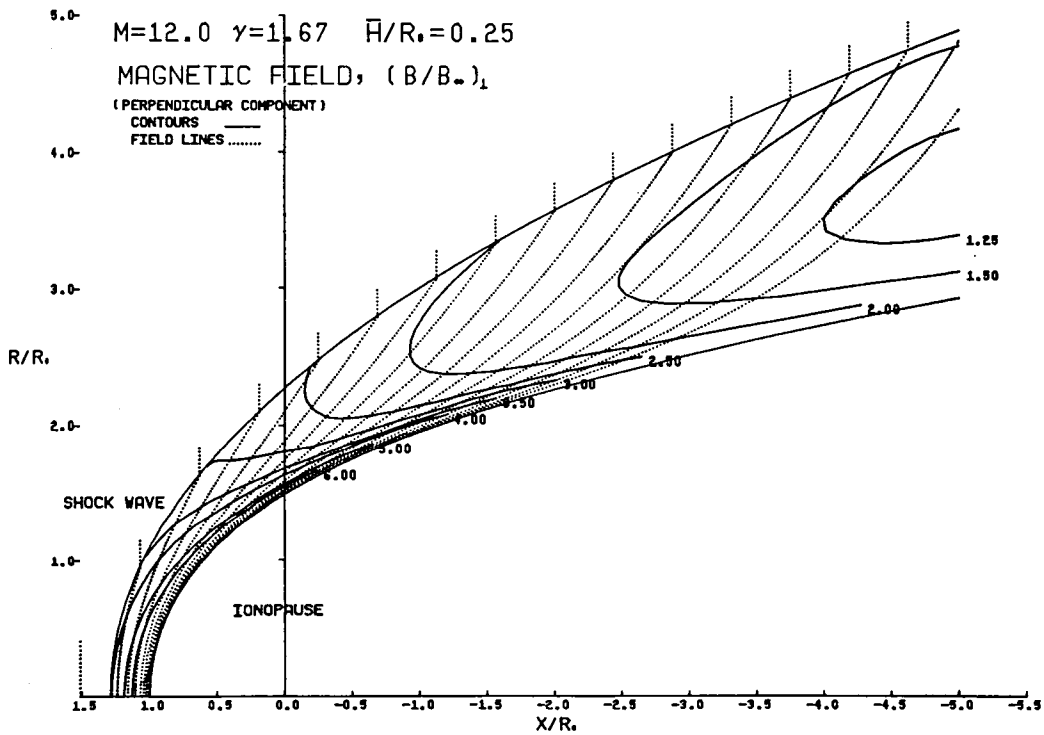
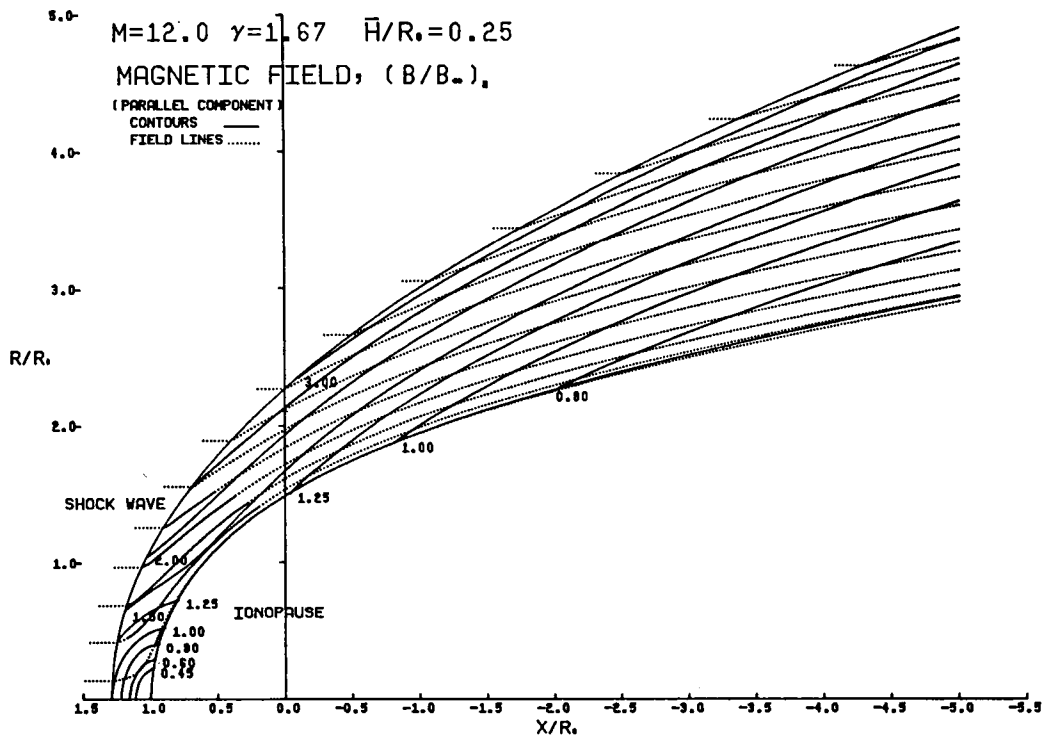


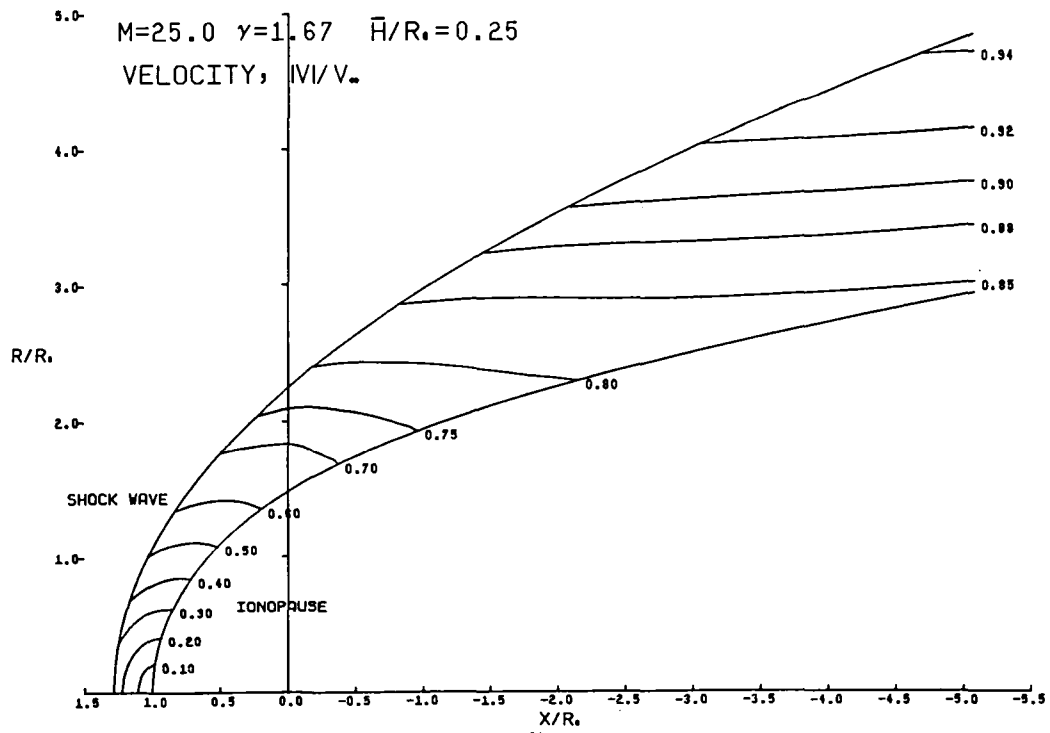
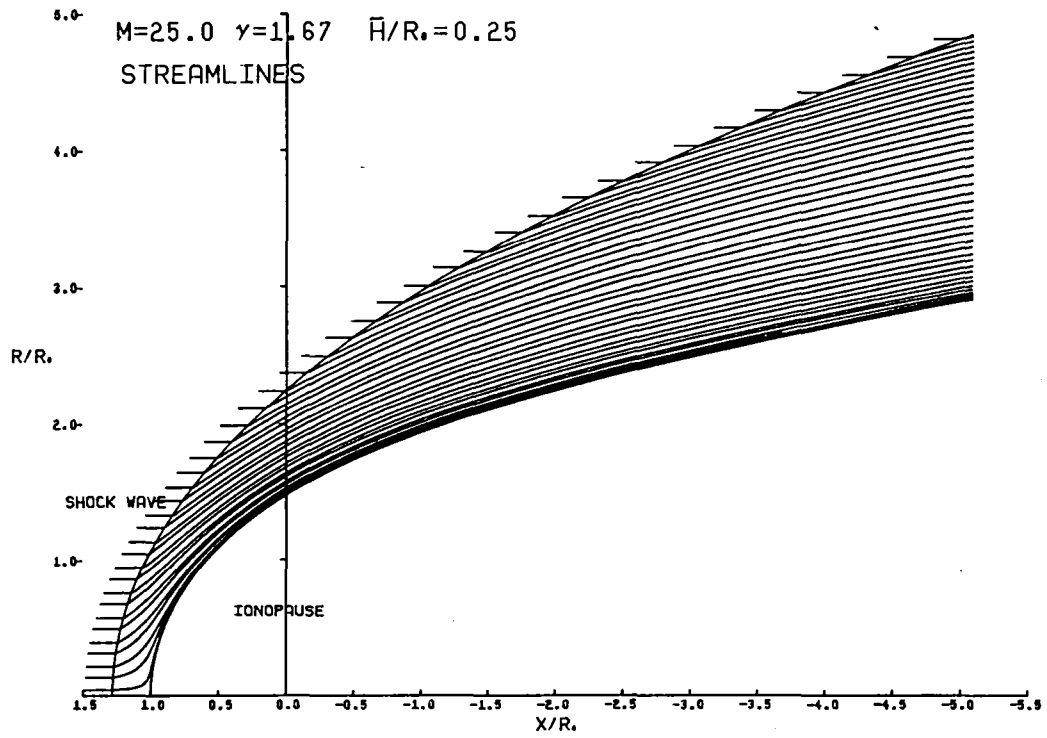


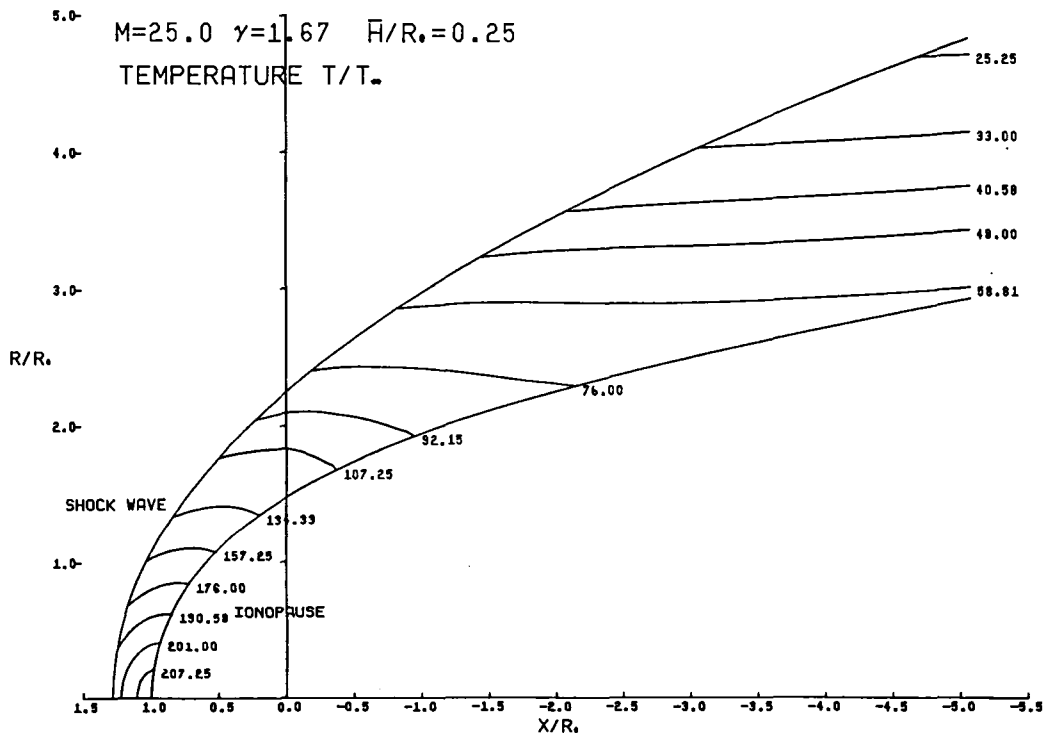
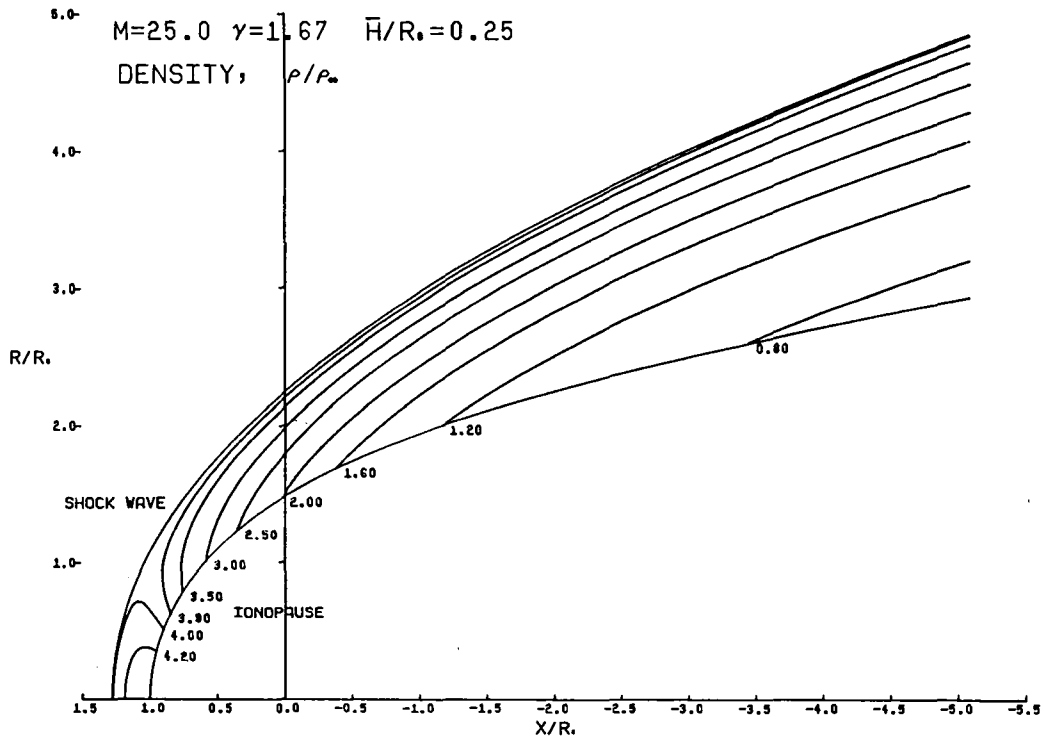


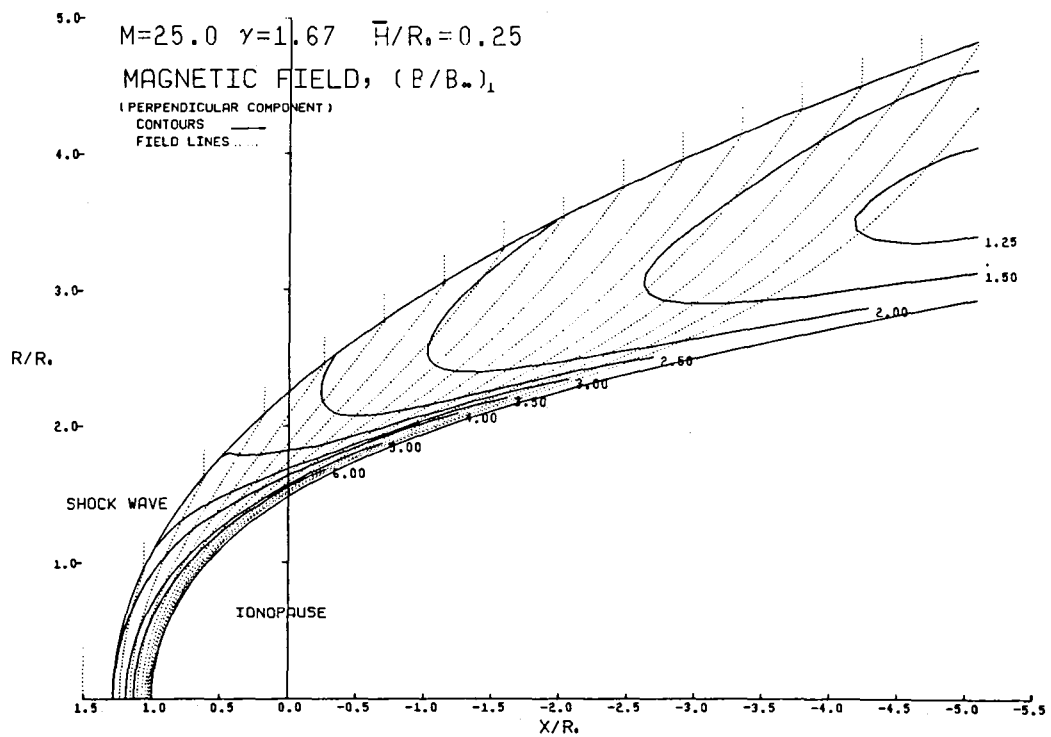
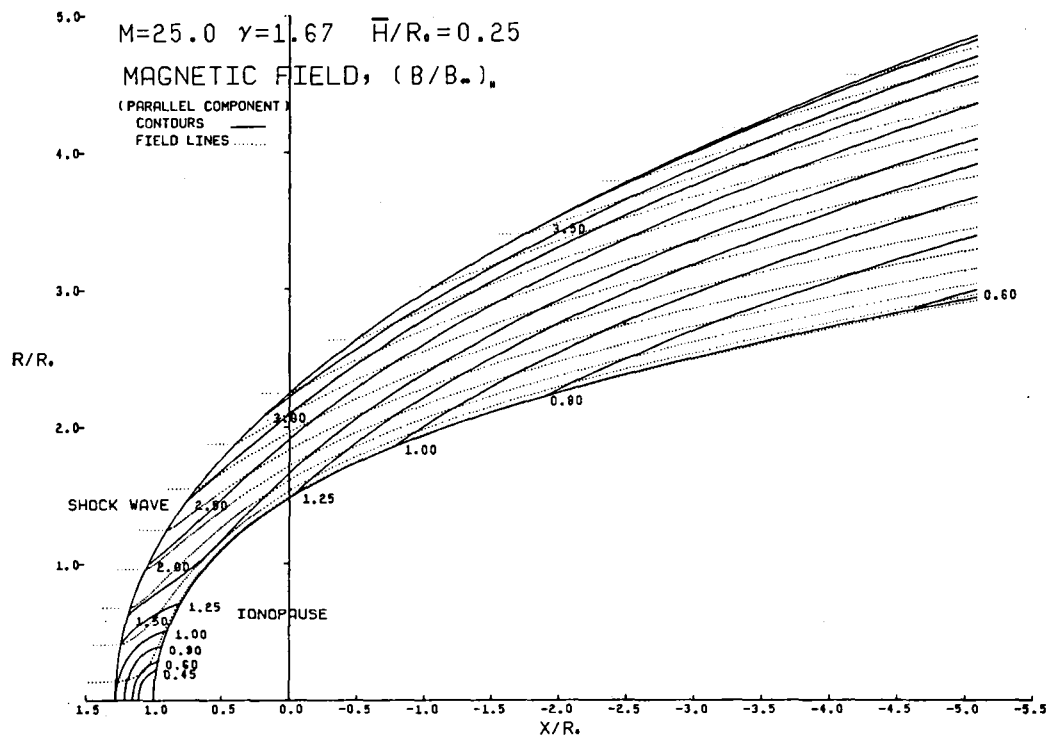












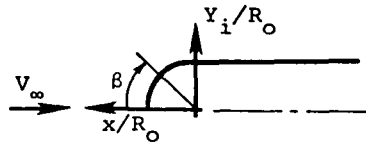
REFERENCES

1. Spreiter, J. R. and Jones, W. P.: On the Effect of a Weak Interplanetary Magnetic Field on the Interaction Between the Solar Wind and the Geomagnetic Field. *J. Geophys. Res.*, Vol. 68, 1963, pp. 3555-3564.
2. Spreiter, J. R., Alksne, A. Y., and Summers, A. L.: Hydromagnetic Flow Around the Magnetopause. *Plan. & Space Sci.*, Vol. 14, 1966, pp. 223-253.
3. Dryer, M. and Faye-Petersen, R.: Magnetogasdynamic Boundary Condition for a Self-Consistent Solution to the Closed Magnetopause. *AIAA Journal*, Vol. 4, 1966, pp. 246-254.
4. Dryer, M. and Heckman, G. R.: Application of the Hypersonic Analogy to the Standing Shock of Mars. *Solar Phys.*, Vol. 2, 1967, pp. 112-120.
5. Spreiter, J. R., Alksne, A. Y., and Summers, A. L.: External Aerodynamics of the Magnetosphere. *Physics of the Magnetosphere* (Ed. R. L. Carovillano, J. F. McClay, and H. R. Radoski), D. Reidel Pub. Co., 1968, pp. 304-378 (also NASA TN 4482, 1968).
6. Spreiter, J. R., Summers, A. L., and Rizzi, A. W.: Solar Wind Flow Past Nonmagnetic Planets - Venus and Mars. *Plan. & Space Sci.*, Vol. 18, 1970, pp. 1281-1289.
7. Spreiter, J. R. and Rizzi, A. W.: Aligned Magnetohydrodynamics Solution for Solar Wind Flow Past the Earth's Magnetosphere. *Acta Astronautica*, Vol. 1, 1974, pp. 15-35.
8. Spreiter, J. R.: Magnetohydrodynamic and Gasdynamic Aspects of Solar-Wind Flow Around Terrestrial Planets: A Critical Review. *NASA SP-397*, 1975, pp. 135-150.
9. Stahara, S. S., Chaussee, D. S., Trudinger, B. C., and Spreiter, J. R.: Computational Techniques for Solar Wind Flows Past Terrestrial Planets - Theory and Computer Programs. *NASA CR-2924*, Nov. 1977.
10. Knudsen, W. C., Spenner, K., Spreiter, J. R., Miller, K. L., and Novak, V.: Thermal Structure and Major Ion Composition of the Venusian Ionosphere: First RPA Results from Venus Orbiter. *Science*, Vol. 203, No. 4382, Feb. 1979, pp. 757-763.
11. Knudsen, W. C., Spenner, K., Whitter, R. C., Spreiter, J. R., Miller, K. L., and Novak, V.: Thermal Structure and Energy Influx to the Day- and Nightside Venus Ionosphere. *Science*, Vol. 205, No. 4401, July 1979, pp. 105-107.
12. Kuhn, G. D., Goodwin, F. K., and Perkins, S. C., Jr.: User's Manual for Space-Shuttle Computer Programs. *NEAR TR 110*, Apr. 1976.

REFERENCES (Concluded)

13. Beam, R. M. and Warming, R. F.: An Implicit Finite-Difference Algorithm for Hyperbolic Systems in Conservation-Law Form. *J. Comp. Phys.*, Vol. 22, No. 1, Sept. 1976.
14. Kentzer, C. P.: Discretization of Boundary Conditions on Moving Discontinuities. Proceedings of the Second International Conference on Numerical Methods in Fluid Dynamics, Lecture Notes in Physics, Vol. 8, M. Holt, ed., Berkeley, CA, 1970, pp. 108-113.
15. Thomas, P. D., Vinokur, M., Bastionon, R., and Conti, R. J.: Numerical Solution for the Three-Dimensional Hypersonic Flow Field of a Blunt Delta Body. *AIAA J.*, Vol. 10, July 1972, pp. 887-894.
16. Kutler, P., Reinhardt, W. A., and Warming, R. F.: Numerical Computations of Multi-Shocked Three-Dimensional Supersonic Flow Fields with Real Gas Effects. *AIAA Paper No. 72-702*, June 1972.
17. Kutler, P., Reinhardt, W. A., and Warming, R. F.: Multi-Shocked, Three-Dimensional Supersonic Flow Fields with Real Gas Effects. *AIAA J.*, Vol. 11, May 1973, pp. 657-664.
18. Chaussee, D. S., Holtz, T., and Kutler, P.: Inviscid Supersonic/Hypersonic Body Flow Fields and Aerodynamics from Shock-Capturing Technique Calculations. *AIAA Paper No. 75-837*, June 1975.
19. MacCormack, R. W.: The Effect of Viscosity in Hypervelocity Impact Cratering. *AIAA Paper No. 69-354*, 1969.
20. Alksne, A. Y. and Webster, D. L.: Magnetic and Electric Fields in the Magnetosheath. *Plan. & Space Sci.*, Vol. 18, 1970, pp. 1203-1212.
21. Wolfe, J., Intriligator, D. S., Mihalov, J., Collard, H., McKibbin, D., Whitten, R., and Barnes, A.: Initial Observations of the Pioneer Venus Orbiter Solar Wind Plasma Experiment. *Science*, Vol. 203, No. 4382, Feb. 1979, pp. 750-752.
22. Intriligator, D. S., Collard, H. R., Mihalov, J. P., Whitten, R. C., and Wolfe, J. H.: Electron Observation and Ion Flows from the Pioneer Venus Orbiter Plasma Analyzer Experiment. *Science*, Vol. 205, No. 4401, July 1979, pp. 116-119.
23. Russell, C. T., Elphic, R. C., and Slavin, J. A.: Initial Pioneer Venus Magnetic Field Results: Dayside Observations. *Science*, Vol. 203, No. 4382, Feb. 1979, pp. 745-748.
24. Russell, C. T., Elphic, R. C., and Slavin, J. A.: Initial Pioneer Venus Magnetic Field Results: Nightside Observations. *Science*, Vol. 205, No. 4401, July 1979, pp. 114-116.

Table 1.- Ordinates of Various Ionopause Shapes



β	IONOPAUSE		IONOPAUSE		IONOPAUSE		IONOPAUSE		IONOPAUSE	
	$\bar{H}/R_o = 0.01$		$\bar{H}/R_o = 0.05$		$\bar{H}/R_o = 0.10$		$\bar{H}/R_o = 0.20$		$\bar{H}/R_o = 0.25$	
	x/R_o	y_i/R_o	x/R_o	y_i/R_o	x/R_o	y_i/R_o	x/R_o	y_i/R_o	x/R_o	y_i/R_o
0°	1.0000	0.0000	1.0000	0.0000	1.0000	0.0000	1.0000	0.0000	1.0000	0.0000
2°	0.9994	0.0349	0.9995	0.0349	0.9995	0.0349	0.9995	0.0349	0.9996	0.0349
6°	0.9946	0.1045	0.9950	0.1046	0.9953	0.1046	0.9958	0.1047	0.9960	0.1047
10°	0.9851	0.1737	0.9861	0.1739	0.9870	0.1740	0.9883	0.1743	0.9888	0.1744
14°	0.9709	0.2421	0.9727	0.2425	0.9746	0.2430	0.9771	0.2436	0.9781	0.2439
18°	0.9520	0.3093	0.9550	0.3103	0.9580	0.3113	0.9622	0.3126	0.9638	0.3132
22°	0.9285	0.3751	0.9330	0.3770	0.9374	0.3787	0.9435	0.3812	0.9459	0.3822
26°	0.9006	0.4393	0.9068	0.4423	0.9127	0.4451	0.9211	0.4492	0.9243	0.4508
30°	0.8684	0.5014	0.8764	0.5060	0.8840	0.5104	0.8949	0.5167	0.8991	0.5191
34°	0.8320	0.5612	0.8419	0.5679	0.8514	0.5743	0.8649	0.5834	0.8701	0.5869
38°	0.7916	0.6185	0.8035	0.6278	0.8148	0.6366	0.8312	0.6494	0.8374	0.6543
42°	0.7474	0.6729	0.7613	0.6854	0.7745	0.6973	0.7935	0.7145	0.8009	0.7211
46°	0.6995	0.7243	0.7153	0.7407	0.7303	0.7563	0.7520	0.7787	0.7604	0.7874
50°	0.6482	0.7725	0.6658	0.7934	0.6824	0.8133	0.7066	0.8421	0.7159	0.8532
54°	0.5937	0.8172	0.6128	0.8435	0.6309	0.8683	0.6571	0.9044	0.6673	0.9184
58°	0.5363	0.8582	0.5565	0.8906	0.5756	0.9212	0.6035	0.9657	0.6143	0.9831
62°	0.4761	0.8954	0.4971	0.9349	0.5168	0.9719	0.5456	1.0261	0.5569	1.0473
66°	0.4135	0.9287	0.4346	0.9761	0.4543	1.0203	0.4504	1.1147	0.4947	1.1744
70°	0.3487	0.9581	0.3691	1.0142	0.3882	1.0665	0.4163	1.1437	0.4274	1.1744
74°	0.2820	0.9833	0.3009	1.0492	0.3184	1.1103	0.3444	1.2010	0.3548	1.2374
78°	0.2135	1.0046	0.2298	1.0811	0.2448	1.1517	0.2673	1.2574	0.2764	1.3001
82°	0.1436	1.0219	0.1560	1.1098	0.1674	1.1908	0.1845	1.3130	0.1915	1.3628
86°	0.0724	1.0354	0.0794	1.1355	0.0858	1.2276	0.0956	1.3677	0.0997	1.4254
90°	0.0000	1.0454	0.0000	1.1583	0.0000	1.2620	0.0000	1.4218	0.0000	1.4883
94°	-0.0736	1.0523	-0.0824	1.1782	-0.0905	1.2943	-0.1032	1.4753	-0.1085	1.5516
98°	-0.1485	1.0566	-0.1680	1.1955	-0.1861	1.3244	-0.2148	1.5284	-0.2271	1.6156
102°	-0.2251	1.0591	-0.2572	1.2102	-0.2875	1.3524	-0.3361	1.5813	-0.3572	1.6807
106°	-0.3040	1.0603	-0.3506	1.2226	-0.3953	1.3785	-0.4686	1.6343	-0.5010	1.7472
110°	-0.3861	1.0607	-0.4488	1.2330	-0.5106	1.4027	-0.6142	1.6875	-0.6608	1.8156
114°	-0.4723	1.0609	-0.5527	1.2415	-0.6346	1.4253	-0.7753	1.7414	-0.8400	1.8866

Table 1.- Concluded.

β	IONOPAUSE		IONOPAUSE		IONOPAUSE		IONOPAUSE		IONOPAUSE	
	$\bar{H}/R_0 = 0.01$		$\bar{H}/R_0 = 0.05$		$\bar{H}/R_0 = 0.10$		$\bar{H}/R_0 = 0.20$		$\bar{H}/R_0 = 0.25$	
	x/R_0	Y_i/R_0	x/R_0	Y_i/R_0	x/R_0	Y_i/R_0	x/R_0	Y_i/R_0	x/R_0	Y_i/R_0
118°	-0.5641	1.0610	-0.6638	1.2484	-0.7690	1.4462	-0.9551	1.7963	-1.0427	1.9610
122°	-0.6630	1.0610	-0.7835	1.2539	-0.9159	1.4657	-1.1578	1.8529	-1.2746	2.0397
126°	-0.7708	1.0610	-0.9142	1.2583	-1.0782	1.4840	-1.3890	1.9118	-1.5434	2.1243
130°	-0.8903	1.0610	-1.0587	1.2617	-1.2597	1.5012	-1.6562	1.9738	-1.8598	2.2165
134°	-1.0246	1.0610	-1.2209	1.2643	-1.4654	1.5175	-1.9703	2.0403	-2.2393	2.3189
138°	-1.1783	1.0610	-1.4064	1.2664	-1.7027	1.5331	-2.3465	2.1128	-2.7047	2.4353
142°	-1.3580	1.0610	-1.6229	1.2679	-1.9817	1.5482	-2.8081	2.1939	-3.2913	2.5715
146°	-1.5730	1.0610	-1.8816	1.2692	-2.3176	1.5632	-3.3909	2.2872	-4.0570	2.7365
150°	-1.8377	1.0610	-2.1999	1.2701	-2.7338	1.5784	-4.1545	2.3986	-5.1025	2.9460
154°	-2.1754	1.0610	-2.6057	1.2709	-3.2686	1.5942	-5.2045	2.5384	-6.6208	3.2292
158°	-2.6262	1.0610	-3.1471	1.2715	-3.9884	1.6114	-6.7470	2.7260	-9.0300	3.6484
162°	-3.3654	1.0610	-3.9152	1.2721	-5.0210	1.6314	-9.2448	3.0038	-13.4322	4.3644
166°	-4.2564	1.0610	-5.1047	1.2727	-6.6450	1.6568	-13.9882	3.4877	-23.9161	5.9630
170°	-6.0204	1.0610	-7.2230	1.2736	-10.1609	1.7004	-26.3596	4.6480		
174°	-10.1111	1.0610	-12.1370	1.2758	-16.8192	1.7678				

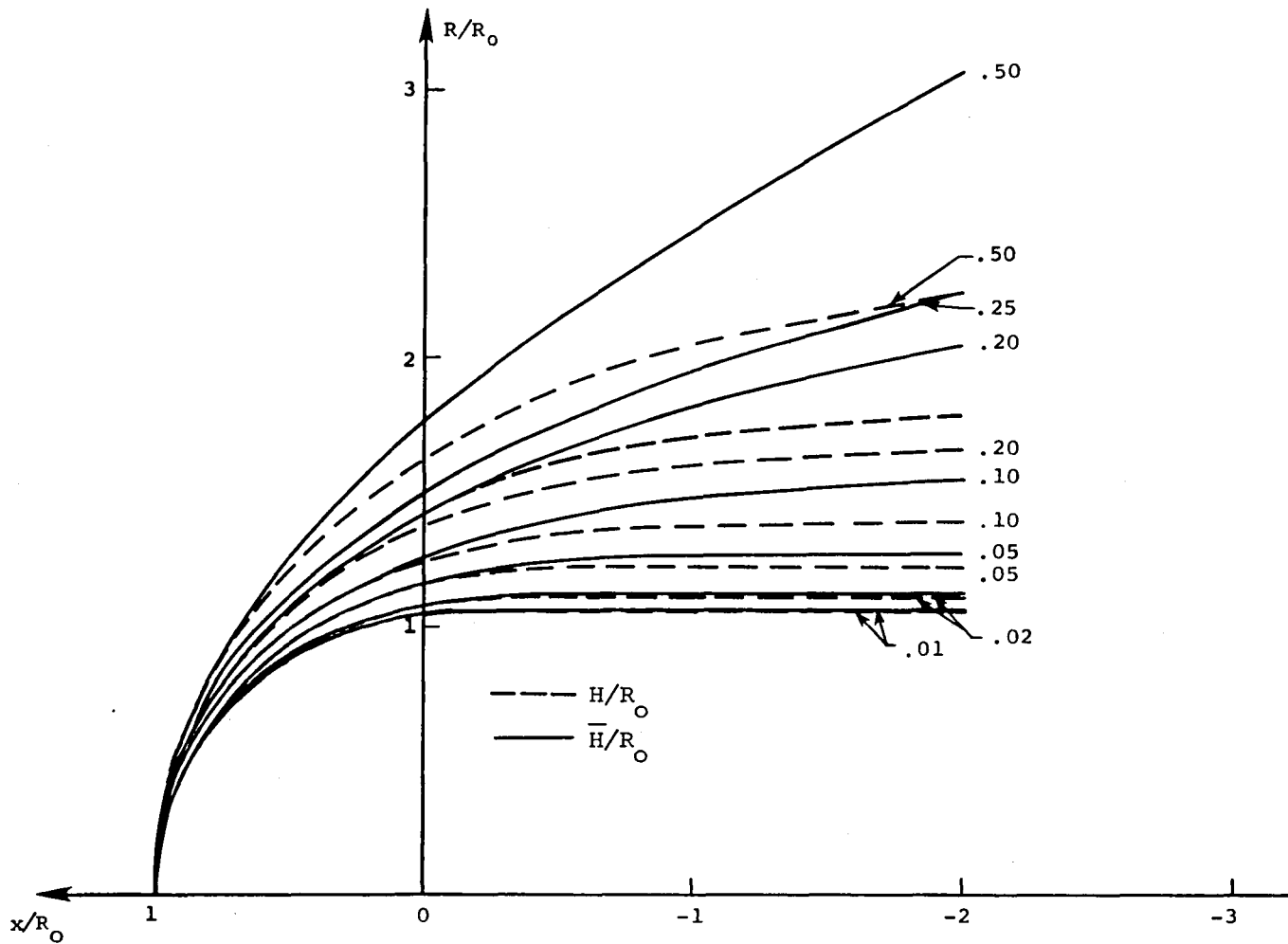
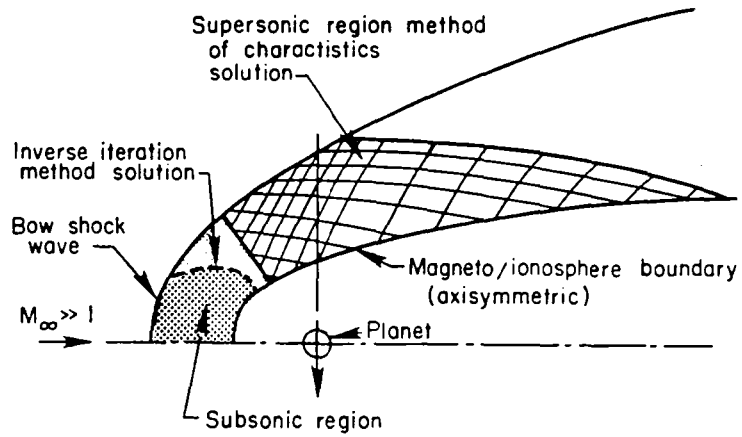
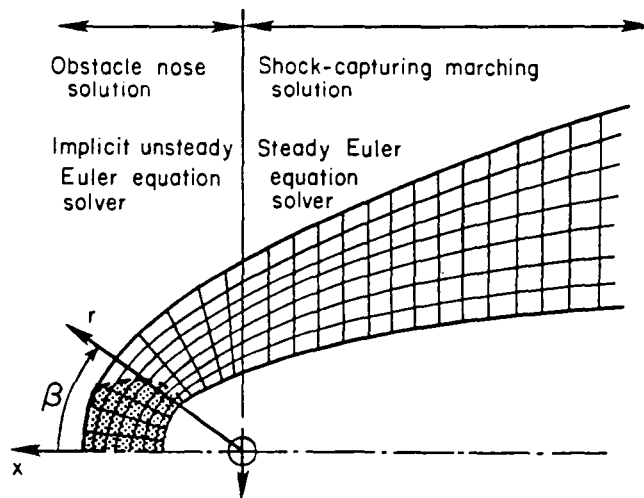


Figure 1.-Illustration of ionopause shapes for atmospheres with various (i) constant scale heights \bar{H}/R_0 and (ii) gravitational variation included in the scale height H/R_0 .



(a) Former method.



(b) Present method.

Figure 2.- Comparison of former and present computational procedures for determining the gasdynamic flow properties of solar wind-magneto/ionopause interactions.

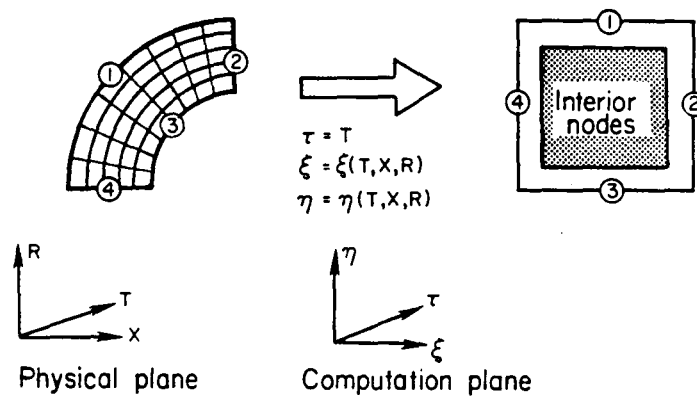


Figure 3.- Transformation from physical domain to rectangular computational domain.

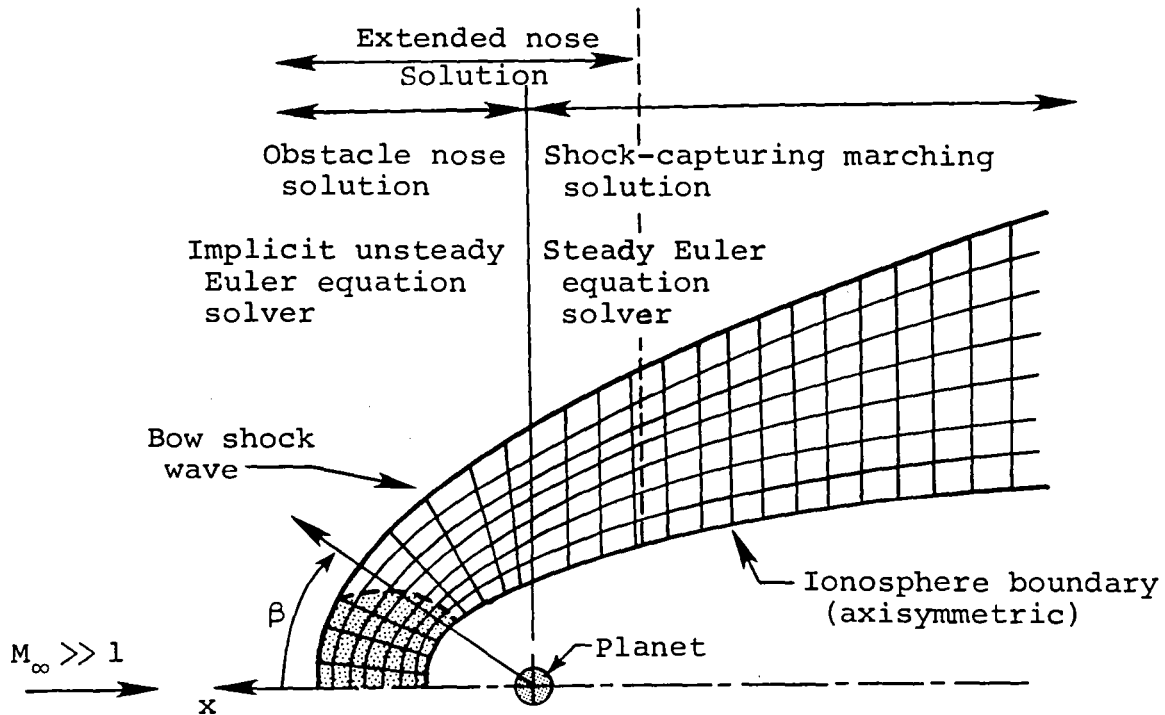


Figure 4.- Illustration of capability for providing an additional flow-field segment to the obstacle nose solution in the computational procedure for determining the gasdynamic flow properties of solar wind-ionopause interactions.

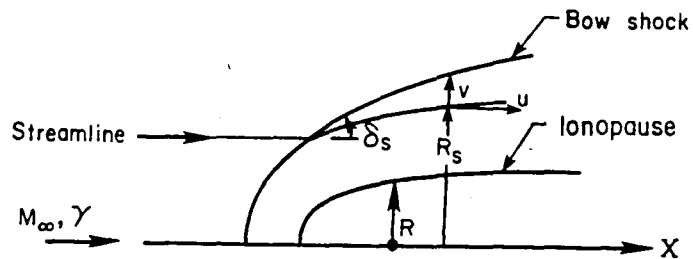


Figure 5.- Illustration of quantities used for streamline calculation.

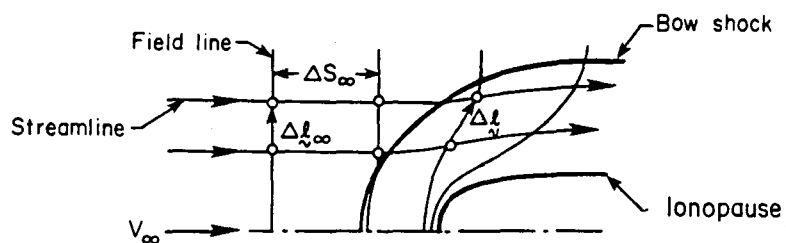


Figure 6.- Illustration of quantities used for magnetic field-line calculation in the plane of magnetic symmetry.

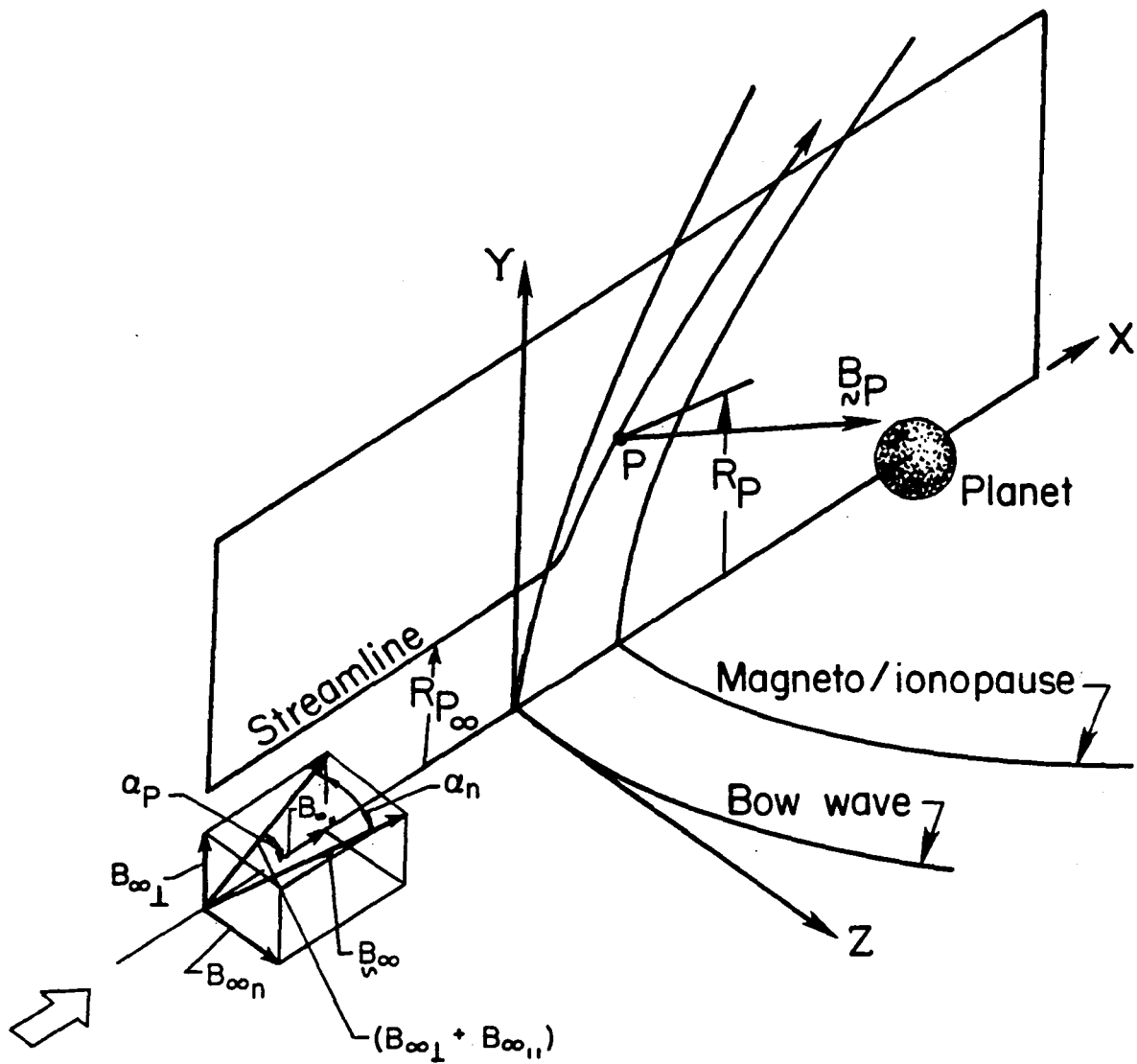


Figure 7.- Illustration of the components of the three-dimensional magnetic field.

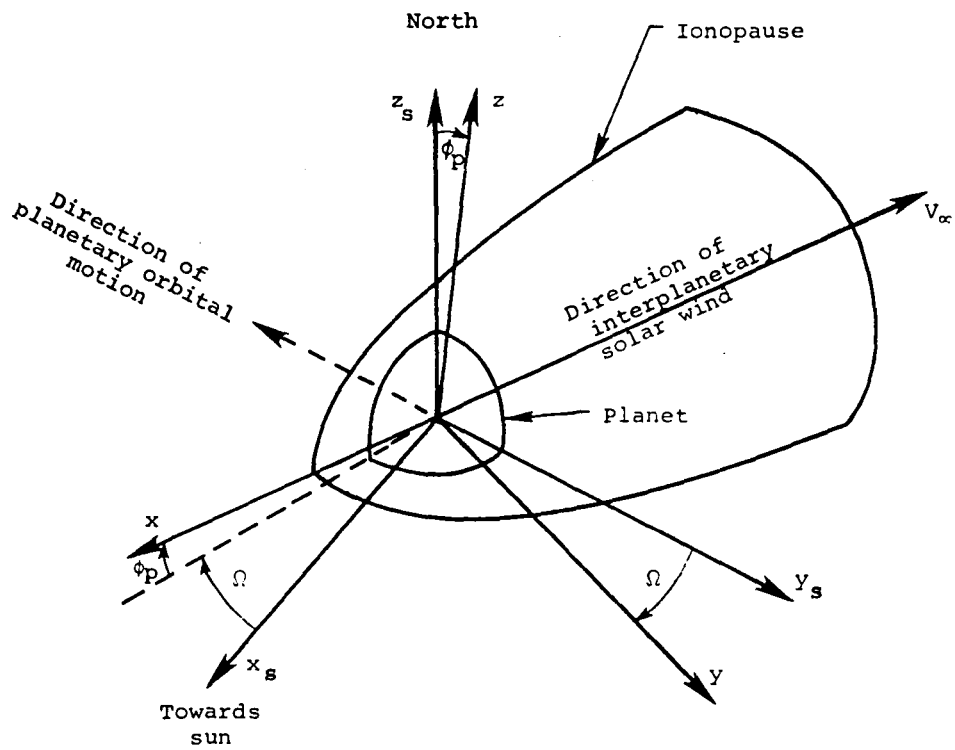


Figure 8.- Illustration of sun-planet (x_s, y_s, z_s) and solar wind (x, y, z) coordinate systems and the azimuthal (Ω) and polar (ϕ_p) solar-wind angles, both shown in a positive sense.

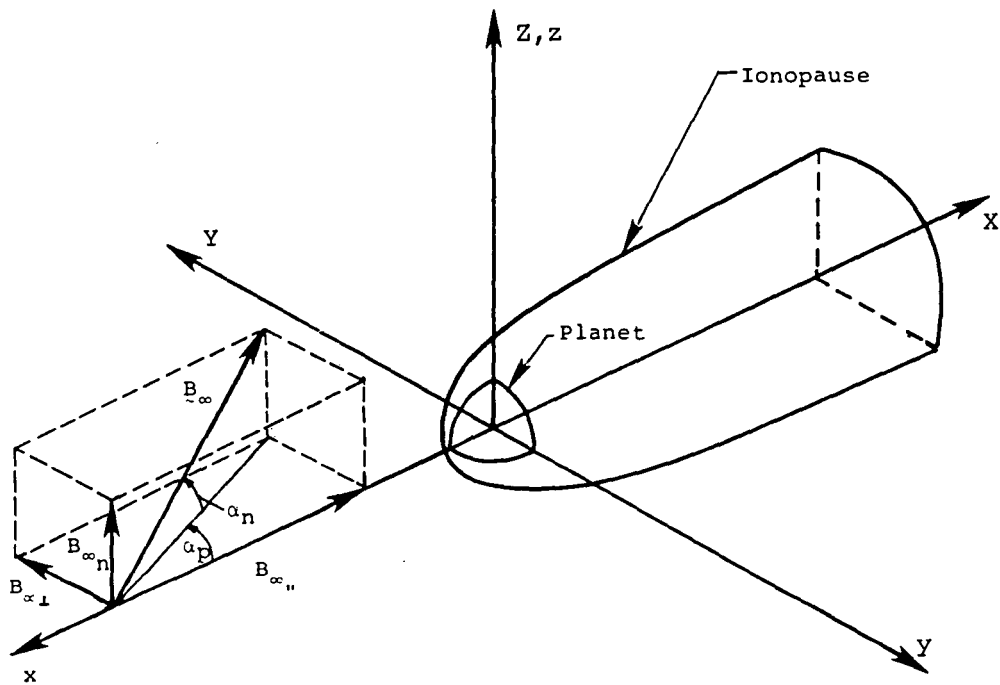


Figure 9.- Illustration of solar-wind (x, y, z) and (X, Y, Z) coordinate systems and the interplanetary magnetic field and magnetic-field angles (α_p, α_n) .

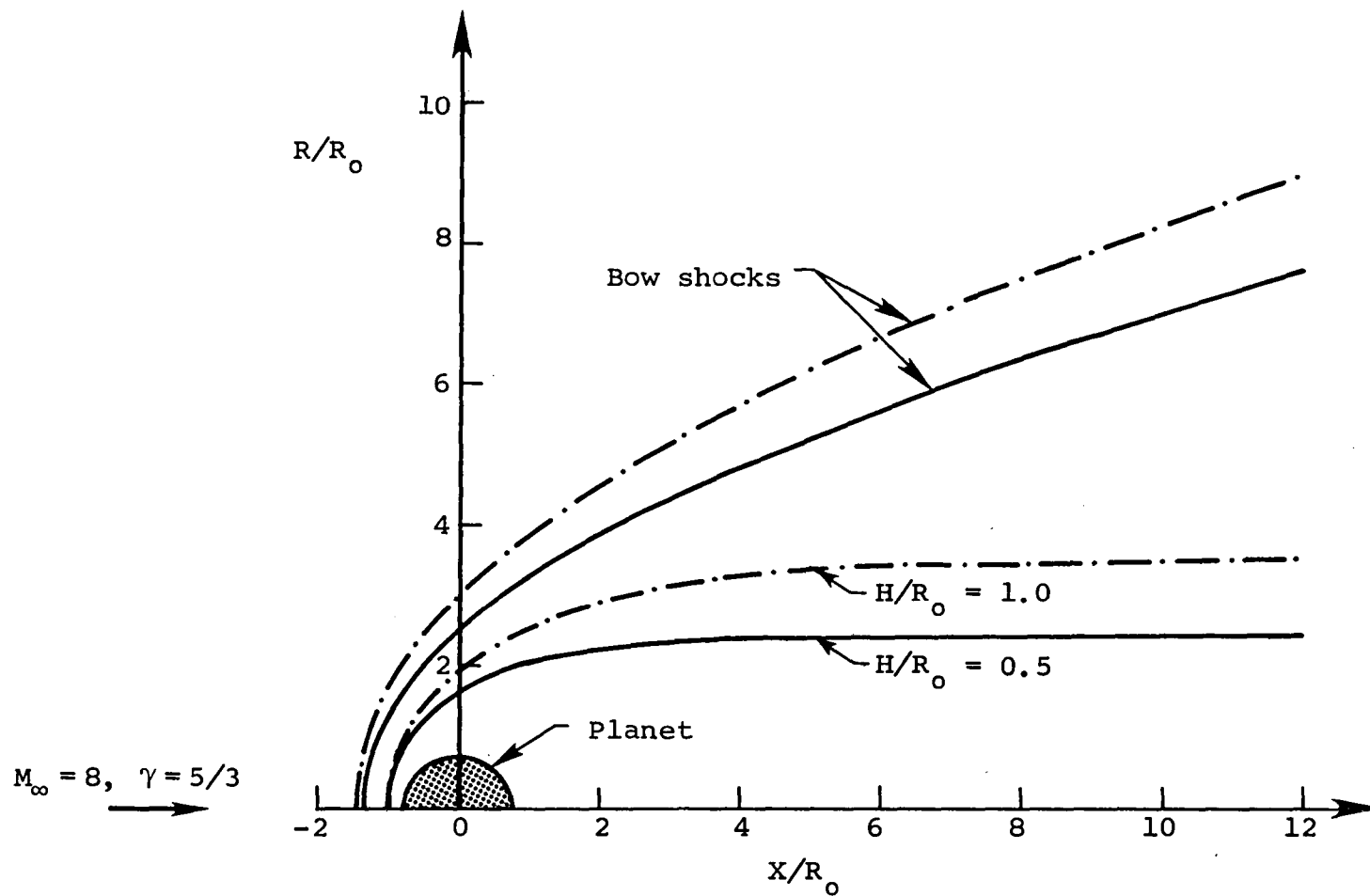


Figure 10.- Bow shock locations for $M_\infty = 8.0, \gamma = 5/3$ flow past constant scale-height ionopause shapes with $H/R_0 = 0.5$ and 1.0 .

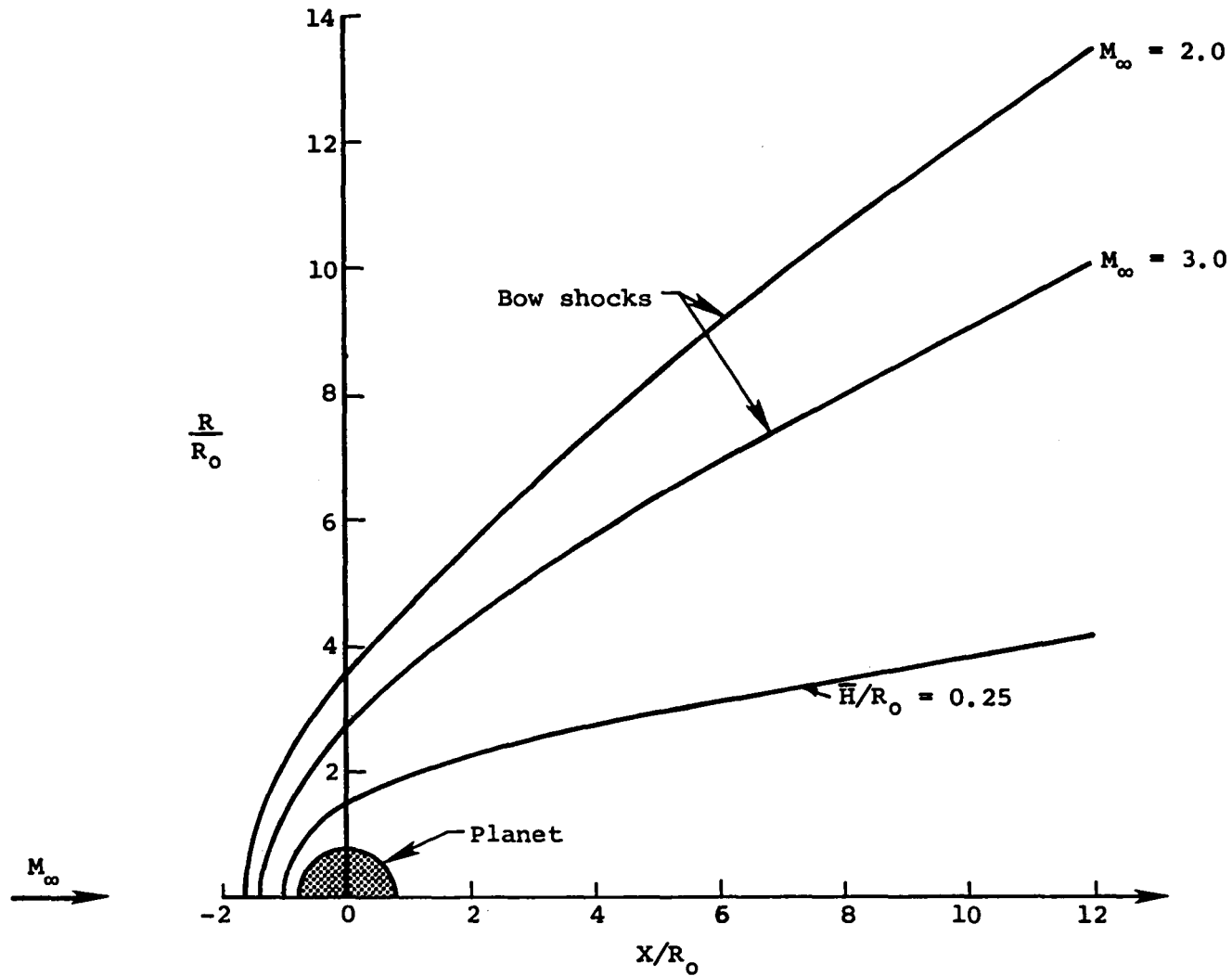


Figure 11.- Bow shock shapes for flow past an ionopause shape with gravitational variation included in scale height with $\bar{H}/R_0 = 0.25$, $\gamma = 5/3$ and $M_\infty = 2.0$ and 3.0 .

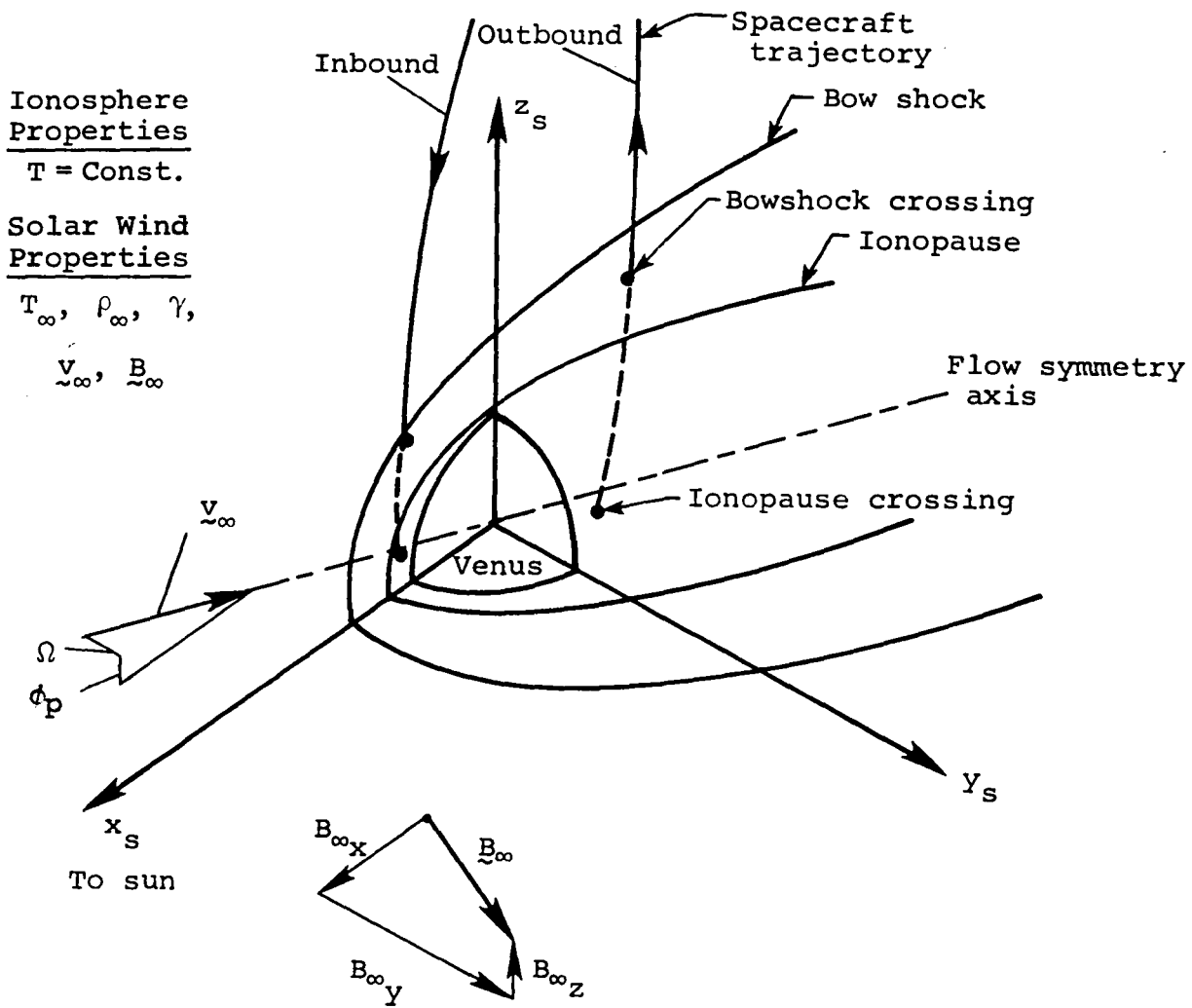


Figure 12.- Overall features of Pioneer-Venus orbiter trajectory crossings of solar-wind/Venus-ionosphere interaction region.

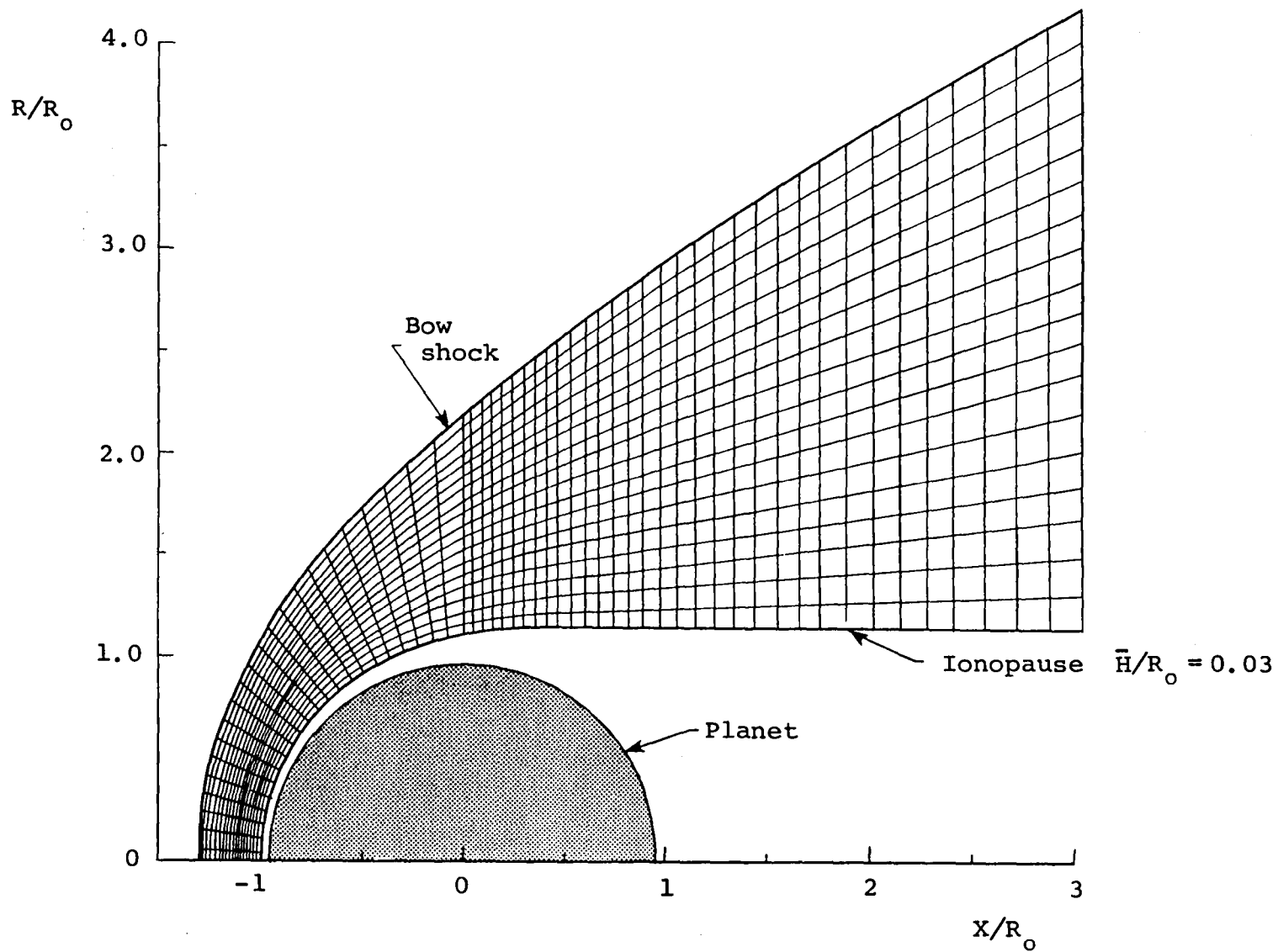


Figure 13.- Illustration of typical flow-field grid density for gasdynamic solution; $M_\infty = 3.0$, $\gamma = 5/3$.

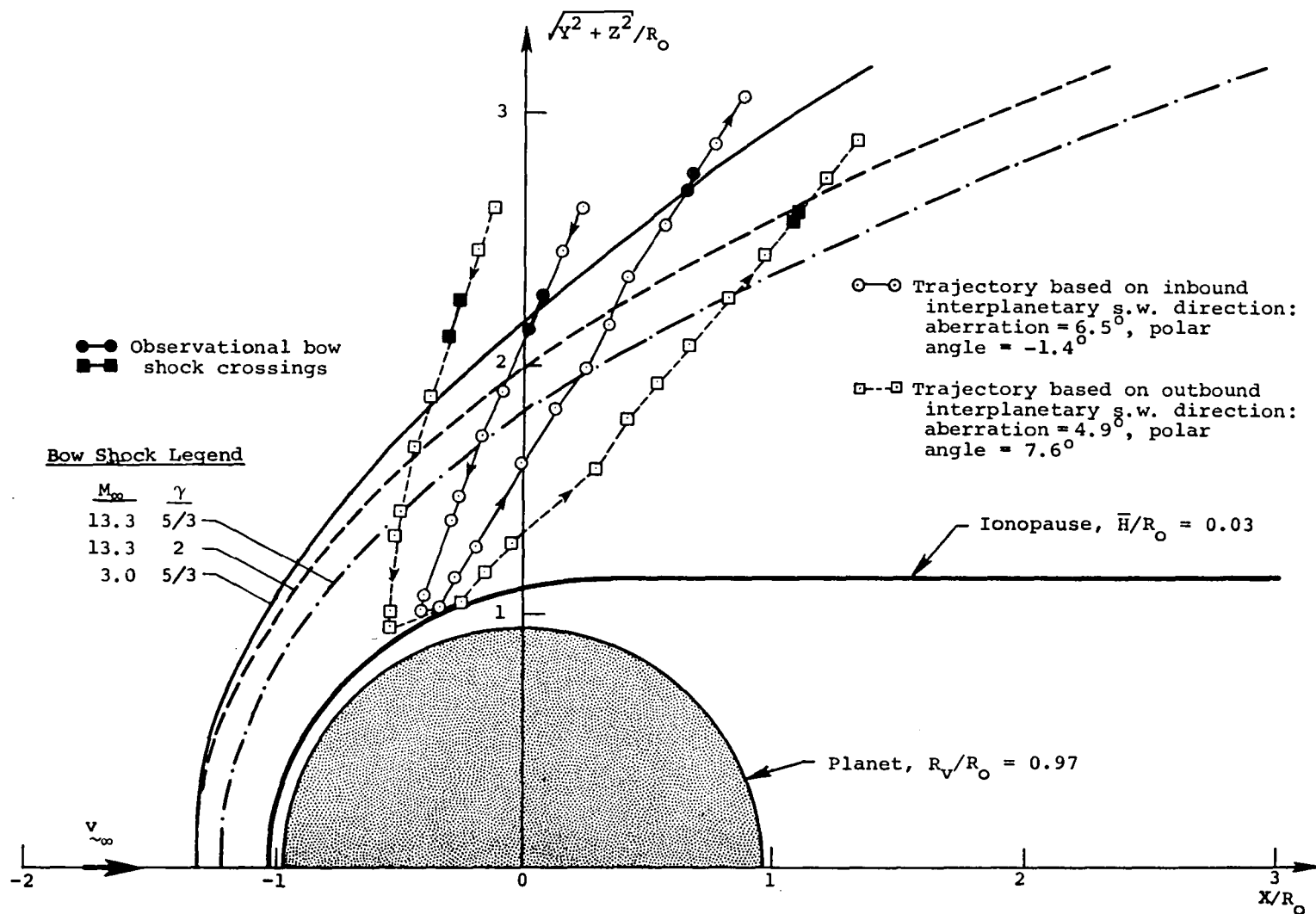


Figure 14.- P-V Orbit 6 trajectories and observational bow shock crossings as viewed in solar-wind coordinates based on inbound and outbound interplanetary solar-wind directions; also, various bow shock shapes for different interplanetary solar-wind conditions.

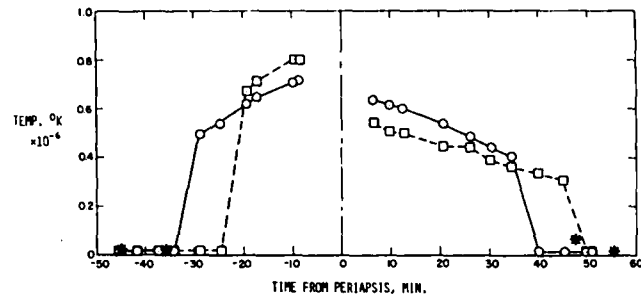
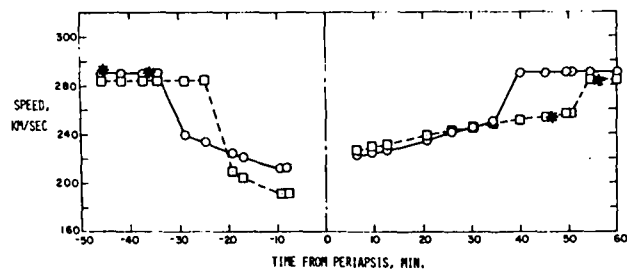
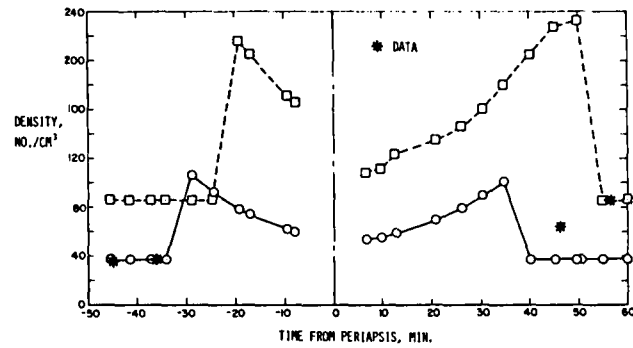
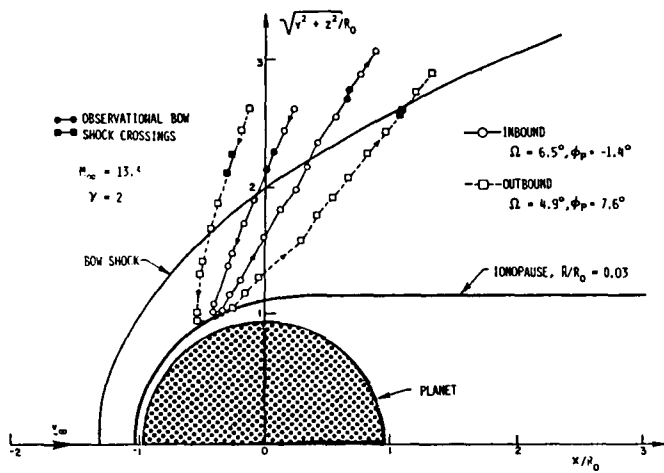
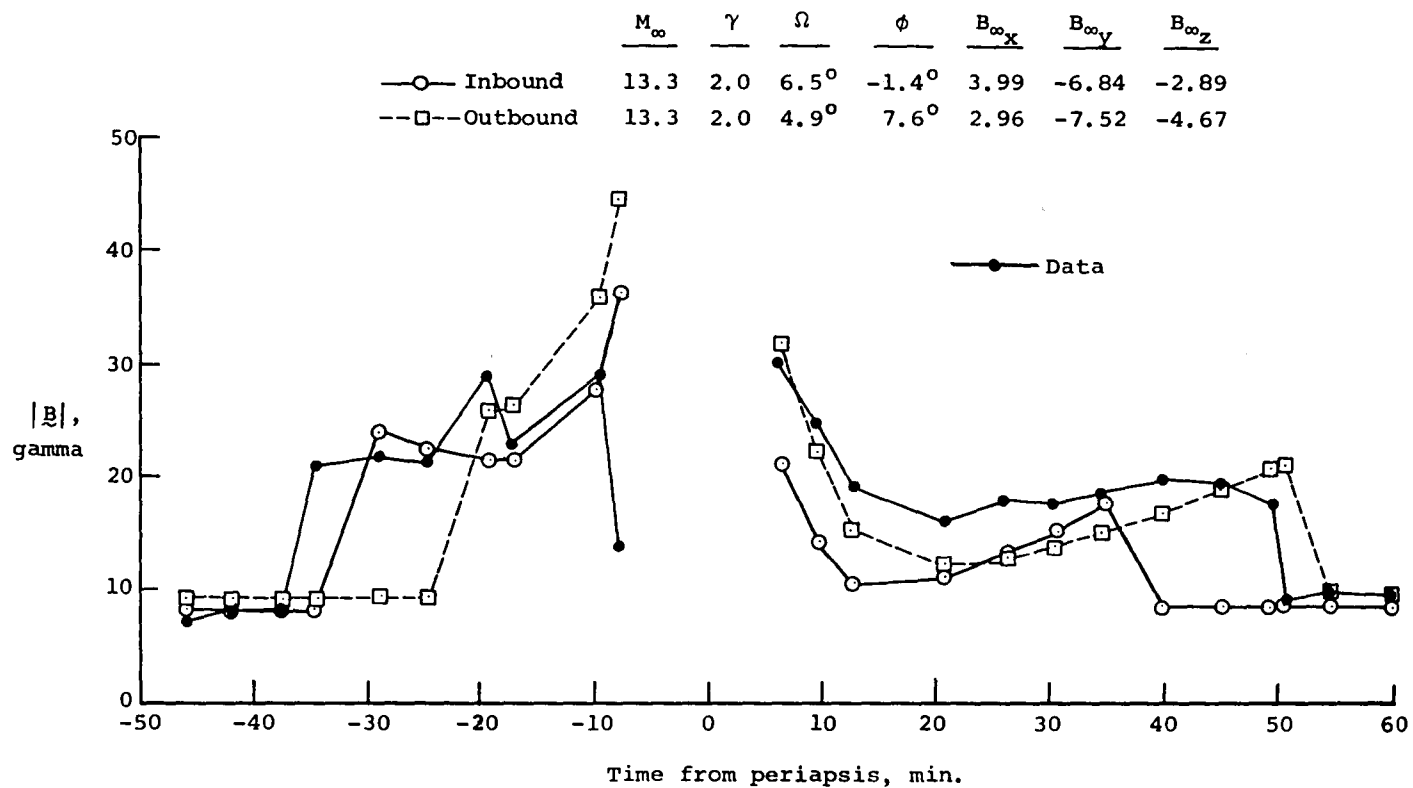
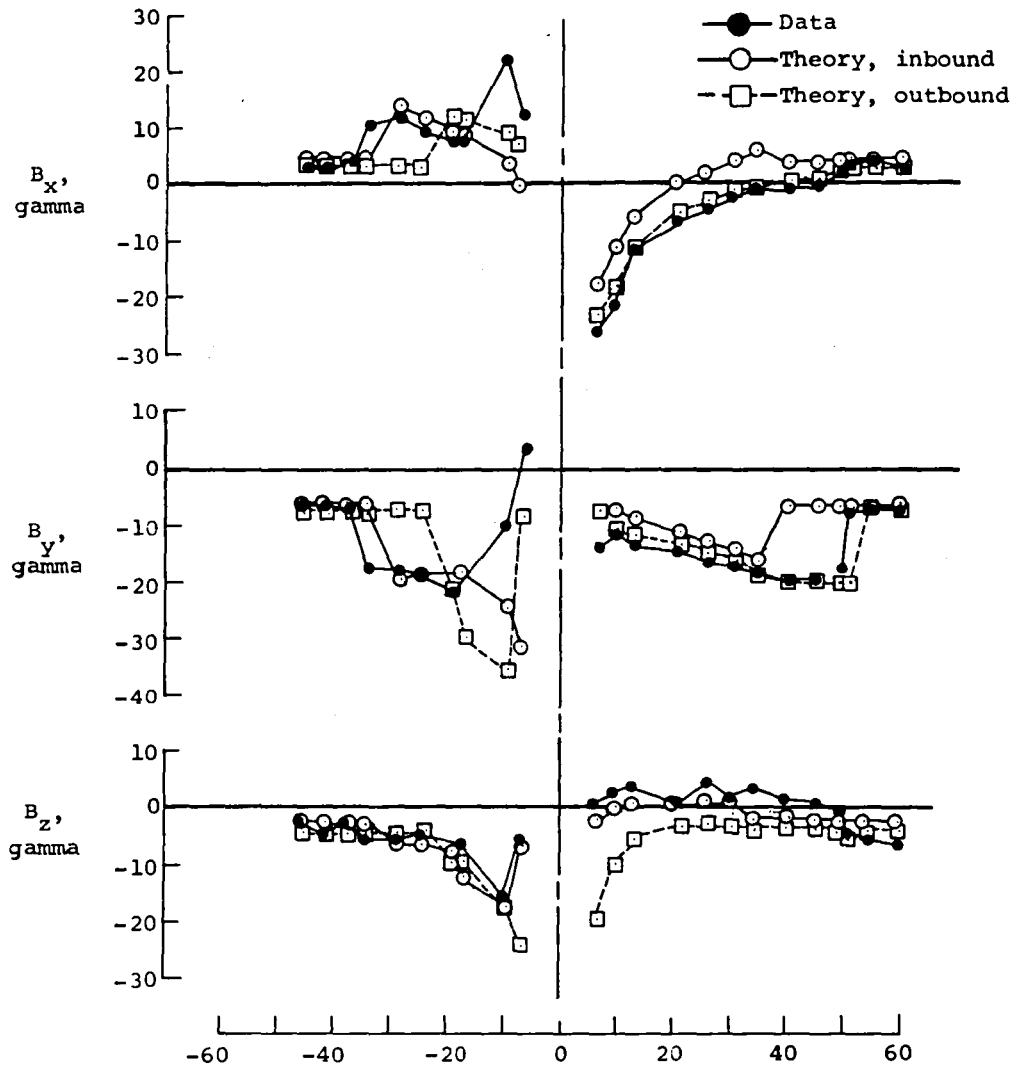


Figure 15.- Comparison of observed (OPA) and theoretical time histories of ionosheath plasma properties for P-V Orbit 6 based on inbound and outbound interplanetary solar-wind conditions using a gasdynamic solution for $M_\infty = 13.3$, $\gamma = 2.0$.



(a) Magnetic-field magnitude.

Figure 16.- Comparison of observed (OMAG) and theoretical time histories for the magnitude of the magnetic field for P-V Orbit 6 based on inbound and outbound interplanetary conditions using gasdynamic solution for $M_\infty = 13.3$, $\gamma = 2$.



Time from periapsis, min.
 (b) Magnetic-field components.

Figure 16.- Concluded.

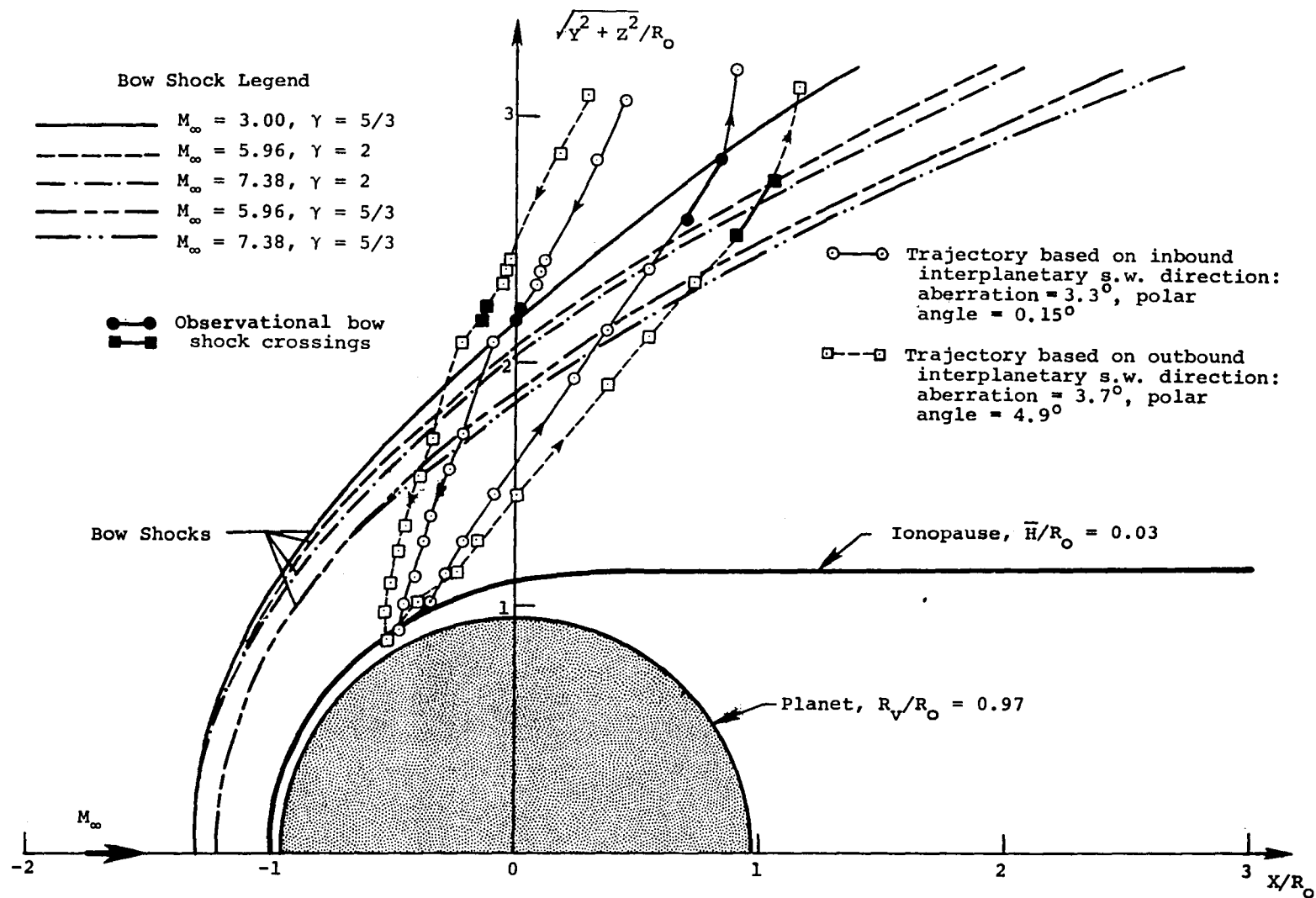


Figure 17.- P-V Orbit 3 trajectories and observational bow shock crossings as viewed in solar-wind coordinates based on inbound and outbound interplanetary solar-wind directions; also, various bow shock shapes for different interplanetary solar wind conditions.

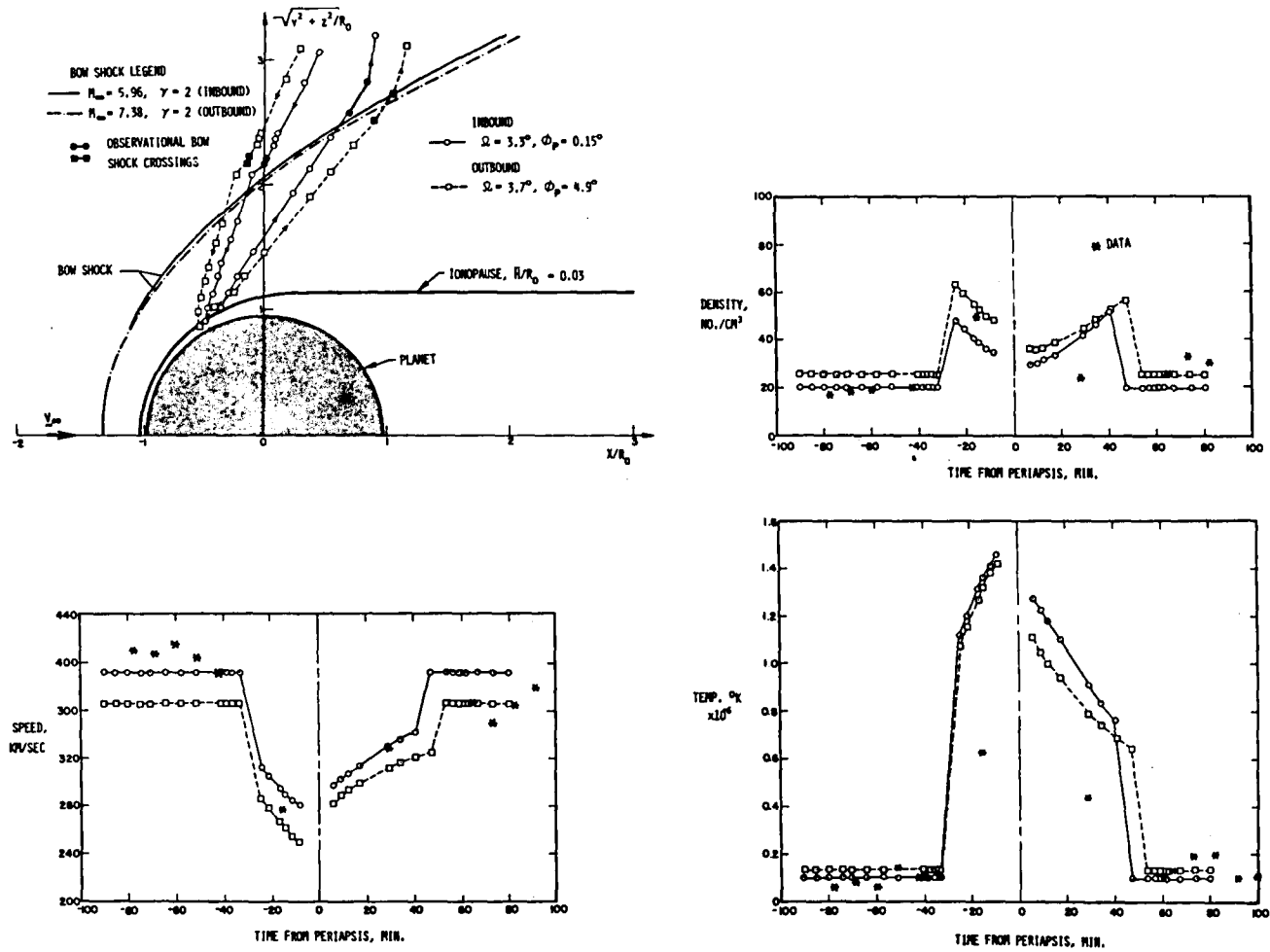
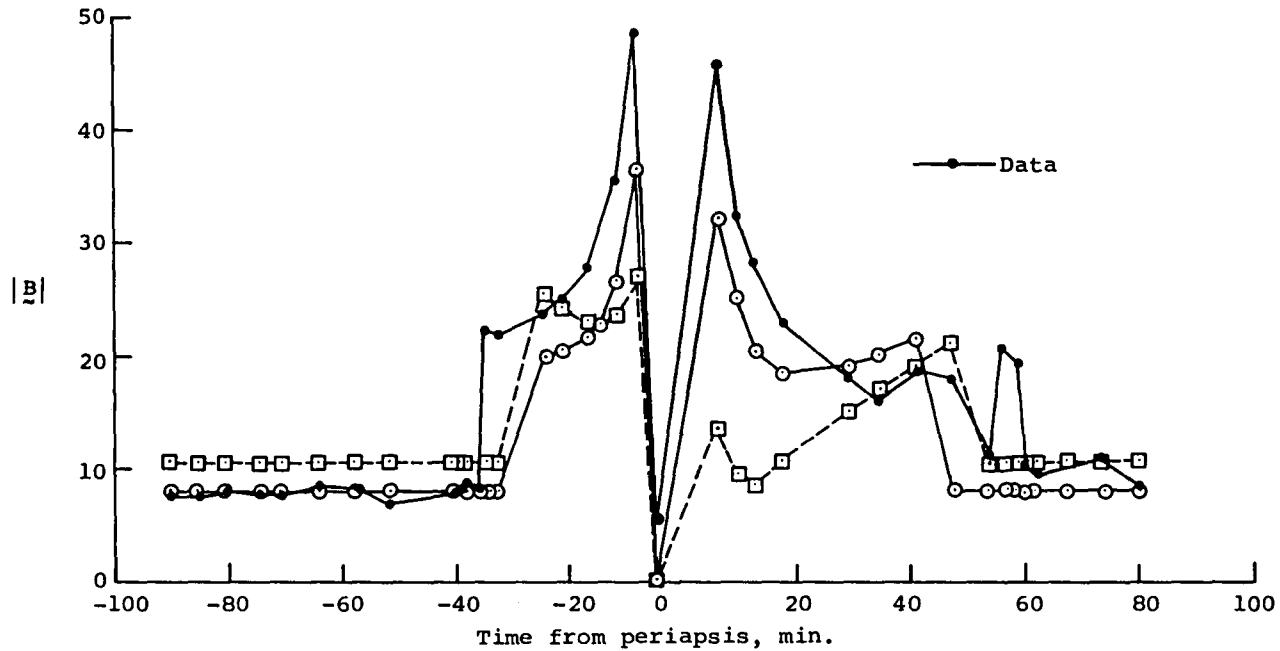


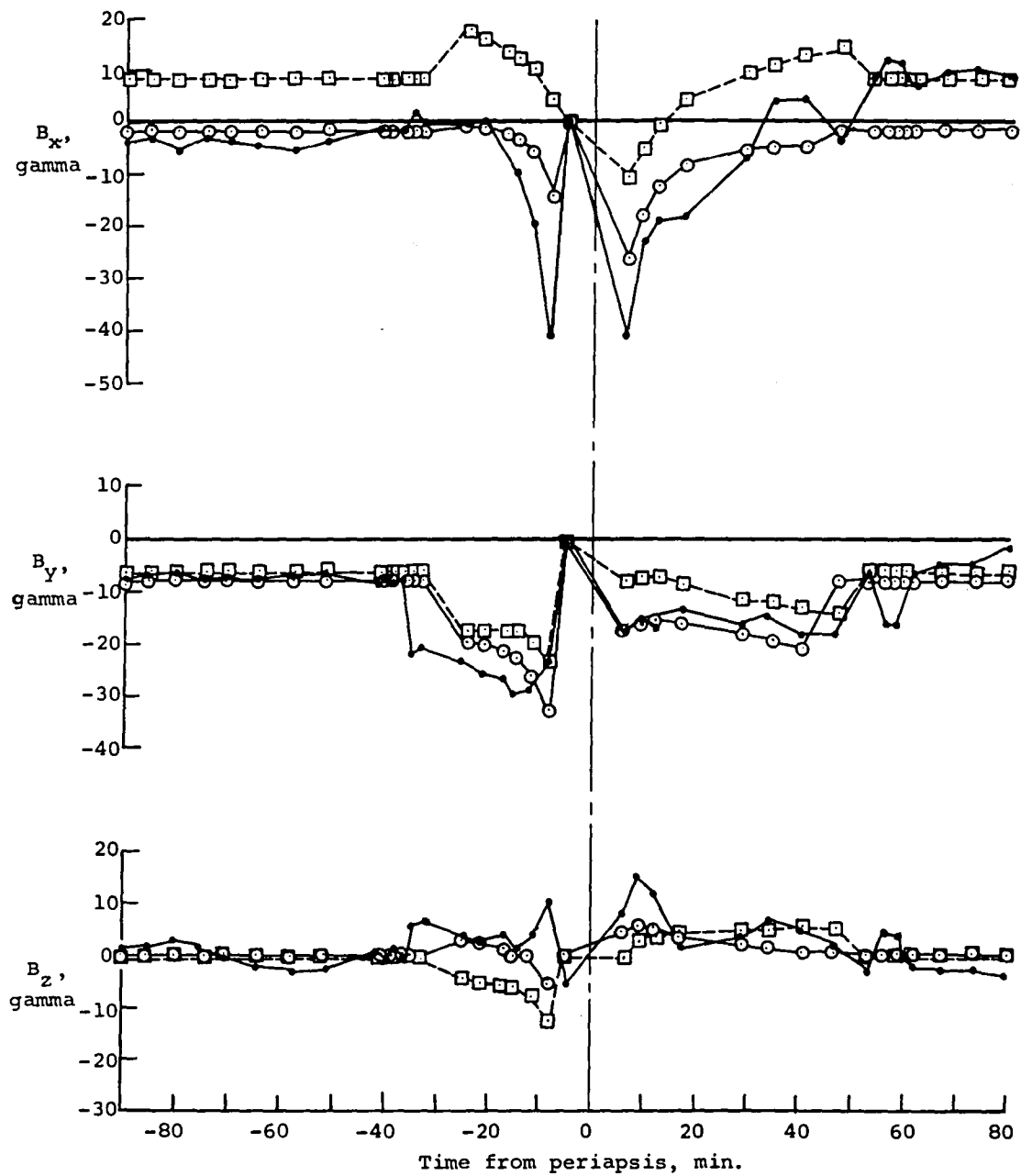
Figure 18.- Comparison of observed and theoretical time histories of ionosheath plasma properties for P-V Orbit 3 based on inbound and outbound interplanetary solar-wind conditions.

Theory	M_∞	γ	Ω	ϕ_P	B_{x_∞}	B_{y_∞}	B_{z_∞}
—○— Inbound	7.38	2.0	3.3°	0.15°	-1.78	-7.86	0.08
—□— Outbound	5.96	2.0	3.7°	4.90°	-8.38	-6.45	-0.31



(a) Magnetic-field magnitudes.

Figure 19.- Comparison of observed (OMAG) and theoretical time histories for the magnetic field for P-V Orbit 3 based on inbound and outbound interplanetary solar-wind conditions using gasdynamic solutions $M_\infty = 7.38$, $\gamma = 2.0$ for inbound and $M_\infty = 5.96$, $\gamma = 2.0$ for outbound calculations.

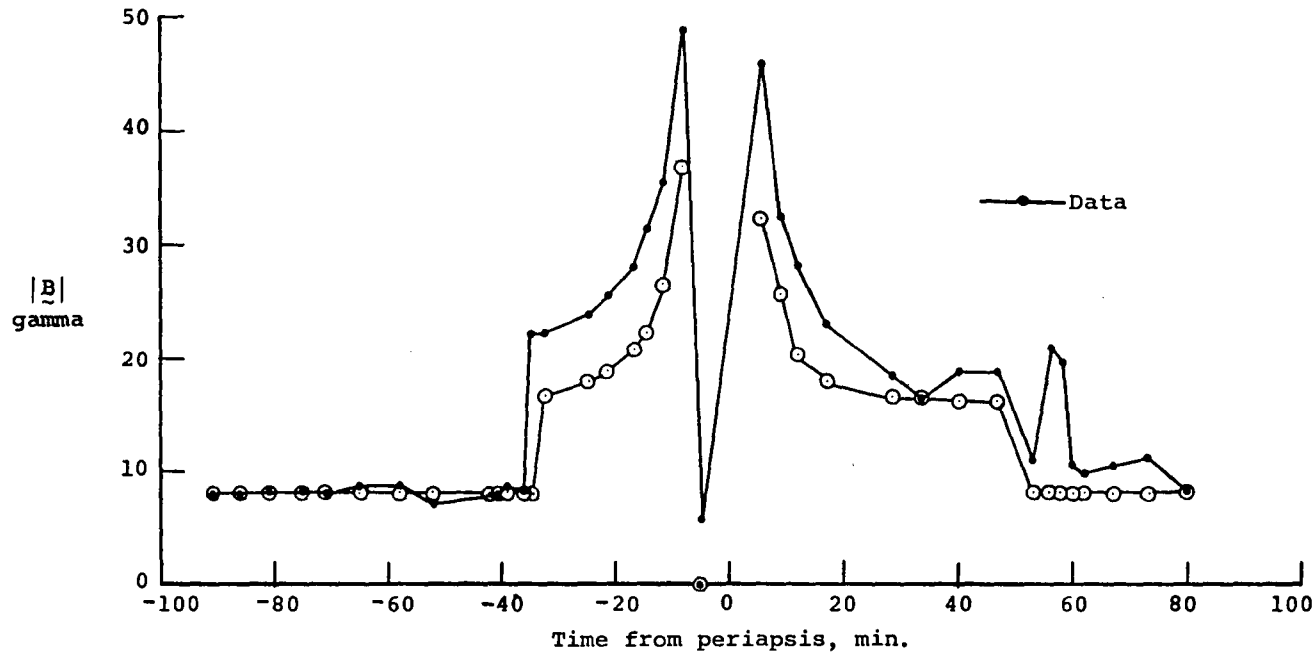


(b) Magnetic-field components.

Figure 19.- Concluded.

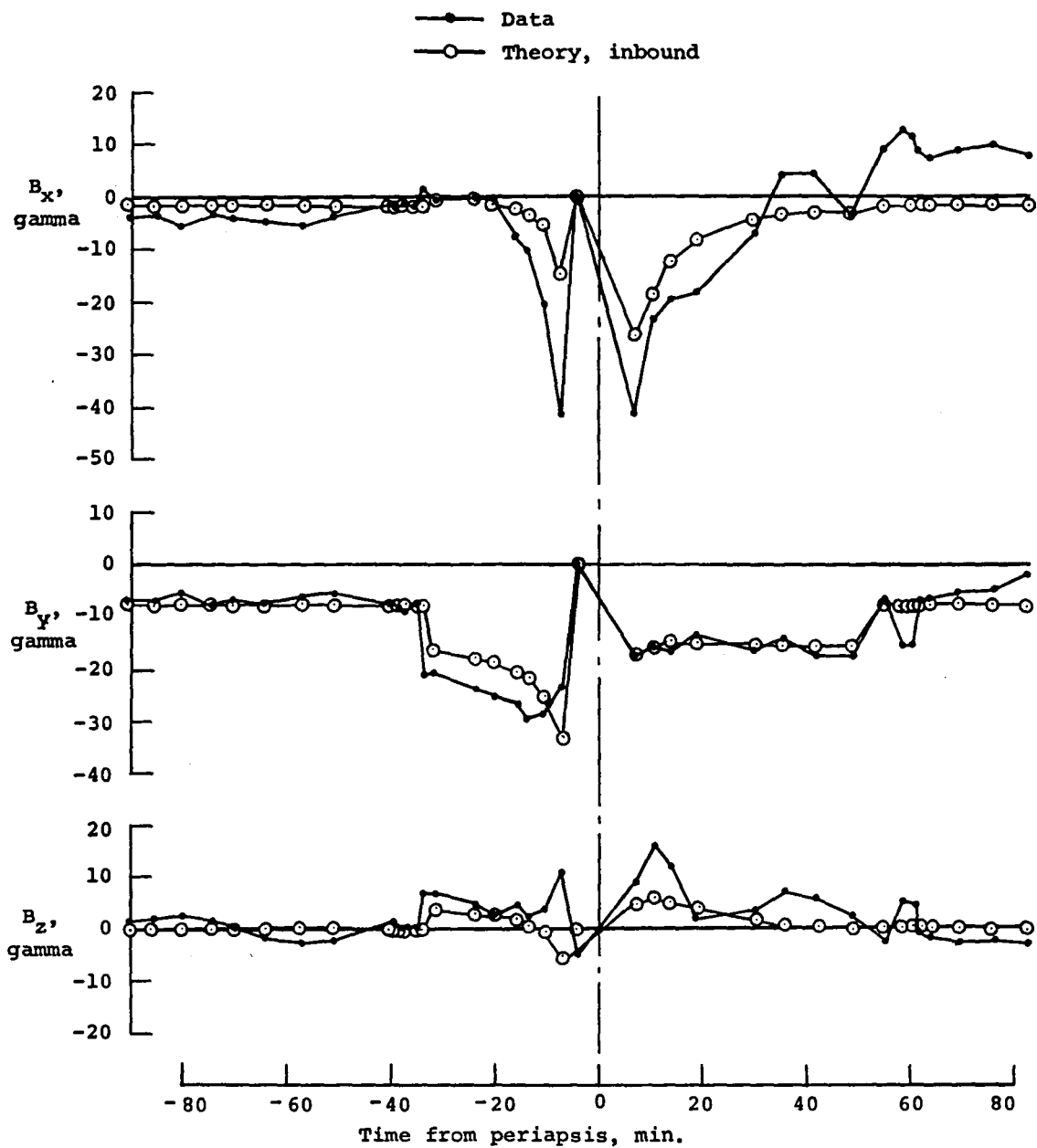
Interplanetary Conditions

<u>Theory</u>	M_∞	γ	Ω	ϕ_p	$B_{x\infty}$	$B_{y\infty}$	$B_{z\infty}$
—○— Inbound	3.0	5/3	3.3°	0.15°	-1.78	-7.86	0.08



(a) Magnetic-field magnitude.

Figure 20.- Comparison of observed (OMAG) and theoretical time histories of the magnetic field for P-V Orbit 3 based on inbound solar wind interplanetary conditions using a gasdynamic solution for $M_\infty = 3.0$, $\gamma = 5/3$.



(b) Magnetic-field components.

Figure 20.- Concluded.

1. Report No. NASA CR-3267	2. Government Accession No.	3. Recipient's Catalog No.	
4. Title and Subtitle APPLICATION OF ADVANCED COMPUTATIONAL PROCEDURES FOR MODELING SOLAR-WIND INTERACTIONS WITH VENUS - THEORY AND COMPUTER CODE		5. Report Date May 1980	6. Performing Organization Code 498/C
		8. Performing Organization Report No. NEAR TR 202	10. Work Unit No.
7. Author(s) Stephen S. Stahara, Daniel Klenke, Barbara C. Trudinger, and John R. Spreiter		11. Contract or Grant No. NASW-3182	
		13. Type of Report and Period Covered Contractor Report 7/78 - 9/79	
9. Performing Organization Name and Address Nielsen Engineering & Research, Inc. 510 Clyde Avenue Mountain View, CA 94043		14. Sponsoring Agency Code	
		12. Sponsoring Agency Name and Address National Aeronautics and Space Administration Washington, DC 20546	
15. Supplementary Notes NASA Headquarters Technical Monitor: Robert E. Murphy			
16. Abstract <p>Advanced computational procedures are developed and applied to the prediction of solar-wind interaction with nonmagnetic terrestrial-planet atmospheres, with particular emphasis to Venus. The theoretical method is based on a single-fluid, steady, dissipationless, magnetohydrodynamic continuum model, and is appropriate for the calculation of axisymmetric, supersonic, super-Alfvénic solar-wind flow past terrestrial planets. The procedures, which consist of finite-difference codes to determine the gasdynamic properties and a variety of special-purpose codes to determine the frozen magnetic field, streamlines, contours, plots, etc. of the flow, are organized into one computational program which has been extensively documented and is presented in a general user's manual included as part of this report.</p> <p>Theoretical results based upon these procedures are reported for a wide variety of solar-wind conditions and ionopause obstacle shapes. Plasma and magnetic-field comparisons in the ionosheath are also provided with actual spacecraft data obtained by the Pioneer-Venus Orbiter. These results have verified the appropriateness of the basic theoretical model, and have indicated the importance of accounting for the variable oncoming direction of the interplanetary solar wind.</p>			
17. Key Words (Suggested by Author(s)) Solar-Wind/Ionosphere Interaction Finite-Difference Methods Steady Flow Frozen Magnetic Field		18. Distribution Statement Unclassified - Unlimited Subject Category 92	
19. Security Classif. (of this report) Unclassified	20. Security Classif. (of this page) Unclassified	21. No. of Pages 316	22. Price* \$11.75

End of Document